Université de Montréal

TITRE:

Characterization of polycystin-1 in ADPKD pathogenetic mechanism: Biogenesis and functional implications by genetic approaches in mouse

Par Almira Kurbegovic

Programme de biologie moléculaire
Faculté de médicine

Thèse présentée à la Faculté des études supérieures
en vue de l'obtention du grade de Philosophiae Doctor (Ph.D.)
en biologie moléculaire

Mars, 2014

Université de Montréal

Faculté des études supérieures

Cette thèse intitulée:

Characterization of polycystin-1 in ADPKD pathogenetic mechanism: Biogenesis and functional implications by genetic approaches in mouse

Présentée par

Almira Kurbegovic

a été évaluée par un jury composé des personnes suivantes:

Président-rapporteur:.....[redacted]……

Directeur de recherche:…..……[redacted]……..

Membre du jury:…….....…[redacted].....…..

Examinateur externe:…..……[redacted].....….

Représentant du doyen de FES:…[redacted]……...…

Thèse acceptée le:……..…… [redacted]……..

RÉSUMÉ

La polykystose rénale autosomique dominante (ADPKD) est une des maladies génétiques les plus communes. ADPKD se manifeste le plus souvent au stade adulte par la présence de kystes rénaux, et bien souvent de kystes hépatiques, avec une progression très variable. ADPKD mène à une insuffisance rénale: les seuls recours sont la dialyse puis la transplantation rénale. Les mutations dispersées sur les gènes *PKD1* (majoritairement; la protéine polycystine-1, PC1) et *PKD2* (la protéine polycystine-2, PC2*)* sont responsables de l'ADPKD. Le mécanisme pathogénétique de perte de fonction (LOF) et donc d'un effet récessif cellulaire est évoqué comme causatif de l'ADPKD. LOF est en effet supporté par les modèles murins d'inactivation de gènes *PKD1/PKD2*, qui développent de kystes, quoique *in utéro* et avec une rapidité impressionnante dans les reins mais pas dans le foie. Malgré de nombreuses études *in vitro*, le rôle de PC1/PC2 membranaire/ciliaire reste plutôt hypothétique et contexte-dépendant. Ces études ont associé PC1/PC2 à une panoplie de voies de signalisation et ont souligné une complexité structurelle et fonctionnelle exceptionnelle, dont l'implication a été testée notamment chez les modèles de LOF. Toutefois, les observations patho-cellulaires chez l'humain dont une expression soutenue, voire augmentée, de *PKD1*/PC1 et l'absence de phénotypes extrarénaux particuliers remet en question l'exclusivité du mécanisme de LOF. Il était donc primordial **1)** d'éclaircir le mécanisme pathogénétique, **2)** de générer des outils *in vivo* authentiques d'ADPKD en terme d'initiation et de progression de la maladie et **3)** de mieux connaitre les fonctions des PC1/PC2 indispensables pour une translation clinique adéquate. Cette thèse aborde tous ces points. **Tout d'abord**, nous avons démontré qu'une augmentation de *PKD1* endogène sauvage, tout comme chez l'humain, est pathogénétique en générant et caractérisant en détail un modèle murin transgénique de *Pkd1* ($Pkd1_{TAG}$). Ce modèle reproduit non seulement les caractéristiques humaines rénales, associées aux défauts du cil primaire, mais aussi extrarénales comme les kystes hépatiques. La sévérité du phénotype corrèle avec le niveau d'expression de *Pkd1* ce qui supporte fortement un modèle de dosage. **Dans un deuxième temps**, nous avons démontré par les études de complémentations

génétiques que ces deux organes reposent sur une balance du clivage GPS de Pc1, une modification post-traductionelle typique des aGPCR, et dont l'activité et l'abondance semblent strictement contrôlées. **De plus,** nous avons caractérisé extensivement la biogénèse de Pc1 et de ses dérivés *in vivo* générés suite au clivage GPS. Nous avons identifié une toute nouvelle forme et prédominante à la membrane, la forme $Pc1^{deN}$, en plus de confirmer deux fragments N- et C-terminal de Pc1 (NTF et CTF, respectivement) qui eux s'associent de manière non-covalente. Nous avons démontré de façon importante que le trafic de $Pc1^{deN}$ *i.e.,* une forme NTF détachée du CTF, est toutefois dépendant de l'intégrité du fragment CTF *in vivo.* **Par la suite,** nous avons généré un premier modèle humanisant une mutation *PKD1* non-sens tronquée au niveau du domaine $NTF^{(E3043X)}$ en la reproduisant chez une souris transgénique (*$Pkd1_{extra}$*). Structurellement, cette mutation, qui mimique la forme $Pc1^{deN}$, s'est également avérée causative de PKD. Le modèle *$Pkd1_{extra}$* a permis entre autre de postuler l'existence d'une cross-interaction entre différentes formes de Pc1. **De plus,** nos deux modèles murins sont tous les deux associés à des niveaux altérés de c-Myc et Pc2, et soutiennent une implication réelle de ces derniers dans l'ADPKD tou comme une interaction fonctionnelle entre les polycystines. **Finalement,** nous avons démontré un chevauchement significatif entre l'ADPKD et le dommage rénal aigüe (ischémie/AKI) dont une expression augmentée de Pc1 et Pc2 mais aussi une stimulation de plusieurs facteurs cystogéniques tel que la tubérine, la β-caténine et l'oncogène c-Myc. Nos études ont donc apporté des évidences cruciales sur la contribution du gène dosage dans l'ADPKD. Nous avons développé deux modèles murins qui serviront d'outil pour l'analyse de la pathologie humaine ainsi que pour la validation préclinique ADPKD. L'identification d'une nouvelle forme de Pc1 ajoute un niveau de complexité supplémentaire expliquant en partie une capacité de régulation de plusieurs voies de signalisation par Pc1. Nos résultats nous amènent à proposer de nouvelles approches thérapeutiques: d'une part, le ciblage de CTF *i.e*., de style chaperonne, et d'autre part le ciblage de modulateurs intracellulaires (c-Myc, Pc2, Hif1α). Ensemble, nos travaux sont d'une importance primordiale du point de vue informatif et pratique pour un avancement vers une thérapie contre l'ADPKD. Le

partage de voies communes entre AKI et ADPKD ouvre la voie aux approches thérapeutiques parallèles pour un traitement assurément beaucoup plus rapide.

Mots clés: ADPKD / Polycystine-1 / Clivage GPS / Dommages rénaux / Souris / Foie/ C-Myc / Pc2/

ABSTRACT

Autosomal dominant polycystic kidney disease (ADPKD) is one of the most common genetic diseases. ADPKD is manifested by the presence of renal cysts detected most often in the adult stage, and frequently liver cysts, with highly variable progression. ADPKD leads to kidney failure with the only recourse of dialysis and eventual kidney transplantation. Mutations dispersed throughout the *PKD1* gene (major player, the polycystin-1 protein, PC1) and the *PKD2* gene (polycystin-2 protein, PC2) are responsible for ADPKD. The loss of function (LOF) pathogenetic mechanism, and therefore a cellular recessive effect, has been suggested as causative of ADPKD. LOF is indeed supported by the *PKD1/PKD2* gene inactivation mouse models, which develop cysts, although *in utero* with impressive speed in the kidney but not in the liver. Despite many *in vitro* studies, the membrane/ciliary role of PC1/PC2 remains rather hypothetical and context-dependent. These studies have associated PC1/PC2 to a variety of signaling pathways and underlined exceptional structural and functional complexity, whose involvement has been tested especially in LOF models. However, pathocellular observations in humans with sustained and even increased expression of *PKD1*/PC1, and the absence of particular human extrarenal phenotypes questions the exclusivity of the LOF mechanism. It was therefore essential **1)** to clarify the pathogenetic mechanism, **2)** to generate *in vivo* tools authentic of ADPKD in terms of initiation and progression of the disease and **3)** to better understand the essential functions of PC1/PC2 for an adequate clinical translation. This thesis addresses all of these issues. **First**, we demonstrated that an increase in endogenous *PKD1*, just like in humans, is pathogenetic by generating and characterizing in detail a transgenic mouse model of *Pkd1* ($Pkd1_{TAG}$). This model not only reproduces the renal human characteristics associated with defects of the primary cilium, but also the extrarenal, namely, liver cysts. The severity of the phenotype correlates with the expression level of *Pkd1,* which strongly supports a dosage model. **Secondly**, we have demonstrated with genetic complementation studies that these two organs rely on a balance of Pc1 GPS cleavage, a typical post-translational modification of aGPCR, whose activity and abundance seem strictly controlled. **Furthermore**, we have extensively characterized

Pc1 biogenesis and its derivatives *in vivo* generated upon GPS cleavage. We have identified a new form, predominantly on the membrane, the $Pc1^{deN}$ form, in addition to confirming the two N- and C-terminal Pc1 fragments (NTF and CTF, respectively), which associate non-covalently. Importantly, we have demonstrated that traffic of $Pc1^{deN}$ *i.e.*, the NTF form detached from the CTF, is still dependant on the integrity of the CTF fragment. **Next**, we generated a first model humanizing a *PKD1* nonsense truncated mutation at the level of the $NTF^{(E3043X)}$ domain by reproducing it in a transgenic mouse ($Pkd1_{extra}$). Structurally, this mutation, which mimics $Pc1^{deN}$, has also been shown to be causative of PKD. The $Pkd1_{extra}$ model allowed the proposition of the existence of a cross-interaction between different forms of Pc1. **In addition**, our two mouse models are both associated with altered levels of c-Myc and Pc2, which is supportive of their involvement in ADPKD and a functional interaction between the polycystins. **Finally**, we have shown a significant overlap between ADPKD and acute renal injury (ischemia/AKI) namely increased expression of Pc1 and Pc2 but also stimulation of several cystogenic factors such as tuberin, β-catenin and the oncogene c-Myc. Our studies have therefore given crucial evidence to the contribution of *PKD1* gene dosage mechanism in ADPKD. We have developed two mouse models, which can serve as a tool for the analysis of human pathology as well as for preclinical validation of ADPKD. The identification of a new form of Pc1 adds an additional level of complexity in part explaining the regulation capacity of Pc1 on several signaling pathways. Our findings lead us to propose new therapeutic approaches: firstly, targeting the CTF *i.e.*, chaperone style, and also targeting intracellular modulators (c-Myc, Pc2, Hif1α). Together, our work is of paramount importance in an informative point of view and practical perspective for progress towards a therapy for treating ADPKD. The sharing of common pathways between AKI and ADPKD paves the way for parallel therapeutic approaches for assured much faster treatment.

Keywords: ADPKD / Polycystin-1 / GPS cleavage/ AKI / mouse models / kidney / liver / c-Myc / Pc2 /

TABLE OF CONTENTS

CHAPTER V

CHAPTER VI

CHAPTER VII

ARTICLE 4: *Acute kidney injury crosstalk with Pkd1/Pkd2 dosage-increased pathogenesis and signalling,* **manuscript in preparation for Nature Communications**

CHAPTER VIII

ARTICLE 5: *Transgenic mice uncover the crucial role of the GPS cleavage in liver homeostasis,* **manuscript in preparation for JASN**

LIST OF FIGURES

LIST OF TABLES

ABBREVIATIONS

A-aa: amino acid(s); **ADPKD:** autosomal dominant polycystic kidney disease; **ADPLD:** autosomal dominant polycystic liver disease; **aGPCR:** adhesion G protein-coupled receptor; **App:** Appendix; **AF:** amniotic fluid; AKI: acute kidney injury; **ARF4:** ADP-ribosylation factor 4; **ARPKD:** autosomal recessive polycystic kidney disease; **APP:** β-amyloid precursor protein (associated with Alzheimer's disease); **AVP:** arginine vasopressin;

B-BAI: brain-specific angiogenesis inhibitor; **BBS**: Bardet-Biedl syndrome; **BFPP:** bilateral frontoparietal polymicrogyria caused by mutations in GPR56 gene (G protein-coupled receptor 56); **BMP:** bone morphogenetic protein; **BSA:** bovine serum albumin.

C-CAKUT: congenital anomalies of the kidney and urinary tract; **cAMP:** cyclic adenosine monophosphate; **CC:** coiled-coil domain; **CF:** cystic fibrosis; **CFTR:** cystic fibrosis transmembrane regulator; **Ch:** Chapter; **ChIP:** chromatin immunoprecilitation; **CHOP:** CCAAT/enhancer binding protein (C/EBP) homologous protein; **CKD:** chronic kidney disease; **CKI:** chronic kidney injury; **CL1/CIRL:** calcium-independent receptor of α-latroxilin (also called latrophilin and lectomedein), Two combined names in CL1=CIRL, binds to latroxin; **CM:** cap mesenchyme; **Col1α1:** collagen 1-α 1; **COS1/COS7**: two forms of COS cells, an immortalized fibroblast-like cell line derived from monkey kidney tissue; **CTF:** C-terminal fragment (following GPS cleavage); **CTGF:** connective tissue growth factor; **CT**: C-terminus; **CTT:** C-terminal tail; **CRISP:** Consortium of Radiologic Imaging Study of PKD.

D-DAB: 3,3'-Diaminobenzidine used for immunohistochemistry with hydrogen peroxydase; **DAPT:** N-[N-(3,5-difluorophenacetyl)-L-alanyl]-S-phenylglycine t-butyl ester (γ-secretase inhibitor); **DBA:** Dolichos biflorus agglutinin; **DDR:** DNA damage

response; dpc: days post-coitum; **Dermo-1 Cre:** mesoderm-specific basic helix-loop-helix transcription factor *Dermo1*; **2DG:** 2-deoxyglucose (glucose analog); **Dmp1:** dentin matrix acidic phosphoprotein gene; **dpf:** days post-fertilization.

E-E/e: embryonic (day); **EBNA2/P100**: ubiquitously expressed transcription factor originally identified as a coactivator of the Epstein, Barr virus nuclear antigen 2; **ECM:** extracellular matrix; **e.g.:** exempli gratia (for the sake of example); **EGF:** epidermal growth factor; **EM:** electron microscopy; **EMSA:** electrophoretic mobility shift assay; **EMT:** epithelial to mesenchymal transition; **ER:** endoplasmic reticulum; **ESC:** embryonic stem cells; **ERK:** regulated kinase; **ERK:** extracellular-signal regulated protein; **ESRD:** end stage renal disease; **etc.:** and other things, and so forth.

F-FACS: fluorescence-activated cell sorting; **FAK:** focal adhesion kinase; FL: full-length; **FGF:** fibroblast growth factor; **FPC:** fibrocystin/polyductin; **FSP:** fibroblast-specific protein.

G-g-force, gravitational; **GAIN:** GPCR-autoproteolytic inducing domain; **GDNF:** glial cell line-derived neurotrophic factor; **GFP:** green fluorescent protein; **GFR:** glomerular filtration rate; **GPCR:** G protein-coupled receptor; **GPS:** GPCR proteolysis site; **GRP98** (Ush2 gene): G protein-coupled receptor 98 gene underlying Usher syndrome; **GOF:** gain-of-function; **GSEA:** gene set enrichment analysis.

H-h: human; **HAEC:** human aortic endothelial cells; **HEK/293/HEK293:** transformed cells derived from normal embryonic human kidneys; **HeLa:** immortal cell line derived from human cervical; **HepG2:** adhesive, epithelial-like human liver hepatocellular carcinoma cell line; **HGF:** hepatocyte growth factor; **HLH:** helix-loop-helix; **HIF:**

Hypoxia inducible factor; **H_2O_2:** hydrogen peroxyde; **Hpf:** hours post fertilization; **hrs:** hours; **HUVEC:** Human umbilical vein endothelial cells.

I-Id2: inhibitor of DNA binding (dominant negative HLH protein); ***i.e.*:** from latin ''id est'' what means ''that is''; **IFT:** intraflagellar transport; **IHC:** immunohistochemistry; **IM:** intermediate mesoderm; **IMDC:** inner medullary collecting duct cells; **Inv:** inversin; **iPS:** induced pluripotent stem cells (generated with retroviral transduction of OSK: Oct4, Sox2, Klf4 and sometimes c-myc); **IRI:** renal ischaemia-reperfusion injury.

K-kDa: kiloDalton; **KIM-1:** kidney injury molecule 1.

L-LEF: lymphoid enhancer-binding factor; **LLC-PK1:** pig kidney epithelial cells; **LNB-TM7:** long N-terminal family G GPCR-related 7TM receptor; **LOF:** loss-of-function; **LOH:** loss-of-heterozygosity; **LOV-1:** location of vulva (Drosophila PKD1 gene).

M-M: molar; **m:** murin; **MAPK:** mitogen-activated protein kinase; **MCP-1:** proinflammatory monocyte chemotactic protein-1 (macrophage chemoattractant); **MDCK:** madin darby canin kidney cell line; **MEFs:** mouse embryonic fibroblasts; **MET:** mesenchyme-to-epithelial transition; **miRNAs:** microRNAs/miR; **MM:** metanephric mesenchyme; **MKS**: Meckel-Gruber syndrome; **MMP:** matrix metalloproteinase; **MMTV-Cre:** the mouse mammary tumor virus (MMTV) long terminal repeat promoter directing expression of P1 Cre recombinase; **mRNA:** messenger ribonucleic acid; **MRI:** magnetic resonance imaging; Meox-Cre: knock-in in mesenchyme homeobox 2 gene locus, very early expression from the epiblast stage; **MTOC:** microtubule organizing center; **MVB:** multivesicular bodies; **MIM**-see **OMIM**.

N-NFAT: nuclear factor of T-cells; **NGS:** normal goat serum; **NLS:** nuclear localization sequence; **NTF:** N-terminal fragment; **NPHP**: nephronophthisis.

O-Oc: osteocalcin; **OCD:** oriented cell division; **Odd1/Osr1:** Odd skipped related1; **OMIM/MIM:** online Mendelian inheritance in man (online continuously updated catalog); **ORF:** open reading frame.

P-P: post-natal (day); **PAC:** P1-derived artificial chromosome; **PC1** (human) **Pc1** (murin): polycystin-1; **PC2** (human), **Pc2** (murin): polycystin-2; **PCP:** planar cell polarity; **PD1:** polyductin; **PI3K:** phosphatidyl-inositol-3-kinase; **PKA:** protein kinase A; **PKD:** polycystic kidney disease(s); **PKD1** (human), **Pkd1** (murin): Polycystic kidney disease gene 1; **PKD2** (human), **Pkd2** (murin): Polycystic kidney disease gene 2; **PLC:** phospholipase C; **PLD:** polycystic liver disease; **PLP1:** proteolipid protein gene 1; **PP1a**: protein phosphatase1 alpha; **PPAR-γ:** peroxisome proliferator-activated receptor γ; **Pu-Py:** polypurine-polypyrimidine.

R-RA: retinoic acid (Vitamin A); **RAR:** retinoic acid receptor; **RCC:** renal cell carcinoma **RCTE:** immortalized normal human renal cortical tubular epithelia; **RIP:** regulated intramembrane proteolysis; **ROCK:** Rho-associated kinase; **RPE:** retinal pigment epithelium; **RPTEC:** renal proximal tubular epithelial cells; **RXR:** retinoic X receptor.

S-SAC: stretch activated ion channels; **SAGE:** serial analysis of gene expression; **SEM:** scanning electron microscopy; **SERCA2:** sarco/endoplasmic reticulum Ca^{2+}-ATPase type 2 isoform; **Shh/SHH:** sonic hedgehog; **shRNA:** short hairpin RNA (for silencing gene expression); **SNARE:** soluble NEM-sensitive factor attachment protein receptor; **SOCE:** Store operated Ca2+ channels.

T-TAL: thick ascending limb (of loop of Henlé); **TCF:** T cell transcription factor; **TEMPO program**: Tolvaptan Efficacy and Safety in Menagement of PKD and Outcomes; **tg:** transgenic; **TGFβ:** transforming growth factor; **THP:** Tamm-Horsfall protein; **TJ:** tight junctions; **TKV:** total kidney volume; **TM:** transmembrane; **mTOR:** Mammalian target of rapamycin; **TRP:** transient receptor potential channel; **TRPP**: transient receptor potential polycystic.

U-UB: ureteric/uretic bud; **UUO:** unilateral ureteral obstruction.

V-V2R: (AVP) V2 receptor; **VHL:** Von Hippel–Lindau disease; **vs:** versus; **VSMC:** vascular smooth muscle cells.

W-WD: Wolffian duct; **Wks:** weaks; **WT:** wild-type; **WT1:** Wilms tumor protein.

Y-Yrs: years.

Z-ZO1: zonula occludens protein-1.

DEDICACE

In loving memory of several members of my family lost during my Ph.D.

ACKNOWLEDGEMENTS

Et puis le moment tant attendu est finalement arrivé!
Tout au long de ces années pendant mon doctorat, j'ai eu l'occasion de grandir sur le plan professionnel mais également de murir inévitablement sur un plan plus personnel, en rencontrant de nombreuses personnes et étudiants qui m'ont enseigné et énormement apporté.....
….
Je souligne la persévérance, l'efficacité, la multifunctionalité et le dévouement irréprochable de Dr. Marie Trudel. Merci de m'avoir accueillie dans votre laboratoire, de m'avoir permis d'assister à une multitude de congrès et de conférences, et d'avoir partagé et transmis généreusement et sans réserve votre savoir.

Et une disponibilité et une générosité irréprochable de Dominique Lauzier (Histologie, IRCM), Dominique Davidson (Laboratoire de Dr. Veillette, Immunologie, IRCM), Dominic Filion (Microscopie, IRCM), Constantin Androne (Animalerie, IRCM), Richard Cimon et Jean-Francois Lauzon (Équipements spécialisés, IRCM) et Carole Marcotte (Aide administratif).

Merci également aux différents laboratoires de l'IRCM et aux autres établissements de recherche de nous avoir fourni de précieux anticorps, les équipements de laboratoire, et d'avoir partagé avec nous leur expertise.

Je remercie le département de biologie moléculaire de l'Université de Montréal, l'IRCM et l'IRSC pour leurs soutients financiers et pour m'avoir donnée l'opportunité d'effectuer un stage scientifique de gros calibre, dans une université américaine de renommée mondiale.

Les membres du comité de thèse pour leur suivi et leur contribution pendant mon cheminement doctoral et leur esprit critique sur mon travail. Depuis le tout début, en partant avec le choix même des articles de mon examen prédoctoral (Hedgehog, Wnt,

cil primaire), l'emphase sur l'importance critique d'usage des contrôles et le choix et l'interprétation de test significatifs se sont avérés très bénéfiques et pertinents, encore plus évident maintenant. Je remercie les membres du jury d'avoir accepté d'évaluer ma thèse ainsi que pour leurs commantaires très constructifs qui m'ont permis d'apprendre davantage.

Dr. Wafaa Lemsaddek, Angela Schneider and Monika Krzywania pour leur géntillesse et leur énorme contribution quant à l'édition et à la correction de ma thèse.

Et, cela va sans dire, mais surtout un gros merci à toute ma famille, mes parents, ma soeur bien-aimée, mon fiancé et sa famille. Leur support, encouragements continuels, leur compréhension et leur patience m'ont permis de mener à terme ce gros projet qui fut le doctorat en biologie moléculaire. Il est temps de passer à d'autres projets avec, à mon avis et donc subjectivement parlant, beaucoup d'expérience et de détermination. Je suis prête à ce que le futur me réserve et de contribuer davantage, avec mes acquis, à l'avancement de la recherche fondamentale!

CHAPTER I - REVIEW OF THE LITERATURE

1) Kidney development

The definitive kidney or metanephros develops through branching morphogenesis much like the lung, mammary gland and submandibular salivary gland. In a manner similar to these other organs, kidney development is a very active process of interactions between different cell types and involvement of multiple nuclear factors and secreted molecules. It requires many critical cellular steps such as epithelial-mesenchymal transition (EMT), stem cell differentiation and renewal, cell migration and polarity, interaction between different cell types or cell autonomous regulation, and on-off switch of developmental programs. Alteration of the aforementioned events can lead to the gamut of kidney defects and anomalies, ranging from kidney agenesis to smaller kidneys to diseased kidneys, dysplasia and polycystic kidney disease.

The metanephric kidney forms from the epithelial ureteric bud (UB) originating from the Wolffian duct (WD) (or mesonephric duct), and the mesenchymal cells derived from the intermediate mesoderm (IM). The initial steps (~E10.5) are thought to involve: **1)** mesenchymal cells induction of the UB; **2)** outpouching of the Wolffian duct/UB; **3)** invasion of the UB into the metanephric mesenchyme (MM) (**Fig. 1**). This early outpouch and subsequent branching and biffurcation rely on interactions and signals between MM and UB. The MM surrounds the UB and forms a histologically distinct region, a so-called cap mesenchyme. This process requires continuous remodeling of the intracellular cell shape, cytoskeleton and extracellular matrix. In mice, the cap mesenchymal cells are believed to represent a pool of kidney multipotent stem cells expressing the factors *Six2* and *Cited* with self-renewal ability. These cells disappear within a few days post-natally at P2-P4. This marks the end of nephrogenesis when no new nephrons are produced but rather existing nephrons mature, a process that seems to conclude before birth in humans. Once the UB has invaded the MM, MET transition occurs with a *WT1* as a master transcriptional gene

for regulation of epithelial E-cadherin and Snail expression (**Fig.1**). The MM aggregates, transits through MET into epithelial structures, the renal vesicle, and comma and S-shaped bodies (which gives rise mainly to proximal and distal tubules, cells of ascending and descending limbs of Henle's loop) and finally connects to the branched UB (which becomes a collecting duct) to generate a functional unit called the nephron (**Fig.1**). The MM cells are also believed to differentiate into other cell types such as mesenchymal cells or the stromal cells and vascular endothelial cells of the kidney. Many repetitive rounds of bifurcation concentrated at the periphery of the kidneys (nephrogenic zone) lead to a mature kidney composed of ~200.000-1.8 million nephrons with essential roles in blood filtration, regulation of blood pressure, urinary excretion, and elimination of waste.

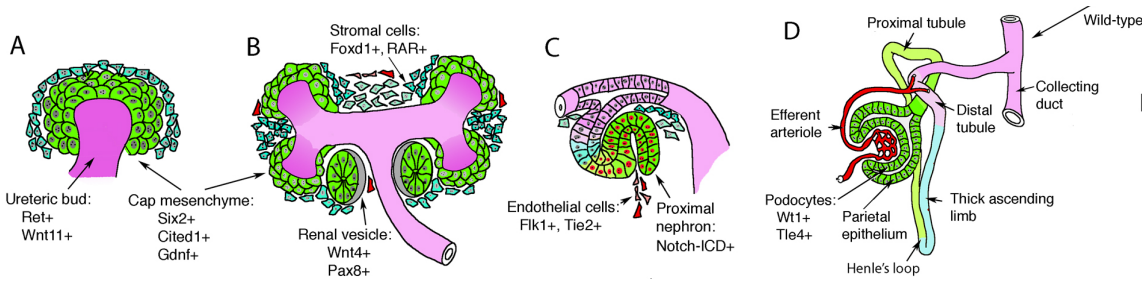

Figure 1: Diagram of different steps during kidney development starting from UB invasion of the MM (green) and some of the important factors implicated in these processes. Modified from (Dressler 2009). Adapted with permission. dev.biologists.org. DOI: 10.1242/dev.034876. See more details in the text.

Key molecular players and pathways for kidney development have been identified using total and conditional Cre/lox inactivation approaches (Reviewed in Chai, Song et al. 2013). For instance, in the IM (*i.e.,* during early kidney development), using different means, *Odd1*/*Osr1* (one of the earliest markers), *Lhx1* (*Lim* family member) and *Pax* genes were found to be very important since their inactivation in most cases leads to absence of UB and consequently kidney agenesis (Tsang, Shawlot et al. 2000, Bouchard, Souabni et al. 2002, Pedersen, Skjong et al. 2005). In the MM, *Gdnf*, *Hgf*, *Wnts*, *Fgf10* and *Bmp4/7*, to name only a few factors, act through their respective receptors on the UB epithelia to induce the ureteric epithelial branching

through signaling pathways such as ERK/MAPK, PI3K, PLCγ and canonical WNT pathway (β-catenin dependent), all well known to be implicated in cell proliferation, migration and ECM degradation (Reviewed in Little and McMahon 2012). Genes such as *WT1* and some members of the *Hox* family are important for MM survival and specification while other genes can be expressed in different compartments and steps throughout nephrogenesis (e.g. *Pax2* in both UB and MM). Stroma appears to be of high importance in nephrogenesis as well. Mendelsohn's group underlined paracrine signaling in stroma/UB axis and, in addition to Gdnf from MM, the importance of retinoic acid from the stroma as a critical player in the maintenance of *c-ret* levels in the UB and consequently in kidney branching and nephron number (Rosselot, Spraggon et al. 2010).

2) Human autosomal dominant polycystic kidney diseases (ADPKD)

2.1) Overview of the disease and genes involved

ADPKD, with autosomal dominant inheritance, is one of the most prevalent monogenic disorders. This chronic renal disease affects 1:500 to 1:1000 people worldwide and accounts for around 8-10% of renal replacement therapies/dialysis cases (Gabow 1993). Originating from a small number of nephrons (1-5%) and affecting all nephron segments, the bilateral kidney cysts can start *in utero.* Although the cysts can be evident very early on, the majority of cysts are detected in adulthood (Waldherr, Zerres et al. 1989, Michaud, Russo et al. 1994). Expansion of the cysts causes compression of noncystic adjacent tubules and eventually leads to ESRD with very variable onset (Grantham, Geiser et al. 1987, Wilson 2004, Torres, Harris et al. 2007). Liver cysts are very common and occur in 50 to 75% of ADPKD patients of 65 years of age and over (Everson 1993). Less frequent but life threatening features of ADPKD include cardiovascular disease such as hypertension, mitral valve prolapse and berry aneurysms in the brain (10X more frequent in ADPKD patients than in the normal population) (Wakabayashi, Fujita et al. 1983, Chapman, Rubinstein et al. 1992, Huston, Torres et al. 1993, Perrone 1997). Abdominal wall hernias have also been reported (Elzinga LW 1996).

ADPKD is a genetically allelically heterogeneous (PKD1 and PKD2) disease. Detected in ~90% of families, *PKD1* gene is mutated ~85% and *PKD2* in ~15% of ADPKD cases (Rossetti, Consugar et al. 2007, Audrezet, Cornec-Le Gall et al. 2012). A potential third PKD locus (PKD3) was proposed based on consistent ~10% of mutations unlinked with either *PKD1* or *PKD2* but its presence was recently not supported by re-evaluation of these families (Daoust, Reynolds et al. 1995, Paul, Consugar et al. 2014). Phenotypically, ADPKD1 (ADPKD caused by mutations in *PKD1* gene) and ADPKD2 (ADPKD caused by mutations in *PKD2* gene) are quite similar, virtually indistinguishable clinically. ADPKD1 kidneys are reported to be slightly larger than ADPKD2 kidneys because of the difference in the initial number of cysts rather than in cyst growth (Harris, Bae et al. 2006) and progression to ESRD is slower in ADPKD2 occurring almost 20 years earlier in ADPKD1 with median age for renal survival and ESRD at 58 years for PKD1 and 79 years for PKD2 patients (Harris, Bae et al. 2006, Cornec-Le Gall, Audrezet et al. 2013). **Table 1** summarizes the evolution and progression of crucial findings in the ADPKD field since the identification of causative genes, which will be addressed throughout this section.

Period (year)	Summary of findings
1988-1995	**PKD1/PKD2 gene locus localized** **PC1/PC2 protein identification**
1996-2000	PC1/PC2 proteins identified Human PC1/PC2 expression analysis **Expression and localization studies** Detection of **LOH** in PKD1 and PKD2, **somatic mutations (2nd hit)** 1997: **1st KO Pkd1** (kidney and pancreatic defects) (LOF) Few PC1 partners identified: RG7, E-cadherin, Phosho-sites in CT **PC1 and PC2 interactions** through PC2 CC domain **Transgenic PKD1 mice (gene dosage)**
2001-2005	Additional KO *Pkd1* in mice with squeletal and cardiovascular defects **Pkd1/Pkd2 hypomorph (gene dosage) and conditional *Pkd1 mice* generated** Signaling pathways for PC1: apoptosis, tubulogenesis, JAK/STAT pathway Localisation of PC1 and PC2 in the **primary cilia** (mechanosensation) **Cleavage in N-terminal PC1 GPS site and C-terminus (RIP) *in vitro*** PC1 and PC2 interactors: NaKATPase (CT), Siah (CT), IP3R
2006-2010	Two *Pkd1* transgenic mouse models (kidney specific and systemic), **gene dosage** **Developmental swich of *Pkd1* function** (P12-13) by conditional inactivations Signaling pathways for PC1: mTOR, PI3K/Akt, ERK (CT), **β-catenin (CT, Wnt)** **Cleavage in N-terminal GPS**: auto-proteolytic and *in vivo* Generation of *Pkd2* (TG) mice (**gene dosage**) Centrosomal and chromosomal defects in *Pkd1* (siRNA) and *Pkd2* (TG) line **Cell polarity defects** (PCP) and the **kidney injury (3rd hit) in ADPKD** Interconnection/**cross-talk ADPKD-ARPKD** **Treatments** tested in mice: triptolide, rapamycin, inhib. glucoceramide **1st clinical trial started** (2007), stopped in 2013
2011-today	Altered **Hippo pathway** in ADPKD Functional PC1 levels (**gene dosage**) affects severity (continuation) PC1 and PC2 relative imbalance, interregulation (continuation)

Table 1: History of crucial advances in ADPKD. Results of Pubmed search narrowed to ''ADPKD'' alone showed 3140 articles while ''ADPKD and *Pkd1*'' accessed ~670 articles. Since the discovery of causative *PKD1* and *PKD2* genes, between ~30-40 articles/year are published by the scientific community. Going from the identification of the causative genes, identification of human mutations, generation of mouse working models used for testing therapies and finally entering human clinical trials, a lot has been achieved and some important questions remain to be answered toward accurate long lasting remedies. Particular topics are represented in bold, some of which are a direct contribution by our work described previously or here within.

2.2) Cellular pathological aspects of ADPKD

2.2.1) Increased proliferation and apoptosis

Normal kidney development and homeostasis rely on a tight balance of cell proliferation/division and cell death with elevated levels during the embryonic stage and very low levels in adulthood during tissue homeostasis. Both processes are disturbed in human ADPKD pathogenesis and targeting pathways that regulate proliferation or apoptosis in mice recapitulate ADPKD-like kidney pathogenesis (**Table 7, Section 7.1.1**). For instance, expression of *c-Myc* oncogene, which is implicated in both proliferation and apoptosis, is upregulated up to 15-fold in human ADPKD tissues (Lanoix, D'Agati et al. 1996). Apoptotic and proliferative indices are increased in non-cystic, dilated tubules and interstitium of human ADPKD kidneys, seemingly even more highly elevated than in cyst-lining epithelia (Lanoix, D'Agati et al. 1996, Prasad, McDaid et al. 2009). Although hyperplasia in the renal cyst epithelial cells is a common hallmark of human ADPKD, the rate of cell proliferation is slower than in neoplastic cells, which is one possible explanation for the similar incidence of ADPKD-associated RCC to that of the general population (Grantham 1990, Keith, Torres et al. 1994, Soderdahl, Thrasher et al. 1997).

2.2.2) Increased secretion

Fluid accumulation and related mechanisms are believed to be responsible for cyst growth and size. One of the potential molecules implicated in this process is Na^+/K^+-ATPase that drives the sodium ion gradients at the basolateral cell membrane. Na^+/K^+-ATPase defects (altered levels and mislocalization) are reported in ADPKD kidneys (Wilson 1997) but only occasionally and hence might not be a driving factor for cyst growth (Brill, Ross et al. 1996, Jiang, Chiou et al. 2006).

Alternatively, in order to grow in size, ADPKD cysts seem to rely on chloride ion secretion. One very important molecule for chloride secretion, in many tissues and potentially also in the kidney cystogenesis, is cAMP-regulated chloride channel, the cystic fibrosis transmembrane regulator CFTR. The CFTR is expressed in the

kidneys; its expression in the normal kidneys is developmentally regulated and decreases in adult (Devuyst, Burrow et al. 1996). Although CFTR expression levels have not been yet assessed in a robustly quantitative manner in ADPKD kidneys, several studies demonstrated the apical localization of CFTR in cyst epithelia derived from human ADPKD kidneys (Brill, Ross et al. 1996, Hanaoka, Devuyst et al. 1996, Lebeau, Hanaoka et al. 2002) and in kidneys from early and late stage ADPKD (Hanaoka, Devuyst et al. 1996). The direct effect of CFTR for epithelia secretion and cyst growth (and not on cell proliferation) was shown *in vitro* in MDCK cells where the rate of secretion of Cl^- and fluid from ADPKD epithelia was directly correlating with the quantity of CFTR on the apical surface of the cystic epithelium (Davidow, Maser et al. 1996, Li, Findlay et al. 2004, Yang, Sonawane et al. 2008). Furthermore, stimulation of secretion in ADPKD epithelia by forskolin (cAMP agonist) is virtually completely dependent on CFTR (Davidow, Maser et al. 1996). Although the mechanism remains unknown, *in vitro* the abundance of cell surface CFTR and Cl^- secretion were shown to be regulated/inhibited by polycystin-1, the *PKD1* gene product (Ikeda, Fong et al. 2006), which would lead to a prediction of altered CFTR levels and/or activity in ADPKD kidney. Consistent with this is the finding that steviol, shown to decrease CFTR levels and activity in MDCK cells, reduces cystogenesis in *Pkd1* mouse model. All of these findings strongly suggest contribution, probably not exclusive, of CFTR in ADPKD cyst formation and enlargement (Yuajit, Muanprasat et al 2014, Yuajit, Homvisasevongsa et al. 2013).

Further support for the implication of CFTR in ADPKD *in vivo* is obtained from the occurrence of CF patients with coexisting *CFTR* and *PKD1* mutations that appear to have milder ADPKD kidney phenotype (O'Sullivan, Torres et al. 1998, Xu, Glockner et al. 2006, Torres, King et al. 2001). Lack of attenuation of the ADPKD phenotype by CFTR mutation in one study (Persu, Devuyst et al. 2000) clearily indicates that further studies are necessary as to the exact implication and mechanistic relationship of CFTR in ADPKD.

2.2.3) Dedifferentiation

Renal cysts negative for any tubular segment marker or with decreased expression of specific differentiated tubular markers are frequently observed in ADPKD and point to altered differentiating epithelia (**Section 2.2.10**) (Song, Di Giovanni et al. 2009). Indeed, expression of embryonic fetal markers in post-natal kidneys is one of the hallmarks of the dedifferentiating ADPKD epithelia. Phenomena typical of embryonic epithelia and developing kidneys, such as re-expression of N-cadherin, Na-K-ATPAse fetal subunit or increased polycystin-1 expression, are frequently observed in ADPKD (**Section 5**) (Wilson 1997, Roitbak, Ward et al. 2004, Jiang, Chiou et al. 2006). Hence, ADPKD is thought to result from reactivation of a developmental process in adult kidneys.

2.2.4) Fibrosis and inflammation

Fibrosis is caused by the abnormally elevated deposition of extracellular matrix components, such as fibrillar collagen and fibronectin, into the tubular interstitium by myofibroblasts. Progression of ADPKD to renal end-stage disease also seems to correlate with increased levels of fibrosis (Zeier, Fehrenbach et al. 1992, Rossetti, Chauveau et al. 2003, Antiga, Piccinelli et al. 2006), but little is known about the exact mechanistic relationship. It is not known if it happens through a direct tubular EMT or through epithelial defects that lead to altered extracellular matrix composition. The principal fibrogenetic cytokine, TGFβ, is upregulated in human and ADPKD mouse kidneys (Wilson, Norman et al. 1996, Schieren, Rumberger et al. 2006, Song, Di Giovanni et al. 2009, Hassane, Leonhard et al. 2010). In Zebrafish, polycystin-1 was suggested to directly regulate collagen production (Mangos, Lam et al. 2010). In *Pkd1*^{nl} hypomorph mutant (**Table 8A)**, upregulation of TGFβ signaling matches with an increase in fibrosis only at the more advanced stage of the disease, suggesting most likely a secondary rather than initiating event, at least in this mouse model (Hassane, Leonhard et al. 2010).

In human and *Pkd1* and *Pkd2* mouse mutants, the environment of the kidney cysts was reported on multiple occasions to be prone to inflammation. The relationship

between the PKD genes and inflammation needs to be characterized and remains rather elusive and likely secondary to the disease. Murine *Pkd1* conditional LOF models enabled the assessment of the contribution of inflammatory macrophages to the cystic phenotype using a macrophage inhibitor. Specifically, macrophage deletion by liposomal clodronate in this mouse model was shown to decrease cyst coverage, decrease cell proliferation, and importantly, increase renal function, underlying/emphasizing the contribution of macrophages to cyst growth (Karihaloo, Koraishy et al. 2011).

2.2.5) Cell trafficking and polarization (mispolarization)

In 2000, two papers issued from collaborative efforts of Wandinger-Ness and Bacallao labs led to conclusions of altered basolateral traffic and cytoarchitecture in human ADPKD kidneys and cyst-derived cells (Charron, Bacallao et al. 2000, Charron, Nakamura et al. 2000). They showed that tight junctions, that separate apical from baso-lateral membrane compartments, are morphologically (by EM) and functionally (by marker occludin) intact. Assessed by the ability of HA influenza to traffic to the apical membrane of infected ADPKD cells, apical membrane sorting appears to occur normally. The overall biochemical infrastructure of tight junctions (TJ) monitored by typical and constitutively expressed TJ molecules, ZO-1 and occludin, is intact even in very advanced ADPKD disease stages, although some anomalies were observed with claudin-7, another TJ protein, specifically being highly expressed in the cysts (Yu and Yang 2009). Of note, however, desmosomes, another type of intercellular junction that mediates proper cell-cell adhesion, were not properly assembled in primary ADPKD cells (Russo, Husson et al. 2005). Since initial studies by Wilson *et al*., 1997 reported that some proteins and pumps mislocalize in ADPKD epithelia, in light of these new findings it is suggested that only selective apical protein trafficking is impaired in ADPKD and possibly dictated by different types of human ADPKD mutations (Wilson 1997).

Anomalies in the adherens junctions, on the other hand, are frequently observed in human ADPKD tissues or cells (Wilson 1997, Roitbak, Ward et al. 2004, Russo,

Husson et al. 2005, Streets, Wagner et al. 2009). Normally localized on the basolateral membrane of epithelial cells and involved in basolateral transport, E-cadherin is virtually absent, although variable, from ADPKD cell membranes, generally decreased in expression and preferentially accumulated inside of the cell. This finding correlates with mislocalization of two components of the basolateral-targeting patch, sec6/8. The lack of E-cadherin on the membrane does not completely prevent cell adhesion since some alternative cadherins, such as mesenchymal N-cadherin, may compensate (Roitbak, Ward et al. 2004). Impaired basolateral sorting and accumulation of proteins within the cell suggests that cargo is potentially stuck in *trans*-Golgi; this would cause significant morphological changes in this organelle. Accordingly, in contrast to the Golgi of cells isolated from normal kidney, ADPKD Golgi exhibit markedly dilated fenestration of the cisternae.

In addition, localization of some ras-like monomeric GTPase family members, previously shown to interface with the vesicular machinery, was also shown to be affected in ADPKD (Simons and Zerial 1993, Jou and Nelson 1998, Jou, Schneeberger et al. 1998, Roth 1999). Rab GTPases for example are involved throughout vesicular transport and docking. Of importance, Rab8, a specific Rab for basolateral traffic normally localized in the Golgi region and in transport vesicles directed to the cell surface, was found to localize in abnormally large dispersed vesicles of ADPKD epithelia. On the other hand, Rab11, 18 or Rab26, which is similar to Rab8 and genomically localized within the *Pkd1* locus, localized similarly or identically as they would in normal cells. Therefore, it is suggested that altered basolateral sorting of proteins in ADPKD is the result of a combination of traffic defects *i.e.,* impairment in various transport effectors including adapter, coat proteins, cytoskeletal components and targeting players.

Together, these studies suggest dysregulation of cell trafficking and adhesion properties, which in ADPKD eventually result in altered cell proliferation, polarity and cystogenesis.

2.2.6) Centrosome amplification, chromosome alterations and genomic instability

Predominantly allelic losses but also DNA copy number gains were found in ADPKD kidneys of 8 patients and 24 cysts by comparative genomic hybridization and LOH analysis (Gogusev, Murakami et al. 2003). This indicated the occurrence of chromosomal rearrangements in ADPKD cystic epithelia (smaller and larger cysts confounded) that potentially affect genes such as oncogenes and tumor suppressors, which might modify the progression and severity of ADPKD. However, a direct relationship between *PKD1* and chromosomal instability could not be made in this study because the authors used cystic epithelia and the findings could be therefore representative of secondary dedifferentiated state or abnormal proliferation.

Insights into direct association between *Pkd1* and genomic alterations and chromosomal instability were gained when *PKD1* was suppressed by lentiviral anti-*Pkd1* siRNA *in vitro* and in human primary renal epithelia (Battini, Macip et al. 2008). *Pkd1* siRNA resulted in abnormal ploidy (polyploidy), rescued by the reintroduction of exogenous *Pkd1*. This pointed to the specificity of siRNA knock-down for *Pkd1* directly, excluded off-side effects and provided causal correlation between dysregulation of *Pkd1* expression and genomic instability. Additionally, supernumerary centrosomes (>2), atypical mitosis and multipolar spindles were also significantly increased in *Pkd1* siRNA transfected cells. *Pkd1* knock-down led to abnormal chromosomal segregation (mitotic catastrophe) and apoptotic cell death. Most importantly, similar findings regarding centrosomal number were observed in human ADPKD renal specimens and in renal specific inactivation of *Pkd1* in mice even despite ‘’*seemingly normal histological appearance*’’ suggesting that these alterations may precede cystogenesis.

2.2.7) Loss-of-heterozygosity (LOH)

Loss of heterozygosity (LOH) in either *PKD1* or *PKD2* genes was reported in ~17-24% of kidney and liver cysts of human ADPKD (Qian, Watnick et al. 1996, Brasier and Henske 1997, Watnick, Torres et al. 1998, Pei, Watnick et al. 1999). LOH seems

to be an attractive model to explain the focal nature, intrafamilial variability and late onset of ADPKD pathogenesis. It principally supports the idea of ADPKD behaving as a recessive etiology at the cellular level where *Pkd1* mutations (germinal and additional somatic) would lead to the disease.

2.2.8) Cyst heterogeneity

Both inter- and intracystic heterogeneity are seen in ADPKD cysts *in vivo*. For instance, by immunohistochemistry some cysts in ADPKD kidneys are negative for *CFTR* but even some cells within the same *CFTR*-positive cyst are also negative (Hanaoka, Devuyst et al. 1996). This kind of heterogeneity in expression is also found for *PKD1*/*PKD2* genes (**Section 5.4**). Accordingly, the future therapies for this disease risk being partial and incomplete since they might target only some cysts (in late or early stage) and will probably require a combination of therapies for successful treatment (**Section 8**).

2.2.9) Modifiers

Much phenotypic variability in ADPKD is ascribed to environmental factors and genetic modifiers (genetic background) but sometimes occurs in almost identical genetic background (Peters and Breuning 2001, Persu, Duyme et al. 2004, Fain, McFann et al. 2005). The threshold of genes of the same network and their redundancy are equally important for the phenotypic outcome (**Section 3.2**). Hypertension is considered as another modifier of ADPKD. Patients with higher blood pressure are more prone to increase in total kidney volume, which inversely correlates with kidney activity, and additionally at increased risk for cardiovascular complications (Chang, Kuok et al. 2010, Chapman, Stepniakowski et al. 2010, Chapman, Torres et al. 2010). Along these lines, type II diabetes was also suggested to influence kidney function, volume, hypertension and life expectancy in ADPKD patients (Reeds, Helal et al. 2012).

2.2.10) Microarrays on human kidney and liver tissues

About 4 studies have reported differential gene expression profiling and signaling networks utilizing **1)** human ADPKD tissues (Schieren, Rumberger et al. 2006), **2)** epithelia from isolated ADPKD cysts (Lee, Park et al. 2004, Lal, Song et al. 2008, Song, Di Giovanni et al. 2009), or **3)** a combination of SAGE of immortalized cystic cells from ADPKD kidney and liver samples, and subsequent confirmation of obtained selected candidates by custom cDNA microarray directly on ADPKD tissues (Husson, Manavalan et al. 2004).

Pathways involved in apoptosis, cell cycle, proliferation, ECM remodeling, inflammation, metabolism, oxidative stress, aging, genome integrity, hypoxic responses, cell adhesion (laminin, collagen, integrins), tissue fibrosis and epithelial-to-mesenchymal transition (SMAα and collagens) all showed differential expression (up-regulated or down-regulated) in ADPKD cystic epithelia. Of interest, one of the most upregulated pathways by GSEA was the canonical β-catenin/Wnt signalling pathway (Lee, Park et al. 2004, Lal, Song et al. 2008, Song, Di Giovanni et al. 2009) and its downstream targets (*c-myc*, *cyclin-D*, etc). Importantly, microarray data also provided indicative information about the pathogenetic mechanism, and showed that in cystic epithelia specific differentiated tubular markers such as *HNBβ1*, *PKHD1*, *IFT* are decreased (*PKD2* modestly increased) while embryonic genes are reactivated, suggesting epithelial dedifferentiation in cystogenesis (Song, Di Giovanni et al. 2009).

These studies provided valuable information about human ADPKD pathobiology that requires confirmation for direct functional relevance in mammalian models (**Section 7**).

3) *PKD1* and *PKD2* genes

3.1) Normal *PKD1* and *PKD2* genes and transcripts

3.1.1) Exons/introns/isoforms

The Polycystic kidney disease 1 locus (*PKD1* in human (OMIM) #17390); *Pkd1* in mouse), the main subject of this thesis, is localized in a complex region on chromosome 16 (16p13.3), encompasses 53kb and, out of 46 exons, produces a full-length 14kb transcript and 4309 aa polycystin-1 protein of ~460 kDa (PC1 in human, Pc1 in mouse). The Polycystic kidney disease 2 locus (*PKD2* in human (OMIM) #173910); *Pkd2* in mouse) is localized on chromosome 4 (4q21-23), produces a 5.4kb full-length transcript and 968aa polycystin-2 protein of ~110kDa (PC2 in human, Pc2 in mouse).
In humans (but not in mouse), around two thirds of the 5' end of *PKD1* gene (Exon1-33), so called pseudogenes, are duplicated approximately six times on the same chromosome. The exact role of any of these *PKD1* pseudogenes is unknown.

The *PKD1/Pkd1* gene contains 45 introns, the first one as long as ~16kb, the introns 16, 26, 30, and 34 of ~1 and 3kb and the remaining introns of much shorter size between ~66 and ~600bp. Unlike the generally low sequence conservation of introns compared to coding parts of a gene (exons), the sequence of human *PKD1* intron 45 (90 nucleotides) is highly conserved with ~94% of overall identity (Guillaume 2000, Rodova, Islam et al. 2003). This intron has a special predicted feature, a so called ''stem loop'', that might be important for its splicing (Rodova, Islam et al. 2003) and was proposed to eventually encode an additional 30 amino acids without a frame-shift, elongating the proposed PC1 protein (Guillaume 2000). Because of its size and chromosomal complexity, detailed studies on *PKD1* transcript(s) are still lacking. *PKD1* was reported to generate a full-length mRNA of about 14kb, but at least three additional transcripts have been suggested (Kimura, Wakamatsu et al. 2006, **App.II**).

3.1.2) Promoter regulatory region

In vitro biochemical studies using ~5kb of the proximal promoter region of *Pkd1*/*PKD1* gene provided important insights about *PKD1* gene regulation.

First, a very proximal region of *PKD1* promoter contains active binding elements for specific transcriptional factors such as Ets/Fli1, Sp1 and a transcriptional repressor p53 (Puri, Rodova et al. 2006, Van Bodegom, Saifudeen et al. 2006, Jeon, Yoo et al. 2007, Islam, Jimenez et al. 2010). Furthermore, a mechanistic feedback loop has been proposed between stress-activated components, the p53 repressor, p53 transcriptional kinase-independent Mekk1 co-factor (eg. both activated during oxidative stress and TNFα signaling) and *Pkd1* promoter (Islam, Jimenez et al. 2010).

Next, within its 3.3kb 5' regulatory elements, the *PKD1* gene contains a consensus sequence for TCF binding elements (TBE) CTTTGA/TA/T. β-catenin was shown to activate and interact directly with this portion of the promoter. These elements also appear to be responsive *in vivo* whereby LiCl, an agonist for canonical β-catenin/Wnt signaling through inhibition of GSK3 kinase, is able to trigger an increase in *PKD1* mRNA levels (Stambolic, Ruel et al. 1996, Rodova, Islam et al. 2002).

Finally, a very proximal ~200bp region of *PKD1* promoter was shown to be responsive to all trans retinoic acid, a derivative of vitamin A, through a non-canonical RAR/RXR motif (Islam, Puri et al. 2008). *PKD1* expression could therefore be influenced by all trans retinoic acid and potentially tight hormonal balance. This would be consistent with a mouse study recently published where inhibition of sirtuin by nicotinamide (vitaminB3) significantly rescued cystogenesis in three *Pkd1* mouse models, loss of function, kidney conditional and *Pkd1* hypomorph (Zhou, Fan et al. 2013).

3.1.3) Particular sequences - Polypurine-polypyrimidine tract

The PKD1 locus contains three non-canonical DNA structures (hairpins, triplexes and G-quandruplexes) at the center of the gene (Intron 21) in a very large 2.5kb long

mirror repeat, a polypurine-polypyrimidine (Pu-Py) stretch of 88bp (Van Raay, Burn et al. 1996, Piontek and Germino 1999). This region is shown to form triplex structures visible by atomic force microscopy (Tiner, Potaman et al. 2001), to affect DNA replication and to activate DDR (Patel, Lu et al. 2004). Recently, it has been shown that the Pu-Py *PKD1* tract is indeed able to **1)** cause a replication stall *in vitro* (by blocking primer extension where it adopts a conformation incompatible with DNA synthesis) as well as *in vivo* (Liu, Myers et al. 2012), **2)** activate DDR and moreover constitutive Chk1 phosphorylation and continued growth by checkpoint adaptation, that allow further accumulation of mutations instead of cell cycle arrest. This data on *PKD1* contributes to the growing literature of cystic proteins, ciliopathies, and their involvement in DNA damage repair processes (ATR-Chk1 checkpoint signalling pathway) (Chaki, Airik et al. 2012, Zhou, Otto et al. 2012). Overall, the presence of the Pu-Py region and increased cell division and proliferation with DNA damage all increase the risk of genome instability and may explain the instability and mutability of the *PKD1* locus.

3.2) Mutated *PKD1* and *PKD2* genes and correlations of genotype/phenotype severity in ADPKD

ADPKD is a heterogeneous disease in many aspects: genic (*PKD1* and *PKD2*), allelic (by the specific type of mutation) and phenotypic with remarkable variability in disease severity. Some ADPKD cases present as mild adult disease while others manifest an early rapid onset with important variability within the same family and even in twins, although more variable in siblings than in monozygotic twins (Milutinovic, Rust et al. 1992, Fick, Johnson et al. 1994, Peral, Ong et al. 1996, Persu, Duyme et al. 2004).

The majority of mutations are proper to a specific family, with only 30% recurrent mutations (Rossetti, Chauveau et al. 2002, Rossetti, Consugar et al. 2007), therefore the total number of mutations presented in **Table 2** is increasing considerably. No hot spots for mutations were identified in the *PKD1* gene other than potentially the long polypyrimidine tract (**Section 3.1.3**) (Watnick, Piontek et al. 1997) and some

clustering at the end of exon 15 to exon 19 (corresponding to the junction of PKD repeats and the REJ domain of PC1 protein) for truncating but not for missense mutations (Rossetti, Consugar et al. 2007).

Table 2: Updated summary of mutations identified in human ADPKD patients

	Percentage of specific type of mutation (number from total 1443)	(number from total 347)
	PKD1	***PKD2***
3'UTR	**0%** *(0)*	**0%** *(0)*
5'UTR	**0%** *(0)*	**0%** *(0)*
Frameshift	**27%** *(389)*	**29%** *(100)*
Insertion or deletion	**8%** *(110)*	**3%** *(12)*
IVS silent	**0%** *(1)*	**0%** *(0)*
IVS unknown	**1%** *(15)*	**0%** *(1)*
Large deletion/duplication	**1%** *(17)*	**1%** *(4)*
Non sense	**22%** *(322)*	**37%** *(128)*
Splice	**9%** *(129)*	**15%** *(53)*
Substitution	**36%** *(512)*	**17%** *(58)*

ADPKD: mutation database http://pkdb.mayo.edu/cgi-bin/mutations.cgi. Obtained from the PKD database in Sept 2013. In the case of PKD1 gene, currently ~20-25% of nonsense, 25-30% of frameshift, 10% deletion (truncating=nonsense+frameshift+deletion=~70%) and 20-25% of missense mutations have been identified.

The variability in severity of ADPKD phenotype was associated with non-genetic elements such as male gender/hormones, caffeine, smoking and several genetic modulators. The proposed genetic modifiers are **1)** co-inheritance of *PKD1* with genetic mutations in particular genes such as ***TSC2*** in *PKD1*/*TSC2* contiguous syndrome (Brook-Carter, Peral et al. 1994), ***CFTR*** (O'Sullivan, Torres et al. 1998, Xu, Glockner et al. 2006), *PKD* genes *i.e.,* ***PKD2*** (Pei, Paterson et al. 2001, Dedoussis, Luo et al. 2008, Losekoot, Ruivenkamp et al. 2012), ***PKHD1*** and ***HNF1β*** (Bergmann, von Bothmer et al. 2011, Menezes, Zhou et al. 2012) and **2)** incompletely penetrant hypomorphic mutations (Rossetti, Kubly et al. 2009, Pei, Lan et al. 2012).

Mutations in the 5' position of the *PKD1* gene have been reported to be **1)** more severe, showing modest but significantly earlier ESRD onset than those in 3' termini

(53 yrs for 5' mutations, median position bp7812 vs 56 yrs for 3' for overall *PKD1* of 14000bp) (Rossetti, Burton et al. 2002), and **2)** associated more frequently with vascular disease *i.e.,* cerebral aneurysm when compared to PKD cohort without vascular phenotype (Rossetti, Chauveau et al. 2003). A study of about 700 ADPKD patients from Western France (ADPKD1 and ADPKD2) with similar thresholds for the 5' and 3' positions found that it is not the position, but rather the type of mutation, (being truncating (frameshift, nonsense, splicing and large rearrangements) *vs* the non-truncating (inframe and missense)), that correlates with the age of onset of ESRD/renal survival (55 yrs for truncating and 67 yrs for non-truncating) (Cornec-Le Gall, Audrezet et al. 2013).

Gender seems to modify the severity in *PKD2* (Hateboer, v Dijk et al. 1999, Hateboer, Veldhuisen et al. 2000, Magistroni, He et al. 2003) and probably *PKD1* (Cornec-Le Gall, Audrezet et al. 2013 , Harris, Bae et al. 2006). Males appear to have more rapid kidney disease while females are more affected by liver cysts with the risk increasing with pregnancy (Sherstha, McKinley et al. 1997). Finally, some rare incompletely penetrant *Pkd1* or *Pkd2* mutations are reported whereby alone, hetero- or homozygous mutants are all viable with variable severity ranging from no phenotype to mild or severe adult disease. However, when present with an additional inactivating null truncating or missense allele, these incompletely penetrant mutations become associated with more severe *in utero* disease and resemble recessive progressive pathogenesis of ARPKD (Rossetti, Kubly et al. 2009, Vujic, Heyer et al. 2010, Bergmann, von Bothmer et al. 2011, Losekoot, Ruivenkamp et al. 2012, Pei, Lan et al. 2012). Although rare and not readily generalized to ADPKD, this data is nonetheless supportive of ADPKD dosage mechanism of *PKD1/PKD2* genes as critical for initiation and progression of cystogenesis and residual allelic roles.

4) Polycystin-1 and polycystin-2 proteins

4.1) Structural characteristics of PC1 and PC2

Polycystins belong to a new, growing family of proteins with 5 members in the PC1-like group including PC1, L1, L2, L3, REJ and 3 members in the PC2-like group

including PC2, L1 and L2 with renal and sometimes exclusively extrarenal expression (Nomura, Turco et al. 1998, Chen, Vassilev et al. 1999, Hughes, Ward et al. 1999, Veldhuisen, Spruit et al. 1999, Guo, Chen et al. 2000, Yuasa, Venugopal et al. 2002, Li, Tian et al. 2003, Reviewed in Kurbegovic 2006).

Both PC1 (7-11TM) and PC2 (TRPP2, 6TM) are integral membrane proteins with a C terminus (for PC1) or both a C and N-termini (for PC2) facing the cytosol. PC1 is a large multipassage transmembrane protein with two thirds extracellular at the N-terminal, ~7-11 transmembrane domains and ~200aa long cytoplasmic tail at the C-terminal. PC1 is a type of chimeric molecule where the N-terminus appears to be involved in cell/cell, matrix or extracellular environment interactions, and the C terminus in downstream intracellular signaling (**Table 3**). The highly glycosylated N-terminal extracellular domain is composed of a signal sequence, leucine rich repeats, C-lectin domain, LDL domain, PKD (IgG-like) domains which could allow PC1 to homodimerize and, of particular relevance for this thesis, the GPS G-protein coupled receptor proteolytic site that results in two covalently associated fragments, the NTF (N terminal fragment) and CTF (C terminal fragment) (**Section 4.1.1, Chapter VI**) (Reviewed in Kurbegovic 2006, Ibraghimov-Beskrovnaya, Bukanov et al. 2000). More studies are slowly adding some structural information using atomic force microscopy about PC1 extracellular ectodomain flexibility, PKD and REJ domains, and conformational consequences following binding of PC2 and PC1 (Qian, Wei et al. 2005, Oatley, Stewart et al. 2012, Oatley, Talukder et al. 2013, Xu, Ma et al. 2013). No protein other than PC1 contains this complex combination of multiple N-terminal motifs, which makes the extrapolation of its function difficult.

TRPP2 was referred to as PC2 since it is a founding member of the Trp channel superfamily (**Table 4**, Montell, Birnbaumer et al. 2002, Qamar, Vadivelu et al. 2007). Despite their identification as causal genes for ADPKD disease, the function as well as the immediate or downstream signaling pathways of the two polycystins remains poorly understood. A description of their specific interacting proteins and possible involvement in downstream signaling is provided later on (**Sections 4.1.3 and 4.2.1**).

4.1.1) Putative and functional cleavages of PC1

4.1.1.1) PC1 N-terminal auto-proteolytic GPS/GAIN process

Because of its particular structure, *i.e.,* very large N terminal extracellular domain involved in cell-cell adhesion and matrix interactions, multiple transmembrane domains (**App.XII**), GPS motif, ability to bind G-proteins and several potential processings at the C-terminus tail (**Fig.2**), PC1 is often compared with aGPCRs GPS family of proteins, with well known and established members such as CL1, BAI and EMR. General mechanism of activation, inactivation and signaling by aGPCRs remains unknown. Recent meeting reports on GPS cleavage finely summarized the current knowledge in the field and proposed possible alternatives: tethered negative, tethered positive, intramolecular, intermolecular (direct or via secretion) and gate keeper, being some of the possible mechanisms (Arac, Aust et al. 2012, Promel, Langenhan et al. 2013). The mechanism of activation and regulation of PC1 through GPS/GAIN cleavage remains unknown.

Identification of PC1 protein and its secondary structure indicated that PC1 contains a GPS motif between the REJ domain and the first transmembrane passage (Moy, Mendoza et al. 1996, Ponting, Hofmann et al. 1999). *In vitro,* exogenous tagged PC1 undergoes autoproteolytic *i.e.,* enzyme-independent cleavage in HL↓T site (↓: cleavage) rapidly after its synthesis and results in two NTF and CTF subunits tethered non-covalently (**Fig.2**) (Qian, Boletta et al. 2002, Wei, Hackmann et al. 2007). Partial or full deletion of the REJ domain abrogates the cleavage. The presence of the residual uncleaved full-length Pc1 form also shows that processing at the GPS site is incomplete. The PC1 GPS cleavage is of functional significance in tubulogenesis whereby transfection with full-length wild-type Pc1 induces tubulogenesis while Pc1 GPS cleavage-defective mutants preferentially form cysts (Qian, Boletta et al. 2002). Uncleavable constructs also showed altered STAT1 transcriptional activity. GPS cleavage mutants with impaired PC1 function suggested that cleavage is important for the biological activity of PC1. This was confirmed *in vivo* by generation of knock-in mice that carries a mutation in the critical HLT GPS cleavage site. Replacement of

threonine by valine abrogates the GPS cleavage and leads to post-natal PKD (**Section 7.1.2.2, Table 8A)** (Yu, Hackmann et al. 2007)**.** *In vivo* data underlined a ‘’critical but restricted’’ role of cleavage and a developmentally regulated function of the cleaved and full-length uncleaved PC1 proteins, as suggested for Notch and latrophilin, respectively. PC1 is the first ‘’member’’ of aGPCRs whose functional role was assessed *in vivo*. PC1 therefore provides a good model to analyze the GPS cleavage that could eventually be extrapolated to other members of aGPCRs and their corresponding pathologies.

Although GPS was considered as a domain, its 3D structure was not yet available Thus, how the autoproteolysis could take place remained quite speculative. Crystallisation of a region that includes the GPS motif, as well as a proceeding ‘’stack/HormR domain’’ of two GPS containing proteins, showed that the GPS motif (~40aa) is a part of much larger highly conserved and very ancient GAIN (~320aa) domain, GAIN standing for **G**PCR-**a**utoproteolytic **in**ducing domain (Arac, Boucard et al. 2012). The crystallisation made it possible to envision the mechanism of intramolecular cleavage where a particular constrained structural conformation of the GAIN domain would lead to autoproteolysis, tethering of two cleaved subunits via conserved disulfide bonds between neighbour β-strands, numerous hydrophobic interactions and the conserved hydrophobic pocket, and finally to a more ‘’relaxed’’ resulting heterodimeric structure. Although the crystal structure of PC1 or its GAIN domain per se is not yet available, its high homology with other GPS/GAIN containing domains is indicative of similar mechanistic properties (**App.XIII**).

Processing(s) at the N-terminus of PC1 other than at the GPS/GAIN domain has not been excluded as suggested by latrophilin, which is cleaved C-terminally to GPS by a yet unidentified protease and by BAI2, cleaved N-terminally by furin (**App.XIV**) (Krasnoperov, Deyev et al. 2009, Okajima, Kudo et al. 2010). In the majority of GPS containing proteins (eg. latrophilin, GPR56), the GPS cleavage seems to be a prerequisite for proper intracellular trafficking. However, the exact role of GPS

cleavage on PC1 intracellular trafficking *in vivo,* and without eventual bias by protein tags or overexpression systems, remains to be determined (**Chapter VI**).

4.1.1.2) PC1 C-terminal proteolytic processings

In addition to GPS cleavage, three groups have evoked several cleavages resulting in much shorter PC1 C terminal tails, summarized in this section (**Fig.2**).

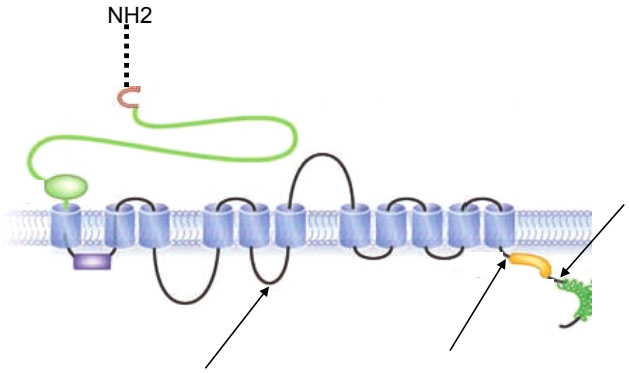

Low e*t al*., 2006

- p111 (aa~4191-4302)
- **~17kDa** (next to PEST domain)
- Accumulates in the nucleus
- Interacts with coactivator of STAT6 (P100)
- No effect on β-catenin signaling

Tools

- Human normal & ADPKD kidneys
- Cos, MDCK

Woodward e*t al*., 2010

- p100 (aa~3645)
- **~100kDa** (within 3rd loop)
- Does not depend on GPS cleavage
- Inhibits STIM/SOCE calcium entry

Tools

- Pkd1WT, Pkd1V/V mice & knock-in mice
- MDCK, CHO

Chauvet *et al*., 2004

- p200 (aa~4100-4300) / mechanical stimuli
- **~28-34kDa**
- Accumulates in the nucleus
- Activates AP-1 pathway
- inhibits β-catenin / Wnt signaling
- PC-2 inhibits PC-1 signaling
- Uncleaved: activates p21/JAK/STAT
- PC2 modulates PC1 cleavage

Tools

- COS, MDCK, HEK, Pkd1TG-BAC^{Somlo}

Figure 2: Putative CTF fragments in PC1. Other than **GPS cleavage at N-terminus** (green oval) that generates N-terminal extracellular (NTF) and C-terminal fragment (CTF) of ~160kDa, **three additional cleavages at C-terminus** have been reported that generate a **~100kDa**, and two quite smaller **~17** and **~34kDa** fragments. PC1 may undergo multiple successive cleavages, which have been described for regulated intramembrane proteolysis. The exact cleavage sites are unknown as well as their functional significance *in vivo*. Arrows: specify putative cleavage site based on the size of the CTF fragment. Tools: Cells or mice used in the study. PC1 structure adapted by permission from Macmillan Publishers Ltd: Kidney International, (Torres and Harris 2009), copyright 2009, doi: 10.1038/ki.2009.128.

4.1.1.2.1) Intramembrane 28-34kDa (Chauvet, Tian et al. 2004)

The first cleavage of PC1 suggested to occur *in vitro* and *in vivo* at the C-terminus cytoplasmic tail was identified by Chauvet *et al*. (**Fig.2**) (Chauvet, Tian et al. 2004). With previously described cleavage at the GPS domain, an additional cleavage, somewhere within the last TM domain of PC1, revealed many similarities with the RIP (*regulated intramembrane proteolysis*) signaling mechanism important for cell fate, cell decision development and response to misfolded proteins during ER stress. This mechanism was described for transmembrane surface receptors (Notch, APP, ARPKD fibrocystin) and intracellular proteins (SREBP, ATF6) where successive processings of the same molecule ultimately generate an active product that translocates to the nucleus and directly affects transcription of downstream genes (Brown and Goldstein 1997, Rawson, Zelenski et al. 1997, Chan and Jan 1999, Haze, Yoshida et al. 1999, Hiesberger, Gourley et al. 2006, Kaimori, Nagasawa et al. 2007).

In the case of PC1, this cleavage generates a ~34kDa CTT (C terminal tail) (last 200aa of the C-terminus tail) in several cell lines stably or transiently transfected with full-length Pc1. CTT is released by γ-secretase where the catalytic subunit of the functional γ-secretase complex, presenilin-2, seems to play a more important role than presenilin-1 (Merrick, Chapin et al. 2012). Pc1 CTT contains a highly conserved putative nuclear localization sequence between the residues 4,134 and 4,154. The short CTT soluble fragment can translocate to the nucleus and activate the AP-1 pathway in coexpressed AP-1 reporter system cells (Chauvet, Tian et al. 2004). PC2 was shown to regulate not only the localization of this cleaved PC1 fragment, but also its biological activity *in vivo* whereby mice with lower expression of Pc2 (**Table 8B**) (*Pkd2*$^{+/-}$ or *Pkd2*$^{WS25/-}$) have detectable nuclear Pc1 expression. Alteration in luminal fluid flow or its sensing, using unilateral ureteral obstruction or lack of cilia in *Kif3A* mice, respectively, induces nuclear abundance of CTT (Chauvet, Tian et al. 2004).

The functional role of this CTT fragment is unknown. *In vitro*, it was suggested to disrupt Wnt canonical pathway (Lal, Song et al. 2008). CTT associates directly to N-terminus of β-catenin, induces β-catenin nuclear translocation whilst inhibiting TCF-

dependent gene transcription by reducing β-catenin affinity for TCF (Lal, Song et al. 2008).

4.1.1.2.2) C-terminal short ~17kDa (Low, Vasanth et al. 2006)

Low *et al*. observed a different half-shorter PC1 CTT fragment that also resulted in nuclear translocation, was relatively unstable and underwent rapid proteosomal degradation (**Fig.2**) (Low, Vasanth et al. 2006). Once anchored to the membrane this 17kDa PC1 fragment constitutively binds to EBNA2 coactivator, also known as P100. This cleaved product is found in a complex, probably via P100, with STAT6 and positively regulates STAT6-dependent transcription. Injection of exogenous soluble full-length C-terminal tail alone was sufficient to induce renal and liver cysts in zebrafish 2-3 dpf in 90% of the embryos *in vivo*. Both the 17kDa CT tail and PC1/STAT6/P100 signaling axis are significantly upregulated in human ADPKD, which suggests a possible functional implication in the human disease.

Neither the soluble nor the membrane form of this specific 17kDa tail had an effect on the Wnt signaling pathway. Only a membrane anchored full-length C-terminal tail of PC1 was able to stimulate AP-1 activity, somewhat inconsistent with a previous report where only the soluble form was shown to translocate to the nucleus and affect AP-1 (Chauvet, Tian et al. 2004).

4.1.1.2.3) C-terminal long ~100kDa (Woodward, Li et al. 2010)

A novel endogenous ~100kDa C-terminal PC1 fragment, referred to as P100, was identified and likely generated by proteolytic cleavage (**Fig.2**) (Woodward, Li et al. 2010). This particular cleavage occurs only in the context of full-length PC1 (not from GPS CTF 160kDa fragment) at a site predicted within the third intracellular loop, a portion of the PC1 that has sequence similarity to PC2. This fragment is also expressed in multiple mouse tissues and its relative levels to 160kDa CTF differed among tissues. The P100 co-immunoprecipitates and inhibits SOCE (*store operated* Ca^{2+} *channels*) currents in Xenopus oocytes. Upon ER store depletion, the P100 fragment in the ER was suggested to interact and inhibit STIM (*an ER localized ER*

store depletion sensor) and consequently block SOCE currents. The presence of P100 CTF fragment, which function could be independent of GPS 160kDa CTF, may explain why *Pkd1*$^{V/V}$ in contrast to *Pkd1*$^{-/-}$ escapes embryonic lethality. The nature of this specific cleavage still remains largely unknown.

4.1.2) Factors that influence PC1 processing and/or trafficking

PC2 seems to be involved in N-terminal GPS cleavage of PC1 (Chapin, Rajendran et al. 2010). Co-expression of mPc1-HA and PC2-Myc tagged proteins in unpolarized non-ciliated fibroblastic HEK293 cell lines results in an increase of Pc1 cell surface localization, mainly the GPS generated CTF 160kDa fragment. Pc1 GPS defective cleavage mutant also abrogates Pc1 membrane localization in MDCK cells (Qian, Boletta et al. 2002, Chapin, Rajendran et al. 2010).

PC2 is also involved in C-terminal cleavage of PC1. PC1 CTT nuclear translocation and activation of AP-1 was inhibited when Pc1 was coexpressed with PC2 (Chauvet, Tian et al. 2004). Coexpression of PC2 and PC1 resulted in nuclear signal of PC1 CTT, which is indicative of increased cleavage of PC1 at its C-terminus (34kDa). The effect of PC2 on PC1 cleavage was shown to be independent of intracellular or extracellular calcium levels or PC2 calcium channel activity (Bertuccio, Chapin et al. 2009). The cleavage (34kDa) could not be detected in WT but interestingly was observed in *Pkd2* haploinsufficient mouse kidneys, suggesting that PC2 directly or indirectly inhibits cleavage. The CTF (160kDa) cleaved fragment was also enhanced when the FL-PC1 construct was co-expressed with PC2, whereas the NTF fragment seemed rather decreased in the presence of PC2 and this was observed in total cell extracts and tissue culture media (secreted form).

PC2 therefore seems able to regulate not only the localization but also generation and abundance of both N- (GPS site) and C-terminus (34kDa and 160kDa) cleavage fragments and most likely PC1 function (Bertuccio, Chapin et al. 2009, Woodward, Li et al. 2010).

4.1.3) Binding partners and signaling pathways of PC1

Using PC1 as an integral or truncated protein in cell systems, PC1 was directly associated with multiple intracellular downstream signaling pathways such as Wnt, G-proteins, mTOR, as well as being found in a PC2 complex, intracellular trafficking, cell-cell and cell-matrix interactions. Here are some of these connections between PC1, signaling cascades and interacting proteins (**Table 3**).

Table 3. PC1 interacting partners

Polycystin-1 binding proteins	Protein complex	Reference
Polycystin-1 (Homophilic)	Polycystin	Ibraghimov-Beskrovnaya *et al.,* 2000
E-cadherin and catenins (α,β,γ)	Adherens junction	Huan *et al.,* 1999; Geng *et al.,* 2000; Streets *et al*., 2009
Collagen I, II, IV and laminin	Extracellular matrix	Weston *et al.,* 2001; Malhas *et al.,* 2002
Vimentin, cytokeratin K8/K18, desmin	Intermediate filaments	Xu *et al.,* 2001
Integrin	Focal adhesion	Geng *et al.,* 2000; Wilson *et al.,* 1999
Vinculin, paxillin	Focal adhesion	Wilson *et al.,* 1999
Annexin A5	Cell contact	Markoff *et al.,* 2007
Flottilin-2	Cell adhesion	Roitbak *et al.,* 2005
Homer-1a/Ves-1s	Synaptic remodelling/plasticity	Stokely *et al.,* 2006
RPTPσ (LAR protein tyrosine phosphatase, E subunit)	Adhesion complex	Boucher *et al.,* 2011
Na-K-ATPase α-subunit	Membrane fluid regulation	Zatti *et al.,* 2005
Polycystin-2	Channel	Tsiokas *et al.,* 1997; Qian *et al.,* 1997
Polycystin-L	Channel?	Bui-Xuan *et al.,* 2006
Siah-1 (Human homolog of Drosophila seven in Absentia)	Ubiquitin-proteasome degradation	Kim *et al.,* 2004
RGS7 (Regulator of G protein signaling)	Signaling	Kim *et al.,* 1999
G protein	Signaling	Parnell *et al.,* 1998
ATP-2 (ATP synthase β-subunit)	Signaling?	Hu *et al.,* 2005
CK2β (β-subunit of casein kinase II)	Phosphorylation/signaling	Hu *et al.,* 2006
β-catenin	Wnt canonical signaling	Lal *et al.,* 2008; Kim *et al.*, 1999
Janus Kinase 2 (JAK2)	Activation of STAT signaling	Bhunia *et al.,* 2002; Low *et al.*, 2006
Tuberin (TSC2)	Membrane localization/ mTOR, PI3K signaling	Kleymenova *et al.,* 2001 Dere *et al.,* 2010 Shillingford *et al.,* 2006
RPTPγ (LAR protein tyrosine phosphatase, P subunit)	Signaling	Boucher *et al.,* 2011
Nephrocystin-1	Regulation of apoptosis	Wodarczyk *et al.,* 2010
Jade-1	Transcriptional coactivator/ubiquitin ligase	Foy *et al*, 2012
TCF (T-cell transcription factor)	Wnt signalling pathway	Merrick *et al.,* 2012
CHOP (C/EBP homologous protein)	Wnt signalling pathway	Merrick *et al.,* 2012
Id2 (Inhibitor of DNA binding)	Cell cycle	Li X *et al.,* 2005
PP1α (protein phosphatase1 α)	Phosphorylation/Pc2 regulation	Streets *et al.,* 2013
Arf4 (ADP-ribosylation factor 4, active bound form)	Cell trafficking	Ward *et al.,* 2011
Rab8, Rab6, Rab11 (not Rab5 or Rab7)	Cell trafficking	Ward *et al.,* 2011
BBS1, 4, 5, 8 (Bardet-Biedl Syndrome)	Trafficking (cilia)	Su *et al.,* 2014
Par3 (not Par6) and aPKC	Cell polarity&convergent extension	Castelli *et al.,* 2013

Legend: Interacting partners of PC1. Updated version from (Kurbegovic 2006).

References: (Boucher, Ward et al. 2011) (Bhunia, Piontek et al. 2002) (Bui-Xuan, Li et al. 2006) (Castelli, Boca et al. 2013) (Dere, Wilson et al. 2010) (Foy, Chitalia et al. 2012) (Geng, Burrow et al. 2000) (Hu, Bae et al. 2006) (Hu and Barr 2005) (Huan and van Adelsberg 1999) (Ibraghimov-Beskrovnaya, Bukanov et al. 2000) (Kim, Arnould et al. 1999) (Kim, Jeong et al. 2004) (Kleymenova, Ibraghimov-Beskrovnaya et al. 2001) (Lal, Song et al. 2008) (Li, Luo et al. 2005) (Low, Vasanth et al. 2006) (Malhas, Abuknesha et al. 2002) (Markoff, Bogdanova et al. 2007) (Merrick, Chapin et al. 2012) (Parnell, Magenheimer et al. 1998) (Qian, Germino et al. 1997) (Roitbak, Surviladze et al. 2005) (Stokely, Hwang et al. 2006) (Shillingford, Murcia et al. 2006) (Streets, Wagner et al. 2009) (Streets, Wessely et al. 2013) (Su, Driscoll et al. 2014) (Tsiokas, Kim et al. 1997) (Ward, Brown-Glaberman et al. 2011) (Weston, Bagneris et al. 2001) (Wilson, Geng et al. 1999) (Wodarczyk, Distefano et al. 2010) (Xu, Sikaneta et al. 2001) (Zatti, Chauvet et al. 2005).

4.1.3.1) Cell adhesion and extracellular matrix

Based on its structure and multiple motifs on its extracellular domain, it is reasonable to speculate functional interaction between PC1 and integral proteins of cell adhesion or the extracellular matrix. In fact, PC1 was detected in important basolateral complexes such as E-cadherin/catenin, collagen and integrins (**Table 3**). Transfection of PC1 N-terminal fragment anchored to the membrane stimulated formation of cell adhesion junctions inhibited by antibodies against PKD domains (Streets, Wagner et al. 2009). Antibodies against PKD domains of PC1 can also disrupt cell adhesion in MDCK monolayers (Ibraghimov-Beskrovnaya, Bukanov et al. 2000). In addition, in Zebrafish, inactivation of *Pkd1* directly modulates the production of collagen which implies a possible compensatory loop or feedback between PC1 and the main component of the extracellular matrix, collagen (Mangos, Lam et al. 2010).

4.1.3.2) Heterotrimeric G-proteins

One of the main characteristics of 7TM GPCRs is the ability to bind and activate heterotrimeric G-proteins that regulate multiple downstream effectors and signaling pathways important for proliferation, survival and motility including cAMP/PKA, calcium, AP-1 and JAK/STAT **(See following paragraphs).** PC1 is often compared to and considered by many to be an atypical adhesion GPCR, a particular subgroup

of GPCR family with GPS cleavage site and a large N-terminal extracellular domain. This comparison for now rests upon structural similarities and the ability of PC1 to bind and activate G-proteins (Parnell, Magenheimer et al. 1998). *In vitro* studies with truncated proteins targeting the C-terminus cytoplasmic tail of PC1 suggested that PC1 might be involved in mediating the G-protein signaling. PC1 contains a 20aa long G-protein activation sequence (RRLRLWMGFSKVKEFRHKVR) conform to that of many GPCR (N' BB.....BBxB C' or N' BB.....BBxxB C' (B standing for basic amino acids R, K, or H)) (Parnell, Magenheimer et al. 1998, Nishimoto, Okamoto et al. 1993). PC1 G-protein activating motif is found in a 74aa minimally required sequence of the C-terminal cytosolic tail of PC1, close to the membrane, that allows direct binding and activation of PC1 to heterotrimeric G-proteins (**Table 3**) (Parnell, Magenheimer et al. 1998, Parnell, Magenheimer et al. 2002).

Similar to GPCRs, PC1 seems to bind a couple of families of Gα proteins, such as $G_{i/o}$, G_q, G_s and G_{12} (Parnell, Magenheimer et al. 1998, Delmas, Nomura et al. 2002, Yuasa, Takakura et al. 2004). Using heterologous systems, the PC1/G-protein binding was shown to mediate, for instance, JNK and AP1 signaling in 293T cells, and, to modulate calcium activity of Ca^{2+} and K^+ channels in neurons, this latest effect being antagonized by co-expression of PC2 (Parnell, Magenheimer et al. 1998, Parnell, Magenheimer et al. 2002, Delmas, Nomura et al. 2002, Yuasa, Takakura et al. 2004). PC1 was also shown to interact and modulate the stability and localization of negative G-protein regulator RGS7 (**Table 3**) (Kim, Arnould et al. 1999). Finally, studies in mice are also suggestive of role of PC1 in G-protein signaling. Reproduction of a human single amino acid deletion L4131Δ in mice (L4122Δ), adjacent to the G-activation sequence disrupts the G-protein signaling, and causes PKD in mice similar to complete deletion of *Pkd1* in LOF models (**Table 8A**) Parnell 2012). Inactivation of GSM1, an accessory G-protein signaling modulator, worsened the phenotype in the $Pkd1^{V/V}$ hypomorphic mouse model (Kwon, Pavlov et al. 2012). Of note, other members of the PC1-like family have also been linked to G-protein signaling (Yuasa, Takakura et al. 2004).

Altogether, it is possible that PC1 acts to transmit the intracellular signal through a G-protein signaling cascade, whereby Pc1/G-protein dysregulation would results in cystic kidney pathogenesis.

4.1.3.3) Calcium homeostasis/cAMP

It is proposed that PC1 and PC2 are implicated in calcium homeostasis. In some studies, both PC1 and PC2 proteins are necessary to act together as a channel protein complex for calcium current and activity *in vitro* (Hanaoka, Qian et al. 2000), and in other studies, PC1 potentiates PC2 channel activity (Xu, Gonzalez-Perrett et al. 2003), but in the majority of studies, PC2 was shown to produce channel activity on its own (Gonzalez-Perrett, Kim et al. 2001, Vassilev, Guo et al. 2001, Koulen, Cai et al. 2002). Interestingly, Pc1 alone, in the absence of PC2, was also reported to confer calcium currents, an event requiring PKD domains of PC1 (Babich, Zeng et al. 2004). Lower levels of steady state calcium have been shown in ADPKD cyst-derived cells (Yamaguchi, Hempson et al. 2006) and in *Pkd1*^{Bei} homozygous osteoblasts (**Table 6**) (Xiao, Zhang et al. 2008). Pc1 was also shown to activate signaling pathways implicated themselves in the modulation of calcium levels and their effectors. For instance, NFAT signaling axis was activated in HEK293 cells by membrane anchored Pc1 terminal tail via G-proteins and PLC (Puri, Magenheimer et al. 2004) or in Pc1 expressing primary human osteoblast-like cells following mechanical stretching sensed most probably through Pc1 NTF portion (Dalagiorgou, Piperi et al. 2012).

Intracellular calcium levels inversely correlate with cAMP levels through downregulation/modulation of Ca^{2+}-dependent adenylate cyclases (Yamaguchi, Wallace et al. 2004). cAMP levels are altered in many orthologous and non-orthologous PKD mouse models and it is generally accepted that cAMP plays an important role in cystogenesis (Torres, Wang et al. 2004, Wang, Gattone et al. 2005, Wang, Wu et al. 2008, Hopp, Ward et al. 2012, Rowe, Chiaravalli et al. 2013, Jiang, Chiou et al. 2006, Gattone, Wang et al. 2003, Torres, Wang et al. 2004, Ahrabi,

Jouret et al. 2010, **Our unpublished data**). The mitogenic cAMP effect on the ADPKD cells can be counteracted/inhibited by restoration of normal calcium levels.

The cAMP/PKA pathway starts with ligand-GPCR-G protein binding and activation, after which the activated G_s α-subunit binds to and activates adenyl cyclase that catalyzes the conversion of ATP into cAMP. In the kidney, vasopressin (AVP) binds to its receptor V2R, expressed in distal tubules and collecting ducts, and this receptor-ligand binding initiates cAMP downstream signaling which includes the B-Raf/MEK/extracellular signal-regulated kinase pathway (B-Raf/MEK/ERK pathway) (Yamaguchi, Wallace et al. 2004). Inactivation of vasopressin in PCK PKD model led to a reduction of cAMP levels and very significant inhibition of cysts (Wang, Wu et al. 2008) while treatment with V2R antagonists leads to improvement of renal functions.

Furthermore, incubation of embryonic wild-type kidney explants with a derivative of cAMP causes proximal and collecting cysts, significantly increased in *Pkd1*$^{-/-}$ kidneys, which suggests that cAMP could play a role in cyst formation by stimulating fluid secretion and proliferation (Magenheimer, St John et al. 2006) (**App.VII**). The CFTR, a channel regulated by cAMP levels, seems very important in cyst growth. In addition to kidney culture *ex vivo* and MDCK cells on collagen gels, inactivation of CFTR in the *Pkd1* conditional mouse model by chemical agent also leads to a delay in kidney cyst growth suggesting the involvement of the cAMP/CFTR pathway in ADPKD (Yang, Sonawane et al. 2008).

4.1.3.4) AP-1, activator protein-1

Activator protein-1 is heterodimeric protein (c-Fos, c-Jun, ATF) activated by stress, cytokines, growth factors and inflammation to control many of the cellular defects reported abberent in PKD, such as proliferation, inflammation and apoptosis, The PC1 C-terminal tail (PC1-CTT) has been associated with regulation of AP-1 in several studies (**Table 3**) (Arnould, Kim et al. 1998, Parnell, Magenheimer et al. 2002, Chauvet, Tian et al. 2004).

4.1.3.5) JAK/STAT

Implication of PC1 C-terminus tail in JAK/STAT pathway was suggested by several groups (Bhunia, Piontek et al. 2002, Low, Vasanth et al. 2006, Talbot, Shillingford et al. 2011). This process seems to depend on *Pkd2* for induction of p21 and cell arrest (Bhunia, Piontek et al. 2002) and on *Jak2* and CTF cytoplasmic processing of Pc1 (Talbot, Shillingford et al. 2011). Phosphorylated levels of STAT3 specifically, signal transducer and activator of transcription 3, are increased in ADPKD human kidneys (Takakura, Nelson et al. 2011), non-orthologous PKD bpk mouse model (Talbot, Shillingford et al. 2011), *Pkd1* conditional mice and ischemic kidneys (Leonhard, van der Wal et al. 2011, Takakura, Nelson et al. 2011, Talbot, Shillingford et al. 2011) and. Treatment of PKD mouse models with curcumin, direct STAT3 inhibitor (S31-201) or anti-parasitic chemical compound (Pyrimethamine) all lead to a decrease in pSTAT3 and concomitantly to improvement of cystogenesis in orthologous *Pkd1* LOF mouse models (Takakura, Nelson et al. 2011, Leonhard, van der Wal et al. 2011).

4.1.3.6) Wnt pathway (canonical)

Mainly through its C-terminus intracellular tail, PC1 was shown to interact with proximal effectors of the canonical Wnt pathway such as β-catenin (Huan and van Adelsberg 1999, Kim, Arnould et al. 1999, Geng, Burrow et al. 2000, Lal, Song et al. 2008, Streets, Wagner et al. 2009), and downstream effectors such as Tcf and CHOP transcriptional factors (Merrick, Chapin et al. 2012). Direct interaction between TCF or CHOP and PC1 was reported with different truncated tagged proteins in cell culture systems. Hence, PC1 could directly, via interaction with critical effectors pathways, modulate the Wnt pathway. Moreover, an indirect role is also possible. For example, Pc1 was also shown to interact with Jade-1, a transcriptional activator but also an ubiquitin ligase for β–catenin (Chitalia, Foy et al. 2008, Foy, Chitalia et al. 2012).

Microarray data on human ADPKD samples and mouse PKD has revealed that many players from the canonical Wnt pathways are dysregulated / mostly upregulated (Lal, Song et al. 2008) (**Section 2.2.10, App.III**). *Pkd1*$^{-/-}$ cells demonstrate significantly

higher β-catenin/Wnt dependent functional stimulation (Merrick, Chapin et al. 2012) and *Pkd1*$^{-/-}$ cyst lining epithelia show increased canonical Wnt signaling *in vivo* using TcfLacZ transgenic reporter (Qin, Taglienti et al. 2012). Unpublished data from our own lab are more consistent with the conclusions that active β-catenin/Wnt canonical downstream signaling is upregulated in *Pkd1*$^{-/-}$ (**App.III**). Further evidence is provided by another PKD mouse model *in vivo* with dysregulation in canonical Wnt downstream effectors, an increase in a positive effector Axin and a decrease in a negative effector Notum in *Pkd1*^{nl} mice (Happe, van der Wal et al. 2013). Activation of the canonical Wnt pathway via overexpression of active β-catenin is sufficient to produce kidney cystogenesis (**Table 7**) (Saadi-Kheddouci, Berrebi et al. 2001, Qian, Knol et al. 2005). C-myc, one of the downstream targets of the canonical Wnt pathway, is also capable of inducing renal cystogenesis (Trudel, D'Agati et al. 1991, Trudel and D'Agati 1992), and was recently reported as a direct transcriptional target of PKD non-orthologous protein cystin (Wu, Yang et al. 2013). Finally, inactivation of c-myc partially rescues kidney cystogenesis in the *SBPkd1*$_{TAG}$ mouse model (Couillard, 2008).

Although all of these studies point to Wnt implication in PKD, they conflict with a recent study that showed unaltered canonical Wnt pathway using *TcfLacZ* β-catenin reporter and two *Pkd1* and *Pkd2* orthologous mutants (Miller, Iglesias et al. 2011). This inconsistency remains to be investigated in the future for better understanding of the degree of involvement of this pathway for eventual therapeutic targeting.

4.1.3.7) Cell polarity (CE-like process, cell migration and orientation)

PCP or planar cell polarity is a process of polarization of cells perpendicular to their apical-basal axis (Karner, Wharton et al. 2006). Two branches of PCP are convergent extension (CE) and oriented cell division (OCD). Convergent extension, as the name implies, is convergence and intercalation of the cells within the plane of epithelium, making structures longer and narrower. The latter involves dynamic changes in cell shape, reorganization of the cytoskeleton and small GTPases, among many other effectors. Both of these processes were brought to the forefront as players in kidney

development or in the diseased-state of PKD (ADPKD and ARPKD) (**Table 7**). A polarizing complex involved in front-rear polarity in mammalian cells and convergent extension process in flies, Par3 (100 and 180kDa isoforms) and aPKC, were recently shown to be interactive partners of the C-terminus of PC1 (**Table 3**) (Castelli, Boca et al. 2013). In wound-healing *in vitro* cellular assay, *Pkd1*$^{-/-}$ MEFs fill the wound in a contorted way with defects in proper orientation of the Golgi and MTOC in contrast to wild-type cells that use a more linear path. This would indicate front-rear polarity and migration defects, closely linked with CE movements. Inactivation of *Par3* in the kidney leads to non-fully penetrant mild cystic phenotype at birth (renal cysts in ≈40% of mice). More direct evidence is starting to appear which argues for CE role in kidney tissue. As cellular shape and cytoskeleton remodeling are necessary for CE, it is reasonable to predict that molecules involved in these processes would affect CE and consequently lead to an abnormal phenotype in mammals. The convergent extension defects associated directly with cystogenic phenotype in mammalian tissues were recently demonstrated for cadherin regulator p120-catenin in the cochlea (Chacon-Heszele, Ren et al. 2012), and p120-catenin and Myosin II in the kidneys (**Table 7**) (Marciano, Brakeman et al. 2011, Lienkamp, Liu et al. 2012).

OCD refers to cell division within the plane of tubular epithelium. Missorientation of the mitotic spindle and altered centrosomal position, normally found in the center of the cell, are indicative of OCD defects (Jonassen, San Agustin et al. 2008, Happe, Leonhard et al. 2009). Defects in oriented cell division were reported in precystic kidney tubules of *Pkd1* mouse model and subjected to kidney injury (Luyten, Su et al. 2010), while alteration in centrosomal angle was described in experimental PKD models with toxic renal injury, notably at the precystic stage and in the *Pkd1* overexpressor mouse model (Happe, Leonhard et al. 2009) (**App.IV**).

Evidence for PCP implication in cystic kidney disease is obtained from a couple of studies in mice. Fischer *et al.* were the first to show that normal tubular elongation in adult kidneys relies on OCD mechanism (Fischer, Legue et al. 2006). Inactivation of PCP component Fat4 cadherin led to cystic kidney phenotype (Saburi, Hester et al. 2008). A follow up of this study led also to inactivation of *Vangl* and *Dsh* (**Table 7,**

App.III). Phenotypical characterization and detection of renal cysts in these mice demonstrated their involvement in normal kidney homeostasis. These findings were explored further using conditional and total *Wnt9b* knock-outs (Karner, Chirumamilla et al. 2009). Karner *et al*. proposed two different mechanisms mediating early *in utero* versus late/post-natal kidney morphogenesis. Before birth, normal tubulogenesis relies on convergent extension, a stage where OCD is completely randomized. Soon after birth (at P1) the regulation of tubular diameter becomes dependent on properly oriented cell division, a process relying on non-canonical Wnt/Rho/JNK pathway (Karner, Chirumamilla et al. 2009).

In summary, the data on the PCP branch of non-canonical Wnt signaling pathway, a very important pathway for kidney development, tubular elongation, oriented cell division and kidney injury/repair, point to the possible cause-effect correlation of PCP and cystogenesis. However, the direct contribution of either the canonical or non-canonical branch of Wnt pathway in ADPKD is still awaiting definitive proof.

4.1.3.8) Phosphorylation/dephosphorylation

Protein phosphorylation/dephosphorylation by kinases and phosphatases, respectively, is a very important post-translational modification that can modulate or dictate protein function. At least four tyrosine (Y)/serines (S) phosphorylation targets have been identified in the COOH tail of PC1 by directed mutagenesis and *in vitro* assays. PKA was suggested to phosphorylate residues hS4251/hS4252 (Li, Geng et al. 1999) and mS4159 corresponding to hS4168 (Parnell, Magenheimer et al. 1999); pp60c-src acts on hY4237 (Li, Geng et al. 1999, Wilson, Geng et al. 1999), PRKX on hS4166 (Li, Burrow et al. 2008) and FAK on a yet unidentified residue target (Geng, Burrow et al. 2000).

Until now, only one phosphatase was reported to act on PC1. PP1α was suggested to dephosphorylate PKA phosphorylated residues of both human S4168 and mouse S4159 PC1 (Parnell, Puri et al. 2012). PC1 was shown to directly interact with this phosphatase. Through PC1/PP1 interaction, PP1 not only targets PC1 but also seems to regulate PC2 PKA phosphorylated levels (Streets, Wessely et al. 2013).

PP1α and its association with PC1 appear necessary for downregulation, via cAMP induced PKA-dependent S829 phosphorylation, of PC2 with functional repercussions (Parnell, Puri et al. 2012, Streets, Wessely et al. 2013). Importantly, phosphorylation of PC2 S829 residue was shown to increase *in vivo* in human ADPKD1 kidneys and *Pkd1* LOF mouse models.

4.1.3.9) Akt/mTOR

mTOR, *mammalian target for rapamycin,* is an atypical kinase found in mTORC1 (rapamycin effective) or mTORC2 protein complex. The mTOR pathway integrates multiple upstream pathways, such as growth factors, cytokines, ATP/energy sensor, amino acids, and nutrients, with downstream biological events, such as RNA translation, autophagy, and cytoskeleton dynamics, that activate either growth and cell proliferation or catabolic metabolism, adipogenesis, and lipogenesis.

PC1 appears to cross-talk with mTOR signaling. Pc1 C-terminus can interact directly with Tuberin, an upstream negative regulator of mTOR pathway encoded by the *Tsc2* gene (Shillingford, Murcia et al. 2006) (**Table 3**). Relevant to human disease, TSC2/PKD1 contiguous syndrome is associated with very severe, early-onset kidney cystic phenotype. Pc1 lateral specific membrane localization was also reported to depend on Tuberin in Eker rat carrying Tsc2 germline null mutation (Kleymenova, Ibraghimov-Beskrovnaya et al. 2001). Critical components of the mTOR pathway have been shown to be upregulated in PKD mouse models (Leonhard, van der Wal et al. 2011). Finally, treatment with sirolimus (commercial form of antagonist) or curcumin (natural product that inhibits both mTOR and Wnt pathways) leads to improvement of cystic phenotype in adult PKD mouse models (Shillingford, Murcia et al. 2006, Wahl, Serra et al. 2006, Shillingford, Piontek et al. 2010, Leonhard, van der Wal et al. 2011) and in embryonic *Pkd1* murine cystogenesis (Stayner, Shields et al. 2012).

AMPK is an energy sensing molecule, a kinase, which when energy *i.e.,* ATP levels are low phosphorylates directly **1)** Tsc2, an upstream negative regulator of proliferative mTOR pathway, and **2)** chloride CFTR channel, important for secretion

and cyst growth (**Section 2.2.2**). Activation of AMPK by metformin in kidney MDCK cells is able to modulate both mTOR and CFTR pathways in mice (Takiar, Nishio et al. 2011). Importantly, treatment of two different ADPKD mouse models with metformin slowed cystogenesis by decreasing proliferation and cyst growth by 10-20%, respectively (Takiar, Nishio et al. 2011).

In comparison to wild-type controls, ATP content is upregulated in *Pkd1*$^{-/-}$ MEFs and *KspCre; Pkd1*$^{flox/-}$ kidneys (Rowe, Chiaravalli et al. 2013) and glucose metabolism altered. The relevance of this observation was assessed using two ADPKD orthologous mouse models, *KspCre; Pkd1*$^{flox/-}$ and *Pkd1*^{V} (**Table 8A**). Treatment with a non-metabolized glucose analogue resulted in moderate effects on kidney weight, volume and cystic index (Rowe, Chiaravalli et al. 2013). This process subsequently implicated ERK phosphorylation that decreased levels of AMPK phosphorylation via LKB1 and activated mTORC1, glycolysis and ATP, further inactivating AMPK and providing mechanistic insight into potentially therapeutic effects of metformin (**See above**).

Given that cell proliferation is a general mechanism for ADPKD cyst growth, targeting the mTOR pathway with an immunosuppressive drug such as rapamycin, already prescribed for other diseases, seems very promising. However, since the clinical trials in humans are not reproducing the positives outcomes of mammalian ADPKD models (**Section 8**), additional studies are undeniably prompted.

4.1.3.10) miRNAs and iPS

miRNA global expression was reported to be altered in some (Pandey, Qin et al. 2011) but not all studies (Menezes, Zhou et al. 2012) using ADPKD models. Hence, the role of miRNA in ADPKD is still in its early days and for now undefined. Nevertheless, miRNA are slowly starting to gain more and more interest in ADPKD with relevance in the kidney (Patel, Hajarnis et al. 2012, Patel, Williams et al. 2013) and in liver disease (Lee, Masyuk et al. 2008). Upregulated in human and mouse ADPKD models, miR17~92 kidney specific transgenesis leads to polycystic kidney disease in mice, through presumably transcriptional repressive control of *Pkd1*, *Pkd2*

and *Hnf-1β*. Furthermore, inactivation of Dicer in the kidney, a critical component of miRNA processing machinery, lead also to late onset of tubular and glomerular cystic phenotype through repression of another miRNA, miR-200. The latter directly targets the 3'UTR of the *Pkd1* locus and, when repressed, results in overall upregulation of *Pkd1* and presentation of the phenotype suggesting gene-dosage regulation by miRNA (Patel, Hajarnis et al. 2012).

Reprogramming of iPS (induced pluripotent stem cells) was put afront in the ADPKD field for at least two reasons: **1)** restoration of heterozygous mutation based on capacity of iPS for increased somatic mutations and **2)** as a model to study the cellular phenotype of human disease given that these cells express ADPKD and ARPKD proteins. For the first purpose, spontaneous mitotic recombination-mediated genetic restoration was obtained from murine *Pkd1* mutant iPS cells and reported to lead to correction of phenotype in chimeric mice (Cheng, Nagata et al. 2012). For the second purpose, iPS cells were generated from keratinocytes and fibroblasts of four ADPKD patients by two independent studies (Thatava, Armstrong et al. 2011, Freedman, Lam et al. 2013) and revealed a phenotype in ciliary PC2 mislocalization independent of somatic hits (Freedman, Lam et al. 2013).

4.1.3.11) Chaperones and proteasomal inhibitors

Chaperones (pharmacological, molecular or chemical) have been elicited for their efficiency in rescuing misfolded proteins, limiting protein degradation, increasing the half-life and allowing their targets the proper localization. This role of chaperones is now beginning to be associated with autosomal dominant polycystic kidney and liver pathogenesis. Molecular chaperones, which target downstream effectors of ADPKD, or inhibitors of proteasomal degradation, which indirectly increase Pc1 half-life in a mouse model of ADPLD, seem promising. HSP90 chaperone is associated with many PKD network genes such as *CFTR*, *c-MYC*, *mTOR*, *HIF1A*, *VIM*, *MAPK1*, *EGFR*, *ERB*, *RGS7*, *CTNNb1*, *TUBULIN*, *HAX1*, *INV* and was shown to be increased in human ADPKD kidneys and in late onset PKD $Pkd1^{fl/fl;}$ $Cre/Esr1^{+}$ mouse model (Seeger-Nukpezah, Proia et al. 2013). Importantly, administration of an inhibitor of

HSP90 (STA-2842) to this mouse model resulted in slower cyst formation and growth in both early and later stages of the disease (cyst % reduced by ~50%, BUN reached normal levels) by targeting a multitude of ADPKD-relevant proteins and effectors *i.e.,* Erk, Akt, Egfr and mTOR.

Interestingly, Pc1 levels and ciliary localization were shown to be decreased in ADPLD causative *Sec63* and *Prkcsh* mutants (Fedeles, Tian et al. 2011). Administration of carfizomib, that inactivates proteasomal degradation, resulted in an increase of Pc1 and significant rescue of their polycystic phenotype (Fedeles, Tian et al. 2011).

Together, bioinformatical prediction, homology analysis, structural examination and *in vitro* studies all point to Pc1 as a membrane protein integrating a yet unknown extracellular signal or ligand and communicating this information at the cellular level through its C-terminus tail(s). It is remarkable how many pathways are activated by *PKD1/PKD2* and altered in ADPKD. Their relevance and the degree of implication in human ADPKD disease need to be further assessed in mouse models authentically reproducing the renal and extrarenal disease. Eventually, for an efficient treatment in humans, it is fundamental to elucidate these pathways in detail, their limitations and regulations.

4.2) Polycystin-2

4.2.1) Binding partners and signaling pathways of PC2

When mutated, PC1 and PC2 both lead to very similar if not identical phenotypical defects; this suggests that these proteins work in parallel, convergent or in the same complex and pathways. PC1 was actually one of the first interacting partners identified for PC2 (**Table 4**). These two polycystins seem to bind through their cytoplasmic tails in order to regulate intracellular calcium levels (**More details about this interaction is found in Section 4.3 and Table 5**).

Table 4. PC2 binding partners

Polycystin-2 binding proteins	Protein complex	Reference
PC2 (Polycystin-2, TRPP2)	Channel	Tsiokas *et al.*, 1997; Qian *et al.*, 1997
PC1 (Polycystin-1)	Channel	Tsiokas *et al.*, 1997; Qian *et al.*, 1997
TRPC1	Channel	Tsiokas *et al.*, 1999
Stx5 (Syntaxin 5)	Modulate channel activity	Geng *et al.*, 2008
EGFR (Epidermal growth factor receptor)	Channel activation	Ma *et al.*, 2005
TRPC4 (Transient receptor potential channel)	Channel	Du *et al.*, 2008
TRPV4	Channel	Kottgen *et al.*, 2008
PLC-γ2 (Phospholipase C-γ2)	Signaling/suppresses PC2 activity	Ma *et al.*, 2005
mDia (Mammalian diaphanous)	Gating, traffic movement	Rundle *et al.*, 2004
FPC (Fibrocystin/Polyductin)	Channel activity	Wang *et al.*, 2007; Kim *et al.*, 2008
KIF3A	Regulates channel activity	Li *et al.*, 2006
KIF3B	Regulates channel activity	Wu *et al.*, 2006
Kim1 (Kidney injury molecule)	Chemosensor	Kuehn *et al.*, 2007
IP_3R (Inositol 1, 4, 5-biphosphate receptor)	Channel	Li *et al.*, 2005
RyR2 (Ryanodine receptor 2)	Channel	Anyatonwu *et al.*, 2007
PATJ (PALS1-associated tight junction protein)	Regulate channel activity	Dunning *et al.*, 2010
RP2 (Retinis-pigmentosa 2)	Channel	Hurd *et al.*, 2010
Pkd1l1 (Polycystic kidney disease 1 like 1)	Mechano/chemosensor	Kamura *et al.*, 2011; Field *et al.*, 2011
Hax-1	Cytoskeleton	Gallagher *et al.*, 2000
CD2AP	Cytoskeleton	Lehtonen *et al.*, 2000
Tropomyosine-1	Cytoskeleton	Li *et al.*, 2003
Troponine-1	Cytoskeleton	Li *et al.*, 2003
α-actinin	Cytoskeleton	Li *et al.*, 2005
Casein kinase 2	Phosphorylation	Cai *et al.*, 2004; Hu *et al.*, 2006
ATPase 97	Degradation	Liang *et al.*, 2008
GSK (Glycogen synthase kinase)	Phosphorylation	Streets *et al.*, 2006
PERK (Pancreatic ER-resident eIF2 kinase)	Signaling/phosphorylation	Liang *et al.*, 2008
HERP (Homocysteine-induced endoplasmic reticulum protein)	Degradation	Liang *et al.*, 2008
TAZ (Trancriptional coactivator with PDZ-linding motif)	Ubiquitination	Tian *et al.*, 2007
Pericentrin	Cilia/centrosome	Yurczyk *et al.*, 2004
Id2 (Inhibitor of DNA binding 2)	Cell cycle	Li *et al.*, 2005
$EIF_2\alpha$ (Eukaryotic translation initiation factor)	Cell proliferation	Liang *et al.*, 2008
PIGEA-14 (Chibby) (PC2 interactor, Golgi and endoplasmic reticulum-associated protein)	Intracellular trafficking	Hidaka *et al.*, 2004
PACS1, PACS2 (Phosphofurin acidic cluster sorting protein 1 and 2)	Trafficking	Kottgen *et al.*, 2005
FIP2 (Family of Rab11-interacting protein 2)	Cilia localization	Li *et al.*, 2008
Collectrin	Intracellular traffic	Zhang *et al.*, 2007
Sec10	Intracellular traffic/ciliary localisation	Fogelgren *et al.*, 2011
Adenyl Cyclase 5/6	cAMP signaling	Choi et *al.*, 2011
Arf4	Cell trafficking	Ward *et al.*, 2011
IFT57	Intraflagellar trasport	Jurczyk *et al.*, 2004
HDAC6 (histone deacetylase 6)	Transport to aggresomes (degradation)	Cebotaru *et al.* 2014
Filamin	Cytoskeleton	Wang et *al.*, 2012 Sharif-Naeini *et al.*, 2009

Legend: Interacting partners of PC2. Updated version from (Kurbegovic 2006).

References: (Anyatonwu, Estrada et al. 2007) (Cai, Anyatonwu et al. 2004) (Cebotaru, Cebotaru et al. 2014) (Choi, Suzuki et al. 2011) (Du, Ding et al. 2008) (Duning, Rosenbusch et al. 2010) (Gallagher, Cedzich et al. 2000) (Geng, Boehmerle et al. 2008) (Hidaka, Konecke et al. 2004) (Field, Riley et al. 2011) (Fogelgren, Lin et al. 2011) (Hu, Bae et al. 2006) (Hurd, Zhou et al. 2010) (Jurczyk, Gromley et al. 2004) (Kamura, Kobayashi et al. 2011) (Kim, Fu et al. 2008) (Kottgen, Benzing et al. 2005) (Kottgen, Buchholz et al. 2008) (Kuehn, Hirt et al. 2007) (Lehtonen, Ora et al. 2000) (Li, Dai et al. 2003) (Li, Luo et al. 2005) (Li, Wright et al. 2005) (Li, Montalbetti et al. 2005) (Li, Montalbetti et al. 2006) (Li, Magenheimer et al. 2008) (Liang, Li et al. 2008) (Ma, Li et al. 2005) (Qian, Germino et al. 1997) (Rundle, Gorbsky et al. 2004) (Sharif-Naeini, Folgering et al. 2009) (Streets, Moon et al. 2006) (Tsiokas, Kim et al. 1997) (Tian, Kolb et al. 2007) (Tsiokas, Arnould et al. 1999) (Wang, Zhang et al. 2007) (Ward, Brown-Glaberman et al. 2011) (Wang, Dai et al. 2012) (Wu, Dai et al. 2006) (Zhang, Wada et al. 2007).

Like PC1, PC2 was also reported to interact with many components of the actin cytoskeleton such as Hax-1, troponin, tropomyosin, α-actinin and filamin A (**Table 4**). In the filamin-dependent context, the balance of polycystins was suggested to play an important role in vascular smooth muscle cells (VSMC) upon intraluminal pressure, similar to the flow that occurs in the renal epithelial tubules. Pc2 inhibits SAC channels (*stretch activated ion channels*) and Pc1 is able to relieve this inhibition, a process requiring Pc1/Pc2 association as well as tightly regulated *PKD1* gene dosage (Sharif-Naeini, Folgering et al. 2009, Wang, Dai et al. 2012).

Multiple (~18) phosphorylation sites are present in PC2 and were summarized recently in detail (Streets, Wessely et al. 2013). Some of the phospho-sites were shown to be recognized by known kinases (CKII, GS3K and PKA) and their phosphorylation dependent on PC1 levels (Streets, Wessely et al. 2013).

PC2 interacting partners point also to regulation of proliferation and apoptosis by PC2 through cross-talk with PERK/eIF2α axis (Liang, Yang et al. 2008). There seems to exist a positive feed-back loop between PC2 and stress induced pathways. After a prolonged ER stress, PC2 protein levels are decreased by a direct interaction with components of the ERAD/proteasome degradation pathway such as Herp and ATPase p97 (Liang, Li et al. 2008). After a milder ER stress, PC2 protein levels became upregulated by ~80% in multiple cell line systems (Yang, Zheng et al. 2013).

Upregulation of PC2 results most probably from phosphorylation of eIF2α, followed by binding of the ribosomes to the 5'ORF of PC2 and skipping the newly identified inhibitory 5'uORF (''u'' for upstream) (a mechanism suggested in some other stress-induced activated genes) for enhanced PC2 translation (Yang, Zheng et al. 2013).

ADPKD PC2 protein has been described in a molecular and *in vivo* functional relationship with fibrocystin/polyductin (FPC), the main player responsible for ARPKD pathogenesis (**Section 6.1**) (Wang, Zhang et al. 2007, Kim, Fu et al. 2008, Kim, Li et al. 2008). Pc2 stability is affected by its ability to interact with fibrocystin, a possible protein complex bridged by the *Kif3B* subunit of kinesin (Wu, Dai et al. 2006). Interactions between polycystin(s) and fibrocystin suggest a cross-talk, a common molecular pathway within PKD related proteins and a reciprocal modifier effect in renal and extrarenal cystogenesis.

Based on interactive proteins, PC2 probably functions in processes, many of which are PC1 dependent, for regulation of calcium with important involvement in actin dynamics, intracellular trafficking and PKD protein cross-talks.

4.3) Common links between polycystin-1 and -2

PC1 and PC2 have been associated and considered as probably the most important physical and functional interactors in ADPKD for multiple reasons. Mutations in both proteins lead to very similar, if not identical, renal pathology in humans and mice (**Section 2.1, 2.2; Table 8A, 8B**). The proposed pathogenetic mechanism(s) of PC1 and PC2 are similar. Importantly, these two proteins interact with each other, and the PC1/PC2 heterodimer is believed to occur through coiled-coil domains found at at carboxyl termini of each protein (**Table 3,4 & 5**).

A.

Domain	Position
CT PC1	4088-4302
CT PC2	687-968
CC PC1	4214-4248
CC1 PC2	772-796
CC2 PC2	833-871

B.

	PC1	PC2	Notes
Tsiokas *et al*,	**CT** (40aa within last 70aa)	**CT** (last 97aa)	PC2 (homo) (but NOT PC1), Y2H, IP, Interaction up-regulates PC1
Feng *et al.*,	**CT** (prob CC 4214-4248))	**CT**	PC2 (homo), PC1 (homo), PC1 and PC2 (hetero), Y2H, IP
Hanaoka *et al.*,	**FL**	**FL**	Tagged
Newby *et al.*,	**FL**	**FL**	Overexpressing TG cell lines, IP with EndoH resistant&sensitive PC1
Chapin *et al.*,	**Other than CT**	**FL**	Deletion of 179aa from the last TM (PC1), tagged
Giamarchi *et al.*,	**NA**	**CT** (833-871)	Homodimerization PC2 (CC2), tagged
Giamarchi *et al.*,	**FL**	**CT** 833-895 (871 to 895)	Heterodimerization PC1 and PC2 (CC2 & more), tagged
Casuscelli *et al.*,	**CT** (short 4202-4243 (CC))	**CT**	PC1 CC alone IP with PC2 CT

Table 5. Putative interaction domain(s) of PC1 and PC2 A. Position of the human PC1 and 2 C-terminus cytoplasmic domain and the coiled-coil motif. **B.** Summary of reported publications evoking PC1 and PC2 interactions and the proposed binding sites. In all studies, when possible, it is the PC2 C-terminus close to/or within coiled-coil domain that interacts with PC1. PC2 homodimerizes through the coiled-coil domain via last 97 aa, that barely affect the CC motif. Similarly to PC2, three studies point to the CC domain of PC1 for interactions with PC2, while one group suggests a site of interaction other than C-terminus all together (aa2,670-~lastTM) (including ours here within) (Chapin *et al.,* 2010). PC2 oligomerisation through its C-termini is a common remark, while PC1 rarely interacts with itself unless through N-terminus PKD domains. CT: C-terminus; FL: full-length; NA: not applicable; CC: coiled-coil; Homo: homodimerization; Hetero: heterodimerization; PC1 and PC2: polycystin 1 and 2; IP: immunoprecipitation; TM: transmembrane; Y2H: yeast two hybrid. All proteins were of human origin except Newby *et al.,* 2002.

References: (Casuscelli, Schmidt et al. 2009) (Chapin, Rajendran et al. 2010) (Giamarchi, Feng et al. 2010) (Hanaoka, Qian et al. 2000) (Newby, Streets et al. 2002) (Qian, Germino et al. 1997) (Tsiokas, Kim et al. 1997).

Co-dependence of PC1/PC2 interaction appears critical, although not always consistent, at least in cell systems, for localization, cleavage, phosphorylation/activity and signaling summarized here below:

1) PC1 localizes to the membrane when PC2 is absent, and to the ER when PC2 is introduced in COS cells (Grimm, Cai et al. 2003);

2) Trafficking of PC1 to the membrane and the cilia requires PC2 in LLC-PK cells (Chapin, Rajendran et al. 2010) and vice versa (Nauli, Alenghat et al. 2003) and in ADPKD iPS cells (Freedman, Lam et al. 2013). In this specific case, mutation of PC1 and reduced PC2 levels at the cilia were proposed to have a ‘’synergetic effect’’ further decreasing the stoichiometry complex and resulting in obvious detrimental effects on kidney morphology;

3) PC2 is observed at the membrane of CHO cells only in the presence of Pc1 where they act together as a calcium channel (Hanaoka, Qian et al. 2000);

4) Pc2 also was reported to regulate not only ER/membrane localization of PC1 but also localization of the Pc1 C-terminus in the nucleus (Chauvet, Tian et al. 2004);

5) PC2 seems to influence GPS cleavage of PC1 assessed by abundance and translocation to the membrane of PC1 NTF GPS cleavage product (Chapin, Rajendran et al. 2010);

6) PC1 targets PC2 to aggresomes and in this way affects its stability and abundance (**Table 3**) (Cebotaru, Cebotaru et al. 2014);

7) Pc1 and PC2 interaction appears critical for the role of Pc1 in dephosphorylation of Pc2 at residue S829, normally recognized and phosphorylated by PKA (Streets, Wessely et al. 2013). This phosphorylation / dephosphorylation complex may be relevant for human pathogenesis since increased phosphorylation of S829 was observed in mouse *Pkd1* LOF mouse model and importantly in human ADPKD;

8) Together PC1 and PC2 are involved in signaling pathways such as G-protein activation and JAK/STAT/p21 to regulate the cell cycle (Bhunia, Piontek et al. 2002, Delmas, Nomura et al. 2002).

Despite available *in vitro* data, the functional *in vivo* relevance of PC1/PC2 association and inter-dynamics still remains quite elusive.

5) Expression of *PKD1*/*PKD2* genes and PC1/PC2 proteins in human and mice

5.1) Expression of *PKD1*/*PKD2* genes and PC1/PC2 proteins in normal human tissues

Several attempts for temporal, spatial and subcellular expression of *PKD1/PKD2* in human tissues were hampered by lack of specific tools and yielded contradictory results by immunohistochemistry, immunofluorescence or biochemical Western blot analysis.

One finding is consistent about *PKD1*/PC1 expression. Human renal PC1 is developmentally regulated with the highest expression at the embryonic stage and the lowest and very weak after birth. Therefore, PC1 does not seem to be required for early nephrogenesis but rather for tubular maturation (Geng, Segal et al. 1996).

In the kidneys, it is generally accepted that S bodies, UB epithelia and proximal tubules show expression of PC1 before birth and collecting/distal convoluting tubules just before birth and post-natally (Ward, Turley et al. 1996, Ibraghimov-Beskrovnaya, Dackowski et al. 1997, Van Adelsberg, Chamberlain et al. 1997, Weston, Jeffery et al. 1997, Chae, Cho et al. 2006). More specifically, PC1 is expressed in medullary collecting ducts and UB (Van Adelsberg, Chamberlain et al. 1997, Ong, Ward et al. 1999, Geng, Segal et al. 1996, Palsson, Sharma et al. 1996). At early stages, mesenchymal (Geng, Segal et al. 1996, Van Adelsberg, Chamberlain et al. 1997) or glomerular PC1 expression is reported as absent (Ibraghimov-Beskrovnaya, Dackowski et al. 1997, Chae, Cho et al. 2006) or low (Palsson, Sharma et al. 1996) but in adults, PC1 can also be detected in the glomeruli (Palsson, Sharma et al. 1996).

PC2 appears to have a somewhat similar pattern of expression to PC1 in the embryonic human kidney. Post-natally, PC2 immunostaining marks all tubular segments, mostly maturing proximal, distal tubules and collecting ducts, and colocalizes with PC1 in medullary collecting ducts (Ong, Ward et al. 1999).

Interestingly, an independent study showed a rather different pattern of expression, with sole co-localization of PC1 and PC2 in a subset of cortical tubules in human adult kidneys (Foggensteiner, Bevan et al. 2000). Thus, the first divergence concerns specific tubular segments expressing polycystins. PC2 expression is strong in medullary TAL and cortical distal tubules, while PC1 is strongest in cortical and medullary collecting ducts. The second divergence of expression between the two polycystins concerns developmental *vs* adult stages. PC1 has highest expression during development and nephrogenesis, which decreases after birth, while PC2 expression is maximal in the adult stage.

Overall, *PKD1/PKD2* and PC1/PC2 are expressed in epithelial cells shown to be frequently affected in ADPKD, *i.e.,* tubules in the kidneys, ducts in pancreas and the biliary tract in the liver (Peters, van de Wal et al. 1999), but also epithelial and non-epithelial cells of many other extrarenal tissues (Reviewed in Kurbegovic 2006, Geng, Segal et al. 1996, Ibraghimov-Beskrovnaya, Dackowski et al. 1997, Palsson, Sharma et al. 1996, Ward, Turley et al. 1996, Ong, Ward et al. 1999). Similar to the kidney, the extrarenal expression of polycystins is also developmentally regulated. For instance, weak levels of PC2 are observed in the fetal pancreatic and liver ducts, with levels increasing after birth (Foggensteiner, Bevan et al. 2000).

5.2) Expression of *Pkd1/Pkd2* and Pc1/Pc2 in murine tissues

Similar to human, murine *Pkd1*, *Pkd2* genes and corresponding Pc1 and Pc2 proteins are widely expressed in renal and extrarenal tissues starting from very early stages (morula) to late stages in adulthood (Guillaume and Trudel, 1999, 2000). They are both developmentally regulated with differential expression in developmental, morphogenic stages and mature adult homeostasis. More specifically, *Pkd1* expression is not detected in pronephros or mesonephros nor in the UB or UB derivates but is detectable in condensed and uninduced mesenchyme at E13.5-E15.5 (Ahrabi, Jouret et al. 2010) and levels increase in differentiated proximal tubules at E15.5 (Boulter, Mulroy et al. 2001). *In utero* at E13.5-16.5, strong Pc1 protein expression is shown in epithelia derived from UB, collecting duct and pelvis with

almost no signal in metanephric mesenchyme. The peak of Pc1 expression occurs between E16-E19 with a drastic drop soon after birth between weeks 1-2 (Geng, Segal et al. 1997, Griffin, O'Sullivan et al. 1997). At E15.5, an increase of Pc1 protein was observed and expression detected in glomerular parietal epithelium, differentiating proximal tubules and collecting ducts (Ahrabi, Jouret et al. 2010). Collecting ducts seem to express more Pc1 than other segments in the kidney (Foggensteiner, Bevan et al. 2000). While Pc1 expression is high during nephrogenesis, Pc2 is highly expressed in mature tubules (Geng, Segal et al. 1997, Markowitz, Cai et al. 1999).

5.3) Subcellular localization of polycystin-1 and polycystin-2

5.3.1) Intracellular and membrane localization

The subcellular localization for both polycystins and especially for PC2 remains quite controversial and seems to be significantly influenced by cell type, cell culture conditions and antibody used (Reviewed in Kurbegovic 2006). PC2 contains an ER retention signal and localizes in the ER (Cai, Maeda et al. 1999, Hanaoka, Qian et al. 2000, Newby, Streets et al. 2002) but also on the plasma membrane and primary cilia (**Section 5.3.3**). PC1 was found to localize in the apical and basolateral membrane, in cell junctions, ER and to co-fractionate with lipid rafts (Roitbak, Surviladze et al. 2005, Van Adelsberg, Chamberlain et al. 1997, Ong, Ward et al. 1999 , Geng, Segal et al. 1996, Palsson, Sharma et al. 1996), whereas the PC1 cleavage products have also been reported in the primary cilia and in the nuclei (Reviewed in Kurbegovic 2006).

5.3.2) Exosomal localization

In addition to removing unnecessary proteins (disposal of unwanted senescent or harmful proteins) as has been suggested for a long time, exosomes are nowadays believed to have a beneficial functional role in intercellular communications (Pisitkun, Shen et al. 2004). Urine contains ‘’exosomes’’ which are 40-100nm secretory organelles originating from MVB (multivesicular bodies) and which have been shown

to be abundant in critical ADPKD and ARPKD genes products (Pisitkun, Shen et al. 2004, Hogan, Manganelli et al. 2008). The PKD ‘’exosome-like’’ *i.e.,* PC1, PC2 and FPC positive vesicles were shown to adhere and interact with the primary cilia, possibly internalize, which lead authors to speculate a novel way of signaling via secreted exosomes through the nephron in the kidney (‘’urocrine’’) or through the biliary tree in the liver (‘’bilocrine’’) (Hogan, Manganelli et al. 2008). However, the role, if any, specifically of PKD proteins in the urinary exosomes, or any other type of exosomes (eg. from the biliary duct), has not yet been directly tested. Nevertheless, exosomes could be eventually envisioned as biomarkers and for the delivery of therapies in PKD.

5.3.3) Expression in the primary cilia

For a very long time, the role of primary cilia was not widely appreciated but nowadays, within the last 10-15 years, the primary cilia is thought to function as an important sensor of the extracellular environment and convertor of the signal into the inside of the cell. Cilia became associated with several human pathologies, such as PKD and blindness, regrouped as ‘’ciliopathies’’.

5.3.3.1) Localization of PC1 and PC2 in the cilia

PC1 was shown to localize in the primary cilia in *C.elegans* sensory neurons and the plasma membrane of the ciliary axoneme in renal epithelial tubular cells. In the cilia, PC1 colocalizes with some other PKD proteins such as PC2 and polaris (Barr and Sternberg 1999, Haycraft, Swoboda et al. 2001, Pazour, San Agustin et al. 2002, Yoder, Hou et al. 2002). The ARPKD protein, fibrocystin was also shown to localize in the primary cilia and centrosome in mammalian cells by a couple of independent groups (Ward, Yuan et al. 2003, Menezes, Cai et al. 2004, Wang, Luo et al. 2004, Zhang, Mai et al. 2004).

5.3.3.2) Mechanism for trafficking of PKD proteins to the cilia

PC1 was shown to contain a conserved K/R/QVxPx sequence, more precisely **KVHPSST** (**VxPx** motif), at its extreme C-terminus, which is necessary, but

insufficient on its own, for trafficking to the primary cilia (Ward, Brown-Glaberman et al. 2011).

PC2 also contains a ciliary targeting signal between aa5-72 at N-terminus of the protein, narrowed down to the first 15 aa and finally refined to the consensus sequence ‘’RVxP’’ necessary for ciliary transport of PC2 in LLC and MDCK cells (Geng, Okuhara et al. 2006, Hoffmeister, Babinger et al. 2011). Contrary to earlier studies (Hanaoka, Qian et al. 2000, Nauli, Alenghat et al. 2003), Geng *et al.* showed that PC2 trafficking, in this case to the primary cilia, was independent of PC1 (Geng, Okuhara et al. 2006).

The ciliary targeting sequence (CTS) of fibrocystin, similar to the lipid raft-targeting signal in SNAP25, was found to reside in the 18aa near the N-terminus of its cytoplasmic tail (Salaun, Gould et al. 2005). Only constructs containing this region were able to co-immunoprecipiate with Rab8 and consequently to localize in the primary cilia (Follit, Li et al. 2010). Of note, Rab8 is also found in a Pc1 protein complex (**Table 3**) (Ward, Brown-Glaberman et al. 2011) whereas both fibrocystin and PC1 have been shown to interact with PC2 (**Table 4**) (Qian, Germino et al. 1997, Tsiokas, Kim et al. 1997, Wang, Zhang et al. 2007, Kim, Fu et al. 2008, Kim, Li et al. 2008). Therefore, these ciliary macromolecules could be part of the same protein complex (Fibrocystin-PC2-PC1-Rab8) that is directed to the primary cilia, Rab8 being the driving force.

5.3.3.3) Putative role of ADPKD gene products in the primary cilia

5.3.3.3.1) Cilia-dependent signaing pathways

Primary cilium has been linked to phototransduction (rhodopsin storage and trafficking to the retina outer segment through the connecting cilium) and signaling pathways such as Hh, Wnt and PCP. The role of primary cilia has recently become a primary field of interest of an increasing number of laboratories working on polycystic kidney disease. Consistent with the primary cilia facing the tubular lumen and exposed to the urinary flow, the primary cilia in the kidney cells is suggested to act as

a mechano-chemo sensor, although the specific ciliary role of polycystins, if any, remains unknown.

Bending of the primary cilia of kidney collecting duct type MDCK cells by a micropipette results in an increase of intracellular calcium levels and hyperpolarization of the membrane but the mechanism responsible for this outcome was unknown (Praetorius and Spring 2001). It was hypothesized that increased intracellular calcium levels lead to membrane hyperpolarization through activation of calcium activated potassium channels on the membrane (Engbretson and Stoner 1987, Breuer, Mack et al. 1988). The putative direct role of Pc1 in cilia was suggested in 2003 where Pc1 or Pc2 mutant epithelia and kidneys were unable to increase calcium influx following shear stress/flow (Nauli, Alenghat et al. 2003, Nauli, Rossetti et al. 2006). *Pkd1* heterozygous, ADPKD non-dilated immortalized or primary cells behaved similarly to the wild-type cells and showed normal change in calcium levels following flow shear stress. However, dilated cystic ADPKD and homozygous mutant cells were not responsive to fluid shear stress and thus could not result in flow-induced calcium signaling. The primary defect relied on polycystins that lost the ability to sense the extracellular tubular flow supporting the role of PC1/PC2 as a mechanosensor complex in the primary cilium of tubular kidney epithelium for calcium homeostasis.

Primary cilia have been also shown to be very important for regulation of the Wnt signaling pathway (Simons, Gloy et al. 2005) and PC1 was shown to interact with and modulate Wnt canonical and non-canonical pathway (**Also see section 4.1.3.6, 4.1.3.7**). On one hand, through Dsh degradation, the ciliary protein inversin is able to down-regulate the β-catenin Wnt canonical pathway. On the other, inversin regulates convergent extension movements of dorsal-mesodermal derived tissues during axis extension (elongation of animal caps), a branch of non-canonical Wnt pathway in Xenopus laevis. Kidney cysts caused by mopholino knock-down of inversin (*i.e.* upregulation of Wnt/β-catenin pathway) are rescued by diversin that negatively regulates canonical and is also implicated in non-canonical Wnt signaling. It has been

proposed that initiation of urine flow during early kidney development increases inversin levels (that occurs before renal electrolyte homeostasis (Friedberg 1955)) to down-regulate β-catenin/Wnt cascade and to activate non-canonical signalling for tubular extension, maturation and differentiation, a process termed a ‘’molecular switch’’. Another very important signaling coordinated by the cilia is the Hedgehog (Hh) signaling pathway, also shown to be associated with polycystic kidney disease. The contribution of Hh in PKD is provided by studies on *Ift* mutants that develop Hh-like phenotypes and on human and/or mice mutations of *Gli2* and *Gli3*, two critical transcriptionnal effectors of Hh cascade, that are associated with polycystic kidney disease (**Table 6, 7**) (Reviewed in Singla & Reiter, 2006).

In summary, the current model of cilia function is that primary cilia act as a sensor of tubule lumen mechanics and flow, which dictates lumen diameter and/or cell proliferation in the kidney through regulation of different signaling pathways. Inactivating primary cilia causes very few cysts before birth in mice (Yu, Carroll et al. 2002, Jonassen, San Agustin et al. 2008) and does not seem to be critical during embryonic development; the role of the cilia is potentially compensated by some other mechanisms such as convergent extension.

cAMP was reported to act as a positive regulator of primary cilia length and its levels are altered in human ADPKD and mouse models (**Section 4.1.3.3**). In normal IMCD cells, activation of cAMP or its critical downstream kinase (PKA), or downregulation of calcium by Gd^{3+} all elongate primary cilia in cell culture (Besschetnova, Kolpakova-Hart et al. 2010). This process of ciliary elongation is independent of protein synthesis and shows significantly accelerated anterograde intraflagellar transport. Potential crosstalk between the two second messengers, calcium and cAMP, which were identified as regulators of this process in different cell types (epithelial and mesenchymal, respectively), suggests coordinated regulation of cilium length, their involvement in ciliogenesis and a common downstream cascade. The authors hypothesized that the flow leads to an increase of cAMP and thus longer cilia. Subsequently, polycystins, which regulate calcium in cilia, would increase calcium

levels as feed-back to adapt and to normalize cilia length. Therefore, this process of adaptation through negative feedback could be regulated by polycystins and altered in *PKD1*/*PKD2* causing mutations disease.

5.3.3.3.2*)* Positive regulators of ciliogenesis common to ADPKD

Other than cAMP, there are many other known positive regulators of the ciliary length reported in the literature, many of which have been associated with PKD. These are cytoskeletal and microtubular dynamics, overexpression of *Rab8*, inactivation of *Nek8*, targeting of *Pkd1* (haploinsufficiency, overexpression or mutation), deficiency of *Tsc1* or *Tsc2,* mutations in some centosomal/transition zone components (*Cep162*) and inflammatory interleukin-1 (IL-1) (Kim, Lee et al. 2010, Sharma, Kosan et al. 2011, Wann and Knight 2012, Bonnet, Aldred et al. 2009, Kurbegovic, Côté et al. 2010, Hopp, Ward et al. 2012, Hartman, Liu et al. 2009, Wang, Tay et al. 2013). The functional and/or pathological role of longer cilia is much less known, compared to the effects of complete absence of cilia. Longer cilia were reported to be either more sensitive to bend and to be activated by fluid-shear stress (Abdul-Majeed and Nauli 2011, Abdul-Majeed, Moloney et al. 2012) or proposed to be less sensitive, owing to their detachement from the cell (Nauli, Jin et al. 2013).

5.3.3.3.3) Potential cilia ‘’cyst promoting signal’’

A recent study in Somlo’s laboratory showed a genetic relationship between the cilia, polycystins and cyst formation. Surprisingly, inactivation of the cilia by targeting *Kif3A* or *Ift20* genes reduced cyst growth in both post-natal developing *Pkd1* and *Pkd2*, in adult inducible *Pkd1* loss-of-function kidneys by *Pax8*^{rtTA}*;TetO-cre* approach (Ma, Tian et al. 2013) in all kidney nephron segments and also in the polycystic liver disease. Instead of a cumulative negative effect due to inactivation of both polycystins and cilia formation, their unexpected data suggest a ciliary ‘’cyst promoting signal’’, which was shown to be independent of MAPK/ERK, mTOR and cAMP effectors and likely polycystins themselves.

5.4) Altered expression of *PKD1/PKD2* and PC1/PC2 in human ADPKD tissues

Multiple labs analyzed the expression levels of PKD1/2 genes, their proteins, as well as their cellular localization. The *PKD1* transcript was shown to be upregulated in ADPKD kidneys (Ward, Turley et al. 1996, Lanoix, D'Agati et al. 1996). Several independent groups classified the PC1 protein signal as ''more intense'', ''strong'' or ''increased'' in kidneys from ADPKD patients with mutations in *PKD1* gene (ADPKD1) in comparison to unaffected normal kidneys **by IHC** (Palsson, Sharma et al. 1996, Ward, Turley et al. 1996, Peters, Spruit et al. 1996, Ibraghimov-Beskrovnaya, Dackowski et al. 1997, Weston, Jeffery et al. 1997, Ong, Harris et al. 1999, Griffin, Torres et al. 1996). High PC1 expression was reported in the cytoplasm of ADPKD1 cystic epithelium (Palsson, Sharma et al. 1996, Van Adelsberg, Chamberlain et al. 1997) and also at the membrane (Geng, Segal et al. 1996). It is PC1 from presumably the wild-type allele that continues to be expressed/increased (Ward, Turley et al. 1996, Ong, Harris et al. 1999, Ong, Ward et al. 1999). Some ADPKD1 cysts (~10-20% kidney and liver, respectively) were heterogeneous with respect to PC1 (Ibraghimov-Beskrovnaya, Dackowski et al. 1997, Ong, Harris et al. 1999) and PC2, and likewise for ADPKD2 cysts (~13%) (Ong, Ward et al. 1999), meaning that within the same tubular cyst, some epithelial cells have a positive signal while other are negative. While increased in most but not all cysts, the complete/total absence of PC1/PC2 could correspond to dedifferentiation of the epithelia. Normal nephrons in ADPKD samples seem to express PC1 similarly to normal kidneys (Ibraghimov-Beskrovnaya, Dackowski et al. 1997). **By Western blot**, in comparison to normal kidneys, the human adult ADPKD kidney homogenates also showed increased PC1 signal similar to that of normal human fetal kidney (Geng, Segal et al. 1996).

In kidneys from patients with mutations in *PKD2* gene (ADPKD2), the cysts expressing PC2 conserved PC1 expression (~65% of cysts) and vice versa (Ong, Ward et al. 1999). Analogous observations were reported for ADPKD1 renal and also liver cysts. When ADPKD human liver samples (the second most frequent manifestation of ADPKD) were available and analyzed, a similar patterns of

expression, with respect to PC2 levels of expression and heterogeneity were demonstrated (Ward, Turley et al. 1996, Ibraghimov-Beskrovnaya, Dackowski et al. 1997, Ong, Harris et al. 1999).

Finally, an elegantly designed study by Ong *et al.,* 1999 (Ong, Harris et al. 1999) quantitatively assessed, using two monoclonal C and N terminal PC1 antibodies in 10 ADPKD1 truncating mutants, the following points: **1**) expression of endogenous wild-type *vs* mutant PC1 protein expression, **2**) liver *vs* kidneys and, **3)** early/rapid (including *TSC2*/*PKD1* deletion) *vs* later onset ADPKD. Using the COOH antibody that consequently recognizes only the normal PC1 (*i.e.,* truncating mutants would not be recognized), ~70% of kidney cysts were found positive for PC1, ~20% negative and 10% heterogenous and this paralleled in liver cysts with ~60% being positive, ~20% negative and ~20% heterogeneous. The negative cysts were very rare to absent in early onset ADPKD samples. Of note, for one truncating human mutation, a very pronounced intense truncating PC1 protein was detected by Western blot using N-terminal antibody (also reported for 2 other truncating mutations).

Altogether, these studies show co-ordinated sustained or increased PKD1/2 gene and protein expression in the ADPKD kidney and liver, with a minority of cysts being negative or heterogeneous.

6) Renal cystic diseases other than ADPKD

6.1) Autosomal recessive polycystic kidney disease (ARPKD)

ARPKD, [MIM 263200] or polycystic kidney and hepatic disease 1 (PKHD), occurs in 1:20,000 births with recessive inheritance. It affects epithelial cells of the kidney, liver and pancreas with detrimental cellular consequences such as kidney cysts, congenital liver fibrosis, ductal plate malformation, pulmonary hypoplasia and lung disease (~11%), portal (30-75%) and systemic (60-100%) hypertension (Guay-Woodford and Desmond 2003). ARPKD is caused by mutations in the *PKHD1* gene encoding for fibrocystin, a one span transmembrane protein with potentially many isoforms. *PKHD1* is localized on chromosome 6 (chromosome 9 in mice) in a region spanning 470kb, and produces an impressive transcript of 67 exons and a protein of

4074aa. This locus was first mapped in PCK ARPKD orthologous rat model (**Table 6**) and then, either by comparative genetics (rat/human) or conventional positional cloning, identified by two different groups in human and consequently named either fibrocystin (Ward, Hogan et al. 2002) or polyductin or fibrocystin/polyductin FPC (Onuchic, Furu et al. 2002). In the kidney, FPC is expressed during kidney development in the branching UB and collecting duct (but not in uninduced or induced mesenchyme) and its expression persists in the adult stage. The pattern of expression of FPC correlates with early onset and the specific fusiform collecting tubules cystic phenotype seen in ARPKD patients (Ward, Yuan et al. 2003). Several studies of inactivation of *Pkhd1* gene in mice all led to severe liver anomalies, but in contrast to the human disease, displayed later onset of kidney cysts (**Table 8C**) (Garcia-Gonzalez, Menezes et al. 2007, Kim, Fu et al. 2008).

6.2) Human diseases reported to show cystic structures

Genes other than PKD1 and PKD2 can be associated with kidney cysts and are considered as potential modulators, modifiers and/or downstream effectors. For example, *TSC1*, *TSC2*, *WT1* and *VHL* are genes involved in cell proliferation, kidney development and hypoxia. When mutated in human or mice, the main characteristic of alteration in these genes is renal tumors (renal cell carcinoma or RCC except for *WT1*) with modest presence of kidney cysts believed to precede tumor formation (**Table 7**). Under normal conditions of oxygenation, the role of *VHL* is to suppress a transcriptional factor *HIF1*α by degradation. Calcium signaling is also reported to affect *HIF1*α levels while both hypoxia and calcium homeostasis are also associated with ADPKD *PKD1/2* pathogenesis. This is one of multiple examples, which suggests a possible convergence of common signaling pathways and cross-talks in PKD. To this group also belong many ciliopathies such as BBS, MKS and NPHP, which are associated with kidney disease but also blindness, obesity, diabetes and neurological phenotypes.

7) System models for functional genomics

7.1) Mouse (*Mus musculus*)

7.1.1) Non-orthologous mouse models

Mouse is an excellent relevant and powerful working model for human pathogenetic polycystic kidney disease and ADPKD. The orthologous genes are highly conserved and they are able to reproduce cellular characteristics of the human polycystic kidney and liver disease.

Initially, several PKD models were obtained either by chemical inducible agents (eg. corticosteroids), insertional mutagenesis (eg. *Nph*, *Tsc2*) or spontaneously (eg. *Pkhd1*, *Nph*, *Bicc1*), and reproduced polycystic kidneys and in some cases extrarenal anomalies (**Table 6**). These models allowed positioning and mapping of important genes, which were linked by comparative genomics and confirmed as causative for some renal cystic diseases including ARPKD.

Table 6: Non-orthologous rodent models for PKD: Spontaneous, insertional or chemically induced mutants

Mutated gene (Protein)	Chr.	Name of the model (specie)	Putative function	Reference
Spontanous				
Cys1 (Cystin)	12	Cpk (s)	Microtubule stabilization?	Fry *et al*., 1985 Hou *et al*., 2002 Preminger *et al*., 1982 Simon *et al*., 1994 Ricker *et al*., 2000
Bicc1 (Bicaudal C)	10	Bpk (s)	miRNA-binding protein	Cogswell *et al*., 2003 Guay-Woodford *et al*., 1996
Nek1 (NIMA-related kinase1)	8	Kat;Kat^{2j} (s)	Cell cycle?	Janaswami *et al*., 1997 Upadhya *et al*., 2000
Nphp3 (Nephrocystin3)	9	Pcy (s)	?	Nagao *et al*., 1995 Takahashi H *et al*., 1991 Takahashi H *et al*., 1986 Olbrich *et al*., 2003
Pkdr1	5	Han:SPRD-cy (r)	?	Bihoreau *et al*., 1997 Cowley *et al*., 1993
Nphp11/Mks3 (Meckelin)	5	Wpk (r)	Ciliogenesis	Nauta *et al*., 2000 Smith *et al*., 2006
Pkhd1 (Fibrocystin)		Pck (r)	Receptor, adhesion	Lager *et al*., 2001 Katsuyama *et al*., 2000
Pkd1 (Polycystin-1)		Pkd1^{m1Bei} (m)	Receptor, channel, adhesion	Herron *et al.*,2002
Insertional				
Nphp9/Nek8 (NIMA-related kinase 8)		Jck (s)	Cell cycle	Atala *et al*., 1993 Liu *et al*., 2002 Holland *et al*., 2002
Nph2 (Inversin)		Inv/Inv (s)	Ciliogenesis	Mochizuki *et al*., 1998 Morgan *et al*., 1998 Otto *et al*., 2003 Phillips *et al*., 2004
Tg737mut (Polaris)	14	Orpk (s)	Ciliogenesis	Moyer *et al*., 1994 Yoder *et al*., 2002a
Tsc2 (Tuberin)	1	Eker (r)	Tumor suppressor	Eker, 1954 Kobayashi *et al*., 1995
Chemically induced				
Chlorambucil	10	Jcpk (m)	Mutation in Bicc1, miRNA-binding protein	Flaherty *et al*., 1995 Cogswell *et al*., 2003
DPT	-	(r)	-	Kanwar *et al*., 1984
NDGA	-	(r)	-	Goodman *et al*., 1970 Evan *et al*., 1979
Corticosteroids	-	(s, r, h, l)	-	McDonald *et al*., 1990 Crooker *et al*., 1976 Filmer *et al*., 1973 Ojeda *et al*., 1986

Legend: NDGA: nordihydroguaiaretic acid; DPT: 2-amino-4,5-diphenyl thiazole; NIMA: never in mitosis A related kinase; r: rat; m: mice; l: rabbit; h: hamster; ?: unknown; -: not applicable; Chr: chromosomal localization; Nphp: nephronophthisis; Han: Hannover; kat: kidney anemia and testis; bpk: BAL/C polycystic kidneys; pcy: polycystic; jck: juvenile cystic kidneys; orpk: Oak Ridge polycystic kidneys; cpk: congenital polycystic kidneys; inv: inversion of embryonic turning. In yellow, the mouse model used here within. Updated from (Kurbegovic 2006) September 2013.

References: (Atala, Freeman et al. 1993) (Bihoreau, Ceccherini et al. 1997) (Cogswell, Price et al. 2003) (Cowley, Gudapaty et al. 1993) (Eker 1954) (Crocker, Stewart et al. 1976) (Evan and Gardner 1979) (Fry, Koch et al. 1985) (Flaherty, Bryda et al. 1995) (Filmer, Carone et al. 1973) (Guay-Woodford, Bryda et al. 1996) (Goodman, Grice et al. 1970) (Holland, Milne et al. 2002) (Janaswami, Birkenmeier et al. 1997) (Herron, Lu et al. 2002) (Hou, Mrug et al. 2002) (Katsuyama, Masuyama et al. 2000) (Kobayashi, Hirayama et al. 1995) (Kobayashi, Nishizawa et al. 1995) (Kanwar and Carone 1984) (Lager, Qian et al. 2001) (Liu, Lu et al. 2002) (Mochizuki, Saijoh et al. 1998) (Morgan, Turnpenny et al. 1998) (Moyer, Lee-Tischler et al. 1994) (McDonald, Crocker et al. 1990) (Nagao, Watanabe et al. 1995) (Nauta, Goedbloed et al. 2000) (Olbrich, Fliegauf et al. 2003) (Otto, Schermer et al. 2003) (Ojeda, Ros et al. 1986) (Phillips, Miller et al. 2004) (Preminger, Koch et al. 1982) (Ricker, Gattone et al. 2000) (Simon, Cook et al. 1994) (Smith, Consugar et al. 2006); (Takahashi, Calvet et al. 1991) (Takahashi, Ueyama et al. 1986) (Upadhya, Birkenmeier et al. 2000) (Yoder, Tousson et al. 2002).

Targeted inactivation or transgenesis are powerful tools in mouse genetics that reveal the role of cystogenic genes and their functional implications *in vivo*. Multiple genes, when inactivated, overexpressed or both, result in kidney cysts or polycystic kidney disease (Complete updated list in **Table 7**). They represent indirect or even direct players in ADPKD cystogenesis and indicate signaling cascades involved. Some of them will be briefly mentioned herein. Starting from defects in the extracellular matrix and cell adhesion (eg., integrins, laminins), primary cilia and ciliogenesis (eg., *Kif3A*, *Ifts*, *Bbs*, *Nphp*), planar cell polarity (eg., *Wnt*, *Fat*, *Vangl*), and moving to downstream proliferative and pro-apoptotic effectors (eg., Wnt canonical, non-canonical, *Cux*, *Myc*, miRNA), they can all result in either cyst formation or recapitulation of polycystic kidney disease in mice. Complexity of this pathology becomes obvious as some candidates appear implicated in cross-talks and feedbacks such as c-Myc. First, c-Myc is considered as a legitimate downstream effector of the β-catenin/Wnt pathway. Second, overexpression of *c-Myc* results in stimulation of *Pkd1*/Pc1 expression, and

conversely, *Pkd1* overexpression is associated with increased levels of c-Myc and β-catenin (**Chapter IV, App.III**). Hypothetically, c-myc gene could also be envisioned as a direct target for PC1 C-terminal tail, if it is eventually shown to behave like cpk/cystin, a protein implicated in ARPKD pathogenesis. Cystin was recently found in a complex with necdin, which binds directly to *c-Myc* promoter to activate *c-Myc* expression (Wu, Yang et al. 2013).

Together, these data from different mouse models are consistent with observations in diseased human tissues and cells and once again add proof for the utility of mouse as an authentic working model of human ADPKD disease.

Table 7: Mouse models of polycystic kidney disease: Genetic inactivations and transgenics

Targeted gene	Putative function	Reference
Inactivation/Hypomorph		
Hnf-1β[1]	Transcriptional factor, embryonic development	Gresh *et al.*, 2004
AP-2β	Transcriptional factor, embryonic development	Moser *et al.*, 2003
Integrin α3β1	Cell adhesion, kidney development	Kreidberg *et al.*, 1996
Integrin β1[1]	Laminin binding receptors/Matrix interactions *(HoxB7Cre collecting duct)*	Wu *et al.*, 2009
Ace	Regulation of blood pressure	Carpenter *et al.*, 1996
Bcl-2	Proto-oncogene, apoptosis, proliferation	Nakayama *et al.*, 1994 Veis *et al.*, 1993 Sorenson, 1999
RhoGDIα	Cytoskeletal organization	Togawa *et al.*, 1999
SOCS/IFNγ	Inflammation	Metcalf *et al.*, 2002
Bmp-7	Proliferation, TGFβ signaling, embryonic development	Jena *et al.*, 1997
Psgs1	Inflammation, vascular contractility	Dinchuk *et al.*, 1995 Morham *et al.*, 1995
APC[1]	Oncogene, Wnt signaling pathway	Qian *et al.*, 2005
Tg737$^{\Delta 2\text{-}3Gal}$	Ciliogenesis	Murcia *et al.*, 2000
Kif3A[1]	Ciliogenesis	Lin *et al.*, 2003
Tensin	Cytoskeletal organization	Lo *et al.*, 1997
Cnb1[1]	NFAT signaling pathway	Chang *et al.*, 2004
Pkd1	Receptor, channel, cell adhesion	Table 8A
Pkd2	Channel	Table 8B
Aqp-11	Channel	Morishita *et al.*, 2005
Flcn[1]	Tumor supressor/cell division *(KspCre)*	Chen *et al.,* 2008
Dlg5	Membrane protein targeting/t-SNARE complex/vesicular tranport *(Cadherin/catenin membrane delivery)*	Nechiporuk *et al.,* 2007
Fh1[1]	Tumor suppressor	Pollard *et al.,* 2007
Cux1 p75	Transcription factor/proliferation *Regulates myc, longer cilia, tg under cytomegalovirus/β-actin enhancer promoter*	Cadieux *et al.,* 2008
Laminin α5	Cell adhesion, kidney development	Shannon *et al.,* 2006
Dsch1	PCP/Hippo signaling, ligand for Fat4 *Atypical myosin*	Mao *et al.,* 2011
Fat4	PCP/Hippo signaling, receptor for Dsch1	Saburi *et al.,* 2008
Vangl2	PCP/Hippo signaling, *Not verified if presence of cysts in adult kidneys*	Yates *et al.,* 2010
Ift88	IFT complex B, ciliogenesis	Pazour *et al.,* 2000
Ift20[1]	IFT complex B, ciliogenesis *HoxB7Cre*	Jonassen *et al.,* 2008

Continuation on the next page

Targeted gene	Putative function	Reference
Inactivation/Hypomorph		
Ift140	IFT complex A, ciliogenesis	Jonassen *et al.,* 2012
Bbs2	Ciliogenesis	Nishimura *et al.,* 2004
Bbs4	Ciliogenesis	Guo *et al.,* 2011
Vegf	Vasculogenesis *(Pax8-rtTA/(tetO)(conditional overexpression)*	Hakroush *et al.,* 2009
p120 catenin	Convergent extension, regulation of E-cadherin *(HoxB7 Cre UB specific : no cysts)* *(Pax3 Cre : proximal tubules cysts)*	Marciano *et al.,* 2011
Wnt9b	Non-canonical Wnt PCP signaling *(CE in utero, OCD after birth)*	Karner *et al.,* 2009
Pkhd1	Receptor, chanel, cell adhesion	Kim *et al.,* 2008 Garcia-Gonzalez *et al.,* 2007
pVhl	Tumor suppressor PEPCK Cre (proximal)	Rankin *et al.,* 2006
Gli3	Transcriptional factor/Hedgehog signaling (Interacts with TAZ/Wwr1 downstream of Hippo signaling)	Kang *et al.,* 2009
Ofd1[1]	Ciliogenesis *(KspCre)*	Zullo *et al.,* 2010
Mxi1	*Tumor suppressor gene* *(Antagonist of c-myc)*	Yoo *et al.,* 2007
Mks1	Ciliogenesis/Hedgehog signaling	Weatherbee *et al.,* 2009
Gli2/Nphp7	Transcriptional factor, Hedgehog signaling	Attanasio et al.,, 2007
RPGRIP1L/Nphp8	Ciliogenesis/Wnt non-canonical pathway	Delous et al., 2007
Nek8/Nphp9	Ciliary kinase/cell cycle	Manning *et al.,* 2013
Erb4[1]	Receptor tyrosine kinase/Proliferation/ apical-basal Par3-Par6-aPKC polarity complex *Specifically larger duct lumens, Pax8-Cre*	Veikkolainen *et al.,* 2012
Cdc42[1]	Small GTPase, exocyst/ciliogenesis *(KspCre)*	Choi *et al.,* 2013
Gpr48	Orphan GPCR *(Wnt/β-catenin and Wnt/PCP signaling)*	Dang *et al*., 2014
Dicer[1]	miRNA processing *PEPCK Cre (proximal): later phenotype (6months)* *KspCre (distal/collecting): numerous cysts at P10*	Wei et al., 2010 Patel *et al.,* 2012
Taz	Wnt non-canonical/Hippo pathway *Cyst originate from proximal tubule segments*	Hossain *et al.,* 2007 Makita *et al.,* 2008
B9d2[1] **and B9d1**	Ciliogenesis/Hedgehog signaling	Tian *et al.,* 2007 Town *et al.,* 2008 Dowdle *et al.,* 2011
Gpc3	Apoptosis, proliferation, IGF signaling	Cano-Gauchi *et al*., 1999
Tsc2$^{+/-}$	mTOR pathway, tumor supressor	Bonnet *et al.,* 2009
Tsc1$^{+/-}$	mTOR pathway, tumor supressor	Wilson *et al.,* 2005
Tsc1[1]	mTOR pathway, tumor supressor *Inducible inactivation by triple crossing :* *transgenic Pax8-rtTA, LC1-Cre and Tsc1flox* *(proximal, distal, collecting)*	Traykova-Brauch *et al.,*2008
Par3[1]	Polarity and convergent extension *Hoxb7Cre in UB (Hoxb7Cre:Par3*$^{flox/-}$ *mice at birth)*	Castelli *et al.,* 2013
Sec63 and Prkcsh	ER protein translocation and protein quality control pathway, *pCX-Cre and KspCre, liver and kidney cysts*	Fedeles *et al.,* 2011

Continuation on the next page

Transgenic		
c-myc[1]	Transcriptional factor, proto-oncogene, apoptosis *Renal specific SB promoter* *Double transgenic: Pax8-rtTA X tetracyclin-responsive c-MYC (TetO-Myc)*	Trudel *et al*., 1991 Traykova-Brauch *et al.,* 2008
α-prothymosin	Apoptosis *(rat β-actin promoter, directly regulates c-myc)*	Li KJ *et al*., 2005
Hnf-1β[1] (Mutant form)	Transcriptional factor, embryonic development	Hiesberger *et al*., 2004 Hiesberger *et al*., 2005
β-catenin (Active form)	Cell adhesion, Wnt signaling pathway	Saadi-Kheddouci *et al*., 2001 Romagnolo *et al*., 1999
Pax-2	Transcriptional factor, embryonic development	Dressler *et al*., 1993
RasT24 oncogene	Proto-oncogene, cell proliferation	Schaffner *et al*., 1993
Simian virus 40 early region	Proto-oncogene, cell proliferation	MacKay *et al*., 1987 Kelley *et al*., 1991
Human αβS	HBS: Sickle cell anemia human hemoglobin S (β^{6Val}) *(One Mouse β-Globin Endogenous Allele)*	Noguchi *et al.,* 2001
c-Erb-B2	Proto-oncogene, cell proliferation	Stöcklin *et al*., 1993
Endothelin-1	Proliferation, vasoconstriction	Hocher *et al*., 1997 Hindo *et al.,* 2002
Hgf	Growth factor, proliferation, kidney development, branching	Takayama *et al*., 1997
Kgf	Growth factor, proliferation	Nguyen *et al*., 1996
Tgf-α	Growth factor, proliferation	Lowden *et al*., 1994
hGH	Growth factor, proliferation	Wanke *et al*., 1991 Brem *et al*., 1989
Alk3	TGFβ signaling, kidney development, branching (dominant negative)	Hu *et al.,* 2003
Hif1a[1]	Transcription factor/Tumor suppressor/Hypoxia inducible *GGT gamma-glutamyltranspeptidase (proximal tubules)*	Fu *et al.,* 2011
Hif2α[1]	Transcription factor/Tumor suppressor/Hypoxia inducible *Ksp cadherin promoter*	Schietke *et al.,* 2012
Erb4[1]	Receptor tyrosine kinase/Proliferation/ Apical-basal Par3-Par6-aPKC polarity complex, tight junction assembly *(Pax8 driven overexpresson)*	Veikkolainen *et al.,* 2012
miR17~92	miRNA, proliferation	Patel *et al.,* 2013
Pkd1 and Pkd1-Tsc2	Pkd1: Receptor, channel, cell adhesion Tsc2: Tumor suppressor	Table 8A
Pkd1[1]	**Receptor, channel, cell adhesion**	Table 8A
Pkd2	Calcium channel	Table 8B

Legend: [1]Specific to kidneys. CE: convergent extension; PCP: planar cell polarity; OCD: oriented cell division; IFT: intraflagellar transport; PEPCK Cre (transgenic): Phosphoenolpyruvate carboxykinase; pVHL: von Hippel-Lindau tumor suppressor; Bbs: Bardet-Biedl syndrome; Mx1: max-interacting protein 1; NPHP: nephronophtisis; Hif: Hypoxia-inducible transcription factor; Fh: fumarate hydratase; folliculin, mutated in Birt-Hogg-Dubé syndrome; Ofd1: oral-facial-digital syndrome; Vegf: vascular endothelial growth factor; Dlg5: Disks large homolog 5; Pkd1 and Pkd2: polycystic kidney disease genes; IGF: insulin growth factor; hGH: human growth hormone; Tgf; transforming growth factor; Kgf: keratinocyte growth factor; Hgf: hepatocyte growth factor; Hnf: hepatocyte nuclear factor; dsch: daschous; cnb: calcineurin; aqp: aquaporin; psgs: prostaglandin; Ace: angiotensin-converting enzyme; SOCS: suppressor of cytokine signalling Gpc3: glypican-3, gene mutated in patients with the Simpson-Golabi-Behmel syndrome (SGBS); rtTA: reverse tetracycline-dependent transactivator (tTA); Tsc: tuberous sclerosis complex. In yellow, the mouse model used here within. Updated from (Kurbegovic 2006), October 2013.

References: (Attanasio, Uhlenhaut et al. 2007) (Brem, Wanke et al. 1989) (Bonnet, Aldred et al. 2009) (Cadieux, Harada et al. 2008) (Cano-Gauci, Song et al. 1999) (Carpenter, Honkanen et al. 1996) (Castelli, Boca et al. 2013) (Chang, McDill et al. 2004) (Chen, Futami et al. 2008) (Choi, Chacon-Heszele et al. 2013) (Delous, Baala et al. 2007) (Dinchuk, Car et al. 1995) (Dowdle, Robinson et al. 2011) (Dressler, Wilkinson et al. 1993) (Fu, Wang et al. 2011) (Garcia-Gonzalez, Menezes et al. 2007) (Gresh, Fischer et al. 2004) (Guo, Beyer et al. 2011) (Jonassen, San Agustin et al. 2008) (Jonassen, SanAgustin et al. 2012) (Hakroush, Moeller et al. 2009) (Hiesberger, Bai et al. 2004) (Hiesberger, Shao et al. 2005) (Hocher, Thone-Reineke et al. 1997) (Hossain, Ali et al. 2007) (Hu, Piscione et al. 2003) (Jena, Martin-Seisdedos et al. 1997) (Kang, Beak et al. 2009) (Karner, Chirumamilla et al. 2009) (Kelley, Agarwal et al. 1991) (Kim, Fu et al. 2008) (Kreidberg, Donovan et al. 1996) (Li, Shiau et al. 2005) (Lin, Hiesberger et al. 2003) (Lo, Yu et al. 1997) (Lowden, Lindemann et al. 1994) (MacKay, Striker et al. 1987) (Makita, Uchijima et al. 2008) (Manning, Sergeev et al. 2013) (Mao, Mulvaney et al. 2011) (Marciano, Brakeman et al. 2011) (Metcalf, Mifsud et al. 2002) (Morham, Langenbach et al. 1995) (Morishita, Matsuzaki et al. 2005) (Moser, Dahmen et al. 2003) (Murcia, Richards et al. 2000) (Nakayama, Nakayama et al. 1994) (Nechiporuk, Fernandez et al. 2007) (Nguyen, Danilenko et al. 1996) (Nishimura, Fath et al. 2004) (Noguchi, Gladwin et al. 2001) (Patel, Hajarnis et al. 2012) (Patel, Williams et al. 2013) (Pazour, Dickert et al. 2000) (Pollard, Spencer-Dene et al. 2007) (Qian, Knol et al. 2005) (Rankin, Tomaszewski et al. 2006) (Saadi-Kheddouci, Berrebi et al. 2001) (Romagnolo, Berrebi et al. 1999) (Saburi, Hester et al. 2008) (Schaffner, Barrios et al. 1993) (Schietke, Hackenbeck et al. 2012) (Shannon, Patton et al. 2006) (Sorenson and Sheibani 1999) (Stocklin, Botteri et al. 1993) (Takayama, LaRochelle et al. 1997) (Togawa, Miyoshi et al. 1999) (Town, Breunig et al. 2008) (Traykova-Brauch, Schonig et al. 2008) (Trudel, D'Agati et al. 1991) (Veikkolainen, Naillat et al. 2012) (Veis, Sorenson et al. 1993) (Wanke, Wolf et al. 2001) (Wei, Bhatt et al. 2010) (Weatherbee,

Niswander et al. 2009) (Wilson, Idziaszczyk et al. 2005) (Wu, Kitamura et al. 2009) (Yates, Papakrivopoulou et al. 2010) (Yoo, Sung et al. 2007) (Zullo, Iaconis et al. 2010).

7.1.2) *PKD1*, *PKD2* and *PKHD1* orthologous mouse models of PKD

Although numerous non-orthologous PKD mouse models were generated (**Table 6,7**), the ideal tools for studying human ADPKD pathogenesis consist of directly targeting the orthologous *Pkd1* or *Pkd2* genes (or *Pkhd1* for ARPKD). Mouse models are beneficial in multiple aspects: **1)** to study the pathogenetic mechanism, **2)** to analyze cellular pathophysiology at different stages of the disease from initiation to progression and end stage, **3)** to delineate important modulators and potential signaling pathways via genetic complementations and **4)** finally for testings in pre-clinical trials. **Tables 8A, B, C** summarize important characteristics of all of these models. For comparison purposes, our own models that contribute extensively to the ADPKD field were included but will be described in detail later on in separate chapters (**Chapters IV-VIII**).

Table 8A. PKD mouse models: *Pkd1* targeting

	Mutant	Exons disrupted	Homozygous Phenotype								Heterozygous Phenotype			Ref
			Lethality	Kidney cyst	Liver cyst	Pancreas cyst	Vascular defect	Heart defect	Skeletal defect	Other defect	Kidney cyst	Liver cyst	Pancreas cyst	
	Targeted Pkd1													
LOF	$Pkd1^{\Delta 34}$	34	E18.5	E15.5	-	+	-	-	+	Lung hypoplasia Skeleton cartilage, Polyhydramnios, Spina bifida occulta	>9	>9	>12 >20m (10%)	(1,4)
	$Pkd1^{L-}$	43-45	E14.5-15.5	E13.5	-	E13.5	Hemorrhage	-	-	Vascular	ND	ND	ND	(2)
	$Pkd1^{\Delta 17-21}$	17-21	E13.5-14.5	ND	ND	ND	Hemorrhage	+	+	Skeleton cartilage	>3m	>19m	-	(3)
	$Pkd1^{Neo1}$	4	E13.5-16.5	E15.5	-	E13.5	Hydrop fetalis	-	+	Skeleton cartilage, Polyhydramnios, Spina bifida occulta	≥2.5m (48%) ≥18mo (100%)	≥2.5m (48%) ≥18mo (100%)	>12.5m	(4)
	$Pkd1^{-/-}$	2-6	E14.5	E15.5	ND	ND	Hemorrhage Hydrop fetalis	+	+	Proglitazone : Partial rescue	ND	ND	ND	(5)
	$Pkd1^{Neo1}$	1	E12.5-birth	E15.5	-	E14.5	Edema, Hemorrhage	-	-	-	>3m	-	ND	(6)
	$Pkd1^{mv10Ahge}$	Rearr 12-26	prior weanning	E16.5	ND	E15.5	Edema	ND	ND	ND	≥6wks	≥40wks	≥40wks	(7)
	$Pkd1^{\Delta 2-4}$	8	E13.5-birth	E15.5			Edema			Polyhydramnios	-	-	-	(8)
	$Pkd1^{\Delta Mys}$	44-46	ND (60% survive to E116.5)	E15.5	ND	ND	Edema, Hemorrhage	ND	ND	Hydroencephalus (E16.5)	- (18mo)	- (18mo)	- (18mo)	(9)
Hypo	$Pkd1^{allo1}$	2	1-15mo	ND	+	+	Hemorrhage	ND	ND	ND	-	NA	NA	(10)
	$Pkd1^{L3}$	30-34	1-12 mo	E15.5	-	+	-	-	+	ND	ND	ND	ND	(11)
	miRNA TG Pkd1	miRNA Pkd1	ND	+ (present at P1)	ND	ND	ND	ND	ND	ND				(12)
	$Pkd1^{V}$	25 (aa 3041)	2-6wks (23dys)	~P3	Fibrosis Dilatatio ns	-	ND	ND	ND	ND	- (13, 22mo)	- (13, 22mo)	- (13, 22mo)	(13)
	$Pkd1^{RC}$	29 (aa R3277)	ND	+ (start at E16.5)	+		ND	ND	ND	$Pkd1^{RC/RC}$ osteopenia and LVH	- (analyzed up to 1yr)	- (analyzed up to 1yr)	ND	(14)
Condi	$Pkd1^{cond}$	2-6 γGt.Cre	<1mo	Severe: P10	NA	NA	NA	NA	NA	NA				(15)
	$Pkd1^{cond}$	21-23 Tamox ind P5	ND	Severe: 1mo	ND	ND	ND	ND	ND	ND				(16)
	$Pkd1^{cond}$	2-11 Ind.KspCre P4 and 3-6mo	ND	P4: Severe 1mo 3-6mo: mild 6-9 mo	ND	ND	ND	ND	ND	ND				(17)
	$Pkd1^{cond}$	1-4 1) Aqp2 Cre 2) B1ATP Cre	1) 8.2wks 2) none	1) severe: wk 1 2) mild: wk 13	NA	NA	NA	NA	NA	NA				(18)
	$Pkd1^{cond}$	2-4 KspCre	P14-17	Severe: P10	NA	NA	NA	NA	NA	NA				(19)
	$Pkd1^{cond}$	45-46 Actin-Cre	E16.5-17.5	E15.5	ND	ND	Edema, hemorrhage	ND	ND	ND				(20)
	$Pkd1^{cond}$	2-4 1) MMTVCre 2) Meox Cre 3) Tamox ind ≤P12 or P14/21	1) None 2) Not viable	1) Rare: 20wks 2) E15.5 3) ≤P12: Severe 1mo P14/21: Mild 6mo	+ E15.5 ND	ND ND ND	ND Edema, hemorrhage ND	ND ND ND	ND ND ND	ND Polyhydramnios ND				(21)
GOF	**TPK**	PKD1/TSC2	None	occasional	+	ND	ND	ND	ND	ND				(22)
	$SBPkd1^{TAG}$	Pkd1 renal-specific	5.9-14.6mo	P1	NA	NA	NA	NA	NA	NA				(23)
	$Pkd1_{TAG}$	Pkd1	5.5-16.7mo	1mo	+	ND	Hemorrhage	+	ND	Intracranial aneurysm				(24)
Human mutant	$Pkd1_{LEXRA}$	Tg Pkd1 Ex1-25 (deleted of 26-end)	17-23mo	Dilatation 2months Cysts 1yr	-	-	-	-	-	-				(25)

Table 8B. PKD mouse models: *Pkd2* targeting

	Mutant	Exons disrupted	Homozygous Phenotype								Heterozygous Phenotype			
			Lethality	Kidney cyst	Liver cyst	Pancreas cyst	Vascular defect	Heart defect	Skeletal defect	Other defect	Kidney cyst	Liver cyst	Pancreas cyst	Ref
	Targeted Pkd2													
LOF	**WS25** (unstable)	Rearr 1-2	>3mo	1-3m	1-2.5m	ND	-	-	-	Intracranial aneurysm	>2.5m (many)	>2.5m	ND	**(26)**
	WS183 (null)	1	E13.5-18.5	E15.5	-	E14.5	Hemorrhage Edema	+	-	-	>3m (rare)	>9m	-	**(27)**
	-/LacZ	1	E12.5-18.5	E15	Abnormal lobulation	L/R defect	Hemorrhage	+	ND	L/R defect	ND	ND	ND	**(28)**
Hypo	**Pkd2^{ad3}**	Intron 2	ND	+ (<12mo)	+	Dilatations	ND	ND	ND	Growth retardation Severe dil. bile ducts				**(29)**
Condi	**Pkd2^{d3}**	3 1) γGt.Cre 2) E11a.Cre 3) Mx1.Cre 4) Pdx1.Cre	perinatal	1) + 2) + 3) + 4) NA	NA + + NA	NA ND + +	NA Edema ND NA	NA ND ND NA	NA ND ND NA	NA L/R defects ND NA				**(30)**
	Pkd2$^{flox11-13}$	11-13 1) Meox2-Cre 2) Tie2-Cre	1) E16.5 (some P0) 2) before birth	+	ND	+	Hemorrhage Edema	-	ND	Situs inversus Placental defects				**(31)**
				-	ND	ND	Hemorrhage N0 Edema	-	ND	Polyhydramnious Placental defects				
GOF	**Pkd2 TG**	Actin PKD2 cDNA	ND	6mo	ND	ND	ND	ND	ND	ND				**(32)**

Table 8C. PKD mouse models: *Pkhd1* targeting

LOF

Mutant	Exons disrupted	Homozygous Phenotype								Heterozygous Phenotype			Ref
		Lethality	Kidney cyst	Liver cyst	Pancreas cyst	Vascular defect	Heart defect	Skeletal defect	Other defect	Kidney cyst	Liver cyst	Pancreas cyst	
Targeted Pkhd1													
Pkhd1^{tTGCFPA16}	15-16	Variable **- 5-10% in utero** **- 25% alive beyond 1 yr**	+ (2-4wks)	+ (2mo)	Dilatations (6mo)	Hemorrhage	ND	ND	Hemorrhage in gastrointestinal tract Brain (vacuoles)				**(33)**
Pkhd1^{LacZ}	1-3	ND	+ (45dys, 100% by 9mo)	+	+ (less frequent)	ND	ND	ND					**(34)**
Pkhd1^{del3-4}	3-4	Variable	Variable (≤ 3mo: 13.7%) (most at 6 mo)	+ (fully penetrant)	+ (≥9mo)	ND	ND	ND	Growth retardation Perinatal pulmonary failure				**(35)**
Pkhd1^{del2}	2	ND	+ (9mo outbred, 3mo inbred)	+ (starts at 1mo, severe at 12-15mo)	+ (48% by 6mo)	-	-	-	Proximal renal cysts Gender (females) preferentially				**(36)**
Pkhd1^{del40}	40	ND	- No cysts (analyzed up to 14mo)	+	ND	ND	ND	ND					**(37)**
Pkhd1^{LSL} (KO)	STOP cassette in intron2	ND	+ (Dilatations at 3-6mo)	+ (At 3mo cysts and fibrosis; At 1mo-cyst start)		ND	ND	ND	Kidney phenotype: - Proximal tubules - Females only Also generated knock-in WT Pkhd1-V5 tagged, **Pkhd1^{V5PK}**				**(38)**

Legend: ND: Not determined; NA: Not applicable; LVH: left ventricular hypertrophy; mo: months; dys: days. Of note, *Pkd1*$_{TAG}$ and *Pkd1*$_{EXTRA}$ are directly generated in this thesis. All mice highlighted in yellow have been subject for different experiments here within.

References: **(1)** (Lu, Peissel et al. 1997) (Lu, Fan et al. 1999); **(2)** (Kim, Drummond et al. 2000); **(3)** (Boulter, Mulroy et al. 2001); **(4)** (Lu, Shen et al. 2001); **(5)** (Muto, Aiba et al. 2002); **(6)** (Wu, Tian et al. 2002); **(7)** (Natoli, Gareski et al. 2008); **(8)** (Starremans, Li et al. 2008); **(9)** (Wodarczyk, Rowe et al. 2009); **(10)** (Lantinga-van Leeuwen, Dauwerse et al. 2004); **(11)** (Jiang, Chiou et al. 2006); **(12)** (Wang, Hsieh-Li et al. 2010); **(13)** (Yu, Hackmann et al. 2007); **(14)** (Hopp, Ward et al. 2012); **(15)** (Starremans, Li et al. 2008); **(16)** (Natoli, Smith et al. 2010); **(17)** (Lantinga-van Leeuwen, Leonhard et al. 2007); **(18)** (Raphael, Strait et al. 2009); **(19)** (Shibazaki, Yu et al. 2008); **(20)** (Wodarczyk, Rowe et al. 2009); **21)** (Piontek, Huso et al. 2004) (Piontek, Menezes et al. 2007); **(22)** (Pritchard, Sloane-Stanley et al. 2000); **(23)** (Thivierge, Kurbegovic et al. 2006); **(24)** (Kurbegovic, Cote et al. 2010); **(25)** (Kurbegovic and Trudel 2013); **(26)** (Wu, D'Agati et al. 1998); **(27)** (Wu, Markowitz et al. 2000); **(28)** (Pennekamp, Karcher et al. 2002); **(29)** (Kim, Fu et al. 2008); **(30)** (Kim, Ding et al. 2009); **(31)** (Garcia-Gonzalez, Outeda et al. 2010); **(32)** (Geng, Boehmerle et al. 2008) (Park, Sung et al. 2009); **(33)** (Kim, Fu et al. 2008); **(34)** (Williams, Cobo-Stark et al. 2008); **(35)** (Garcia-Gonzalez, Menezes et al. 2007); **(36)** (Woollard, Punyashtiti et al. 2007); **(37)** (Moser, Matthiesen et al. 2005); **(38)** (Bakeberg, Tammachote et al. 2011).

7.1.2.1) *Pkd1* Loss-of-function (LOF)

After the discovery of the 2 main genes linked to ADPKD, multiple groups aimed to generate complete *Pkd1* and *Pkd2* null mutants in mice in order to verify the causal relationship between the loss-of-function and the disease (**Table 8A, B**).

Renal and extrarenal phenotypes

The homozygous *Pkd1* mouse models reproducibly develop renal and pancreatic cysts from E13.5-E15.5 and several extrarenal vascular, skeletal and cardiac anomalies (**Table 8A**). Homozygous embryos die *in utero* or perinataly, within a few hours after birth (Lu, Peissel et al. 1997). Expected Mendelian ratio is obtained until E18.5 (Lu, Peissel et al. 1997) and even at birth (**Our unpublished data**). Overall, *Pkd1*$^{-/-}$ embryos have normal early kidney morphogenesis with normal overall pattern of initial UB branching and mesenchymal induction. Because cysts occur quite late in kidney development and since the 1st phase of UB branching and metanephric

mesenchyme induction appears normal, Pc1 is suggested to participate in epithelial cell differentiation and tubular extension (Lu, Peissel et al. 1997) (**See also Section 7.1.2.1** - *Putative roles in morphogenesis and branching morphology*).

Cysts in the kidney are first observed at E15.5 and, in pancreatic ducts occur simultaneously or even before kidney defects at E13.5 (Lu, Peissel et al. 1997). In both organs, cysts grow in size and number. Often, in the pancreas only one enormous yellow filled cyst is detected at birth with almost no intact parenchyma. Consistent with Pc1 pattern of expression, pancreatic islets and acini (exocrine and endocrine structures), derived from proto-differentiated progenitor cells of ductal origin (Madsen, Jensen et al. 1996), are present but reduced in number (Lu, Peissel et al. 1997). Interestingly, *Pkd1* LOF models present many phenotypical similarities to another very common genetic disease, cystic fibrosis (CF) with cystic disease and fibrosis (Oppenheimer and Esterly 1975).

Homozygous pups demonstrate various extrarenal cardiovascular and skeletal/bone/cartilage defects. The bone phenotype in *Pkd1*$^{-/-}$ (skeletal, vertebrate and intramembranous ossification) with less bone mineralization, shorter and thinner long bones was probably caused by defects in chondrocyte maturation (Lu, Shen et al. 2001) correlating with data from conditional inactivation in the bone (**Section 7.1.2.2**). However, in contrast to the human disease, but analogous to all murine mutants, no liver cysts were observed in the absence of full-length Pc1 or Pc2.

The heterozygous mice, on the other hand, do not develop any discernible fully penetrant cystic phenotypes. It is important to note that some subtle anomalies were reported in heterozygous *Pkd1* or *Pkd2* mice and thus represent pre-cystic anomalies: increased proliferation, fibrosis and inflammation (Chang, Parker et al. 2006, Prasad, McDaid et al. 2009).

Cyst origin

The segmental origin of renal cysts was investigated in detail in *Pkd1*$^{-/-}$ mutants (Lu, Peissel et al. 1997, Ahrabi, Jouret et al. 2010). Lu *et al*. demonstrated the

involvement of proximal tubules at the onset of cystogenesis (E15.5) and a more broad implication later on in collecting tubules of the inner medulla and cortex (Lu, Peissel et al. 1997, Lu, Shen et al. 2001). Similarly, another group using megallin staining for proximal tubule identification showed that cysts mostly originate from proximal tubules and glomeruli at E15.5 and, eventually to a lesser extent, DBA distal/collecting positive tubules (Ahrabi, Jouret et al. 2010).

Genetic background and residual proteins as modifiers of PKD

Manifestation of the PKD phenotype was reported as more or less influenced by the genetic background (not really (Lu, Peissel et al. 1997); modestly (Lu, Shen et al. 2001)) and potentially by residual protein mutant expression (**App.VIII**) (Lu, Peissel et al. 1997, Kim, Drummond et al. 2000, Boulter, Mulroy et al. 2001, Lu, Shen et al. 2001).

Putative causes of death

The exact cause of embryonic/perinatal death in the *Pkd1/2*$^{-/-}$ mice is unknown. Since, very early during development, embryos develop haemorrhage, edema, hydrops fetalis (generalized oedema, most visible in the back of the body) and polyhydramnious (excess of amniotic fluid in the amniotic sac), the embryonic cause of death could reside in vascular/cardiac pathology, or hydrops fetalis, caused generally by either cardiac, anemic or skeletal anomalies (Van Maldergem, Jauniaux et al. 1992 , Arcasoy and Gallagher 1995). Defects in the placenta are also a good causative candidate. Indeed, Pc1 and Pc2 are both shown to be expressed in the placenta (Garcia-Gonzalez, Outeda et al. 2010) and important *Pkd1*$^{-/-}$ placental vascular defects are displayed, which include disorganized fetal arteriole and capillary networks, a significant decrease in the number of vascular branches and dilatations of the trophoblast lining maternal vascular channels (Bhunia, Piontek et al. 2002).

Putative roles in morphogenesis and branching morphology

Expression and localization of *PKD1/PKD2* genes and proteins are developmentally regulated and hence ADPKD could be of a developmental origin (**Section 5.1 and 5.2**). There is a couple of evidence for this. **First,** inactivation of *Pkd1* in mice does not affect initial steps of kidney development but rather terminal renal tubular differentiation and thereby leads to formation of renal cysts in the second-half of embryogenesis when tubules normally undergo tubular lengthening and maturation (Lu, Peissel et al. 1997, Wu, D'Agati et al. 1998, Lu, Fan et al. 1999, Wu, Markowitz et al. 2000, Kim, Drummond et al. 2000). **Second,** introduction of *PKD1* into mammalian MDCK or IMCD cells that spontaneously form cysts in 3D type I collagen gels induces spontaneous kidney epithelial branching / tubulogenesis (Boletta, Qian et al. 2000, Nickel, Benzing et al. 2002). **Third,** disruption of PC1 in the ureteric cell membrane and uretic bud lumen of kidney explants leads to a reduction in kidney and UB volume, number of UB branch points, branch tips, UB length and total area, number of glomeruli and increase in volume of terminal branches while the overexpression of the PC1 C-terminus has the opposite effect (Polgar, Burrow et al. 2005). **Finally,** in contrast to PC1, the absence of PC2 results in modest but significant increase in the branching and this process is partially dependent on its calcium activity (Grimm, Karihaloo et al. 2006).

These studies suggest that PC1 and PC2 are implicated in kidney epithelial differentiation and morphogenesis, tubulogenesis and ureteric branching where their relative expression needs to be tightly regulated.

7.1.2.2) *Pkd1* hypomorphs

Two different *Pkd1* hypomorph mouse models, $Pkd1^{nl}$ and $Pkd1^{L3}$, were generated (Lantinga-van Leeuwen, Dauwerse et al. 2004, Jiang, Chiou et al. 2006). The $Pkd1^{nl}$ hypomorph allele interferes with normal splicing (only 13-20% of correctly spliced *Pkd1*), and leads to a frameshift and a premature stop codon at the 5' end (exon1-2) of the murine *Pkd1* gene (**Table 8A**). The construct of $Pkd1^{L3}$ hypomorph allele was intended for conditional targeting by introducing one loxP site in the intron 30 and a

second LoxP-neao cassette site into the intron 34, in a reverse orientation to *Pkd1* gene. Before excision by Cre recombinase, *Pkd1*^{L3} allele led to decreased levels of wild-type *Pkd1*/Pc1 and is considered, by the authors, as a ''pure knockdown'' for *Pkd1*. In both *Pkd1*^{nl} and *Pkd1*^{L3}, hypomorph mice escape *Pkd1*$^{-/-}$ embryonic lethality and the majority of mice live to ~1-2 months with some mice reaching 1 year (~10%) or rarely up to 15 months. These mice develop bilateral cystic kidneys with high variability in phenotype severity. The majority of cysts affect loops of Henlé, distal tubules and collecting ducts with rare proximal (~10%) and glomerular cysts (Lantinga-van Leeuwen, Dauwerse et al. 2004, Happe, van der Wal et al. 2013, Jiang, Chiou et al. 2006) or no proximal cysts (Jiang, Chiou et al. 2006). In addition to a kidney phenotype, *Pkd1*^{nl} hypomorph mice also develop mild liver and pancreatic duct dilatations, cardiovascular defects and saccular intracranial aneurysms (Lantinga-van Leeuwen, Dauwerse et al. 2004); these pathologies are not seen in *Pkd1*^{L3} hypomorphs (Jiang, Chiou et al. 2006). Of note, by Northern blot and QPCR of the 5' end, the *Pkd1* transcript was reduced as expected in the *Pkd1*^{nl} mutant. Unexpectedly and currently without explanation, the 3′ *Pkd1* transcript on the other hand was still produced and even upregulated which could be in part responsible for the survival and delay in the cyst progression to ESRD (Lantinga-van Leeuwen, Dauwerse et al. 2004, Trudel M 2011, Happe, van der Wal et al. 2013) (**App.II**).

miRNA transgenic (tg) knock-down approach was attempted in mice to decrease Pc1 expression and successfully led to kidney phenotype similar to two other ''hypomorph/haploinsufficient'' mouse models (Wang, Hsieh-Li et al. 2010). In this latter study, the extrarenal phenotype was not addressed despite having a human ubiquitin B promoter driving the miRNA.

Two groups used a knock-in approach that resulted in functional Pc1 ''hypomorphs'' (**Table 8A**). In the first study, Yu *et al.* introduced a substitution in one critical amino acid of the GPS cleavage site of Pc1 called *Pkd1*^{V} (HL↓**T** to HL↓**V;** ↓ representing the position of the cleavage). This resulted in sole production of full-length uncleaved

Pc1, and in contrast to *Pkd1*$^{-/-}$, *Pkd1*^{V} homozygotes escaped embryonic lethality, developed exclusively distal postnatal cystogenesis and biliary duct fibrosis and dilatations, and died between 3 and 4 wks of age (Yu, Hackmann et al. 2007) with an intact pancreas. The second study reproduced an incompletely penetrant *Pkd1* variant R3277C in mice and led to decreased levels of functional exosomal Pc1 (Hopp, Ward et al. 2012). Pc1^{RC} was mostly retained in the cell (without triggering ER stress), and less efficiently cleaved at the GPS motif. This Pc1 folding mutant was temperature sensitive and, at a more permissive temperature, was able to traffic more efficiently, for example into the exosomes. These *Pkd1*$^{RC/RC}$ mice developed kidney cysts (early stage: proximal>>>collecting; late stage: collecting>>>proximal tubules) with higher proliferation, deranged ciliary ultrastructure by SEM with longer primary cilia in precystic stage, and liver, bone and cardiac anomalies. Importantly, in comparison to *Pkd1*$^{del2/RC}$ with ~20% of mature Pc1 and rapidly progressive early-onset ADPKD, the *Pkd1*$^{RC/RC}$ with ~40% of mature Pc1 showed slower and adult progressive disease.

This data on *Pkd1* hypomorphs and decrease in Pc1 functional levels being associated with PKD are suggestive of ADPKD being directly related to PC1 dosage and *PKD1*/PC1 threshold.

7.1.2.3) *Pkd1* conditional

7.1.2.3.1) Spatial/temporal conditional inactivations of *Pkd1*

A couple of conditional *Pkd1* floxed alleles were produced in mice, and when crossed with an ubiquitously or widely expressed Cre recombinases (eg., Actin, Meox), resulted in *Pkd1*^{null}-like phenotypes (**Table 8A**). Some of them are mentioned here below with particular relevance to the tissue-specific and developmentally regulated role of *Pkd1*.

Kidney- Inactivation of *Pkd1* with KspCre (transgenic Cre under expression of Ksp cadherin promoter in the distal/collecting tubules at ~E15.5) leads to severe kidney cystogenesis, and death at ~P17 (Shibazaki, Yu et al. 2008). Use of other Cre

recombinase with less specific expression in the kidney (eg. Colα1(3.6)-Cre, Dermo1-Cre, Col2-Cre and Nestin-Cre) were also associated with kidney cysts (Wodarczyk, Rowe et al. 2009, Qiu, Xiao et al. 2012, Kolpakova-Hart, Nicolae et al. 2008, Kolpakova-Hart, McBratney-Owen et al. 2008).

Inducible- Inducible tamoxifen-Cre^{+} *Pkd1* inactivation allowed the narrowing down of a developmental window of *Pkd1* requirement for kidney response. Inactivation of *Pkd1* in mice at P11-P12 (before P13) resulted in severely cystic kidneys within 3 weeks, whereas inactivation at day P14-P15 and later resulted in cysts only after 5 months (Piontek, Menezes et al. 2007). This window of *Pkd1* requirement coincides with significant changes in gene expression profile/patterns (involved in transport, catalytic activities, kidney development and proliferation) and suggests *Pkd1* as regulator of these processes that acts as a ''developmental brake'' of the kidney for the terminal renal maturation process.

Liver- Using MMTV transgenic Cre, which is weakly expressed among other tissues in kidney and liver with only ~10% of recombination, all *Pkd1*$^{cond/cond}$;MMTV-cre mice develop moderate bilateral kidney and severe liver cysts by 20wks of age (Piontek, Huso et al. 2004).

Brain- Inactivation of *Pkd1* using Nestin-Cre highly expressed in the brain caused ventricular dilatations by P7-P10 and hydrocephalus (Wodarczyk, Rowe et al. 2009).

Bone- Bone defects in *Pkd1*$^{-/-}$ mutants raised the question of whether bone phenotype was directly and specificaly due to the role of *Pkd1* in the bone. This hypothesis was tested by multiple Cre recombinases specific for different types of bone forming cells: **1)** mature osteoblasts using Oc-Cre, **2)** osteocytes using Dmp1-Cre (Xiao, Zhang et al. 2010, Xiao, Dallas et al. 2011) or **3)** earlier precursors of osteoblast lineage that originate from mesenchymal cells using Col1α1(3.6)-Cre (Qiu, Xiao et al. 2012). While *Pkd1* inactivation in osteoblast/osteocyte led to postnatal osteopenia *i.e.,* lower bone mineral density, the early inactivation of *Pkd1* in the osteoblast bone cells precursors, the mesenchyme, led to increase in mRNA

expression of mesenchymal/EMT and fibrosis markers such as snail1, vimentin, α-SMA and Col1α1. Nonetheless, this study linked Pc1 once again with potential functional involvement in EMT process, fibrosis and mesenchymal cells. In osteoblasts, *Pkd1* function appears to rely on regulation of calcium levels and osteoblast bone-specific transcription factor, RunxII (Xiao, Zhang et al. 2008). In the bone, but also possibly relevant in the kidney, Pc1 thus seems to act as a sensor to transduce the extracellular signal into intracellular signaling effects.

Furthermore, the role of Pc1 in craniofacial development was assessed by Dermo1-Cre and Wnt1-Cre expressed respectively in osteochondroprogenitor cells in the cranial, axial and appendicular skeleton and neural crest cells (NCC) (Kolpakova-Hart, McBratney-Owen et al. 2008). Finally, using chondrocytic-specific Col2Cre transgenic Cre, the resulting mice also developed skeletal defects (Kolpakova-Hart, Nicolae et al. 2008).

Vessel integrity- Data from tetraploid aggregation (placental *vs* embryo proper) and endothelial Tie2-Cre conditional inactivation of *Pkd1* and *Pkd2* suggested that the placental vessel integrity by Pc1/Pc2 contributed to embryonic demise in these respective mouse models (Bhunia, Piontek et al. 2002).

Epididymis- Finally, using Pax2-cre, a role of *Pkd1* was also uncovered in the epithelia of the male reproductive system, namely the epididymis, with mutants developing dilatation of the efferent duct and coiling defect (Nie and Arend 2013).

7.1.2.3.2) Kidney injury as a ‘’third-hit’’ for cystogenesis

The ‘’second-hit’’ hypothesis was widely accepted for focal cysts and late-onset of ESRD in ADPKD. However, the rate of somatic mutations should be elevated and PKD is very mild in the adult inactivated *Pkd1* mouse model. Some additional factors, so called ‘’third-hits’’ other than somatic second-hits such as genetic modifying genes (modifiers) and environmental factors (ischemia, toxic injury, irradiation, hormones, gender) were suggested to exert an influence on the cystic phenotype and account,

for instance, for the variability of the intrafamilial phenotype in ADPKD (Grantham, Chapman et al. 2006).

Studies in mice suggest that ADPKD kidneys might be more susceptible to kidney injury. The rationale behind acute kidney injury and the ADPKD mechanistic inter-relationship is the following:

First, two late kidney conditionally inactivated *Pkd1* models, which result in slow and late onset of PKD, become much more rapid and severe when submitted to ischemic or nephrotoxic (1,2-dichlorovinyl-cysteine-DCVC) kidney injury (Happe, Leonhard et al. 2009, Takakura, Contrino et al. 2009).

Second, the *Pkd1*$^{+/-}$ heterozygous haploinsufficient mice that rarely develop kidney cysts late in adulthood, form dilatations of the tubules and show increased fibrosis and microcysts 6 weeks following IRI induction at 10-12wks old mice (Bastos, Piontek et al. 2009).

Third, Pc1 and Pc2 membrane levels (Segment S3, the most affected by ischemia-reperfusion-injury) are upregulated shortly after acute renal injury during kidney repair in rat and mouse (Prasad, McDaid et al. 2009, Zhao, Haylor et al. 2002, Obermuller, Cai et al. 2002, Verghese, Weidenfeld et al. 2008).

Finally, interstitial fibrosis and infiltrates (leukocytes such as neutrophils and macrophages) are more severe in *Pkd2*$^{+/-}$ heterozygous kidneys following ischemia than in control mice (Prasad, McDaid et al. 2009).

Pkd1 was thus suggested to protect renal epithelia from kidney injury, or to accelerate the repair, or both, whereby its inactivation would render the cell more susceptible for cyst formation. The study of kidney injury in mouse models overexpressing *Pkd1/2* genes should provide more evidence in this direction.

7.1.2.4) *Pkd1* overexpressors

All expression studies in humans reported sustained expression of *PKD1*/PC1 in the kidneys and liver and therefore the loss-of-function pathogenetic mechanism may not

necessarily apply as the sole mechanism, unless if all mutations were missense and potentially detected by the selected antibodies. LOF could likewise not explain the increased expression of the remaining wild-type allele, which could actually be one of the initiating factors (**Section 5.4**).

One group attempted to verify if increased expression of *PKD1* could be pathogenetic by overexpression of human *PKD1-PAC* in mice (Pritchard, Sloane-Stanley et al. 2000). Since their transgene also contained the full-length *TSC2* gene, which is associated with polycystic kidneys (**Table 8A, Section 3.2**), the causal relationship between the *PKD1* expression and ADPKD (kidney and liver) could not have been unequivocally established.

Our study definitively showed that increased expression of *Pkd1* using untagged *Pkd1* and BAC transgenesis leads to kidney cystogenesis but also reproduces human extrarenal anomalies (Thivierge, Kurbegovic et al. 2006) (Kurbegovic, Côté et al. 2010) (**Chapter IV**). Three transgenic lines with ~2 to 15X levels of endogenous *Pkd1* expression developed polycystic kidney disease with earlier and more severe occurrence correlating with higher expression levels. Overall, data on *Pkd1* hypomorph, *Pkd1* loss of function and *Pkd1* transgenic mice strongly favour the gene-dosage ADPKD pathogenetic mechanism.

7.1.2.5) *Pkd2* and *Pkhd1* targeting

Analogous to *Pkd1* (**Table 8A**), total germline, conditional targeting or overexpression of *Pkd2* gene resulted in very similar renal and extrarenal manifestations and progression (**Table 8B**). These observations in mice are also consistent with similarities in phenotype manifestations of ADPKD1 and ADPKD2 human pathology.

Targeting *Pkhd1* gene in mice using different experimental strategies and constructs resulted mainly in hepatic phenotype (**Table 8C**). Kidney phenotype was observed in some but not all mutants, occurred very late, in some cases affected proximal tubules and was significantly modified by genetic background and gender whereby males

appeared protected from kidney disease. Human ARPKD is a recessive, early, fast progressing disease in humans, thus mice for multiple possible reasons *i.e.,* alternative splicing, possible cleaved forms or potential gene redundancy, do not reproduce the fast progressing human distal/collecting segments of ARPKD. Hence, correlation between mouse and human ARPKD awaits further investigations to resolve those discrepancies.

7.2) Functional working systems other than *Mus musculus*

In addition to the mouse, there are some other model organisms that can be used as experimental tools for analysis and to better our understanding of PKD1 gene function. The most relevant are Tetrahymena chlamydomonas, zebrafish, C. elegans, drosophila and rat. They are summarized here below, with emphasis on unique characteristics of each working model.

Tetrahymena chlamydomonas

Tetrahymena chlamydomonas is a simple unicellular eukaryotic organism with flagella formation. Although it has very limited functional relevance for human polycystic kidney pathology, it is a very useful model for the study of cilia formation and maintenance. The lack of flagella in the *Tetrahymena chlamydomonas* IFT88 mutant (mouse orthologue of PKD Tg737/Polaris gene) suggested for the first time that the ciliary defects could be involved in kidney malfunction and human polycystic kidney disease (**Table 6, 7**) (Pazour, Dickert et al. 2000).

Zebrafish (*Danio rerio*)

This non-mammalian vertebrate model has been extensively studied as a model system of cystogenesis. The pronephric kidney is the functional kidney of zebrafish embryo and larvae and consists only of a glomerulus, pro-nephric tubules and paired pronephric ducts (Drummond, Majumdar et al. 1998, Drummond 2005).
Ventral axis curvature, edema and bilateral pronephric cysts are hallmarks of ciliary defects and pronephric development in zebrafish. Many genes affecting the primary

cilia (eg. *Nek8*, *Inversin*, *Pkd2*, *HNF1β*) when mutated in zebrafish lead to these aforementioned anomalies. Structural defects underlying curvatures are not known. Knockdown of the *Pkd1* genes in Zebrafish (*Pkd1a*/*b*), results in typical ciliary phenotypes such as kidney cysts, hydrocephalus, skeletal abnormalities and dorsal body axis curvature, the latest being the most reliable marker and highly penetrant characteristic of *Pkd1* knockdown (Mangos, Lam et al. 2010). *Pkd2* morpholino treated embryos also present hydrocephalus, kidney cysts and curly tail (Obara, Mangos et. 2006).

Worm (The nematode *Caenorhabditis elegans*)

C. elegans is a non-mammalian multicellular organism, the first to be genomically sequenced in 1998. It has a rapid life cycle (3dys) and simple cellular complexity of only 1,000 cells, and powerful genetic tools are available for its study (siRNA, transgenics) (Reviewed in Barr 2003). C. elegans contain a structure called a duct/channel that has an excretory function similar to the mammalian kidney. In both Zebrafish and C. elegans, the so-called ‘’kidney’’, is implicated in osmoregulation, balance of water and salt. Duct dilatations and cysts can occur but interestingly, the only ciliated cells in the C. elegans are neurons (White 1986) and this is where *LOV-1*/*Pkd1* (location of vulva) and *Pkd2*, are found to co-localize, and whose mutants give rise to similar phenotypes (Barr and Sternberg 1999). Together with the studies in *Tetrahymena chlamydomonas,* C. elegans provided one of the first pieces of evidence of a link between cilia dysfunction and the human ADPKD ciliopathy (Barr and Sternberg 1999). Of note, even though C. elegans contain many of the PKD, IFT, and BBS proteins, it does not contain some other human-disease ciliary related proteins such as fibrocystin, the product of the *PKHD1* gene involved in ARPKD.

Fruit fly (*Drosophila melanogaster)*

Drosophila is a non-mammalian organism studied, among other purposes, for the function of *Pkd2* gene given that an orthologue was identified in Drosophila males and named *amo* for almost there (Watnick, Jin et al. 2003). Sperm storage is an important step for maximal reproductive process in this experimental system. Some of

the non-used sperm can be stored (20%) and used in the absence of additional mating. The *amo/pkd2* mutant causes a dramatic reduction in progeny due to the sperm storage defects but motility, function, architecture of the testis or implantation / transfer are unaffected. The same group has recently shown that *amo*/*pkd2* is indeed responsible for beating of the sperm flagellum and backward movement of the sperm in the reproductive tract of Drosophila (tail first) (Kottgen, Hofherr et al. 2011), two functions abrogated in the amo mutant. Drosophila also has a kidney-like structure called a Malpighian tube, four tubules consisting of two sets of tubules with principal active and smaller intercalated cells (For development see Beyenbach, Skaer et al. 2010). A limitation of this model for studying the kidney function is that is aglomerular, with no circulatory system and presumably no primary cilia in cells other than sensory neurons and sperm, which are used mostly as a tool to assess the function of ciliary proteins, as described in C. elegans. However, Drosophila has a structure somewhat similar to a vertebrate glomeruli, a nephrocyte, of two types: pericardial and garland (Weavers, Prieto-Sanchez et al. 2009). Malpighian tubules function to constitutively form uric acid crystals *i.e.,* urate nephrolithiasis and therefore, in addition to abovementioned conditions, reproduce some kidney conditions and disease (Munn 1886).

Rat (*Ratus norvegicus*)

By CLUSTALW multiple sequence alignment, rat *Pkd1* gene has high homology with human (80%) and mouse (93%) nucleotide sequence and predicted 78% and 93% sequence analogy with human and mouse PC1/Pc1 protein (Xu, Shen et al. 2001). Rat *Pkd1* gene maps on the rat chromosome 10-10q12. Multiple similarities between rat and mouse/human *Pkd1* genes are reported: **1)** separation by 63bp at 3' end between *Pkd1* and *Tsc2* genes, **2)** alternatively spliced exon 12 with a couple isoforms in the brain and kidney (Lohning, Nowicka et al. 1997) and **3)** an additional splice isoform identified in exon 31 that might result in a shorter Pc1 variant (Xu, Shen et al. 2001).

Although rat models for PKD linked directly to inactivation of *Pkd1* and *Pkd2* genes have not been described yet, Han-SPRD (Nagao, Ushijima et al. 1999), wpk (Nauta, Goedbloed et al. 2000), chi/chi and Crj/CD (Ohno and Kondo 1989, Katsuyama, Masuyama et al. 2000) or rat overexpressor of truncated *Pkd2* develop polycystic kidneys and extrarenal defects (**Table 6**) (Guay-Woodford 2003 , Gallagher, Hoffmann et al. 2006).

8) Probationary therapeutic approaches and biomarkers in ADPKD

Currently, there is a lack of effective clinical therapies for ADPKD. An ideal therapy would consist of absent or minimal side effects, maximal long-term efficiency, and potentially simultaneous treatment of renal and extrarenal manifestations such as kidney and liver cysts. From the previous section on ADPKD cellular pathology, avenues that have been undertaken to halt this disease either in completed or undergoing clinical trials mainly target the cell proliferation, fluid secretion or regulation of cAMP levels (Detailed review by Chang and Ong 2012).

To evaluate the efficiency of the tested drug, TKV (total kidney volume suggested by CRISP study where kidney volume correlates with decline in renal function) by MRI and GFR (glomerular filtration rate) are currently used as endpoints, *i.e.,* early and late biomarkers of disease activity, respectively. Using these endpoints, human clinical trials in ADPKD were not very successful. Inhibitors of mTOR, that regulate cell proliferation and cyst growth, did not produce positive results, with no significant change in TKV or GFR when treatment lasted 6-24 months (Perico, Antiga et al. 2010, Serra, Poster et al. 2010, Walz, Budde et al. 2010). Moreover, trials with an inhibitor against V2 receptors under the TEMPO program (Tolvaptan Efficacy and Safety in Management of PKD and Outcomes) (Torres 2008) was recently stopped because of ‘’unacceptable surrogate endpoints’’ (TKV change) and concerns about ‘’drug-induced liver damage’’ (Brown 2013) (FDA Cardiovascular and Renal Drugs Advisory Committee Meeting. Silver Spring, Maryland. August 5, 2013). However, somatostatin that targets the cAMP pathway was successful in improving TKV in a 6-12 month treatment and will require further longer-term trials (van Keimpema, Nevens

et al. 2009, Hogan, Masyuk et al. 2010). There is also an ongoing long-term large clinical trial for ACE inhibitors under the HALT study (Chapman, Torres et al. 2010).

Currently in the pre-clinical stage for ADPKD therapy are drugs for cell proliferation/apoptosis (rosocovitine, HDAC inhibitors), secretion (small molecule CFTR inhibitors, KCa3.1 blockers), and calcium regulation (Triptolide/PC2 dependent, calcimimetics) (**Section 4.1.3.3 and 5.3.3.3.1**). All of these preclinical aspiring possibilities still have to be tested in ADPKD orthologous models.

Appropriate disease biomarkers, with higher sensitivity other than GFR and TKV, generation of authentic orthologous mouse models representative of slow progressive human ADPKD and unraveling potentially more relevant signaling pathways still await discovery; lack thereof may underlie the limited success in human ADPKD clinical trials to date.

CHAPTER II
AIMS OF THE PROJECT AND INSTRUCTIONS FOR FACILITATED LECTURE OF THIS THESIS

ADPKD is a very common but complex multiorgan pathology. Even though the causative genes were discovered many years ago and important advances were made, effective therapies are still lacking and sole invasive alternatives consist of dialysis or kidney transplantation. This reality is a result of our limited understanding of the *PKD1/PKD2* causative genes, uncertainty about the prevailing pathogenetic mechanism and insufficient characterization of polycystin's function *in vivo*. The role of PC1/PC2 was particularly studied *in vitro* in heterologous systems and mainly as truncating fusion proteins. These studies resulted in context-dependent and sometimes conflicting results. Interpretation of PC1 connection with downstream signalling and cellular processes is complicated due to the structural and most likely multifunctional property of the protein. ***Here are the goals of this thesis for better understanding of PKD1/PC1 function in normal conditions and ADPKD disease:***

AIM 1: ***Test if gain-of-function/increased expression of Pkd1 is pathogenetic in renal and extrarenal tissues (generate an ADPKD mouse model).*** Kidney cystic phenotype is reproduced in the *Pkd1/Pkd2* loss-of-function mouse models, which die before or at birth. However, murine *Pkd1* LOF does not reflect sustained or even increased *PKD1*/PC1 expression, adult onset and slow progression nor extrarenal hepatic phenotype observed in human ADPKD. To consolidate both human and mouse findings for the ADPKD pathogenetic mechanism, it is reasoned that imbalance of any of the polycystins, is sufficient to lead to ADPKD via a gene dosage mechanism. We therefore tested if *PKD1* overexpression (GOF) can also be a pathogenic renal and extrarenal mechanism. For this, we generated and characterized a *Pkd1* transgenic mouse model, named $Pkd1_{TAG}$. In addition to our previous kidney-specific transgene ($SBPkd1_{TAG}$) associated with PKD, *Pkd1* renal but also extrarenal expression in this case was conferred by ~25kb of endogenous *Pkd1* promoter from a *Pkd1*-BAC. Extrarenal (over)expression of *Pkd1* could be associated

with extrarenal phenotypes observed in human such as the liver cyst, the second most frequent manifestation of ADPKD, and would strongly suggest a gene dosage mechanism in organs other than kidney (**Chapter IV**). Physiopathological characterisation of the transgenic mice and the cellular processes would lead to generation of an *in vivo* model to study the human disease and possibly allow better translation in human (**Chapter IV, Chapter VIII, Appendix**). Detailed characterization of previously reported kidney specific and, here within generated, systemic *Pkd1* dosage increase mouse models on $Pkd1^{Null}$ genetic background would supply further decisive evidence for functional gene dosage pathogenetic mechanism. Providing insight into the consequences of the effects of modulation of *PKD1/PC1* is of essence for human gene therapy (**Chapter VIII**).

AIM 2: ***Gain insights into the PC1 function following GPS cleavage in the kidney and liver.*** GPS cleavage is a typical characteristic of aGPCRs that results in generation of N- and C- terminal fragments (NTF and CTF, respectively). The mechanism underlining the GPS cleavage and biogenesis of this group of proteins is still puzzling. PC1 contains a GPS motif and was shown to undergo an incomplete cleavage. Similar to many aGPCRs, *in vivo* biogenesis and the functional role of the cleavage or its derived products remains to to be established. Pc1 GPS cleavage was shown to be critical for adult kidney homeostasis by data from $Pkd1^{V}$ mouse mutant. $Pkd1^{V}$ mice, which produce the uncleaved full-length Pc1, survive embryonic lethality but develop kidney cystogenesis and die at ~1 month. However, the mechanism by which the uncleaved Pc1 protein or lack of the cleaved forms leads to cystogenesis in adult kidneys is unknown. Since these mice die prematurely, the contribution of the GPS cleavage and different Pc1 forms to the liver phenotype cannot be assessed either. Here, in a collaborative study, we studied and characterized in more detail the biogenesis of endogenous Pc1 by biochemical means. Using various murine tissues at different ages and different biochemical approaches, we aimed to identify different Pc1 GPS cleavage products and study their localization and trafficking *in vivo* (**Chapter VI**). Knowing more about PC1 localisation and biogenesis, as well as interdependence of different PC1 forms following GPS cleavage may also help

envision therapeutic approaches to target specific PC1 forms. Genetic complementation of uncleaved *Pkd1*^{V} mutant by various *Pkd1* transgenes would also allow for the study of the dynamics and reciprocal functional contribution of each form in the kidney and liver (**Chapter VI, VIII**, **Appendix**).

AIM 3: ***Investigate the role of NTF-like PC1 GPS cleavage product in vivo****.* The N-terminal motif accounts for ~2/3 of the PC1 protein, was suggested to interact with components of the extracellular matrix, and is cleaved/processed *in vivo*. However, its contribution to the overall function of PC1 remains elusive. To begin understanding how the PC1 NTF fragment behaves with potential relevance for human mutations, we generated a transgenic mouse of N-terminal extracellular ectodomain of Pc1, named *Pkd1*$_{extra}$. *Pkd1*$_{extra}$ transgene was deleted of intracellular and transmembrane domains by homologous recombination and designed to mimic several truncating human mutations (**Chapter V**). Analysing the ability to traffic and properly localize (or lack thereof) under various *Pkd1* genetic backgrounds will provide insight into how this construct may lead to a phenotype in transgenic mice and in human ADPKD. Backcrossing *Pkd1*$_{extra}$ on *Pkd1*$^{+/-}$ or *Pkd1*$^{-/-}$ (dosage reduce) allows us to assess the nature of the mutation (dominant negative *vs* gain of function). The functional mechanism and potential interaction of Pc1$_{extra}$ with endogenous Pc2 or Pc1 are assessed for a possible interacting or modulating effect by this human mutant. Attempt of genetic complementation *in vivo* of uncleaved *Pkd1*^{V} and *Pkd1*^{Null} by *Pkd1*$_{extra}$ would test the autonomous caracteristics of Pc1$_{extra}$ NTF-like human mutant protein (**Chapters V**, **VI, Appendix**).

AIM 4: ***Study the effect of kidney injury in slow progressive adult Pkd1 transgenic mouse models***. Presence of kidney injury seems sufficient to amplify the adult phenotype of *Pkd1* conditional loss-of-function likely by reactivating developmental programs of the kidney repair process. Here we aimed to analyze the repercussions of kidney injury in *Pkd1* transgenic mice reproducing the progression of human ADPKD. To test this, we induced unilateral acute kidney ischemia in *Pkd1*$_{TAG}$ *and Pkd1*$_{extra}$ mice (**Chapter VII**). We analyzed the consequences of ischemia on

several signaling pathways to try to dissect molecular interactions triggered in non-transgenic and *PKD1* transgenic mice.

AIM 5: ***Assess downstream modulators and signaling pathways using PKD1 orthologous mouse models of GOF and LOF for more efficient drug targeting.*** To begin establishing a link between PC1 and downstream signaling and cellular processes *in vivo*, we used our two GOF models, and two LOF mice obtained from other labs. Studying signaling pathways in several models may allow a better and broader translation for the human PKD pathology. Through protein expression analysis, we introduce potential effectors and/or modulators and hence possible therapeutic targets for PKD (**Chapters IV, V, VIII, Appendix).** Numerous examples are provided in **Chapter I** and point to Wnt pathway as a very promising target. We therefore studied the expression of some of the main components of the canonical Wnt/β-catenin pathway by Western blot. We also began assessing the contribution of non-canonical Wnt/PCP branch. Additional studies are however required and will consist of targeting these pathways in ADPKD mouse models to confirm their implication as a direct or downstream functional partner. Moreover, given that PC1/Pc1 and PC2/Pc2 mutations lead to a similar phenotype in humans and mice, we investigated the relationship between PC1 and PC2 in wild-type and *Pkd1* transgenic mice via a biochemical approach. Analysing how PC1 and PC2 interact *in vivo*, under which conditions, and how they modulate each other's expression and stability in normal and ADPKD-like conditions will bring more insight into the involvement of the PC1/PC2 complex for proper tubular morphology. Finally, structural analysis of PC1/Pc1 and comparison with other proteins containing a GPS motif may open up new avenues for PC1 targeting in ADPKD.

CHAPTER III

Papers published, submitted or in preparation with specific contributions of the author of this thesis

Article 1: *Pkd1 transgenic mice: adult model of polycystic kidney disease with renal and extrarenal phenotypes,* **published Human Molecular Genetics 2010.** Almira Kurbegovic, Olivier Côté, Martin Couillard, Christopher J Ward, Peter C Harris, Marie Trudel.

Article 1: Contribution of AK to generation and characterization of transgenic mice, extensive expression analysis via molecular and biochemical approaches, preparation of figures and tables.

Article 2: *Progressive development of polycystic kidney disease in the mouse model expressing Pkd1 extracellular domain,* **published Human Molecular Genetics 2013.** Almira Kurbegovic and Marie Trudel.

Article 2: Contribution of AK to generation and characterization of transgenic mice, extensive expression analysis via molecular and biochemical approaches, preparation of figures and tables.

Article 3: *Novel Functional Complexity of Polycystin-1 by GPS Cleavage In Vivo: Role in Polycystic Kidney Disease,* **published in Molecular and Cellular Biology 2014.** Almira Kurbegovic, Hyunho Kim, Hangxue Xu, Shengqiang Yu, Julie Cruanès, Robin L. Maser, Alessandra Boletta, Marie Trudel and Feng Qian.

Article 3: Contribution of AK to biochemical experiments, mouse genetic complementation, preparation of figures and tables, interpretation of results and writing of the manuscript.

Article 4: *Effect of acute kidney injury in transgenic Pkd1 mice: from initiation to ESRD,* **manuscript in preparation for Am J Physiol Renal Physiol.** Almira Kurbegovic and Marie Trudel.

Article 4: Contribution of AK to induction of unilateral ischemia in the kidney (IRI), characterization of the phenotype, biochemical analysis, preparation of figures and tables, interpretation of results and writing of the manuscript.

Article 5: *Transgenic mice uncover the crucial role of the GPS cleavage in liver homeostasis,* **manuscript in preparation for JASN.** Almira Kurbegovic, and Marie Trudel.

Article 5: Contribution of AK to study design, characterization of the phenotype, expression analysis, biochemistry, preparation of figures and tables, interpretation of results and writing of the manuscript.

CHAPTER IV – ARTICLE 1

PKD1 TRANSGENIC MICE: ADULT MODEL OF POLYCYSTIC KIDNEY DISEASE WITH EXTRARENAL AND RENAL PHENOTYPES

Almira Kurbegovic†[1], Olivier Côté†[1], Martin Couillard[1], Christopher J. Ward[2], Peter C. Harris[2], Marie Trudel*[1]

† both authors contributed equally

[1]Institut de Recherches Cliniques de Montreal, Molecular Genetics and Development, Faculte de Medecine, Universite de Montreal, Montreal, Quebec, Canada [2] Mayo Clinic, Rochester, MN, USA

*Correspondence:

Dr. Marie Trudel

[redacted]

This article was accepted for publication in Human Molecular Genetics following peer review. The definitive publisher-authenticated version [Hum. Mol. Genet. (2010) 19 (7): 1174-1189] is available online [doi:10.1093/hmg/ddp588].

ABSTRACT

While high levels of Pkd1 expression are detected in tissues of patients with autosomal dominant polycystic kidney disease (ADPKD), it is unclear whether enhanced expression could be a pathogenetic mechanism for this systemic disorder. Three transgenic mouse lines were generated from a Pkd1-BAC modified by introducing a silent tag via homologous recombination to target a sustained wild type genomic Pkd1 expression within the native tissue and temporal regulation. These mice specifically overexpressed the Pkd1 transgene in extrarenal and renal tissues from ~2- to 15-fold over Pkd1 endogenous levels in a copy-dependent manner. All transgenic mice reproducibly developed tubular and glomerular cysts leading to renal insufficiency. Interestingly, $Pkd1_{TAG}$ mice also exhibited renal fibrosis and calcium deposits in papilla reminiscent of nephrolithiasis as frequently observed in ADPKD. Similar to human ADPKD, these mice consistently displayed hepatic fibrosis and ~15% intrahepatic cysts of the bile ducts affecting females preferentially. Moreover, a significant proportion of mice developed cardiac anomalies with severe left ventricular hypertrophy, marked aortic arch distention and/or valvular stenosis and calcification that had profound functional impact. Of significance, $Pkd1_{TAG}$ mice displayed occasional cerebral lesions with evidence of ruptured and unruptured cerebral aneurysms. This $Pkd1_{TAG}$ mouse model demonstrates that overexpression of wildtype Pkd1 can trigger the typical adult renal and extrarenal phenotypes resembling human ADPKD.

INTRODUCTION

Human autosomal dominant polycystic kidney disease (ADPKD) is one of the most prevalent monogenic diseases with an incidence of 1:400 to 1:1000 individuals. It is a multisystemic disorder characterized by numerous bilateral renal epithelial cysts affecting all segments of the nephron. Eventually, progression of these multiple cysts in kidneys leads to renal insufficiency and end-stage renal disease by late mid-age. Extrarenal clinical manifestations are also common with hepatic cysts being the most frequent, and predominately so, in women. Non-cystic features include cardiac and valvular anomalies and, less frequently, intracranial aneurysms (1).

The majority of patients (85-90%) with ADPKD have a mutation in the PKD1 gene. The gene spans 54kb and encodes a very large protein of 4302 amino acids, polycystin-1. Polycystin-1 is a transmembrane protein that has a large N-terminal extracellular domain with a unique combination of motifs and was reported to undergo partial autocleavage at the G-protein coupled receptor proteolytic site (GPS) (2). Polycystin-1 has been implicated in signal transduction, in mechanosensation, and in cell-cell/cell-matrix interactions. Human PKD1 and polycystin-1 expression have been analyzed in normal and ADPKD tissues. PKD1 and polycystin-1 are normally expressed in a wide range of adult tissues including epithelial and non-epithelial cell types (3-8). Interestingly, PKD1 expression is developmentally regulated, particularly in the kidneys. Polycystin-1 has highest levels in fetal life and is readily detected in glomerular and tubular epithelial cells (reviewed in (9) and reference therein). In normal adult kidneys, the RNA transcript and protein levels of polycystin-1 are decreased to lower levels, most notably in the collecting and distal tubules. By contrast, PKD1 expression levels were increased (~2-fold) in ADPKD kidneys (3, 10) and consistently, the majority of renal epithelial cysts displayed persistent or enhanced levels of polycystin-1 (4).

Although ADPKD is a dominant disease, the stochastic nature of the renal cysts in ADPKD suggests that the mutational mechanism for PKD1 could result from a two-hit phenomenon or a loss of heterozygosity. This mechanism is supported by detection of PKD1 clonal somatic mutations in cells from a significant proportion of cysts (11-13). Moreover, loss of heterozygosity could account for the widely varying phenotype commonly observed in individual families. This mechanism would however be at variance with the persistent or enhanced expression of PKD1 seen in the majority of human renal cysts, unless a mechanism of gain-of-function/overexpression may also be operant.

The mouse Pkd1 gene has very close similarities to the human PKD1 and may provide important insights into PKD1 function(s). During normal development, murine Pkd1 is expressed at high levels from the morula stage and detected in all neural crest cell derivatives including adult brain, aortic arch, cartilage, and mesenchymal condensation (14, 15). Homozygous mutant mice targeted for Pkd1 deletion have been reported to develop renal and pancreatic cysts (16-21). These attempts to generate mouse models, unfortunately, did not produce viable animals. Nevertheless, the occurrence of renal cysts in these homozygous Pkd1 mutant mice would be consistent with the hypothesis of a two-hit mutational mechanism in humans that involves a germline mutation and somatic inactivation of the normal allele. This mechanism is also supported by conditional ablation of Pkd1 in mice few days after birth (22) but not upon later ablation since cysts developed only focally (23, 24). However, evidence of a mechanism of haploinsufficiency or gene dosage reduction for cystogenesis was provided in mice homozygous for a Pkd1 hypomorphic allele or heterozygous for a Pkd1 deleted allele (25, 26). Moreover, Pkd1 gain of function may also be an additional mechanism for ADPKD pathogenesis as determined by the renal-targeted Pkd1 in SBPkd1$_{TAG}$ mice with renal cystogenesis (27). These findings would support a gene dosage dependent mechanism for ADPKD where mutations of loss of heterozygosity,

haploinsufficiency, or overexpression could trigger a renal phenotype and thereby provide an explanation for the high penetrance found for a range of different mutations in this disease.

To interrogate increased Pkd1 dosage as an ADPKD pathogenetic mechanism, Pkd1 in the native genomic context purified from a murine BAC was targeted in transgenic mice. We generated three transgenic lines that expressed systemically increase Pkd1 at proportional gene dosage levels in different tissues. These mice not only develop polycystic kidneys and renal failure but also all the prevalent extrarenal manifestations observed in ADPKD patients including liver cysts, cardiac and valvular anomalies as well as the dreadful complication of ruptured intracranial aneurysms. Our study reproduces the first orthologous ADPKD mouse model with the entire spectrum of adult extrarenal and renal phenotypes.

RESULTS

Production of Pkd1$_{TAG}$-BAC by homologous recombination

To investigate the role of Pkd1 overexpression/gain-of-function in renal and extrarenal tissues, we have used a genomic clone containing the entire Pkd1 gene in a BAC vector 129/Sv library that we previously isolated (27). This BAC contains a ~121kb insert with ~37kb of upstream and ~39kb of downstream sequences of the Pkd1 gene including the entire adjacent Tsc2 gene. This Pkd1-BAC was modified by two successive homologous recombination events. First, the Pkd1 gene was tagged in exon 10 by substituting a nucleotide (G to A) to create a novel EcoRI site at position 2355 on the cDNA map. This silent point mutation was produced to readily distinguish the Pkd1 gene and transcript of the BAC from that of endogenous origin. Second, we have deleted the Tsc2 gene (~34.5kb) of the Pkd1-BAC to prevent introducing the Tsc2 gene exogenously and to reduce the BAC size (Figure S1). This new Pkd1$_{TAG}$-BAC was digested with MluI, a unique site located at ~24.8kb upstream of the Pkd1 translation

initiation site, and NotI site in the BAC polylinker sequences to remove the prokaryotic BAC vector sequences (Supplemental Figure 1, Figure 1). This ~75kb MluI-NotI fragment was isolated, purified and quantified for oocytes microinjection (28).

Production and analysis of Pkd1$_{TAG}$ transgenic mice

Three transgenic founders carrying several copies (2 to 15) of the Pkd1$_{TAG}$ transgene as determined by Southern analysis, served to derive three transgenic lines. Characterization of the transgene chromosomal integrity in these lines was performed with 5', internal, and 3' probes (a to g) used for BAC analysis in Supplemental Figure 1. Transgene 5' flanking sequence was monitored for presence of a specific polymorphism from the 129/Sv genetic background by a band at 100bp compared to the 113bp and/or 133bp typical of the inbred C57Bl/6J and CBA/J strains used to produce these transgenic mice (Figure 1). To verify the transgene 3' end, a probe consisting of the Pkd1 gene exon 45-46 was used to detect the endogenous 7.0kb Pkd1 band as well as the transgene 5.0kb (Figure 1). The Pkd1$_{TAG}$ mice contained complete copies of the Pkd1 transgene based also on the internal genomic overlapping structure analysis.

Pkd1 expression in adult Pkd1$_{TAG}$ transgenic mice

Analysis of Pkd1$_{TAG}$ transgene and Pkd1 endogenous gene expression was carried out in several tissues. To first quantify the transcript levels from the transgene comparatively to the endogenous gene, Northern blots were performed on kidneys (n=4) of each transgenic line (Figure 2A). The transgene transcript size was identical to the endogenous transcript of 14.2kb. All Pkd1$_{TAG}$ transgenic mice showed systematically increased transcript Pkd1 levels in kidneys relative to controls. In fact, Pkd1$_{TAG}$ transgene renal expression increased with the number of Pkd1$_{TAG}$ copies (2, 6, 15) in each line compared to controls (n=2): line 6 (n=4), 18 (n=3), 26 (n=3) displayed ~1.9±0.8, 6.0±0.9 and 17.9±1.9 fold increase respectively.

Quantification of transgene expression levels was carried out by real-time PCR in the three transgenic lines at adult age, by using primers in the exon 1 and 2 of Pkd1 (Figure 2B). The $Pkd1_{TAG}$ expression in transgenic mice was compared to S16 ribosomal protein gene product as internal standard. Analysis of Pkd1 renal expression showed similar fold increase for transgenic kidneys as those obtained by Northern blot. Since endogenous Pkd1 expression levels are modulated in various tissues, we quantified $Pkd1_{TAG}$ expression levels to determine whether the transgene followed the endogenous gene expression pattern. Transgene expression by real-time PCR consistently and specifically showed highest expression in the brain of all transgenic lines relative to other organs (Figure 2B). The heart, lung, and brain displayed higher Pkd1 levels than in the kidneys whereas the other organs including spleen, liver, and pancreas levels were lower. Interestingly, the three transgenic lines demonstrated, within all tissues analyzed, a comparable increase in transgene to endogenous expression, indicating that the $Pkd1_{TAG}$ transgene contained all the appropriate regulatory elements for tissue expression.

To monitor whether gene expression correlated with the levels of Pkd1 protein or polycystin-1 (Pc-1), Western blot was performed on various tissues of the $Pkd1_{TAG}26$ line using the 7e12 Pc-1 monoclonal antibody and Gapdh as control. The $Pkd1_{TAG}26$ showed several fold increase of Pc-1 for all extrarenal and renal tissues relative to non-transgenic control mice (Figure 2C). Subsequently, phenotype caused by transgene expression was characterized in the $Pkd1_{TAG}$ mice by gross and histology analysis of tissues frequently affected in human ADPKD.

Renal anomalies in $Pkd1_{TAG}$ mice

$Pkd1_{TAG}$ transgenic adult kidneys of all three lines were generally pale and exhibited bilateral cysts studding the cortical surface. Histologically, transgenic mice developed multiple microscopic and macroscopic cysts affecting cortex and medulla as well as glomerular cysts (Figure 3A-F). Anomalies were detected at 1 month of age for $Pkd1_{TAG}$ 6 and 26 mice as mild tubular dilatation and scattered

tubular microcysts with epithelial hyperplasia respectively, suggesting abnormal features early on as observed in ADPKD patients. The renal phenotype in $Pkd1_{TAG}$ 26 developed much more rapidly than in the $Pkd1_{TAG}$ 6 mice. Consistently, $Pkd1_{TAG}$ 26 kidneys at 2-months had tubular and glomerular cysts that became very severe by 3-months of age whereas $Pkd1_{TAG}$ 6 displayed glomerular and tubular dilatation at 7 months of age that progressed to cysts at 9 months and were severely cystic by 12-16 months of age. Cystic and even non-cystic tubules frequently displayed epithelial hyperplasia and hypertrophy and occasional presence of polyps with variable severity between mice. Hemorrhagic cysts consistent with some hematuria, proteinaceous casts in tubular cysts as well as interstitial fibrosis were commonly observed (Figure 3B). To evaluate levels of fibrosis, we quantified the density of Sirius red staining in $Pkd1_{TAG}$6 (n=6, 7-16months) at 5.7% and 26 kidneys (n=6, 2-8months) at 9.6% that was markedly elevated by ~4.8- and 8-fold respectively compared to controls (n=5; 1.2%). Further, partial and total sclerosis of glomeruli was detected in all three transgenic lines. To define more precisely the origin of the renal cysts, we used specific nephron segment markers of the proximal, distal, and collecting tubules. As shown in Figure 3C and D, cysts originated from all segments of the nephron with highest and similar proportion in proximal and collecting tubules (~30-35%). A significant proportion of cysts (~20%) were unstained, some of which with presence of mesangial tuft could be identified of glomerular origin whereas others could be from undifferentiated tubular epithelial cells. Analysis of $Pkd1_{TAG}$26 mice (7/18) with highly invasive renal cysts also displayed calcium deposits that were mainly localized to the papilla, reminiscent of the renal calculi described frequently in ADPKD (29-31) (Figure 3E versus F). Since we observed the presence of renal epithelial hyperplasia and polyps, we monitored cell proliferation with the nuclear antigen Ki67 marker by immunostaining in $Pkd1_{TAG}$ 6 and 26 lines (Figure 3G, H). Proliferation was calculated as a percentage of tubules with 0, 1 or ≥2 Ki67-positive cells in the kidneys. In control animals, >92% of tubules (n=941) had no Ki67-positive cells and 5.4% or 2.1% of tubules displayed 1 or ≥2 positive cells respectively. By contrast, the $Pkd1_{TAG}$ 26 line displayed 22.6%

and 27.5% of cystic tubules with 1 and ≥2 Ki67 positive cells, a significant increase of 4 to 10-fold relative to controls ($p<0.01$). Similar levels of proliferation were also observed for the $Pkd1_{TAG}$ 6 line (16% and 26% of 1 and ≥2 Ki67 positive cells). To determine whether c-myc is implicated in the $Pkd1_{TAG}$ renal phenotype, c-myc expression was analyzed by real-time PCR and immunohistochemistry. Expression of c-myc was increased by ~4.8-fold in the $Pkd1_{TAG}$ 26 mice (n=4) relative to controls (n=4) (≤0.02). Consistently, renal sections of $Pkd1_{TAG}$ 6 and 26 mouse lines also revealed diffusely elevated levels of c-myc relative to controls and frequently more pronounced nuclear staining in cystic epithelium (Figure 3I, J), suggesting that c-myc could be an indirect effector of $Pkd1_{TAG}$.

Since cilia anomalies have been associated with cyst formation, cilia of renal epithelial cells were monitored by α-acetylated tubulin staining in $Pkd1_{TAG}$ 26 line and control mice at few weeks of age prior to overt cystogenesis (Figure 3K, L). Most strikingly, the cilia size distribution (at 1 μm interval) in all $Pkd1_{TAG}$ mice showed significantly longer cilia length relative to controls (Figure 3L). Indeed, most cilia of the $Pkd1_{TAG}$ mice (n=346) (Figure 3L) were >5 μm whereas cilia in controls (n=266) (Figure 3K) were mainly 2-3 μm in length. Cilia from $Pkd1_{TAG}$ renal epithelium were often of kinky structure and occasionally displayed 2 or multicilia by EM. These mice consistently developed PKD features pointing to the induced expression from the transgene as specifically responsible for the pathogenesis.

Altered renal physiology in $Pkd1_{TAG}$ mice

Renal function was monitored in the low and high expressor $Pkd1_{TAG}$ 6 and 26 transgenic lines. Animals were monitored for urinary levels of urea nitrogen, creatinine, protein, and urine osmolality and volume (Table 1). In comparison to negative controls of same genetic background, the low and high expressors exhibited significant increase in urine volume similar to the positive PKD controls SBM mice (28).

These urinary and blood analysis are consistent with mild concentrating defects but cannot exclude AVP deficiency. Accordingly, urinary urea nitrogen, creatinine, and protein were significantly decreased. In addition, $Pkd1_{TAG}$ mice had urinary calcium (0.8±0.2; n=8, 9-14 months) and urinary pH (6.0±0.1, n=16, 7-18 months) comparable to controls (0.9±0.2; n=4, 11 months) (5.9±0.1, n=4, 11 months). Mice from all three $Pkd1_{TAG}$ lines were also monitored for hematocrit levels since patients with progressive renal insufficiency commonly develop anemia. Consistently, the three $Pkd1_{TAG}$ mouse lines at 5 to 7 months of age displayed significantly reduced hematocrit levels (Table 1 and data not shown). Mice from the three transgenic $Pkd1_{TAG}$ lines were also analyzed qualitatively for proteinuria from urine samples on SDS-PAGE (Figure 4 A). Despite the reduced concentration level of protein in urine, $Pkd1_{TAG}$ animals at 4 months of age appeared to display non-selective proteinuria that was most pronounced in the high transgene expressor. To determine whether Pc-1 in $Pkd1_{TAG}26$ transgenic mice were present in urine, we prepared total crude protein from urine (T), urine devoided of exosome or uromodulin aggregates (supernatant 1, S1), the resuspended pellet was separated in two additional fractions the surpernatant containing uromodulin (supernatant 2, S2) and urinary exosome following the protocol of (32, 33). Western analysis of total crude urinary protein with the LRR Pc-1 antibody (7e12) showed a similar pattern to that of total kidney extracts from native untreated (N) and deglycosylated (DG) samples (Figure 4B). While samples in the native form displayed two protein bands estimated by migration at ~360-380kDa and slightly above ~420kDa, in the deglycosylated form a unique product was detected corresponding to the lower band. Pc-1 was detected in three urine fractions (T, S1, and exosomes) whereas it appears absent in the supernatant (S2) for both control and transgenic mice. In exosomal pellet fraction, Pc-1 was present mainly in the glycosylated form, as observed in human ADPKD urinary exosomes (33). Interestingly, significant proportion of Pc-1 was also found in the S1 supernatant in both $Pkd1_{TAG}$ transgenic mice and controls in both glycosylated and unglycosylated forms, suggesting that the N-terminal domain of Pc-1 is likely excreted in the urine. Importantly, similar fold enrichment in Pc-

1 was observed in $Pkd1_{TAG}26$ transgenic mice relative to controls in all three Pc-1 containing fractions, indicating that the Pc-1 from the transgene follow a normal physiological process.

Hepatic anomalies in $Pkd1_{TAG}$ mice similar to PKD

Since human ADPKD frequently developed biliary dysgenesis, we investigated whether enhanced $Pkd1_{TAG}$ gene expression could induce hepatic abnormalities in mice. Readily from macroscopic liver examination, hepatic cysts could be detected in both transgenic 6 and 26 lines (low and high Pkd1 expressors): 5 of 34 $Pkd1_{TAG}$ transgenic mice from line 26 and in 1 of 32 from line 6 (Figure 5A, B). Histologically, these liver developed cysts likely of cholangiocyte origin that ranged from mild to very severe (Figure 5C, D). Interestingly, these characteristic cystic features affected mainly female mice (4 out of 5) as in human ADPKD. Further, hepatic parenchyma from both transgenic 6 and 26 lines showed presence of a broad band of fibrosis along the intrahepatic ducts that was systematically observed and in some mice, fibrosis was widespread (Figure 5E, F). Quantification of fibrosis over the liver sections showed ~4- to 5-fold increased respectively for the $Pkd1_{TAG}$ 6 (9.8±9.3%; n=10; $p \leq 0.02$) and 26 lines (11.1±7.9%; n=12; $p < 0.002$) compared to controls (1.9±0.8%; n=10). Similar to $Pkd1_{TAG}$ 6 and 26 renal analysis, we evaluated whether proliferation could be implicated in the hepatic cysts, liver sections were stained with Ki67. The epithelial linings of cysts were uniformly delineated by enhanced Ki67 staining and/or by strong nuclear staining (Figure 5G, H). These $Pkd1_{TAG}$ livers also displayed elevated c-myc expression in the cystic areas with more intense signal in cell lining the cysts (Figure 5I, J). Interestingly, this increased proliferation and myc expression paralleled the marked fibrosis in regions of liver cysts. Since the $Pkd1_{TAG}$ 6 and 26 transgenic mice develop typical hepatic ADPKD characteristics, it is likely that Pkd1 overexpression in the liver may be a pathogenetic mechanism through potentially modulating c-myc.

Cardiac anomalies in Pkd1$_{TAG}$ mice

Because a proportion of ADPKD patients develop cardiac anomalies, we performed physiologic studies using non-invasive ultrasound imaging in Pkd1$_{TAG}$ 6 and 26 relative to control mice (Figure 6A, B; Table 2). The M-mode dimensions showed significantly increased left ventricular posterior wall thickness at diastole and at systole indicating left ventricular hypertrophy (Table 2A). The interventricular septa thickness was also increased. Further, the aortic root diameter and area were significantly increased in the Pkd1$_{TAG}$ mice showing important dilatation as described in ADPKD patients. At necropsies, gross heart anatomy of mice from the three Pkd1$_{TAG}$ lines showed significant and extensive enlargement relative to that of negative control littermates (Figure 6C, D; Table 2A), providing evidence of eccentric dilated cardiac hypertrophy. Hearts of Pkd1$_{TAG}$ relative to controls also showed important alteration in the cardiac structure and morphology as analyzed by Microfil casting that fills the body entire vasculature providing a three-dimensional visualization of organ circulation (Figure 6E, F). Substantial abnormalities of the ventricular vasculature were readily detectable under different angles, suggesting injury to the myocardium with possible development of fibrosis (Figure 6F vs E). We then verified by histology and detected that 35-40% of Pkd1$_{TAG}$ mice (lines 18 and 26) displayed to 2-to 4-fold increase in cardiac fibrosis.

Functional analysis by echographic measurements consistently showed a marked increased in stroke volume as well as in the cardiac output by almost 2-fold in Pkd1$_{TAG}$26 mouse lines (Table 2B). While the heart rates of Pkd1$_{TAG}$ and control mice were similar, cardiac valves displayed some anomalies in the Pkd1$_{TAG}$ mice (Table 2B) (Figure 6A, B). As shown in Table 2, the significant increase in mean and peak velocity downstream of the aortic valve suggested stenosis. This increased velocity measurement was consistent with the abnormal aortic valve leaflets detected by ultrasound imaging as opaque in some Pkd1$_{TAG}$ 6 and 26 mice rather than delicate and translucent (Figure 6B). Upon heart sectioning, large

areas within the ventricular lining exhibited change in pigmentation, indicative of ventricular lining calcification (Figure 6G, H). To determine whether the valves opacity and ventricular lining anomalies resulted from calcium deposits, cardiac histologic sections were stained individually with Alizarin and VonKossa. Analysis revealed presence of calcification in 6 of the 15 aortic valves, 4 of which also had staining in ventricular lining (Figure 6I, J). Furthermore, 3 of these 6 $Pkd1_{TAG}$ mice exhibited staining in the myocardium as well. Since observations of valvular, vascular, and myocardium calcification in individuals with chronic kidney disease has been associated with higher serum phosphate (34), we determined the levels of phosphate in serum of $Pkd1_{TAG}$ mice. Analogously to human, the $Pkd1_{TAG}$ mice (1.9±0.3 mmol/L; n=8) had significantly increased serum phosphate relative to controls (1.4±0.2 mmol/L; n=4), supporting the hypothesis that elevation in serum phosphate concentration may contribute to calcification risk and cardiovascular events.

Vascular anomalies in $Pkd1_{TAG}$ mice

To investigate whether adult $Pkd1_{TAG}$ mouse lines exhibited altered cardiovascular response, we measured blood pressure in two $Pkd1_{TAG}$ lines (26 and 18) and control mice using the tail cuff method. Two groups of $Pkd1_{TAG}$ mice were readily distinguishable in both lines. In $Pkd1_{TAG}$26 line (6-7 months of age), the first group of mice (n=5) exhibited systolic blood pressure at 113.5±11.0 mmHg comparable to control mice (n=4) of systolic blood pressure at 116.2± 3.1 mmHg. The second group of $Pkd1_{TAG}$ 26 mice (n=3) had significantly increased blood pressure at 161.1±5.1 mmHg ($p<0.001$). Similarly, evidence of hypertension in two of six $Pkd1_{TAG}$18 mice (132.3±1.3 mmHg; $p<0.0009$) indicated that the $Pkd1_{TAG}$ mouse lines can progress to severe hypertension as in human ADPKD.

Upon signs of distress in three mice of $Pkd1_{TAG}$ 26 line, we macroscopically observed severe hemorrhage and severe intracranial edema. These mice at dissection did not show closure of the cranial

bone at the sutura sagitalis and have evidence of hydrocephalus with ventricle dilatation (Figure 7A and B). No control mice exhibited this phenotype. In the $Pkd1_{TAG}$ 26 mice, subarachnoid hemorrhages were observed in different areas of the brain and were so severe in some cases that a significant portion of the brain was completely destroyed/obliterated. Further, the cerebellum of these $Pkd1_{TAG}$ 26 mice at histologic examination was underdeveloped, reduced in size or constricted, providing signs of prior compression of this region and adjacent structures (Figure 7D). To visualize and analyze the vasculature, we introduced Microfil casting to model the entire vasculature of $Pkd1_{TAG}$ 26 (n=5) and control (n=7) mice. As illustrated in Figure 7E-F, two $Pkd1_{TAG}$26 mice compared to none in controls showed unruptured cerebral aneurysm, the most dreadful complication of ADPKD.

Lifespan in $Pkd1_{TAG}$ mice

Lifespan of mice from the three transgenic $Pkd1_{TAG}$ lines was also quantified. Animals died at 5.5 ± 2.8 months (n=18) for the high expressing $Pkd1_{TAG}$ 26 line presumably due at least in part to renal failure, at older age of 16.7±5.5 months (n=9) and 16.6±1.8 months (n=12) for the lower expressors $Pkd1_{TAG}$ 18 and 6 lines respectively.

DISCUSSION

This study reports generation and characterization of the first Pkd1 mouse model of ADPKD that develops the typical renal and extrarenal pathologic spectrum. This model was produced by expressing a "wild type" full length Pkd1 gene and proximal regions purified from a BAC that produces a functional polycystin-1 (Pc-1) protein. Since this mouse model reproduces both the entire phenotypic spectrum and at the similar frequency occurrence as in ADPKD, a systemic Pkd1 enhanced expression is most likely a pathogenetic mechanism.

The three transgenic $Pkd1_{TAG}$ mouse lines generated showed a copy-number dependent expression of the full-length Pkd1 transgene in all tissues. Since the regulatory pattern of transgene expression was similar to that of the endogenous gene, it is likely that the transgene includes all the necessary transcriptional regulatory regions of the Pkd1 gene. Consistently, the Pc-1 protein is also similarly overexpressed in these mice. Of importance, gene dosage or expression correlated with the progression of phenotypic severity.

The $Pkd1_{TAG}$ mice are the first model among the mice with dysregulated or mutated Pkd1 gene that develops the typical multicystic "bosselated" cortical surface with tubular and glomerular cysts as in ADPKD. Renal insufficiency was detected in $Pkd1_{TAG}$ mice at 5-6 months of age by altered urinary and blood analysis. Severe cystogenesis with loss of renal function and increase kidney fibrosis are hallmarks of ADPKD renal pathology. In addition to frequent hemorrhagic cysts and hematuria, an incidence of ~39% of $Pkd1_{TAG}$ mice with pronounced cystic disease displayed intraluminal but also parenchymal calcium deposits limited to the papilla. Presence of this localized nephrocalcinosis in $Pkd1_{TAG}$ mice is compatible with the nephrolithiasis observed in 20-36% of patients with ADPKD (30, 31). While the mechanism responsible for these calcium deposits is unknown, the urinary concentration defect should in theory have a protective effect but urinary stasis within the distorted anatomy and compressed tubules may predispose to calcium precipitation.

Of particular interest was the significantly longer primary cilium of renal epithelial cells in $Pkd1_{TAG}$ prior to cyst appearances. This indicated that increased expression of normal functional polycystin-1 protein might promote ciliogenesis. Since endogenous Pc-1 was localized to the cilia (35), this finding suggests that it can occur via a direct effect of Pc-1 overexpression and/or through indirect Pc-1 cellular effectors modulating proteins of the cilia and axoneme assembly. Since cilia anomalies preceded

cystogenesis, it raises the question whether it is a prerequisite for cyst formation in $Pkd1_{TAG}$ mice. In addition, the increased cilia length distribution also persisted during cystogenesis and this, in spite of significantly elevated renal epithelial proliferation. While defects in the primary cilia have been observed in other cystic diseases, most of cilia anomalies have been attributed to shorter or absence of cilia (35-38) except for the Nek8 and p75/cux genes (39, 40).

The consistent increase in Pc-1 in equivalent proportion from crude urine to subfractionated exosomes of the $Pkd1_{TAG}$ over control mice argues that Pc-1 in transgenic kidneys undergoes the normal *in vivo* physiologic protein processing. The shed Pc-1 protein both glycosylated and unglycosylated in crude urine corresponded approximately in size to a N-terminal cleaved form of Pc-1 at the G protein-coupled receptor proteolytic site (GPS at aa 3041). Strikingly, similar size Pc-1 glycosylated and unglycosylated forms were free in urine itself whereas only the glycosylated form was detected in the exosome fraction. This finding is consistent with the cleaved form of PC-1 present in human urinary exosomes (33, 41). While the role of Pc-1 in exosomes remains to be elucidated, we speculate that the increased frequency of interaction between free Pc-1, exosome and cilia in flow of $Pkd1_{TAG}$ mice could influence intercellular and intracellular signaling. Alternatively, exosomes if in close proximity of cilia as shown *in vitro* (33) could interact, fuse and consequently, induce longer cilia with profound impact on mechanosignaling and tubular integrity.

The spectrum of extrarenal phenotypes in the $Pkd1_{TAG}$ mice closely recapitulates that of human ADPKD. Indeed, the high frequency of hepatic cysts in $Pkd1_{TAG}$ mice affecting mainly females is reminiscent of ADPKD. Cysts affecting intrahepatic bile ducts are consistent with the endogenous pattern of Pkd1 expression (14, 16) and likely due to enhanced transgene expression in $Pkd1_{TAG}$ mice. The systematic increased fibrosis surrounding the biliary ducts in $Pkd1_{TAG}$ mice indicated that fibrosis precedes cyst formation. Furthermore, it also suggests that Pkd1 overexpression interferes with the extracellular

environment and results in active remodeling of the extracellular matrix. Regions of hepatic cysts and fibrosis were associated with elevated proliferation. Interestingly, such association of liver fibrosis and cyst development has also been observed when Pkd1 gene dosage expression is reduced from a hypomorphic allele (42).

The concomitant features of fibrosis and cyst formation in the liver and in kidneys of $Pkd1_{TAG}$ mice correlated with substantial stimulation of proliferation. Such phenotypic similarities to the SBM transgenic mice (43) produced by targeted c-myc expression prompted analysis of c-myc expression in liver and kidneys of $Pkd1_{TAG}$ mice. This study demonstrates that Pkd1 overexpression activates c-myc in both tissues and with a higher signal in cysts. Hence, it is likely a critical component of this signaling event. While the molecular mediators immediately downstream of Pkd1 protein are not yet delineated, c-myc appears to play a central role in the signaling pathway cascade triggered by Pkd1.

Cardiovascular anomalies are the most prevalent non-cystic extrarenal manifestation of ADPKD and of $Pkd1_{TAG}$ mice. $Pkd1_{TAG}$ mice structural cardiac defects are consistent with enhanced Pkd1 transgene expression following the Pkd1 endogenous pattern. We and others have shown that endogenous Pkd1 expression was high in the aortic arch, valve leaflets, atrioventricular cushion, and low in myocardium of wild type mice (8, 14-16, 44). Accordingly, the generalized cardiac anomalies in $Pkd1_{TAG}$ transgenic mice included frequent left ventricular hypertrophy, thickening of the myocardial wall associated with significantly increased aortic root dilatation. In addition, the cardiac aortic and mitral valve morphologic anomalies, particularly stenosis and calcification revealed severe functional impact and suggested signs of valvular regurgitation. In fact, this would be consistent with a compensatory mechanism of heart dilatation/cardiomegaly and increased cardiac output with similar heart rate. In parallel to these anomalies, systemic hypertension in $Pkd1_{TAG}$ mice could be responsible indirectly for the marked aortic

insufficiency as well as the cardiac hypertrophy. However, the strong Pkd1 expression in the aortic valve and root is likely to have a direct contributory role. Together, these cardiac and aortic anomalies with important complications are analogous to those of ADPKD patients (45, 46).

Probably the most devastating extrarenal manifestation in ADPKD is intracranial aneurysm. Given that Pkd1 is expressed in endothelial cells and vascular smooth muscle (8, 47), the presence of cerebral aneurysms in $Pkd1_{TAG}$ was consistent with a primary defect in vascular structure. Similarly, this Pc-1 expression may also be the cause of hypertension independently of renal cystogenesis. Development of cerebral aneurysms in $Pkd1_{TAG}$ mice as in humans is asymptomatic and could be exacerbated by systemic hypertension. However, rupture of aneurysms was detected in a few $Pkd1_{TAG}$ mice at one month of age upon very brief exposure, if any, to hypertension. Rupture of cerebral aneurysms was evident by compression of adjacent structures, focal brain ischemia, and subarachnoid hemorrhage as well as by morbidity.

Systemic enhanced expression of $Pkd1_{TAG}$ mice leads to abnormalities in various organs/tissues as well as in kidneys. Anomalies in a particular organ of $Pkd1_{TAG}$ mice likely result from direct expression of Pkd1 in this organ per se. Evidence for this direct effect instead of a secondary consequence of renal defects, is provided by the renal-targeted Pkd1 mice, $SBPkd1_{TAG}$, that essentially displays a renal restricted PKD disorder (27) similar to that of $Pkd1_{TAG}$ kidney phenotype.

The mutational mechanism of ADPKD was initially proposed as a two-hit model for cyst formation and thereby could explain the focal nature of cyst and the disease variable severity. However, this mechanism is at variance with the continuing expression of PKD1/PC-1 in the majority of ADPKD renal cysts (3-5, 10, 48-50), hepatic cysts (6, 44, 51), and cerebral aneurysms (47). A more inclusive model

would be that an imbalance or dysregulated PKD1/PC-1 would be sufficient to elicit a cystic phenotype. This model is supported by the increase in disease severity correlating with the increase Pkd1 gene dosage in $Pkd1_{TAG}$ and $SBPkd1_{TAG}$ mice (27, 52) and reciprocally with the progressive decrease in expression from haploinsufficiency to hypomorphic Pkd1 allele in mice (23, 25, 42, 53). In fact, both human ADPKD and murine Pkd1 studies have provided evidence for, although opposite, gain-of-function as well as loss-of-function and haploinsufficiency/dosage effect as pathogenetic mechanisms. Hence, a Pkd1 dose imbalance model mechanism would be compatible with a dominantly inherited mutation as seen in humans and could also explain the high prevalence of ADPKD in the population. Importantly, the cystic focal nature in our $Pkd1_{TAG}$ study as in human ADPKD, supports a pathogenetic mechanism that combines Pkd1 dysregulation with an additional mutational step or stochastic event/threshold level to determine whether a cell will enter a cystic cascade and develop cystogenesis.

This study demonstrates that "wild type" full-length Pkd1 overexpression/gain-of-function in the $Pkd1_{TAG}$ mouse is sufficient to reproduce the ADPKD systemic clinical manifestations. Enhanced Pkd1 gene expression recapitulates a physiologic bona fide murine ADPKD disorder with renal and extrarenal phenotypes. Thus, these transgenic mice may be instrumental for numerous studies including the design of novel therapeutic strategies to modulate in vivo progression of ADPKD.

MATERIALS AND METHODS

Constructs for homologous recombination of Pkd1-BAC clone

The Pkd1-BAC clone from the bacterial host strain DH10B ($RecA^-$; $RecBC^+$) was isolated from a 129/Sv mouse pBelo11BAC library (Research Genetics) and was orthologous to the human PKD1 gene as described in (27). To modify the original wild-type Pkd1-BAC by homologous recombination, two constructs were produced in the pLD53.SC-AB BAC recombination vector (54). The first construct was carried out in order to introduce a silent point mutation by substitution of a G to A nucleotide as we did for $SBPkd1_{TAG}$ (27). This substitution created a new EcoRI restriction site in Pkd1 exon 10 that distinguished the transgene from the endogenous gene/transcript. The second construct was performed to delete Tsc2 gene body and consisted of two homology arms, the Tsc2 promoter-intron 2 linked directly to Tsc2 exon 42-exon 46 Pkd1 in a BAC recombination vector. The first homology arm was obtained by PCR amplification of 1116bp fragment (Tsc2 promoter-intron2) with the primers: 5'-TCAGATGCTGCGGCCCGGGACGCA-3' (forward Tsc2 promoter) and 5'-GGACAGCATGCCCTATGCAGATG (reverse intron2) followed by a restriction enzyme digest SmaI-SpHI. The second arm was also generated from a PCR product of 1.2kb with the following primers: 5'-TTCAGCACATGCTCATGCC-3' (reverse Tsc2 intron 40) and 5'-GCTGAAAATGGGCCCATTGTTACC-3' (forward Pkd1 exon 46) followed by a SpHI- BamHI restriction digest that produce 0.9kb from Tsc2 exon42 to exon46 Pkd1. Both these arms were introduced into the pLD53.SC-AB BAC recombination vector.

Modification of BAC clones by homologous recombination in E. coli

Each of the two BAC recombination vectors was used in a two-step RecA strategy for BAC modifications, as previously described (27). Approximately 64 co-integrates were analyzed for each recombination by Southern blot to monitor for appropriate integration event. Two proper co-integrates

were chosen for the second recombination event and positive clones from the resolved BACs were further analyzed by Southern following standard and PFGE using seven probes spanning the entire sequence of the modified BAC. The probes were designed in (14, 27): a. genomic exon 1, b. genomic exon 2-3, c. genomic exon 7-15, d. cDNA exon 15-20, e. cDNA exon 25-34, f. cDNA exon 36-45, g. genomic exon 45-46. Subsequently, modified Pkd1 gene regions were sequenced to confirm that the intended recombined BAC clones were achieved. Following these two modifications the BAC clone was referred as $Pkd1_{TAG}$-BAC.

Production and analysis of $Pkd1_{TAG}$-BAC transgenic mice

The $Pkd1_{TAG}$-BAC (40-50 μg of DNA) was digested with the restriction enzymes MluI and NotI. The ~75kb transgene fragment was isolated on low melt agarose by PFGE. The $Pkd1_{TAG}$ linearized DNA fragment was purified as in (27). The fragment preparation was verified for integrity by PFGE and was microinjected as described (28). Transgenic founder mice and progenies were identified by Southern analysis of DNA from tail biopsies digested with HindIII, EcoRI and/or KpnI and respectively hybridized with the 7 mouse Pkd1 probes to verify integrity of the transgene. The 5' transgene integrity was verified by a polymorphism at 4.47 kb of the murine Pkd1 gene specific for 129/sv that can be distinguished from the C57BL/6J and CBA/J inbred strains that served to produce the transgenic mice. PCR amplification of genomic DNA from transgenic mice at the polymorphic region was carried out with the primers: (forward) 5'-CTGCACCCATGTCAGGTGTA-3' and (reverse) 5'-GTTCTAGGCCAGCCAACTC-3' and expected fragment for 129sv, C57Bl6/J and CBA/J are 100bp, 133bp, and 113bp respectively. All transgenic mouse lines were backcrossed onto C57Bl6/J. Animal procedures were approved by the Animal Care Committee of the IRCM and conducted according to the guidelines of the Canadian Council on Animal Care.

RNA expression analysis

Total RNA was extracted from various tissues, including kidneys, lungs, spleen, brain, heart, pancreas and liver, of 4 to 9 month old animals using guanidium thiocyanate or trizol/chloroform method (55). The integrity of all RNA preparations was monitored by electrophoresis on formaldehyde-agarose gels prior to analysis (56).

$Pkd1_{TAG}$ transgene expression in all tissues was analyzed by quantitative real-time PCR. All RNA samples were reversed transcribed as previously described (10). The primers used were as follows: 5'-TCAATTGCTCCGGCCGCTG- 3' (forward Pkd1 exon 1) and 5'-CCAGCGTCTGAAGTAGGTTGTGGG-3' (reverse Pkd1 exon 2) that detect endogenous and transgene. The S16 ribosomal gene product served as an internal control with the following primers: 5'-AGGAGCGATTT-GCTGGTGTGGA-3' (forward S16 exon 3) and 5'-GCTACCAGGCCTTTGAGATGGA-3' (reverse S16 exon 4). Each pair of primers was designed such that only spliced mRNA would produce the predicted amplification products of 101bp for Pkd1 total (endogenous gene and transgene) and 102bp for S16. All reactions for quantitative real-time PCR analysis were performed in triplicate in a master mix (Qiagen, Mississauga, Canada) using a MX4000 Multiplex quantitative PCR analyser.

Expression analysis of Pkd1 (endogenous gene and transgene) was also performed by Northern blot. Total RNA from each sample (30 μg) was electrophoresed on agarose/formaldehyde gel, transferred to nylon membranes and hybridized with "g" probe for Pkd1 and with glyceraldehyde 3-phosphate dehydrogenase (Gapdh) as internal control (14). Membranes were exposed to X-ray film (Biomax MS) for 24-48 hours, scanned and quantified with the Image Quant 5.0 software.

Protein expression analysis

Total protein extracts from multiple organs, kidney, lung, brain, liver, pancreas and heart, were produced in RIPA buffer (20mM Tris pH8; 2mM EDTA; 150mM NaCl; Triton 0.5%) supplemented by cocktail of inhibitors of proteases (1X, SIGMA) and PMSF (1mM). Protein concentration was measured by Bradford assay (BioRad). Total protein extracts (40 or 80µg) was reduced in NuPAGE loading dye for 7min at 65°C and loaded on 4-12% NuPage Bis-Tris gel using 1X MES SDS Invitrogen migration buffer. Urinary proteins were prepared as described (32, 33). In brief, urine was supplemented with cocktail inhibitors, centrifuged to remove cell debris and supernatant was considered total urinary fraction (T). Total fraction was then centrifuged, the new supernatant is the S1 fraction and pellet resuspended for recentrifugation, resulting in non-clustered uromodulin (S2) in the supernatant and the exosomes (Exo) in the pellet. Total urinary and S1 fractions (50ug) were precipitated by trichloroacetic acid and resuspended in loading dye. Exosomes were directly resuspended in loading dye with half the volume analyzed under the native form and the other half following deglycosylation with 750U of PNGase (New England Biolabs). Proteins were transferred on PVDF membranes that were hybridized with mouse monoclonal antibodies, 7e12 against N-terminal of polycystin-1 (51) and secondary goat anti-mouse IgG (SIGMA) coupled to horseradish peroxidase or with mouse monoclonal antibody Gapdh (Abcam, Cambridge, MA) and revealed with Amersham ECL Advance Plus (GE HealthCare) on X-Omat films.

Renal and Cardiac physiological function analysis

Renal function was evaluated by analysis of urine samples collected in metabolic cages for 24 hours with non-restricted water supply. Urinary urea nitrogen, creatinine and ion concentrations were measured with a CX9 Beckmann apparatus whereas urine osmolality was determined with a radiometer.

Proteinuria was qualitatively analyzed using 50 μg of total urinary protein on a 10 % SDS-PAGE stained with Coomassie blue as described (57).

Echocardiographic measurements on transgenic and control mice were carried out using the Vevo 770 (Visualsonics) with a probe transducer of 35MHz as in (58). Preheated ultrasound transmisson gel (Aquasonic 100) was placed on heart region to provide acoustic coupling between the probe and the mice. Cardiac dimensions including aortic root and left ventricle wall thickness and diameter were monitored in the M-mode. Functional analysis of stroke volume and cardiac output was determined from aortic Doppler measurements whereas the heart rate was obtained from ECG. Mitral and aortic valvular velocities upstream and downstream were measured using Doppler to evaluate their functional efficiency.

Morphologic, histologic, and cellular analysis

Different tissues including kidneys, heart, pancreas, lung, liver, brain, spleen were analyzed from adult transgenic mice aged between 1 to 20 months. Four-μm-thick paraffin sections of paraformaldehyde- or formalin-fixed tissues were deparaffinized and stained with hematoxylin and eosin. Detection of calcium deposits was monitored with specific stains by Alizarin red or Von Kossa and fibrosis by Sirius red.

Cysts from renal tissue were immunostained to identify the origin of the nephron segment affected. Sections (4-μm) were incubated with three primary antibodies α-calbindin (Sigma) for collecting ducts, lycopersicon esculentum lectin (Vector Lab) for distal convoluted tubules and lotus tetragonolobus lectin linked to fluorescein (Vector Lab) for proximal tubules and then with secondary antibodies a goat α-mouse IgG Alexa 255 (Invitrogen) and AMCA-streptavidin (Vector Lab). Slides were visualized with Axiovert S100TV microscope. Characterization of primary cilia in renal tissues was performed with α-

acetylated tubulin (Sigma) as primary antibody and goat α-mouse IgG Alexa 255 (Invitrogen) as secondary antibody and slides were mounted with vectashield and DAPI.

Analysis of cellular c-myc expression and proliferation using Ki67 marker was performed by immunohistochemistry (59). Kidney and liver adult mice fixed tissues from transgenic and control mice were incubated with rabbit c-myc (Upstate) or rabbit Ki67 (Novocastra) O/N at 4^0C, then for 1 hour with secondary anti-rabbit biotinylated antibody and signal detected using Vectastain ABC kit (Vector Lab) and diaminobenzinide. Proliferation rate was evaluated according to the number of renal tubules normal (control) or cystic ($Pkd1_{TAG}$) with 0, 1, ≥2 nuclei positive for Ki67 on multiple non-overlapping images (≥5) using Axiophot (Zeiss) microscope.

Vasculature analysis was performed from anesthetized animals perfused intracardiac with paraformaldehyde and Microfil media (Flow Tech Inc, Mass). Fixation was carried out overnight and tissues collected were cleared with methyl salicylate and photograph with Nikon SMZ-U using Q-capture software.

Statistical analysis

Values were expressed as mean ± standard deviation. A 2-tailed unpaired Student's t-test was used for statistical analysis; $p < 0.05$ was considered significant.

ACKNOWLEDGMENTS

We thank Dr. V. Gattone and the Indiana University School of Medicine EM Center and the generous support of that facility by the Polycystic Kidney Disease Foundation. The authors thank K. Jani for technical support and Dr C. Deschepper for critical reading of the manuscript. This work was supported by the Canadian Institutes of Health Research (CIHR) [MOP-81325 to MT] and a CIHR Frederick Banting and Charles Best studentship to AK and a Fonds de la Recherche en Santé du Québec (FRSQ) studentship to MC.

REFERENCES

1. Chapman, A.B., Rubinstein, M.D., Hughes, R., Stears, J.C., Earnest, M.P., Johnson, A.M., Gabow, P.A. and Kaehny, W.D. (1992) Intracranial aneurysms in autosomal dominant polycystic kidney disease. *N. Engl. J. of Med.,* **327,** 916-920.
2. Wei, W., Hackmann, K., Xu, H., Germino, G. and Qian, F. (2007) Characterization of cis-autoproteolysis of polycystin-1, the product of human polycystic kidney disease 1 gene. *J. Biol. Chem.,* **282,** 21729-21737.
3. Ward, C.J., Turley, H., Ong, A.C.M., Comley, M., Biddolph, S., Chetty, R., Ratcliffe, P.J., Gatter, K. and Harris, P.C. (1996) Polycystin, the polycystic kidney disease 1 protein, is expressed by epithelial cells in fetal, adult and polycystic kidney. *Proc. Natl. Acad. Sci. USA,* **93,** 1524-1528.
4. Ong, A.C.M., Ward, C.J., Butler, R.J., Biddolph, S., Bowker, C., Torra, R., Pei, Y. and Harris, P.C. (1999) Coordinate expression of the autosomal dominant polycystic kidney disease proteins, polycystin-2 and polycystin-1, in normal and cystic tissue. *Am. J. Pathol.,* **154,** 1721-1729.

5. Geng, L., Segal, Y., Peissel, B., Deng, N., Pei, Y., Carone, F., Rennke, H.G., Glücksmann-Kuis, A.M., Schneider, M.C., Ericsson, M. *et al.* (1996) Identification and localization of polycystin, the PKD1 gene product. *J. Clin. Invest.,* **98,** 2674-2682.

6. Ibraghimov-Beskrovnaya, O., Dackowski, W.R., Foggensteiner, L., Coleman, N., Thiru, S., Petry, L.R., Burn, T.C., Connors, T.D., Van Raay, T., Bradley, J. *et al.* (1997) Polycystin: In vitro synthesis, in vivo tissue expression, and subcellular localization identifies a large membrane-associated protein. *Proc. Natl. Acad. Sci. USA,* **94,** 6397-6402.

7. Chauvet, V., Qian, F., Boute, N., Cai, Y., Phakdeekitacharoen, B., Onuchic, L.F., Attie-Bitach, T., Guicharnaud, L., Devuyst, O., Germino, G.G. *et al.* (2002) Expression of *PKD1* and *PKD2* Transcripts and Proteins in Human Embryo and during Normal Kidney Development. *Am. J. Pathol.,* **160,** 973-983.

8. Peters, D.J.M., Van De Wal, A., Spruit, L., Saris, J.J., Breuning, M.H., Bruijn, J.A. and de Heer, E. (1999) Cellular Localization and Tissue Distribution of Polycystin-1. *J. Pathol.,* **188,** 439-446.

9. Trudel, M. and Guillaume, R. (2000) Molecular biology of autosomal dominant polycystic kidney disease. *Pediatr. Pathol. Mol. Med.,* **18,** 483-499.

10. Lanoix, J., D'Agati, V., Szabolcs, M. and Trudel, M. (1996) Dysregulation of cellular proliferation and apoptosis mediates human autosomal dominant polycystic kidney disease (ADPKD). *Oncogene,* **13,** 1153-1160.

11. Qian, F., Watnick, T.J., Onuchic, L.F. and Germino, G.G. (1996) The molecular basis of focal cyst formation in human autosomal dominant polycystic kidney disease type I. *Cell,* **87,** 979-987.

12. Brasier, J.L. and Henske, E.P. (1997) Loss of the polycystic kidney disease (PKD1) region of chromosome 16p13 in renal cyst cells supports a loss-of-function model for cyst pathogenesis. *J. Clin. Invest.,* **99,** 194-199.

13. Koptides, M., Constantinides, R., Kyriakides, G., Hadjigavriel, M., Patsalis, P.C., Pierides, A. and Deltas, C.C. (1998) Loss of heterozygosity in polycystic kidney disease with a missense mutation in the repeated region of PKD1. *Hum. Genet.,* **103,** 709-717.

14. Guillaume, R., D'Agati, V., Daoust, M. and Trudel, M. (1999) Murine Pkd1 is a developmentally regulated gene from morula to adulthood: Role in tissue condensation and patterning. *Dev. Dyn.,* **214,** 337-348.

15. Guillaume, R. and Trudel, M. (2000) Distinct and common developmental expression patterns of the murine PKD2 and PKD1 genes. *Mech. Dev.,* **93,** 179-183.

16. Boulter, C., Mulroy, S., Webb, S., Fleming, S., Brindle, K. and Sandford, R. (2001) Cardiovascular, skeletal, and renal defects in mice with a targeted disruption of the *Pkd1* gene. *Proc. Natl. Acad. Sci. USA,* **98,** 12174-12179.

17. Kim, K., Drummond, I., Ibraghimov-Beskrovnaya, O., Klinger, K. and Arnaout, M.A. (2000) Polycystin 1 is required for the structural integrity of blood vessels. *Proc. Natl. Acad. Sci. USA,* **97,** 1731-1736.

18. Lu, W., Peissel, B., Babakhanlou, H., Pavlova, A., Geng, L., Fan, X., Larson, C., Brent, G. and Zhou, J. (1997) Perinatal lethality with kidney and pancreas defects in mice with a targetted PKD1 mutation. *Nat. Genet.,* **17,** 179-181.

19. Lu, W., Shen, X., Pavlova, A., Lakkis, M., Watrd, C.J., Pritchard, L., Harris, P.C., Genest, D.R., Perez-Atayde, A.R. and Zhou, J. (2001) Comparison of *Pkd1*-targeted mutants reveals that loss of polycystin-1 causes cystogenesis and bone defects. *Hum. Mol. Genet.,* **10,** 2385-2396.

20. Muto, S., Aiba, A., Saito, Y., Nakao, K., Nakamura, K., Tomita, K., Kitamura, T., Kurabayashi, M., Nagai, R., Higashihara, E. *et al.* (2002) Pioglitazone improves the phenotype and molecular defects of a targeted *Pkd1* mutant. *Hum. Mol. Genet.,* **11,** 1731-1742.

21. Wu, G., Tian, X., Nishimura, S., Markowitz, G.S., D'Agati, V., Park, J.H., Yao, L., Li, L., Geng, L., Zhao, H. *et al.* (2002) *Trans*-heterozygous *Pkd1* and *Pkd2* mutations modify expression of polycystin kidney disease. *Hum. Mol. Genet.,* **11,** 1845-1854.

22. Starremans, P.G., Li, X., Finnerty, P.E., Guo, L., Takakura, A., Neilson, E.G. and Zhou, J. (2008) A mouse model for polycystic kidney disease through a somatic in-frame deletion in the 5' end of Pkd1. *Kidney Int.,* **73,** 1394-1405.

23. Lantinga-van Leeuwen, I.S., Leonhard, W.N., van der Wal, A., Breuning, M.H., de Heer, E. and Peters, D.J.M. (2007) Kidney-specific inactivation of the Pkd1 gene induces rapid cyst formation in developing kidneys and a slow onset of disease in adult mice. *Hum. Mol. Genet.,* **16,** 3188-3196.

24. Takakura, A., Contrino, L., Beck, A.W. and Zhou, J. (2008) Pkd1 inactivation induced in adulthood produces focal cystic disease. *J. Am. Soc. Nephrol.,* **19,** 2351-2363.

25. Lantinga-van Leeuwen, I.S., Dauwerse, J.G., Baelde, H.J., Leonhard, W.N., van de Wal, A., Ward, C.J., Verbeek, S., Deruiter, M.C., Breuning, M.H., de Heer, E. *et al.* (2004) Lowering of *Pkd1* expression is sufficient to cause polycystic kidney disease. *Hum. Mol. Genet.,* **13,** 3069-3077.

26. Lu, W., Fan, X., Basora, N., Babakhanlou, H., Law, T., Rifai, N., Harris, P.C., Perez-Atayde, A.R., Rennke, H.G. and Zhou, J. (1999) Late onset of renal and hepatic cysts in *Pkd1*-targeted heterozygotes. *Nat. Genet.,* **21,** 160-161.

27. Thivierge, C., Kurbegovic, A., Couillard, M., Guillaume, R., Cote, O. and Trudel, M. (2006) Overexpression of PKD1 Causes Polycystic Kidney Disease. *Mol. Cell. Biol.,* **26,** 1538-1548.

28. Trudel, M., D'Agati, V. and Costantini, F. (1991) C-myc as an inducer of polycystic kidney disease in transgenic mice. *Kidney Int.,* **39,** 665-671.

29. Torres, V.E., Erickson, S.B., Smith, L.H., Wilson, D.M., Hattery, R.R. and Segura, J.W. (1988) The association of nephrolithiasis and autosomal dominant polycystic kidney disease. *Am. J. Kidney Dis.,* **11,** 318-325.

30. Torres, V.E., Wilson, D.M., Hattery, R.R. and Segura, J.W. (1993) Renal stone disease in autosomal dominant polycystic kidney disease. *Am. J. Kidney Dis.,* **22,** 513-519.

31. Levine, E. and Grantham, J.J. (1992) Calcified renal stones and cyst calcifications in autosomal dominant polycystic kidney disease: clinical and CT study in 84 patients. *Am. J. Roentgenol.,* **159,** 77-81.

32. Gonzales, P.A., Pisitkun, T., Hoffert, J.D., Tchapyjnikov, D., Star, R.A., Kleta, R., Wang, N.S. and Knepper, M.A. (2009) Large-scale proteomics and phosphoproteomics of urinary exosomes. *J. Am. Soc. Nephrol.,* **20,** 363-379.

33. Hogan, M.C., Manganelli, L., Woollard, J.R., Masyuk, A.I., Masyuk, T.V., Tammachote, R., Huang, B.Q., Leontovich, A.A., Beito, T.G., Madden, B.J. *et al.* (2009) Characterization of PKD protein-positive exosome-like vesicles. *J. Am. Soc. Nephrol.,* **20,** 278-288.

34. Adeney, K.L., Siscovick, D.S., Ix, J.H., Seliger, S.L., Shlipak, M.G., Jenny, N.S. and Kestenbaum, B.R. (2009) Association of serum phosphate with vascular and valvular calcification in moderate CKD. *J. Am. Soc. Nephrol.,* **20,** 381-387.

35. Yoder, B.K., Hou, X. and Guay-Woodford, L.M. (2002) The Polycystic Kidney Disease Proteins, Polycystin-1, Polycystin-2, Polaris, and Cystin, Are Co-Localized in Renal Cilia. *J. Am. Soc. Nephrol.,* **13,** 2508-2516.

36. Pazour, G.J., Dickert, B.L., Vucica, Y., Seeley, E.S., Rosenbaum, J.L., Witman, G.B. and Cole, D.G. (2000) Chlamydomonas IFT88 and its mouse homologue, polycystic kidney disease gene tg737, are required for assembly of cilia and flagella. *J. Cell. Biol.,* **151,** 709-718.

37. Lin, F., Hiesberger, T., Cordes, K., Sinclair, A.M., Goldstein, L.S.B., Somlo, S. and Igarashi, P. (2003) Kidney-specific inactivation of the KIF3A subunit of kinesin-II inhibits renal ciliogenesis and produces polycystic kidney disease. *Proc. Natl. Acad. Sci. USA,* **100,** 5286-5291.

38. Masyuk, T.V., Huang, B.Q., Ward, C.J., Masyuk, A.I., Yuan, D., Splinter, P.L., Punyashthiti, R., Ritman, E.L., Torres, V.E., Harris, P.C. *et al.* (2003) Defects in cholangiocyte fibrocystin expression and ciliary structure in the PCK rat. *Gastroenterology,* **125,** 1303-1310.

39. Smith, L.A., Bukanov, N.O., Husson, H., Russo, R.J., Barry, T.C., Taylor, A.L., Beier, D.R. and Ibraghimov-Beskrovnaya, O. (2006) Development of polycystic kidney disease in juvenile cystic kidney mice: insights into pathogenesis, ciliary abnormalities, and common features with human disease. *J. Am. Soc. Nephrol.,* **17,** 2821-2831.

40. Cadieux, C., Harada, R., Paquet, M., Cote, O., Trudel, M., Nepveu, A. and Bouchard, M. (2008) Polycystic kidneys caused by sustained expression of Cux1 isoform p75. *J. Biol. Chem.,* **283,** 13817-13824.

41. Pisitkun, T., Shen, R.F. and Knepper, M.A. (2004) Identification and proteomic profiling of exosomes in human urine. *Proc. Natl. Acad. Sci. U S A,* **101,** 13368-13373.

42. Jiang, S.-T., Chiou, Y.-Y., Wang, E., Lin, H.-K., Lin, Y.-T., Chi, Y.-C., Wang, C.-K.L., Tang, M.-J. and Li, H. (2006) Defining a Link with Autosomal-Dominant Polycystic Kidney Disease in Mice with Congenitally Low Expression of Pkd1. *Am. J. Pathol.,* **168,** 205-220.

43. Trudel, M. and D'Agati, V. (1992) A model of polycystic kidney disease in SBM transgenic mice. In Berlyne, G.M. (ed.), *Contrib. Nephrol.* Karger, S., Basel, Brooklyn, NY, Vol. 97, pp. 47-59.

44. Griffin, M.D., Torres, V.E., Grande, J.P. and Kumar, R. (1996) Immunolocalization of polycystin in human tissues and cultured cells. *Proc. Assoc. Am. Physicians,* **108**.

45. Leier, C.V., Baker, P.B., Kilman, J.W. and Wooley, C.F. (1984) Cardiovascular abnormalities associated with adult polycystic kidney disease. *Ann. Intern. Med.,* **100,** 683-688.

46. Hossack, K.F., Leddy, C.L., Johnson, A.M., Schrier, R.W. and Gabow, P.A. (1988) Echocardiographic findings in autosomal dominant polycystic kidney disease. *The New England Journal of Medicine,* **319,** 907-912.

47. Griffin, M.D., Torres, V.E., Grande, J.P. and Kumar, R. (1997) Vascular Expression of Polycystin. *J. Am. Soc. Nephrol.,* **8,** 616-626.

48. Peters, D.J.M., Spruit, L., Klingel, R., Prins, F., Baelde, H.J.J., Giordano, P.C., Bernini, L.F., de Heer, E., Breuning, M.H. and Bruijn, J.A. (1996) Adult, fetal, and polycystic kidney expression of polycystin, the polycystic kidney disease-1 gene product. *Lab. Invest.,* **75,** 221-230.

49. Weston, B.S., Jeffery, S., Jeffrey, I., Sharaf, S.F.A., Carter, N., Saggar-Malik, A. and Price, R.G. (1997) Polycystin expression during embryonic development of human kidney in adult tissues and ADPKD tissue. *Histochem. J.,* **29,** 847-856.

50. Palson, R., Sharma, C.P., Kim, K., McLaughlin, M., Brown, D. and Arnaout, M.A. (1996) Characterization and cell distribution of polycystin, the product of autosomal dominant polycystic kidney disease gene 1. *Mol. Med.,* **2,** 702-711.

51. Ong, A.C.M., Harris, P.C., Davies, D.R., Pritchard, L., Rossetti, S., Biddolph, S., Vaux, D.J.T., Migone, N. and Ward, C.J. (1999) Polycystin-1 expression in PKD1, early onset PKD1 and TSC2/PKD1 cystic tissue: implications for understanding cystogenesis. *Kidney Int.,* **56,** 1324-1333.

52. Pritchard, L., Sloane-Stanley, J.A., Sharpe, J.A., Aspinwall, R., Lu, W., Buckle, V., Strmecki, L., Walker, D., Ward, C.J., Alpers, C.E. *et al.* (2000) A human *PKD1* transgene generates functional polycystin-1 in mice and is associated with a cystic phenotype. *Hum. Mol. Genet.,* **9,** 2617-2627.

53. Ahrabi, A.K., Terryn, S., Valenti, G., Caron, N., Serradeil-Le Gal, C., Raufaste, D., Nielsen, S., Horie, S., Verbavatz, J.M. and Devuyst, O. (2007) PKD1 haploinsufficiency causes a syndrome of inappropriate antidiuresis in mice. *J. Am. Soc. Nephrol.,* **18,** 1740-1753.

54. Gong, S., Yang, X.W., Li, C. and Heintz, N. (2002) Highly Efficient Modification of Bacterial Artificial Chromosomes (BACs) Using Novel Shuttle Vectors Containing the R6Kγ Origin of Replication. *Genome Res.,* **12,** 1992-1998.

55. Couillard, M., Guillaume, R., Tanji, N., D'Agati, V. and Trudel, M. (2002) c-myc-induced Apoptosis in Polycystic Kidney Disease is Independent of FasL/Fas Interaction. *Cancer Res.,* **62,** 2210-2214.

56. Trudel, M., Lanoix, J., Barisoni, L., Blouin, M.-J., Desforges, M., L'Italien, C. and D'Agati, V. (1997) C-myc-induced Apoptosis in Polycystic Kidney Disease is Bcl-2 and p53 Independent. *J. Exp. Med.,* **186,** 1873-1884.

57. De Paepe, M.E. and Trudel, M. (1994) The transgenic SAD mouse: A model of human sickle cell glomerulopathy. *Kidney Int.,* **46,** 1337-1345.

58. Stoyanova, E., Trudel, M., Felfly, H., Garcia, D. and Cloutier, G. (2007) Characterization of circulatory disorders in beta-thalassemic mice by noninvasive ultrasound biomicroscopy. *Physiol. Genomics,* **29,** 84-90.

59. Couillard, M. and Trudel, M. (2009) C-myc as a modulator of renal stem/progenitor cell population. *Dev. Dyn.,* **238,** 405-414.

FIGURE LEGENDS

Figure 1 Genomic analysis of Pkd1 $_{TAG}$ transgenic mice

Representative analysis of the 5' regulatory region of Pkd1$_{TAG}$ transgenic mice was carried out based on a polymorphism at ~ 4.5 kb upstream of the translation initiation codon of the murine *Pkd1* gene. Since Pkd1$_{TAG}$ transgenic mice were produced on a mixed C57Bl6/J and CBA/J inbred background, the BAC of 129sv origin could be detected by 100bp amplification band whereas the C57Bl6/J and CBA/J displayed a 133 and 113bp, respectively. Analysis of the 3' Pkd1$_{TAG}$ region was verified on Southern using a KpnI digestion with the Pkd1 "g" probe (exon 45-46). Bands are expected at 7kb for the endogenous Pkd1 gene and at 5kb for the Pkd1$_{TAG}$ transgene (5kb). The 5' and the 3' ends of the transgene were intact for the three transgenic mouse lines. M: 100 bp marker; C: negative control; C57: C57Bl/6J mice; CBA: CBA/J mice; 129:129sv mice; Ma: lambda HindIII marker; WT: wild type control mice; Tg: Pkd1$_{TAG}$ transgene; Endo: endogenous Pkd1 gene; E: EcoRI; K: Kpnl; E* = tag silent point mutation.

Figure 2 Expression analysis of Pkd1 $_{TAG}$ transgenic mice

(**A**) Renal expression analysis of total *Pkd1* (endogenous and transgene: ~14.2kb) transcript of Pkd1$_{TAG}$ transgenic mice assessed by Northern blotting using Pkd1 probe "f" (exon 36-45) and Gapdh (1.2 kb). One representative kidney sample from each transgenic line 6, 18 and 26 is compared to endogenous *Pkd1* transcript of control (C) genetic background and age-matched mice. Quantification of renal transcripts from transgenic Pkd1$_{TAG}$ mouse lines were increased compared to endogenous Pkd1 transcript as indicated below the blot (control refers to 1).

(**B**) Quantitative real-time PCR of Pkd1 expression from renal and extrarenal tissues was carried out using primers in exons 1 and 2. Transgenic mice (n=3; * n= 2) from each of the 3 different lines and non-transgenic age-matched control mice (4-12 mo) were analyzed in triplicata for Pkd1 and S16 that served as an internal control. Quantification of renal expression in these transgenic mice ranged from 1.3

to 15.5-fold relative to endogenous levels of control mice arbitrarily set at 1. Extrarenal tissue expression levels were established in function of Pkd1 levels in control kidneys. Number in parentheses refers to the ratio of transgene expression levels to the organ control. Similar gene expression ratio or fold-increase was detected for each transgenic line across the tissues analyzed.

(**C**) Renal and extrarenal polycystin-1 protein expression analysis in $Pkd1_{TAG}$ 26 mice (6 mo.) by Western blot using the N-terminal Pc-1 7e12antibody. In $Pkd1_{TAG}$ organs, Pc-1 expression was intact and at higher expression levels than controls (6 mo.). Of the organs tested, highest Pc-1 signal was detected in lungs, heart and kidney. Quantities of protein loaded (40 or 80 ug prot) are indicated below the blot. C: non-transgenic control mice; Tg: $Pkd1_{TAG}$ transgenic mice, line 26. Gapdh was used as an internal loading control.

Figure 3 Renal phenotype in $Pkd1_{TAG}$ mice

(**A, B**) Overview of renal cortical sections from adult 20 month-old control and $Pkd1_{TAG}6$ mice, respectively. While control exhibited normal glomeruli (g) and tubule (t), $Pkd1_{TAG}6$ mice showed presence of numerous glomerular and tubular cysts associated with frequent proteinaceous casts (pc) and of tubulointerstitial fibrosis (H&E). Original magnification, x10.

(**C, D**) High power view of renal sections of $Pkd1_{TAG}6$ and 26 mice (26 and 16 mo.) that show epithelial hyperplasia and hypertrophy (H) as well as presence of polyps (arrowhead) in cystic tubules. Original magnification, x 40.

(**E, F**) Assessment of nephron segment origin in control and $Pkd1_{TAG}26$ mice (7 mo.) respectively was determined by immunofluorescence using specific markers of proximal (Lotus tetragonolobus, green), distal (Esculentum Lycopersicon, blue) and collecting ducts (α-Calbindin D28K, red). Transgenic mice displayed cysts from all nephron segments and in higher proportion in proximal and collecting tubules. Noticeably, epithelial hyperplasia and hypertrophy (H) were frequently observed in dilated collecting ducts. Original magnification, x20.

(**G, H**) Analysis of calcium deposits from renal sections of control and $Pkd1_{TAG}26$ (10 mo.) respectively was evaluated by Alizarin red staining. Intense extracellular calcium deposits were detected in the renal papilla of $Pkd1_{TAG}26$ mice (inset) but absence of signal in cysts or in kidneys of non-transgenic mice. Original magnification, x10.

(**I, J**) Proliferation was assessed from control and $Pkd1_{TAG}26$ renal sections (13 mo.) respectively with the Ki67 nuclear proliferation marker. Epithelial cells from normal and dilated tubules displayed higher rate of proliferation in $Pkd1_{TAG}26$ mice compared to control. Original magnification, x40.

(**K, L**) Detection of c-myc in renal tissues of control and $Pkd1_{TAG}6$ (13 mo.) respectively correlated with higher proliferation rate. Increased nuclear and even cytoplasmic staining in cystic and non-cystic regions in $Pkd1_{TAG}6$ relative to control. Original magnification, x40.

(**M, N**) Primary cilia of renal epithelial cells from control and $Pkd1_{TAG}$ mice (1 mo.) respectively were assessed. Triplet figure consists of staining by α-acetylated tubulin (left panel) marker for cilia, DAPI (middle panel) for nucleus and merge (right panel). In control mice, the average length of cilia was estimated to 2-3 μm whereas in $Pkd1_{TAG}26$ mice a significant shift in cilia length distribution to longer cilia of ≥ 5 μm was measured. Original magnification, x100.

Figure 4 Analysis of urinary proteins in $Pkd1_{TAG}$ mice

(**A**) Protein urine samples from all $Pkd1_{TAG}$ mice lines (4 mo.) were compared to non-transgenic age-matched control (C) and SBM transgenic mice (positive control that develop PKD) in addition to serum protein sample (S) from non-transgenic mice on SDS-PAGE stained by Coomassie blue. Albumin normally present in serum was detected at abnormally high levels in $Pkd1_{TAG}26$ urine comparable to SBM urine. $Pkd1_{TAG}$ mice like SBM mice exhibit non-selective proteinuria. Mice also displayed normal excretion of the major urinary proteins (MUPs). M: molecular mass markers of 31 to 200 kDa.

(**B**) Polycystin-1 was analyzed in fractioned urinary samples by Western blot using the N-terminal 7e12 Pc-1 antibody. Two bands (slightly above ~420kDa and ~360-380kDa) were typically detected in native

(N, without treatment) samples whether from total kidney protein extracts of $Pkd1_{TAG}26$, from total urinary proteins (T) or exosome-free fraction (S1) of $Pkd1_{TAG}26$ and of control mice (mean ~9 mo.). A unique Pc-1 band slightly above ~420kDa was observed in exosome (Exo) fractions from $Pkd1_{TAG}$ and control urine whereas the uromodulin-positive (S2) fraction appears devoided of Pc-1. Noticeably, $Pkd1_{TAG}$ transgenic mice in comparison to age-matched control mice consistently showed more intense Pc-1 bands and likely higher Pc-1 excretion. Upon deglycosylation (DG) of protein extracts with PNGase, a unique band is detected at the size of the lowest native band (~360-380kDa), showing strong glycosylation of Pc-1 and indicating that the band above ~420kDa is likely the cleaved form of Pc-1 (predicted mass of 448kDa and 328kDa in glycosylated and deglycosylated respectively).

Figure 5 $Pkd1_{TAG}$ mice hepatic phenotypes

(**A, B**) Macroscopic view of livers is shown from adult control and $Pkd1_{TAG}$ 26 mice (20 mo.) respectively. In comparison to normal liver of control mice, liver of $Pkd1_{TAG}$ mice appeared abnormal with clusters of cysts. Original magnification, x5.

(**C, D**) Overview of liver histologic sections from adult control and $Pkd1_{TAG}26$ mice (14 and 23 mo.), respectively. Notably, a $Pkd1_{TAG}$ mouse shows presence of numerous cysts (c) lined by cuboid epithelium, suggesting tubular cholangiocyte origin. Cluster of cysts are formed focally around the periportal region tubular structures (H&E). Original magnification, x10.

(**E, F**) Liver sections from adult control and $Pkd1_{TAG}26$ mice (11and 14 mo.), respectively. Liver of $Pkd1_{TAG}$ mice displayed severe periportal fibrosis with various levels of increased interstitial fibrosis (Sirius red). Original magnification, x10.

(**G, H**) Proliferation was assessed from liver sections of control and $Pkd1_{TAG}26$ (21 mo.) respectively with the Ki67 nuclear proliferation marker. Cystic epithelium of the liver was associated with higher rate of proliferation compared to non-cystic control. Original magnification, x40.

(**I, J**) Analysis of c-myc in hepatic tissues of control and $Pkd1_{TAG}26$ (16 and 23 mo.) respectively correlated with higher proliferation rate. Increased nuclear and even cytoplasmic staining is observed in cystic regions in $Pkd1_{TAG}$ relative to control. Original magnification, x40.

Figure 6 Cardiac phenotypes in $Pkd1_{TAG}$ mice

(**A, B**) Non-invasive ultrasound of cardiac function of adult control mice and $Pkd1_{TAG}$ 26 mice (16 mo.), respectively. Echocardiography of $Pkd1_{TAG}$ mice detected presence of aortic valve of hyperechoic, indicating calcification and probably stenosis (white arrow). Attached video imaging shows the inability of the aortic valves to fully open.

(**C, D**) Anatomy of hearts from adult control mice and $Pkd1_{TAG}$ mice (8 and 7 mo.), respectively. The heart size of $Pkd1_{TAG}$ mice (0.32g and body weight 16.7g) is readily larger than non-transgenic control (0.27g and body weight 31.5g). Original magnification, x2.5.

(**E, F**) Heart vasculature from adult control mice and $Pkd1_{TAG}$ 26 mice (11 and 13 mo.) respectively, filled with Microfil latex. $Pkd1_{TAG}$ mouse left ventricle hypertrophy was clearly visible under 3D angles by different segmentation and the substantial decreased vascularization of ventricular wall (*).

(**G, H**) Longitudinally sectioned heart from adult control and $Pkd1_{TAG}$ mice (11 and 12 mo.), respectively. View of sectioned heart of $Pkd1_{TAG}$ 26 mouse displays changes in color pigmentation of the left ventricle wall (arrow) due to calcium deposits as defined with specific histology stains. Original magnification, x5.

(**I, J**) Higher-power view of aortic valves from adult control and $Pkd1_{TAG}$ mice (11 and 12 mo.), respectively. $Pkd1_{TAG}$ mouse exhibited severe calcified valves (arrow) stained with Alizarin red consistent with echocardiography. Original magnification, x20.

Figure 7 $Pkd1_{TAG}$ mice vascular defect: intracranial aneurysm.

(**A, B**) Macroscopic view of scalped head is shown from adult control and $Pkd1_{TAG}$26 mice (1 mo.) respectively. Evidence of enlarged skull associated with abnormal brain/ventricle morphology, sagital suture, intracranial hemorrhages and edema in $Pkd1_{TAG}$ mice.

(**C, D**) Overview of brain sections from adult control and $Pkd1_{TAG}$ mice (1 mo.), respectively. Evidence of $Pkd1_{TAG}$ cortex (c) thinning is shown with a major cavity associated with elongated and compressed cerebellum (ce) due to hemorrhage and excessive fluid (H&E). Original magnification, x1.25.

(**E, F**) Brain vasculature from adult control mice and $Pkd1_{TAG}$ 26 mice (11 and 13 mo.) respectively filled with Microfil latex. Evidence of unruptured cerebral aneurysm (arrow) was observed in a $Pkd1_{TAG}$ mouse whereas not detected in vasculature of control mice. Original magnification, x5.

Table 1

A) Urine Analysis

Mice*	Age (mo)	n	Volume (mL)	n	Urea Nitrogen (mmol/L)	n	Creatinine (mmol/L)	n	Protein (g/L)	n	Osmolality (mOsm/kg)
Control	16	5	**0.5** ± 0.2	5	**682** ± 407	5	**4.9** ± 0.6	5	**1.4** ± 0.8	5	**2026** ± 160
$Pkd1_{TAG}$ 6	15	6	**1.6** ± 0.5[b]	6	**309** ± 148[c]	6	**1.1** ± 0.3[d]	6	**0.7** ± 0.3	6	**627** ± 166[d]
Control	4-9	12	**0.7** ± 0.4	12	**809** ± 320	15	**3.9** ± 1.8	11	**6.9** ± 5.5	11	**1426** ± 547
SBM	4-10	10	**2.7** ± 1.3[b]	7	**328** ± 76[c]	8	**1.3** ± 0.6[c]	5	**3.4** ± 1.4	4	**843** ± 265[a]
$Pkd1_{TAG}$ 26	5-7	7	**2.4** ± 1.5[b]	8	**461** ± 267[a]	10	**1.6** ± 1.3[b]	8	**1.1** ± 0.7[b]	6	**985** ± 566

*Urine analysis of $Pkd1_{TAG}$ with control mice at severe renal phenotype time points.
[a] P≤0.02; [b] P≤0.01; [c] P≤0.001; [d] P≤0.0001

B) Blood Analysis

Mice	Age (mo)	n	Hematocrit (%)	n	BUN range (mmol/L)	Creatinine (mmol/L)	Sodium (mmol/L)	Osmolality (mOsm/kg)
Control	6	5	**54** ± 3	5	**6.3 – 8.4** (mean 7.5 ± 0.8)	**19.6** ± 2.6	**151** ± 2	**329** ± 5
$Pkd1_{TAG}$ 6	15	6	**40** ± 3[e]	6	**9.0 – 12.8**	**20.1** ± 3.2	**157** ± 2[d]	**340** ± 4[b]
$Pkd1_{TAG}$ 26	6	7	**35** ± 6[c]	8	**5.5 – 10.8**	**29.8** ± 7.5[b]	**156** ± 2[b]	**336** ± 6[a]

[a] P≤0.05; [b] P≤0.005; [c] P≤0.001; [d] P≤0.0005; [e] P≤0.0001

Table 2

A) Cardiac Dimension Analysis

Mice		Heart wt/ Body wt		Echocardiographic measurement: Left ventricle pw d	Left ventricle pw s	Inter-ventricular septum d	Inter-ventricular septum s	Aortic root diam.	Aortic root area	Left ventricle volume d	Left ventricle volume s	Ventricle diameter d	Ventricle diameter s
		%		10^{-2} mm/wt		10^{-2} mm/wt		10^{-2} mm/wt		µl/wt		10^{-2} mm/wt	
	n		n										
Control	21	**0.7** ±0.1	6	**2.0** ±0.3	**2.8** ±0.6	**2.1** ±0.4	**3.0** ±0.5	**3.5** ±0.2	**4.1** ±0.3	**2.21** ±0.23	**1.01** ±0.24	**10.7** ±0.7	**7.7** ±0.9
$Pkd1_{TAG}6$	26	**0.9**[a] ±0.3	6	**3.8**[c] ±0.6	**5.1**[d] ±0.7	**3.6**[d] ±0.4	**4.9**[d] ±0.5	**5.0**[b] ±0.8	**5.3**[a] ±1.0	**2.17** ±0.35	**0.73** ±0.23	**13.9**[c] ±1.2	**8.8** ±1.1
$Pkd1_{TAG}26$	27	**1.0**[e] ±0.2	4	**3.3**[c] ±0.4	**4.6**[b] ±0.6	**3.2**[a] ±0.6	**4.0** ±1.3	**5.0**[d] ±0.2	**5.7**[d] ±0.2	**3.11** ±1.06	**1.51** ±0.97	**15.2**[a] ±2.4	**10.9** ±3.0

[a] P≤0.05; [b] P≤0.003; [c] P≤0.002; [d] P≤0.0002; [e] P≤10^{-6}
wt = weight; pw = posterior wall; d = diastolic; s = systolic; diam. = diameter

B) Echocardiographic Functional Analysis

Mice		Stroke vol. aorta	Fractional ejection	Fractional shortening	Cardiac output	Heart rate		Aortic valve velocity: Upstream mean	Aortic valve velocity: Upstream peak		Aortic valve velocity: Downstream mean	Aortic valve velocity: Downstream peak		Mitral valve velocity: Upstream mean	Mitral valve velocity: Upstream peak		Mitral valve velocity: Downstream mean	Mitral valve velocity: Downstream peak
		10^{-2} mL/wt	%	%	ml/min/wt	bpm		mm/s			mm/s			mm/s			mm/s	
	n						n			n			n			n		
Control	6	**0.27** ±0.03	**54.8** ±6.5	**28.5** ±4.3	**1.29** ±0.16	**474** ±16	4	**554** ±56	**977** ±140	6	**1152** ±134	**1901** ±247	4	**557** ±79	**899** ±105	6	**743** ±77	**1247** ±133
$Pkd1_{TAG}6$	6	**0.31** ±0.06	**66.6**[b] ±8.1	**36.4**[b] ±6.2	**1.49** ±0.32	**482** ±22	6	**486** ±104	**776** ±170	6	**1155** ±343	**1861** ±565	6	**511** ±74	**851** ±135	6	**800** ±117	**1318** ±208
$Pkd1_{TAG}26$	4	**0.53**[b] ±0.13	**53.6** ±17.1	**28.5** ±12.2	**2.59**[c] ±0.46	**487** ±43	4	**581** ±251	**965** ±431	4	**1705**[a] ±344	**2772**[a] ±562	4	**454** ±103	**817** ±156	4	**714** ±109	**1233** ±205

[a] P≤0.05; [b] P≤0.03; [c] P≤0.01
bpm = beats per minute

Figure 1

5' analysis:

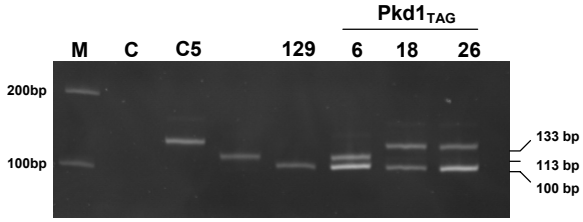

3' analysis: Pkd1 Probe/KpnI

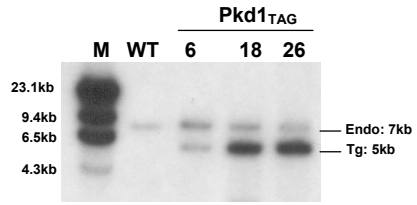

Figure 2

A

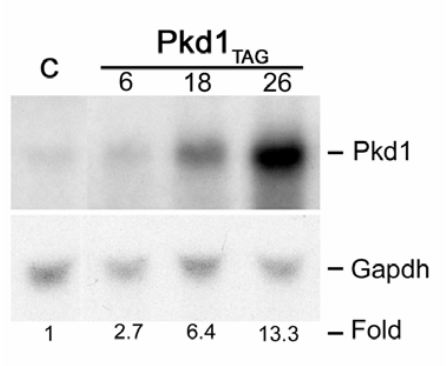

B

Mice	n	Pkd1 expression relative to control kidneys (relative to organ control)						
		Kidneys	Brain	Heart	Lungs	Spleen	Liver	Pancreas
Control	3	1.0	3.5 (1.0)	1.5 (1.0)	2.9 (1.0)	0.5 (1.0)	0.6 (1.0)	0.8 (1.0)
$Pkd1_{TAG}$ 6	3	1.3	5.6 (1.6)	2.3 (1.5)	3.1 (1.1)	0.7 (1.4)	0.8 (1.2)	1.0 (1.2)
$Pkd1_{TAG}$ 18	3	8.0	24.7 (7.1)	13.6 (8.8)	13.9 (4.9)	3.5 (6.6)	3.2 (5.3)	3.0 (3.6)
$Pkd1_{TAG}$ 26	3	15.5	37.7 (10.8)	20.6 (13.3)	22.6 (7.9)	5.8 (11.0)	5.3 (8.7)	10.9 (13.2) *

C

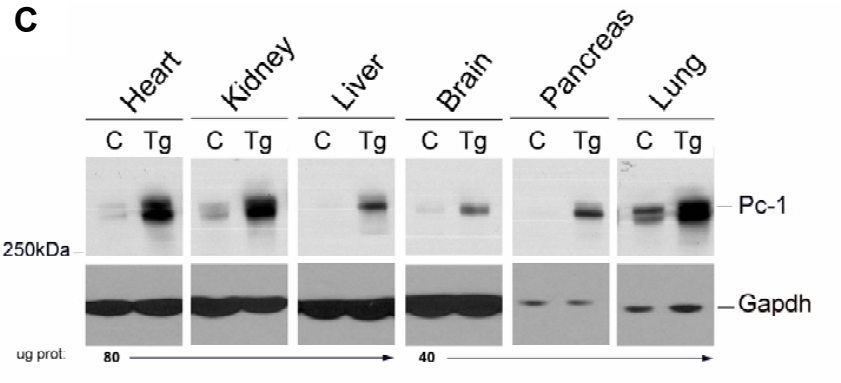

Figure 3

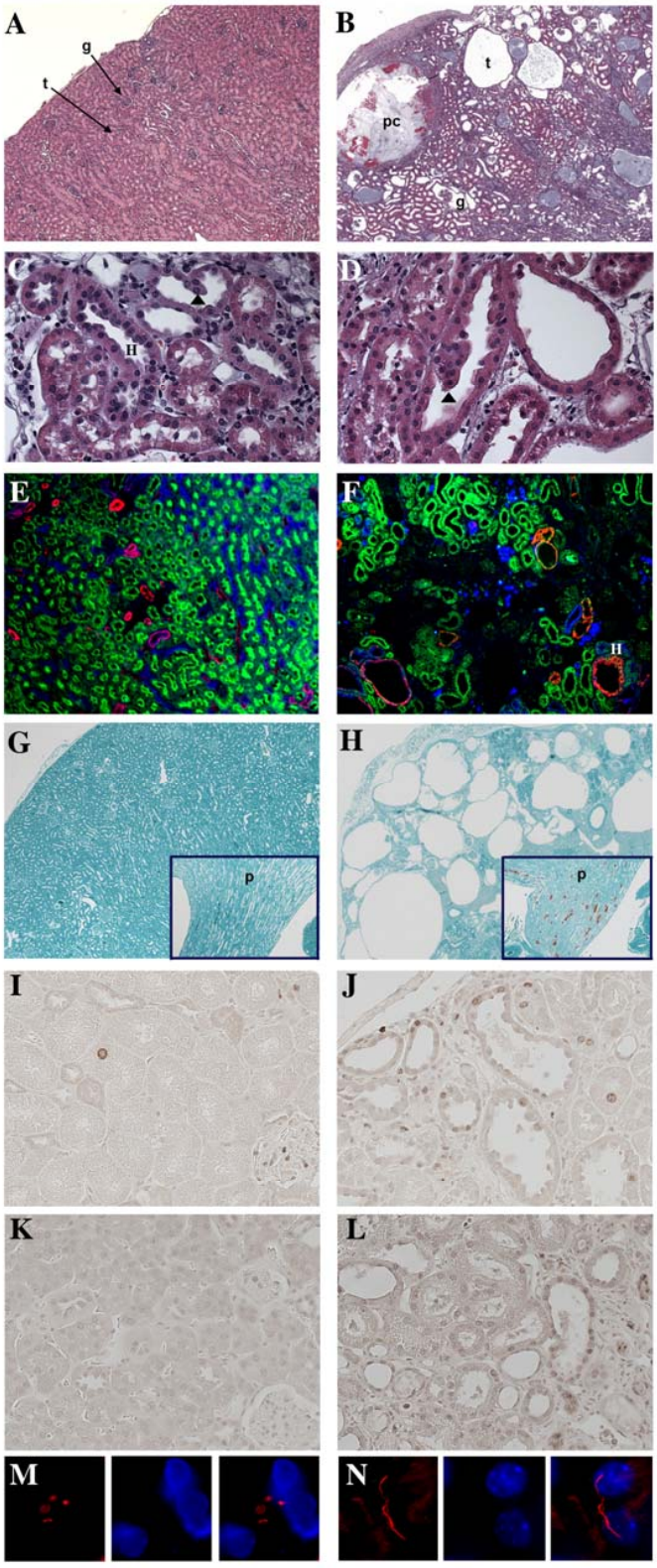

Figure 4

A

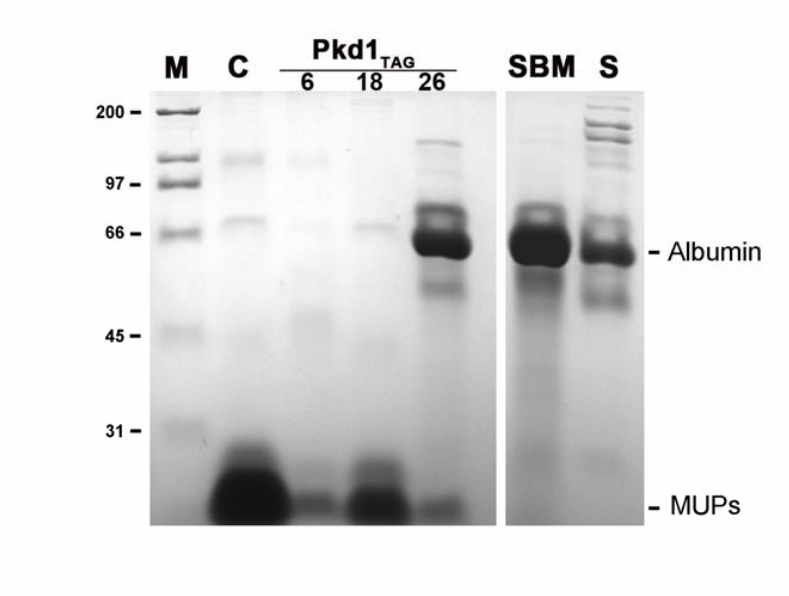
M
C
Pkd1TAG
6
18
26
SBM
S
200
97
66
45
31
Albumin
MUPs

B

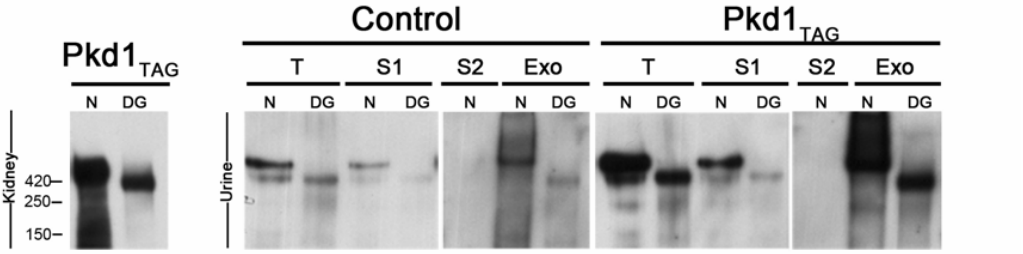
Pkd1TAG
N
DG
Kidney
420
250
150
Control
T
S1
S2
Exo
Urine
Pkd1TAG

Figure 5

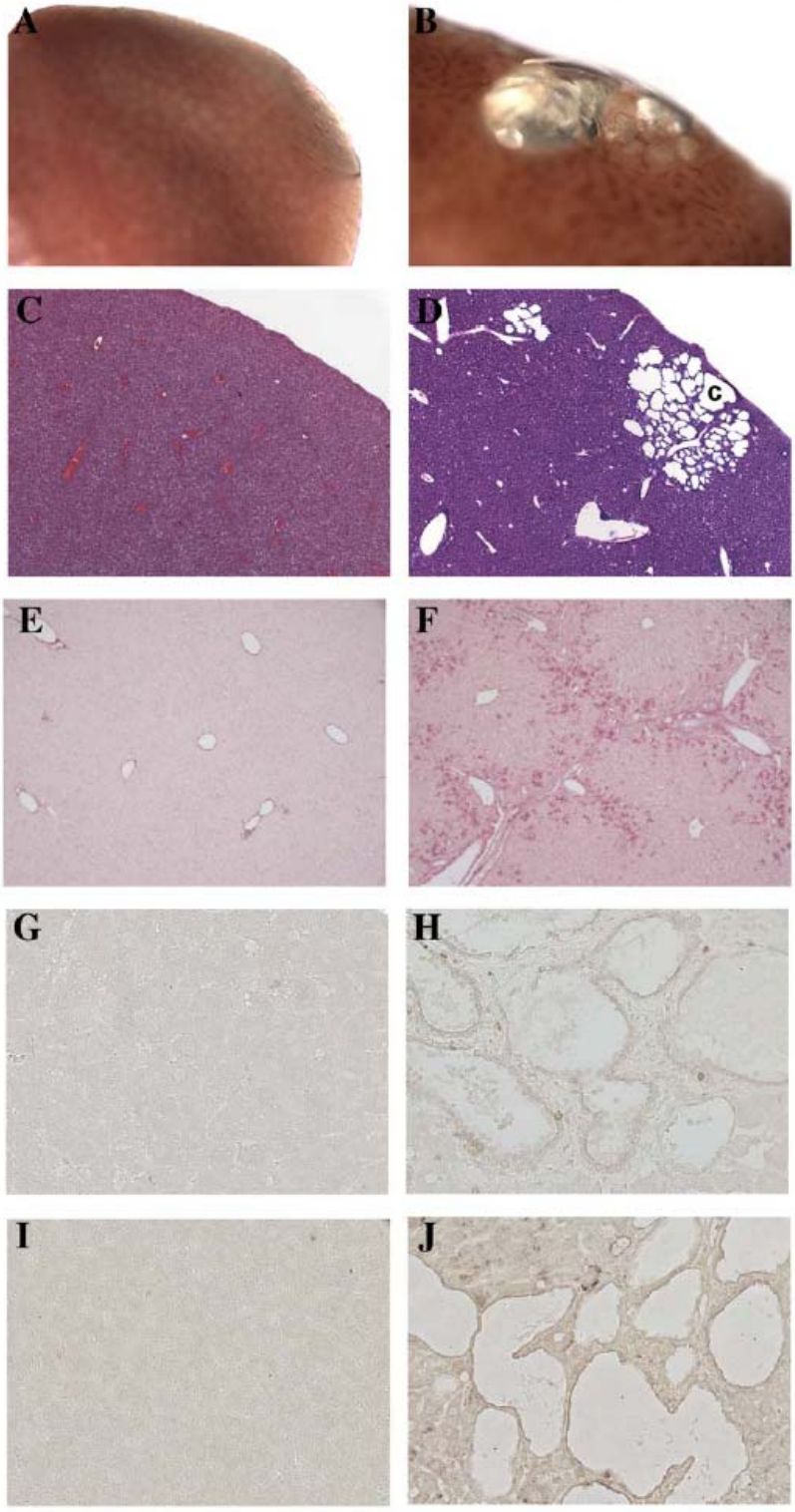

Figure 6

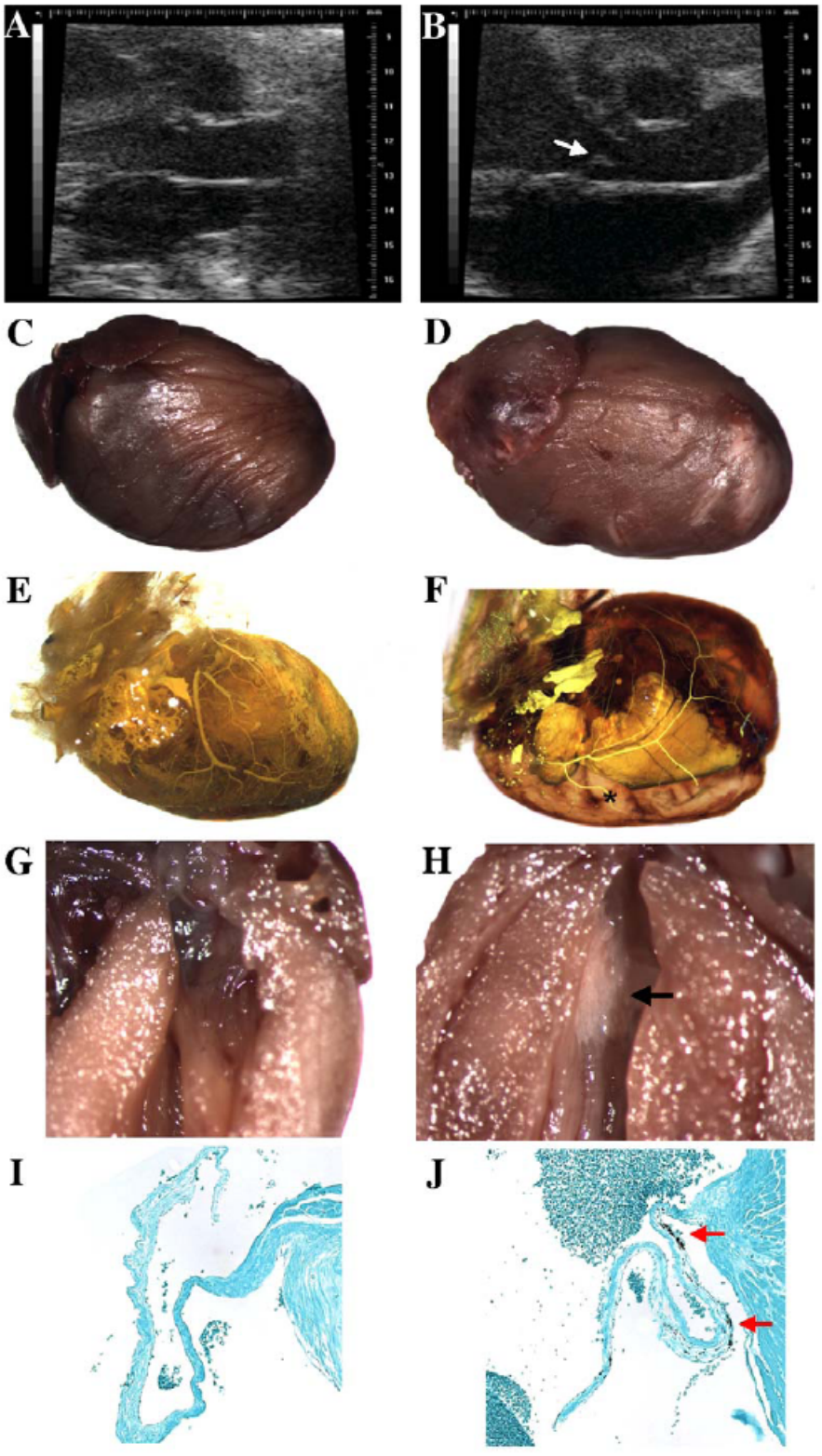

Figure 7

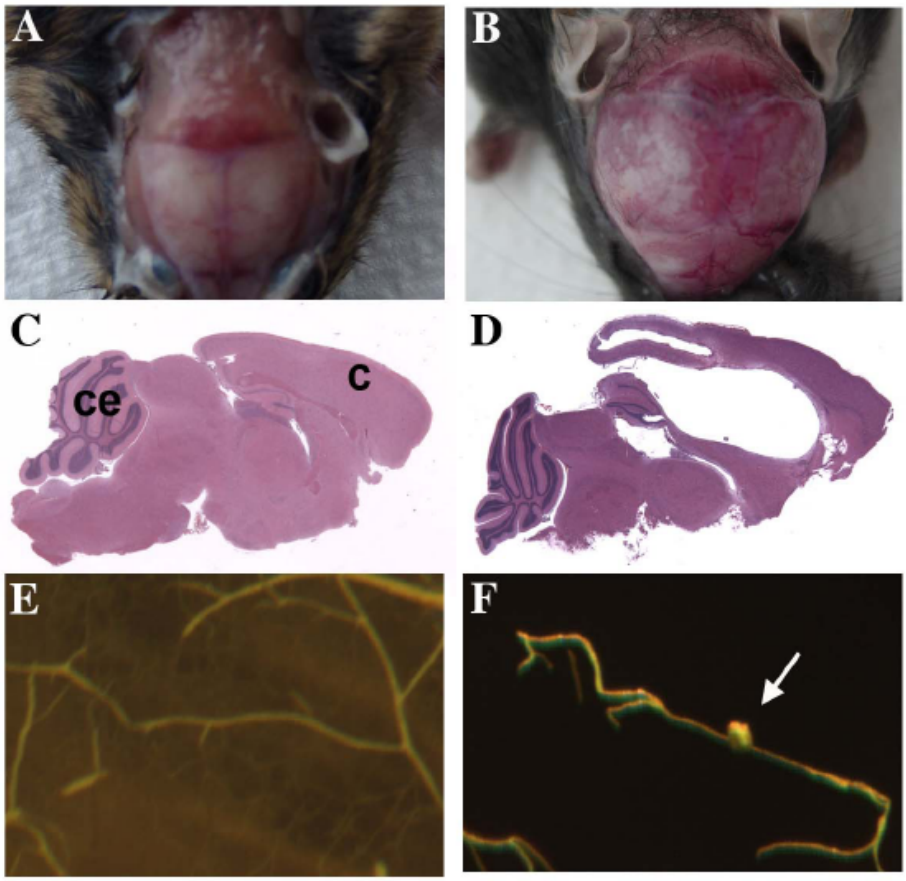

Suppl. Fig 1

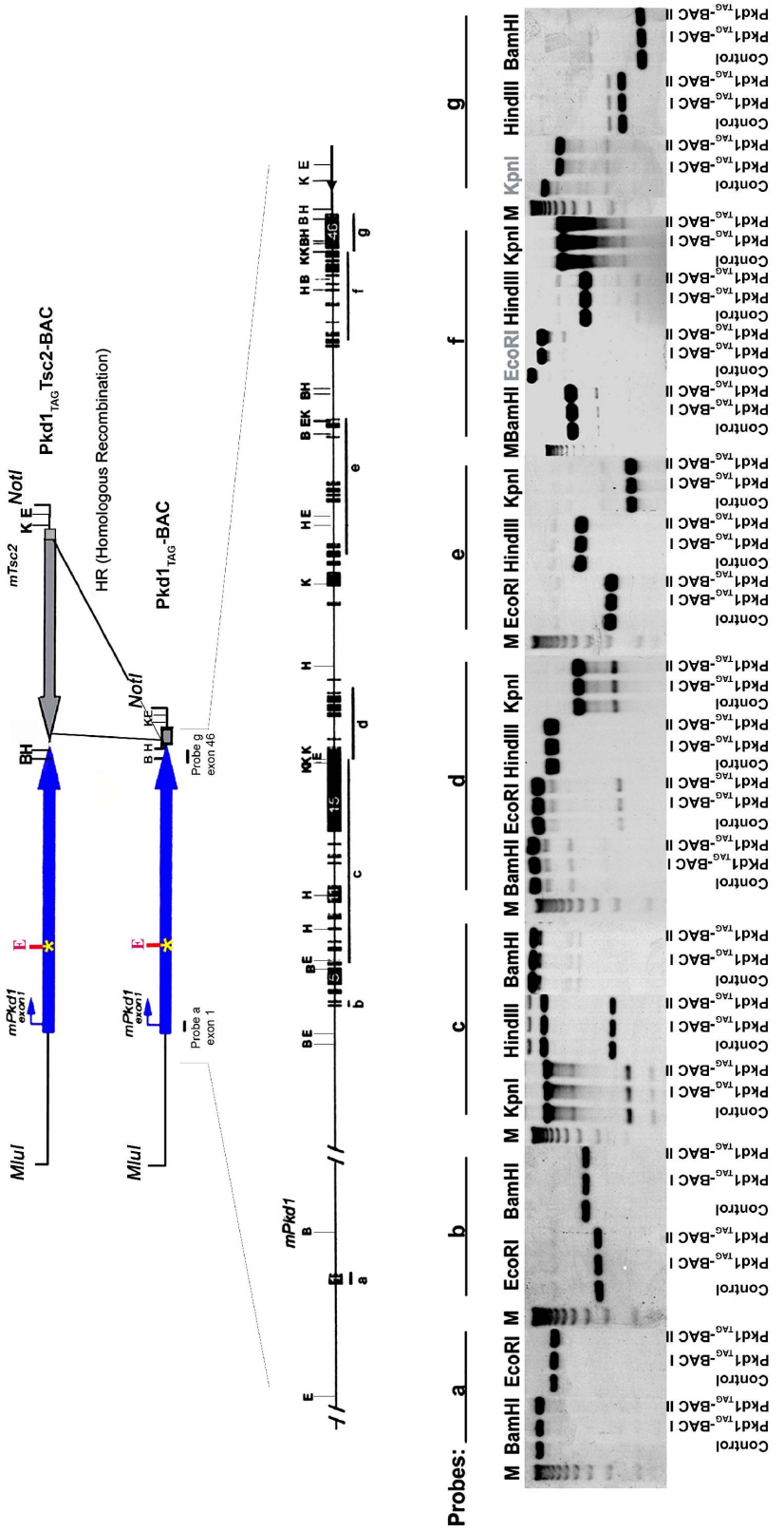
Pkd1TAG-Tsc2-BAC
HR (Homologous Recombination)
Pkd1TAG-BAC
mTsc2
NotI
MluI
mPkd1 exon1
Probe a exon 1
Probe g exon 46
mPkd1
Probes: a b c d e f g
M BamHI EcoRI BamHI M KpnI HindIII BamHI EcoRI HindIII KpnI M EcoRI HindIII KpnI M BamHI EcoRI HindIII KpnI M KpnI HindIII BamHI
Control
Pkd1TAG-BAC I
Pkd1TAG-BAC II

List of Abbreviations

ADPKD	autosomal dominant polycystic kidney disease
Gapdh	glyceraldehyde 3-phosphate dehydrogenase
GPS	G-protein coupled receptor proteolytic site
Pc-1	Pkd1 protein or polycystin-1

CHAPTER V - ARTICLE 2

PROGRESSIVE DEVELOPMENT OF POLYCYSTIC KIDNEY DISEASE IN THE MOUSE MODEL EXPRESSING PKD1 EXTRACELLULAR DOMAIN

Almira Kurbegovic & Marie Trudel*

Institut de Recherches Cliniques de Montreal, Molecular Genetics and Development, Faculte de Medecine, Universite de Montreal, Montreal, Quebec, Canada

Correspondence and proofs:
Dr. Marie Trudel
[redacted]

This article was accepted for publication in Human Molecular Genetics following peer review. The definitive publisher-authenticated version [Hum Mol Genet. 2013 Jun 15;22(12):2361-75] is available online [doi:10.1093/hmg/ddt081].

ABSTRACT

Autosomal dominant polycystic kidney disease (ADPKD) is characterized by slow progression of multiple cysts in both kidneys that lead to renal insufficiency in mid-life or later. ADPKD is associated with mutations mainly in the PKD1 gene (encoding polycystin-1 or PC1) and less frequently, in PKD2 gene (encoding polycystin-2 or PC2). To mimic naturally occurring human PKD1 mutations and gain insight into the PC1 extracellular domain function, four transgenic mouse lines were established with exclusively the extracellular domain of the Pkd1 gene ($Pkd1_{extra}$) under endogenous transcriptional regulation. Expression of the $Pkd1_{extra}$ transgene was 2 to 80 fold above endogenous levels. Strikingly, the $Pc1_{extra}$ protein was more abundant, proportionally to the endogenous. All four transgenic mouse lines consistently displayed progressive renal cystic phenotype. Consequently, these transgenic mice reproducibly developed renal functional alterations similar to human ADPKD with proteinuria, renal insufficiency, anemia and died of renal failure late in life. In precystic kidneys, the $Pkd1_{extra}$ transgene modulated Pc2 expression and thereby, uncovered a potential Pc1-mutant/Pc2 pathogenic crosstalk mechanism. Moreover, the pathophysiologic mechanism also implicates c-myc, a major modulator of cystogenesis. Altogether, the novel $Pkd1_{extra}$ mouse model is the first Pc1 extracellular mutant that reproduces human ADPKD clinical progression and physiopathology.

INTRODUCTION

Human autosomal polycystic kidney disease (ADPKD) is one of the most common genetic diseases. ADPKD is characterized by the presence of many renal epithelial cysts in all segments of the nephron that affect both kidneys. The cystic dilatations of tubules and glomeruli in these kidneys ultimately result in remodeling of the renal architecture and alter renal physiologic functions. Consequently, ADPKD patients develop renal insufficiency during the fifth to sixth decade of life that accounts for ~10% of all individuals requiring renal replacement therapy.

Mutations in the PKD1 or PKD2 genes are associated with ADPKD. The PKD1 gene, the most frequently mutated, is large and spans 54kb consisting of 46 exons, generates a 14kb transcript and encodes a 4302 amino acid protein called polycystin-1 (PC1) (1-4). In silico, PC1 analysis revealed that the amino terminal portion consists of multimodular domains described as: leucine-rich repeats flanked by cysteine-rich structures (LRR), a LDL-A domain, a C-type lectin domain, 16 PKD (Ig-like) tandem repeats, a REJ-like domain (receptor for egg jelly), a G protein-coupled receptor proteolytic site or GPCR-autoproteolysis inducing (GPS or GAIN) (1, 3, 5, 6) just prior to the first transmembrane domain. These motifs are followed by 11 transmembrane domains. The first intracellular/cytoplasmic loop contains a so-called PLAT domain (for PC1, lipoxygenase and alpha toxin) (7-10) whereas the last intracellular loop contains a potential PEST sequence and at the carboxy terminal end, a coiled-coil domain comprised of 5 heptad-repeats. Based on these predictions, the PC1 protein could act as a cell surface receptor or participate in a large membrane protein complex that could be involved in cell-cell and/or cell-matrix interactions. However the role of PC1 and in particular that of the extracellular domain, remains elusive.

A wide spectrum of mutations for the PKD1 gene has been reported and most of them belong to a unique family. Frequently, these PKD1 mutations are predicted to cause truncated transcripts

due to frameshift, deletion, nonsense or splicing defects, although a significant minority is missense (11-14). Some of these mutated PKD1 transcripts have also been shown to produce truncated proteins (15, 16). Notably, patients expressing both a PKD1 truncated allele and a wild type allele developed PKD.

While ADPKD transmission is dominant, the pathogenic mechanism leading to the disease is still not clearly established. Few groups have proposed that a PKD1 gene-dosage or -imbalance dependent mechanism, based on either amorphic/loss-of-gene-function, hypomorphic and hypermorphic/gain-of-gene-function alleles, is responsible for PKD1 pathogenesis. Evidence for recessive inactivation of PKD1 was provided by somatic mutations, in addition to an inherited germ line mutation, found in a subset of renal cysts (17-19). Hypomorphic alleles have also been identified in some ADPKD patients (20). Evidence also points to a gain-of-function mechanism underlying human ADPKD pathogenesis that is supported from overexpression of the normal PKD1 allele as well as by the majority of cysts staining positively for PC1 (15, 21, 22).

In mice, cystogenesis can result from various Pkd1 mutations. A loss-of-heterozygosity, hypomorphic allele has been shown to be associated with the formation of renal cysts (23-30). More recently, we have produced transgenic mice with specific renal and systemic Pkd1 overexpression that developed a cystic phenotype (31, 32). Altogether, these results indicated that a renal imbalance in Pc1 levels could lead to PKD phenotype and suggest that a similar mechanism may prevail in human ADPKD.

To mimic a human ADPKD mutation in mice and gain insight into the role of PC1 extracellular domain in mice, we have generated a truncated form of the Pkd1 gene based on four described truncated ADPKD mutations (p130/E3020X, WS219, Y2991X, W3001X). These mutations are located between the extracellular region and the membrane junction (11, 14) and PC1 lacks

specifically both the membrane-spanning and intracellular domains. Using homologous recombination on our characterized Pkd1-BAC, we have engineered a truncated Pkd1 gene ($Pkd1_{extra}$) that produces only the extracellular Pc1 domain ($Pc1_{extra}$). Expression of this truncated $Pkd1_{extra}$ transgene caused a slow, progressive, cystic phenotype associated with renal insufficiency recapitulating the development of human ADPKD.

RESULTS

Production of $Pkd1_{extra}$-BAC and transgenic mice

To investigate the Pc1 extracellular domain pathogenic role and function, we mimicked a truncated form of PC1 that was previously documented in ADPKD patients namely, WS219, p130/E3020X, Y2991X, W3001X (11, 12, 14, 33). The Pkd1 gene was truncated to delete the protein region just prior the first transmembrane, the membrane-spanning and intracellular domains (Fig. 1A), using homologous recombination on the Pkd1-BAC that we have isolated and characterized (31). The Pkd1-BAC was modified with a recombination vector that contained Pkd1 exon23-25 gene till nucleotide 31,129 corresponding to amino acid 3043 just prior to the first transmembrane region, followed by two point mutations to create a stop codon (F3043X) and adjoined directly to the non-coding sequences of Pkd1 exon 46, poly A and flanking sequences for appropriate transcript processing (Supplementary material, Fig. S1A). This vector served to produce the $Pkd1_{extra}$-BAC that was then analyzed for integrity with four restriction enzyme digestions and seven probes as described for wild type Pkd1-BAC (31) (Supplementary material Fig. S1B). The $Pkd1_{extra}$ fragment (77 kb) was isolated from $Pkd1_{extra}$-BAC (Fig. 1A) that removed BAC vector sequences, Tsc2 regulatory elements and 5' half of the gene to avoid altered expression and was purified for transgenic mice production.

Four $Pkd1_{extra}$ transgenic mouse lines were generated carrying multiple copies of the transgene (~2, 12, 50, 85). These transgenic lines were analyzed for transgene integrity by genomic DNA analysis using polymorphisms, Southern and PCR (32). All lines showed intact flanking sequences of the 5' $Pkd1_{extra}$ transgene based on the presence of a polymorphism (~4.5kb upstream) specific to the 129/Sv strain from which the Pkd1-BAC derives compared to the C57BL/6J and CBA/J strains that served to generate transgenic mice (Fig. 1B). The $Pkd1_{extra}$ transgene integrity was demonstrated by Southern blot analysis using three restriction enzymes and five probes (Fig. 1C, D).

$Pkd1_{extra}$ transgene expression analysis

Transcript analysis was carried out by various complementary means. First, Northern blotting using a two-step agarose gel showed that $Pkd1_{extra}$ kidneys from the different transgenic lines expressed a 9.76kb specific transcript of the expected size whereas the endogenous transcript was detected at 14.14kb (Fig. 2A). Among the four different transgenic lines (n=3-5 mice per line), ~2- to ~80–fold renal expression levels were obtained for the $Pkd1_{extra}$ transgene above the endogenous expression level. Noticeably, the $Pkd1_{extra}$ transgene levels did not appear to alter the endogenous Pkd1 expression levels. Second, semi-quantitative RT-PCR was performed for the 4 transgenic lines at adult age and was designed to distinguish the transgenic from the endogenous transcript by using primers in exon 24 and 3'UTR due to the novel 3' $Pkd1_{extra}$ junction (Fig. 2B). Expression of the truncated $Pkd1_{extra}$ transgene was evaluated relative to the S16 ribosomal protein gene product as internal control. Various quantities of RT aliquots were used to determine the linear range for expression analysis. The $Pkd1_{extra}$ transgene was expressed in all tested tissues (kidneys, brain, liver, lung, spleen) of the four transgenic mouse lines with highest expression in brain and lung (Fig. 2B). The transgene expression pattern essentially followed that of the Pkd1 endogenous gene. Third, quantitative expression analysis for total endogenous and transgene expression were carried out by real-time PCR with primers in exon1 and 2, on transcript from numerous tissues including kidneys, brain, heart, lung, spleen, liver and pancreas. As shown in Figure 2C, renal

expression of total Pkd1 increased proportionally with transgene copy number. In comparison to the kidneys, total Pkd1 expression was generally higher in brain, heart and lung whereas levels were lower in spleen, liver and pancreas.

$Pc1_{extra}$ protein expression analysis

We then monitored protein expression in the $Pkd1_{extra}$ transgenic mice. We first verified by using a Tsc2 antibody against the C-terminal domain that the transgene did not alter Tsc2 protein (tuberin) expression levels since it can induce cyst formation (34-36). As shown in Figure 3A, Tsc2 protein levels were similar both in the lowest and highest $Pkd1_{extra}$ transgenic expressors as in the controls. Significantly, no truncated Tsc2 protein was detected in the transgenic kidneys. These findings confirmed that the transgene did not modify Tsc2 expression levels.

Expression of the protein from the $Pkd1_{extra}$ transgene Pc1 extracellular domain ($Pc1_{extra}$) in comparison to endogenous and full length transgenic Pc1 controls was quantified in adult kidneys (n=5-6/transgenic line) of the four transgenic lines. Pc1 and $Pc1_{extra}$ were detected by immunoblotting with the monoclonal antibody 7e12 that recognize the extrarenal LRR domain (Fig. 3B). The protein specificity was confirmed by the presence of a strong Pc1 band in transgenic kidney extracts of $Pkd1_{TAG}26$ mice overexpressing the native Pkd1 gene (~15-fold) as positive control (32). Truncated $Pc1_{extra}$ protein encoded by the transgene has a predicted mass without post-transcriptional modification of 328kDa same as the N-terminal Pc1 GPS/GAIN domain in comparison to the 466kDa full length Pc1. Levels of $Pc1_{extra}$ in the kidneys increased with transgene copy numbers and RNA expression levels, indicating that this truncated protein is relatively stable (Fig. 3B). Notably, renal expression in the $Pkd1_{extra}$ 11 line displayed markedly higher levels of protein than in the $Pkd1_{TAG}26$ line, despite having similar transgene copy numbers (~12 vs ~15-copies) (Fig. 3B). In fact, the $Pkd1_{TAG}26$ line had comparable levels to the ~2-copy transgene of $Pkd1_{extra}$ 39 line. Interestingly, transgenic $Pkd1_{extra}$ kidneys showed at a given

transgene copy number, a disproportional increase in the levels of the $Pc1_{extra}$ protein relative to the native Pc1. This suggests that the $Pc1_{extra}$ protein is protected from degradation, more stable and/or not secreted in comparison to the native Pc1.

To determine whether this increased expression was characteristic of the $Pc1_{extra}$ protein or peculiar to expression in renal cells, extrarenal tissues were monitored for $Pc1_{extra}$ and Pc1 expression in the $Pkd1_{extra}$ 39 and 11 transgenic mice. Levels of $Pc1_{extra}$ and Pc1 protein for extrarenal tissues followed approximately $Pkd1_{extra}$ transcript levels except for the brain as previously detected in the $Pkd1_{TAG}$ lines (32). Similar to the kidneys, extrarenal tissues of the $Pkd1_{extra}$ lines exhibited higher protein levels of $Pc1_{extra}$ relative to Pc1 for equivalent transcript levels or transgene copy number (Fig. 3C). The similar expression range from the $Pkd1_{extra}$ 39 and $Pkd1_{TAG}$26 lines in Figure 3C suggest that either $Pc1_{extra}$ processing or stability is increased and sustained in renal as well as in extrarenal tissues.

Since the Pc1/$Pc1_{extra}$ band appears as a doublet in wild type and transgenic mice and Pc1 has many glycosylation sites, we examined the glycosylation status of Pc1/$Pc1_{extra}$. Western analysis of total kidney protein extracts was performed with untreated (non-deglycosylated, ND) samples, treated with PNGase that removes all N-linked carbohydrate groups or treated with Endoglycosidase H that cleaves high mannose. To monitor Pc1/$Pc1_{extra}$ within a same set of experiments, significantly less protein (~2.5- to 25-fold) were used for $Pkd1_{extra}$ kidneys relative to controls thereby resulting mainly in the analysis of the transgenic protein. $Pc1_{extra}$ or native Pc1 in $Pkd1_{extra}$, controls and $Pkd1_{TAG}$ mice are heavily glycosylated as indicated by the major shift in size upon treatment with PNGase (Fig. 3D). Further, Pc1/$Pc1_{extra}$ from $Pkd1_{extra}$, controls and $Pkd1_{TAG}$ mice displayed apparently same molecular weight protein. Of interest, transgenic $Pkd1_{extra}$ and controls treated with Endo H generated both forms, Endo H sensitive Pc1/$Pc1_{extra}$ that is presumably localized in the ER and Endo H resistant that has reached the medial-Golgi and potentially the plasma membrane. Notably, the $Pc1_{extra}$ appears to have lower

proportion of Endo H resistant to Endo H sensitive relative to controls suggesting that the overexpressed $Pc1_{extra}$ post-translational maturation is delayed.

To further investigate Pc1 and $Pc1_{extra}$ localization, we established MEF cells from transgenic $Pkd1_{extra}$ 11 and control mice. MEF cells were grown in serum-free media and Pc1/$Pc1_{extra}$ proteins monitored in the media for secretion and in the cells. From cell culture media, the exosomes and exosome-free subfractions were isolated via ultracentrifugation or exoquick. As shown in Figure 3E, Pc1/ $Pc1_{extra}$ proteins were present in exosomes from both non-transgenic control and $Pkd1_{extra}11$ MEFs. In addition, exosomes from $Pkd1_{extra}11$ MEFs displayed substantially higher levels (~10- to 12-fold) of Pc1/ $Pc1_{extra}$ than the controls, consistent with $Pc1_{extra}$ overexpression. In non-transgenic control and $Pkd1_{extra}11$ media devoided of exosomes, free Pc1/ $Pc1_{extra}$ protein levels seems increased (~3-fold) in $Pkd1_{extra}11$ relative to controls, though in decreased proportion based on total expression levels of $Pkd1_{extra}11$ and controls (Figure 3B). An aliquot of MEF cells from $Pkd1_{extra}$ 11 and non-transgenic controls were fractionated in cytosol and triton-soluble membrane (Figure 3F). Marked increase in Pc1/ $Pc1_{extra}$ expression (>10-fold) was detected in total MEF extracts of $Pkd1_{extra}11$ in comparison to controls. In both the cytosol and the triton-soluble membrane fractions, Pc1/ $Pc1_{extra}$ was detected in $Pkd1_{extra}11$ as well as in controls (Figure 3F), correlating with the renal Pc1/ $Pc1_{extra}$ glycosylation analysis.

Histopathologic anomalies in $Pkd1_{extra}$ mice

To evaluate progression of the cystogenic disorder in the $Pkd1_{extra}$ transgenic mouse lines, we carried out non-invasive imaging by ultrasound measurements using a VisualSonics Vevo 660 Imaging System with a 40-MHz scanhead. Analysis of $Pkd1_{extra}$ transgenic lines 11 and 39 (n=8) at ≥15 months showed readily detectable multiple macro and microcysts (Fig. 4A, B).

To investigate the phenotype induced by the transgene expression, we subjected the four $Pkd1_{extra}$ transgenic mouse lines (n>16 per line; n=141) including founders and progenies to complete histological analysis. While our analysis was performed on various organs, anomalies were mainly confined to the kidneys. All transgenic mouse lines exhibited characteristic features of PKD whereas non-transgenic controls did not develop these disorders. Interestingly, very mild renal tubular dilatation can be detected in ~2 month old $Pkd1_{extra}$ mice. With advancing age, the renal tubular dilatation phenotype progressed similarly for both the lowest and highest $Pkd1_{extra}$ expressing lines, a key characteristic of ADPKD (Supplementary material, Fig. S2). Both kidneys of $Pkd1_{extra}$ transgenic mice over time became pale with an embossed surface and were severely affected by macro- and micro-cysts (Fig. 4C, D). Glomeruli displayed prominent cysts associated with hyperplasia of the parietal epithelial cells (Fig. 4F, G, H). The glomerular tufts were hypocellular and became sclerotic. The renal parenchyma displayed tubular cysts but also, loss of tubules as well as presence of mild to extensive interstitial fibrosis (Fig. 4I, J) with localized lymphoid infiltrates often perivascular. Thus the $Pkd1_{extra}$ transgenic mice developed typical PKD manifestations that progressed akin with age in all four lines.

Because defects in tubulogenesis can occur from inhibition of Pc1 cleavage (5), ex vivo incubation of peptides against the Pkd1 extracellular domain (37), and was recently associated with renal cysts formation (38), we queried whether $Pkd1_{extra}$ expression could alter regulation of ureteric branching in vivo. To evaluate ureteric branching or tubulogenesis, we quantified the number of glomeruli/nephron per mm^2 from stained sections in young $Pkd1_{extra}$ transgenic mice at 1.5 months of age as described (39). Analysis of mice with low $Pkd1_{extra}$ (line 39: 12.1± 2.96 glomeruli/mm^2; n=3) and high $Pkd1_{extra}$ expression (line 9: 13.9±0.91 glomeruli/mm^2; n=3) revealed that $Pkd1_{extra}$ transgenic kidneys have similar number of glomeruli relative to wild type controls (12.9±1.55 glomeruli/mm^2; n=5), suggesting that the renal developmental program is not affected by expression

of the $Pkd1_{extra}$ transgene. This finding was also consistent with the kidney size that was comparable in the $Pkd1_{extra}$ and the wild type control at this age.

Since $Pkd1_{TAG}$ mice displayed cilia anomalies prior overt cystogenesis (32), cilia of renal epithelial cells were monitored by α-acetylated tubulin staining in $Pkd1_{extra}$ and control mice. The cilia size distribution measured at μm interval in $Pkd1_{extra}$ 39 and 2 lines at precystic age showed that most cilia (n=389) were of 2-4μm in length (55-61%) similar to controls (n=428; 54%). At cystic age, cilia in $Pkd1_{extra}$ 11 and 2 lines displayed no difference in cilia size distribution or structure relative to controls. This data suggests that the cilia length is not implicated in $Pkd1_{extra}$ cystogenesis.

Altered renal physiologic function in $Pkd1_{extra}$ transgenic mice

Mice from the $Pkd1_{extra}$ transgenic lines exhibited renal functional anomalies resembling those in ADPKD compared to age-matched controls. The renal physiology was investigated by urine analysis in comparison to the severe PKD mouse model SBM (40) as well as by blood analysis (Tables 1, 2). Transgenic mice displayed 3-4-fold increase in urine volume, a concentrating defect that progressed with age (≥15 months). Consequently, renal parameters in these mice also exhibited decrease in urine osmolality, urea nitrogen, creatinine, protein and ion excretion (Table 1). Notably, these alterations are frequent also in human ADPKD. In addition, we qualitatively analyzed the urine protein composition from the four $Pkd1_{extra}$ transgenic mouse lines by SDS-PAGE. As shown in Figure 5A, transgenic mice of all lines displayed non-selective proteinuria. This abnormal protein leakage was already detectable at 12 months and increased further with age. Consistent with these altered urine parameters, the levels of serum BUN and serum creatinine were elevated, indicating renal insufficiency (Table 2). Since renal insufficiency frequently causes hematologic anomalies in both mice and humans, hematocrit was measured in all of our $Pkd1_{extra}$ transgenic mouse lines.

These mice showed important decrease in hematocrit levels, providing evidence for chronic renal insufficiency (Table 2), similar to human ADPKD pathogenesis.

To determine whether $Pc1_{extra}$ in $Pkd1_{extra}$ transgenic mice is present in urinary exosomes and/or free in the urine, as native Pc1 in non-transgenic and $Pkd1_{TAG}26$ controls, we isolated urinary exosomes. $Pc1/Pc1_{extra}$ was detected in exosomes of $Pkd1_{extra}$ lines 2, 11 and 39 and of non-transgenic control and transgenic $Pkd1_{TAG}26$. In transgenic $Pkd1_{extra}$ lines and $Pkd1_{TAG}26$ mice, exosomal $Pc1/Pc1_{extra}$ levels appear to increase in parallel with the range of overexpression (Fig. 5B). In urine free exosome, secreted $Pc1/Pc1_{extra}$ was detected in transgenic $Pkd1_{extra}$ and $Pkd1_{TAG}26$ mice (Fig. 5C). Since non-transgenic control mice had very low to barely detectable Pc1 levels, this implies that mainly $Pc1_{extra}$ is the secreted form in the urine of $Pkd1_{extra}$ lines. Noticeably, levels of $Pc1_{extra}$ in urine free-exosome, upon comparison of total expression in $Pkd1_{extra}$ lines to $Pkd1_{TAG}26$ (Figure 3B), suggest that the $Pc1_{extra}$ protein is not as efficiently secreted as the native Pc1.

Animals from these $Pkd1_{extra}$ transgenic lines manifested late-onset of renal failure. Indeed, the mean lifespan in mice of line 2 (n=10) was ~17.3±4.5 months of age, line 9 (n=9) 23.0±5.5, line 11 (n=20) 17.7±4.4 and line 39 (n=15) 17.4±6.9 months whereas for controls of the same genetic background the mean survival age ranged between 23-29 months.

Functional analysis of $Pkd1_{extra}$ mice on hemizygous Pkd1 background

In an attempt to genetically mimic the human context, the $Pkd1_{extra}$ 39 line was mated to mice with a Pkd1 null allele (41) to produce compound heterozygous $Pkd1_{extra}$ 39; $Pkd1^{+/-}$ mice. Histomorphologic analysis of kidneys in the double heterozygote adult mice (n=12; 11-23 months) was compared to $Pkd1_{extra}$ 39 (n=22; 15-29 months) and $Pkd1^{+/-}$ mice (n=9; 13-26 months). Despite some variability between mice, the $Pkd1_{extra}$ 39; $Pkd1^{+/-}$ kidneys exhibited tubular and glomerular

cysts in late adulthood reminiscent of $Pkd1_{extra}$ 39 mice perhaps with a trend toward more pronounced phenotype as evidenced by general tubular dilatations (Fig. 6). While the $Pkd1^{+/-}$ mice displayed limited renal cysts in a minority of old individuals as reported previously (42, 43), both the double heterozygote and the $Pkd1_{extra}$ 39 adult mice develop a severe phenotype. To assess whether this phenotype results from the transgene expression or from the imbalanced between $Pkd1_{extra}$ to Pkd1 expression, the strongest expressing line $Pkd1_{extra}$ 2 was mated onto the $Pkd1^{+/-}$ background. The $Pkd1_{extra}2$; $Pkd1^{+/-}$ kidneys (n=11; 7-26 months) exhibited slightly more severe phenotype than in the $Pkd1_{extra}2$ (n=31; 13-31months), as observed in the $Pkd1_{extra}$ 39; $Pkd1^{+/-}$ kidneys. This experiment supports that the $Pkd1_{extra}$ transgene is likely responsible for the phenotype. These double heterozygous mice seem to display a more severe PKD phenotype than the $Pkd1_{extra}$ transgenic mice by exhibiting more invasive phenotype and/or occasional earlier onset as a possible effect of $Pkd1^{+/-}$ phenotype.

Identification of $Pkd1_{extra}$ renal molecular targets

Since Pc1 is implicated in a large complex with Pc2 in the kidneys (44-48) and Pkd2 dysregulation can cause cysts (41, 49, 50), we queried whether Pkd2 renal expression levels might be altered in $Pkd1_{extra}$ mice. Expression analysis was performed by Northern on kidneys of all transgenic $Pkd1_{extra}$ mouse lines (n=16). In comparison to control (n=6), there is no increase expression of endogenous Pkd2 transcript in $Pkd1_{extra}$ mice (Fig. 7A). In contrast, the protein expression levels of Pc2 determined by immunoblot was increased (mean ~6- to 8-fold) in pre-cystic kidneys of all four $Pkd1_{extra}$ lines (n≥4/line; n=18) relative to control (n=4) mice (Fig. 7B). Similar range of Pc2 increased was observed in compound heterozygous $Pkd1_{extra}$; $Pkd1^{+/-}$ mice (data not shown). These experiments suggest that the $Pc1_{extra}$ could prevent Pc2 degradation or could modulate Pc2 protein stabilization, and thereby lead to cyst formation. Underlying these hypotheses is whether $Pc1_{extra}$ potentially can interact with Pc2. To monitor for this interaction, coimmunoprecipitation

experiments were performed with Pc2 in $Pkd1_{extra}$ mice in comparison to $Pkd1_{TAG}$ and control mice (Supplementary material, Fig. S3). Our results shows that Pc1 interacts with Pc2 in kidneys of $Pkd1_{TAG}$ 26 line in higher proportion than wildtype controls, consistent with increase Pc1 expression. Intriguingly, there seems also increased interaction in kidneys of $Pkd1_{extra}$ 39 mice relative to controls. Although we demonstrate the existence of a protein complex, this result does not distinguish interaction of $Pc1_{extra}$ and/or Pc1 with Pc2 but both could be possible based on cellular studies (48). Of significance, the $Pc1_{extra}$ protein at the very least does not hamper Pc1-Pc2 interaction. Overall, the analogous Pc2 enhanced expression in these $Pkd1_{extra}$ transgenic lines is particularly striking and correlates with the similar slow progression and development of PKD phenotype in these mice.

Because we have previously detected increase c-myc renal expression in human ADPKD kidneys and in a PKD transgenic mouse model due to Pkd1 overexpression, we next evaluated renal c-myc expression levels in the four transgenic $Pkd1_{extra}$ mouse lines. When very mild renal phenotype was observed at 2-4 months of age, these mice had little to no difference in endogenous c-myc transcript expression relative to control (data not shown). However, c-myc expression increased up to 6-fold at 19-26 months of age associated with cystogenesis defects (Fig. 7C). This result is also consistent with the increased c-myc expression detected in the Pkd2 transgenic mice (51).

DISCUSSION

This study reports the first Pkd1 mutant mouse model, $Pkd1_{extra}$, of ADPKD. This mutant $Pkd1_{extra}$ model addresses concomitantly the pathogenic role of the Pc1 extracellular domain since the Pkd1 gene in a BAC was truncated to delete the protein membrane spanning and intracellular domains. Four $Pkd1_{extra}$ transgenic mouse lines with ~2- to ~80-fold increase in transcript and protein expression of the Pkd1 extracellular domain reproducibly developed late

renal morphological alterations typical of the human ADPKD. Renal insufficiency is apparent at late age and mice die of renal failure. The Pc2 overexpression in the precystic $Pkd1_{extra}$ transgenic mice, a known PKD pathogenic mechanism, correlated with the comparable phenotype and revealed a potential novel regulatory crosstalk between $Pc1_{extra}$ and Pc2. Our results also indicate that the cystogenic mechanism responsible for the $Pkd1_{extra}$ phenotype is associated with activation of c-myc signaling. The gradual recruitment of cysts with clinical progression makes this human-like $Pkd1_{extra}$ mouse mutant, a relevant model of ADPKD pathophysiology.

The design of our truncated Pc1, $Pc1_{extra}$, homologous to characterized human ADPKD mutations, corresponds to the encoded form documented in four patients with different truncated mutations at the extracellular domain/membrane junction or in proximity of the natural GPS/GAIN cleavage site (11, 14). This $Pc1_{extra}$ mutant form devoided of the membrane-spanning and intracellular regions should be normally glycosylated, maintain its structural conformation/folding, potentially tethered to the membrane and/or secreted, based on previous truncated receptor analysis (5, 52-55). Consequently, we have addressed the role of $Pc1_{extra}$ function within the Pkd1 systemic regulation. The four different $Pkd1_{extra}$ transgenic founder mice and lines expressed the transgene in a copy dependent manner. The expression pattern of the $Pkd1_{extra}$ transgene in various tissues, generally paralleled that of the endogenous Pkd1 gene, albeit for slightly lower levels in the brain as observed in Pkd1 full-length transgenic mice (32). This pattern suggests that the flanking regions of the $Pkd1_{extra}$ transgene contain most of the necessary regulatory elements for proper expression and regulation. Of interest, expression of the $Pkd1_{extra}$ transgene at 2-80 fold that of endogenous did not affect the transcriptional regulation of the endogenous Pkd1 gene, consistent with no autoregulatory feedback as suggested (46).

The $Pkd1_{extra}$ transgenic mouse lines in presence of endogenous gene had complete penetrance of the phenotype and shared several physiopathologic features with ADPKD. These include the development of cysts in the cortex, medulla and glomeruli, together with epithelial hyperplasia, interstitial fibrosis and focal interstitial inflammation. In parallel, alterations in renal function progressed with time and at mid-age, $Pkd1_{extra}$ mice had signs of renal insufficiency. Since the PKD phenotype was consistently observed in all 4 different transgenic mouse lines and the transgene integration into the mouse genome is a random phenomenon, the phenotype cannot simply be a consequence of chromosomal position effect but results from $Pkd1_{extra}$ expression. Moreover, we showed that $Pkd1_{extra}$ cystogenesis does not occur from an indirect role that targets a stage in the process of ciliogenesis or of ureteric branching during development. Hence our results provide clear evidence that overexpression of the mutated Pkd1 transgene, $Pkd1_{extra}$, can produce multiple renal cysts. These $Pkd1_{extra}$ mice are the most valuable orthologous mouse models generated by mimicking natural, pathologically relevant, mutations of the human PKD1 gene that can also recapitulate the slow progression of PKD.

Noticeably, the protein levels of $Pc1_{extra}$ in the kidneys correlated with the $Pkd1_{extra}$ transcript levels, indicating that a stable truncated $Pc1_{extra}$ protein was produced and reached substantial expression levels in some lines. The cellular levels of $Pc1_{extra}$ were however, in considerable excess relative to native Pc1 for similar transcript levels. The higher levels of $Pc1_{extra}$ protein than expected in comparison to native Pc1 suggested at least two explanations that are not mutually exclusive. The first is that $Pc1_{extra}$ is protected from degradation, potentially from the loss of the PEST motif localized in the truncated intracellular domain. The second possibility is that $Pc1_{extra}$ is not efficiently secreted and/or excreted from renal epithelial exosomes in contrast to the native Pc1 (32). This latter mechanism is consistent with the lower levels of secreted $Pc1_{extra}$ relative to the native Pc1 in urine and MEF cells and correlated with the apparent delay in $Pc1_{extra}$ post-

translational maturation determined by glycolysation status. These results correlated with cell studies that expressed an analogous truncated human PKD1 due to premature termination codon at p130/E3020X and showed a small amount of PC1 extracellular domain secreted in media whereas most remained tethered or intracellular (5). Furthermore, we show that the difference in levels of secreted $Pc1_{extra}$ relative to native Pc1 in urine and MEF cells occurred independently of Tsc2 dysregulation previously associated with mislocalization of Pc1 (56). Nevertheless, $Pc1_{extra}$ like some truncated receptors appears to proceed via the typical secretory pathway, as it is heavily glycosylated, excreted in exosomes and secreted. In fact, a considerable amount of $Pc1_{extra}$ was excreted in exosomes and freely secreted that may interfere with the normal Pc1 extracellular function (57). In addition, altered $Pc1_{extra}$ protein distribution may be pathogenic by not localizing to a site of functional task.

Few hypothetical mechanisms for $Pkd1_{extra}$ cystogenesis may prevail. One plausible mechanism is that the $Pc1_{extra}$ protein virtually indistinguishable from the naturally cleaved GPS/GAIN-Pc1 may interfere with the native Pc1 autoproteolytic cleavage and/or alter Pc1 downstream signaling. Alternatively, one mechanism may be attributed to the imbalance between the cleaved Pc1 extracellular domain and the transmembrane and intracellular domains. A dynamic interaction between the extra- and intra-cellular domains may require tight regulation to transmit changes from the microenvironment through channel activity or signaling pathways. Nonetheless, an intriguing finding is that expression of the $Pkd1_{extra}$ transgene in the kidneys at various RNA or protein levels lead to similar progression and severity of the phenotype. This result indicates that $Pc1_{extra}$ could be sufficient to produce the phenotype but may be limited by the availability of ligands, interacting partners and/or downstream targets and therefore the disruptive signal cannot be increased further in a dose-dependent mechanism as reported for the Pkd1 full-length transgenic mice (32). Moreover, the onset and phenotypic progression of PKD

in the $Pkd1_{extra}$ mice are milder than in the Pkd1 full-length transgenic mice. Consequently, this raises the question of $Pkd1_{extra}$ pathogenetic mechanism(s) triggered in these mice in comparison to the Pkd1 overexpressing mice.

Insights into these $Pkd1_{extra}$ potential pathogenic mechanism(s) was provided by analysis of renal Pc1 interacting partner Pc2. While no difference in Pc2 expression was noted in the $Pkd1^{-/-}$ and $Pkd1^{+/-}$ embryos (29), all four $Pkd1_{extra}$ transgenic lines displayed increase Pc2 expression which argues for a $Pc1_{extra}$ specific effect. Interestingly, the significantly enhanced Pc2 expression occurred despite similar Pkd2 transcript levels and indicates that $Pc1_{extra}$ may modulate directly or indirectly Pc2 protein levels through a post-transcriptional mechanism. This response may result from a compensatory mechanism, reduced Pc2 protein secretion and/or decreased Pc2 degradation mechanism. Of importance, the remarkably similar range of Pc2 elevated levels correlated with the comparable PKD developmental progression in these $Pkd1_{extra}$ transgenic lines. Compelling support for this interrelation is provided from the Pc2 overexpressing transgenic mice that developed very similar onset and progression of renal PKD phenotype (50). These correlations extend to the absence of liver or pancreatic anomalies in $Pkd1_{extra}$ mice as observed in transgenic Pkd2 mice (51). Such results, combined with the observation that Pkd1 expression in cells was able to modulate the localization and perhaps the function of Pc2 (47), suggest that $Pkd1_{extra}$ pathogenic mechanism may be triggered by the dysregulation of Pc2 that in turn control cystogenic threshold.

Both Pc1 and Pc2 form complexes with many signaling molecules, hence abnormally high Pc1 or Pc2 levels likely disrupt downstream signaling. Consistent with this rationale, Pkd2 transgenic mice revealed stimulation of c-myc expression (51) one of the major mediator of cystogenesis in both human and mouse (21, 40). Likewise, c-myc expression was also elevated in $Pkd1_{extra}$

kidneys (herein) as well as in kidneys of Pkd1 overexpressing transgenic mice (31, 32). This data indicates that $Pc1_{extra}$ directly and/or via Pc2 can modulate a downstream signaling pathway that cause dysregulation of c-myc.

From the $Pkd1_{extra}$ mice analyses, it is plausible that the interactions of the expressed mutant $Pc1_{extra}$ promote Pc2 expression. Activation of such crosstalk regulation provides evidence for a novel cystogenic mechanism. These findings suggest that other truncated PC1 mutants may also trigger this pathogenic crosstalk. Together with previous human and mouse studies on PKD mutational mechanism, this cystogenic crosstalk mechanism is not only consistent, but substantiates a dosage dependent mechanism for ADPKD.

In conclusion, the $Pkd1_{extra}$ mice constitute the first Pc1 extracellular mutant that can reproduce the clinical renal phenotypes progression of human ADPKD disease. This model has established the basis for future studies to dissect the functions of the multimodular Pkd1 extracellular domain. Most importantly, our results provide major insights into a novel PKD pathogenic mechanism implicating a regulatory crosstalk between a truncated Pc1 mutant and Pc2. This model will be invaluable for the characterization of multiple facets of Pkd1 pathophysiology and devise innovative therapeutic strategies.

MATERIALS AND METHODS

DNA constructs and homologous recombination in $Pkd1_{extra}$-BAC

List of all primers used is provided in supplementary materials Table1.

We have previously isolated a murine Pkd1-BAC derived from a murine 129/Sv library that contained ~129 kb insert with the entire Pkd1 gene (31) as well as ~37 kb of upstream and ~39.1 kb of downstream flanking sequences including the Tsc2 gene body. To create a BAC with only

Pc1 extracellular domain, we removed Pc1 transmembrane and cytoplasmic domain by homologous recombination in the Pkd1-BAC, adjoining amino acid 3042 (exon 25, nt 9442-9444, accession number: U70209), a translation termination codon (UAA) and the native 3'UTR of the Pkd1 gene (exon 46, nt 13819). To produce the truncation, Exon23-25 fragment including the stop codon was obtained by amplification (1.25kb), digested with ClaI (NEB) and BamHI (Invitrogen) (nt 9445) and introduced into the same corresponding sites of p-Bluescript. A second fragment containing the 3'UTR Pkd1/3'UTR Tsc2-intron39 was amplified (1.163kb) and then was subsequently digested with BamHI/BclI (nt 13820/4980) and inserted in BamHI of p-Bluescript. The novel junctions of the resulting exon23-25/3'UTR Pkd1/3'UTR Tsc2-intron39 plasmid were sequenced to confirm appropriate cloning. This plasmid was then digested with PvuII (2.45 kb) and introduced into the SmaI site of the BAC recombination vector (PLD53.SC-AB) (58). This BAC recombination vector containing Pkd1 exon23-25/3'UTR Pkd1/3'UTR Tsc2-intron39 served to modify the wild type Pkd1-BAC by homologous recombination protocol as previously described (31, 32). DNA from resolved BACs were analysed by Southern for appropriate modifications by four probes: exon 1 (nt 1-509); exon 7-15 (nt. 1752-6622); exon 23-25 (nt. 8579-9443) and exon 46 (nt. 12760-13820). The integrity of the modified $Pkd1_{extra}$-BAC was also confirmed by PFGE and by sequencing the junction between the exons 25 and 46.

Production and genotyping of transgenic mice

The new $Pkd1_{extra}$-BAC was digested to isolate the $Pkd1_{extra}$ gene away from the murine Tsc2 gene and the BAC vector sequences with MluI a unique site ~24.8 kb upstream of Pkd1 initiation codon and ClaI site ~21.6 kb downstream of Pkd1 stop codon. The 77 kb $Pkd1_{extra}$ fragment was isolated and purified for microinjection into fertilized (C57BL/6JXCBA/J)F2 mouse eggs as described previously (40).

Transgenic mice were analyzed for transgene integrity. The 5' upstream sequence was monitored by a polymorphic sequence located in the murine Pkd1 gene at 4.47 kb upstream of the ATG translation initiation codon. A PCR protocol was designed to distinguish the 129/Sv of the Pkd1-BAC from the C57BL/6J and CBA/J inbred strains that served to produce transgenic mice (32). Integrity of $Pkd1_{extra}$ transgene sequences were monitored by signal intensity from Southern Blot of genomic DNA digested with EcoRI and hybridized with 6 genomic probes: exon 1, exons 2-3, exons 7-15, exons 15-20, exons 25-34, exon 46. To verify transgene integrity in the 3' downstream sequences, genomic DNA from founder mice and progenies of the four transgenic mouse lines were analysed by Southern Blot. Three restriction enzymes (EcoRI, BamHI and HindIII (Invitrogen)) that distinguished the endogenous Pkd1 gene from the $Pkd1_{extra}$ transgene were used with the exons 23-25 Pkd1 genomic probe.

Renal function analysis

Blood urea nitrogen (BUN), creatinine, urinary proteins and osmolality levels were determined from urine of transgenic (n>3/line) and non-transgenic age-matched control mice (n>4). For urine analysis, 350 to 500 µl were collected per mouse. BUN and creatinine were measured with a CX9 Beckmann apparatus while osmolality was evaluated with a radiometer. Qualitative assessment of urinary proteins was also performed with ~50 µg of proteins on 8% SDS-PAGE as described (59) and stained with Coomassie Blue. Blood serum from transgenic and control mice was also analysed for BUN and creatinine levels.

Histopathological analysis

Transgenic and non-transgenic age-matched control mice were sacrificed and tissues kidney, lung, liver, brain, spleen, heart and pancreas readily removed. Tissues were immediately placed in formalin or paraformaldehyde and following fixation were embedded in paraffin. Five-µm-thick

sections were stained with hematoxylin & eosin (H&E) for morphological evaluation. Fibrosis analysis was carried out on both kidneys of transgenic and age-matched control mice (n= 4-5 mice/line). Five µm sections were stained with Sirius red to evaluate fibrosis. Levels of renal fibrosis were quantified in function of μm^2 with a 10X objective from 4 cortical fields of each kidney using the Northern Eclipse.

RNA expression analysis

Total RNA from transgenic and age-matched control tissues including kidneys, brain, lung, spleen, heart, liver and pancreas was extracted with guanidium thiocyanate or trizol/chloroform method (60). RNA integrity was verified by electrophoresis on formaldehyde-agarose gel (61). Expression of the $Pkd1_{extra}$ transgene was analyzed by both semi-quantitative RT-PCR and real-time PCR approaches. Each pair of primers was designed such that only spliced mRNA would produce the predicted amplification products of 290, 94 and 103 bp for $Pkd1_{extra}$, Pkd1 total (endogenous and transgene) and S16 respectively. For semi-quantitative PCR, control reactions were first performed using a wide range of RT aliquots to test for linearity amplification. PCR reactions were carried out for both $Pkd1_{extra}$ and S16 internal control were run on 10% polyacrylamide/TBE1X gel and visualized by ethidium bromide staining. Image Quant 5.0 software was used for the semiquantitative evaluation. For real-time PCR, all reactions were carried out in triplicate in a Quanti Tech SYBR Green PCR master mix (Qiagen and Quanta) using Mx4000/3005 multiplex PCR apparatus (Stratagene).

Expression analyses of $Pkd1_{extra}$ transgene and Pkd1 endogenous gene were monitored by Northern blotting. Total kidney RNA from adult transgenic and non-transgenic mice of approximately same age (30µg) was DNAse digested and separated by electrophoresis on a two-step 0.8%/1.5 % formaldehyde-agarose gel and transferred to nylon membranes (Osmonics inc.) and were hybridized with Pkd1 exon 15-20 cDNA probe (1.55kb) for transgene, Pkd1 exon36-45

cDNA probe (1.6kb) for endogenous Pkd1 and for internal control a Gapdh cDNA probe (1.2kb) as previously described (62). Pkd2 expression analysis was performed by Northern blotting and evaluated by hybridization with Pkd2 cDNA probe (2.2kb) (generous gift from Dr. S. Somlo) and Gapdh as control. Expression analysis of c-myc in $Pkd1_{extra}$ mice was evaluated by Northern blot analysis as described for Pkd2. RNA (20μg) was hybridized with a c-myc probe consisting of exons 2 and 3 and the ribosomal protein L32 (rpL32) that served as loading control. Both scanned films or phosphoimager were quantified by with Image Quant 5.0 software

Protein analysis

Total protein extract was prepared from transgenic and non-transgenic renal and extrarenal tissues, homogenized in RIPA buffer and cocktail of proteases inhibitors (SIGMA). Protein extracts (36μg extrarenal, 48μg renal) were loaded on 4-12% Tris-Glycine SDS-polyacrylamide gels (NUPAGE, Invitrogen) and transfer at 4^0C overnight, 30 Volts using Biotrace™ PVDF membrane (Pall). Membranes were hybridized with the monoclonal 7e12 antibody (16) for detection of Pc1 (generous gift of Drs C. Ward and P. Harris). Secondary HRP-conjugated antibodies allowed detection by ECL Plus Western Blotting Detection System (Amersham Biosciences). Deglycosylation analysis was performed with PNGase and EndoH (New England Biolabs) as described in (32) and monitored on 4-12% Bis-Tris gels. For Tsc2 protein/tuberin analysis, proteins (8μg) were loaded on a two-step 6.25%/12.25 % polyacrylamide gel and detected using a rabbit polyclonal SC893 that recognize the carboxy-terminal fragment (20aa). For Pc2 analysis, immunoblotting was similar to Pc1, protein extracts (200μg) were used on 8% Tris-Glycine SDS-polyacrylamide gel (BIORAD) and transfer on nitrocellulose membrane. Hybridization was carried out with the YCC2 polyclonal antibody (generous gift of Drs Y. Cai and S. Somlo) (41). Gapdh (Abcam), β-tubulin and β-actin (Sigma) served as loading controls.

MEF cells were isolated from $Pkd1_{extra}$ transgenic and non-transgenic embryos (e14.5), incubated for 2-3 days with FBS until confluency. MEF cells were replated in serum-free media for 3 days to analyze free-secreted Pc1 in the media and Pc1 in exosomes. Both Exoquick™ (System Biosciences, Medicorp) for exosomes as described by the manufacturer and ultracentrifugation for exosomal and exosomal-free fractions were carried out as described in (32). PBS-washed MEF cells were centrifuged at 100000g, supernatant fraction (cytosolic) was collected and the unsoluble pellet resuspended and incubated in lysis buffer containing 1% Triton (Triton-soluble fraction, membrane). Proteins were analyzed on 3-8% Tris acetate gel (Nu-Page, Invitrogen) and as controls for exosomes, the Alix/αAIP1 mouse monoclonal antibody (BD Transduction Lab) was used. Urinary protein from exosomes were obtained from 600-650µl of pooled adult urine and precipitated with Exoquick™ and processed as MEF cells. Similarly, exosomal and exosomal-free fractions (250µg) were isolated by ultracentrifugation and processed as above and with sheep anti-THP antibody (Abcam).

Coimmunoprecipitation analysis was performed on adult kidney samples (600µg) incubated with 2µg of the monoclonal anti-rat Pc2 antibody, generously provided by Alabama University PKD core facility and with Protein A/G Plus-Agarose beads (SantaCruz Biotechnology). Material was analyzed on 4-12% Bis-Tris (Invitrogen), controls consist of non-specific binding to the beads alone (-) without Pc2 antibody.

ACKNOWLEDGMENTS

This work was supported by grants from the Canadian Institutes of Health Research, The Polycystic Kidney Disease Foundation of Canada and of USA and the Kidney Foundation of Canada to M. T. and a Frederick Banting and Charles Best of Canada Graduate Scholarship Award to A.K. We acknowledge kind gifts of antibodies from Drs Y. Cai, S. Somlo, C. Ward, P. Harris and the Alabama University PKD Core facility and of $Pkd1^{+/-}$ mice from Dr. S. Somlo. The authors are grateful to Dr Chiara Gamberi and Nicolas Ah-Son for critical reading of the manuscript.

REFERENCES

1 Consortium, E.P.K.D. (1993) Identification and characterization of the tuberous sclerosis gene on chromosome 16. *Cell*, **75**, 1305-1315.

2 Consortium, E.P.K.D. (1994) The polycystic kidney disease 1 gene encodes a 14 kb transcript and lies within a duplicated region on chromosome 16. *Cell*, **77**, 881-894.

3 Burn, T.C., Connors, T.D., Dackowski, W.R., Petry, L.R., Van Raay, T.J., Millholland, J.M., Venet, M., Miller, G., Hakim, R.M., Landes, G.M. *et al.* (1995) Analysis of the genomic sequence for the autosomal dominant polycystic kidney disease (PKD1) gene predicts the presence of a leucine-rich repeat. *Hum. Mol. Genet.*, **4**, 575-582.

4 Consortium, I.P.K.D. (1995) Polycystic Kidney Disease: The complete structure of the PKD1 gene and its protein. *Cell*, **81**, 289-298.

5 Qian, F., Boletta, A., Bhunia, A.K., Xu, H., Liu, L., Ahrabi, A.K., Watnick, T.J., Zhou, F. and Germino, G.G. (2002) Cleavage of polycystin-1 requires the receptor for egg jelly domain and is disrupted by human autosomal-dominant polycystic kidney disease 1- associated mutations. *Proc. Natl. Acad. Sci. USA*, **99**, 16981-16986.

6 Arac, D., Boucard, A.A., Bolliger, M.F., Nguyen, J., Soltis, S.M., Sudhof, T.C. and Brunger, A.T. (2012) A novel evolutionarily conserved domain of cell-adhesion GPCRs mediates autoproteolysis. *EMBO J.*, **31**, 1364-1378.

7 Bateman, A. and Sandford, R. (1999) The PLAT domain: a new piece in the PKD1 puzzle. *Current Biology*, **9**, R588-R590.

8 van Tilbeurgh, H., Egloff, M.P., Martinez, C., Rugani, N., Verger, R. and Cambillau, C. (1993) Interfacial activation of the lipase-procolipase complex by mixed micelles revealed by X-ray crystallography. *Nature*, **362**, 814-820.

9 Gillmor, S.A., Villasenor, A., Fletterick, R., Sigal, E. and Browner, M.F. (1998) The structure of mammalian 15-lipoxygenase reveals similarity to the lipases and the determinants of substrate specificity. *Nat. Struct. Biol.*, **4**, 1003-1009.

10 Naylor, C.E., Eaton, J.T., Howells, A., Justin, N., Moss, D.S., Titball, R.W. and Basak, A.K. (1998) Structure of the key toxin in gas gangrene. *Nat. Struct. Biol.*, **5**, 738-746.

11 Peral, B., Gamble, V., Stron, C., Ong, A.C.M., Sloane-Stanley, J., Zerres, K., Winearls, C.G. and Harris, P.C. (1997) Identification of mutations in the duplicated region of the polycystic kidney disease 1 gene (PKD1) by a novel approach. *Am. J. Hum. Genet.*, **60**, 1399-1410.

12 Rossetti, S., Chauveau, D., Walker, D., Saggar-Malik, A., Winearls, C.G., Torres, V.E. and Harris, P.C. (2002) A complete mutation screen of the ADPKD genes by DHPLC. *Kidney Int.*, **61**, 1588-1599.

13 Thomas, R., McConnell, R., Whittacker, J., Kirkpatrick, P., Bradley, J. and Sandford, R. (1999) Identification of mutations in the repeated part of the autosomal dominant polycystic kidney disease type 1 gene, PKD1, by long-range PCR. *Am. J. Hum. Genet.*, **65**, 39-49.

14 Brook-Carter, P.T., Peral, B., Ward, C.J., Thompson, P., Hughes, J., Maheshwar, M.M., Nellist, M., Gamble, V., Harris, P.C. and Sampson, J.R. (1994) Deletion of the TSC2 and PKD1 genes associated with severe infantile polycystic kidney disease - a contiguous gene syndrome. *Nature Genet.*, **8**, 328-332.

15 Ward, C.J., Turley, H., Ong, A.C.M., Comley, M., Biddolph, S., Chetty, R., Ratcliffe, P.J., Gatter, K. and Harris, P.C. (1996) Polycystin, the polycystic kidney disease 1 protein, is expressed by epithelial cells in fetal, adult and polycystic kidney. *Proc. Natl. Acad. Sci. USA*, **93**, 1524-1528.

16 Ong, A.C.M., Harris, P.C., Davies, D.R., Pritchard, L., Rossetti, S., Biddolph, S., Vaux, D.J.T., Migone, N. and Ward, C.J. (1999) Polycystin-1 expression in PKD1, early onset PKD1

and TSC2/PKD1 cystic tissue: implications for understanding cystogenesis. *Kidney Int.*, **56**, 1324-1333.

17 Qian, F., Watnick, T.J., Onuchic, L.F. and Germino, G.G. (1996) The molecular basis of focal cyst formation in human autosomal dominant polycystic kidney disease type I. *Cell*, **87**, 979-987.

18 Brasier, J.L. and Henske, E.P. (1997) Loss of the polycystic kidney disease (PKD1) region of chromosome 16p13 in renal cyst cells supports a loss-of-function model for cyst pathogenesis. *J. Clin. Invest.*, **99**, 194-199.

19 Koptides, M., Constantinides, R., Kyriakides, G., Hadjigavriel, M., Patsalis, P.C., Pierides, A. and Deltas, C.C. (1998) Loss of heterozygosity in polycystic kidney disease with a missense mutation in the repeated region of PKD1. *Hum. Genet.*, **103**, 709-717.

20 Rossetti, S., Kubly, V.J., Consugar, M.B., Hopp, K., Roy, S., Horsley, S.W., Chauveau, D., Rees, L., Barratt, T.M., van't Hoff, W.G. *et al.* (2009) Incompletely penetrant PKD1 alleles suggest a role for gene dosage in cyst initiation in polycystic kidney disease. *Kidney Int.*, **75**, 848-855.

21 Lanoix, J., D'Agati, V., Szabolcs, M. and Trudel, M. (1996) Dysregulation of cellular proliferation and apoptosis mediates human autosomal dominant polycystic kidney disease (ADPKD). *Oncogene*, **13**, 1153-1160.

22 Ong, A.C.M., Ward, C.J., Butler, R.J., Biddolph, S., Bowker, C., Torra, R., Pei, Y. and Harris, P.C. (1999) Coordinate expression of the autosomal dominant polycystic kidney disease proteins, polycystin-2 and polycystin-1, in normal and cystic tissue. *Am. J. Pathol.*, **154**, 1721-1729.

23 Pritchard, L., Sloane-Stanley, J.A., Sharpe, J.A., Aspinwall, R., Lu, W., Buckle, V., Strmecki, L., Walker, D., Ward, C.J., Alpers, C.E. *et al.* (2000) A human *PKD1* transgene generates functional polycystin-1 in mice and is associated with a cystic phenotype. *Hum. Mol. Genet.*, **9**, 2617-2627.

24 Boulter, C., Mulroy, S., Webb, S., Fleming, S., Brindle, K. and Sandford, R. (2001) Cardiovascular, skeletal, and renal defects in mice with a targeted disruption of the *Pkd1* gene. *Proc. Natl. Acad. Sci. USA*, **98**, 12174-12179.

25 Kim, K., Drummond, I., Ibraghimov-Beskrovnaya, O., Klinger, K. and Arnaout, M.A. (2000) Polycystin 1 is required for the structural integrity of blood vessels. *Proc. Natl. Acad. Sci. USA*, **97**, 1731-1736.

26 Lu, W., Peissel, B., Babakhanlou, H., Pavlova, A., Geng, L., Fan, X., Larson, C., Brent, G. and Zhou, J. (1997) Perinatal lethality with kidney and pancreas defects in mice with a targetted PKD1 mutation. *Nat. Genet.*, **17**, 179-181.

27 Lu, W., Shen, X., Pavlova, A., Lakkis, M., Watrd, C.J., Pritchard, L., Harris, P.C., Genest, D.R., Perez-Atayde, A.R. and Zhou, J. (2001) Comparison of *Pkd1*-targeted mutants reveals that loss of polycystin-1 causes cystogenesis and bone defects. *Hum. Mol. Genet.*, **10**, 2385-2396.

28 Muto, S., Aiba, A., Saito, Y., Nakao, K., Nakamura, K., Tomita, K., Kitamura, T., Kurabayashi, M., Nagai, R., Higashihara, E. *et al.* (2002) Pioglitazone improves the phenotype and molecular defects of a targeted *Pkd1* mutant. *Hum. Mol. Genet.*, **11**, 1731-1742.

29 Wu, G., Tian, X., Nishimura, S., Markowitz, G.S., D'Agati, V., Park, J.H., Yao, L., Li, L., Geng, L., Zhao, H. *et al.* (2002) *Trans*-heterozygous *Pkd1* and *Pkd2* mutations modify expression of polycystin kidney disease. *Hum. Mol. Genet.*, **11**, 1845-1854.

30 Lantinga-van Leeuwen, I.S., Dauwerse, J.G., Baelde, H.J., Leonhard, W.N., van de Wal, A., Ward, C.J., Verbeek, S., Deruiter, M.C., Breuning, M.H., de Heer, E. *et al.* (2004) Lowering of *Pkd1* expression is sufficient to cause polycystic kidney disease. *Hum. Mol. Genet.*, **13**, 3069-3077.

31 Thivierge, C., Kurbegovic, A., Couillard, M., Guillaume, R., Cote, O. and Trudel, M. (2006) Overexpression of PKD1 Causes Polycystic Kidney Disease. *Mol. Cell. Biol.*, **26**, 1538-1548.

32 Kurbegovic, A., Cote, O., Couillard, M., Ward, C.J., Harris, P.C. and Trudel, M. (2010) Pkd1 transgenic mice: adult model of polycystic kidney disease with extrarenal and renal phenotypes. *Hum. Mol. Genet.*, **19**, 1174-1189.

33 Phakdeekitcharoen, B., Watnick, T.J. and Germino, G.G. (2001) Mutation analysis of the entire replicated portion of *PKD1* using genomic DNA samples. *J. Am. Soc. Nephrol.*, **12**, 955-963.

34 Kobayashi, T., Minowa, O., Kuno, J., Mitani, H., Hino, O. and Noda, T. (1999) Renal Carcinogenesis, Hepatic Hemangiomatosis, and Embryonic Lethality Caused by a Germ-Line *Tsc2* Mutation in Mice. *Cancer Res.*, **59**, 1206-1211.

35 Onda, H., Lueck, A., Marks, P.W., Warren, H.B. and Kwiatkowski, D.J. (1999) $Tsc2^{+/-}$ mice develop tumors in multiple sites that express gelsolin and are influenced by genetic background. *J. Clin. Invest.*, **104**, 687-698.

36 Cheadle, J.P., Reeve, M.P., Sampson, J.R. and Kwiatkowski, D.J. (2000) Molecular genetic advances in tuberous sclerosis. *Hum. Genet.*, **107**, 97-114.

37 Van Adelsberg, J. (1999) Peptides from the PKD repeats of polycystin, the PKD1 gene product, modulate pattern formation in the developing kidney. *Dev. Gen.*, **24**, 299-308.

38 Mao, Y., Mulvaney, J., Zakaria, S., Yu, T., Morgan, K.M., Allen, S., Basson, M.A., Francis-West, P. and Irvine, K.D. (2011) Characterization of a Dchs1 mutant mouse reveals requirements for Dchs1-Fat4 signaling during mammalian development. *Development*, **138**, 947-957.

39 Couillard, M. and Trudel, M. (2009) C-myc as a modulator of renal stem/progenitor cell population. *Dev. Dyn.*, **238**, 405-414.

40 Trudel, M., D'Agati, V. and Costantini, F. (1991) C-myc as an inducer of polycystic kidney disease in transgenic mice. *Kidney Int.*, **39**, 665-671.

41 Wu, Q., D'Agati, V., Cai, Y., Markowitz, G., Park, J.H., Reynolds, D.M., Maeda, Y., Le, T.C., Hou JR., H., Kucherlapati, R. *et al.* (1998) Somatic inactivation of Pkd2 results in polycystic kidney disease. *Cell*, **93**, 177-188.

42 Ahrabi, A.K., Terryn, S., Valenti, G., Caron, N., Serradeil-Le Gal, C., Raufaste, D., Nielsen, S., Horie, S., Verbavatz, J.M. and Devuyst, O. (2007) PKD1 haploinsufficiency causes a syndrome of inappropriate antidiuresis in mice. *J. Am. Soc. Nephrol.*, **18**, 1740-1753.

43 Lu, W., Fan, X., Basora, N., Babakhanlou, H., Law, T., Rifai, N., Harris, P.C., Perez-Atayde, A.R., Rennke, H.G. and Zhou, J. (1999) Late onset of renal and hepatic cysts in *Pkd1*-targeted heterozygotes. *Nat. Genet.*, **21**, 160-161.

44 Tsiokas, L., Kim, E., Arnould, T., Sukhatme, V.P. and Walz, G. (1997) Homo- and heterodimeric interactions between the gene product of PKD1 and PKD2. *Proc. Natl. Acad. Sci. USA*, **94**, 6965-6970.

45 Qian, F., Germino, F.J., Cai, Y., Zhang, X., Somlo, S. and Germino, G.G. (1997) PKD1 interacts with PKD2 through a probable coiled-coil domain. *Nat. Genet.*, **16**, 179-183.

46 Newby, L.J., Streets, A.J., Zhao, Y., Harris, P.C., Ward, C.J. and Ong, A.C. (2002) Identification, characterization, and localization of a novel kidney polycystin-1-polycystin-2 complex. *J. Biol. Chem.*, **277**, 20763-20773.

47 Hanaoka, K., Qian, F., Boletta, A., Bhunia, A.K., Plontek, K., Tslokas, L., Sukhatme, V.P., Guggino, W.B. and Germino, G.G. (2000) Co-assembly of polycystin-1 and -2 produces unique cation-permeable currents. *Nature*, **408**, 990-994.

48 Chapin, H.C., Rajendran, V. and Caplan, M.J. (2010) Polycystin-1 surface localization is stimulated by polycystin-2 and cleavage at the G protein-coupled receptor proteolytic site. *Mol. Biol. Cell*, **21**, 4338-4348.

49 Wu, G., Markowitz, G.S., D'Agati, V.D., Factor, S.M., Geng, L., Tibara, S., Tuchman, J., Cai, Y., J.H., P., van Adelsberg, J. *et al.* (2000) Cardiac defects and renal failure in mice with targeted mutations in *PKD2*. *Nat. Gen.*, **24**, 75-78.

50 Park, E.Y., Sung, Y.H., Yang, M.H., Noh, J.Y., Park, S.Y., Lee, T.Y., Yook, Y.J., Yoo, K.H., Roh, K.J., Kim, I. *et al.* (2009) Cyst formation in kidney via B-Raf signaling in the PKD2 transgenic mice. *J. Biol. Chem.*, **284**, 7214-7222.

51 Burtey, S., Riera, M., Ribe, E., Pennekamp, P., Passage, E., Rance, R., Dworniczak, B. and Fontes, M. (2008) Overexpression of PKD2 in the mouse is associated with renal tubulopathy. *Nephrol. Dial. Transplant.*, **23**, 1157-1165.

52 Ahn, K., Herman, S.B. and Fahnoe, D.C. (1998) Soluble human endothelin-converting enzyme-1: expression, purification, and demonstration of pronounced pH sensitivity. *Arch. Biochem. Biophys.*, **359**, 258-268.

53 Horan, T.P., Simonet, L., Jacobsen, R., Mann, M., Haniu, M., Wen, J., Arakawa, T., Kuwamoto, M. and Martin, F. (1998) Coexpression of G-CSF with an unglycosylated G-CSF receptor mutant results in secretion of a stable complex. *Protein Expr. Purif.*, **14**, 45-53.

54 Okamoto, T., Sekiyama, N., Otsu, M., Shimada, Y., Sato, A., Nakanishi, S. and Jingami, H. (1998) Expression and purification of the extracellular ligand binding region of metabotropic glutamate receptor subtype 1. *J. Biol. Chem.*, **273**, 13089-13096.

55 Robbins, M.J., Ciruela, F., Rhodes, A. and McIlhinney, R.A. (1999) Characterization of the dimerization of metabotropic glutamate receptors using an N-terminal truncation of mGluR1alpha. *J. Neurochem.*, **72**, 2539-2547.

56 Kleymenova, E., Ibraghimov-Beskrovnaya, O., Kugoh, H., Everitt, J., Xu, H., Kiguchi, K., Landes, G., Harris, P. and Walker, C. (2001) Tuberin-dependent membrane localization of polycystin-1: a functional link between polycystic kidney disease and the TSC2 tumor suppressor gene. *Mol. Cell*, **7**, 823-832.

57 Hogan, M.C., Manganelli, L., Woollard, J.R., Masyuk, A.I., Masyuk, T.V., Tammachote, R., Huang, B.Q., Leontovich, A.A., Beito, T.G., Madden, B.J. *et al.* (2009) Characterization of PKD protein-positive exosome-like vesicles. *J. Am. Soc. Nephrol.*, **20**, 278-288.

58 Gong, S., Yang, X.W., Li, C. and Heintz, N. (2002) Highly Efficient Modification of Bacterial Artificial Chromosomes (BACs) Using Novel Shuttle Vectors Containing the R6Kγ Origin of Replication. *Genome Res.*, **12**, 1992-1998.

59 De Paepe, M.E. and Trudel, M. (1994) The transgenic SAD mouse: A model of human sickle cell glomerulopathy. *Kidney Int.*, **46**, 1337-1345.

60 Couillard, M., Guillaume, R., Tanji, N., D'Agati, V. and Trudel, M. (2002) c-myc-induced Apoptosis in Polycystic Kidney Disease is Independent of FasL/Fas Interaction. *Cancer Res.*, **62**, 2210-2214.

61 Trudel, M., Lanoix, J., Barisoni, L., Blouin, M.-J., Desforges, M., L'Italien, C. and D'Agati, V. (1997) C-myc-induced Apoptosis in Polycystic Kidney Disease is Bcl-2 and p53 Independent. *J. Exp. Med.*, **186**, 1873-1884.

62 Guillaume, R., D'Agati, V., Daoust, M. and Trudel, M. (1999) Murine Pkd1 is a developmentally regulated gene from morula to adulthood: Role in tissue condensation and patterning. *Dev. Dyn.*, **214**, 337-348.

FIGURE LEGENDS

1. Production of $Pkd1_{extra}$ transgenic mice

A) Schematic representation of the Pkd1 wild type and $Pkd1_{extra}$ -BAC construct deleted of transmembrane and intracellular domains. The $Pkd1_{extra}$-BAC is shown in dark grey (exons: boxes and introns: lines) and the deleted Pkd1 domains are indicated as open boxes/lines. The STOP on $Pkd1_{extra}$-BAC corresponds to the insertion of a termination translation codon in exon 25. Six probes used for analysis of genomic integrity span exons 1, 7-15, 15-20, 23-25, 36-45, 46 are illustrated below the $Pkd1_{extra}$-BAC construct. Restriction sites are indicated above the construct as follows: E, EcoRI; B, BamHI; H, HindIII; C, ClaI; M, MluI.

B) Genomic analysis of the 5' regulatory region of transgenic $Pkd1_{extra}$ mice was monitored using a polymorphism at ~4.5kb upstream of the ATG translation initiation codon of murine Pkd1 gene. The 100bp band corresponds to the 5' region of Pkd1 gene of 129/Sv origin that indicates integrity of this region in $Pkd1_{extra}$ transgene. M: 100bp DNA ladder; C: H_2O, control for PCR reaction; C57: C57BL/6J mice; CBA: CBA/J mice; 129: 129/Sv mice.

C) Genomic analysis of the $Pkd1_{extra}$ transgene was carried out on Southern blot using EcoRI digestion with the exon 7-15 probe. The 9.6kb band indicates integrity of the Pkd1 gene in this region. M: λ HindIII marker.

D) Analysis of the 3' exon 25-46 junction of $Pkd1_{extra}$ transgene by Southern blot was accomplished using BamHI, EcoRI and HindIII digestions with exon 23-25 probe. The hybridization pattern highlights the differences between endogenous Pkd1 and $Pkd1_{extra}$ in the truncated region. M: λ HindIII marker.

2. Transcript expression analysis of $Pkd1_{extra}$ transgene

A) Analysis of the renal adult tissues (n=2; 19-26 months) of the four transgenic lines and two age-matched non-transgenic mouse controls monitored by Northern blot for $Pkd1_{extra}$ transcript

($Pkd1_{extra}$) using exon 15-20 probe and endogenous Pkd1 ($Pkd1_{endo}$) using exon 36-45 probe. Expression of Gapdh served as internal loading control. $Pkd1_{extra}$ expression range was from ~2- to 80-fold over endogenous Pkd1 expression.

B) Semi-quantitative RT-PCR expression studies were carried out to detect the $Pkd1_{extra}$ transcript specifically. Representative analysis from $Pkd1_{extra}$ transgenic line 2 is shown for kidney, lung, brain, liver and spleen, using primers in exon 24 and in 3' UTR. Highest expression was consistently observed in kidney, lung and brain for all lines. Ribosomal protein S16 served as internal control. M: 100bp DNA ladder; Ki: kidney, Lu: lung, Br: brain, Li: liver, Sp: spleen.

C) Quantitative real-time PCR was carried out in triplicata for adult $Pkd1_{extra}$ mice (n=3) of all transgenic lines. Expression analysis on kidney, lung, brain, liver, heart, spleen and pancreas was performed using primers in exon 1 and exon 2 of Pkd1 gene. Control kidneys were set at 1. Transgene expression analysis followed the Pkd1 endogenous expression pattern and was relatively proportional to transgene copy number. *: n=2.

3. Analysis of $Pc1_{extra}$ expression in mice

A) Expression of Tsc2 protein (tuberin) was monitored in kidneys of the lowest and highest expressing $Pkd1_{extra}$ lines 39 and 2 (n=3/per line). Expression of Gapdh served as internal loading control. No detectable difference in Tsc2 expression was observed in the $Pkd1_{extra}$ compared to the non-transgenic control kidneys.

B) Endogenous and transgenic Pc1/$Pc1_{extra}$ protein expression levels analyzed on a gel gradient by Western blot are shown for adult kidneys (n=2-3) of three $Pkd1_{extra}$ mouse lines. Pc1 was detected using 7e12 monoclonal antibody with both long and short exposures along with internal control Gapdh. Expression of the truncated Pc1 protein, $Pc1_{extra}$ was within similar range as

transcript levels. Highest levels were obtained in line 2 and lowest in line 39. The $Pc1_{extra}$ protein band appears to migrate as the Pc1 protein from endogenous control and transgenic $Pkd1_{TAG}$ 26.

C) Analysis of transgenic Pc1/$Pc1_{extra}$ protein expression levels in adult extrarenal tissues of $Pkd1_{extra}$ 39 transgenic mice. Pc1 was detected using 7e12 monoclonal antibody with both long and short exposures along with internal Gapdh control. Transgenic kidneys of $Pkd1_{extra}$ 39 showed approximately equivalent Pc1 protein levels as $Pkd1_{TAG}$ 26 transgenic kidneys. Lu: lung, Ki: kidney, Pa: pancreas, Br: brain, He: heart, Li: liver.

D) Analysis of Pc1 and transgenic $Pc1_{extra}$ protein glycosylation status. Pc1/$Pc1_{extra}$ was detected with the 7e12 monoclonal antibody and β-tubulin as internal control. Adult transgenic renal extracts of $Pkd1_{extra}$ 2 (3.5µg), 11(15µg) and 39 (35µg), control $Pkd1_{TAG}$ 26 (35µg) and control non-transgenic (90µg) were treated with PNGase (P) and Endo H (E) and compared to untreated non-deglycosylated (ND). The larger Pc1/$Pc1_{extra}$ band corresponds to the mature glycosylated form in all transgenic and controls. Both controls and transgenic mice have Endo H sensitive and resistant Pc1/$Pc1_{extra}$, the ratio of $Pkd1_{TAG}$ and non-transgenic control appear similar whereas it seems increased in $Pkd1_{extra}$.

E) Pc1 and transgenic $Pc1_{extra}$ protein secretion from MEF cells. Pc1/$Pc1_{extra}$ was detected with the 7e12 monoclonal antibody and internal control Alix. Serum-free media of MEFs from $Pkd1_{extra}$ 11 and non-transgenic control was fractionated in exosomes and exosome-free supernatant. Isolated exosomes (Exoquick or ultracentrifugation) showed in $Pkd1_{extra}$ 11 marked increased Pc1/$Pc1_{extra}$ levels relative to control. Pc1/$Pc1_{extra}$ was also secreted in the media free of exosomes for both $Pkd1_{extra}$ 11 and non-transgenic control. For the same volume of media obtained from confluent MEF cells, the amount of Pc1/$Pc1_{extra}$ in the exosome-free samples appears proportionally much lower (at least 3-fold) than in the exosomal fraction.

F) Pc1 and transgenic $Pc1_{extra}$ protein expression in MEF cells. Pc1/$Pc1_{extra}$ was detected with the 7e12 monoclonal antibody and as internal controls β-tubulin and β-actin. Pc1/$Pc1_{extra}$ was

detected in total MEF extracts, the cytosolic fraction and the triton-soluble membrane fraction. Levels of Pc1/Pc1$_{extra}$were substantially elevated in MEFs obtained from the transgenic Pkd1$_{extra}$ 11 compared to the non-transgenic control.

4. Renal pathology in Pkd1$_{extra}$ transgenic mice

A, B) High-resolution ultrasound imaging of kidneys. Comparison of control non-transgenic (A) with Pkd1$_{extra}$ mice (B) was performed during lifespan. Attached video imaging shows representative renal echographies used to monitor cysts progression in Pkd1$_{extra}$ transgenic mice relative to control, at similar age (~20 months).

C, D) Kidneys from a non-transgenic control mouse (C) were compared to kidneys of Pkd1$_{extra}$ transgenic mouse line (D). Transgenic kidneys were pale and displayed pronounced macrocysts with completely remodeled renal architecture. Red arrowhead indicates protruding cysts.

E, F) Histologic analysis of renal cortex from adult non-transgenic control (E) and transgenic Pkd1$_{extra}$ (F) mice (~20 months). Pkd1$_{extra}$ transgenic mice showed numerous tubular and glomerular cysts (black arrow) as well as presence of hyperplasia (double arrow), lymphoid infiltrates (star) and protein deposits (arrowhead) in tubular cysts. Sections were stained with Hematoxylin and Eosin. Original magnification, 50X.

G) Higher magnification of the boxed area from 4F. Original magnification, 320X.

H) Higher magnification of an adjacent region from the same transgenic Pkd1$_{extra}$ renal section shown in 4F. Original magnification, 400X.

I, J) Analysis of interstitial fibrosis in kidney sections from adult non-transgenic control (I) and transgenic Pkd1$_{extra}$ (J) mice (~20 months). Pkd1$_{extra}$ transgenic mice exhibited intense Sirius red staining in comparison to control indicative of marked fibrosis. Original magnification, 50X. Insets show higher magnification of the boxed area. Original magnification, 320X.

5. Proteinuria and Pc1 urine excretion in $Pkd1_{extra}$ transgenic mice

A) Urinary protein analysis of the four $Pkd1_{extra}$ transgenic mouse lines (15-22 months) was monitored qualitatively on SDS-PAGE. Urine protein from all mice showed low molecular weight bands that represent the normally excreted major urinary proteins (MUPs). In addition, urine samples from mice of the four $Pkd1_{extra}$ transgenic lines 2, 9, 11 and 39 showed severe spillage of a ~ 66 kDa protein, probably albumin, indicative of proteinuria reaching levels comparable to the SBM control mouse with pronounced PKD. SBM: PKD mouse model, control for proteinuria; C: non-transgenic mice, normal control; M: protein molecular weight marker; MUPs: major urinary proteins.

B) Immunoblot of protein urinary exosomes from $Pkd1_{extra}$ transgenic lines 2, 11 and 39, non-transgenic control and $Pkd1_{TAG}$ 26. Pc1/$Pc1_{extra}$ was analyzed on a 3-8% gel and detected using 7e12 monoclonal antibody with both long and short exposures along with exosomal marker Alix. Protein extracts of Pc1/$Pc1_{extra}$ was detected in urinary exosomes of $Pkd1_{extra}$ 11 and 39 (11 µg) $Pkd1_{extra}$ 2 (13µg), non-transgenic control (11 µg) and $Pkd1_{TAG}$ (13 µg) mice. Levels of Pc1/$Pc1_{extra}$ appear more abundant in the highest transgenic $Pkd1_{extra}$ expressors.

C) Analysis of Pc1/$Pc1_{extra}$ protein secretion in the urine. The ''exosomal-free'' urinary fraction (250 µg) obtained after ultracentrifugation from $Pkd1_{extra}$ transgenic lines 2, 11 and 39, non-transgenic control and $Pkd1_{TAG}$ 26 were analyzed on 3-8% Tris acetate gel. Pc1/$Pc1_{extra}$ was detected using 7e12 monoclonal antibody with both long and short exposures along with internal control THP for exosome-free and negative control Alix for exosome. In exosome-free urine, non-transgenic control had low levels of Pc1/$Pc1_{extra}$ whereas higher levels were observed for $Pkd1_{extra}$ and $Pkd1_{TAG}$ mouse lines. Levels of secreted Pc1/$Pc1_{extra}$ from $Pkd1_{extra}$ exosome-free samples are much lower proportionally than in the $Pkd1_{TAG}$ urine.

6. Comparison of renal phenotype of $Pkd1_{extra}39$ and $Pkd1_{extra}39$; $Pkd1^{+/-}$ transgenic mice

A) Histopathological analysis of $Pkd1_{extra}$ 39 transgenic kidneys (~15 months) exhibited tubular and glomerular cysts, epithelial hyperplasia, focal inflammation. Sections were stained with Hematoxylin and Eosin. Original magnification, 80X.

B) Higher magnification of the boxed area in 6A.

C) Double heterozygous $Pkd1_{extra}$ 39; $Pkd1^{+/-}$ transgenic kidneys (~15 months) displayed similar tubular and glomerular cysts to $Pkd1_{extra}$ 39, the main difference in the renal parenchyma of double heterozygous is that tubular dilatations or cysts appear to be slightly more widespread. Sections were stained with Hematoxylin and Eosin. Original magnification, 80X.

D) Higher magnification of the boxed area in 6C.

7. Expression analysis of Pkd2 and polycystin-2 in $Pkd1_{extra}$ transgenic mice

A) Expression analysis of Pkd2 in $Pkd1_{extra}$ transgenic mouse lines (n=1-2; 3-14 months). Transcript expression of Pkd2 was analyzed by Northern blot using a 2.2Kb cDNA murine probe. Levels of Pkd2 expression appeared unaltered in transgenic relative to control renal tissues of comparable age. Expression of Gapdh served as internal loading control. Ctrl: non-transgenic mice from same genetic background.

B) Protein expression analysis of Pc2 was carried out by Western blot using YCC2 antibody on kidneys of precystic $Pkd1_{extra}$ transgenic mice and controls (1-7months). All $Pkd1_{extra}$ transgenic mouse lines showed increased Pc2 expression in renal tissues relative to control. Actin served as internal loading control. Ctrl: non-transgenic mice from same genetic background.

C) Expression analysis of c-myc in $Pkd1_{extra}$ transgenic mice. Expression levels of c-myc were analyzed by Northern blot in kidneys of 19-26 months old $Pkd1_{extra}$ transgenic mice (n=2). Transcript levels of c-myc were increased up to 6.3-fold above renal control RNA. Ctrl: non-transgenic mice of same genetic background used as control; SBM: transgenic mice

overexpressing c-myc used as positive control. 1, 2: different mice from the same mouse line. rpL32: ribosomal protein L32 served as loading control.

Table 1: Evidence of altered renal physiology in $Pkd1_{extra}$ transgenic mice

Mice	n	Volume ml	n	Osmolality mosmol/kg	n	Urea nitrogen mmoL/L	n	Creatinine mmoL/L	n	Protein g/L
Control	4	**0.9** ± 0.3	4	**1907.3** ± 551.3	5	**1316.5** ± 570.3	5	**3.8** ± 1.1	4	**8.6** ± 3.8
SBM	3	**3.9** ± 1.0	2	**485.5** ± 60.1	2	**268.8** ± 36.4	2	**0.7** ± 0.4	2	**4.4** ± 4.0
$Pkd1_{extra}$ 2	4	**2.8** ± 0.6**	5	**737.2** ± 150.9*	5	**407.7** ± 86.9*	5	**1.1** ± 0.3**	4	**0.7** ± 0.4*
$Pkd1_{extra}$ 9	4	**2.8** ± 1.4	5	**731.2** ± 86.9*	5	**455.4** ± 73.8*	5	**0.8** ± 0.4**	5	**0.4** ± 0.2*
$Pkd1_{extra}$ 11	4	**3.5** ± 1.6*	6	**633.8** ± 89.1*	5	**312.6** ± 49.0*	6	**1.0** ± 0.3**	3	**0.8** ± 0.4*
$Pkd1_{extra}$ 39	4	**3.5** ± 0.8**	3	**523.0** ± 17.5*	3	**278.1** ± 47.8*	3	**0.7** ± 0.4**	3	**0.4** ± 0.2*

Control: non-transgenic mice used as normal control; SBM: transgenic PKD mouse model used as control for renal insufficiency; four $Pkd1_{extra}$ transgenic lines: $Pkd1_{extra}$ 2, 9, 11, and 39. The mice age range was for controls (21-22 mo), $Pkd1_{extra}$2 (23-25.5 mo), $Pkd1_{extra}$9 (17.5-22 mo), $Pkd1_{extra}$11 (21.5-22.5 mo), $Pkd1_{extra}$39 (19.5-23.5 mo), SBM (5-5.5 mo). Values are mean ± standard deviation; *: $p \leq 0.05$; **: $p \leq 0.005$.

Table 2: Chronic renal insufficiency in $Pkd1_{extra}$ transgenic mice

Mice	n	BUN µmoL/L	Creatinine µmoL/L	n	Hematocrit %
Control	3	**5.6** ± 0.7	**18.3** ± 1.2	3	**45.5** ± 1.4
$Pkd1_{extra}$ 2	6	**20.2** ± 7.4**	**31.8** ± 8.2*	2	**37.6** ± 2.9*
$Pkd1_{extra}$ 9	4	**12.0** ± 2.1*	**21.3** ± 2.4	2	**27.4** ± 11.9
$Pkd1_{extra}$ 11	4	**18.3** ± 13.9	**44.0** ± 32.1	3	**30.9** ± 6.2*
$Pkd1_{extra}$ 39	5	**20.3** ± 17.6	**32.0** ± 22.0	3	**38.9** ± 1.7*

Control: non transgenic mice used as normal control; four $Pkd1_{extra}$ transgenic lines: $Pkd1_{extra}$ 2, 9, 11, and 39. The mice age range was for controls (22 mo), $Pkd1_{extra}$2 (20-22 mo), $Pkd1_{extra}$9 (26 mo), $Pkd1_{extra}$11 (21-24 mo), $Pkd1_{extra}$39 (19.5-23.5 mo). Values are mean ± standard deviation; * p: ≤ 0.05; ** p: ≤ 0.005.

Figure 1

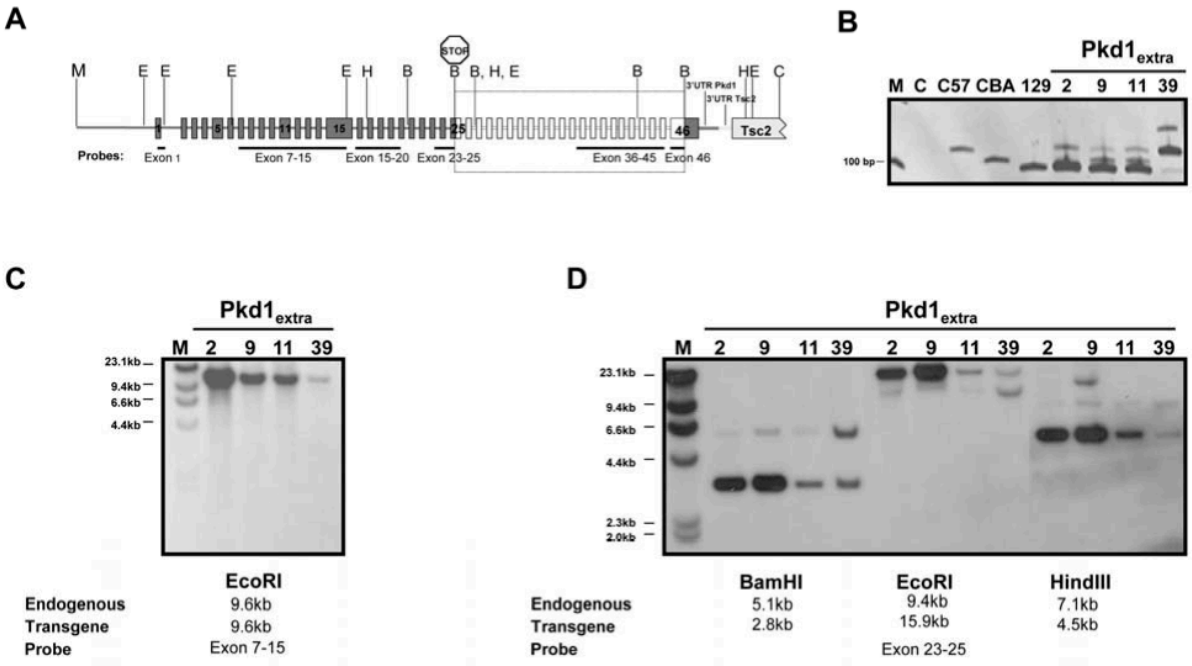
A
M E E E E H B B B, H, E B B HE C
STOP
3'UTR Pkd1
3'UTR Tsc2
1 5 11 15 25 46 Tsc2
Probes: Exon 1 Exon 7-15 Exon 15-20 Exon 23-25 Exon 36-45 Exon 46
B
Pkd1extra
M C C57 CBA 129 2 9 11 39
100 bp
C
Pkd1extra
M 2 9 11 39
23.1kb
9.4kb
6.6kb
4.4kb
EcoRI
Endogenous 9.6kb
Transgene 9.6kb
Probe Exon 7-15
D
Pkd1extra
M 2 9 11 39 2 9 11 39 2 9 11 39
23.1kb
9.4kb
6.6kb
4.4kb
2.3kb
2.0kb
BamHI EcoRI HindIII
Endogenous 5.1kb 9.4kb 7.1kb
Transgene 2.8kb 15.9kb 4.5kb
Probe Exon 23-25

Figure 2

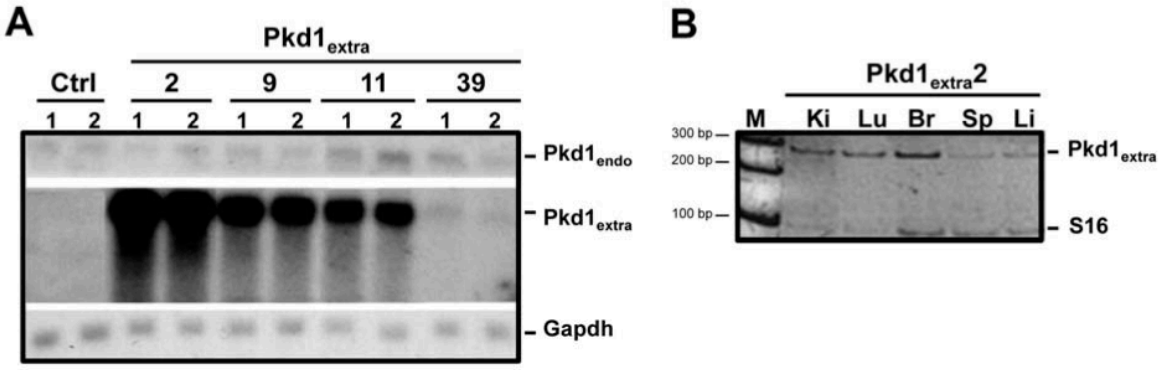

C

Mouse	n	Quantitative Pkd1 expression						
		kidney	*brain*	*heart*	*lungs*	*liver*	*pancreas*	*spleen*
Control	3	1.0	3.2	1.8	2.3	0.5	0.7*	0.4
$Pkd1_{extra}2$	3	86.9	113.1	174.0	121.8	26.1	43.5	17.4
$Pkd1_{extra}9$	3	61.4	61.0	85.4	61.0	30.5	18.3	6.1
$Pkd1_{extra}11$	3	13.9	11.2	26.6	9.8	2.8	7.0	2.8
$Pkd1_{extra}39$	3	2.5	3.0	4.0	3.1	1.0	0.8	1.0

Figure 3

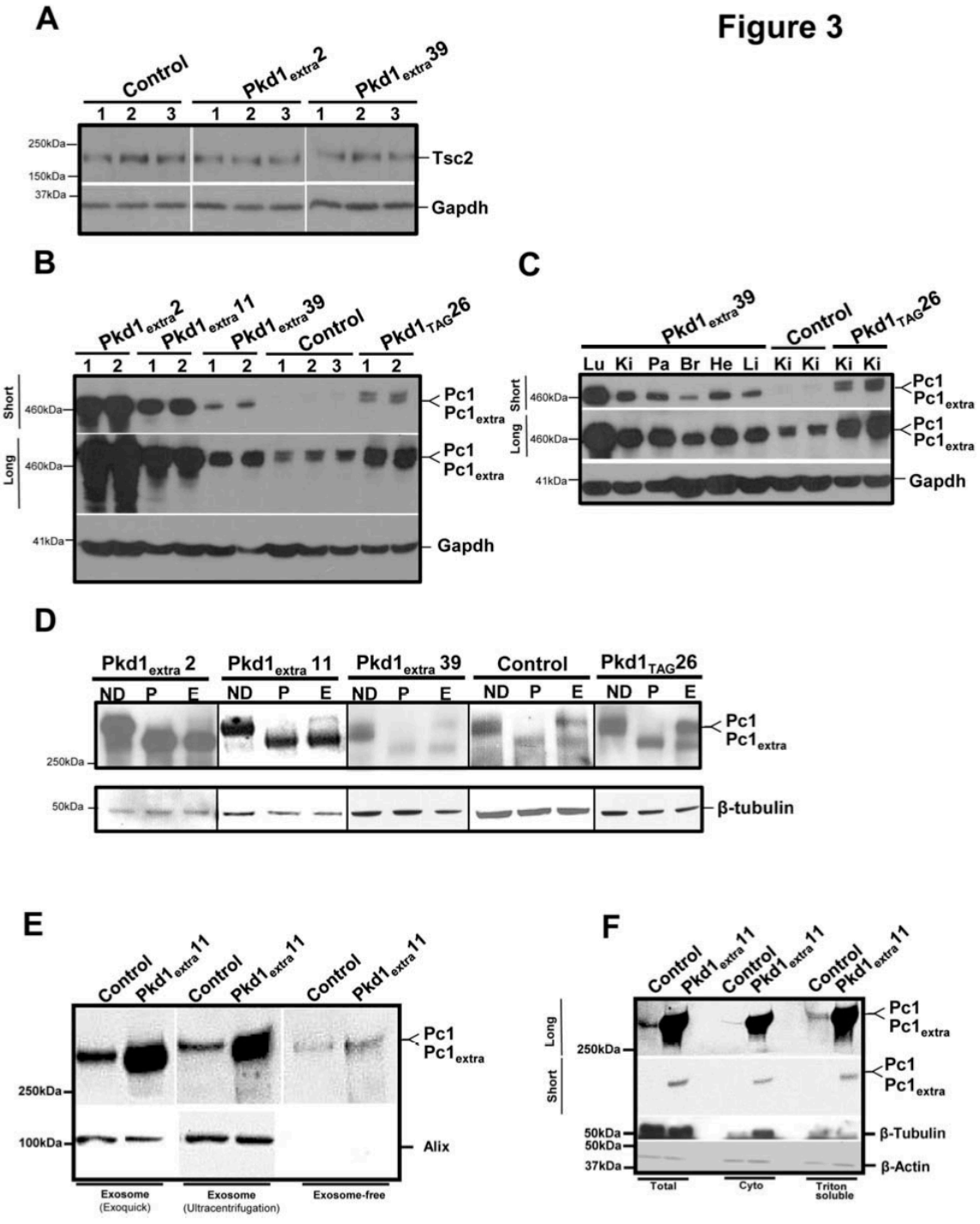
A
Control
Pkd1extra2
Pkd1extra39
1 2 3 1 2 3 1 2 3
250kDa
150kDa
37kDa
Tsc2
Gapdh
B
Pkd1extra2
Pkd1extra11
Pkd1extra39
Control
Pkd1TAG26
1 2 1 2 1 2 1 2 3 1 2
Short
Long
460kDa
460kDa
41kDa
Pc1
Pc1extra
Pc1
Pc1extra
Gapdh
C
Pkd1extra39
Control
Pkd1TAG26
Lu Ki Pa Br He Li Ki Ki Ki Ki
Short
Long
460kDa
460kDa
41kDa
Pc1
Pc1extra
Pc1
Pc1extra
Gapdh
D
Pkd1extra 2
Pkd1extra 11
Pkd1extra 39
Control
Pkd1TAG26
ND P E ND P E ND P E ND P E ND P E
250kDa
50kDa
Pc1
Pc1extra
β-tubulin
E
Control
Pkd1extra11
Control
Pkd1extra11
Control
Pkd1extra11
250kDa
100kDa
Pc1
Pc1extra
Alix
Exosome
(Exoquick)
Exosome
(Ultracentrifugation)
Exosome-free
F
Control
Pkd1extra11
Control
Pkd1extra11
Control
Pkd1extra11
Long
Short
250kDa
50kDa
50kDa
37kDa
Pc1
Pc1extra
Pc1
Pc1extra
β-Tubulin
β-Actin
Total
Cyto
Triton soluble

Figure 4

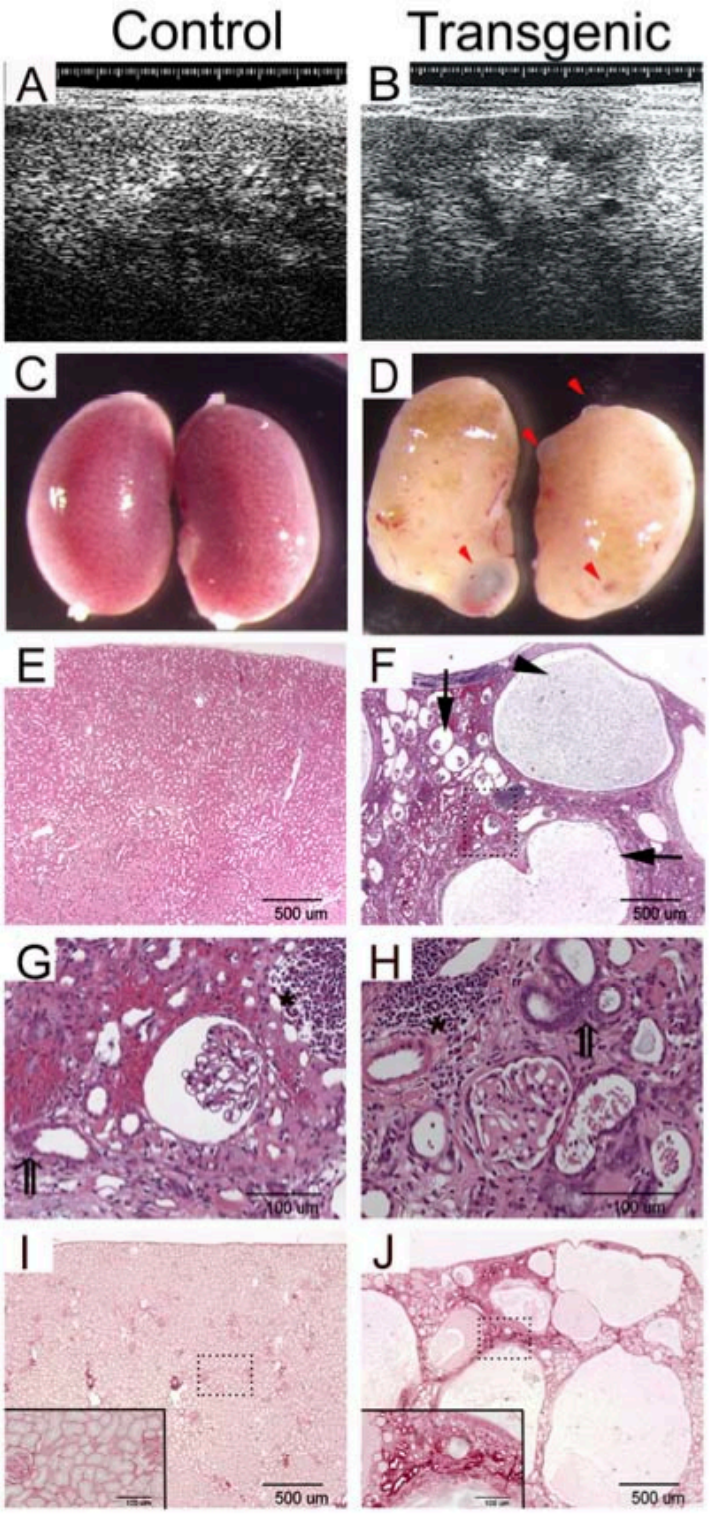
Control
Transgenic
A
B
C
D
E
F
500 um
500 um
G
H
100 um
100 um
I
J
500 um
500 um

Figure 5

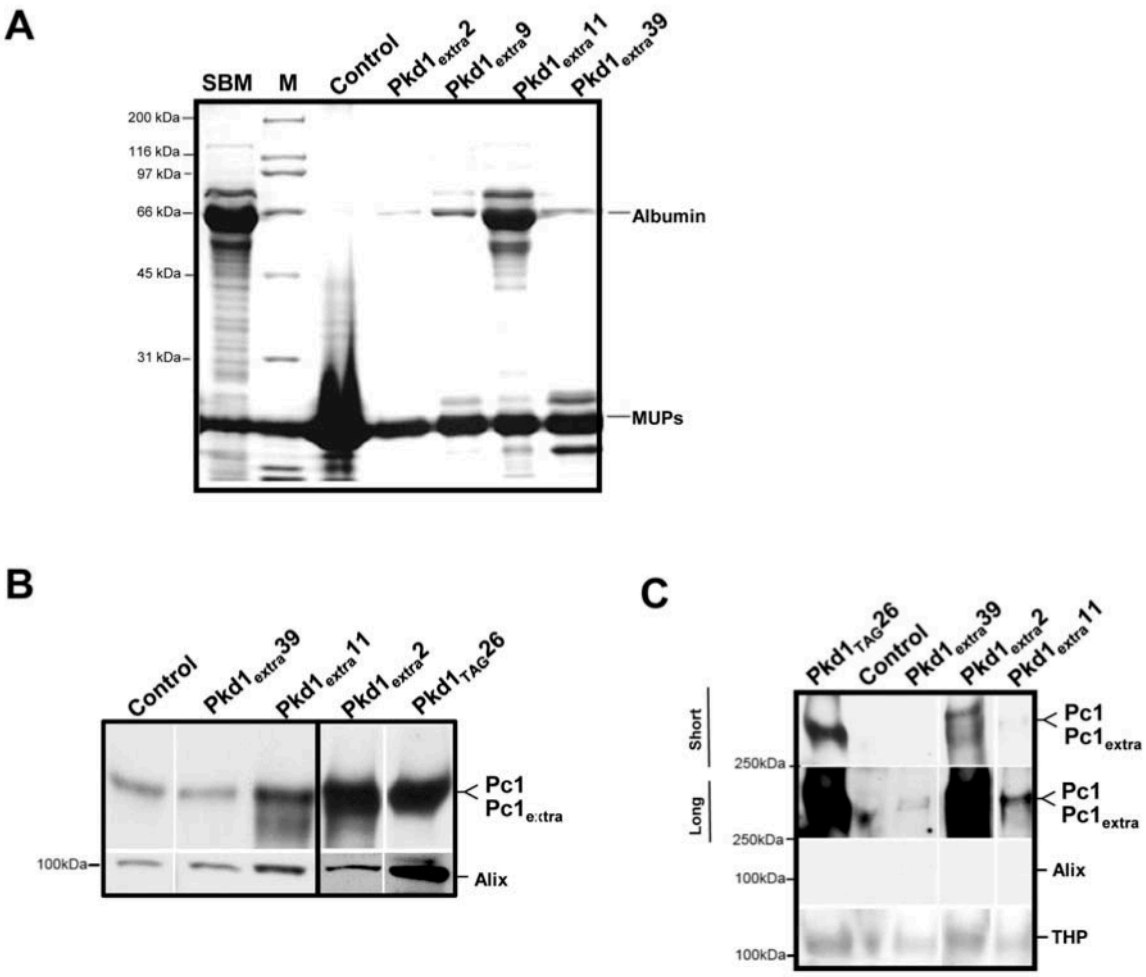
A
SBM
M
Control
Pkd1extra2
Pkd1extra9
Pkd1extra11
Pkd1extra39
200 kDa
116 kDa
97 kDa
66 kDa
45 kDa
31 kDa
Albumin
MUPs
B
Control
Pkd1extra39
Pkd1extra11
Pkd1extra2
Pkd1TAG26
Pc1
Pc1extra
100kDa
Alix
C
Pkd1TAG26
Control
Pkd1extra39
Pkd1extra2
Pkd1extra11
Short
Long
250kDa
250kDa
Pc1
Pc1extra
Pc1
Pc1extra
100kDa
Alix
100kDa
THP

Figure 6

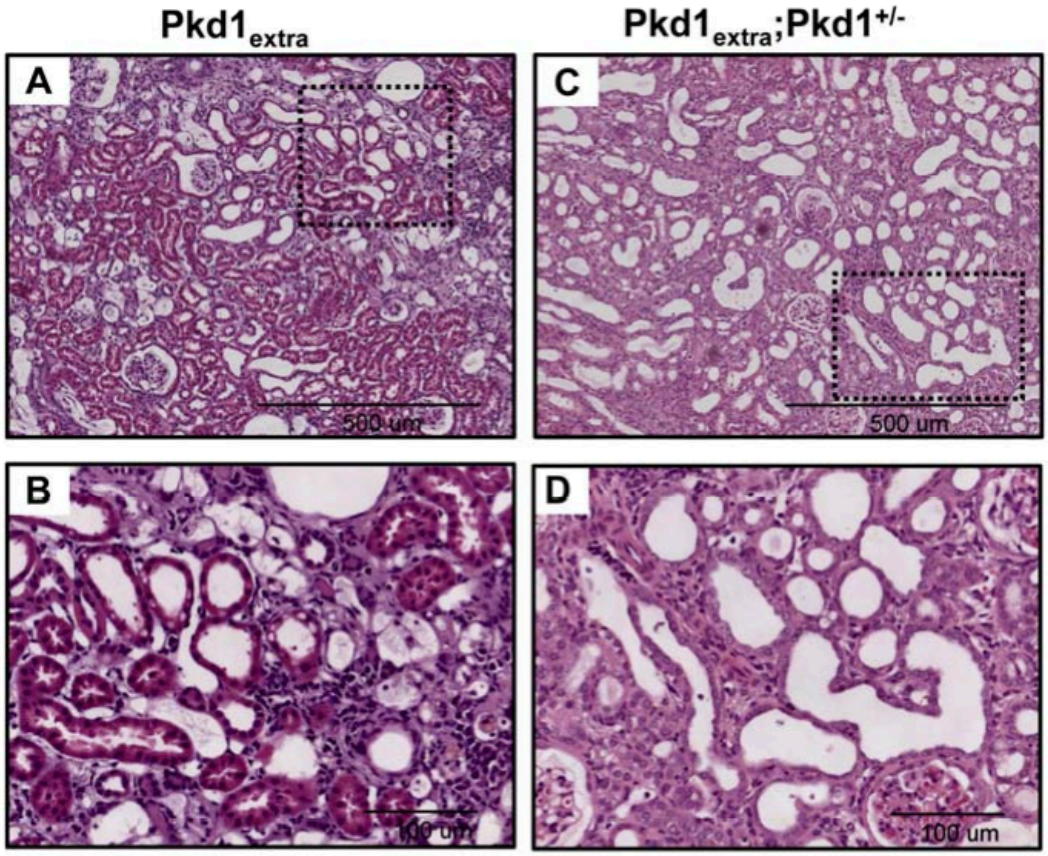

Figure 7

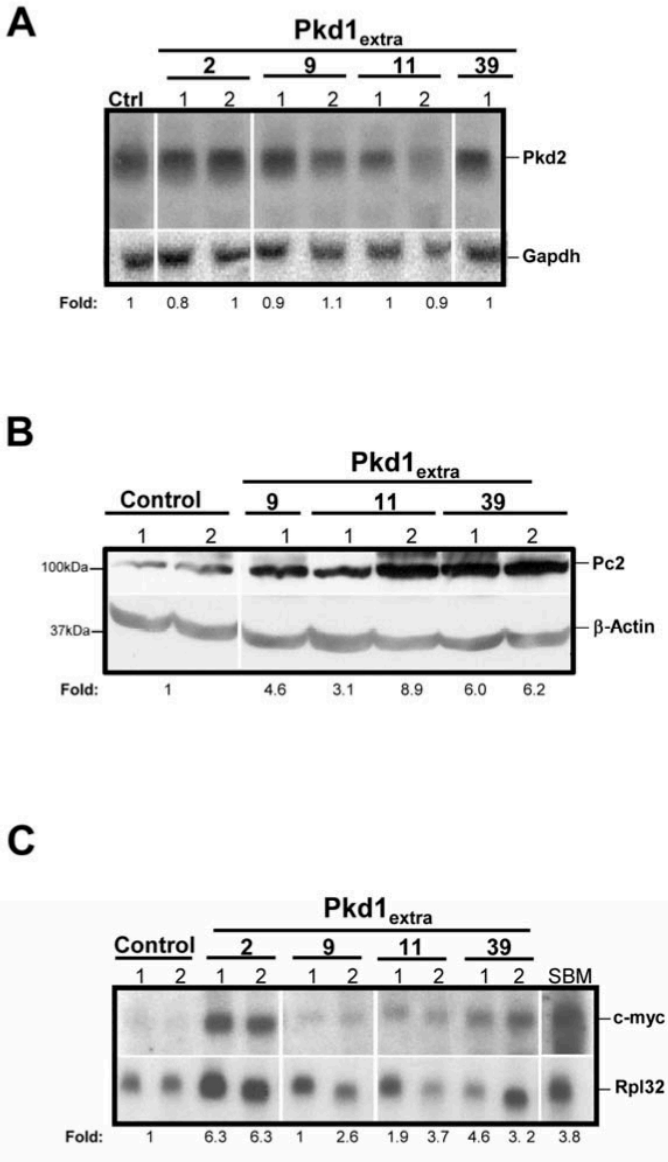
A
Pkd1extra
2
9
11
39
Ctrl
1 2 1 2 1 2 1
Pkd2
Gapdh
Fold: 1 0.8 1 0.9 1.1 1 0.9 1
B
Pkd1extra
Control
9
11
39
1 2 1 1 2 1 2
100kDa
37kDa
Pc2
β-Actin
Fold: 1 4.6 3.1 8.9 6.0 6.2
C
Pkd1extra
Control
2
9
11
39
1 2 1 2 1 2 1 2 1 2 SBM
c-myc
Rpl32
Fold: 1 6.3 6.3 1 2.6 1.9 3.7 4.6 3. 2 3.8

Supplementary Figure 1

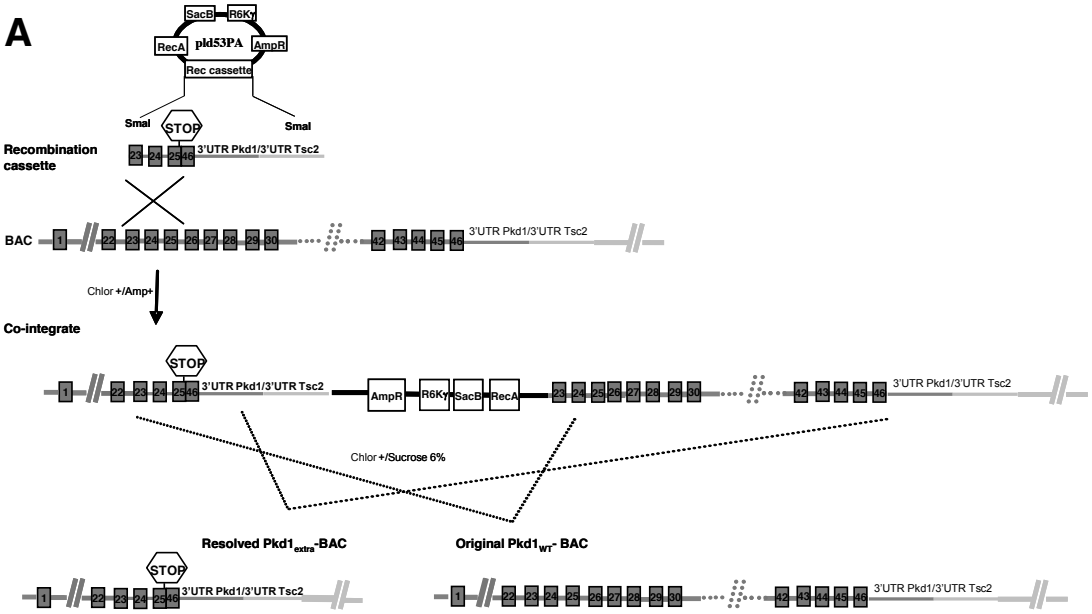

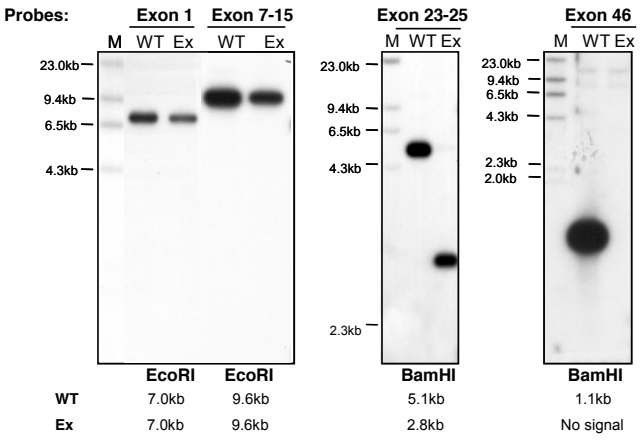

Supplementary Figure 2A

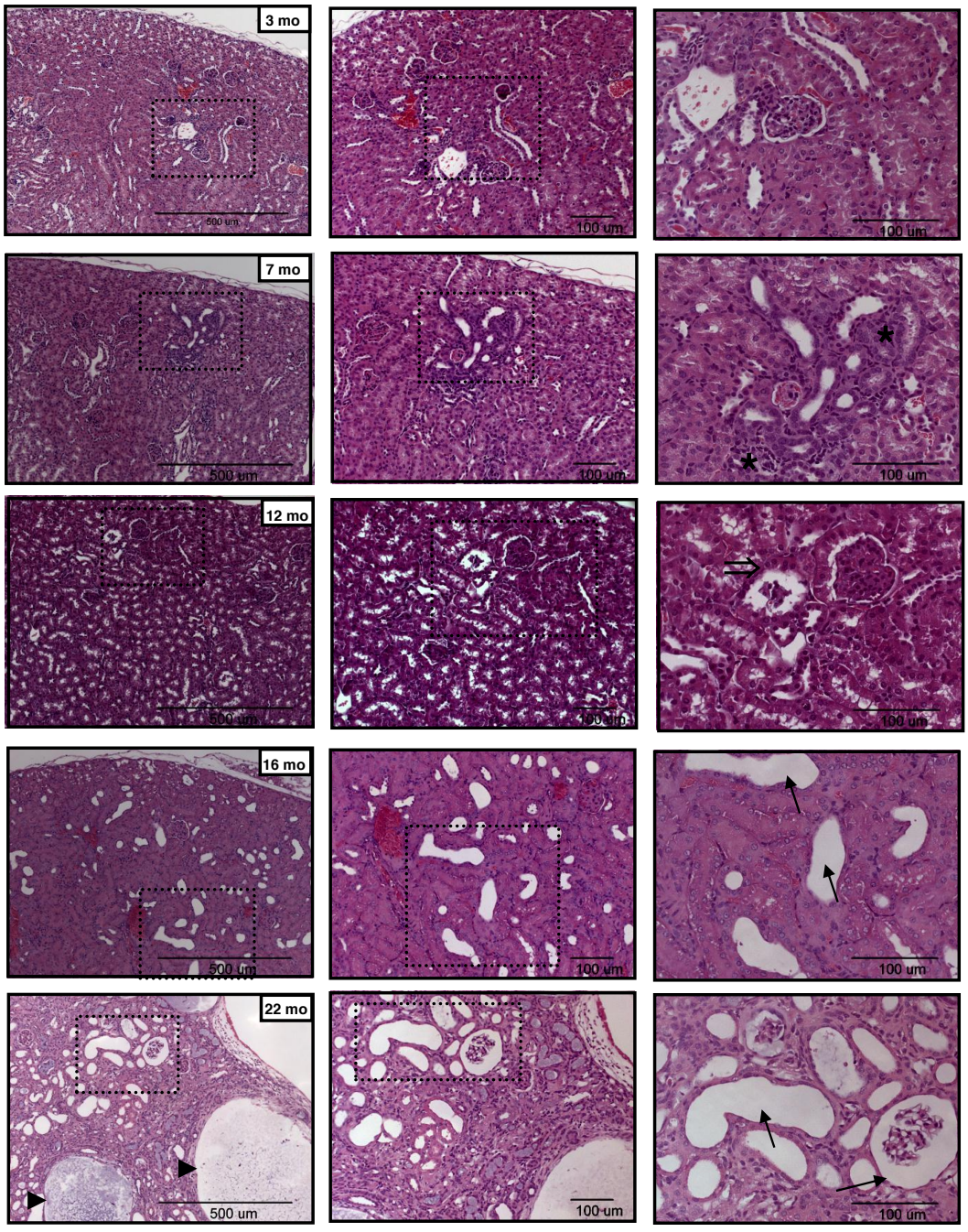

Supplementary Figure 2B

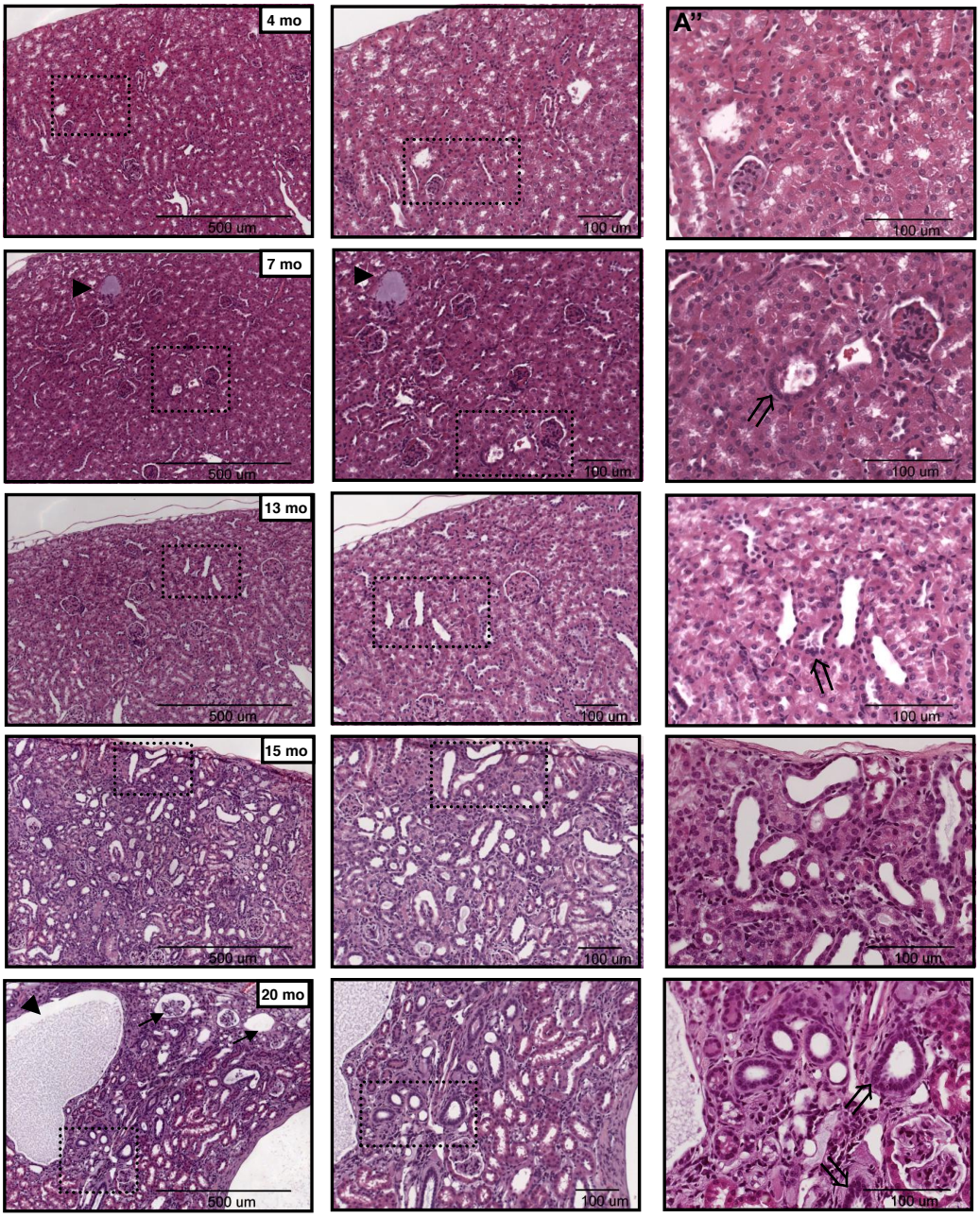

Supplementary Figure 3

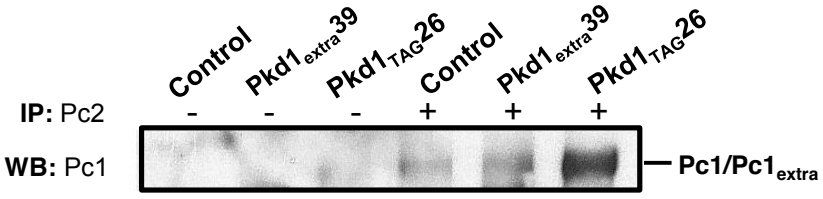

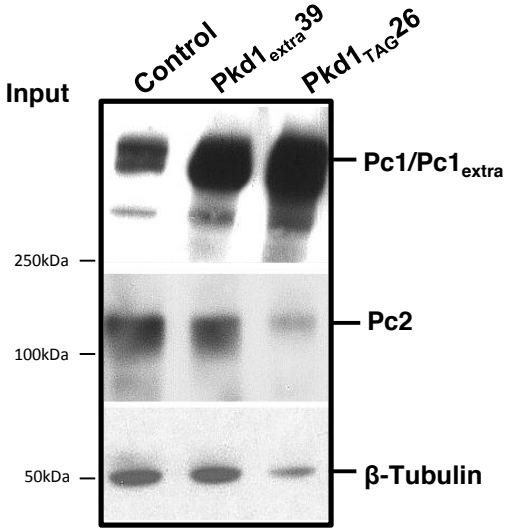

Supplementary Table 1. Oligonucleotide primers used in *Material and Methods* protocols

Description	Position (nt)	Sequence
Pkd1 promoter, forward	promoter	5’ CTG CAC CCA TGT CAG GTG TA
Pkd1 promoter, reverse	promoter	5’ GTT CTA GGC CAG CCA ACT C
Pkd1 exon 1, forward	461-479	5’ TCA ATT GCT CCG GCC GCT G
Pkd1 exon 2, reverse	539-562	5’ CCA GCG TCT GAA GTA GGT TGT GGG
Pkd1 exon 23, forward	Reverse primer pbluescript	
Pkd1 exon 24, forward	9198-9218	5’ AGG GTG CTG ACC ACA GGC TCT A
Pkd1 exon 25, reverse, stop codon	9456-9433	5’AAG GCT GGA TCC **TTA** GGC AGT GAGG
Pkd1 exon 46, reverse	13840-13861	5’ CCA ATT GCT GTC CAG CAC CTG
Pkd1 3’UTR, forward	13608-13628	5’ CAC TTC TCC TTT ATC CGT CCC
Pkd1 3’UTR, reverse	14126-14145*	5’ GAC AGC AGT CAG ACA GCT TC
TSC2-intron 39, reverse	Intron**	5’ TTC AGC ACA TGC TCA TGC C
S16 ribosomal protein exon 3, forward	1799-1819	5’ AGG AGC GAT TTG CTG GTG TGG
S16 ribosomal protein exon 4, reverse	1969-1990	5’ GCT ACC AGG GCC TTT GAG ATG

Accession number: U70209 (Pkd1), M11408 (S16),* NM_013630.2, **NT_039649.8/ENSMUST00000097373.

CHAPTER VI - ARTICLE 3

Novel Functional Complexity of Polycystin-1 by GPS Cleavage In Vivo: Role in Polycystic Kidney Disease

Almira Kurbegovic[1,5], Hyunho Kim[2,5], Hangxue Xu[2], Shengqiang Yu[2,6], Julie Cruanès[1], Robin L. Maser[3], Alessandra Boletta[4], Marie Trudel[1*] and Feng Qian[2*]

1. *Molecular Genetics and Development, Institut de Recherches Cliniques de Montreal, Universite de Montreal, Faculte de Medecine, Montreal, Quebec, Canada*
2. *Department of Medicine, Division of Nephrology, University of Maryland School of Medicine, Baltimore, Maryland, USA*
3. *Department of Clinical Laboratory Sciences, and the Kidney Institute, University of Kansas Medical Center, Kansas City, Kansas, USA*
4. *Dulbecco Telethon Institute at Dibit-San Raffaele, Milan, Italy*
5. *These authors contributed equally to this work.*
6. *Present address: Division of Nephrology, Shanghai Changzheng Hospital, Second Military Medical University, Shanghai, China.*

Running title: Novel polycystin-1 complexity by GPS cleavage

*Drs. Trudel and Qian contributed equally as co-senior authors

Correspondence to:

Feng Qian, [redacted]

Key words (5 alphabetic order): adhesion-GPCRs/ADPKD/ biogenesis/GPS-cleavage/Polycystin-1

This article was accepted for publication in Molecular and Cellular Biology following peer review. The definitive publisher-authenticated version [Mol Cell Biol 34 (17): 3341-53 (2014)] is available online [doi: 10.1128/MCB.00687-14].

ABSTRACT

Polycystin-1 (Pc1) cleavage at the G protein-coupled receptor (GPCR) proteolytic site (GPS) is required for normal kidney morphology in humans and mice. We found a complex pattern of endogenous Pc1 forms by GPS cleavage. GPS cleavage generates not only the heterodimeric cleaved full-length Pc1 ($Pc1^{cFL}$) in which the N-terminal fragment (NTF) remains noncovalently associated with the C-terminal fragment (CTF) but also a novel (Pc1) form ($Pc1^{deN}$) in which NTF becomes detached from CTF. Uncleaved Pc1 ($Pc1^{U}$) resides primarily in the endoplasmic reticulum (ER), whereas both $Pc1^{cFL}$ and $Pc1^{deN}$ traffic through the secretory pathway in vivo. GPS cleavage is not a prerequisite, however, for Pc1 trafficking in vivo. Importantly, $Pc1^{deN}$ is predominantly found at the plasma membrane of renal epithelial cells. By functional genetic complementation with five *Pkd1* mouse models, we discovered that CTF plays a crucial role in $Pc1^{deN}$ trafficking. Our studies support GPS cleavage as a critical regulatory mechanism of Pc1 biogenesis and trafficking for proper kidney development and homeostasis.

INTRODUCTION

Polycystin-1 (PC1) is encoded by the PKD1 gene that is mutated in autosomal dominant polycystic kidney disease (ADPKD), characterized by the development of numerous cysts in both kidneys and progressive renal failure (1). PC1 regulates terminal differentiation of tubular structures in kidney and liver (2–4), as well as maintaining the structural integrity of the kidney (5) and vasculature (6). Expression studies in human and mouse showed spatiotemporal regulated expression for PC1/Pc1 (7–10). In the fetal kidney, immunolocalization of endogenous PC1/Pc1 was observed at apical (most predominant) and basolateral plasma membranes of ureteric bud and collecting ducts (CDs) (11–13). During late renal morphogenesis, Pc1 expression increases significantly during planar cell polarity (PCP)-dependent convergent extension and late collecting duct branching elongation (9, 14). In adult kidney and other tissues or cell lines, PC1/Pc1 localization was reported in a range of subcellular compartments to apical and basal lateral plasma membranes (12), cell-cell junctions (15, 16), and primary cilia (17, 18). Based on its complex structure and expression patterns, native Pc1 is thought to act on the cell surface and may have multiple cellular functions in vivo.

PC1 is a 4,302-amino-acid (aa) glycoprotein with a huge N-terminal extracellular region containing protein-protein interaction motifs, an 11-transmembrane (TM) domain, and an ~200-aa C-terminal cytoplasmic tail that can activate a number of signaling pathways (19, 20) (Fig. 1A). The N-terminal extracellular region is separated from the 11-TM domain by the G protein-coupled receptor (GPCR) proteolytic site (GPS) motif of ~50 aa (19, 20). Initial studies with recombinant PC1 showed that PC1/Pc1 is cleaved within the GPS motif (21) at the tripeptide HL↓T^{3041} located ~20 aa before the first TM domain, resulting in an ~370-kDa N-terminal fragment (NTF) and an ~150-kDa C-terminal fragment (CTF) (22). Following GPS cleavage, Pc1 NTF remains noncovalently associated with the CTF. In addition, a significant proportion of the overexpressed recombinant PC1/Pc1 remains uncleaved in various mammalian cells.

Missense mutations in the GPS or GPCR autoproteolysis-inducing (GAIN) domain of *PKD1* disrupt cleavage of PC1 in recombinant systems (22–24) and prevent activation of the JAK-STAT pathway and induction of tubulogenesis in MDCK three-dimensional (3D) cultures (22). The first evidence for a functional and physiologic role of GPS cleavage for Pc1 came from analysis of mice homozygous for the knock-in missense change T3041V at the HL↓T^{3041} cleavage site (*Pkd1*$^{V/V}$; the position of cleavage is indicated by the downward arrow), which produces a noncleavable Pc1 ($Pc1^{V}$) (25, 26). In contrast to the embryonic-lethal *Pkd1* null mice, which develop severely cystic kidneys starting at embryonic day 15.5 (E15.5) (2–4), *Pkd1*$^{V/V}$ mutant mice are viable with virtually normally appearing kidneys at birth. However, from postnatal day 3 (P3), *Pkd1*$^{V/V}$ mice develop massive cysts mainly in distal nephron segments, leading to death by ~1 month (26). Therefore, GPS cleavage of Pc1 is not essential in embryonic kidneys but is fundamental in postnatal kidneys. Additionally, uncleaved full-length Pc1 ($Pc1^{U}$) and GPS-cleaved Pc1 molecules appear to possess distinct biological functions. While $Pc1^{U}$ appears important for embryonic kidney development and postnatally for proximal tubule integrity, cleaved Pc1 is indispensable for intact structure of distal nephron segments after birth.

The GPS motif was first identified as an internal cleavage site in the neuronal GPCR protein latrophilin and was later found to be part of the ~300-aa-long GAIN domain (23) present in ~30 adhesion GPCRs (aGPCRs), the second largest GPCR subfamily characterized by an unusually large and complex ectodomain (27– 29). A unique property of GPS cleavage is that the two resulting fragments remain associated noncovalently to form a stable but dissociable heterodimer via extensive networks of hydrophobic side chain interactions between the GPS/GAIN domain and the N-terminal stalk of the C-terminal fragment (23, 30–33). Previous studies on aGPCRs have suggested that GPS cleavage promotes efficient trafficking and signaling (34–36). It was also proposed that the NTF of the aGPCR heterodimers might inhibit

receptor signaling (35, 37). Such inhibition can be relieved by conformational changes induced by ligand binding and activation of the G-protein-mediated signaling by the seven-TM CTF. Further, ligands that stabilize the heterodimer may antagonize aGPCR signaling while others may induce adhesion without dissociation of the NTF and CTF or inhibition of CTF signaling (38, 39). The NTF itself can serve additional functions independently of the CTF (40, 41). However, it remains unknown how cleavage affects the biochemical composition and the trafficking of these proteins *in vivo* to regulate the signaling pathways of the cleaved fragments.

In this study, we defined the molecular composition of endogenous Pc1 arising from GPS cleavage in the tissues and cells from postnatal and adult mice and describe its intracellular trafficking *in vivo*. We discovered novel complexity of endogenous Pc1 molecules arising from GPS cleavage and identified two distinct cleaved Pc1 molecules in vivo: (i) the heterodimeric cleaved full-length ($Pc1^{cFL}$) form, in which the NTF subunit remains noncovalently associated to the CTF subunit, and (ii) the novel $Pc1^{deN}$ form, in which the NTF subunit is detached from the CTF. We show for the first time that GPS cleavage of endogenous Pc1 occurs in the endoplasmic reticulum (ER) and is not an absolute prerequisite for Pc1 trafficking to the Golgi compartment in vivo. Analysis using bacterial artificial chromosome (BAC) transgenesis establishes that $Pc1^{deN}$ does not traffic autonomously but is “carried” via $Pc1^{cFL}$. This study on Pc1 biogenesis and trafficking leads to a model in which individual Pc1 forms play multiple roles in kidney development and homeostasis.

RESULTS

Characterization of endogenous polycystin-1 (Pc1) products generated by GPS cleavage

The cleaved polycystin-1 form consisting of the NTF associated with the CTF ($Pc1^{cFL}$) (22) and the uncleaved full-length Pc1 ($Pc1^{U}$) have previously been described *in vitro* and are illustrated in Fig. 1A. To identify the endogenous forms of Pc1 and their spatiotemporal expression patterns *in vivo*, we performed immunoprecipitation (IP) with a chicken antibody directed to the CTF (anti-cCC) from lysates of embryos, kidneys at different postnatal ages, and numerous tissues from adult mice, followed by immunoblot (IB) analysis with anti-rCC and anti-LRR separately. Embryo and adult tissues probed with anti-rCC showed a prominent ~150-kDa band of Pc1, corresponding to the CTF subunit (Fig. 1B) as reported by Yu et al. (26). In addition, a weak but distinct ~520-kDa Pc1 band corresponding to the $Pc1^{U}$ was observed. In kidneys, the $Pc1^{U}$ and the CTF subunit were detectable during postnatal development from P3 to P14, but their levels waned considerably thereafter, in contrast with the very high levels in adult lungs (Fig. 1B, bottom panel). Probing with anti-LRR detected a weak $Pc1^{U}$ band in the embryos and adult tissues, consistent with anti-rCC results (Fig. 1B, top panel), and, additionally, a strong Pc1 doublet (~450 and ~370 kDa) that is not recognized by anti-rCC (lower panel). Based on their molecular masses (MM) and coimmunoprecipitation (co-IP) with CTF, the doublet bands most likely represent the NTF subunits of $Pc1^{cFL}$ (a 450-kDa band [NTF^{450}] and a 370-kDa band [NTF^{370}], according to their MM) that is associated with the CTF (Fig. 1B, schematic right side). Decreased levels were observed for both coimmunoprecipitated NTF and CTF from the postnatal period to adulthood in the kidney samples. Together, these results indicate that $Pc1^{cFL}$ expression is developmentally regulated in the embryonic kidneys and in the adult tissues. Of interest, the stoichiometry of NTF^{450} and NTF^{370} varied among the samples examined; i.e., NTF^{370} was more abundant in the embryos and adult brain, while the

NTF^{450} band was conversely more predominant in the others (Fig. 1B).

The consistent observation of a Pc1 NTF doublet raised the question of whether these bands represent two distinct $Pc1^{cFL}$ isoforms or result from differential N-glycosylation of $Pc1^{cFL}$. To address this point, wild-type MEF cells, which express high endogenous levels of Pc1, were used to analyze the N-glycan modification of $Pc1^{cFL}$ with the N-deglycosylases PNGase F and endo-H (endoglycosidase H), which also serves to monitor protein trafficking along the secretory pathway (49–51). This approach is based on the characteristic nonuniform distribution of glycosylation enzymes along the intracellular secretory pathway, making the glycosylation pattern a useful marker indicating the localization of glycoproteins. The general rationale is that N-glycans of glycoproteins in the endoplasmic reticulum (ER) are all high mannose and are susceptible to removal by cleavage using PNGase F or endo-H, whereas complex N-glycans acquired in the medial/ trans-Golgi compartment are resistant to removal by endo-H but remain sensitive to PNGase F. Sensitivity to endo-H is therefore indicative of proteins that are still in the ER, whereas proteins that acquire endo-H resistance have egressed the ER and transited through the Golgi compartment (49–51). Anti-cCC IP products from MEF protein extracts were treated with PNGase F or endo-H or left untreated (controls) and analyzed by IB with anti-rCC or -LRR antibodies (Fig. 1C). As seen with embryo and tissue samples (Fig. 1B, bottom panel), the Pc1 CTF in MEFs migrates as a pronounced band at ~150 kDa (Fig. 1C, bottom panel). Treatment with PNGase F shifted the CTF to a slightly faster-migrating band at ~140 kDa (the predicted MM of the CTF), whereas endo-H digestion resulted in appearance of two distinct bands at ~150 and ~140 kDa. These data indicate that the Pc1 CTF is composed of distinct species of very similar MW and different N-glycan types. Noticeably, the $Pc1^{U}$ was extensively N-glycosylated and exclusively sensitive to endo-H, as shown by its shift to ~460 kDa (the predicted MM of full-length Pc1) upon treatment (Fig. 1C, bottom panel). The shift of $Pc1^{U}$ upon PNGase F treatment was also observed with anti-LRR (Fig. 1C, top panel). This

result indicates that $Pc1^{U}$ is mainly localized to the ER. Importantly, both the NTF^{450} and NTF^{370} bands were reduced to a single one at ~320 kDa, the predicted MM of NTF, by PNGase F treatment (Fig. 1C, top panel, lane 3). Analysis with endo-H indicated that NTF^{450} was endo-H resistant, while NTF^{370} was endo-H sensitive, as revealed by its shift to ~320 kDa. Hence, the NTF doublet bands do not correspond to two distinct $Pc1^{cFL}$ isoforms but rather result from differential N-glycosylation modification in the NTF subunits of $Pc1^{cFL}$. The NTF subunit therefore consists of both endo-H-resistant and -sensitive pools, as was found for the CTF subunits. Collectively, these data provide evidence for one single endogenous $Pc1^{cFL}$ form that could traffic from the Golgi compartment to the plasma membrane.

To determine whether differential N-glycosylation of endogenous $Pc1^{cFL}$ also occurs in the kidney, similar experiments were performed using P5 wild-type kidneys. Anti-LRR detected three bands from untreated kidney samples: the $Pc1^{U}$ and the more abundant doublet of NTF subunits from $Pc1^{cFL}$ (Fig. 1D). $Pc1^{U}$ was sensitive to both PNGase F and endo-H, as observed in MEFs, thereby pointing to ER localization. The NTF^{450} and NTF^{370} bands were reduced to a single band of ~320 kDa by PNGase F treatment and exhibited endo-H resistance and sensitivity, respectively, supporting the presence of differential N-glycan modifications of $Pc1^{cFL}$ in the kidney. Analogous results were obtained with the lung (see Fig. 2C) and embryo (see Fig. 6). Collectively, these results show one single endogenous $Pc1^{cFL}$ form present in the ER and post-ER/Golgi compartments of kidneys and multiple tissues/cells and argue that Pc1 GPS cis-autoproteolytic cleavage occurs in the ER *in vivo*.

To define the nature of the association between CTF and NTF in the endogenous $Pc1^{cFL}$ form, lysates from MEFs were immunoprecipitated with anti-cCC antibody either under denaturing conditions (Fig. 1E, lane D, 0.1% SDS) to dissociate noncovalent protein interactions or nondenaturing conditions (Fig. 1E, lane Non-D,

0.5% Triton X-100). While Pc1 CTF and $Pc1^{U}$ were detected under both conditions (Fig. 1E, bottom panel), both NTF^{450} and NTF^{370} were detected only under nondenaturing conditions (Fig. 1E, top panel). Therefore, the endogenous $Pc1^{cFL}$ complex consists of NTF and CTF associated via noncovalent interactions.

Pc1 GPS cleavage is not a prerequisite for intracellular trafficking to the Golgi compartment

Two possible mechanisms could be responsible for the lack of endo-H-resistant $Pc1^{U}$. First, GPS cleavage is essential for Pc1 trafficking out of the ER. Second, $Pc1^{U}$ does exit the ER but becomes rapidly cleaved before or upon reaching the cis-Golgi network, consequently preventing detectable levels of endo-H-resistant $Pc1^{U}$ to be achieved at steady state. To differentiate between these two possibilities, we examined the N-glycosylation status of the noncleavable $Pc1^{V}$ in renal collecting duct cells from mutant *Pkd1*$^{V/V}$ mice (Table 1 and Fig. 2A). Two bands of ~600 kDa and ~520 kDa were detected with anti-LRR for $Pc1^{V}$ in untreated samples, whereby the lower band migrated to a similar position as the upper NTF band of wild-type collecting duct cells (Fig. 2B, lanes 1 and 4). Both $Pc1^{V}$ forms collapsed to a single band at the predicted MM of ~460 kDa upon PNGase F treatment (lane 5). Importantly, the ~600-kDa $Pc1^{V}$ was resistant to endo-H digestion, indicating that $Pc1^{V}$ localizes to a post-ER or -Golgi compartment. The ~520-kDa $Pc1^{V}$ band, in contrast, was endo-H sensitive and shifted to ~460 kDa upon endo-H treatment (Fig. 2B, lane 6). Similar results were obtained with the lungs of *Pkd1*$^{V/V}$ mice, whereby the lower $Pc1^{V}$ band comigrated with the $Pc1^{U}$ band of wild-type lung (Fig. 2C). Together, our data suggest that noncleavable $Pc1^{V}$ can traffic to the Golgi compartment as the endogenous cleaved form, $Pc1^{cFL}$. These results, while divergent from models based on recombinant Pc1 and aGPCRs (52, 53), indicate that GPS cleavage is not a prerequisite for endogenous Pc1 intracellular trafficking to the Golgi

compartment *in vivo*.

Characterization of Pc1 products at the cell surface

To identify the specific Pc1 forms localized to the cell surface, surface biotinylation experiments were performed in wild-type collecting duct cells. Intact monolayers were treated with or without a membrane-impermeant biotinylation reagent, and cell lysates were incubated with avidin-agarose and analyzed by IB (Fig. 3). The avidin-bound proteins from surface biotinylated cells contained the upper but not the lower Pc1 NTF product (Fig. 3, LRR blot, lane 4), consistent with their endo-H reactivity patterns (Fig. 2B, lane 3). CTF could also be detected in the biotinylated sample on the same blot after stripping (Fig. 3, CC blot, lane 4). The relative NTF or CTF quantity at the cell surface was determined by comparing the signal intensity of the NTF or CTF detected in the surface protein population relative to that in total lysates. We found that surface Pc1 NTF (NTF^{450}) makes up about 50% of total cellular endo-H-resistant Pc1 NTF, whereas only about 5% of Pc1 CTF was located at the cell surface. This result indicates that while a small amount of Pc1 NTF can be associated with the CTF in the form of $Pc1^{cFL}$ at the cell surface, Pc1 NTF appeared predominantly as a stand-alone Pc1 molecule that is detached from the CTF.

A novel endogenous detached form of Pc1 NTF: $Pc1^{deN}$

To determine whether a novel detached form of Pc1 NTF, here termed $Pc1^{deN}$, exists *in vivo*, we devised an immunodepletion strategy that would specifically separate $Pc1^{deN}$ from other Pc1 forms (Fig. 4A). In this approach, $Pc1^{cFL}$ and $Pc1^{U}$ were quantitatively removed from total lysates by IP with anti-cCC under non-denaturing conditions, and the putative $Pc1^{deN}$ was assessed in flowthrough lysate (Fig. 4, L^{Δ}) after depletion. Depletion efficiency was assessed by reprecipitation of the flowthrough lysate with anti-cCC and IB with anti-rCC or -LRR. We confirmed that the immunodepletion was complete by the absence of $Pc1^{cFL}$ and $Pc1^{U}$ signals in the unbound fraction via reprecipitation with anti- cCC (data not shown). Western blots of

the depleted lysate (Fig. 4B, L^{Δ}) with anti-LRR readily identified two $Pc1^{deN}$ products at ~450 kDa ($Pc1^{deN450}$) and ~370 kDa ($Pc1^{deN370}$) as in the original total lysate (Fig. 4B, L) in inner medullary collecting duct (IMCD) cells or kidney tissues (Fig. 4C). $Pc1^{deN450}$ was endo-H resistant, $Pc1^{deN370}$ was endo-H sensitive, and both had the same mobilities as the two NTF bands in the total lysate. Semiquantification of the signal intensities of Pc1 NTF bands in the flowthrough lysate and total lysate indicates that the relative ratio of $Pc1^{deN}$ to $Pc1^{cFL}$ is ~10:1. $Pc1^{deN}$ was also found in the wild-type lung and MEF cells (data not shown), suggesting that this may be functional *in vivo*. These data show that GPS cleavage of Pc1 gives rise both to the $Pc1^{cFL}$ form and to a distinct and significant pool of $Pc1^{deN}$ that traffics from the ER to the Golgi compartment and to the cell surface (Fig. 3).

Nonautonomous intracellular trafficking of the $Pc1^{deN}$ form

The finding of $Pc1^{deN}$ as a significant form of endogenous GPS-cleaved Pc1 suggests that $Pc1^{deN}$ has a functional role in renal homeostasis. Consistent with this idea, the $Pkd1^{V/V}$ mouse mutant, which expresses a noncleavable Pc1 and therefore lacks the $Pc1^{deN}$ and $Pc1^{cFL}$ forms, gradually acquires cysts in the distal tubules and collecting ducts after birth (26). To determine if the cystic disease caused by the $Pkd1^{V/V}$ mutation could be rescued or ameliorated by coexpression of a Pc1 NTF-like protein, we crossed $Pkd1^{V/V}$ mice with two different lines of the $Pkd1_{extra}$ transgenic mouse model. The $Pkd1_{extra}$ transgenic mouse model expresses a Pc1 protein ($Pc1_{extra}$) truncated at the GPS cleavage site by introduction of a stop codon at aa 3043 in a *Pkd1*-BAC vector (Table 1 and Fig. 5A) (44). The two different transgenic lines express $Pc1_{extra}$ with the correct temporal pattern of wild-type *Pkd1* but at different levels in the kidney: the $Pkd1_{extra}39$ line expresses $Pc1_{extra}$ at ~15-fold over the endogenous Pc1 level, whereas the $Pkd1_{extra}2$ line levels are ~10 times that of the $Pkd1_{extra}39$ line (Fig. 5B). Importantly, the transgenic $Pkd1_{extra}39$ and

Pkd1$_{extra}$*2* lines do not display any renal morphological abnormalities in the first few months of age.

Each *Pkd1*$_{extra}$ line was bred with the *Pkd1*$^{V/+}$ mice to generate compound *Pkd1*$^{V/V}$*; Pkd1*$_{extra}$*2* and *Pkd1*$^{V/V}$*; Pkd1*$_{extra}$*39* animals. The compound *Pkd1*$^{V/V}$*; Pkd1*$_{extra}$ mice expressed transgenic Pc1$_{extra}$ molecules in the kidney tissues similar to their respective Pkd1$_{extra}$ lines (Fig. 5B). Despite the high levels of Pc1$_{extra}$, both lines of compound *Pkd1*$^{V/V}$*; Pkd1*$_{extra}$ mice exhibited high kidney-to-body weight ratios similar to the *Pkd1*$^{V/V}$ mice, and these ratios were ~7- to 8-fold increased over those of age-matched control wild-type mice (Fig. 5C). Further, these *Pkd1*$^{V/V}$*; Pkd1*$_{extra}$ mice developed renal cystic expansion indistinguishable from the *Pkd1*$^{V/V}$ littermates at P10 (Fig. 5D). Analysis of the cystic index for these *Pkd1*$^{V/V}$*; Pkd1*$_{extra}$ kidneys was comparable to that of the *Pkd1*$^{V/V}$ controls and significantly increased relative to age-matched wild-type controls ($P < 0.0001$) (Fig. 5E). Histomorphologic analysis of the cortex and medulla revealed significantly lower cystic involvement in the cortex than the medulla for both *Pkd1*$^{V/V}$ and *Pkd1*$^{V/V}$; *Pkd1*$_{extra}$ kidneys ($P < 0.0003$), consistent with the preponderant distal nephron cystogenesis (Fig. 5F). Consequently, these compound *Pkd1*$^{V/V}$*; Pkd1*$_{extra}$ mice had similar life expectancies as the *Pkd1*$^{V/V}$ littermates as determined from Kaplan-Meier curves (Fig. 5G). These results show that Pc1$_{extra}$ expression was not sufficient to prevent postnatal renal cystogenesis or affect the life span of the *Pkd1*$^{V/V}$ mice and suggest that Pc1^{deN} acquires a critical property through GPS cleavage of nascent Pc1^{U} .

To determine the reason for the absence of *Pkd1*$^{V/V}$ rescue by Pc1$_{extra}$, the expression and posttranslational modification of Pc1 were examined. In *Pkd1*$^{V/V}$*; Pkd1*$_{extra}$ kidneys, the Pc1 product was expressed at levels similar to those of *Pkd1*$_{extra}$ kidneys (Fig. 5B). However, it appeared as a single and intense band in

both lines, whereas endogenous Pc1 from kidney tissues of nontransgenic mice migrated as a doublet. Moreover, the $Pc1_{extra}$ band in *Pkd1*$^{V/V}$*; Pkd1*$_{extra}$ kidney lysates of both transgenic lines was N-glycosylated, similar to the NTF band in nontransgenic kidney, but was mainly endo-H sensitive (Fig. 5H). This result indicates that most $Pc1_{extra}$ molecules in the *Pkd1*$^{V/V}$ background do not exit the ER efficiently, unlike the endogenous wild-type $Pc1^{deN}$ derived via GPS cleavage, which moves throughout the secretory pathway. Our result suggests that the CTF of Pc1 is required for the $Pc1^{deN}$ to exit the ER.

Intact CTF is required for nonautonomous intracellular trafficking of the $Pc1^{deN}$ form

To examine the dependence of $Pc1^{deN}$ trafficking on the Pc1 CTF, we undertook biochemical analysis of Pc1 forms in two different *Pkd1* mouse models with mutations within the CTF, which we postulated impaired trafficking of the CTF. Importantly for this approach, the NTF of these *Pkd1* mutants must have a wild-type GPS/GAIN domain that can undergo normal GPS cleavage.

The *Pkd1*^{m1Bei} mouse was the first mutant CTF model examined. *Pkd1*$^{m1Bei/m1Bei}$ mice carry only a single amino acid substitution, M3083R, within the first TM domain of CTF^{m1Bei} (Table 1 and Fig. 6A), which results in renal cyst formation starting at E15.5 (42, 54). Western blot analysis of *Pkd1*$^{m1Bei/m1Bei}$ embryo lysates with anti-LRR detected a single endo-H-sensitive NTF band (Fig. 6B, B/B) that comigrated with the Pc1 NTF^{370} in wild-type embryos. In addition, the $Pc1^{U\text{-}m1Bei}$ was exclusively endo-H sensitive (Fig. 6B). The cleavage pattern of the mutant Pc1 products was examined by immunodepletion (Fig. 4A). As shown in Fig. 6C, the $Pc1^{cFL\text{-}m1Bei}$ form is generated in the *Pkd1*$^{m1Bei/m1Bei}$ embryos, as evidenced by co-IP of NTF by the CTF^{m1Bei}. The ability to undergo GPS cleavage suggests that $Pc1^{m1Bei}$ is able to fold properly within the GPS/GAIN domain. Notably, the CTF^{m1Bei} appeared

as a doublet, and both bands shifted similarly upon endo-H or PNGase F treatment (Fig. 6C, bottom panel). This doublet likely corresponds to the previously reported CTF isoforms resulting from alternative splicing of *Pkd1* exon 31 (38 aa, 3.9 kDa) (55). Hence, both the NTF and CTF subunits of $Pc1^{cFL\text{-}m1Bei}$ appear exclusively endo-H sensitive, as was the $Pc1^{U\text{-}m1Bei}$ form (Fig. 6C), suggesting that the mutant $Pc1^{cFL\text{-}m1Bei}$ form, as well as the $Pc1^{U\text{-}m1Bei}$ form, is unable to egress from the ER despite proper cleavage. Most importantly, the $Pc1^{deN}$ form generated from $Pc1^{cFL\text{-}m1Bei}$ was essentially endo-H sensitive and appeared as a single band comigrating with the wild-type Pc1 NTF^{370} (Fig. 6D). Thus, despite having wild-type sequence, the $Pc1^{deN}$ of $Pc1^{m1Bei}$ was retained in the ER due to CTF^{m1Bei}. Therefore, the wild-type CTF appears required for proper ER-Golgi compartment trafficking of both $Pc1^{cFL}$ and $Pc1^{deN}$.

The second mutant mouse investigated, *Pkd1* $^{\Delta CMYC/\Delta CMYC}$ (Fig. 6, ΔC/ΔC), expresses cleavable Pc1 that is truncated by replacement of the C-terminal 257 aa of Pc1 with a Myc-epitope tag (45) (Table 1 and Fig. 6E). The phenotypically normal *Pkd1*$^{MYC/MYC}$ knock-in (Fig. 6, M/M) littermates, which express Myc-tagged full-length Pc1, served as controls. Similar to the *Pkd1*^{m1Bei} mutation, this C-terminal truncation did not prevent formation of $Pc1^{cFL}$ but impaired its trafficking, as $NTF^{\Delta CMYC}$ and $CTF^{\Delta CMYC}$ were exclusively endo-H sensitive (Fig. 6F). Of note, it cannot be excluded that $CTF^{\Delta CMYC}$ may have a misfolded motif but with minor effect on the stability of the $CTF^{\Delta CMYC}$ doublet level. The mutant $Pc1^{U\text{-}\Delta CMYC}$ form was also entirely endo-H sensitive, implying that the C-terminal domain of Pc1 is critical for intracellular trafficking of $Pc1^{U}$ as well as for $Pc1^{cFL}$. The $Pc1^{deN\text{-}\Delta CMYC}$ generated in *Pkd1*$^{\Delta CMYC/\Delta CMYC}$ embryos was detected as a single endo-H-sensitive band corresponding to the lower band of the $Pc1^{deN\text{-}MYC}$ doublet of the *Pkd1*$^{MYC/MYC}$ controls (Fig. 6G), as in the *Pkd1*$^{m1Bei/m1Bei}$ mutant. Together, the

data from the two *Pkd1* mutant mice exclude autonomous trafficking of $Pc1^{deN}$ and support the model that $Pc1^{deN}$ is carried to the Golgi compartment via $Pc1^{cFL}$. Furthermore, these results highlight that the CTF is likely critical for proper trafficking of all Pc1 forms *in vivo*.

Functional rescue of $Pkd1^{V/V}$ phenotype by Pkd1-BAC transgenesis

To provide evidence for the importance of an intact CTF in Pc1 trafficking, we determined whether the $Pkd1^{V/V}$ mouse phenotype could be rescued by the $Pkd1_{TAG}26$-BAC transgene (Table 1 and Fig. 7A) that expresses wild-type Pc1 15-fold over endogenous levels in renal tissue (Fig. 7B). The $Pkd1_{TAG}26$ mice were bred with $Pkd1^{V/+}$ mice to generate the compound $Pkd1^{V/V}$; $Pkd1_{TAG}$ animals. As shown in Fig. 7C, the $Pkd1^{V/V}$; $Pkd1_{TAG}$ mice exhibited a normal kidney-to-body weight ratio (n=8; 1.2 ± 0.1) that is similar to that of age-matched wild-type controls (n=15; 1.3 ± 0.2) and is significantly decreased compared to that of $Pkd1^{V/V}$ controls (n=10; 7.6 ± 2.4; $P < 0.0001$) at P10. Consistently, the $Pkd1^{V/V}$; $Pkd1_{TAG}$ mice displayed normal kidney structure and function when analyzed at P10 and 3 months. The renal cystic area in $Pkd1^{V/V}$; $Pkd1_{TAG}$ mice was significantly decreased (n=7; 1.8 ± 0.9) compared to that of $Pkd1^{V/V}$ controls (n=10; 32.2 ± 11.1; $P < 0.0001$) and was similar to that of age-matched normal controls (n=6; 0.7 ± 0.3). Importantly, the $Pkd1^{V/V}$; $Pkd1_{TAG}$ mice had a prolonged life expectancy compared to both the $Pkd1^{V/V}$ and the $Pkd1_{TAG}26$ mice of up to 1 year. In addition, the $Pkd1^{V/V}$; $Pkd1_{TAG}$ mice express the full complement of Pc1 cleaved products with N-glycosylation patterns for both the NTF and CTF identical to those of the endogenous Pc1 in nontransgenic kidneys (Fig. 7D and E). These data demonstrate that overexpression of wild-type Pc1 by the $Pkd1_{TAG}26$ transgene can compensate for the mutant $Pc1^{V}$ and prevent $Pkd1^{V/V}$ renal cystogenesis. Our data provide evidence that the normal CTF is necessary for $Pc1^{deN}$ intracellular trafficking via $Pc1^{cFL}$.

DISCUSSION

Cis-autoproteolytic cleavage at the juxtamembrane GPS motif plays an essential role for the biological function of Pc1 (25, 26) and is disrupted by an increasing number of disease-associated *PKD1* mutations (22–24). This study uncovered significant complexity of endogenous Pc1 biogenesis by GPS cleavage, with at least two distinct and coexisting cleaved Pc1 molecules in normal mouse tissues: (i) the heterodimeric $Pc1^{cFL}$ form that consists of the NTF noncovalently associated to the CTF and (ii) the novel $Pc1^{deN}$ form that represents the NTF detached from the CTF. Our results reveal that a small amount of uncleaved $Pc1^{U}$ resides primarily in the ER, whereas both $Pc1^{cFL}$ and $Pc1^{deN}$ molecules are generated early in the ER and progress through the secretory pathway. We found that $Pc1^{deN}$ is located at the cell surface. Moreover, the CTF plays a crucial and transient role for $Pc1^{deN}$ trafficking as determined by genetic and biochemical experiments in mice that express transgenic $Pc1_{extra}$ mimicking $Pc1^{deN}$ on a $Pkd1^{V/V}$ background or express two cleavable Pc1 proteins with different CTF mutations. The critical function of CTF for $Pc1^{deN}$ trafficking was shown by complementation analysis of the $Pkd1^{V/V}$ mouse mutant with the $Pkd1_{TAG}$-BAC transgene.

The cleaved forms of Pc1 are predominant in whole embryos, in postnatal kidneys, and in various adult tissues. The finding of significant amounts of endo H-sensitive and -resistant populations of $Pc1^{cFL}$ indicate that GPS cleavage occurs early in the ER in vivo and that the resulting $Pc1^{cFL}$ then transits through the Golgi compartment. $Pc1^{deN}$ appears as abundant as, or in greater quantity than, $Pc1^{cFL}$. Hence, $Pc1^{cFL}$ and $Pc1^{deN}$ together or independently are key contributors in renal development during postnatal periods and/or maintenance of homeostasis.

A surprising finding of the study is that GPS cleavage per se is not a prerequisite for endogenous Pc1 to exit the ER and transit through the Golgi compartment as

determined by the identification of endo-H resistance of $Pc1^{V}$. A dissociation of GPS cleavage from trafficking was previously shown for the native PKDREJ, a member of the polycystin-1 family, known to be naturally uncleaved and yet localized at the plasma membrane (56). Other reports, in contrast, suggested an essential role for GPS cleavage in progressing into the Golgi compartment based on impaired targeting of recombinant noncleavable GPS mutants in $Pc1^{L3040H}$ (52) and GPR56 (57), but the causal relationship was questioned due to possible protein misfolding. It is plausible that, for wild- type Pc1, $Pc1^{U}$ might also exit the ER as $Pc1^{V}$ but be efficiently converted to the cleaved forms by GPS cleavage before achieving endo-H resistance to detectable levels. The resulting $Pc1^{cFL}$ population is likely the predominant form that exits the ER. The trafficking and relative distribution of various Pc1 molecules in vivo are thus probably affected by the rate of GPS cleavage. Together, our results show that native Pc1 undergoes GPS cleavage prior to trafficking from the ER to the Golgi compartment but has the potential to transit independently of the GPS cleavage mechanism.

The identification of native $Pc1^{deN}$ as a major endogenous Pc1 molecule in tissues that are predominantly endo-H resistant and present at the plasma membrane of renal epithelial cells was striking. $Pc1^{deN}$ cannot be distinguished from the NTF subunits of $Pc1^{cFL}$ electrophoretically in total lysate and is only recognized using the immunodepletion strategy that specifically removes the other Pc1 forms. $Pc1^{deN}$ is more abundant than $Pc1^{cFL}$ at the plasma membrane of renal epithelial cells. This finding initially suggested that $Pc1^{deN}$ might traffic autonomously to reach the plasma membrane and play a critical functional role in renal ho- meostasis. However, BAC transgenic expression of $Pc1_{extra}$, a Pc1 NTF-like protein, was unable to complement renal cystic progression and early postnatal death in the *Pkd1*$^{V/V}$ mice. While this finding precludes us from a functional evaluation of endogenous $Pc1^{deN}$, it uncovered a novel trafficking mechanism for $Pc1^{deN}$ conferred by GPS cleavage that

likely relies on a protein carrier or cofactor. Our biochemical analyses of mutant Pc1 with mutations in either the proximal or distal CTF region from the two Pkd1 mouse models, *Pkd1*$^{m1Bei/m1Bei}$ and *Pkd1*$^{\Delta CMYC/\Delta CMYC}$, provided evidence that Pc1 CTF may be such a carrier for Pc1^{deN} trafficking. Both Pc1^{deN} and Pc1^{cFL} were retained in the ER despite proper GPS cleavage in both mutants. This characterization not only demonstrates the molecular mechanism responsible for the null phenotype in these mouse mutants but also suggests the presence of at least two determinants within the proximal and distal regions of the CTF subunit. The requirement of the CTF for Pc1^{deN} trafficking and function was demonstrated from biochemical and phenotypical complementation of the *Pkd1*$^{V/V}$ mouse mutant with the *Pkd1*$_{TAG}$-BAC transgene. Together, our data thus show that early trafficking of Pc1^{deN} does not occur autonomously but that Pc1^{deN} is carried to intracellular compartments indirectly via Pc1^{cFL}, followed by subsequent subunit dissociation.

Our finding of a small amount of Pc1^{cFL} coexisting at the surface is consistent with the previous results in recombinant studies (16, 22, 52). One possible explanation for the observed Pc1^{deN} excess (about 10-fold) is that Pc1^{cFL} at the plasma membrane continuously undergoes subunit dissociation followed by internalization and degradation of the resulting dissociated CTF via its cytoplasmic PEST domain (58–60). An alternative explanation for the finding is the previously described cleavage events in the C-terminal tail of the CTF (59, 61, 62), which may result in C-terminal fragments that are translocated to the nucleus for signaling (59, 61). Since Pc1^{deN} is predicted to contain no TM domain, it may be associated to the membrane via another cell surface receptor(s) and/or by lipid modifications, as previously proposed for CIRL/ latrophilin and Sonic hedgehog (63, 64). Our result does not exclude the possibility that some of the CTF is dissociated from the NTF at the surface as described for CIRL/latrophilin (63, 64).

Based on these findings, we propose a GPS cleavage-based biogenesis and

trafficking model for Pc1 with diverse functions (Fig. 8). Wild-type $Pc1^{cFL}$ dissociates to produce $Pc1^{deN}$ in the ER or traffics to the Golgi compartment (Fig. 8, step 1) and subsequently to the plasma membrane/cell-cell junctions (step 2), where it undergoes subunit (NTF and CTF) dissociation. The resulting $Pc1^{deN}$ may be associated to the membrane via another cell surface receptor(s) and/or by lipid modifications, but the released CTF from $Pc1^{cFL}$ may activate a signal pathway and then is quickly degraded. $Pc1^{cFL}$ may also traffic from the Golgi compartment to cilium for the GPS-dependent function (Fig. 8, step 3). The $Pc1^{cFL\text{-}Bei/\Delta CMYC}$ mutants lacking the intact CTF cannot traffic from the ER to the Golgi compartment and to the plasma membrane and cilium.

Our findings also shed light on human ADPKD pathogenic mechanisms triggered by various *PKD1* mutations within the CTF subunit and show that these mutations can have as severe consequences as mutations in the NTF. This is consistent with results of a recent report showing that the type of *PKD1* mutation, but not its protein location, correlated strongly with renal survival of the patients (65). Moreover, our data predict that a subset of *PKD1* mutations affecting the CTF sequence would retain both $Pc1^{cFL}$ and $Pc1^{deN}$ in the ER without affecting GPS cleavage. Alleviation of such CTF carrier defects by providing a substitute could restore trafficking and function of both $Pc1^{cFL}$ and $Pc1^{deN}$. This study paves the way toward understanding the biochemical complexity and functions of the GPS-cleaved forms of endogenous Pc1. Crucial insights were devised for the functional role of the different Pc1 forms in renal development and homeostasis. Moreover, we identified for the first time that the CTF subunit can be a promising novel pharmacological target. Future studies will center on the development of innovative designs for therapeutic strategies that promote the trafficking and function of Pc1 forms affected by *PKD1* mutations in ADPKD.

MATERIALS AND METHODS

Animals. We previously produced the transgenic *Pkd1*$_{extra}$ and *Pkd1*$_{TAG}$ mouse lines, the knock-in *Pkd1*$^{V/V}$ and *Pkd1*$^{MYC/MYC}$ mice, and the knockout *Pkd1*$^{\Delta CMYC/\Delta CMYC}$ mice as well as obtained the N-ethyl-N-nitrosourea (ENU)-induced *Pkd1*$^{m1Bei/m1Bei}$ mice (26, 42–45). These mouse models were bred to a C57BL/6J genetic background. All animal experiments conformed to the standards of the Canadian Council of Animal Care of Institut de Recherches Cliniques de Montréal and of the Animal Care and Use Committees of Johns Hopkins School of Medicine and the University of Maryland School of Medicine.

Genotype analysis. Mouse genotyping was accomplished on DNA extracted from tail biopsy specimens. The *Pkd1*$_{TAG}$ and *Pkd1*$_{extra}$ transgenes were genotyped by Southern blots using EcoRI (Pkd1 probe exon 7 to 15) and BamHI (Pkd1 probe exon 23 to 25), respectively (43, 46). To identify *Pkd1*^{V} heterozygous mice, we used PCR amplification with the following oligonucleotides: forward, Pkd1 exon 23 (5'-CCA AAC AACTCA GAC CAG G-3'), and reverse, Pkd1 intron 23 (5'-ACC AGG ACA GCA AGA AAA C-3'). These produce amplicons of 280 bp (wild-type [WT] *Pkd1*) and 320 bp (*Pkd1*^{V} allele). The heterozygous or homozygous *Pkd1*^{V} allele on the transgenic *Pkd1*$_{extra}$ or *Pkd1*$_{TAG}$ mouse background was distinguished by TaqMan gene copy number assay. Quantitative PCR (qPCR) was performed with the forward primer (Intron 23 Pkd1) 5'-TGC CTT TCT TCC CTC CTT GTC-3', reverse primer (Flp recognition target [FRT] and linker from *Pkd1*^{V} construct) 5'-GCC GAA GTT CCT ATT CTC TAG AAA GTA T-3', and a TaqMan probe (FRT and linker from *Pkd1*^{V} construct), 6FAM-CTC GAC GAA GTT CC-MGBNFQ (where FAM is 6-carboxyfluorescein and MGBNFQ is minor groove binder and nonfluorescent quencher). We used as a normalizer the Dolt gene with the forward primer (intron 1) 5'-GCC CCA GCA CGA CCA TT-3', reverse primer (Intron 1) 5'-TAG TTG GCA TCC TTA TGC TTC ATC-3', and a TaqMan probe with Dolt (VIC-CCA GCT CTC AAG TCG-MGBNFQ; Life Technologies). The PCRs were carried out with the PerfeCTa

qPCR SuperMix (Quanta Biosciences) in an Mx4000, 3005P (Stratagene), or Viia7 apparatus (Life Technologies).

Histopathological analysis. Transgenic *Pkd1*$^{V/V}$; *Pkd1*$_{extra}$ mice, *Pkd1*$^{V/V}$; *Pkd1*$_{TAG}$ mice, knock-in *Pkd1*$^{V/V}$ mice, and nontransgenic age-matched control *Pkd1*$^{+/+}$ mice from different ages were sacrificed, and kidney tissues were readily removed. Kidneys were immediately placed in formalin or paraformaldehyde and then embedded in paraffin. Tissue sections (4 to 5 μm thick) were stained with hematoxylin and eosin (H&E) for morphological evaluation using an Axiophot Zeiss microscope (47). Cystic areas of kidneys at P10 from *Pkd1*$^{V/V}$; *Pkd1*$_{extra}$, *Pkd1*$^{V/V}$; *Pkd1*$_{TAG}$, and littermate *Pkd1*$^{V/V}$ and Pkd1$^{+/+}$ controls were quantified at a magnification of ~X1.5 to X1.6 as a function of cyst percentage to total surface using a Leica MX12 microscope and Northern Eclipse software. In addition, cystic surface of the cortex versus medulla was evaluated for *Pkd1*$^{V/V}$; *Pkd1*$_{extra}$*2* and *Pkd1*$^{V/V}$ controls using the same approach.

Protein analysis. Immunoprecipitation (IP) studies of the endogenous polycystin-1 were accomplished on mouse tissue samples, embryos, or cells (murine embryonic fibroblasts [MEFs], collecting duct cells, and inner medullary collecting duct [IMCD] cells) homogenized in lysis buffer (20 mM sodium phosphate [pH 7.2], 150 mM NaCl, 1 mM EDTA, 10% glycerol, 0.5 to 1% Triton X-100) and a cocktail of protease inhibitors (Sigma-Aldrich) (22). The homogenate was incubated for 1 h on ice and cleared of debris by centrifugation at 17,000X g for 10 min at 4°C. Ten milligrams of protein lysates in 1 ml was typically used for IP with the chicken C-terminal Pc1 antibody (anti-cCC) and goat anti-chicken IgY–agarose beads (PrecipHen; Aves Labs) as described previously (26). The resulting IP products were loaded on 3 to 8% Tris-acetate-SDS-polyacrylamide precast gels or 4 to 12% Tris-glycine-SDS-polyacrylamide precast gels (Invitrogen) and transferred to polyvinylidene difluoride (PVDF) membrane (Bio-Rad). The membranes were incubated with rabbit poly-

clonal or rat monoclonal C-terminal anti-CC (anti-rCC) and a horseradish peroxidase (HRP)-conjugated secondary antibody as previously described (26). ECL Prime (GE Health Care Life Sciences) was used for detection on Kodak film or a ChemiDoc XRS+ Pharos imaging system (Bio-Rad). The membranes were then stripped using Restore Western blot buffer (Pierce, VWR) and reprobed with the anti-LRR (7e12) antibody directed to the LRR domain of Pc1 (Santa Cruz Biotechnology) (48). A similar protocol was performed for analysis of Pc1 in the *Pkd1*$^{MYC/MYC}$ and *Pkd1*$^{\Delta CMYC/\Delta CMYC}$ embryos, but the protein lysates were immunoprecipitated with a polyclonal anti-Myc (Cell Signaling Technology) and detected with a rabbit polyclonal anti-Myc (Cell Signaling Technology) or anti-LRR (7e12).

The immunodepletion studies were performed on kidneys, lungs, embryos, MEFs, and IMCD cells. According to the endogenous polycystin-1 expression levels, up to five rounds of immunoprecipitation were carried out to achieve complete depletion of both Pc1^{U} and Pc1^{cFL}. These IP products were monitored for intact Pc1^{cFL} by coprecipitation of NTFs throughout the depletion procedure. The flowthrough fraction was immunoprecipitated with anti-CC (cCC) followed by Western blot analysis with anti-CC (rCC) and anti-LRR (7e12) to verify efficiency of immunodepletion.
Analysis of total protein lysates was carried out on kidneys, lungs, embryos, MEFs, and IMCD cells. Protein extracts were prepared as described previously (43, 44); usually, *Pkd1*$_{extra}$ (alone or with *Pkd1*$^{V/V}$) was loaded at 1/10 of other samples for immunoblotting (IB). Membranes were incubated with anti-LRR (7e12) antibody and the internal control β-tubulin or glyceraldehyde-3-phosphate dehydrogenase (GAPDH; Sigma-Aldrich and Abcam), followed by ECL Prime or ECL (GE Health Care Life Sciences) for detection. Total protein or IP samples were deglycosylated using peptide N-glycosidase F (PNGase F) or endoglycosidase H (endo-H; New England BioLabs) according to the manufacturer's instructions.

Cell and surface biotinylation studies. Collecting duct (CD) cells were derived from *Pkd1* WT postnatal kidneys for endogenous Pc1 analysis. Surface biotinylation

experiments for CD monolayers were performed using a Pierce cell surface protein isolation kit (Thermo Scientific) according to the manufacturer's instructions. Anti-GM130 (Novus biologicals), a cis-Golgi marker, was used as a negative control for surface protein detection. Proteins on the blots were quantified using Quantity One software of the Pharos imaging system (Bio-Rad). The relative amounts of Pc1 NTF and CTF, detected by anti-LRR and CC, respectively, were determined by adjusting their signal intensities to those of noncleavable $Pc1^{V}$ loaded on the same blot.

Statistical analysis. Values were expressed as means ± standard deviations. Statistical analysis was performed by one-way analysis of variance (ANOVA) with a Tukey correction test for multiple comparisons of the mean of each column to the mean of every other column and computed by Prism 6 software. A P value of 0.05 with a 95% confidence interval was considered significant.

ACKNOWLEDGMENTS

We thank J. Calvet, Chiara Gamberi, and Owen Woodward for reading and commenting on the manuscript and B. Magenheimer and M. Chiaravalli for technical assistance.

This work was supported by grants from the Canadian Institutes of Health Research and the Polycystic Kidney Disease Foundation of Canada (to M.T.), by grants from the NIH (R01 DK062199 and P30 DK090868) and National Kidney Foundation of Maryland (to F.Q.), by a Frederick Banting and Charles Best of Canada Graduate Scholarship Award (to A.K.), and by a Korea Research Foundation grant by the Korean Government (KRF-2008-357-E00030, to H.K.).

REFERENCES

1. Gabow PA. 1993. Autosomal dominant polycystic kidney disease. N. Engl. J. Med. 329:332–342.

2. Ahrabi AK, Jouret F, Marbaix E, Delporte C, Horie S, Mulroy S, Boulter C, Sandford R, Devuyst O. 2010. Glomerular and proximal tubule cysts as early manifestations of Pkd1 deletion. Nephrol. Dial. Transplant. 25:1067–1078.

3. Lu W, Shen X, Pavlova A, Lakkis M, Ward CJ, Pritchard L, Harris PC, Genest DR, Perez-Atayde AR, Zhou J. 2001. Comparison of Pkd1 targeted mutants reveals that loss of polycystin-1 causes cystogenesis and bone defects. Hum. Mol. Genet. 10:2385–2396.

4. Piontek KB, Huso DL, Grinberg A, Liu L, Bedja D, Zhao H, Gabrielson K, Qian F, Mei C, Westphal H, Germino GG. 2004. A functional floxed allele of Pkd1 that can be conditionally inactivated in vivo. J. Am. Soc. Nephrol. 15:3035–3043.

5. Piontek K, Menezes LF, Garcia-Gonzalez MA, Huso DL, Germino GG. 2007. A critical developmental switch defines the kinetics of kidney cyst formation after loss of Pkd1. Nat. Med. 13:1490 –1495.

6. Kim K, Drummond I, Ibraghimov-Beskrovnaya O, Klinger K, Arnaout MA. 2000. Polycystin 1 is required for the structural integrity of blood vessels. Proc. Natl. Acad. Sci. U. S. A. 97:1731–1736.

7. Chauvet V, Qian F, Boute N, Cai Y, Phakdeekitacharoen B, Onuchic LF, Attie-Bitach T, Guicharnaud L, Devuyst O, Germino GG, Gubler MC. 2002. Expression of PKD1 and PKD2 transcripts and proteins in human embryo and during normal kidney development. Am. J. Pathol. 160:973–983.

8. Foggensteiner L, Bevan AP, Thomas R, Coleman N, Boulter C, Bradley J, Ibraghimov-Beskrovnaya O, Klinger K, Sandford R. 2000. Cellular and subcellular distribution of polycystin-2, the protein product of the PKD2 gene. J. Am. Soc. Nephrol. 11:814 – 827.

9. Guillaume R, D'Agati V, Daoust M, Trudel M. 1999. Murine Pkd1 is a developmentally regulated gene from morula to adulthood: role in tissue condensation and patterning. Dev. Dyn. 214:337–348.

10. Guillaume R, Trudel M. 2000. Distinct and common developmental expression patterns of the murine Pkd2 and Pkd1 genes. Mech. Dev. 93: 179 –183.

11. Van Adelsberg J, Chamberlain S, D'Agati V. 1997. Polycystin expression is temporally and spatially regulated during renal development. Am. J. Physiol. 272:F602–F609.

12. Geng L, Segal Y, Peissel B, Deng N, Pei Y, Carone F, Rennke HG, Glucksmann-Kuis AM, Schneider MC, Ericsson M, Reeders ST, Zhou J. 1996. Identification and localization of polycystin, the PKD1 gene product. J. Clin. Invest. 98:2674 –2682.

13. Palsson R, Sharma CP, Kim K, McLaughlin M, Brown D, Arnaout MA. 1996. Characterization and cell distribution of polycystin, the product of autosomal dominant polycystic kidney disease gene 1. Mol. Med. 2:702–711.

14. Geng L, Segal Y, Pavlova A, Barros EJ, Lohning C, Lu W, Nigam SK, Frischauf AM, Reeders ST, Zhou J. 1997. Distribution and developmentally regulated expression of murine polycystin. Am. J. Physiol. 272:F451–F459.

15. Kleymenova E, Ibraghimov-Beskrovnaya O, Kugoh H, Everitt J, Xu H, Kiguchi K, Landes G, Harris P, Walker C. 2001. Tuberin-dependent membrane localization of polycystin-1: a functional link between polycystic kidney disease and the TSC2 tumor suppressor gene. Mol. Cell 7:823– 832.

16. Boletta A, Qian F, Onuchic LF, Bragonzi A, Cortese M, Deen PM, Courtoy PJ, Soria MR, Devuyst O, Monaco L, Germino GG. 2001. Biochemical characterization of bona fide polycystin-1 in vitro and in vivo. Am. J. Kidney Dis. 38:1421–1429.

17. Nauli SM, Alenghat FJ, Luo Y, Williams E, Vassilev P, Li X, Elia AE, Lu W, Brown EM, Quinn SJ, Ingber DE, Zhou J. 2003. Polycystins 1 and 2 mediate mechanosensation in the primary cilium of kidney cells. Nat. Genet. 33:129 –137.

18. Yoder BK, Hou X, Guay-Woodford LM. 2002. The polycystic kidney disease proteins, polycystin-1, polycystin-2, polaris, and cystin, are colocalized in renal cilia. J. Am. Soc. Nephrol. 13:2508 –2516.

19. Hughes J, Ward CJ, Peral B, Aspinwall R, Clark K, San Millan JL, Gamble V, Harris PC. 1995. The polycystic kidney disease 1 (PKD1) gene encodes a novel protein with multiple cell recognition domains. Nat. Genet. 10:151–160.

20. Ponting CP, Hofmann K, Bork P. 1999. A latrophilin/CL-1-like GPS domain in

polycystin-1. Curr. Biol. 9:R585–R588.

21. Wei W, Hackmann K, Xu H, Germino G, Qian F. 2007. Characteriza- tion of cis-autoproteolysis of polycystin-1, the product of human polycystic kidney disease 1 gene. J. Biol. Chem. 282:21729 –21737.

22. Qian F, Boletta A, Bhunia AK, Xu H, Liu L, Ahrabi AK, Watnick TJ, Zhou F, Germino GG. 2002. Cleavage of polycystin-1 requires the receptor for egg jelly domain and is disrupted by human autosomal-dominant polycystic kidney disease 1-associated mutations. Proc. Natl. Acad. Sci. U. S. A. 99:16981–16986.

23. Arac D, Boucard AA, Bolliger MF, Nguyen J, Soltis SM, Sudhof TC, Brunger AT. 2012. A novel evolutionarily conserved domain of cell-adhesion GPCRs mediates autoproteolysis. EMBO J. 31:1364 –1378.

24. Garcia-Gonzalez MA, Jones JG, Allen SK, Palatucci CM, Batish SD, Seltzer WK, Lan Z, Allen E, Qian F, Lens XM, Pei Y, Germino GG, Watnick TJ. 2007. Evaluating the clinical utility of a molecular genetic test for polycystic kidney disease. Mol. Genet. Metab. 92:160–167.

25. Qian F. 2012. Polycystin-1, p 3728–3736. In Rawlings ND, Salvesen G (ed), The handbook of proteolytic enzymes, 3rd ed. Academic Press, San Diego, CA.

26. Yu S, Hackmann K, Gao J, He X, Piontek K, Garcia-Gonzalez MA, Menezes LF, Xu H, Germino GG, Zuo J, Qian F. 2007. Essential role of cleavage of polycystin-1 at G protein-coupled receptor proteolytic site for kidney tubular structure. Proc. Natl. Acad. Sci. U. S. A. 104:18688 –18693.

27. Fredriksson R, Lagerstrom MC, Hoglund PJ, Schioth HB. 2002. Novel human G protein-coupled receptors with long N-terminals containing GPS domains and Ser/Thr-rich regions. FEBS Lett. 531:407–414.

28. Lin HH, Stacey M, Yona S, Chang GW. 2010. GPS proteolytic cleavage of adhesion-GPCRs. Adv. Exp. Med. Biol. 706:49 –58.

29. Sugita S, Ichtchenko K, Khvotchev M, Sudhof TC. 1998. α-Latrotoxin receptor CIRL/latrophilin 1 (CL1) defines an unusual family of ubiquitous G-protein-linked receptors. G-protein coupling not required for triggering exocytosis. J. Biol. Chem. 273:32715–32724.

30. Abe J, Fukuzawa T, Hirose S. 2002. Cleavage of Ig-Hepta at a “SEA” module and

at a conserved G protein-coupled receptor proteolytic site. J. Biol. Chem. 277:23391–23398.

31. Gray JX, Haino M, Roth MJ, Maguire JE, Jensen PN, Yarme A, Stetler-Stevenson MA, Siebenlist U, Kelly K. 1996. CD97 is a processed, seven-transmembrane, heterodimeric receptor associated with inflammation. J. Immunol. 157:5438 –5447.

32. Krasnoperov VG, Bittner MA, Beavis R, Kuang Y, Salnikow KV, Che- purny OG, Little AR, Plotnikov AN, Wu D, Holz RW, Petrenko AG. 997. alpha-Latrotoxin stimulates exocytosis by the interaction with a neuronal G-protein-coupled receptor. Neuron 18:925–937.

33. Lin HH, Chang GW, Davies JQ, Stacey M, Harris J, Gordon S. 2004. Autocatalytic cleavage of the EMR2 receptor occurs at a conserved G protein-coupled receptor proteolytic site motif. J. Biol. Chem. 279:31823– 31832.

34. Hsiao CC, Chen HY, Chang GW, Lin HH. 2011. GPS autoproteolysis is required for CD97 to up-regulate the expression of N-cadherin that promotes homotypic cell-cell aggregation. FEBS Lett. 585:313–318.

35. Paavola KJ, Stephenson JR, Ritter SL, Alter SP, Hall RA. 2011. The N terminus of the adhesion G protein-coupled receptor GPR56 controls receptor signaling activity. J. Biol. Chem. 286:28914 –28921.

36. Promel S, Frickenhaus M, Hughes S, Mestek L, Staunton D, Woollard A, Vakonakis I, Schoneberg T, Schnabel R, Russ AP, Langenhan T. 2012. The GPS motif is a molecular switch for bimodal activities of adhesion class G protein-coupled receptors. Cell Rep. 2:321–331.

37. Ward Y, Lake R, Yin JJ, Heger CD, Raffeld M, Goldsmith PK, Merino M, Kelly K. 2011. LPA receptor heterodimerizes with CD97 to amplify LPA-initiated RHO-dependent signaling and invasion in prostate cancer cells. Cancer Res. 71:7301–7311.

38. Paavola KJ, Hall RA. 2012. Adhesion G protein-coupled receptors: signaling, pharmacology, and mechanisms of activation. Mol. Pharmacol. 82:777–783.

39. Promel S, Langenhan T, Arac D. 2013. Matching structure with function: the GAIN domain of Adhesion-GPCR and PKD1-like proteins. Trends Pharmacol. Sci. 34:470–

478.

40. Kaur B, Brat DJ, Devi NS, Van Meir EG. 2005. Vasculostatin, a proteolytic fragment of brain angiogenesis inhibitor 1, is an antiangiogenic and antitumorigenic factor. Oncogene 24:3632–3642.

41. Kaur B, Cork SM, Sandberg EM, Devi NS, Zhang Z, Klenotic PA, Febbraio M, Shim H, Mao H, Tucker-Burden C, Silverstein RL, Brat DJ, Olson JJ, Van Meir EG. 2009. Vasculostatin inhibits intracranial glioma growth and negatively regulates in vivo angiogenesis through a CD36-dependent mechanism. Cancer Res. 69:1212–1220.

42. Herron BJ, Lu W, Rao C, Liu S, Peters H, Bronson RT, Justice MJ, McDonald JD, Beier DR. 2002. Efficient generation and mapping of recessive developmental mutations using ENU mutagenesis. Nat. Genet. 30:185–189.

43. Kurbegovic A, Cote O, Couillard M, Ward CJ, Harris PC, Trudel M. 2010. Pkd1 transgenic mice: adult model of polycystic kidney disease with extrarenal and renal phenotypes. Hum. Mol. Genet. 19:1174 –1189.

44. Kurbegovic A, Trudel M. 2013. Progressive development of polycystic kidney disease in the mouse model expressing Pkd1 extracellular domain. Hum. Mol. Genet. 22:2361–2375.

45. Wodarczyk C, Rowe I, Chiaravalli M, Pema M, Qian F, Boletta A. 2009. A novel mouse model reveals that polycystin-1 deficiency in ependyma and choroid plexus results in dysfunctional cilia and hydrocephalus. PLoS One 4:e7137.

46. Thivierge C, Kurbegovic A, Couillard M, Guillaume R, Cote O, Trudel M. 2006. Overexpression of PKD1 causes polycystic kidney disease. Mol. Cell. Biol. 26:1538 – 1548.

47. Couillard M, Trudel M. 2009. C-myc as a modulator of renal stem/ progenitor cell population. Dev. Dyn. 238:405– 414.

48. Ong AC, Harris PC, Davies DR, Pritchard L, Rossetti S, Biddolph S, Vaux DJ, Migone N, Ward CJ. 1999. Polycystin-1 expression in PKD1, early-onset PKD1, and TSC2/PKD1 cystic tissue. Kidney Int. 56:1324– 1333.

49. Freeze HH. 2001. Use of glycosidases to study protein trafficking. Curr. Protoc. Cell Biol. Chapter 15:Unit 15.2.

50. Kornfeld R, Kornfeld S. 1985. Assembly of asparagine-linked oligosaccharides. Annu. Rev. Biochem. 54:631– 664.

51. Stanley P. 2011. Golgi glycosylation. Cold Spring Harb. Perspect. Biol. 3:a005199.

52. Chapin HC, Rajendran V, Caplan MJ. 2010. Polycystin-1 surface localization is stimulated by polycystin-2 and cleavage at the G protein-coupled receptor proteolytic site. Mol. Biol. Cell 21:4338 – 4348.

53. Krasnoperov V, Lu Y, Buryanovsky L, Neubert TA, Ichtchenko K, Petrenko AG. 2002. Post-translational proteolytic processing of the calcium-independent receptor of alpha-latrotoxin (CIRL), a natural chimera of the cell adhesion protein and the G protein-coupled receptor. Role of the G protein-coupled receptor proteolysis site (GPS) motif. J. Biol. Chem. 277:46518 – 46526.

54. Magenheimer BS, St John PL, Isom KS, Abrahamson DR, De Lisle RC, Wallace DP, Maser RL, Grantham JJ, Calvet JP. 2006. Early embryonic renal tubules of wild-type and polycystic kidney disease kidneys respond to cAMP stimulation with cystic fibrosis transmembrane conductance regulator/Na^+, K^+, $2Cl^-$ Co-transporter-dependent cystic dilation. J. Am. Soc. Nephrol. 17: 3424 –3437.

55. Xu H, Shen J, Walker CL, Kleymenova E. 2001. Tissue-specific expression and splicing of the rat polycystic kidney disease 1 gene. DNA Seq. 12:361–366.

56. Butscheid Y, Chubanov V, Steger K, Meyer D, Dietrich A, Gudermann T. 2006. Polycystic kidney disease and receptor for egg jelly is a plasma membrane protein of mouse sperm head. Mol. Reprod. Dev. 73:350 –360.

57. Jin Z, Tietjen I, Bu L, Liu-Yesucevitz L, Gaur SK, Walsh CA, Piao X. 2007. Disease-associated mutations affect GPR56 protein trafficking and cell surface expression. Hum. Mol. Genet. 16:1972–1985.

58. Kim H, Jeong W, Ahn K, Ahn C, Kang S. 2004. Siah-1 interacts with the intracellular region of polycystin-1 and affects its stability via the ubiquitin-proteasome pathway. J. Am. Soc. Nephrol. 15:2042–2049.

59. Low SH, Vasanth S, Larson CH, Mukherjee S, Sharma N, Kinter MT, Kane ME, Obara T, Weimbs T. 2006. Polycystin-1, STAT6, and P100 function in a pathway that

transduces ciliary mechanosensation and is activated in polycystic kidney disease. Dev. Cell 10:57–69.

60. Tsiokas L, Kim E, Arnould T, Sukhatme VP, Walz G. 1997. Homo- and heterodimeric interactions between the gene products of PKD1 and PKD2. Proc. Natl. Acad. Sci. U. S. A. 94:6965– 6970.

61. Chauvet V, Tian X, Husson H, Grimm DH, Wang T, Hiesberger T, Igarashi P, Bennett AM, Ibraghimov-Beskrovnaya O, Somlo S, Caplan MJ. 2004. Mechanical stimuli induce cleavage and nuclear translocation of the polycystin-1 C terminus. J. Clin. Invest. 114:1433–1443.

62. Woodward OM, Li Y, Yu S, Greenwell P, Wodarczyk C, Boletta A, Guggino WB, Qian F. 2010. Identification of a polycystin-1 cleavage product, P100, that regulates store operated Ca entry through interactions with STIM1. PLoS One 5:e12305.

63. Porter JA, Young KE, Beachy PA. 1996. Cholesterol modification of hedgehog signaling proteins in animal development. Science 274:255– 259.

64. Volynski KE, Silva JP, Lelianova VG, Atiqur Rahman M, Hopkins C, Ushkaryov YA. 2004. Latrophilin fragments behave as independent proteins that associate and signal on binding of LTX(N4C). EMBO J. 23: 4423– 4433.

65. Cornec-Le Gall E, Audrezet MP, Chen JM, Hourmant M, Morin MP, Perrichot R, Charasse C, Whebe B, Renaudineau E, Jousset P, Guillodo MP, Grall-Jezequel A, Saliou P, Ferec C, Le Meur Y. 2013. Type of PKD1 Mutation Influences Renal Outcome in ADPKD. J. Am. Soc. Nephrol. 24:1006 –1013.

FIGURE LEGENDS

Figure 1. Characterization of endogenous $Pc1^{U}$ and $Pc1^{cFL}$ molecules in normal mouse tissues

(A) Schematic structure of mouse polycystin-1 (Pc1). LRR, leucine-rich repeat; CL, C-type lectin; L, LDL-A; PKD, polycystic kidney disease repeats; REJ, receptor for egg jelly; GPS, G-protein-coupled receptor proteolytic site. Pc1 cleavage occurs at $HL2T^{3041}$ site in the GPS motif, resulting in NTF and CTF fragments. Epitope positions of anti-LRR and anti-CC (chicken, cCC; rabbit, rCC) are shown by black boxes. The uncleaved full-length $Pc1^{U}$ (red) and the full-length cleaved $Pc1^{cFL}$ (blue) are schematized. The color code is maintained throughout the figures.

(B) Endogenous Pc1 products were analyzed by immunoprecipitation (IP) with anti-cCC from wild-type (WT) mouse embryos (E14.5 and E18.5), kidneys (P3 to P21), and adult (2-month-old) tissues (Br, brain; Li, liver; Ki, kidney; Lu, lung; He, heart; Sp, spleen) and detected by immunoblotting (IB) with anti-LRR (upper panel) and anti-rCC (lower panel). The schematic diagram (right panel) provides an identification guide.

(C) N-glycosylation modification of endogenous Pc1 from WT MEFs was monitored by IB on anti-cCC immunoprecipitates, either untreated (-) or treated with PNGase F (P) or endo-H (E). Pc1 products were detected with anti-LRR and anti-rCC from different exposures. The exclusive endo-H sensitivity of $Pc1^{U}$ contrasts with the partial endo-H sensitivity of $Pc1^{cFL}$. Note that endo-H-deglycosylated $Pc1^{U}$ overlapped with the intense endo-H-resistant NTF^{450} band (lane 3). A schematic diagram provides an identification guide.

(D) N-glycosylation modification of endogenous Pc1 from WT kidneys at P5 was analyzed as described for panel C and detected by IB with anti-LRR. Endogenous $Pc1^{U}$ is endo-H sensitive, whereas the Pc1 NTF subunit is both endo-H resistant and sensitive.

(E) Noncovalent association of $Pc1^{cFL}$ subunits. MEF lysates were subjected to IP with anti-cCC under either nondenaturing conditions with 0.5% Triton X-100 (Non-D)

or denaturing conditions with de- tergent SDS (0.1%; D), followed by IB with anti-LRR or anti-rCC. The NTF subunit was coprecipitated by the CTF subunit only under nondenaturing conditions. The schematic diagram provides an identification guide.

Figure 2. GPS cleavage is not a prerequisite for Pc1 intracellular trafficking

(A) Schematic structure of WT Pc1 and noncleavable $Pc1^{V}$ with a T3041V substitution at the $HL{\downarrow}T^{3041}$ cleavage consensus site, corresponding to the length of $Pc1^{U}$.

(B) N-glycosylation modification of Pc1 from collecting duct (CD) cells derived from WT and *Pkd1*$^{V/V}$ (V/V) postnatal kidneys was analyzed by IP with anti-cCC, either untreated (-) or treated with PNGase F (P) or endo-H (E), and then detected by IB with anti-LRR. In *Pkd1*$^{V/V}$ CD cells, the upper $Pc1^{V}$ band is endo-H resistant (arrow), and the lower $Pc1^{V}$ band is endo-H sensitive, as indicated in the schematic diagram. Note that $Pc1^{U}$ from WT CD cells was not detectable (lane 1).

(C) N-glycosylation modification of Pc1 from WT and *Pkd1*$^{V/V}$ (V/V) postnatal lungs was analyzed for anti-cCC IP products with anti-LRR and anti-rCC, similarly as described for panel B. Of note, $Pc1^{U}$ is weakly detected in the WT lungs, indicated by a red line in the right diagram.

Figure 3. Identification and characterization of Pc1 products on cell surfaces of collecting duct (CD) cells

Confluent CD monolayers were untreated (lane 3) or treated with sulfo-NHS-SS-biotin [sulfosuccinimidyl 2-(biotinamido)-ethyl-1,3-dithiopropionate] (lane 4). Protein lysates were prepared and incubated with NeutrAvidin-agarose (Avi, lanes 3 and 4). The bound proteins were eluted and analyzed by Western blotting using antibodies as indicated. The lack of detection of GM130 (a cis-Golgi protein) in the biotinylated protein population (lane 4) indicates that surface proteins were exclusively biotinylated. Total cell lysate (L) treated with biotin served as a positive control for NTF and CTF (lane 2), with an amount loaded that is equivalent to 1/20 of the amount

used for NeutrAvidin-agarose binding. Recombinant $Pc1^{V}$ served to indicate the position of uncleaved Pc1 (lane 1). The schematic diagram at right provides an identification guide. The asterisk indicates a nonspecific band that is seen in the surface protein population (lane 4).

Figure 4. Identification of a novel endogenous Pc1 form: $Pc1^{deN}$

(A) Immunodepletion strategy to identify the Pc1 NTF detached from the CTF subunit, $Pc1^{deN}$. $Pc1^{U}$ and $Pc1^{cFL}$ are exhaustively immunoprecipitated from total lysates (L) with anti-cCC, and the putative $Pc1^{deN}$ is analyzed from immunodepleted lysates (LΔ) with anti-LRR.

(B) N-glycosylation of endogenous $Pc1^{deN}$ in IMCD cells was analyzed from total lysate (L) and immunodepleted lysates (LΔ) by IB with anti-LRR, after deglycosylation with PNGase F (P) or endo-H (E) or no treatment (-). Note that the $Pc1^{U}$ form was not detectable. The depleted lysate (LΔ) is devoid of $Pc1^{cFL}$ (data not shown). Of interest, $Pc1^{deN}$ was detected in both endo-H-resistant (upper band) and -sensitive (lower band) forms, as schematically depicted at right. GAPDH was used as a loading control.

(C) N-glycosylation of endogenous $Pc1^{deN}$ in P5 WT kidney was analyzed from total lysate (L) and immunodepleted lysates (LΔ) as described for IMCD cells in panel B. In total lysate, $Pc1^{cFL}$ overlapped with $Pc1^{deN}$. The schematic diagram provides an identification guide.

Figure 5. Analysis of $Pc1^{deN}$ functional role by a $Pc1_{extra}$-BAC transgene in *Pkd1*$^{V/V}$ mice

(A) Schematic structure of endogenous Pc1 (*Pkd1*$^{+/+}$), $Pc1^{V}$ (*Pkd1*$^{V/V}$), and $Pc1_{extra}$ (*Pkd1*$_{extra}$) proteins. $Pc1_{extra}$ protein was generated by insertion of a termination translation codon in exon 25 of *Pkd1* at aa 3043 immediately following the GPS cleavage site. The epitope recognized by anti-LRR is indicated as a black box.

(B) Pc1/Pc1^{V}/Pc1$_{extra}$ protein expression levels in P10 kidneys were analyzed by IB with anti-LRR from mice with the genotypes indicated. Protein loading for *Pkd1$_{extra}$2* and *Pkd1$^{V/V}$; Pkd1$_{extra}$2* mice was decreased by 10-fold (0.9 μg/lane) relative to all other kidney samples (9 μg). Pc1$_{extra}$ exhibits higher expression levels in line *Pkd1$_{extra}$2* than in line *Pkd1$_{extra}$39* and appears in both lines as a single band in comparison to the doublet detected in the wild-type Pc1. β-Tubulin was used as a loading control.

(C) Histogram of the kidney weight-to-body weight ratio (KBW) for all genotypes as indicated. The ratios for the *Pkd1$^{V/V}$; Pkd1$_{extra}$39*, *Pkd1$^{V/V}$; Pkd1$_{extra}$ 2*, and *Pkd1$^{V/V}$* mice at P10 were significantly increased in comparison to the value for WT mice (*, $P < 0.0001$). n, number of mice.

(D) Histopathological analysis (H&E staining) of *Pkd1$^{V/V}$; Pkd1$_{extra}$* kidneys at P10. *Pkd1$^{V/V}$; Pkd1$_{extra}$39* and *Pkd1$^{V/V}$; Pkd1$_{extra}$2* mice displayed numerous cysts throughout the kidney parenchyma comparable to Pkd1$^{V/V}$ mice. Scale bar, 100 μm.

(E) Histogram of renal cystic index of *Pkd1$^{V/V}$; Pkd1$_{extra}$* kidneys at P10. Cystic involvement (percentage of cystic area) in the *Pkd1$^{V/V}$; Pkd1$_{extra}$39* and *Pkd1$^{V/V}$; Pkd1$_{extra}$2* lines shows no significant difference from that in the *Pkd1$^{V/V}$* kidneys, but values were highly significant compare to control values (*, $P < 0.0001$). n, number of mice.

(F) Renal cystic involvement in medulla versus cortex in *Pkd1$^{V/V}$* and *Pkd1$^{V/V}$; Pkd1$_{extra}$2* mouse lines at P10. For both *Pkd1$^{V/V}$* and *Pkd1$^{V/V}$; Pkd1$_{extra}$2* mouse lines, cyst surface area (%) is significantly higher in the medulla than in cortex (*, $P < 0.0003$). Values for the *Pkd1$^{V/V}$; Pkd1$_{extra}$2* line are not significantly different from those of *Pkd1$^{V/V}$* mice in cortex or medulla. n, number of mice.

(G) Kaplan-Meier survival curves of the *Pkd1$^{V/V}$*, *Pkd1$^{V/V}$; Pkd1$_{extra}$39*, and *Pkd1$^{V/V}$; Pkd1$_{extra}$2* mice revealed similar life expectancies.

(H) Pc1/Pc1^{V}/Pc1$_{extra}$ N-glycosylation status at P10 kidneys was analyzed by IB with anti-LRR on kidney lysates from control *Pkd1*$^{+/+}$, *Pkd1*$^{V/V}$; *Pkd1*$_{extra}$*39*, and *Pkd1*$^{V/V}$; *Pkd1*$_{extra}$*2* mice, either untreated (-) or deglycosylated with PNGase F (P) or endo-H (E). Pc1 NTF in WT kidneys displayed both Pc1 endo-H-resistant and -sensitive forms, whereas Pc1$_{extra}$ in *Pkd1*$^{V/V}$; *Pkd1*$_{extra}$*39* and *Pkd1*$^{V/V}$; *Pkd1*$_{extra}$*2* kidneys is mainly endo-H sensitive. Protein loading for *Pkd1*$^{V/V}$; *Pkd1*$_{extra}$*2* mice was decreased by 10-fold in comparison to other kidney samples. GAPDH served as a loading control.

Figure 6. Intact CTF is required for intracellular trafficking of the Pc1^{deN} form

(A) Schematic diagram of Pc1 from WT *Pkd1* and *Pkd1*^{m1Bei} alleles. The Pc1^{m1Bei} contains a single substitution (M3083R) in the first TM domain of CTF (black triangle). Epitope positions of anti-LRR and anti-CC are indicated (black boxes).

(B) Endogenous Pc1 forms from WT and homozygous *Pkd1*$^{m1Bei/m1Bei}$ (B/B) embryos (E12.5) were monitored by IB on total lysates either untreated (-) or deglycosylated with PNGase F (P) or endo-H (E) using anti-LRR. *Pkd1*$^{m1Bei/m1Bei}$ embryos express mutant full-length Pc1$^{U\text{-}m1Bei}$, with exclusive endo-H sensitivity, similar to Pc1^{U} in WT embryos (red). Pc1 NTF in *Pkd1*$^{m1Bei/m1Bei}$ embryos lacks endo-H resistance relative to WT embryos (arrows). Schematic diagram identifies the corresponding bands.

(C) N-glycosylation status of endogenous Pc1^{U} and Pc1^{cFL} forms from WT and mutant *Pkd1*$^{m1Bei/m1Bei}$ embryos was monitored by IB on anti-cCC immunoprecipitates, either untreated (-) or treated with PNGase F (P) or endo-H (E). Pc1 products were detected with anti-LRR and anti-rCC as indicated. The absence of endo-H resistance of both Pc1 NTF (as observed for total NTF in panel B) and CTF subunits in *Pkd1*$^{m1Bei/m1Bei}$ embryos contrasts with endo-H resistance in WT embryos (blue, arrows). Re-IP of the flowthrough fractions with anti-cCC (LΔ) confirmed complete depletion of Pc1^{U} and Pc1^{cFL} from both WT and

Pkd1$^{m1Bei/m1Bei}$ embryo lysates. The schematic diagram depicts corresponding bands.

(D) N-glycosylation status of endogenous Pc1^{deN} was analyzed by IB with anti-LRR from depleted lysates (LΔ) of WT and *Pkd1*$^{m1Bei/m1Bei}$ embryos following deglycosylation. Pc1^{deN} of the *Pkd1*$^{m1Bei/m1Bei}$ embryos lacks endo-H resistance relative to WT embryos (arrows), as indicated by the schematic diagram at right.

(E to G) Results of N-glycosylation analysis for endogenous Pc1 forms from E12.5 *Pkd1*$^{MYC/MYC}$ knock-in (M/M) and *Pkd1*$^{\Delta CMYC/\Delta CMYC}$ knockout (ΔC/ΔC) embryos using the same method as for the *Pkd1*$^{m1Bei/m1Bei}$ (B/B) embryos in panels A to C, except that anti-Myc was used to immunoprecipitate and detect endogenous Myc-tagged Pc1 molecules.

Figure 7. Functional complementation of *Pkd1*$^{V/V}$ by Pkd1-BAC transgenic mice

(A) Schematic diagram of Pc1$_{tg}$ (*Pkd1*$_{TAG}$) and Pc1^{V} (*Pkd1*$^{V/V}$). The epitopes recognized by anti-LRR and anti-CC are indicated as black boxes.

(B) Protein expression of P10 kidneys from *Pkd1*$^{+/+}$, *Pkd1*$_{TAG}$, *Pkd1*$^{V/V}$, and *Pkd1*$^{V/V}$; *Pkd1*$_{TAG}$ mice were analyzed by IB using anti-LRR. Pc1 expression in *Pkd1*$_{TAG}$ and *Pkd1*$^{V/V}$; *Pkd1*$_{TAG}$ mice was increased, and Pc1 migrated as a doublet, like endogenous Pc1. β-Tubulin served as a loading control.

(C) Kidney histology (H&E staining) of *Pkd1*$^{+/+}$, *Pkd1*$^{V/V}$, and *Pkd1*$^{V/V}$; *Pkd1*$_{TAG}$ mice. *Pkd1*$^{V/V}$; *Pkd1*$_{TAG}$ mice showed complete rescue of the *Pkd1*$^{V/V}$ renal phenotype, similar to the WT controls at P10 and 3 months of age. Scale bar, 100 μm.

(D) N-glycosylation status of Pc1 from *Pkd1*$^{V/V}$; *Pkd1*$_{TAG}$ P10 kidneys was monitored by IB on anti-cCC immunoprecipitates, either untreated (-) or treated with PNGase F (P) or endo-H (E). Pc1 products were detected with anti-LRR and anti-rCC

as indicated. Pc1^{cFL} and Pc1^{U} patterns in *Pkd1$^{V/V}$; Pkd1$_{TAG}$* kidneys are identical to those of the endogenous Pc1 in WT kidneys shown in Fig. 1D. The schematic diagram indicates different Pc1 forms.

(E) Pc1 N-glycosylation status of wild-type *Pkd1$^{+/+}$* and *Pkd1$^{V/V}$; Pkd1$_{TAG}$* P10 kidneys was analyzed using total lysate (L) and immunodepleted lysate (LΔ) by IB with anti-LRR following deglycosylation. *Pkd1$^{V/V}$; Pkd1$_{TAG}$* kidneys produce both endo-H-resistant and -sensitive Pc1^{deN} forms as in WT kidneys (left panel). The schematic diagram provides an identification guide.

Figure 8. Model for the role of GPS cleavage in Pc1 biogenesis, trafficking, and functions.

In wild-type kidneys (left panel), Pc1^{U} is rapidly converted to Pc1^{cFL} by GPS cleavage in the ER, resulting in small amounts that may exit the ER (open arrow). The resulting Pc1^{cFL} is the main form that exits the ER (1) and traffics to the plasma membrane/cell-cell junctions (2) or other locations, possibly the primary cilium (3). Some of the Pc1^{cFL} in the ER and Golgi compartment undergoes subunit dissociation, producing Pc1^{deN}. The Pc1^{cFL} on the plasma membrane/cell-cell junctions could also dissociate. The released CTF is likely rapidly degraded, as indicated by dots. The Pc1^{deN} remains associated on the membrane, likely through the interaction with other membrane proteins or lipid modification, and accumulates over time (curved arrow). Pc1^{deN}/ Pc1^{cFL} probably plays an important role at the cell membrane and/or at the cilium. In *Pkd1$^{m1Bei/m1Bei}$* or *Pkd1$^{\Delta CMYC/\Delta CMYC}$* pups (right panel) the mutant Pc1 is unable to exit the ER (black bar), leading to the development of massive cysts despite proper GPS cleavage. Schematized Pc1 forms in wild-type and mutant mice are illustrated below.

Fig1.

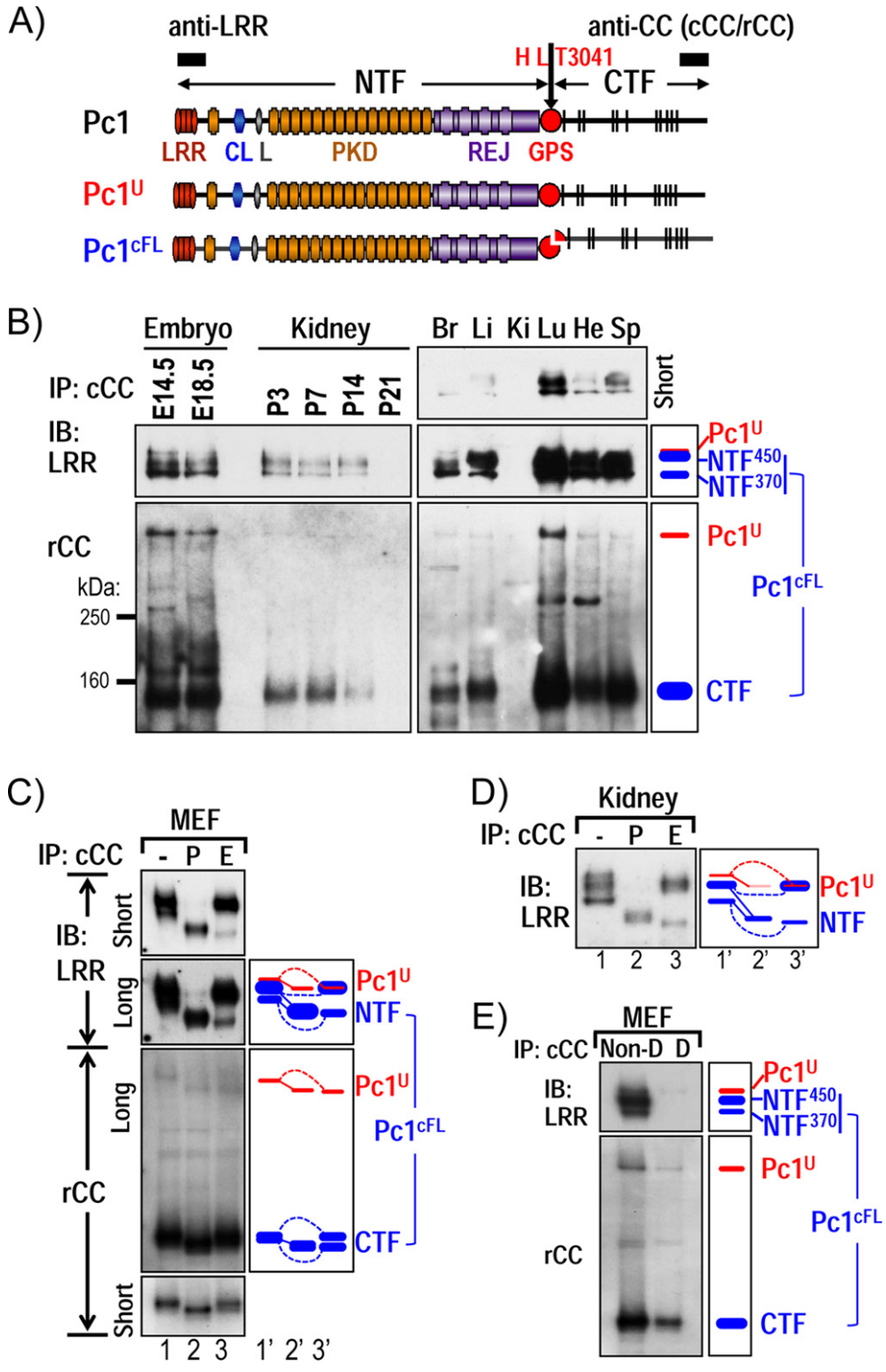
A)
anti-LRR
anti-CC (cCC/rCC)
H L T3041
NTF
CTF
Pc1
LRR CL L
PKD
REJ
GPS
Pc1U
Pc1cFL
B)
Embryo
Kidney
Br Li Ki Lu He Sp
IP: cCC
E14.5
E18.5
P3
P7
P14
P21
Short
IB: LRR
rCC
kDa:
250
160
Pc1U
NTF450
NTF370
Pc1cFL
CTF
C)
MEF
IP: cCC
- P E
IB: LRR
Short
Long
Long
rCC
Short
Pc1U
NTF
Pc1U
Pc1cFL
CTF
1 2 3 1' 2' 3'
D)
Kidney
IP: cCC
- P E
IB: LRR
1 2 3 1' 2' 3'
Pc1U
NTF
E)
MEF
IP: cCC
Non-D D
IB: LRR
rCC
Pc1U
NTF450
NTF370
Pc1U
Pc1cFL
CTF

Fig2.

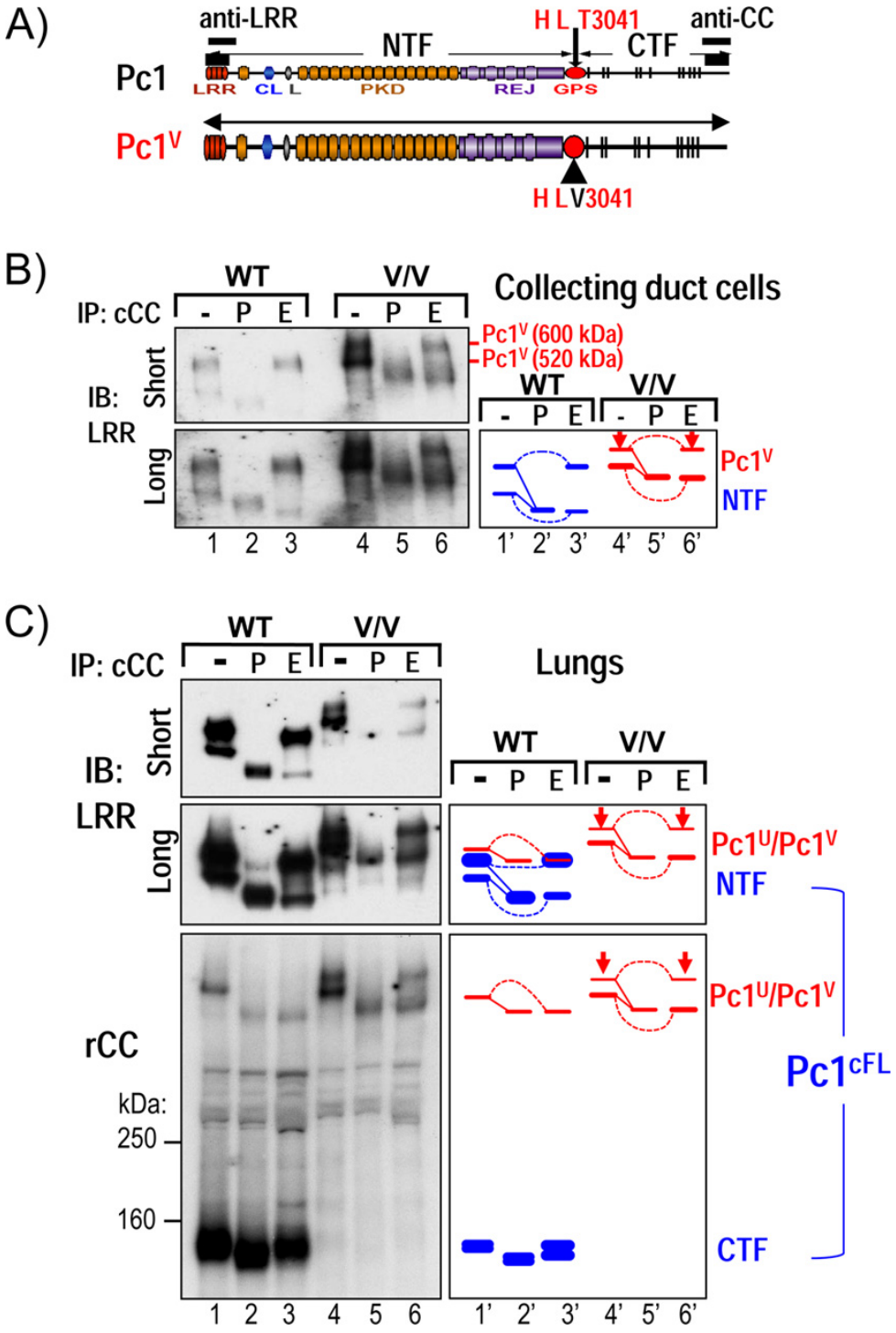
A)
anti-LRR
NTF
H L T3041
CTF
anti-CC
Pc1
LRR CL L
PKD
REJ GPS
Pc1V
H LV3041
B)
WT
V/V
Collecting duct cells
IP: cCC
- P E
- P E
Pc1V (600 kDa)
Pc1V (520 kDa)
IB: LRR
Short
Long
WT
V/V
- P E
- P E
Pc1V
NTF
1 2 3 4 5 6
1' 2' 3' 4' 5' 6'
C)
WT
V/V
IP: cCC
- P E
- P E
Lungs
IB: LRR
Short
Long
WT
V/V
- P E
- P E
Pc1U/Pc1V
NTF
Pc1U/Pc1V
rCC
kDa:
250
160
Pc1cFL
CTF
1 2 3 4 5 6
1' 2' 3' 4' 5' 6'

Fig3.

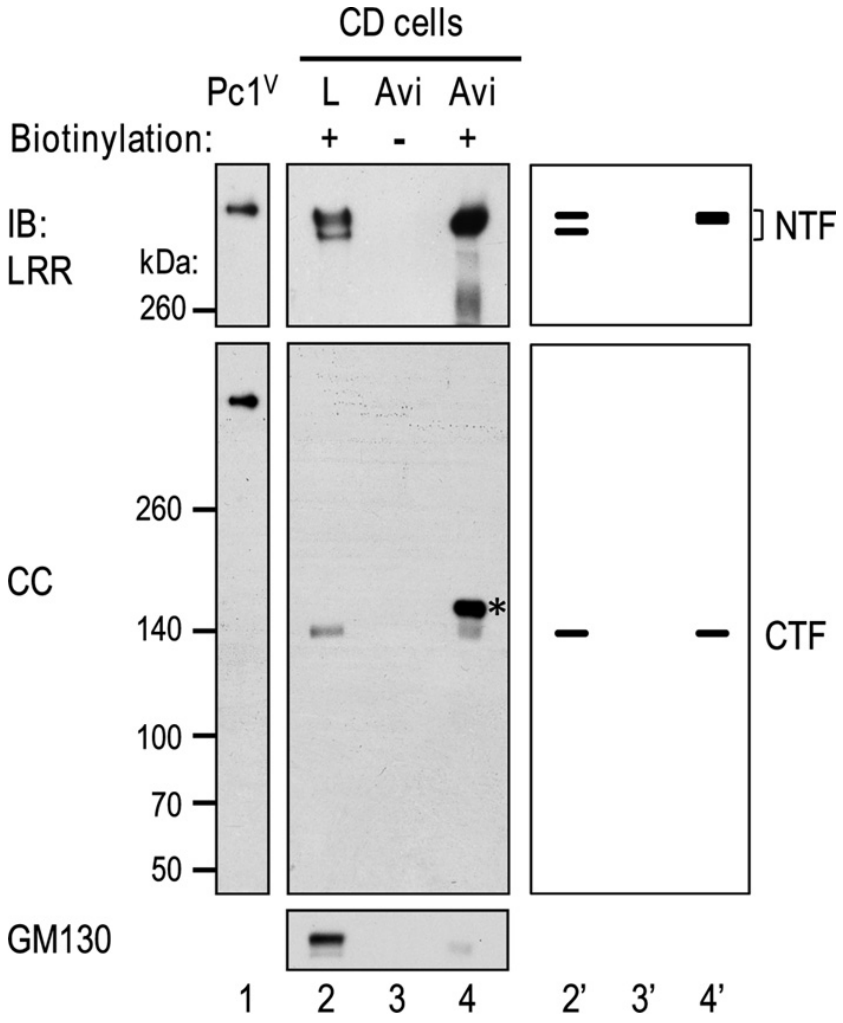
CD cells
Pc1V
L
Avi
Avi
Biotinylation:
+
-
+
IB:
LRR
kDa:
260
NTF
260
CC
140
*
CTF
100
70
50
GM130
1
2
3
4
2'
3'
4'

Fig4.

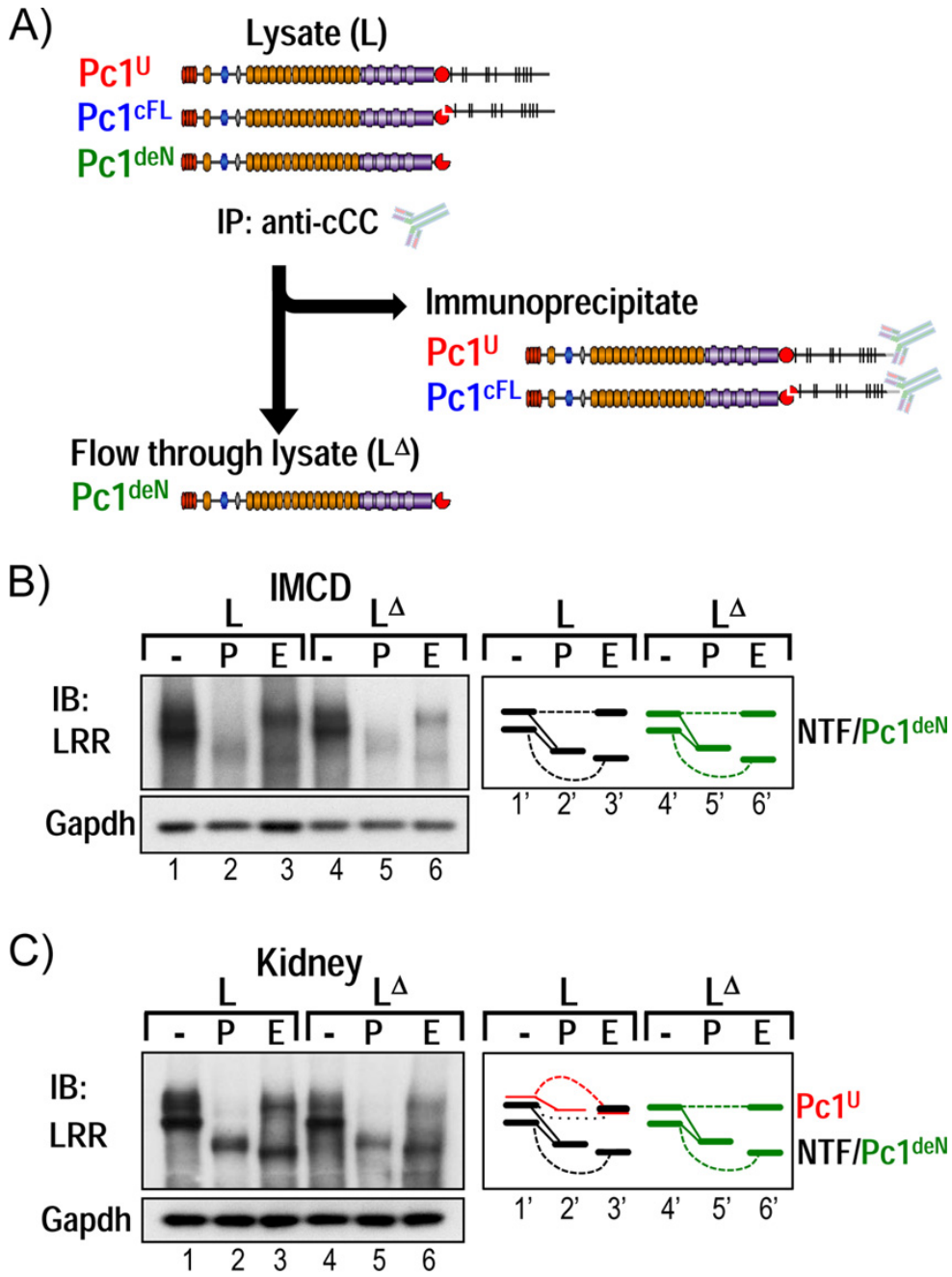
A)
Lysate (L)
Pc1U
Pc1cFL
Pc1deN
IP: anti-cCC
Immunoprecipitate
Pc1U
Pc1cFL
Flow through lysate (LΔ)
Pc1deN
B)
IMCD
L
LΔ
- P E
IB:
LRR
Gapdh
1 2 3 4 5 6
1' 2' 3' 4' 5' 6'
NTF/Pc1deN
C)
Kidney
Pc1U
NTF/Pc1deN

Fig5.

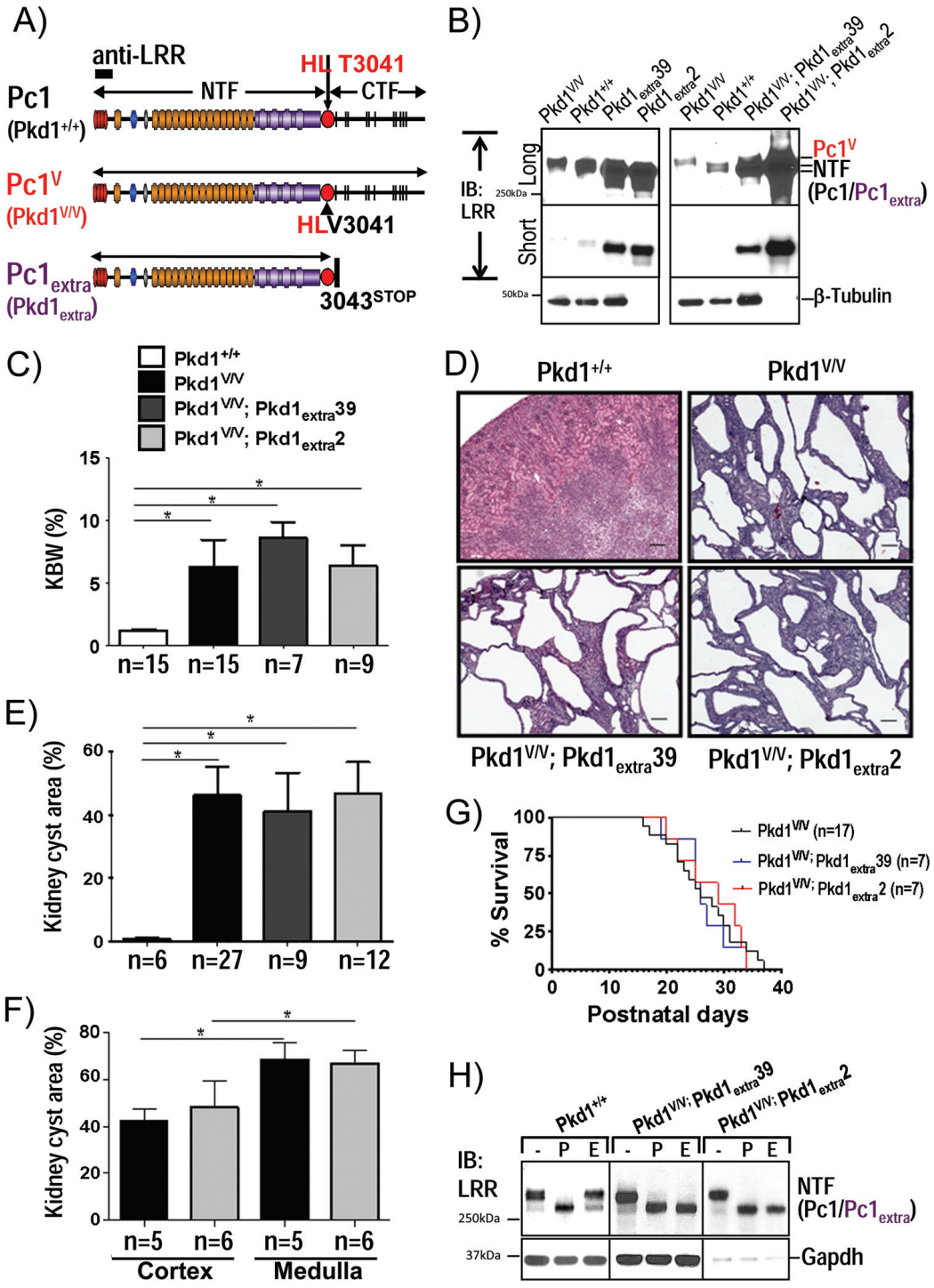
A)
anti-LRR
HL T3041
NTF
CTF
Pc1
(Pkd1+/+)
Pc1V
(Pkd1V/V)
HLV3041
Pc1extra
(Pkd1extra)
3043STOP
B)
Pkd1V/V
Pkd1+/+
Pkd1extra39
Pkd1extra2
Pkd1V/V; Pkd1extra39
Pkd1V/V; Pkd1extra2
IB: LRR
Long
Short
250kDa
50kDa
Pc1V
NTF
(Pc1/Pc1extra)
β-Tubulin
C)
Pkd1+/+
Pkd1V/V
Pkd1V/V; Pkd1extra39
Pkd1V/V; Pkd1extra2
KBW (%)
n=15
n=15
n=7
n=9
D)
Pkd1+/+
Pkd1V/V
Pkd1V/V; Pkd1extra39
Pkd1V/V; Pkd1extra2
E)
Kidney cyst area (%)
n=6
n=27
n=9
n=12
F)
Kidney cyst area (%)
n=5
n=6
n=5
n=6
Cortex
Medulla
G)
% Survival
Postnatal days
Pkd1V/V (n=17)
Pkd1V/V; Pkd1extra39 (n=7)
Pkd1V/V; Pkd1extra2 (n=7)
H)
Pkd1+/+
Pkd1V/V; Pkd1extra39
Pkd1V/V; Pkd1extra2
- P E
IB: LRR
250kDa
37kDa
NTF
(Pc1/Pc1extra)
Gapdh

FIG.6

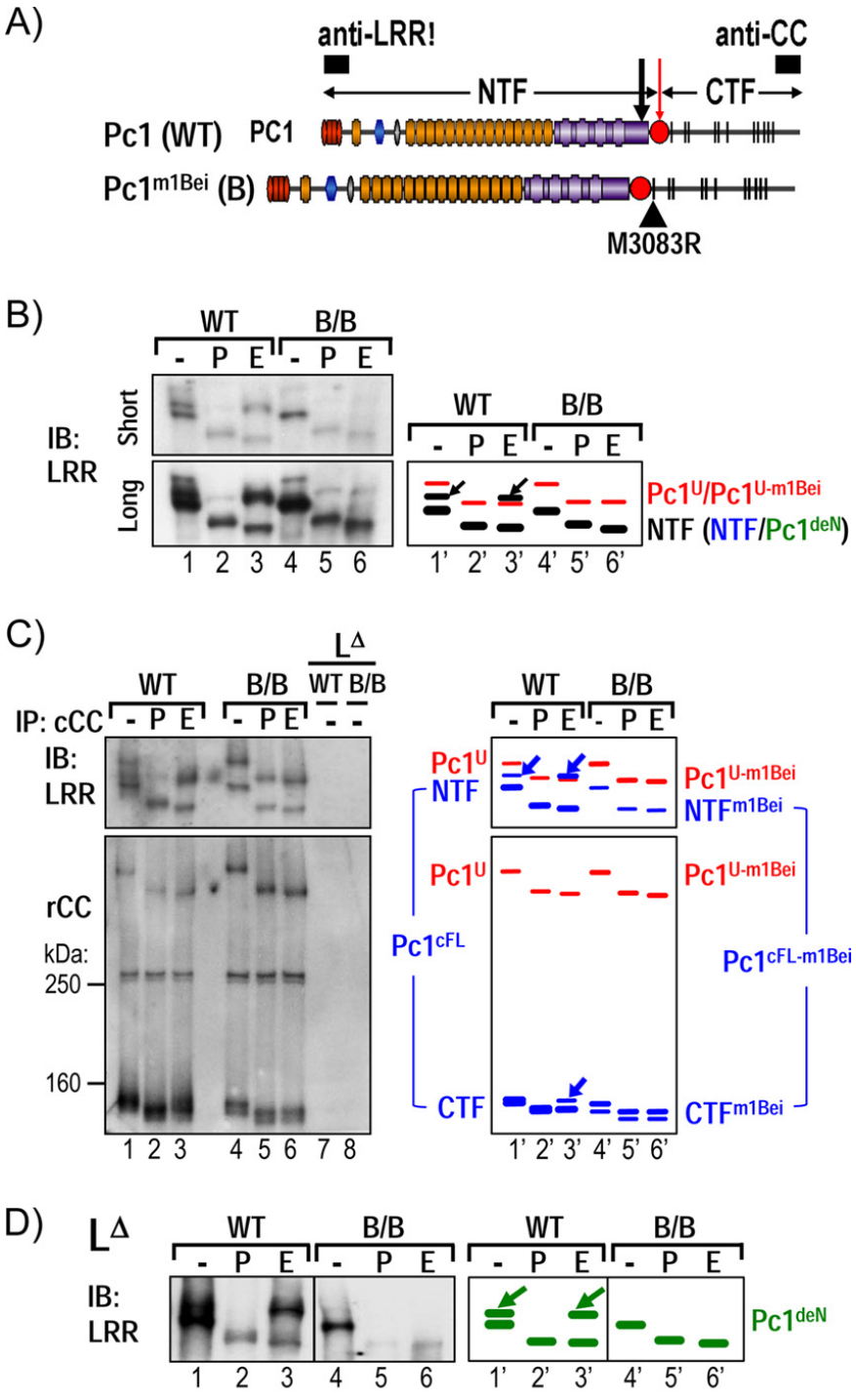
A)
anti-LRR!
anti-CC
NTF
CTF
Pc1 (WT)
PC1
Pc1m1Bei (B)
M3083R
B)
WT
B/B
- P E
IB:
LRR
Short
Long
1 2 3 4 5 6
1' 2' 3' 4' 5' 6'
Pc1U/Pc1U-m1Bei
NTF (NTF/Pc1deN)
C)
LΔ
IP: cCC
rCC
kDa:
250
160
1 2 3 4 5 6 7 8
1' 2' 3' 4' 5' 6'
Pc1U
NTF
Pc1U-m1Bei
NTFm1Bei
Pc1cFL
Pc1cFL-m1Bei
CTF
CTFm1Bei
D)
LΔ
Pc1deN

Fig6.

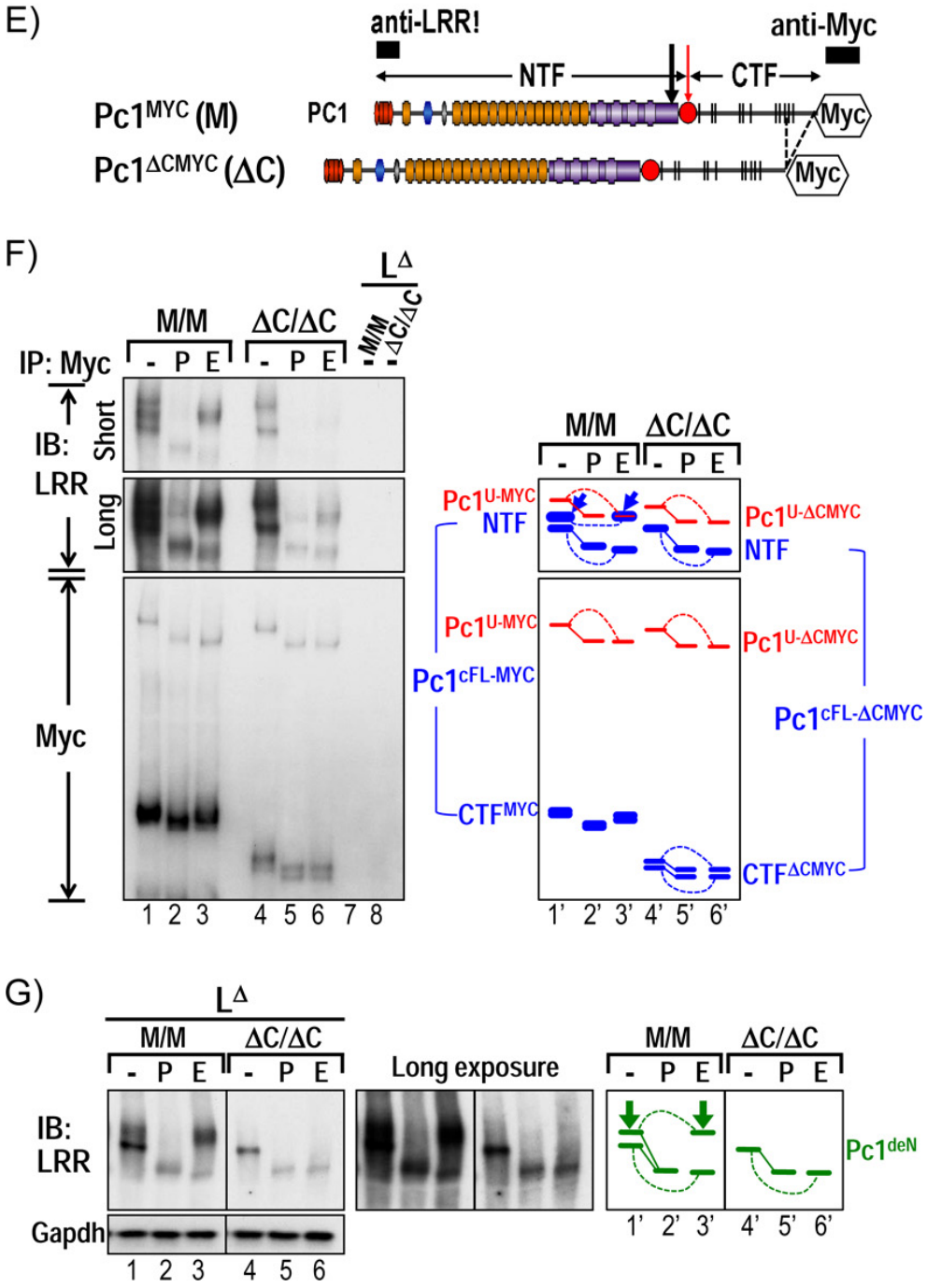
E)
anti-LRR!
anti-Myc
NTF
CTF
Pc1MYC (M)
PC1
Myc
Pc1ΔCMYC (ΔC)
Myc
F)
LΔ
M/M
ΔC/ΔC
M/M
ΔC/ΔC
IP: Myc
- P E
- P E
IB:
LRR
Short
Long
Myc
1 2 3 4 5 6 7 8
M/M
ΔC/ΔC
- P E
- P E
Pc1U-MYC
NTF
Pc1U-ΔCMYC
NTF
Pc1U-MYC
Pc1U-ΔCMYC
Pc1cFL-MYC
Pc1cFL-ΔCMYC
CTFMYC
CTFΔCMYC
1' 2' 3' 4' 5' 6'
G)
LΔ
M/M
ΔC/ΔC
- P E
- P E
IB:
LRR
Gapdh
1 2 3 4 5 6
Long exposure
M/M
ΔC/ΔC
- P E
- P E
Pc1deN
1' 2' 3' 4' 5' 6'

Fig7.

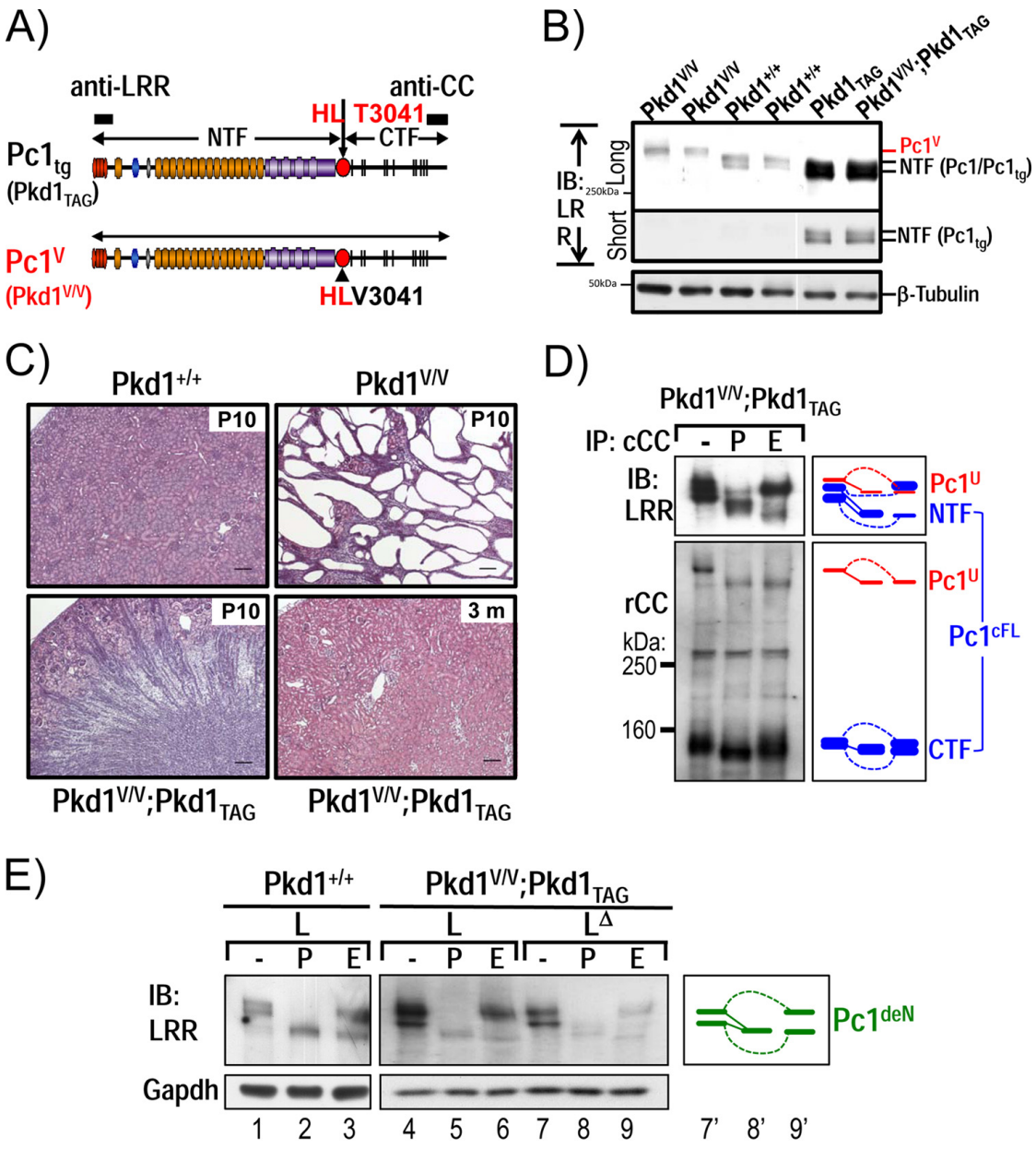
A)
anti-LRR
anti-CC
HL T3041
NTF
CTF
Pc1tg
(Pkd1TAG)
Pc1V
(Pkd1V/V)
HLV3041
B)
Pkd1V/V
Pkd1V/V
Pkd1+/+
Pkd1+/+
Pkd1TAG
Pkd1V/V;Pkd1TAG
IB:
LR
Long
Short
250kDa
50kDa
Pc1V
NTF (Pc1/Pc1tg)
NTF (Pc1tg)
β-Tubulin
C)
Pkd1+/+
Pkd1V/V
P10
P10
P10
3 m
Pkd1V/V;Pkd1TAG
Pkd1V/V;Pkd1TAG
D)
Pkd1V/V;Pkd1TAG
IP: cCC
- P E
IB:
LRR
rCC
kDa:
250
160
Pc1U
NTF
Pc1U
Pc1cFL
CTF
E)
Pkd1+/+
Pkd1V/V;Pkd1TAG
L
L
LΔ
- P E
- P E
- P E
IB:
LRR
Gapdh
Pc1deN
1 2 3 4 5 6 7 8 9 7' 8' 9'

Fig8.

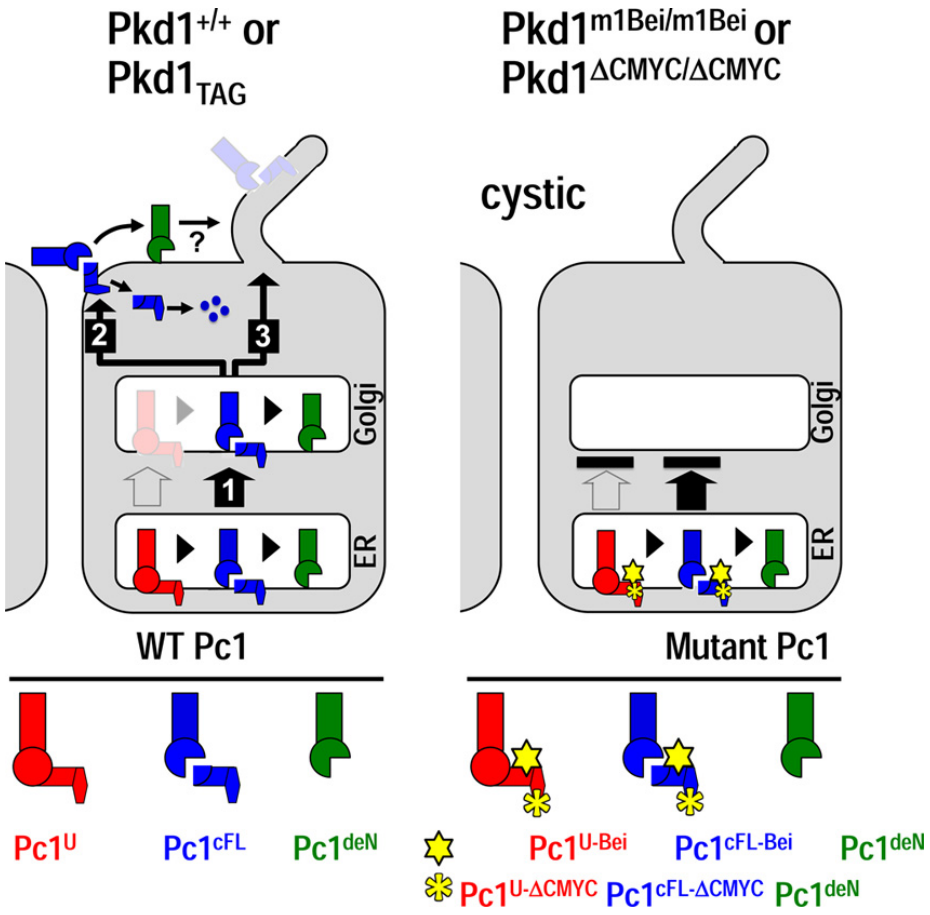

Table 1

TABLE 1 Pkd1 mouse lines

Mouse line	Genetic modification	Description	Reference
$Pkd1^{V/V}$	Knock-in	T3041V at GPS/GAIN domain produces noncleavable $Pc1^{V}$	26
$Pkd1_{extra}2$	Transgenic (~80 copies)	F3043X in Pkd1-BAC produces NTF-like protein	44
$Pkd1_{extra}39$	Transgenic (~2 copies)	F3043X in Pkd1-BAC produces NTF-like protein	44
$Pkd1_{TAG}26$	Transgenic (~15 copies)	Full-length $Pkd1_{WT}$-BAC overexpresses endogenous Pc1	43
$Pkd1^{m1Bei/m1Bei}$	ENU mutagenesis	M3083R within the first transmembrane domain of CTF	42
$Pkd1^{MYC/MYC}$	Knock-in	Produces fully functional Pc1 with a C-terminal 5×Myc tag	45
$Pkd1^{\Delta CMYC/\Delta CMYC}$	Knockout	Produces 5×Myc-tagged Pc1 lacking C-terminal 257 aa	45

CHAPTER VII - ARTICLE 4

Acute kidney injury crosstalk with Pkd1/Pkd2 dosage-increased pathogenesis and signaling

Almira Kurbegovic & Marie Trudel*

Molecular Genetics and Development, Institut de Recherches Cliniques de Montréal, Université de Montréal, Faculté de Médecine, Montréal, Québec, Canada

Word count:

Key words: Acute kidney injury, IRI, polycystin-1, polycystin-2, ADPKD, mTOR signaling, Wnt cascade

*Correspondence:

Dr. Marie Trudel

[redacted]

ABSTRACT

Acute kidney injury and autosomal dominant polycystic kidney disease (ADPKD) are a frequent cause for ESRD. Since ADPKD is triggered by altered Pc1- or Pc2 dosage-dependent mechanism in the mouse, we investigated whether slow progression of cystogenesis in Pkd1 dosage-increase mouse models can be accelerated with mild to moderate ischemia-reperfusion injury (IRI). Transient unilateral left ischemic kidney in both non-transgenic and transgenic mice revealed long-term and important stimulation of Hif1α expression. Control and transgenic mice systematically develop renal cysts associated with substantial and sustained Pc1 and Pc2 expression that can be causative. Activation of the mTOR cascade by phosphorylation of Erk and of AKT likely contributes to the cystogenic phenotype. Moreover, induction of the Wnt canonical pathway with markedly elevated b-catenin and c-Myc expression is a potential modulator of mTORC1 cascade and a key mechanism in the IRI cystogenic phenotype. This study shows for the first time that acute kidney injury crosstalk with Pc1/Pc2 signaling and pathogenic mechanisms.

INTRODUCTION

Acute kidney injury (AKI) is described as a sudden loss of renal function that is of high incidence in critically ill patients with multiple organ failure and sepsis. One of the most common causes of AKI is ischemia-reperfusion injury (IRI) that occurs in different clinical settings like kidney transplantation. Patients that recover from AKI are at significant increase risk to develop chronic kidney disease [1].

Human autosomal dominant polycystic kidney disease (ADPKD) is one of the most common genetic diseases manifested by bilateral renal cysts. ADPKD patients progress to end-stage renal failure frequently at mid-age and then require renal support or replacement therapy. ADPKD is caused in most cases by mutations in *PKD1* gene, encoding the protein polycystin-1 (PC1) or by mutations in *PKD2*, encoding polycystin-2 (PC2). The exact cystogenic mechanism is not clearly defined in human. In fact, loss-of-heterozygosity of *PKD1* was reported in a significant minority of the cysts whereas sustained and even increased PKD1 transcript and PC1 protein levels are detected in kidney homogenates and in majority of cysts [2,3]. Studies have suggested that PC1 may act as a receptor, mechanosensor and cell-cell/matrix interactive protein while PC2 functions as a non-selective calcium channel either independently or together with PC1. A more severe PKD phenotype was described in the contiguous gene syndrome due to mutations in both *PKD1* and the *TSC2* gene adjacent to each other in the human genome. Tuberin, the product of the *TSC2* gene was found to physically interact with PC1 [4]. This data suggested that both PC1 and Tuberin are implicated in the same pathway.

In the mouse, homozygous deletion of *Pkd1* result in rapid renal cystic disease whereas hypomorphic alleles of *Pkd1* have variable cystic disease progression [4-6]. *Pkd1* renal conditional inactivation in adulthood however leads to mild or focal cysts [7,8]. In parallel, we produced *SBPkd1*$_{TAG}$ transgenic mice that specifically express full-length *Pkd1* in kidneys and cause a cystic phenotype within few months [9]. *Pkd1*$_{TAG}$ mice with systemic full-length *Pkd1* gene consistently develop not only renal cysts associated with longer primary cilia in epithelial cells but also extrarenal phenotypes

[10]. Severity of cyst formation and renal insufficiency in the *Pkd1*$_{TAG}$ mouse lines progressed with Pkd1 dosage-increased expression. It showed that altered Pc1 levels in the kidney lead to a PKD phenotype and in a dose-dependent mechanism, consistent with human ADPKD studies. More recently, we generated mouse models that mimic a clinical *PKD1* allele by expressing the N-terminal extracellular domain of Pc1, *Pkd1*$_{extra}$ (Pkd1^{3043X}). These *Pkd1*$_{extra}$ mouse lines develop gradual progressive renal cystogenesis with severe disease at >1.5 year of age, recapitulating ADPKD characteristics, possibly via a Pc2 dosage-increased mechanism [11].

Upon induction of injury, adult kidneys in dosage-reduced mouse models from *Pkd1* ablation or haploinsufficiency were found to acquire cysts more rapidly [12-14]. Renal regeneration from AKI in normal mice is believed to occur within few days, probably via activation of a repair program associated with cellular proliferation, as in renal development [15]. In the *Pkd1* dosage-reduced kidneys however, AKI would trigger injury-induced cystogenesis by failing to switch out of the repair mechanism or by activation of large number of genes that would result in a pathologic process [16]. The injury-induced *Pkd1* deficient mouse models implicate possibly many signaling pathways of which only the Wnt and planar cell polarity pathways are reported [13,17]. Presently, kidney injury is considered as a "modifier'' of *Pkd1* dosage-reduced murine models. However, the exact mechanisms underlying this effect and the interconnection between AKI and Pkd1 dosage-dependent cystogenesis remain to be elucidated.

We investigated whether AKI is a modifier of cystogenesis from clinical-like and dosage-increased *Pkd1* alleles toward dissection of the global cellular and molecular interaction(s). Transient IRI induced in a low Pkd1 dosage-increased mouse line, *Pkd1*$_{TAG}$6 and in two *Pkd1*$_{extra}$ lines with slow progression of cyst formation in late adulthood [10,11] as well as in non-transgenic controls developed typical PKD cystogenesis. The cystogenic mechanism was associated not only with markedly elevated Pc1 and Pc2 but also with persistent increased Hif1α levels and stimulation of both the Wnt and mTOR signaling pathways. Our studies provide evidence that AKI

lead to cystogenesis and progressive chronic kidney disease and to identification of a novel crosstalk between AKI and Pc1/Pc2 signaling pathways.

RESULTS

Opposite renal bilateral response from IRI unilateral exposure

Since ischemia reperfusion injury (IRI) in *Pkd1* dosage reduce mouse models was reported to promote cystogenesis, we questioned whether cystogenesis could be accelerated in *Pkd1* dosage increase mouse models and interrogated the molecular signaling mechanism. Two sets of transgenic mouse lines were selected one set expressed the full-length *Pkd1* dosage increase $Pkd1_{TAG}$ (line 6) at mild level and the second set the extracellular domain $Pkd1_{extra}$ at mild (line39) and high (line2) level. Transient unilateral left renal IRI for 30 minutes was performed in all mice including control littermates at 3-months of age (median 90 ±3.0days) and mice sacrificed at different time points following reperfusion (**Fig.1A**).

We first examined kidney size relative to body weight as a surrogate to kidney volume since kidney volume is a prognostic biomarker for cystogenesis and renal function [18]. At the onset of renal injury in 3 month-old wild type mice, the left kidney size (0.61%±0.06; n=7) are non-significantly different from the right kidney (0.64% ±0.05; n=7) relative to body weight but tended to be slightly smaller (**Fig.1B**). At 23 days following reperfusion, the left IRI kidneys (0.33±0.03; n=5) was decreased by ~45% in size whereas the contralateral right kidneys (0.86±0.09; n=5) was increased by ~30%. Unexpectedly, we observed similar response for the relative left (0.30±0.07; n=3) and right (0.80±0.04; n=3) kidney sizes of the two transgenic $Pkd1_{extra}$ mouse lines following 23 days post-reperfusion.

Analysis of the $Pkd1_{TAG}$ and $Pkd1_{extra}$ transgenic lines and non-transgenic littermate controls were compared at 3 and 4 months post-IRI or ~6 months of age. Controls non-IRI at ~6 months of age showed no significant difference between the relative right and left kidneys size of wild type mice (n=4). Like at 23 days post-reperfusion, a similar pattern was detected for the IRI kidneys of non-transgenic (n=45) and transgenic $Pkd1_{TAG}$ and $Pkd1_{extra}$ lines with mild or high Pkd1 expression as shown in figure 1B. Following IRI, the relative kidney size of non-transgenic right kidneys was increased by ~34% comparable to the hypertrophy detected at 23 days post-IRI of the

right kidneys. In contrast, the non-transgenic left IRI kidneys seem to regress further than at 23 days decreasing to ~56% (**Fig.1B**). Data for the slow progressive development of PKD phenotype in the two *Pkd1*$_{extra}$ mouse lines was analogous and regrouped. The relative right kidney size of transgenic *Pkd1*$_{extra}$ (n=24) and *Pkd1*$_{TAG}$ *6* (n=9) was increased by ~37%, similar to right kidneys from the IRI control mice. Comparison of the post-IRI left kidney size of the *Pkd1*$_{extra}$ lines and *Pkd1*$_{TAG}$ *6* to the non-ischemic control littermates showed a decrease by ~50 and 60% respectively, analogous to the non-transgenic IRI left kidneys. This indicated that within 23 days of IRI and in the following months, the left kidneys undergo atrophy and the right kidneys a compensatory hypertrophy independently of the genotype.

Renal cystogenesis in both transgenic and non-transgenic mice

To gain insight into the cellular mechanism, histological analysis of the kidneys was performed. At 16 and 23 days post-reperfusion, the left kidneys of non-transgenic mice (n=6) showed evidence of tubular and glomerular dilatations and cysts, epithelial hyperplasia, infiltrates, tubular damage, protein hyaline casts, and fibrosis (**Fig.2A**). From 23 days to ~3 months post-IRI, all left kidneys from non-transgenic (n=37) developed renal cysts some of which were detected macroscopically while the right kidneys were unaffected (**Fig.2A**). Similarly, all left IRI kidneys from transgenic *Pkd1*$_{extra}$ (n=24) and *Pkd1*$_{TAG}$ *6* (n=8) mice displayed at 23 days and 3 months post-reperfusion tubular dilatations and cysts in the kidneys (**Fig.2B**). Interestingly, cysts were detected in the cortex, cortico-medullary junction but as well in the papilla of the left kidneys from the non-transgenic and transgenic *Pkd1*$_{extra}$ and *Pkd1*$_{TAG}$ *6* mice. Since all non-transgenic and transgenic left IRI kidneys develop cysts but with variable severity, renal cystic involvement was evaluated by ratio of cystic surface relative to the total surface using histo-morphometry. The cystic surface area of left IRI kidneys at 3 months post-reperfusion was classified as mild (0-5%), intermediate (5-15%) or severe (>15%) for each mouse genotype. Figure 2C show that non-transgenic controls and transgenic mouse lines had a similar proportion of mice in the corresponding cystic severity groups. Non-transgenic and transgenic left IRI kidneys were then monitored for mean number of cysts per surface area and then subdivided

into groups of low (<2 cysts/mm^2), moderate (2-5 cysts/mm^2) and high (>5 cysts/mm^2) number of cysts for each murine genotype. As shown in fig 2C, the proportion of mice in the three groups did not appear very different. Notably, mice cystic surface involvement, mild, intermediate or severe significantly correlated with mice in the low, moderate or high mean number of cysts, respectively. The similar proportion of mice with various severity of cystic surface or mean cyst number in controls IRI kidneys indicate that the transgene had minimal to no effect on the cystic phenotype at 3-mont post-reperfusion.

We also monitored fibrosis and interstitial scarring in transgenic and non-transgenic IRI kidneys with Sirius red staining. Both IRI non-transgenic and transgenic *Pkd1$_{extra}$* left kidneys showed intense positive staining over the cortical-medullary junction in the outer medulla, the most susceptible region to ischemia as well as signals within the cortex and papilla at 3-months post-reperfusion (**Supp Fig.1A**). To substantiate the increase levels of fibrosis, we performed immunoblot with collagen type IV antibody and obtained two major bands (160kDa and >250kDa) from the non-transgenic and transgenic left IRI kidneys whereas it was barely detectable in the right contralateral kidneys (**Supp Fig.1B**). The abundance of collagen deposits did not correlate directly with severity of renal cysts. Together, fibrosis and collagen deposits appeared independent of the genotype and severity of cystogenesis.

Because cilia anomalies have been associated with renal cyst and stress-response [19,20], we monitored cilia of renal epithelial cells in the non-transgenic control (n=3) and transgenic *Pkd1$_{extra}$* mice (n=3) by α-acetylated tubulin staining at 3 months post-reperfusion. The cilia size distribution in the epithelia of the left IRI kidneys of both control (6.1%) and transgenic (8.1%) mice tended to show a higher proportion of longer cilia (>5um) than the non-IRI left kidneys (0.7%). This result suggests that the ischemia-induced cystic anomalies of the left kidneys elicit mild stimulation of ciliogenesis.

Persistent ischemic response following post-reperfusion

To determine whether IRI induced a persistent hypoxic and/or repair response in non-transgenic control and transgenic mice, we monitored Hif1α expression levels from 16 days post-reperfusion. Expression of Hif1α in left IRI kidney non-transgenic control was readily observed whereas it was undetectable in the right kidneys or in the non-IRI left kidneys (**Fig.3A**), confirming that the signal is triggered by induced ischemia. Strikingly, levels remain elevated and was increased at 23 days and ~3 months post-reperfusion in left IRI kidney non-transgenic control (n=2 and 5) by at least 2-fold. Similar to the controls, the left IRI *Pkd1*$_{extra}$ transgenic kidneys (n=4) also exhibited increase in Hif1α expression levels at 23 days and ~3 months following ischemia (**Fig.3B**) compared to non-IRI control. The persistent ischemic response suggests that renal damage is not declining substantially and presumably, the Hif1α transcription factor could play a role in a number of transcriptional regulatory pathways.

Stimulation of Pc1/Pc2 signaling pathways

Since Pc1 or Pc2 dysregulation induce cystogenesis [9,10,21-25], we investigated whether Pc1 and/or Pc2 expression levels could be altered in IRI kidneys post-reperfusion. Analysis of the left IRI kidneys from control non-transgenic mice showed notable increased Pc1 expression (~460kDa) at 16days (~3- to 4-fold) post-IRI prior to overt pathocellular changes or cystogenesis (**Fig.4A**). The overexpression of Pc1 in the left IRI kidneys was sustained at 23 days and at 3-4 months post-IRI (n=2 and 5) (**Fig.4A**). In contrast, the right kidneys from IRI non-transgenic mice showed comparable Pc1 expression levels to control mice without IRI at these different ages. We then monitored Pc1 expression in the kidneys of the lowest expressor *Pkd*$_{extra}$ 39 transgenic line. As expected Pc1/Pc1$_{extra}$ expression levels were elevated in the right kidneys of *Pkd*$_{extra}$ *39* relative to control non-IRI as previously reported [11]. Nevertheless, levels of Pc1 expression were systematically increased by ~3- to 6-fold in the left kidneys in comparison to the right *Pkd*$_{extra}$ 39 kidneys at 23 days and 3 months post-reperfusion (n=2 per age). Of interest, levels appeared equally stimulated

in the mild and highly cystic (annoted L^c) left kidneys, as observed in the control non-transgenic IRI mice.

We next addressed whether Pc2 expression could be modulated. Analysis of the control non-transgenic mice showed a striking increase in Pc2 expression (~130kDa) between 8- and 15-fold in the left IRI kidneys compared to age-matched non-IRI left kidneys at 16, 23 days and 3 months post-reperfusion (**Fig.4B**). As shown for Pc1 upregulated levels, levels of Pc2 in severely cystic IRI non-transgenic kidneys were within the same range as the mildly cystic kidneys. The contralateral right kidneys displayed comparable Pc2 expression levels at 23 days and 3 months post-reperfusion as in the control without IRI of same age. Pc2 expression levels were also assessed in the left kidneys of the *Pkd*$_{extra}$ 39 and 2 transgenic lines from overtly or non-overtly cystic mice. Independently of the genotype or cyst severity, the Pc2 levels were elevated to the same magnitude in the left IRI kidneys of *Pkd1*$_{extra}$ lines as determined for the IRI non-transgenic control kidneys (**Fig.4B**).

AKI as a modulator of Tuberin and mTOR cascade

To determine whether the expression pattern of known key factors associated with cystogenesis were modulated following acute kidney injury, we quantified levels of the gene product of Tsc2, Tuberin that is also an interacting partner of Pc1 [26]. Noticeably, Tuberin (~200kDa) expression was not decreased as expected for a role in cystogenesis but strongly stimulated (>10-fold) from the early tubular dilatation stages onward in the left IRI kidneys relative to non-IRI kidneys or to right IRI kidneys (**Fig.5A**). Tuberin overexpression was maintained at 23days and 3 months post-reperfusion in the left IRI control kidneys. Similarly, *Pkd1*$_{extra}$ 39 and 2 transgenic lines from overtly or non-overtly cystic mice exhibited increased Tuberin (~8- to 11-fold) in the left IRI kidneys at 3 months post-reperfusion. Noticeably, overtly cystic kidneys consistently displayed highest levels of Tuberin. These data suggest that AKI stimulate Pc1-Tuberin complex.

To identify the potential regulator of Tuberin stimulation, we first investigated the extracellular signal-regulated kinase, ERK (phospho- and total levels) activation status subsequent to AKI. As shown in Figure 5B, both phospho-Erk (42/44kDa) and total Erk expression was substantially elevated in the left IRI kidneys of non-transgenic and transgenic mice compared to the contralateral right kidneys at 16, 23 and 3 months post-reperfusion. The ratio of phospho-Erk to total Erk of the non-transgenic left IRI kidneys was not significantly reduced relative to the non-IRI kidneys. The absolute increase in p-Erk suggests that Erk signaling via negative control can be a major regulator of Tuberin.

To monitor whether phospho-AKT through negative regulation could be responsible for Tuberin stimulation, we assessed levels of p-Akt^{308}, p-Akt^{473} and total Akt. The immunoblot results on total AKT showed consistently increased levels in the left IRI kidneys by ~ 10-20-fold compared to the contralateral right kidneys and to the non-IRI kidneys. Interestingly, the p-Akt^{308} levels revealed a limited increase in the non-transgenic left IRI kidneys relative to both the contralateral right kidneys and to non-IRI kidneys at 16, 23 days post-reperfusion (**Fig.5C**). Analysis of p-Akt^{473} levels showed a major increase in the non-transgenic left IRI kidneys compared to the contralateral right kidneys at 16, 23 days post-reperfusion but is only equivalent or slightly increase compare to non IRI kidneys. Noticeably, at 3-months post-reperfusion both p-Akt^{308} and p-Akt^{473} and total Akt displayed highest levels (**Fig.5C**). In contrast, the hypertrophic right kidneys displayed lower p-Akt^{473} levels and tended to have lower p-Akt^{308} and total Akt relative to both kidneys of control non-IRI mice. Since phospho-Akt plays a negative regulatory role on Tuberin, the pattern of increase p-Akt indicated that mTORC1 could be modulated.

To determine whether the mTOR pathway was modulated, we analyzed the phosphorylation status of the downstream effector ribosomal subunit protein phospho-S6K (Thr412/389) and total S6K. Levels of total S6K were similar in both the IRI and non-IRI kidneys (**Fig.5D**). By contrast, p-S6k levels were strongly induced in the left IRI kidneys relative to the contralateral right kidneys and to the non-IRI kidneys. This

data indicated important activation of the mTORC1 pathway and is likely to be targeted by AKI.

AKI stimulate Wnt canonical signaling pathway

Since Tuberin was shown to crosstalk with the Wnt canonical pathway via GSK3 [27], we monitored β-catenin activation. Analysis of control non-transgenic mice showed a striking increase in total β-catenin expression of >10-fold in the left IRI kidneys compared to the barely detectable levels in the contralateral right kidneys from early stages of tubular dilatations to 3 months post-reperfusion (**Fig.6A**). Levels of active β-catenin were equivalent or even more enhanced than the total β-catenin in the left IRI kidneys but was scarcely observed in the contralateral right kidneys. AKI appears to stimulate markedly the Wnt canonical pathway.

A major downstream target of the Wnt canonical pathway, c-myc was then evaluated in particular as we showed previously increase c-myc renal expression in human ADPKD kidneys and in *Pkd1* dosage-increased transgenic mouse models [2,9,10]. Normally c-myc expression is virtually undetectable in normal wild type mice as in the control non-IRI left or in the contralateral right IRI kidneys (**Fig.6B**). However, renal c-myc (~60kDa) expression in the left IRI kidneys from non-transgenic and transgenic mice was markedly upregulated (**Fig.6B**). Noticeably, a second band was also elevated that likely corresponds to the c-myc cytoplasmic cleaved form called myc-nick (~42kDa) [28]. Overtly cystic kidneys displayed even higher c-myc expression levels, implicating a cystogenic role of c-myc in AKI.

DISCUSSION

The original intent of these studies was to determine whether AKI is a modifier of cystogenesis in late onset clinical and dosage-increased *Pkd1* alleles with a focus on progressive and long-term consequences. Our studies show in fact, that ischemia is not only a modifier but also an inducer of cystogenesis in non-transgenic and in late onset *Pkd1* dosage-dependent mouse models with similar PKD cellular responses. AKI-induced cystogenesis mechanism crosstalks with Pc1 and Pc2 signaling cascade and shares similar global molecular network.

The occurrence of renal atrophy of the left kidneys upon unilateral IRI in parallel with the hypertrophy of the right kidneys is a striking characteristic. This is the first time that such opposite response of the two kidneys is noted despite similar or more severe experimental ischemic conditions used for *Pkd1* dosage-reduced mouse models [12,14] and other models [15,29]. This renal atrophy occurred rapidly in less than 2-weeks following IRI possibly via increase cell death and/or tubular necrosis within few days after ischemic exposure [12,30]. In contrast, development of hypertrophy in the right kidneys of non-transgenic and transgenic animals support a compensatory mechanism probably in response to the altered function of the left ischemic kidneys. Similar observations of hypertrophic response of the contralateral kidneys in cases of uninephrectomy was reported in human [31] but also observed in mice, as a result of hyperfiltration [32].

Particularly striking is the 100% penetrance of renal tubular and glomerular cystogenesis in the transgenic and non-transgenic IRI kidneys. The comparable range of cystic severity from the transgenic as well as non-transgenic mice indicates that the transgene does not significantly potentiate the phenotype. The mild to moderate ischemic conditions led to systematic renal abnormalities of hyaline casts, inflammation and epithelial hyperplasia that are highly alike to those described in the *Pkd1* dosage-reduced mouse models. Interestingly, we observed for the first time to our knowledge, increase epithelial cilia length in response to mild ischemia in kidneys, analogously to the dosage-increased *Pkd1* mouse models [10]. The phenotype of renal

permanent interstitial scarring or fibrosis in the IRI kidneys resemble those found in other IRI mouse and rat models and in human kidney transplantation [33-35]. Independently of the genotype, our data show that despite presumably active renal repair programs following IRI [4], kidneys were incapable of complete recovery from injury and progress to cystic disease within weeks of reperfusion.

While stimulation of the hypoxia inducible factor, Hif1α, a sensor for oxygen-deprived levels was anticipated subsequent to ischemia or cellular hypoxia, the elevated levels for several weeks revealed a transition from acute renal injury to chronic renal injury. It is expected that Hif1α should be transiently stabilized in the early phase of post-reperfusion following injury during kidney repair process [36,37] to transcriptionally regulate crucial pathways [38]. However, the persistence of Hif1α expression detected from the early tubular dilatation stage onwards suggests absence of switching off the repair process, maladaptive repair or activation of injury-associated secondary cascades [16]. Interestingly, increased expression of Hif1α was detected in late stages of human ADPKD but also in PKD animal models as the cpk mice and rat Han:Sprd [39,40]. The sustained increase in Hif1α expression alone is unlikely responsible of the injury-induced cystogenesis in our IRI control and transgenic mice since overexpression of Hif1a cause renal cysts at and beyond 1 year of age [41]. Nevertheless, Hif1α overexpression could be a significant modifier or contributor to IRI cystogenic pathway.

Our results demonstrate persistent and substantial renal upregulation of Pc1 and Pc2 expression in control and transgenic mice following acute ischemic injury. Much attention has focused on the early IRI mechanism that show stimulation of Pc1 and/or Pc2 expression for 2 days, possibly as a repair process [29,42-44]. However, the sustained and high levels of Pc2 detected for several weeks are likely to have cystogenic potential since *Pkd2*/Pc2 mild upregulation in transgenic mice can cause cysts by 6-18 months of age [21]. Concurrently, the presence of increased Pc1 levels can also trigger cystogenesis within 3 months as previously shown with *Pkd1*

transgenic mice targeted specifically to the kidney or systemically [9,10]. Our data show that acute ischemic injury upregulate both genes responsible for ADPKD after reperfusion, and could account for the cystogenic phenotype or at least, are important modifiers.

Of importance, our studies show dysregulation of mTOR signaling cascade in ischemic kidneys few weeks after reperfusion as observed in cystic mouse models and human ADPKD tissues [26,45-47]. Our data provide evidence that AKI in late post-reperfusion stages lead to physiologic activation of both phospho Akt^{308} and Akt^{473} that are upstream of mTORC1 and target of mTORC2, respectively. Elevated renal Akt^{308} in IRI kidneys is consistent with prosurvival signaling and ongoing repair process via Tuberin and the mTOR effectors [4]. Interestingly, the late increase in p-Akt mimics the age-related increase detected in renal cystic mouse model [45]. In parallel, AKI activates uniformly p-Erk and total Erk from early to late stages post-reperfusion and possibly regulates mTORC1 pathway [48]. While Erk play an important role in cell survival, our data are also in line with the early activation of Erk toward an anti-inflammatory response and inhibition of fibrosis progression [49]. Early activation of Erk after IRI is as well consistent with cystic mouse model [45]. Of interest, the ischemia-induced mouse models with marked overexpression of Pc1 also indicate that physiologically Pc1 do not or is not sufficient to inhibit Erk signaling as previously suggested in vitro [50]. The molecular mechanisms by which IRI kidneys lead to increase phospho and total Akt and Erk are still uncertain but independently or together, activation of Erk and Akt upstream effectors of the mTOR can lead to activation of the cascade. It is likely based on their activation patterns that Erk controls early stages whereas both Erk and Akt prevail later in the mechanism through which IRI activates S6K, the downstream target of mTOR. The strong implication of mTORC1 in response to ischemic stress is further supported by the more pronounced tubular damage by IRI in mTORC1 deficient kidneys and in rapamycin-treated animals [51,52]. Our finding in renal ischemic stress remarkably parallels the mTOR cascade activation and delayed cystogenesis by mTOR inhibitors in several cystic non- and orthologous Pkd1 mouse models [26,45,53,54]. An important insight into our analysis is that

in the face of markedly elevated Pc1, mTORC1 pathway is not downregulated but in fact is upregulated *in vivo*. Co-activation of Erk, mTOR and Hif1α in renal IRI and down-regulation of Hif1α with inhibitors of mTOR [55,56] indicate that Hif1α signals into the mTOR pathway to adapt cell metabolism and protein synthesis responses upon hypoxia. Collectively our data clearly suggest that the mTOR pathway is involved in progression of the ischemic renal cystic pathology.

Our studies determine that the Wnt canonical pathway in IRI is possibly a modulator of the mTORC1 cascade and a key and critical mechanism in the ischemic-induced phenotype. While it was proposed that Wnt stimulation can activate mTORC1 cascade through inhibition of coordinate regulation of the Wnt effector GSK3 and AMPK on Tuberin [27], our Pc1 upregulation results suggest alternatively, that Pc1 negatively regulate GSK3 function [57] to counteract Tuberin role. Consistently, the strong and sustained activation of the b-catenin from early to late post-reperfusion showed that the Wnt canonical pathway is stimulated during renal injury and/or repair. This finding correlated with a more severe AKI response in β-catenin deficient animals [58]. However, persistent upregulation of β-catenin can be responsible for development of the cystogenic phenotype as previously observed [59]. In addition, the increase fibrosis in ischemic kidneys may result from β-catenin activation since it was associated with TGF-β signaling in response to injury [60]. Similar to mTOR stimulation in cystic mouse models and human ADPKD tissues, activation of Wnt canonical pathway is modulated upon dysregulation of Pc1 expression [61-63] (AK and MT data unpublished). Most significantly, the strong induction of c-myc, a downstream effector of β-catenin [64] supports the implication of the Wnt canonical pathway. Upregulation of both full-length c-myc and myc-nick could play a role following ischemic stress in transcriptional regulation and in cell survival/metabolism [28,65], respectively. Interestingly, upregulation of c-myc was shown in several cystic mouse models [66,67] including renal or systemic dosage-increase *Pkd1* mouse models [9,10] and in human ADPKD tissues [2]. Most importantly, targeted c-myc overexpression in the kidneys was shown to induce PKD in transgenic mice [68,69], thereby c-myc could be the causative cystogenic factor in IRI.

Noticeably, there is also a bidirectional cross-regulation between c-myc and Hif1α where c-myc upregulate Hif1α by controlling stability [70] and Hif1α inhibit c-myc transcriptional activity [71]. Since both c-myc and Hif1α are upregulated following ischemic stress, it is likely that an additional regulator of c-myc as β-catenin contributes to sustained activation of c-myc. While mTOR is a known regulator of c-myc [72,73], the feedback control of Hif1α on mTOR in IRI condition could not promote c-myc upregulation. Together these results indicate that the Wnt canonical pathway is determinant in the IRI-induced signaling network.

Particularly striking is the parallel between the long-term signaling and response of acute kidney injury and ADPKD. These similarities suggest that ischemic stress plays an important role in ADPKD. Recently, Chawla and Kimmel have proposed that acute kidney injury and chronic kidney disease are interconnected human syndromes and that acute kidney injury increases risk of developing chronic kidney disease and vice-versa [1]. In this study, we provide *in vivo* experimental evidence that acute ischemic injury lead to cystogenesis and a progressive chronic kidney disease. These findings suggest that the recurrent injury in ADPKD and *Pkd1* orthologous dosage-dependent mouse models triggered by cystogenesis involve an ischemic chronic kidney disease state. Molecularly, the convergence of several causative cystogenic/PKD factors of Pc1, Pc2, Hif1α, β-catenin and c-myc induced few weeks after reperfusion support a crosstalk between IRI and the Pc1 and Pc2 signaling pathways.

In conclusion, we demonstrated that ischemia-induced injury in mice reproduces several of the typical ADPKD characteristics. Both mTOR and Wnt pathways are early responders upon ischemic injury and play important roles in cyst development and progression. Most importantly, our study also shows that renal injury crosstalk with Pc1/Pc2 signaling mechanisms.

MATERIAL AND METHODS

Unilateral ischemia-reperfusion injury

Experiments were carried out on ischemia-induced transgenic *Pkd1$_{extra}$2/39* (n=27), *Pkd1$_{TAG}$6* (n=9) and control non-transgenic littermate (n=51) male mice at 3 months of age as well as on C57Bl6/JL sham-operated (15). All transgenic mice were backcrossed on C57Bl6/JL background for several generations. Briefly, mice were anesthetized with isoflurane and placed on a heating pad during surgery. A vascular clamp (Roboz) was applied only on the left renal pedicle to obstruct blood flow and to induce a transient mild to moderate ischemia for 30 minutes. Reperfusion was confirmed by visualization and mice were monitored for few minutes under heating lamp and in the subsequent days. Mice were sacrificed at different time points following IRI. The protocols for in vivo experiments were reviewed and approved by the IRCM Animal Care Committee (ACC), which follow the regulations and requirements of the Canadian Council on Animal Care.

Histology

Mice were sacrified at different stages of reperfusion and both kidneys (ischemic left and non-ischemic right) first weighted and subsequently fixed in formalin. Paraffin embedded blocks were sectioned in 4-to-5 micrometer-thick slices and stained with hematoxylin and eosin for morphological analysis and sirius red for evaluation of fibrosis.

Semi-quantitative analysis of % cystic surface and number of cyst on the total renal surface area was performed using formalin-fixed H&E stained sections of left IRI kidneys from non-transgenic (n=38), transgenic *Pkd1$_{extra}$2/39* (n=19) and *Pkd1$_{TAG}$6* (n=8) mice. The images were first taken by Leica MZ12 microscope. The threshold was set using Northern Eclipse to delimit and measure the total kidney surface, and then to identify the cysts as white objects on a grey intact kidney surface. The surface of cysts per section and hence the total number of cyst per surface is obtained automatically through Northern Eclipse software and data exported in Excel file for compilation.

Cilia length was evaluated on formalin fixed right and left kidneys from IRI non-transgenic (n=3), IRI transgenic (n=3) and wild-type kidneys (n=1) by immunofluorescence using acetylated a-tubulin antibody as described in [10]. The slides were mounted with Prolong Antifade Gold (Invitrogen) and images were taken by DM5500 B Microscope and the cilia length (n ›200 cilia/mouse) measured by Volocity software.

Western blot analysis

Total protein extracts were extracted from frozen kidneys. Extracts for Pc1 were migrating on 4-12% precast Bis-Tris NuPAGE gels and MES buffer (Invitrogen) and all other proteins analyzed on 8% Tris-Glycine homemade gels. Proteins were transferred on PVDF membranes (VWR) that were blocked with PBST1X/milk 5% or TBST1X/BSA5% and incubated with antibody, followed by PBST1X or TBST1X washes as described in [10,11]. For analysis of expression of phospho-proteins with different periods of reperfusion (16 days, 23 days and 3 months), we also added a cocktail of inhibitors of phosphatases. Following antibodies were used: Pc1 anti-LRR (7^e12) monoclonal antibody, rabbit monoclonal against c-Myc from Epitomics (Cedarlane #1472-1), Tuberin rabbit polyclonal from Santa Cruz Biotechnology (sc-893), Pc2 YCC2 rat monoclonal from PKD core (Gift of Drs. Lisa Guay-Woodford and Mary Ann Accavitti-Loper, University of Alabama, P30 PKD Core), Hif1α mouse monoclonal from Novus Biologicals (#NB100-123), total β-catenin rabbit polyclonal from Upstate (#06-734) and active β-catenin mouse monoclonal from Upstate (#05-665), total Erk rabbit polyclonal from Millipore (#06-182) and phospho-Erk mouse monoclonal from Cell Signaling (#9106, both generous gifts of Dominique Davidson, IRCM), Collagen type IV rabbit polyclonal from Abcam (#ab-19808), total Akt, total S6K, Akt308 and Akt473 from Cell Signaling (#9272, 9202, 9275, 9271 generous gift of Dr. Jean Vacher). Detection by ECL Prime (Amersham) and BioRad Chemi-Doc XRS+Imaging system was used for quantification of intensity of the bands for all gels.

Statistical analysis

Data on kidney to body weight ratio (KBW) is represented as mean ± standard deviation and statistical significance analyzed using Student T test. For cystic surface and cystic number, the data is represented in a % of mice of a particular genotype in either category of cystic invasion or number of cysts. Correlation between cystic surface and cystic number within the same genotype was assessed by Pearson ‘’r’’ test using Prism 6 software. $p \leq 0.05$ was considered as significant.

ACKNOWLEDGMENTS

We thank Mrs Cindy Baldwin and Dr. Serge Lemay at McGill U. for advice on kidney ischemia experiments. The authors thank Samuel St-Jacques, Rosa Jiménez, Angela Schneider for technical support. This work was supported by grants from the Canadian Institutes of Health Research (CIHR) and The Polycystic Kidney Disease Foundation of Canada (to MT) and from a Frederick Banting and Charles Best of Canada Graduate Scholarship Award (to AK).

REFERENCES

1 Chawla, L. S. & Kimmel, P. L. Acute kidney injury and chronic kidney disease: an integrated clinical syndrome. *Kidney Int* 82, 516-524, doi:10.1038/ki.2012.208 (2012).

2 Lanoix, J., D'Agati, V., Szabolcs, M. & Trudel, M. Dysregulation of cellular proliferation and apoptosis mediates human autosomal dominant polycystic kidney disease (ADPKD). *Oncogene* 13, 1153-1160 (1996).

3 Ward, C. J. *et al.* Polycystin, the polycystic kidney disease 1 protein, is expressed by epithelial cells in fetal, adult and polycystic kidney. *Proc Natl Acad Sci USA* 93, 1524-1528 (1996).

4 Weimbs, T. Polycystic kidney disease and renal injury repair: common pathways, fluid flow, and the function of polycystin-1. *Am J Physiol Renal Physiol* 293, F1423-1432, doi:10.1152/ajprenal.00275.2007 (2007).

5 Jiang, S.-T. *et al.* Defining a Link with Autosomal-Dominant Polycystic Kidney Disease in Mice with Congenitally Low Expression of Pkd1. *Am J Pathol* 168, 205-220 (2006).

6 Lantinga-van Leeuwen, I. S. *et al.* Lowering of *Pkd1* expression is sufficient to cause polycystic kidney disease. *Hum Mol Genet* 13, 3069-3077 (2004).

7 Lantinga-van Leeuwen, I. S. *et al.* Kidney-specific inactivation of the Pkd1 gene induces rapid cyst formation in developing kidneys and a slow onset of disease in adult mice. *Hum Mol Genet* 16, 3188-3196 (2007).

8 Piontek, K. B., Menezes, L. F., Garcia-Gonzalez, M. A., Huso, D. L. & Germino, G. G. A critical developmental switch defines the kinetics of kidney cyst formation after loss of *Pkd1*. *Nat Med* 13, 1490-1495 (2007).

9 Thivierge, C. *et al.* Overexpression of PKD1 Causes Polycystic Kidney Disease. *Mol Cell Biol* 26, 1538-1548 (2006).

10 Kurbegovic, A. *et al.* Pkd1 transgenic mice: adult model of polycystic kidney disease with extrarenal and renal phenotypes. *Hum Mol Genet* 19, 1174-1189 (2010).

11 Kurbegovic, A. & Trudel, M. Progressive development of polycystic kidney disease in the mouse model expressing Pkd1 extracellular domain. *Hum Mol Genet* 22, 2361-2375, doi:10.1093/hmg/ddt081 (2013).

12 Bastos, A. P. *et al.* Pkd1 haploinsufficiency increases renal damage and induces microcyst formation following ischemia/reperfusion. *J Am Soc Nephrol* 20, 2389-2402 (2009).

13 Happe, H. *et al.* Toxic tubular injury in kidneys from Pkd1-deletion mice accelerates cystogenesis accompanied by dysregulated planar cell polarity and canonical Wnt signaling pathways. *Hum Mol Genet* 18, 2532-2542 (2009).

14 Takakura, A. *et al.* Renal injury is a third hit promoting rapid development of adult polycystic kidney disease. *Hum Mol Genet* 18, 2523-2531 (2009).

15 Patel, V. *et al.* Acute kidney injury and aberrant planar cell polarity induce cyst formation in mice lacking renal cilia. *Hum Mol Genet* 17, 1578-1590, doi:10.1093/hmg/ddn045 (2008).

16 Zhou, J. *et al.* Kidney injury accelerates cystogenesis via pathways modulated by heme oxygenase and complement. *J Am Soc Nephrol* 23, 1161-1171, doi:10.1681/asn.2011050442 (2012).

17 Luyten, A. *et al.* Aberrant regulation of planar cell polarity in polycystic kidney disease. *J Am Soc Nephrol* 21, 1521-1532 (2010).

18 Chapman, A. B. *et al.* Kidney volume and functional outcomes in autosomal dominant polycystic kidney disease. *Clinical journal of the American Society of Nephrology : CJASN* 7, 479-486, doi:10.2215/cjn.09500911 (2012).

19 Yoder, B. K. Role of primary cilia in the pathogenesis of polycystic kidney disease. *J Am Soc Nephrol* 18, 1381-1388, doi:10.1681/asn.2006111215 (2007).

20 Chavali, P. L. & Gergely, F. Cilia born out of shock and stress. *EMBO J* 32, 3011-3013, doi:10.1038/emboj.2013.241 (2013).

21 Park, E. Y. *et al.* Cyst formation in kidney via B-Raf signaling in the PKD2 transgenic mice. *J Biol Chem* 284, 7214-7222 (2009).

22 Wu, G. *et al. Trans*-heterozygous *Pkd1* and *Pkd2* mutations modify expression of polycystin kidney disease. *Hum Mol Genet* 11, 1845-1854 (2002).

23 Kim, K., Drummond, I., Ibraghimov-Beskrovnaya, O., Klinger, K. & Arnaout, M. A. Polycystin 1 is required for the structural integrity of blood vessels. *Proc Natl Acad Sci USA* 97, 1731-1736 (2000).

24 Lu, W. *et al.* Comparison of *Pkd1*-targeted mutants reveals that loss of polycystin-1 causes cystogenesis and bone defects. *Hum Mol Genet* 10, 2385-2396 (2001).

25 Muto, S. *et al.* Pioglitazone improves the phenotype and molecular defects of a targeted *Pkd1* mutant. *Hum Mol Genet* 11, 1731-1742 (2002).

26 Shillingford, J. M. *et al.* The mTOR pathway is regulated by polycystin-1, and its inhibition reverses renal cystogenesis in polycystic kidney disease. *Proc Natl Acad Sci U S A* 103, 5466-5471, doi:10.1073/pnas.0509694103 (2006).

27 Inoki, K. *et al.* TSC2 integrates Wnt and energy signals via a coordinated phosphorylation by AMPK and GSK3 to regulate cell growth. *Cell* 126, 955-968, doi:10.1016/j.cell.2006.06.055 (2006).

28 Conacci-Sorrell, M., Ngouenet, C., Anderson, S., Brabletz, T. & Eisenman, R. N. Stress-induced cleavage of Myc promotes cancer cell survival. *Genes Dev* 28, 689-707, doi:10.1101/gad.231894.113 (2014).

29 Zhao, Y., Haylor, J. L. & Ong, A. C. Polycystin-2 expression is increased following experimental ischaemic renal injury. *Nephrol Dial Transplant* 17, 2138-2144 (2002).

30 Matsuda, H., Lavoie, J. L., Gaboury, L., Hamet, P. & Tremblay, J. HCaRG accelerates tubular repair after ischemic kidney injury. *J Am Soc Nephrol* 22, 2077-2089, doi:10.1681/asn.2010121265 (2011).

31 Takagi, T. *et al.* Compensatory Hypertrophy after Partial and Radical Nephrectomy in Adults. *The Journal of urology*, doi:10.1016/j.juro.2014.06.018 (2014).

32 Liu, B. & Preisig, P. A. Compensatory renal hypertrophy is mediated by a cell cycle-dependent mechanism. *Kidney Int* 62, 1650-1658, doi:10.1046/j.1523-1755.2002.00620.x (2002).

33 Basile, D. P., Donohoe, D., Roethe, K. & Osborn, J. L. Renal ischemic injury results in permanent damage to peritubular capillaries and influences long-term function. *Am J Physiol Renal Physiol* 281, F887-899 (2001).

34 Isoniemi, H. M. *et al.* Histopathological findings in well-functioning, long-term renal allografts. *Kidney Int* 41, 155-160 (1992).

35 Pagtalunan, M. E., Olson, J. L., Tilney, N. L. & Meyer, T. W. Late consequences of acute ischemic injury to a solitary kidney. *J Am Soc Nephrol* 10, 366-373 (1999).

36 Conde, E. *et al.* Hypoxia inducible factor 1-alpha (HIF-1 alpha) is induced during reperfusion after renal ischemia and is critical for proximal tubule cell survival. *PLoS One* 7, e33258, doi:10.1371/journal.pone.0033258 (2012).

37 Heyman, S. N., Rosenberger, C. & Rosen, S. Experimental ischemia-reperfusion: biases and myths-the proximal vs. distal hypoxic tubular injury debate revisited. *Kidney Int* 77, 9-16, doi:10.1038/ki.2009.347 (2010).

38 Gunaratnam, L. & Bonventre, J. V. HIF in kidney disease and development. *J Am Soc Nephrol* 20, 1877-1887, doi:10.1681/asn.2008070804 (2009).

39 Bernhardt, W. M. *et al.* Involvement of hypoxia-inducible transcription factors in polycystic kidney disease. *Am J Pathol* 170, 830-842, doi:10.2353/ajpath.2007.060455 (2007).

40 Belibi, F. *et al.* Hypoxia-inducible factor-1alpha (HIF-1alpha) and autophagy in polycystic kidney disease (PKD). *Am J Physiol Renal Physiol* 300, F1235-1243, doi:10.1152/ajprenal.00348.2010 (2011).

41 Fu, L., Wang, G., Shevchuk, M. M., Nanus, D. M. & Gudas, L. J. Generation of a mouse model of Von Hippel-Lindau kidney disease leading to renal cancers by expression of a constitutively active mutant of Hif1αlpha. *Cancer Res* 71, 6848-6856, doi:10.1158/0008-5472.can-11-1745 (2011).

42 Prasad, S., McDaid, J. P., Tam, F. W., Haylor, J. L. & Ong, A. C. Pkd2 dosage influences cellular repair responses following ischemia-reperfusion injury. *Am J Pathol* 175, 1493-1503, doi:10.2353/ajpath.2009.090227 (2009).

43 Obermuller, N. *et al.* Altered expression pattern of polycystin-2 in acute and chronic renal tubular diseases. *J Am Soc Nephrol* 13, 1855-1864 (2002).

44 Verghese, E., Weidenfeld, R., Berttram, J. F., Ricardo, S. D. & Deane, J. A. Renal cilia display length alterations following tubular injury and are present early in epithelial repair. *Nephrol Dial Transplant* 23, 834-841 (2008).

45 Gattone, V. H., 2nd, Sinders, R. M., Hornberger, T. A. & Robling, A. G. Late progression of renal pathology and cyst enlargement is reduced by rapamycin in a

mouse model of nephronophthisis. *Kidney Int* 76, 178-182, doi:10.1038/ki.2009.147 (2009).

46 Tao, Y., Kim, J., Schrier, R. W. & Edelstein, C. L. Rapamycin Markedly Slows Disease Progression in a Rat Model of Polycystic Kidney Disease. *J Am Soc Nephrol* 16, 46-51 (2005).

47 Qian, Q. *et al.* Sirolimus reduces polycystic liver volume in ADPKD patients. *J Am Soc Nephrol* 19, 631-638, doi:10.1681/asn.2007050626 (2008).

48 Ma, L., Chen, Z., Erdjument-Bromage, H., Tempst, P. & Pandolfi, P. P. Phosphorylation and functional inactivation of TSC2 by Erk implications for tuberous sclerosis and cancer pathogenesis. *Cell* 121, 179-193, doi:10.1016/j.cell.2005.02.031 (2005).

49 Jang, H. S. *et al.* Activation of ERK accelerates repair of renal tubular epithelial cells, whereas it inhibits progression of fibrosis following ischemia/reperfusion injury. *Biochim Biophys Acta* 1832, 1998-2008, doi:10.1016/j.bbadis.2013.07.001 (2013).

50 Distefano, G. *et al.* Polycystin-1 regulates extracellular signal-regulated kinase-dependent phosphorylation of tuberin to control cell size through mTOR and its downstream effectors S6K and 4EBP1. *Mol Cell Biol* 29, 2359-2371, doi:10.1128/mcb.01259-08 (2009).

51 Grahammer, F. *et al.* mTORC1 maintains renal tubular homeostasis and is essential in response to ischemic stress. *Proc Natl Acad Sci U S A* 111, E2817-2826, doi:10.1073/pnas.1402352111 (2014).

52 Lieberthal, W., Fuhro, R., Andry, C., Patel, V. & Levine, J. S. Rapamycin delays but does not prevent recovery from acute renal failure: role of acquired tubular resistance. *Transplantation* 82, 17-22, doi:10.1097/01.tp.0000225772.22757.5e (2006).

53 Shillingford, J. M., Piontek, K. B., Germino, G. G. & Weimbs, T. Rapamycin ameliorates PKD resulting from conditional inactivation of Pkd1. *J Am Soc Nephrol* 21, 489-497, doi:10.1681/asn.2009040421 (2010).

54 Novalic, Z. *et al.* Dose-dependent effects of sirolimus on mTOR signaling and polycystic kidney disease. *J Am Soc Nephrol* 23, 842-853, doi:10.1681/asn.2011040340 (2012).

55 Hudson, C. C. *et al.* Regulation of hypoxia-inducible factor 1alpha expression and function by the mammalian target of rapamycin. *Mol Cell Biol* 22, 7004-7014 (2002).

56 Minet, E. *et al.* ERK activation upon hypoxia: involvement in HIF-1 activation. *FEBS letters* 468, 53-58 (2000).

57 Kim, E. *et al.* The Polycystic Kidney Disease 1 Gene Product Modulates Wnt Signaling. *Journal of Biological Chemistry* 8, 4947-4953 (1999).

58 Zhou, D. *et al.* Tubule-specific ablation of endogenous beta-catenin aggravates acute kidney injury in mice. *Kidney Int* 82, 537-547, doi:10.1038/ki.2012.173 (2012).

59 Saadi-Kheddouci, S. *et al.* Early development of polycystic kidney disease in transgenic mice expressing an activated mutant of the β-catenin gene. *Oncogene* 20, 5972-5981 (2001).

60 Lam, A. P. & Gottardi, C. J. beta-catenin signaling: a novel mediator of fibrosis and potential therapeutic target. *Current opinion in rheumatology* 23, 562-567, doi:10.1097/BOR.0b013e32834b3309 (2011).

61 Pandey, P., Qin, S., Ho, J., Zhou, J. & Kreidberg, J. A. Systems biology approach to identify transcriptome reprogramming and candidate microRNA targets during the progression of polycystic kidney disease. *BMC Syst Biol* 5, 56 (2011).

62 Merrick, D. *et al.* The gamma-Secretase Cleavage Product of Polycystin-1 Regulates TCF and CHOP-Mediated Transcriptional Activation through a p300-Dependent Mechanism. *Dev Cell* 22, 197-210 (2012).

63 Lal, M. *et al.* Polycystin-1 C-terminal tail associates with beta-catenin and inhibits canonical Wnt signaling. *Hum Mol Genet* 17, 3105-3117 (2008).

64 He, T.-C. *et al.* Identification of *c-MYC* as a Target of the APC Pathway. *Science* 281, 1509-1512 (1998).

65 Gordan, J. D., Thompson, C. B. & Simon, M. C. HIF and c-Myc: sibling rivals for control of cancer cell metabolism and proliferation. *Cancer cell* 12, 108-113, doi:10.1016/j.ccr.2007.07.006 (2007).

66 Cowley, B. D., Smardo, F. L., Grantham, J. J. & Calvet, J. P. Elevated c-myc protooncogene expression in autosomal recessive polycystic kidney disease. *Proc Natl Acad Sci USA* 84, 8394-8398 (1987).

67 Wu, M., Yang, C., Tao, B., Bu, S. & Guay-Woodford, L. M. The ciliary protein cystin forms a regulatory complex with necdin to modulate Myc expression. *PLoS One* 8, e83062, doi:10.1371/journal.pone.0083062 (2013).

68 Trudel, M., D'Agati, V. & Costantini, F. C-myc as an inducer of polycystic kidney disease in transgenic mice. *Kidney Int* 39, 665-671 (1991).

69 Trudel, M., Barisoni, L., Lanoix, J. & D'Agati, V. Polycystic Kidney Disease in SBM Transgenic Mice: Role of c-myc in Disease Induction and Progression. *Am. J. Pathol.* 152, 219-229 (1998).

70 Doe, M. R., Ascano, J. M., Kaur, M. & Cole, M. D. Myc posttranscriptionally induces HIF1 protein and target gene expression in normal and cancer cells. *Cancer Res* 72, 949-957, doi:10.1158/0008-5472.can-11-2371 (2012).

71 Koshiji, M. *et al.* HIF-1alpha induces cell cycle arrest by functionally counteracting Myc. *EMBO J* 23, 1949-1956, doi:10.1038/sj.emboj.7600196 (2004).

72 Hosoi, H. *et al.* Studies on the mechanism of resistance to rapamycin in human cancer cells. *Molecular pharmacology* 54, 815-824 (1998).

73 West, M. J., Stoneley, M. & Willis, A. E. Translational induction of the c-myc oncogene via activation of the FRAP/TOR signalling pathway. *Oncogene* 17, 769-780, doi:10.1038/sj.onc.1201990 (1998).

74 Bernstein, J., Evan, A. P. & Gardner, K. D. Epithelial hyperplasia in human polycystic kidney disease. *Am J Pathol* 129, 92-100 (1987).

FIGURES AND TABLES LEGENDS

Figure 1. Unilateral ischemia leads to opposite kidney response in mice

(A) Schematic illustration of the time course experiment. Unilateral ischemia was induced for 30 minutes in the left kidney of 3-month-old male mice from Pkd_{extra} and $Pkd1_{TAG}$ transgenic lines, and the non-transgenic controls. Operated mice were sacrified at the three indicated time points: 16 days, 23 days and 3-4 months post-ischemia.

(B) Kidney to body weight ratio of the left and right kidneys was measured. Non-IRI control mice were used at two ages corresponding at the onset and end of the experiment: at 3 months (n=7; thick open bar) and at 6 months (n=4; thin open bar). The IRI kidney samples monitored at 3-4 months post-reperfusion were as follows: non-transgenic control (n=45; black bar), transgenic $Pkd1_{extra}$2/39 expressing a clinical Pkd1 allele (n=24; dark grey bar) and transgenic $Pkd1_{TAG}$6 slight upregulation of Pkd1 allele (n=9; light grey bar). Renal ischemia leads to significant atrophy of the left kidney for control and transgenic mice within the same range. In contrast, significant hypertrophy of the right kidney was observed for control and transgenic mice.

Figure 2. Progression of the cystogenic phenotype in control and transgenic mouse models post-reperfusion.

(A) Sections of ischemic left kidneys (LK) from non-transgenic IRI control mice after 16 days, 23 days or 3-4 months reperfusion compared to their contralateral right kidneys (RK). At 16 days post-reperfusion, evidence of tubular dilatations can readily be observed. At 23 days and 3-4 months, presence of protein deposits (white arrowhead), tubular cysts (star), glomerular (two stars), hyperplasia (black arrowhead) and infitrates (arrow) were detected in kidneys, but not in contralateral right kidneys. H&E staining, all sections from RK and sections from LK at 16 days and 3 months post-reperfusion are 10X magnification, LK at 23 days post-reperfusion are 32X magnification.

(B) Kidney sections of left IRI kidneys (LK) from transgenic $Pkd1_{extra}$ and $Pkd1_{TAG}$ mice in comparison to the non-ischemic right kidneys. While the RK do not show any

obvious defects in any transgenic mice at 3-4 months post-reperfusion, all transgenic mouse lines similar to the non-transgenic controls (A) displayed renal infiltrates, hyperplasia, fibrosis and renal cysts in the left kidneys. Representative sections of mild, intermediate and severe phenotypes are illustrated. m: months, H&E staining.

(C) Semi-quantification of the cystic phenotype variability was assessed in both control and transgenic mice following renal ischemia. Total cystic surface area (left histogram) in each ischemic kidneys of non-transgenic (n=38) and transgenic mice ($Pkd1_{extra}$2/39 lines n=19; $Pkd1_{TAG}$6 line n=8) was determined at 3-4 months post-injury. Mice were subdivided in three groups: ‘’mild’’ with 0-5% of cystic surface, ‘’intermediate’’ with 5-15% and ‘’invasive’’≥15%. The proportion of mice in each subgroup was comparable between control and transgenic lines. Mean number of cyst per surface (mm^2) (right histogram) for each left kidneys was performed and subdivided into low <2 cysts/mm^2, moderate 2-5 cysts/mm^2 and high ≥5 cysts/mm^2. The proportion of mice in each mean cyst number subgroups did not seem more severe in the transgenic than in controls.

Figure 3. Persistent expression of Hif1α in IRI non-transgenic and transgenic mice

(A) Hif1α immunoblot was performed on right (R) and left (L) kidneys in non-transgenic mice with (IRI +) and without (IRI -) unilateral IRI. In both kidneys of non-IRI control (non-transgenic) adult mice, Hif1α expression is barely detectable at two ages corresponding to the onset of ischemia 3 months (the “0” timepoint) and end of experiment 6 months (the “3m” analogous to the 3-4 months post-ischemia) of age; these points corresponded to our non-IRI baseline levels. As early as 16 days post-reperfusion (*left panel*) Hif1α was readily detectable and was sustained until 3-4 months (*right panel*). Levels of Hif1α□ were comparable in overtly cystic left kidneys (L^c) to left kidneys (L) following IRI.

(B) Similarly to non-transgenic IRI left kidneys, Hif1α expression pattern was persistent and elevated in the transgenic $Pkd1_{extra}$ kidneys. Blots were monitored for Gapdh as equal loading control. d: days. m: months.

Figure 4. Persistent renal upregulation of Pc1 and Pc2 after IRI in control and transgenic mice.

(A) Polycystin-1 (Pc1) expression levels were analyzed by immunoblot in right and left kidneys of non-transgenic control and transgenic $Pkd1_{extra}$ (line 39) mice with and without unilateral IRI. Non-IRI control and transgenic adult kidneys were monitored for expression of Pc1 at 3 months (the "0" timepoint), age at which ischemia was induced and/or end of experiment 6 months (the "3m" analogous to the 3-4 months post-ischemia). In IRI control mice at 16 days post-reperfusion, Pc1 levels were markedly increased and remained elevated at 23 days and 3-4 months after reperfusion in left kidneys compare to right kidneys and to non-IRI left kidney(*left panel*). Since the transgenic $Pkd1_{extra}$ lines have enhanced Pc1 expression, Pc1 levels without IRI were monitored at baseline ("3m" or 6 months of age). At 23 days and 3 months post-reperfusion, the left kidneys of transgenic $Pkd1_{extra}$ line 39 displayed even more pronounced Pc1 expression levels than the right kidneys. At the late stage of post-reperfusion, levels of Pc1 do not seem further increased in the left overtly cystic kidneys when compared to left kidneys of the same genotype (*right panel*). Gapdh served as equal loading control.

(B) Expression analysis of polycystin-2 (Pc2) by immunoblot was performed in non-transgenic control and transgenic $Pkd1_{extra}$ (lines 39 and 2) mice using the same identification key as stated above in A and Fig 3. Left IRI kidneys in both control and transgenic exhibit strikingly elevated Pc2 expression at 23 days and 3-4 months post-IRI (left panel) relative to contralateral right kidneys and non-IRI kidneys baseline levels. Pc2 levels were within similar range in overtly cystic (L^c) as in all left IRI kidneys (left and right panel). In all blots, Gapdh was used as loading control.

Figure 5. Activation of the mTOR signaling cascade after kidney ischemia in control and Pkd1 transgenic mice.

(A) Expression analysis of Tsc2 gene product, Tuberin, is increased at all time points following IRI in the left kidneys of control and transgenic mice in comparison to the right kidneys and non-IRI baseline levels. Same identification key was used as Fig 3 and 4.

(B) Levels of Erk1/2 (44, 42kDa) expression in right and left kidneys of control non-transgenic and transgenic $Pkd1_{extra}$ (line 39) mice were analyzed by immunoblot using same identification key as Fig 3 and 4. An increase in both phospho-Erk (P-Erk) and total Erk levels in left kidneys is observed starting from the earliest timepoint (16 days) to 3-4 months post-reperfusion relative to the right kidneys and to non-IRI baseline levels in control non-transgenic mice. Expression of P-Erk or total Erk does not seem significantly different in overtly cystic versus left kidneys.

(C) Immunoblot of total and phosphorylated Akt levels (Akt^{T308} and Akt^{S473}) on right and left kidneys of control non-transgenic mice and transgenic $Pkd1_{extra}$ (line 39) mice. Left IRI kidneys exhibit an increase of phospho- and total Akt levels relative to the contralateral right kidneys. In comparison to non-IRI baseline levels, the left IRI kidneys display equivalent or mild stimulation of P-Akt at 16 and 23 days but a considerable increase after 3-4 months post-IRI whereas total Akt is enhanced from 16 days onwards. Notably, the contralateral right hypertrophic kidneys have decrease levels of both P-Akt and total Akt.

(D) S6K expression levels were analyzed by Western blots on right and left control non-transgenic kidneys at different timepoint post-reperfusion. Total S6K levels in right or left kidneys seem unchanged at all times post-reperfusion in comparison to non-IRI kidneys. Levels of phospho-S6K ($S6K^{Thr389}$) are systematically upregulated in left IRI kidneys relative to right kidneys and non-IRI baseline levels.

All blots were monitored for Gapdh for equal loading.

Figure 6. Stimulation of the Wnt signaling pathway following IRI.

(A) Levels of active and total β-catenin expression in right and left kidneys of non-transgenic control and transgenic $Pkd1_{extra}$ (line 39) mice with and without unilateral IRI were analyzed by immunoblot using same identification key as Fig 3 and 4. Left IRI kidneys in both control and transgenic display markedly enhanced active and total β-catenin expression from 16 days onwards whereas the contralateral right kidney has barely detectable levels. Active and total β-catenin levels were within similar range in overtly cystic (L^c) as in all left IRI kidneys (left and right panel). Gapdh was used as loading control.

(B) Immunoblot of c-myc the downstream target of β-catenin at different time-points after reperfusion in non-transgenic and $Pkd1_{extra}$ transgenic mice. From the early 16 days post-reperfusion, c-myc expression (both full-length ~60kDa and myc-nick ~42kDa) is importantly increased relative to the contralateral right kidneys and non-IRI baseline levels. Notably, c-myc pattern of expression correlated with the activation of β-catenin. Levels of c-myc appear highest in overtly cystic (L^c) in comparison to the left IRI kidneys (left and right panel).
In both blots, Gapdh was used to monitor equal loading m: months, d: days.

Supplementary figure 1. Increased collagen expression in ischemic kidneys

(A) Presence of collagen was analyzed by Sirius red staining on left IRI kidneys to evaluate involvement of fibrosis. Positive signal is particularly intense at the cortico-medullary border but is also detected in the cortex and the papilla as shown by a representative section from the $Pkd1_{extra}39$ line at 3-4 months post-IRI. Scale, 100 μm.

(B) Evaluation of collagen deposits by Western blot on total extracts from left IRI and contralateral right kidneys at 3-4 months post-IRI using collagen IV antibody. Control non-transgenic and $Pkd1_{extra}$ transgenic mice exhibit major increased collagen IV expression levels in left IRI kidneys compare to right kidneys. Gapdh was used as loading control.

Fig.1

A.

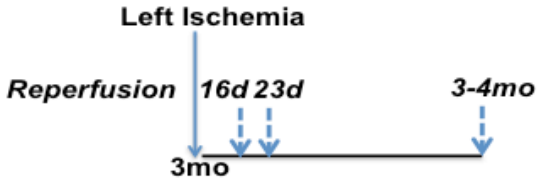
Left Ischemia
Reperfusion
16d
23d
3-4mo
3mo

B.

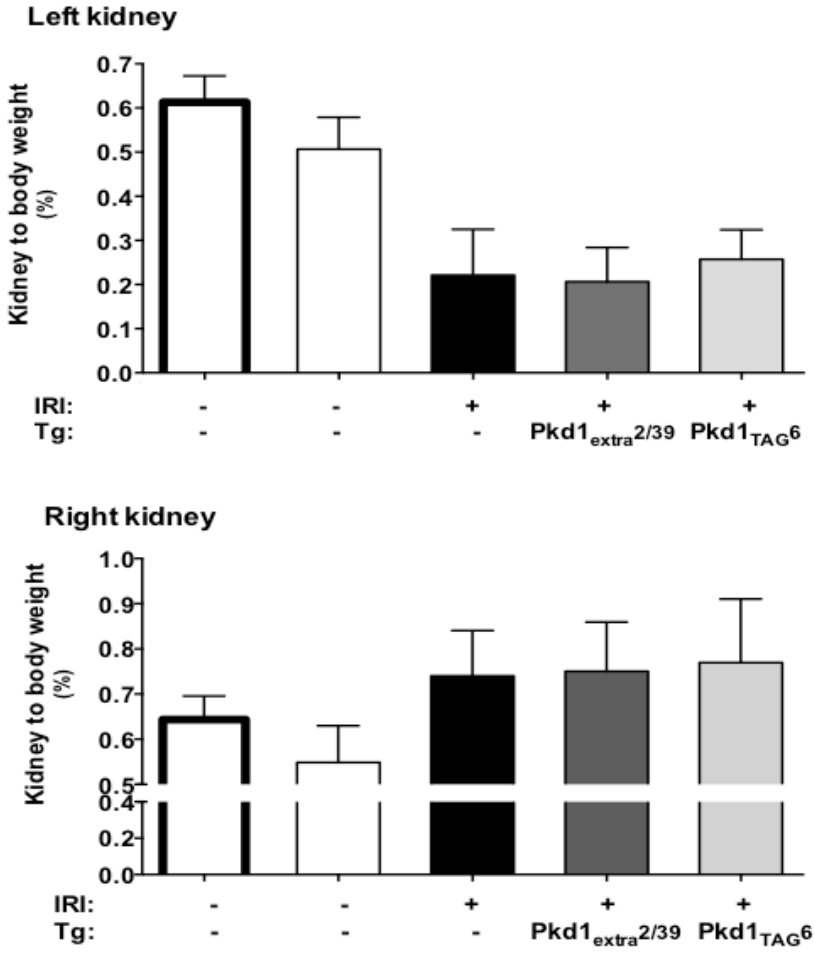
Left kidney
Kidney to body weight (%)
0.7
0.6
0.5
0.4
0.3
0.2
0.1
0.0
IRI: - - + + +
Tg: - - - Pkd1extra2/39 Pkd1TAG6
Right kidney
Kidney to body weight (%)
1.0
0.9
0.8
0.7
0.6
0.5
0.4
0.2
0.0
IRI: - - + + +
Tg: - - - Pkd1extra2/39 Pkd1TAG6

Fig.2

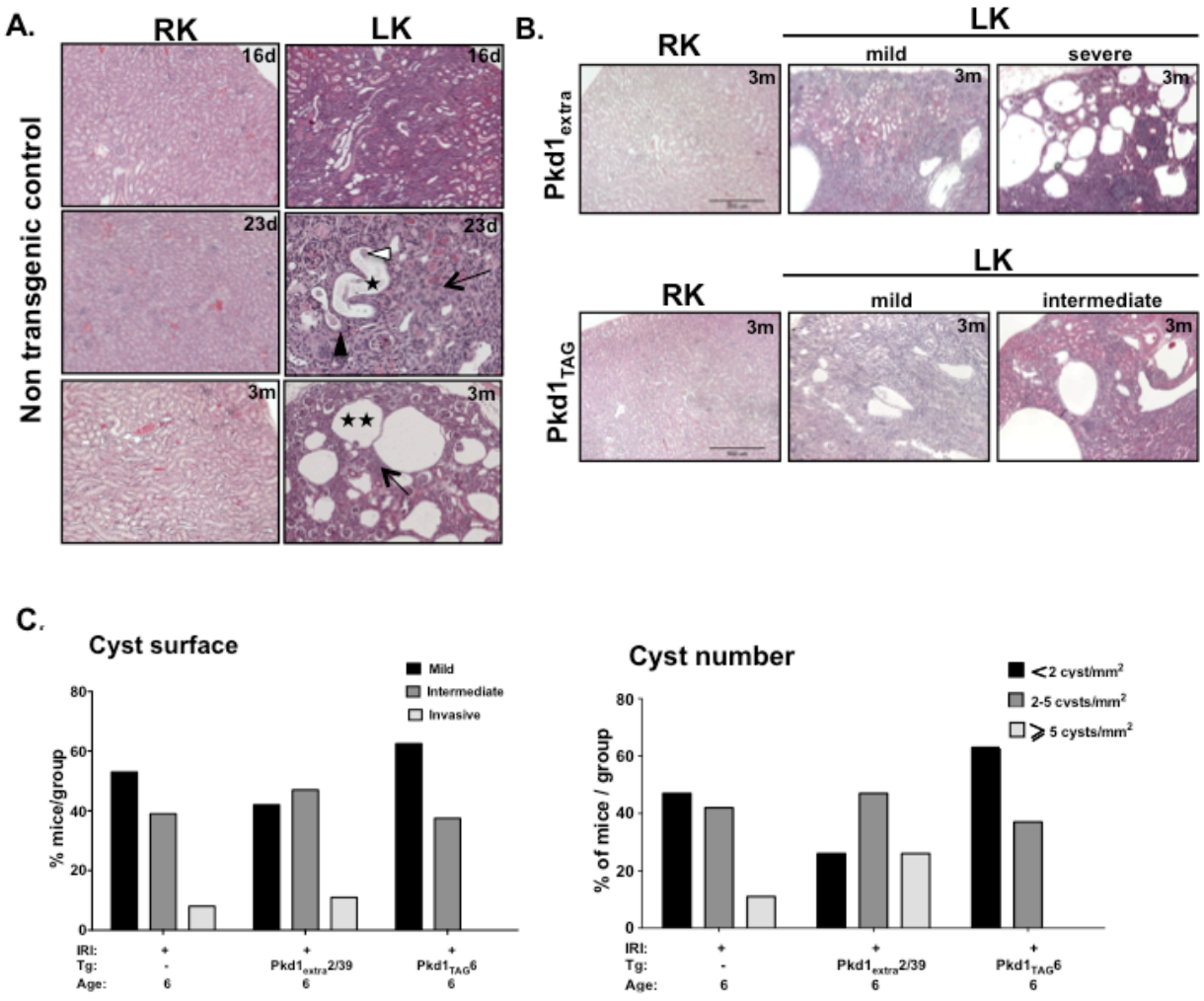
A.
RK
LK
Non transgenic control
16d
23d
3m
B.
LK
RK
mild
severe
Pkd1extra
intermediate
Pkd1TAG
C.
Cyst surface
Mild
Intermediate
Invasive
% mice/group
IRI:
Tg:
Age:
Pkd1extra2/39
Pkd1TAG6
Cyst number
<2 cyst/mm2
2-5 cysts/mm2
⩾ 5 cysts/mm2
% of mice / group

Fig.3

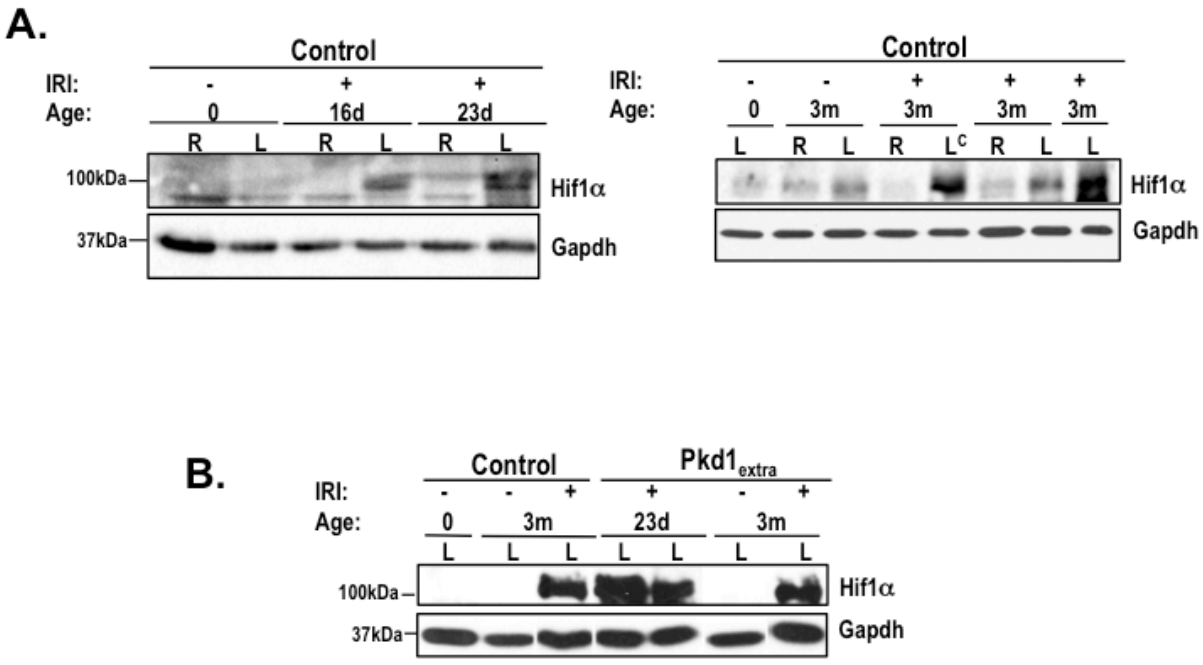
A.
Control
IRI:
Age:
0
16d
23d
R L R L R L
100kDa
37kDa
Hif1α
Gapdh
Control
IRI:
Age:
0
3m
3m
3m
3m
L R L R L^C R L L
Hif1α
Gapdh
B.
Control
Pkd1extra
IRI:
Age:
0
3m
23d
3m
L L L L L L L
100kDa
37kDa
Hif1α
Gapdh

Fig.4

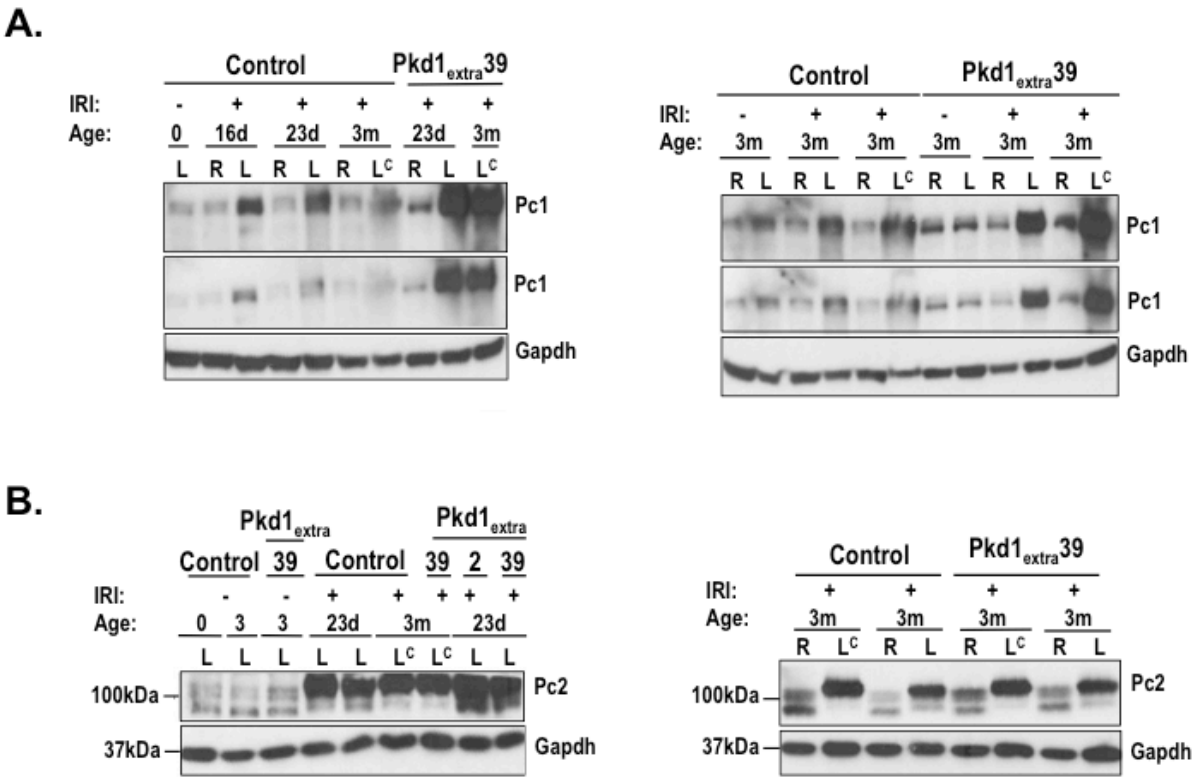
A.
Control
Pkd1extra39
IRI:
Age:
0
16d
23d
3m
23d
3m
L R L R L R LC R L LC
Pc1
Pc1
Gapdh
Control
Pkd1extra39
IRI:
Age:
3m
3m
3m
3m
3m
3m
R L R L R LC R L R L R LC
Pc1
Pc1
Gapdh
B.
Pkd1extra
Pkd1extra
Control
39
Control
39
2
39
IRI:
Age:
0
3
3
23d
3m
23d
L L L L L LC LC L L
100kDa
Pc2
37kDa
Gapdh
Control
Pkd1extra39
IRI:
Age:
3m
3m
3m
3m
R LC R L R LC R L
100kDa
Pc2
37kDa
Gapdh

Fig.5

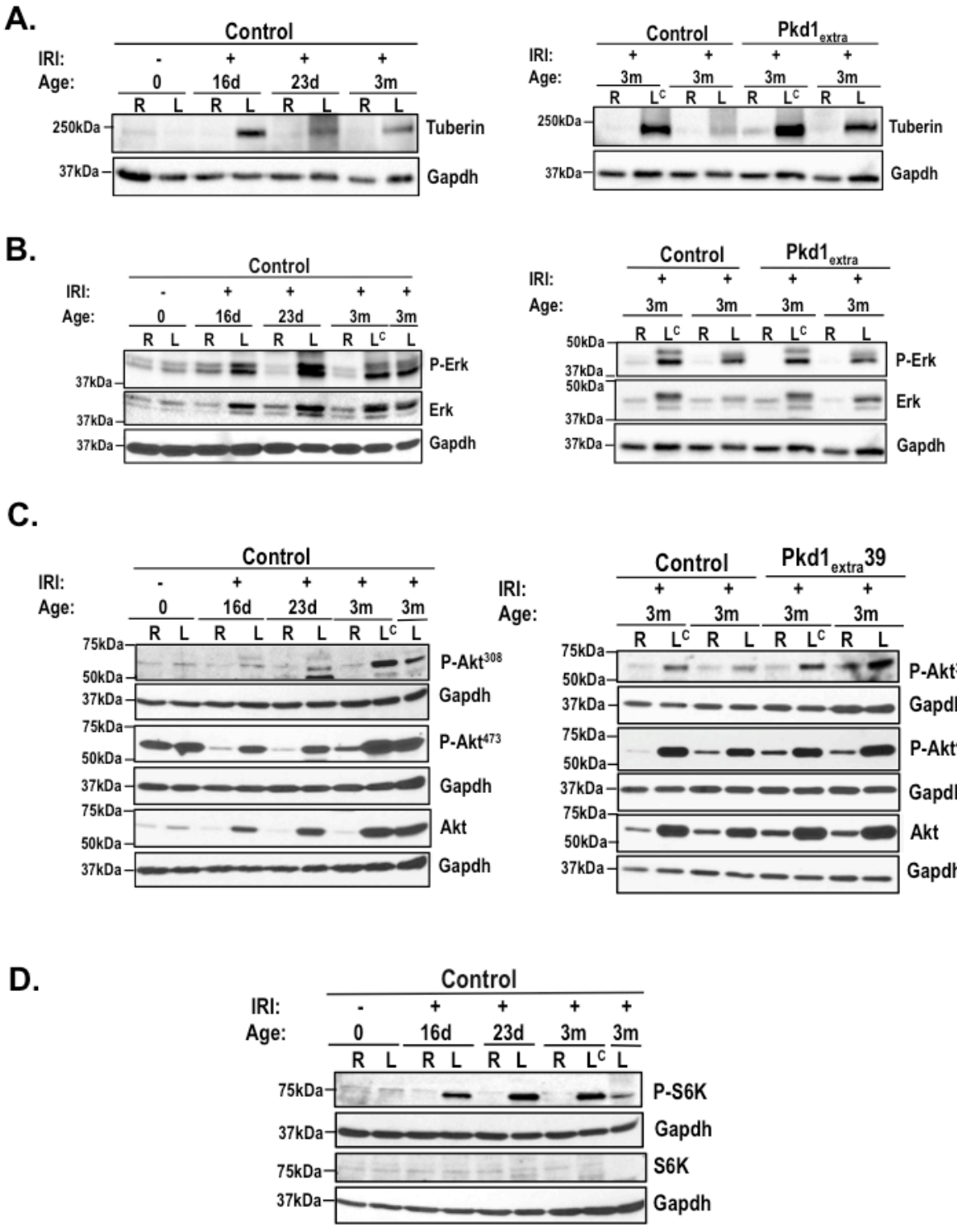
A.
Control
IRI: - + + +
Age: 0 16d 23d 3m
R L R L R L R L
250kDa
Tuberin
37kDa
Gapdh
Control
Pkd1extra
IRI: + + + +
Age: 3m 3m 3m 3m
R LC R L R LC R L
250kDa
Tuberin
37kDa
Gapdh
B.
Control
IRI: - + + + +
Age: 0 16d 23d 3m 3m
R L R L R L R LC L
37kDa
P-Erk
37kDa
Erk
37kDa
Gapdh
Control
Pkd1extra
IRI: + + + +
Age: 3m 3m 3m 3m
R LC R L R LC R L
50kDa
37kDa
P-Erk
50kDa
37kDa
Erk
37kDa
Gapdh
C.
Control
IRI: - + + + +
Age: 0 16d 23d 3m 3m
R L R L R L R LC L
75kDa
50kDa
37kDa
P-Akt308
Gapdh
75kDa
50kDa
37kDa
P-Akt473
Gapdh
75kDa
50kDa
37kDa
Akt
Gapdh
Control
Pkd1extra39
IRI: + + + +
Age: 3m 3m 3m 3m
R LC R L R LC R L
75kDa
50kDa
37kDa
P-Akt308
Gapdh
75kDa
50kDa
37kDa
P-Akt473
Gapdh
75kDa
50kDa
37kDa
Akt
Gapdh
D.
Control
IRI: - + + + +
Age: 0 16d 23d 3m 3m
R L R L R L R LC L
75kDa
P-S6K
37kDa
Gapdh
75kDa
S6K
37kDa
Gapdh

Fig.6

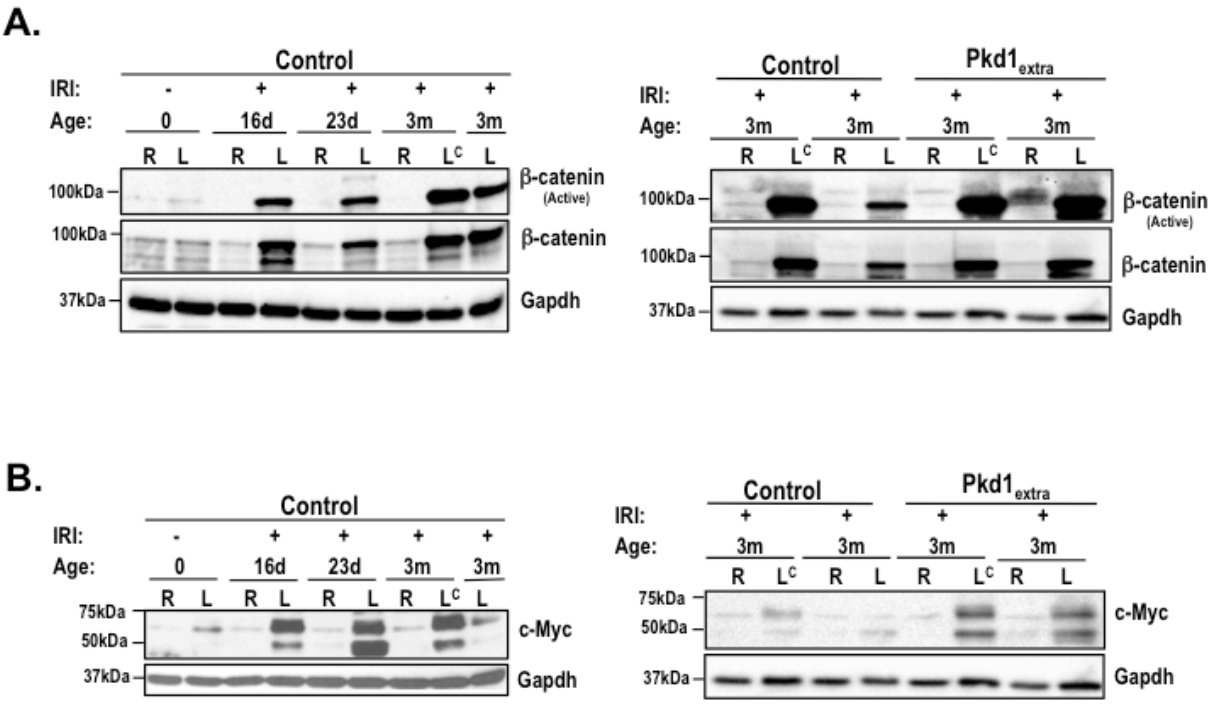
A.
Control
IRI: - + + + +
Age: 0 16d 23d 3m 3m
R L R L R L R L^C L
100kDa
β-catenin (Active)
100kDa
β-catenin
37kDa
Gapdh
Control
Pkd1extra
IRI: + + + +
Age: 3m 3m 3m 3m
R L^C R L R L^C R L
100kDa
β-catenin (Active)
100kDa
β-catenin
37kDa
Gapdh
B.
Control
IRI: - + + + +
Age: 0 16d 23d 3m 3m
R L R L R L R L^C L
75kDa
50kDa
c-Myc
37kDa
Gapdh
Control
Pkd1extra
IRI: + + + +
Age: 3m 3m 3m 3m
R L^C R L R L^C R L
75kDa
50kDa
c-Myc
37kDa
Gapdh

Suppl. Fig 1

A.

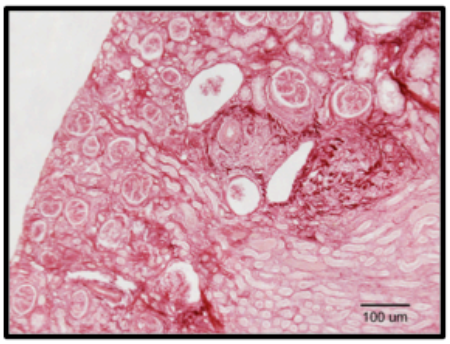

B.

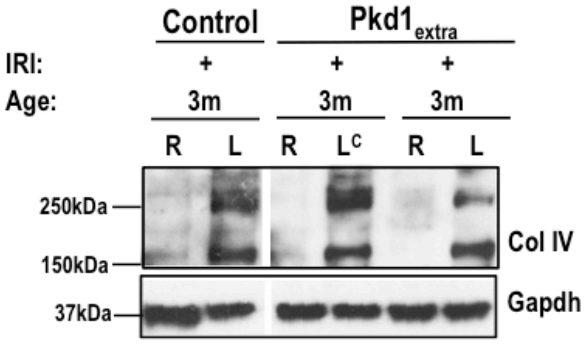

LIST OF ABBREVIATIONS

ADPKD: Autosomal dominant polycystic kidney disease

AKI: Acute kidney injury

CKI: Chronic kidney injury

Hif: Hypoxia inducible factor

PKD: Polycystic kidney disease

IRI: Ischemia reperfusion injury

CKD: Chronic kidney disease

KBW: Kidney weight to body weight ratio in %

LK: Left kidney (IRI)

RK: Right kidney (non-IRI)

***PKD1* and *2*:** Polycystic kidney disease gene 1 and gene 2

PC1 and PC2: polycystin-1 and polycystin-2

CHAPTER VIII - ARTICLE 5

Transgenic mice uncover the crucial role of the GPS cleavage in liver homeostasis

Almira Kurbegovic and Marie Trudel*

Molecular Genetics and Development, Institut de Recherches Cliniques de Montreal,

Universite de Montreal, Faculte de Medecine, Montreal, Quebec, Canada

*Correspondence:

Dr. Marie Trudel

[redacted]

Total character count (including spaces): 56K (including M&M and Figure legends)

ABSTRACT

Autosomal dominant polycystic kidney disease (ADPKD) is one of the most frequent genetic diseases with important renal but also extrarenal manifestations. From mouse studies, it is believed that causative *PKD1* mutations eventually with additional hits lead to LOF pathogenetic mechanism. Accordingly to observations in human, we have previously demonstrated, that even an increase in *PKD1* by systemic or ''SB'' kidney specific BAC-transgenesis is cystogenic in mice strongly pointing to the gene dosage disease. In this report, we provide additional arguments for this by genetic approaches of complementation of loss-of-function $Pkd1^{-/-}$ and GPS cleavage-deficient $Pkd1^{V/V}$ mice, morphometrics, extensive morphology analysis and biochemical assays. We show that a systemic *Pkd1*/Pc1 transgenic protein ($Pc1_{TAG}$) behaves as wild-type protein, is functional and can rescue *Pkd1* LOF kidney and extrarenal anomalies. Furthermore, a full rescue of *Pkd1* LOF confirms that *Pkd1*-BAC transgene contains all temporal/spatial regulatory elements. The *Pkd1* renal-specific construct ($SBPkd1_{TAG}$) only rescued partially the $Pkd1^{-/-}$ kidney phenotype and died prematurely. Interestingly, the low copy line developed renal and pancreatic disease much earlier than the high copy line. These findings revealed ''SB'' kidney specific elements temporarily/spatial regulation with total levels of Pc1 being critical for initiation and modulation of the progression. Importantly, while the liver rescue was complete on $Pkd1^{-/-}$ background in both *Pkd1* kidney-specific or systemic transgenic expressors, surprisingly it was only partial and lead to progressive cystogenesis on $Pkd1^{V/V}$ genetic background. These data strongly confirm *PKD1* gene dosage, but also strongly suggest the importance of GPS-cleavage balance/abundance for adult liver homeostasis. Inadequate regulation of the cleavage and long-term presence of uncleaved Pc1 form might act as one of ''additional cystogenic hits''. Our data is very encouraging for the future aims to rescue the GPS-cleavage as therapy for kidney and liver human ADPKD.

INTRODUCTION

ADPKD affects around 12.5 million people worldwide and accounts for around 10% of all ESRD requiring renal transplantation. It is characterized with cysts in both kidneys and very frequently in the liver with ESRD disease in late fifties. No efficient therapies are currently available but only the aggressive and invading approaches: dialysis and renal transplantation for the kidney and partial hepatectomy or transplant for the liver.

ADPKD is caused by mutations in two genes, *PKD1* (85%) and *PKD2* (15%) encoding for polycystin-1, a GPS-cleavage processed protein, and polycystin-2, a well-accepted calcium channel, respectively (1994, 1995, Hughes, Ward et al. 1995, Mochizuki, Wu et al. 1996). Deletion, missense and truncating mutations are found throughout the causative genes. Some groups have reported associations between the position of the mutation and the severity of the renal or specific extrarenal phenotype (Rossetti, Burton et al. 2002, Rossetti, Chauveau et al. 2003) but for others the nature of mutation seems more critical than the position on the locus (Cornec-Le Gall, Audrezet et al. 2013).

The exact ADPKD pathogenetic mechanism in the kidney and liver is of particular interest for development of accurate therapies. While observations from the human ADPKD kidney and liver tissues show loss of *PKD1* and *PKD2* in a minority of cysts, a sustained or increased expression of *PKD1* or *PKD2* is detected in early and late stage of ADPKD cystic epithelia (Geng, Segal et al. 1996, Lanoix, D'Agati et al. 1996, Ward, Turley et al. 1996, Weston, Jeffery et al. 1997). Absence of *PKD1*/*PKD2* and encoding proteins expression in some cysts is consistent with loss-of-heterozygocity in some cysts and observation of renal and extrarenal anomalies in mouse models with total inactivation of *Pkd1*/*Pkd2* (Lu, Peissel et al. 1997, Wu, Markowitz et al. 2000, Pennekamp, Karcher et al. 2002, Wu, Tian et al. 2002, Natoli, Gareski et al. 2008). Given that important divergences are observed in mouse loss-of-function manifestations and human ADPKD *i.e.,* early and rapid onset, pancreatic cysts at birth as the most frequent extrarenal anomaly and importantly unexplained increased

expression in human tissues, the proposed loss-of-function pathogenetic mechanism might not be the sole responsible.

Our group has previously shown that *Pkd1*-BAC transgene downstream of ''SB'' regulatory (the combinatory SV40 enhancer and β-globin promoter) resulted in high expression of *Pkd1* in the adult kidney with low to almost undetectable levels in extrarenal tissues and consequently kidney cystogenesis (Thivierge, Kurbegovic et al. 2006). This study provided the first evidence that even an increase in *Pkd1* exclusively could be cystogenetic. Not only murine *Pkd1* transgenesis was able to lead to kidney phenotype but also to very similar human extrarenal defects and adult-onset using *Pkd1*-BAC under control of ~25kb downstream endogenous regulatory region (Kurbegovic, Cote et al. 2010). Together with hypomorphic alleles of *Pkd1* (Lantinga-van Leeuwen, Dauwerse et al. 2004, Wang, Hsieh-Li et al. 2010), *Pkd2* (Kim, Fu et al. 2008), and more recently reports on partially functional hypomorphic human mutations (Hopp, Ward et al. 2012), the gene-dosage pathogenetic mechanism appears very relevant in this, to say the least, very complex pathology at the cellular level.

In this study, we confirmed that our *Pkd1*-BAC transgene contains proper regulatory elements for proper overall tissue, cell-type and temporal expression of *Pkd1*. The Pc1 transgenic protein produced behaves as functional wild-type endogenous Pc1 with appropriate trafficking and independently of endogenous protein. In addition, the kidney-specific overexpressor showed to be cell-specific and resulted in hypomorph phenotype on *Pkd1*$^{-/-}$ genetic background. We thus provide ultimate evidence for implication of gene-dosage as pathogenetic for ADPKD1. Furthermore, using our full-length transgenic lines and a *Pkd1* mutant mimicking NTF GPS cleaved product, we uncovered that GPS cleavage is critical for liver homeostasis in mice. As we recently proposed for the kidney (Kurbegovic *et al*. 2014, **Chapter VI**), rescuing the GPS cleavage and modulating the abundance of the cleaved and uncleaved molecules could be perceived as more global therapeutic avenue for synchronous treatment/prevention of both kidney and liver ADPKD features.

RESULTS

Characterization of the renal and extrarenal phenotype in *Pkd1*$^{-/-}$; *Pkd1* transgenic mice at different timepoints

In our previous studies, we showed that transgenic *Pkd1* can lead to adult polycystic kidney in mice and we characterized and detailed the extrarenal disease with similar frequencies to the human (Kurbegovic, Cote et al. 2010). To confirm that our *Pkd1*-BAC transgene behaves as a full length reminiscent of wild-type endogenous Pc1, we undertook crossings of two different *Pkd1*$_{TAG}$ systemic lines (18 and 26, **Suppl Fig.1, Fig.1B**) and *Pkd1*$^{+/-}$ mouse and backcrossed to obtain and characterize ultimately the *Pkd1*$^{-/-}$; *Pkd1*$_{TAG}$ binary compound. When backcrossed with *Pkd1*$^{+/-}$;*Pkd1*$_{TAG}$, potential homozygous for the transgene were possible and are identified as *Pkd1*$^{-/-}$;*Pkd1*$_{TG}^{1\text{-}2X}$. In contrast to the *Pkd1*$^{-/-}$ kidneys, *Pkd1*$^{-/-}$;*Pkd1*$_{TAG}$*18* and *Pkd1*$^{-/-}$;*Pkd1*$_{TAG}$*26* express more than 10X of endogenous *Pkd1* mRNA at birth (**Fig.2A**). Consistently, kidney to body weight ratio (KBW) for both lines was very similar to the wild-type controls of the corresponding age until P30 (**Fig.3A**) At P30, KBW had tendency to be slightly decreased in *Pkd1*$^{-/-}$;*Pkd1*$_{TAG}$*26* but this did not reach statistical significance with the available number of mice.

Kidney

Renal histology showed that both *Pkd1* systemic lines on *Pkd1*$^{-/-}$ background have normal kidneys from birth to P30 (**Fig.5A,B**).

In more details, when compared to the wild-type kidneys (n=9), the *Pkd1*$^{-/-}$;*Pkd1*$_{TAG}$*18* compound did not show any distinguishable renal phenotype at birth (*Pkd1*$^{-/-}$;*Pkd1*$_{TAG}$*18*^{1X} (n=2); *Pkd1*$^{-/-}$;*Pkd1*$_{TAG}$*18*$^{1\text{-}2X}$ (n=2)). At P10, the kidneys of these mice were similar to those of *Pkd1*$_{TAG}$*18* transgenic alone at the same age (*Pkd1*$^{-/-}$;*Pkd1*$_{TAG}$*18*^{1X} (n=3); *Pkd1*$^{+/+}$;*Pkd1*$_{TAG}$*18*^{1X} (n=2), respectively). Identical observations were obtained at 1 month of age (*Pkd1*$^{-/-}$;*Pkd1*$_{TAG}$*18*^{1X} (n=8)). Of note, some obvious infiltrates were found in the kidneys. Finally, three mice were analysed at ~7-8months and did not show cystic phenotype (*Pkd1*$^{-/-}$;*Pkd1*$_{TAG}$*18*^{1X}; n=3, 1male, 2 females)),

only a couple of very few small dilatations/cysts (glomerular size) and again some infiltrates (**Fig.5A**).

As for the high-copy *Pkd1$_{TAG}$26* systemic transgenic line, at birth, the kidney histology appeared normal (**Fig.5B**) (*Pkd1$^{-/-}$;Pkd1$_{TAG}$26^{1X}*; (n=4); *Pkd1$^{-/-}$;Pkd1$_{TAG}$26^{1-2X}* (n=3)). Small dilatations are seen and probably due to undergoing postnatal nephrogenesis and were also observed in wild-type kidneys at birth (n=6). At P10, *Pkd1$_{TAG}$26^{1X}* transgenic kidneys look like wild-type kidneys (*Pkd1$^{+/+}$;Pkd1$_{TAG}$26^{1X}*). Similarily, at P10, the *Pkd1$^{-/-}$;Pkd1$_{TAG}$26^{1X}* shows no kidney cysts at all (n=2/3) or very small dilatations (n=1/3) (*Pkd1$^{-/-}$;Pkd1$_{TAG}$26^{1X}* (n=3)). At P10, small cysts and dilatations observed in *Pkd1$^{-/-}$;Pkd1$_{TAG}$26^{1-2X}* are probably due to the excess of transgene (n=4/4). At P30, kidneys were relatively normal-looking with some infiltrates/dilatations in one mice (*Pkd1$^{-/-}$;Pkd1$_{TAG}$26^{1X}* (n=5), 3 females, 2 males; *Pkd1$^{-/-}$;Pkd1$_{TAG}$26^{1-2X}* (n=1, male)).

Later on, in adult mice, some cystic anomalies could be observed (**Fig.6**). From 1 to 4 months of age, no kidney phenotype was observed in the *Pkd1$^{-/-}$;Pkd1$_{TAG}$26* mice analyzed ((n=4), 2 males, 2 females). Interestingly, at 7-8 months, two *Pkd1$^{-/-}$;Pkd1$_{TAG}$26* mice showed kidney cysts while one was normal (n=3 females). Identically, in the 10 to 13 months range (n=3 females), three mice were analysed from which 2 showed kidney cysts and one was intact. At 15-17 months, five out of seven mice (6 males, 1 female), were cystic while 2 other appeared normal. Two *Pkd1$^{-/-}$;Pkd1$_{TAG}$26* mice died at ~9 months probably from kidney failure since they had no obvious extrarenal phenotype. One mouse died very young soon after weaning at age of 5 weeks presumably because of teeth problem. Both parents for all these mating were heterozygous for the *Pkd1$_{TAG}$* transgene and thus it is highly possible that the mice that continue to show cysts at the adult stage are homozygous for the *Pkd1$_{TAG}$* transgene.

In sum, thoroughfull analysis of the kidney histology in systemic *Pkd1$^{-/-}$;Pkd1$_{TAG}$* compounds 18 and 26 show complete rescue of the kidney cystogenesis caused by *Pkd1* LOF until later adulthood where transgene levels appear critical.

Liver and pancreas

Regarding the extrarenal phenotype, when compared with wild-type controls (pancreas n=8, liver n=4), at P0 the *Pkd1*$^{-/-}$*;Pkd1*$_{TAG}$18 compound did not show pancreatic (*Pkd1*$^{-/-}$*;Pkd1*$_{TAG}$18^{1X} (n=2); *Pkd1*$^{-/-}$*;Pkd1*$_{TAG}$18^{1-2X} (n=2)) or liver anomalies (*Pkd1*$^{-/-}$*;Pkd1*$_{TAG}$*18*^{1X} (n=1); *Pkd1*$^{-/-}$*;Pkd1*$_{TAG}$*18*$^{1-2X}$ (n=2)), was similar to the *Pkd1*$^{+/+}$*;Pkd1*$_{TAG}$*18* transgenic at P10 and continued to be normal at P30 (*Pkd1*$^{-/-}$*;Pkd1*$_{TAG}$*18*^{1X}; (n=8)) (**Fig.5A**). Some obvious infiltrates were noted in the kidney and liver but importantly no cyst-like structures or dilatations were present. Additionally, for the mice sacrificed at ~7-8 months extrarenal morphology did not show liver or pancreas defects, other than pancreatic vacuoles and liver infiltrates, as observed in older *Pkd1*$^{-/-}$*;Pkd1*$_{TAG}$26 tissues (*Pkd1*$^{-/-}$*;Pkd1*$_{TAG}$*18*^{1X}, (n=3), 2 females, 1 male).

As for *Pkd1*$^{-/-}$*;Pkd1*$_{TAG}$*26* (**Fig.5B**), at birth, the liver and pancreas were intact (liver- *Pkd1*$^{-/-}$*;Pkd1*$_{TAG}$*26*^{1X}; (n=5); pancreas- *Pkd1*$^{-/-}$*;Pkd1*$_{TAG}$*26*^{1X} (n=3) and *Pkd1*$^{-/-}$*;Pkd1*$_{TAG}$*26*$^{1-2X}$ (n=1)). At P10, analogously to the *Pkd1*$_{TAG}$*26* transgenic alone (*Pkd1*$^{+/+}$*;Pkd1*$_{TAG}$*26*^{1X} liver (n=7), pancreas (n=6)), pancreas of the high *Pkd1*$^{-/-}$*;Pkd1*$_{TAG}$*26* expressor (n=5 total; *Pkd1*$^{-/-}$*;Pkd1*$_{TAG}$*26*^{1X} (n=3) & *Pkd1*$^{-/-}$*;Pkd1*$_{TAG}$*26*$^{1-2X}$ (n=2)) and liver ((n=6 total; *Pkd1*$^{-/-}$*;Pkd1*$_{TAG}$*26*^{1X} (n=3) & *Pkd1*$^{-/-}$*;Pkd1*$_{TAG}$*26*$^{1-2X}$ (n=3)) seemed normal, albeit some dilatations were seen in the pancreas which could be due to the section/infusion. In the early adulthood at P30/P31, normal appearance of the liver and pancreas was observed (*Pkd1*$^{-/-}$*;Pkd1*$_{TAG}$*26*^{1X}; n=5; 2 females, 3 males) and no pancreatic cysts were detected in mice ranging from 2-17 months (*Pkd1*$^{-/-}$*;Pkd1*$_{TAG}$*26*^{1X} n=10) (**Fig.6**). We could detect some patches of fat adipose-like regions in the pancreas of 5 out of 10 mice analyzed. Lipid-like structures could be seen and for 1 mice at 15 months some important dilatations in one part of the pancreas only. Importantly, the invasive liver phenotype in these same mice was absent (n=11) (**Fig.6**). Of note, two mice showed small non-invasive anomalies and in one a cluster of smaller cysts/dilatatations around the biliary duct. One mouse at 17 months of age had only solitary large cysts and the other one at 15 months had a cluster of cysts in the periphery of only one hepatic lobe. Overall, similarly to the kidney, *Pkd1*$^{-/-}$*;Pkd1*$_{TAG}$ compounds that express exogenous full-length *Pkd1* had a

rather normal renal and extrarenal histology all ages, albeit with some anomalies such as lipid-like, fibrotic regions and infiltrates.

To analyse if a truncated human mutation is able to rescue the *Pkd1*$^{-/-}$ kidney and pancreas cystic phenotype, we analysed the *Pkd1*$^{-/-}$*;Pkd1*$_{extra}$ *39* compound. Based on human mutation, *Pkd1*$_{extra}$ transgenic line 39 (2 copies) leads to a stabilized expression of Pc1$_{extra}$ protein at birth and in adulthood and closely mimics GPS Pc1 NTF cleaved form associated with late-onset of kidney cystogenesis in mice (**Suppl Fig.1, Fig.4A**) (Kurbegovic and Trudel 2013). Unlike the full-length *Pkd1*$_{TAG}$ transgene, the truncated human-like *Pkd1*$_{extra}$ mutant was unable to improve *Pkd1* loss-of-function kidney nor pancreatic cysts at birth despite at least 2X fold increase in mRNA and Pc1 protein when compared to normal endogenous levels (**Fig4B-D**). We therefore analysed the glycosylation pattern of *Pkd1*$_{extra}$ transgene in *Pkd1*$^{-/-}$ background at birth (**Fig.4E**). Unlike wild-type Pc1 and transgenic Pc1$_{TAG}$ that show partial EndoH resistance at P0, the *Pc1*$_{extra}$ appears solely Endo sensitive. Thus, on the *Pkd1*$^{-/-}$ genetic background, the Pc1$_{extra}$ human truncating mutation appears to behave as a loss-of-function.

Characterization of the renal and extrarenal phenotype in *Pkd1*$^{-/-}$*; SBPkd1* transgenic mice at different timepoints

Since the systemic full-lengh *Pkd1* expressor was able to fully complement *Pkd1*$^{-/-}$ kidney and pancreas cystic phenotype shown by *Pkd1*$^{-/-}$*;Pkd1*$_{TAG}$ compound, we aimed to confirm this with two lines of our previously published kidney specific *SBPkd1*$_{TAG}$ transgenic mice (**Suppl Fig.1**) (Thivierge, Kurbegovic et al. 2006). The low-copy line corresponds to *SBPkd1*$_{TAG}$*3* and high-copy to *SBPkd1*$_{TAG}$*41*. In addition, double mating would allow us to uncover the *Pkd1* kidney specific phenotypes and potentially the most frequent human extrarenal liver cysts in the *Pkd1*$^{-/-}$ LOF context.

Kidney

First, by QPCR we confirmed that kidneys of compounds of both lines express sufficient *Pkd1* levels. Indeed, both lines expressed *Pkd1* to at least similar levels of *Pkd1* in wild-type kidneys. The low copy *Pkd1*$^{-/-}$*;SBPkd1*$_{TAG}$*3* compound express ~1.5-fold while *Pkd1*$^{-/-}$*;SBPkd1*$_{TAG}$41 more than 10-fold increase when compared to *Pkd1* levels in *Pkd1*$^{+/+}$ wild-type kidneys (**Fig.2B)**. This is somewhat similar to the protein expression in the transgenic kidneys at the same age (**Fig.1C**). At birth, KBW ratio of *Pkd1*$^{-/-}$*;SBPkd1*$_{TAG}$*3 and Pkd1*$^{-/-}$*;SBPkd1*$_{TAG}$ 41 compounds was very similar to the wild-type kidneys and significantly different from the *Pkd1*$^{-/-}$. However, at P5, *Pkd1*$^{-/-}$*;SBPkd1*$_{TAG}$*3* compound had tendency to increase and actually become significantly increased at P10 (**Fig.3B)**. At P5, the KBW increased to ~2-fold (n=3) and at P10 increased significantly to ~3-fold (n=4) for the *Pkd1*$^{-/-}$*;SBPkd1*$_{TAG}$*3* while it remained similar to the wild-type controls for *Pkd1*$^{-/-}$*;SBPkd1*$_{TAG}$*41*. The *Pkd1*$^{-/-}$*;SBPkd1*$_{TAG}$*41* compound on the other hand become significantly increased at P30. We then proceeded with extensive analysis of the kidney histology at P0, P5, P10 and P30 (**Fig7A, 7B**). The *SBPkd1*$_{TAG}$ mice develop kidney cystogenesis in adulthood and kidney anomalies are reported very minimal in young mice (Thivierge, Kurbegovic et al. 2006). At P5 the *Pkd1*$^{+/+}$*;SBPkd1*$_{TAG}$*3*^{1X} transgenic alone showed kidneys overall very comparable to the wild-type, with 2-3 small dilatations equivalent or smaller than a size of glomeruli (n=5) and at P10 (n=5/6) kidneys continue to show only mild dilatations while some (n=1/6) show multiple smaller cysts ranging from ~0.003-0.005mm2. In contrast to *SBPkd1*$_{TAG}$ transgenics, already at P0, the earliest age analyzed, the *Pkd1*$^{-/-}$*;SBPkd1*$_{TAG}$*3* compound showed some glomerular and tubular cysts (*Pkd1*$^{-/-}$*;SBPkd1*$_{TAG}$*3*^{1X} (n=9)) which did not significantly influence the kidney to body ratio versus the wild-type controls (n=5) (**Fig.7A-a**). At P5, the *Pkd1*$^{-/-}$*;SBPkd1*$_{TAG}$*3* showed obvious kidney cysts that seemed bigger in size and number (n=2) than at birth and seemed to be confined more to the periphery (cortex). At P10, the cystic phenotype was affecting almost all kidney architecture (n=4). Numerous cysts of different size (small to very big) are present in the cortex and the medulla with pronounced epithelial hyperplasia. An undifferentiated, fibroblastic-like

(nephrogenic) zone could also be seen in the outer cortex, protruding from the medulla to cortex. Some tubules and glomeruli were however intact. No *Pkd1*$^{-/-}$*;SBPkd1*$_{TAG}$*3* mice were analysed later than P10 but are not expected to reach post-weaning stage/early adulthood.

In the higher overexpressor, *Pkd1*$^{-/-}$*;SBPkd1*$_{TAG}$*41* some dilatations/cysts could also be seen at birth (*Pkd1*$^{-/-}$*;SBPkd1*$_{TAG}$*41*^{1X} (n=6); *Pkd1*$^{-/-}$*;SBPkd1*$_{TAG}$*41*$^{1-2X}$ (n=1)) (**Fig.7B**) and were similar to *Pkd1*$^{+/+}$*;SBPkd1*$_{TAG}$*41* transgenic (*Pkd1*$^{+/+}$*;SBPkd1*$_{TAG}$*41*^{1X} (n=4)) or heterozygous *Pkd1*$^{+/-}$*; SBPkd1*$_{TAG}$*41*^{1X} (n=1)). At P5, the high *Pkd1*$^{+/+}$*;SBPkd1*$_{TAG}$*41* transgenic mice present already at this age small cysts/dilatations and some are very cystic (small cysts) (*Pkd1*$^{+/+}$*;SBPkd1*$_{TAG}$*41*^{1X}*,* (n=8)). Relative to the size of the glomeruli at this stage (~1600μm^2=1.6mm^2), small dilatations go from ~0.08-0.5mm^2 and up to cystic 2-4mm^2. At P5, for *Pkd1*$^{-/-}$*;SBPkd1*$_{TAG}$*41* kidneys showed multiple dilatations/cysts of ~0.014mm^2 (glomerular size) (*Pkd1*$^{-/-}$*;SBPkd1*$_{TAG}$*41*^{1X} (n=4/5) therefore somewhat similar to their transgenic counterparts. At P10, for the high expressor *Pkd1*$^{-/-}$*;SBPkd1*$_{TAG}$*41* smaller cysts were present (*Pkd1*$^{-/-}$*;SBPkd1*$_{TAG}$*41*^{1X} ((n=6)) similarly to the transgenic kidneys with 9 out of 11 manifesting multiple small cysts and 2 out of 11 with no cysts at all, as the wild-type (*Pkd1*$^{+/+}$*;SBPkd1*$_{TAG}$*41*^{1X} (n=11)). At P30, *Pkd1*$^{+/-}$*;SBPkd1*$_{TAG}$*41* showed a few rather smaller cysts (*Pkd1*$^{+/-}$*;SBPkd1*$_{TAG}$*41*^{1X} (n=2)) and 4 out 5 mice manifested kidney hydronephrosis (*Pkd1*$^{+/-}$*;SBPkd1*$_{TAG}$*41*^{1X}). Interestingly, while kidneys were not severely affected prior and at P10, at P30/P31, the *Pkd1*$^{-/-}$*;SBPkd1*$_{TAG}$*41* kidneys presented multiple cysts and extensive cystogenesis (n=7/7), further amplified at 3-4 months (n=3). When it was possible to determine, at least 4 out of 7 *Pkd1*$^{-/-}$*;SBPkd1*$_{TAG}$*41* mice (*Pkd1*$^{-/-}$*;SBPkd1*$_{TAG}$*41*^{1X}) showed severe hydronephrosis. Together, these data show that both ''SB'' kidney specific transgenic *Pkd1* lines partially rescue the kidney phenotype of *Pkd1* LOF model with important variability in the severity of the cystic phenotype.

Liver and pancreas

As previously reported, *Pkd1*$^{-/-}$ mice develop pancreatic cysts, one of the most obvious macroscopic phenotypes in this mouse model along obvious kidney cysts at birth (n=6). Interestingly, the SB kidney-specific compound, at birth, showed no macroscopic (n=4) or microscopic (n=4) cysts in the pancreas of *Pkd1*$^{-/-}$*;SBPkd1*$_{TAG}$*3 (Pkd1*$^{-/-}$*;SBPkd1*$_{TAG}$*3*^{1X}*)* (**Fig.7A-a**). No obvious anomalies or cysts were seen in the liver (n=5). At P5, the stage where no *Pkd1*$^{-/-}$ is alive, the *Pkd1*$^{-/-}$*;SBPkd1*$_{TAG}$*3* pancreas seemed to have normal appearance in one mouse, while the second showed were multiple pancreatic cysts (*Pkd1*$^{-/-}$*;SBPkd1*$_{TAG}$*3*^{1X}). Liver (n=1) is similar to wild-type (n=5). At P10, however the pancreatic phenotype is completely penetrant in *Pkd1*$^{-/-}$*;SBPkd1*$_{TAG}$*3* that show simple (n=1/4) or in most cases (n=3/4) multiple numerous cysts, which appear bigger in size than at P5 (*Pkd1*$^{-/-}$*;SBPkd1*$_{TAG}$*3*^{1X} (n=4)). Almost every cyst has epithelial hyperplasia (multiple layers of cells), and structural cystic epithelia in the pancreas are very similar to those in the kidney (hyperplasia, fibrosis, proteinous casts). Pancreatic cysts seem to be filled with proteinous/lipid casts. Endocrine/exocrine cells are visible, and some are intact but not many left probably because of the invasiveness of cysts. Similar to the kidney, pancreatic cysts were surrounded by fibroblastic/mesenchymal/lipidous like tissue. We did not see any obvious anomalies in the liver of *Pkd1*$^{-/-}$*;SBPkd1*$_{TAG}$*3* mice at P10 (n=4) other than some infiltrates around vein/ducts .

As for a much higher overexpressor (**Fig.7B**), at P0, neither *Pkd1*$^{-/-}$*;SBPkd1*$_{TAG}$*41* pancreas (*Pkd1*$^{-/-}$*;SBPkd1*$_{TAG}$*41*^{1X} *(n=2)*; *Pkd1*$^{-/-}$*;SBPkd1*$_{TAG}$*41*$^{1-2X}$ (n=1)) or liver (*Pkd1*$^{-/-}$*;SBPkd1*$_{TAG}$*41*$^{1-2X}$ (n=1)) presented cystic anomalies. At P5, the liver seems intact (*Pkd1*$^{+/-}$*;SBPkd1*$_{TAG}$*41*^{1X}(n=7)) and pancreas overall normal, although obvious fibrotic/connective tissue at different extent is present in all 7 mice analysed. At P10 the liver does not contain important gross anomalies or cysts (*Pkd1*$^{-/-}$*;SBPkd1*$_{TAG}$*41*^{1X} (*n*=3)) other that infiltrates/inflammation around veinous/ductal network which could also be seen in some wild-type mice and caused by infusion/fixation conditions. In the pancreas on the other hand, although important variability is to be noted and no cysts are detected, some anomalies could be observed at P10: small

pseudocysts/dilatations (n=2/6), disorganization of the structures (n=1/6), increase in the sclerotic /connective tissue (n=4/6) while in some cases pancreas seemed almost normal (n=2/6).

At P30/P31, the liver of high expressor *Pkd1*$^{-/-}$*;SBPkd1*$_{TAG}$*41* (*Pkd1*$^{-/-}$*;SBPkd1*$_{TAG}$*41*^{1X} n=7/7) showed a lot of infiltrates around biliary ducts and some dilatations which could be seen also in the *Pkd1*$^{+/-}$*;SBPkd1*$_{TAG}$*41* (*Pkd1*$^{+/-}$*;SBPkd1*$_{TAG}$*41*^{1X} (n=5)) with similar severity. The severity of this observation did not seen to correlate with a specific gender. At P30/31, the *Pkd1*$^{-/-}$*;SBPkd1*$_{TAG}$*41* pancreas did not show any cysts (*Pkd1*$^{-/-}$*;SBPkd1*$_{TAG}$*41*^{1X} (n=6/6)) but rather a lot of adipose-like fat tissue (n=3/6), which could also be seen in *Pkd1*$^{+/-}$*;SBPkd1*$_{TAG}$*41 (Pkd1*$^{-/-}$*;SBPkd1*$_{TAG}$*41*^{1X} (n=1/1)). At 3-4 months, livers from the *Pkd1*$^{-/-}$*;SBPkd1*$_{TAG}$*41* mice show important infiltrates around the biliary ducts but no cystic alterations.

ADPKD is associated with increased levels of fibrosis, proliferation and smooth muscle actin. Given that H&E staining was suggesting of these alterations in our transgenic compounds, we performed specific colorimetric staining for collagene using Sirius Red, antibody detection for SMA and Ki67 on P10 kidneys (**Fig.7A-b**). Both staininig with Sirius red and immunofluorescence using α-SMA specific antibody showed increased positive signal around the cysts (wild-type controls n=3; *Pkd1*$^{-/-}$*;SBPkd1*$_{TAG}$*3* (n=4)). The cystic regions in the *Pkd1*$^{-/-}$*;SBPkd1*$_{TAG}$*3* pancreas were thus found to be positive for myofibroblastic smooth muscle actin marker (SMA). Immunohistochemistry using the proliferative marker Ki67 on these same samples showed important basal proliferation in wild-type kidneys and many positive nuclei in the long cystic epithelia from *Pkd1*$^{-/-}$*;SBPkd1*$_{TAG}$*3* kidneys. Of note, some cyst cell epithelia were flat while other very elongated.

In sum, unexpectedly, the adult kidney-specific *Pkd1*$^{-/-}$*;SBPkd1*$_{TAG}$ compound, that partially rescues the kidney cystogenesis, also improves pancreatic cystic phenotype. The liver phenotype expected potentially from *Pkd1* absence in the liver (if LOF was cystogenic in extrarenal tissues) does not occur at the latest time-point analysed, 1 month.

Characterization and progression of the liver phenotype in *Pkd1$^{V/V}$;Pkd1 transgenic compounds*

The full-complementation of *Pkd1* LOF extrarenal phenotype by *Pkd1$_{TAG}$* transgene, and premature death and absence of liver cysts in kidney specific *SBPkd1$_{TAG}$* compound, precluded us from assessing if loss-of function is directly causative pathogenetic mechanism in liver cystogenesis. Since this could only be tested until ~1 month of age, we decided to mate our *Pkd1* transgenic mice with *Pkd1$^{V/V}$* GPS-deficient knock-in mutant (**Suppl Fig.1**). Pc1 GPS cleavage leads to generation of NTF and CTF cleaved products and was shown as developmentally regulated in the kidneys in mice (Yu, Hackmann et al. 2007, Castelli, Boca et al. 2013). The Pc1 uncleaved form is sufficient for *in utero* but insufficient for post-natal distal segment homeostasis in kidneys (Yu, Hackmann et al. 2007). In contrast to *Pkd1* LOF model, the *Pkd1$^{V/V}$* survive until around P27-P30 and die most probably of kidney failure. The *Pkd1$^{V/V}$* mice were reported with some liver fibrosis few days after (P14) birth but the progression of hepatic phenotype was not characterized in further details.

At P10, further analysis of liver sections show that *Pkd1$^{V/V}$* mice indeed develop liver cysts obvious at P30 (**Fig.8A)**. The liver cysts cannot be corrected by the presence of only NTF-like cleaved form provided by *Pkd1$_{extra}$* transgene shown by *Pkd1$^{V/V}$;Pkd1$_{extra}$39* binary mice. The *Pkd1$^{V/V}$;SBPkd1$_{TAG}$41* mice showed very cystic kidneys (**App.V**) and importantly biliary ducts dilatations and cysts at P30 (*Pkd1$^{V/V}$;SBPkd1$_{TAG}$41^{1X}*, n=1) and over hepatic cystogenesis later at 3months (n=3) (**Fig.8B**). At P31/33, one female low copy *Pkd1$^{V/V}$;SBPkd1$_{TAG}$3* mice homozygous for the transgene (*Pkd1$^{V/V}$;SBPkd1$_{TAG}$3^{2X}* (n=1/1)) showed minimally affected kidneys and apparently more severe liver cystogenesis (bigger cysts) than in *Pkd1$^{V/V}$;SBPkd1$_{TAG}$41^{1X}*. Of note, two very old *Pkd1$^{V/+}$;SBPkd1$_{TAG}$41* mice (*Pkd1$^{V/+}$;SBPkd1$_{TAG}$41^{1-2X}*, n=2/2, 1 female, 1 male) at 18.5-19 months both showed imposing/invasive liver cysts, in some ways similar to one *Pkd1$^{V/V}$; Pkd1$_{TAG}$26* mice at 19 months of age (see above). These data suggest that the kidney-specific transgene *SBPkd1$_{TAG}$* is not able to significantly rescue liver cystogenesis in *Pkd1$^{V/V}$*, but appears to delay the process.

Since the kidney phenotype was completely rescued by the *Pkd1*$_{TAG}$ transgene in *Pkd1*$^{-/-}$ and *Pkd1*$^{V/V}$ genetic background (**Chapter VI**), we expected that the liver of the *Pkd1*$^{V/V}$*;Pkd1*$_{TAG}$*26* would be fully complemented as well (**Fig.8C**). However, already at ~3months of age (n=4 females), two (50%) demonstrated 1 or more clusters of liver cysts whereas the *Pkd1*$^{V/+}$*;Pkd1*$_{TAG}$*26* littermate controls *(Pkd1*$^{V/+}$*; Pkd1*$_{TAG}$*26*^{1X} (n=3)) at this age did not show any anomalies. Furthermore, later on, the liver showed completely penetrant cystic phenotype (n=12; 9 females, 3 males, 6-14 months). The cystic phenotype seemed progressive in the number of clusters and the size of the cysts in contrast to the absence of any liver anomalies in controls *Pkd1*$^{V/+}$*; Pkd1*$_{TAG}$*26* (*Pkd1*$^{V/+}$*;Pkd1*$_{TAG}$*26*^{1X}, n=7, 3 females, 4 males, 12.5-14.5 months), *Pkd1*$_{TAG}$ transgenic (*Pkd1*$_{TAG}$^{1X} n=3) and *Pkd1*$^{-/-}$*;Pkd1*$_{TAG}$*26 (***Fig.5B,6***)*. Of importance, incomplete although significant penetrance of liver cysts was reported in aged *Pkd1*$_{TAG}$ transgenic mice, no liver cysts could be detected at 7 months of age (n=2 females, 1 male).

For the small number of males available, when compared with females of the same age (6-7months), the males seem to have lesser number of clusters and clusters seems overall smaller. Two *Pkd1*$^{V/V}$*;Pkd1*$_{TAG}$*26* males (*Pkd1*$^{V/V}$*;Pkd1*$_{TAG}$*26*$^{1-2X}$) at 6-7 months were phenotypically somewhat comparable to females at 3 months, consistent with PKD liver cystogenesis being modulated by oestrogen. One *Pkd1*$^{V/V}$*;Pkd1*$_{TAG}$*26* male (*Pkd1*$^{V/V}$*;Pkd1*$_{TAG}$*26*^{1X}) was sacrificed at 19 months of age and also showed impressively massive liver cysts consistent with the previous reports that liver cysts also affect males, but with a slower pace. When females are compared within different ages, the number of cluster is not significantly increased while the size of the cluster is. These findings underline the role of the cleavage and specifically the abundance of uncleaved Pc1 form in adult liver homeostasis.

Renal and extrarenal polycystin-1 expression in transgenic *Pkd1* LOF and *Pkd1$^{V/V}$* compounds

We previously showed almost undetectable levels of *Pkd1* in adult extrarenal tissues in *SBPkd1$_{TAG}$* model by Q-PCR and semi-quantitative PCR (Thivierge, Kurbegovic et al. 2006). However, rescue of pancreatic phenotype in *SBPkd1$_{TAG}$41 s*uggests extrarenal Pc1 expression at earlier stage. To analyse Pc1 expression in extrarenal tissues, we performed Western blot analysed in the total extracts of the kidney, liver and pancreas from birth to P30 (**Fig.9**). Similar to results obtained for the *Pkd1* transcript by Q-PCR (**Fig.2**), the expression of Pc1 in the kidney was detectable in all lines at similar or higher levels to the endogenous Pc1 in wild-type control (**Fig.9A**). Both systemic *Pkd1$^{-/-}$;Pkd1$_{TAG}$* transgenic compounds showed elevated extrarenal Pc1 expression (**Fig.9A-D**) with higher expression in the kidneys and pancreas and lower in the liver (**Fig.9D**). In the low-copy kidney-specific *Pkd1$^{-/-}$;SBPkd1$_{TAG}$3*, Pc1 expression was undetectable in the pancreas and extremely low in the liver (a faint band only seen after very long exposition in the liver). Surprisingly, in the high-copy kidney-specific *Pkd1$^{-/-}$;*SBPkd1$_{TAG}$41 at P0 Pc1 was detected in both liver and pancreas (**Fig.9B,C**) to levels similar to endogenous wild-type expression. The hepatic expression of Pc1 in *Pkd1$^{-/-}$;SBPkd1$_{TAG}$41* compound at P0 was also detected in *Pkd1$^{V/V}$; SBPkd1$_{TAG}$41* compound at P10 (**Fig.9G**). When compared at different stages, the *SBPkd1$_{TAG}$* total kidney expression of Pc1 was similar to endogenous Pc1 regulation with descending levels from P0, P10 to P30 (**Fig.9E**). Notably less expressed, this decreasing expression pattern seems also conserved in the liver for the wild-type mice and *Pkd1$^{-/-}$;*SBPkd1$_{TAG}$41 (**Fig.9F**).

DISCUSSION

In this study we provide an ultimate evidence for gene-dosage pathogenetic mechanism for ADPKD. We show that our *Pkd1*-BAC transgenic product behaves as a wild-type endogenous Pc1 protein and is able to functionally fully rescue the *Pkd1* LOF kidney and extrarenal anomalies. Our study also leads to further temporal and spatial characterization of ''SB'' kidney-specific elements. The *Pkd1*$^{-/-}$*;SBPkd1*$_{TAG}$ compounds develop hypomorph-like phenotypes but with significant difference in pace of disease progression in low and high-copy *Pkd1*$^{-/-}$ compounds. Furthermore, we uncover the critical importance of the GPS cleavage and particularly of Pc1 uncleaved form for an extrarenal homeostasis. Together, we believe these findings are of great impact for better understanding the pathocellular processes in the kidney and liver polycystic disease towards specific and efficient therapies.

We and other groups have previously shown that transgenic systemic or kidney-specific expression of *Pkd1*-BAC or *Pkd1*-*Tsc2*-PAC causes kidney and liver cystogenesis in mice (Pritchard, Sloane-Stanley et al. 2000, Thivierge, Kurbegovic et al. 2006, Kurbegovic, Cote et al. 2010). To exclude the possibility that the transgene behaves as a mutant, backcrossing of the transgenes on *Pkd1*$^{-/-}$ genetic background confirmed the increase of wild-type full-length Pc1 proteins as a direct cause. Genetic complementation in mice thus indicates that ADPKD is a disease of abnormal (increase/decrease) regulation of *PKD1* levels and definitively places *PKD1* in a category of gene-dosage diseases.

The low-copy *Pkd1* kidney-specific overexpressor reproduces kidney and pancreatic anomalies and, although later, the high expressor develops kidney cysts likewise. These observations are in agreement with our gene-dosage hypothesis. Additionally, they also suggest restrained cell-specific expression of Pc1 provided by SB regulatory elements in comparison to the endogenous *Pkd1*. While pancreatic cyst are completely penetrant in *Pkd1*$^{-/-}$ mice at birth, no cysts are observed at P0 for low copy *Pkd1*$^{-/-}$*;SBPkd1*$_{TAG}$*3*. Thus, not only SB promoter is cell-specific, but also appears somewhat developmentally regulated. With undetectable levels of Pc1 at

this stage in *Pkd1*$^{-/-}$*;SBPkd1*$_{TAG}$*3*, this could also point to earlier *in utero* subtle non-cystic pancreatic developmental defects prior birth and/or requirement of very low levels of Pc1 for normal for perinatal pancreas development. The second possibility is consistent with very low levels of *Pkd1* in *Pkd1*^{nl} hypomorph (~20% in the kidney) associated with only mild pancreatic cystogenesis (Lantinga-van Leeuwen, Dauwerse et al. 2004). Cell-specific expression of Pc1 could not have been undertaken given the absence of available biochemical reliable tools. Future studies using laser-capture microscopy, specific cell-sorting in parallel with determination of cyst origin in the kidney and pancreas of *Pkd1*$^{-/-}$*;SBPkd1*$_{TAG}$ will help to answer these concerns.

Frequent pancreatic phenotype observed in the *Pkd1* LOF mouse models are rarely reported in human ADPKD or adult ADPKD mouse models. Therefore, the loss of *Pkd1* in the pancreas could be of limited translational interpretation of human disease. However, specific epithelial cystic characteristics and cellular defects, such as fibrosis, SMA accumulations and proliferation, that we report in the pancreas of *Pkd1*$^{-/-}$*;SBPkd1*$_{TAG}$ compound are also associated with polycystic kidney disease and therefore could be informative. In addition, pancreatic phenotype is similar to the one observed in patients with cystic fibrosis with CFTR mutations and CFTR inhibitors are promising kidney cystogenesis treatment in mice (Yang, Sonawane et al. 2008, Oppenheimer and Esterly 1975).

The ‘’*Pkd1* gene-dosage’’ not only seems to imply levels of *Pkd1* transcript and Pc1 protein levels, but also levels of specific Pc1 (iso)forms. We previously showed that Pc1 GPS cleaved forms and intact CTF fragment were necessary for kidney homeostasis whereby kidney cystogenesis of *Pkd1*$^{V/V}$ was completely rescued by *Pkd1*$_{TAG}$ transgene (**Chapter VI**). In the liver on the other hand, *Pkd1*$^{V/V}$ cystogenesis is significantly diminished however not completely rescued. The presence of uncleaved form in *Pkd1*$^{V/V}$*;Pkd1*$_{TAG}$ seems adverse to adult liver homeostasis. As it was shown for some other GPS non-constitutively cleaved molecules, one possibility is that the uncleaved full-length Pc1 is functionally active and independent of the cleaved forms as suggested for Shh (Tokhunts, Singh et al. 2010) with potential

competition with cleaved forms for downstream signalling targets as suggested for Jade-1 (Foy, Chitalia et al. 2012). Why would the *Pkd1* transgene rescue kidney but not liver phenotype? It is possible that the uncleaved form binds to the ligand, which is more expressed in adult liver. Since neither kidney (**Chapter VI**) nor liver could be corrected by NTF-like form, we suggest that in general there needs to be enough available endogenous CTF fragments for instance for proper trafficking and function of Pc1. This would be consistent with lack of rescue of the $Pkd1^{-/-}$ and $Pkd1^{V/V}$ but late-onset of cystogenesis on $Pkd1^{+/+}$ by the $Pkd1_{extra}$ transgene. Presence of liver phenotype in the $Pkd1^{V/V};Pkd1_{TAG}$ most likely does not result from potential lack of the $Pkd1_{TAG}$ expression in some cell types because the $Pkd1^{-/-};Pkd1_{TAG}$ do not develop liver phenotype. Alternatively, Pc1 full-length could be a ''reservoir'' of P100, another C-terminal fragment independent of GPS cleavage that could have particular roles (Woodward, Li et al. 2010). Finally, Pc2 was reported to affect the GPS cleavage *in vitro* (Chapin, Rajendran et al. 2010). In contrast to Pc1, the Pc2 expression remains more easily detectable after birth and this could be to maintain the differential levels of the cleaved and uncleaved products. These important questions could be addressed in future by generating $Pkd1^{V}$ transgenic lines or by using with $Pkd1^{V/-};Pkd1_{TAG}$ binary mice to modulate the levels of the uncleaved Pc1.

Liver cystogenesis is the most frequent human extrarenal ADPKD defect of epithelial origin in the biliary ducts, the cholangiocytes, and affects more females than males. Similarly to the human, liver cysts in our binary models on $Pkd1^{V/V}$ genetic background localize around biliary ducts and seem more severe in females. Although quantitative assessment of the cluster area/cyst area in multiple consecutive sections will be required for further evaluation of the progression of liver disease and influence of the gender, cysts appear more severe in females than in males. Interestingly, the $Pkd1^{V/V};SBPkd1_{TAG}$ do not seem to have a completely identical pattern to liver cysts in $Pkd1^{V/V}$ and for now, we cannot exclude or include $SBPkd1_{TAG}$ as potentially also expressed in cells other than cholangiocytes because of the nonidentical pattern. The focal almost random nature of $Pkd1^{V/V};Pkd1_{TAG}$ mice points to cleavage as potentially focal-regulated process. Exosomes were suggested to play a role in biliary

cholangiocytes and shown to affect signalling pathways such as ERK/MAPK and cell proliferation (Masyuk, Huang et al. 2010). With this in mind, an attractive hypothesis would be the presence of an exosomal transport and delivery of specific Pc1 forms that might counterbalance threshold levels of uncleaved Pc1. Finally, our findings are consistent with both, altered efficiency of the cleavage reported in *Pkd1* hypomorph kidney extracts that was associated with kidney and liver cystogenesis (Hopp, Ward et al. 2012), and *Pkd1* being the critical determinant in the liver of five PKD diseases caused by *Pkd1*, *Pkd2*, *Prkch*, *Sec63* and *Pkhd1* (Fedeles, Tian et al. 2011). We suggest that successful rescue of the cystic liver phenotype by improving the Pc1 GPS cleavage may not be due uniquely to the indispensable presence of GPS-cleaved forms but also a necessary decrease of potentially hyperactive uncleaved form.

Overall, these studies support the crucial role of *Pkd1* in the PKD liver disease. As we suggested previously for the kidney (**Chapter VI**), the GPS cleavage seems indeed a promising approach not only for kidney but also liver disease therapy alternatives.

MATERIAL AND METHODS

Mice

Pkd1^{Null}, *Pkd1*$_{extra}$, *Pkd1*$_{TAG}$, *SBPkd1*$_{TAG}$ and *Pkd1*$^{V/V}$ mouse models were previously described (Wu, Tian et al. 2002, Thivierge, Kurbegovic et al. 2006, Yu, Hackmann et al. 2007, Kurbegovic, Cote et al. 2010, Kurbegovic and Trudel 2013). All work using animals was accomplished following standards of the Canadian Council of Animal Care of Institut de Recherches Cliniques de Montréal.

Genotyping analysis

Genotyping of mice were done on DNA extracted from the tails and consisted of 3 different steps. First, by regular PCR amplification we identified Pkd1 heterozygous mice using the following oligos: **Forward** (6-48): 5'CAG GGT CTC CGG CCA G 3' and **Reverse** (6-49): 5' AGC GCA TCG CCT TCT ATC GC 3' allowing an amplicon of around 400bp (presence of neo allele). Then, the Pkd1$_{TAG}$ and Pkd1$_{extra}$ transgenes were genotyped by Southern blots using EcoRI (ex7-15 Pkd1 probe) and BamHI (ex 23-25 probe) respectively. Finally, we identified Pkd1$^{-/-}$; transgenic compound by quantitative PCR using the Taqman approach for gene copy number (homozygous vs heterozygous for ''Null/Neo'' allele).

Taqman Dolt gene as a normalizer (Life Technologies): **Forward primer** (Intron 1, #9-19): 5' GCC CCA GCA CGA CCA TT 3'; **Probe ''Dolt''**: VIC CCA GCT CTC AAG TCG MGBNFQ; **Reverse primer** (Intron 1, #9-20): 5'TAG TTG GCA TCC TTA TGC TTC ATC3' amplifying a product of 68bp.

Taqman Neo gene: **Forward primer** (Neo gene #9-17): 5' TCG ACC ACC AAG CGA AAC A3', **Probe ''NEO''**: 6FAM CGC ATC GAG CGA GC MGBNFQ; **Reverse primer** (Neo gene #9-18): 5' CCG GCT TCC ATC CGA GTA C 3' amplifying a product of 55bp.

For the genotyping of *Pkd1*$^{V/V}$*;Pkd1* transgenic compounds, we followed the same steps as described in Chapter 4 (Manuscript in preparation).

For both PCRs, the conditions were: 0.45μM of each primer, 0.125μm of the probe, 10ng of genomic DNA in a total volume of 10ul. PCRs were done in duplicates using PerfeCTa qPCR SuperMix (Quanta Biosciences) and run either in Mx4000, 3005P (Stratagene) or Viia7 (Life Technologies) apparatus with 45C 5min, 95C 5min, 95C 15sec, 60 45sec, two last steps repeated 40 times.

Histology

Tissues were fixed in formalin and dehydrated in increasing % of ethanol, xylene and embedded in paraffin. Paraffin blocks were sectioned and stained by Hematoxilin&Eosin (4μm thick) or Sirius red (5μm thick). Stained sections of renal and extrarenal tissues of each mouse (each ''n'') and of specific genotype were observed using Axiophot Zeiss microscope and then pictures for each one of them taken using MicroPublisher 3.3. RTV Imaging/Nikon camera and Northern eclipse software. Images were analyzed at different magnifications (2.5, 5X and 20X) and representative images selected for the histology figures.

Q-PCR

Kidneys were harvested at birth and RNA isolated using Trizol reagent (Invitrogen). The integrity was confirmed on agarose gel. 1μg of RNA was treated by DNAse and followed by RT-PCR reaction. Samples were quantified/analyzed as triplicates for Pkd1 expression using ViiA7 (Life technologies) apparatus and 384-plate. Pkd1 expression at 5' end was analyzed using the primers in exon1/2 (Forward 5' TCA ATT GCT CCG GCC GCT G; Reverse 5' CCA GCG TCT GAA GTA GGT TGT GGG) and 3' end using primers in exon39/40 (Forward 5' CTG ATG AGT TCT GGC CAT GGA TG; Reverse 5' 5' CTG CCA GCC AAT GCC ATA GTC AC) of Pkd1 gene. S16 was used as normalizer with following primers: Forward 5' AGG AGC GAT TTG CTG GTG TGG and Reverse 5' GCT ACC AGG GCC TTT GAG ATG. Data was analyzed as follows: **1**) Analyze the triplicates (remove bad); **2**) Get the ΔCt for each mouse; **3**) Calculate the mean of ΔCt of the $Pkd1^{+/+}$ (calibrator); **4**) Calculate ΔΔCt for each

mouse versus mean ΔCt of the Pkd1$^{+/+}$; **5**) Calculate $2^{-\Delta\Delta Ct}$; **6**) Average of $2^{-\Delta\Delta Ct}$ for each particular genotype; **7**) Standard deviation of ΔΔCt for each particular genotype.

Biochemical studies

Immunoblots were performed as previously published (Kurbegovic, Cote et al. 2010, Kurbegovic and Trudel 2013). Total proteins extract were quantified either by Bradford (Bio-Rad) or BCA assay (Pierce, Fisher), loaded on 4-12% Bis-Tris NuPage gels with MES migration buffer (Invitrogen). We used mouse monoclonal 7e12 antibody against Pc1, mouse monoclonal against smooth muscle actin (Milipore), rabbit antibody against Ki67 (Novacastra), and three different mouse monoclonal antibodies as loading controls *i.e.,* Gapdh (Abcam), β-actin and β-tubulin (SIGMA). ECL Prime was used for detection. Quantification of the intensity of bands was performed by scanning the Kodak films and processing with ImageQuant software, or directly by BioRad Chemi-Doc XRS+Imaging system. Deglycosylation of the protein extracts using PNGase and EndoH enzymes from NEB was performed following manufacturer's instructions.

Immunofluorescence and Immunohistochemistry

For smooth muscle actin, we used paraffin-embedded sections (4μm) which were first deparaffinised, washed in TBS buffer (Tris pH7.5, 0.1M; NaCl 0.15M), incubated 30 min with NaBH4 (0.01%) and permeabilized with SDS (1%) for 7min. After blocking the endogenous mouse IgGs (JacksonImmunoresearch) at dilution 1:5 in blocking solution (10X goat serum; 0.1% BSA in TBS) O/N at 4°C, slides were then incubated with mouse monoclonal antibody against SMA (Milipore) at 1:250 dilution, 4°C, O/N. Secondary goat anti-mouse antibody (Alexa 555, Invitrogen) was used at 1:300 dilution at 4°C for 2hours. Finally, nuclei were stained with DAPI (SIGMA) at 1:10 000 dilution in PBS1X buffer for 2min at room temperature. Slides were mounted with ProLong Gold antifade reagent mounting media (Invitrogen). Slides that underwent exactly the same conditions except addition of the first antibody were used as negative control for assessment of background signal due to the secondary

antibody or inefficient mouse IgG blocking. Images for immunofluorescence were taken by Leitz DMRB (Leica) microscope using Northern Eclipse software.

For Ki67 staining, we followed a protocol as previously published with slight modifications (Kurbegovic, Cote et al. 2010). Briefly, paraffin-embedded sections (4μm) were deparafinized, endogenous peroxidase activity inhibited with H_2O_2 for 10min, antigene retrieved using pressure cocker for 15min (Citric acid 1.8mM; Sodium citrate 8.2mM) and blocking step for 30 min at room temperature (10% goat serum, 1% BSA, 0.02%Tween). We used with Ki67 antibody (rabbit, Novacastra) at 1:100 O/N at 4°C and secondary biotinylated antibody (anti-IgG rabbit, Vector) at dilution 1:300 for 2 hours at room temperature. The signal was detected after 30 min of incubation with ABC kit and 6min fresh DAB (Vector Laboratories). Images for were taken using Axiophot Zeiss microscope.

Statistical analysis

Graphs are presented as mean ± standard deviation. A 2-tail unpaired Student's t-test (excel software 2,3) was used for statistical analysis and $p < 0.05$ considered as significant.

ACKNOWLEDGMENTS

The authors would like to acknowledge help from Andréea Milasàn with dissections of mice, genotyping and Western blots. This work was supported by grants from the Canadian Institutes of Health Research and The Polycystic Kidney Disease Foundation of Canada (to MT), and from a Frederick Banting and Charles Best of Canada Graduate Scholarship Award (to AK).

REFERENCES

(1994). "The polycystic kidney disease 1 gene encodes a 14 kb transcript and lies within a duplicated region on chromosome 16. The European Polycystic Kidney Disease Consortium." Cell **77**(6): 881-894.

(1995). "Polycystic kidney disease: the complete structure of the PKD1 gene and its protein. The International Polycystic Kidney Disease Consortium." Cell **81**(2): 289-298.

(2011). "[Clinical guidelines for the management of polycystic kidney disease]." Nihon Jinzo Gakkai Shi **53**(4): 556-578.

Castelli, M., M. Boca, M. Chiaravalli, H. Ramalingam, I. Rowe, G. Distefano, T. Carroll and A. Boletta (2013). "Polycystin-1 binds Par3/aPKC and controls convergent extension during renal tubular morphogenesis." Nat Commun **4**: 2658.

Chapin, H. C., V. Rajendran and M. J. Caplan (2010). "Polycystin-1 surface localization is stimulated by polycystin-2 and cleavage at the G protein-coupled receptor proteolytic site." Mol Biol Cell **21**(24): 4338-4348.

Cornec-Le Gall, E., M. P. Audrezet, J. M. Chen, M. Hourmant, M. P. Morin, R. Perrichot, C. Charasse, B. Whebe, E. Renaudineau, P. Jousset, M. P. Guillodo, A. Grall-Jezequel, P. Saliou, C. Ferec and Y. Le Meur (2013). "Type of PKD1 Mutation Influences Renal Outcome in ADPKD." J Am Soc Nephrol **24**(6): 1006-1013.

Fedeles, S. V., X. Tian, A. R. Gallagher, M. Mitobe, S. Nishio, S. H. Lee, Y. Cai, L. Geng, C. M. Crews and S. Somlo (2011). "A genetic interaction network of five genes for human polycystic kidney and liver diseases defines polycystin-1 as the central determinant of cyst formation." Nat Genet **43**(7): 639-647.

Foy, R. L., V. C. Chitalia, M. V. Panchenko, L. Zeng, D. Lopez, J. W. Lee, S. V. Rana, A. Boletta, F. Qian, L. Tsiokas, K. B. Piontek, G. G. Germino, M. I. Zhou and H. T. Cohen (2012). "Polycystin-1 regulates the stability and ubiquitination of transcription factor Jade-1." Hum Mol Genet.

Geng, L., Y. Segal, B. Peissel, N. Deng, Y. Pei, F. Carone, H. G. Rennke, A. M. Glucksmann-Kuis, M. C. Schneider, M. Ericsson, S. T. Reeders and J. Zhou (1996). "Identification and localization of polycystin, the PKD1 gene product." J Clin Invest **98**(12): 2674-2682.

Hopp, K., C. J. Ward, C. J. Hommerding, S. H. Nasr, H. F. Tuan, V. G. Gainullin, S. Rossetti, V. E. Torres and P. C. Harris (2012). "Functional polycystin-1 dosage governs autosomal dominant polycystic kidney disease severity." J Clin Invest **122**(11): 4257-4273.

Hughes, J., C. J. Ward, B. Peral, R. Aspinwall, K. Clark, J. L. San Millan, V. Gamble and P. C. Harris (1995). "The polycystic kidney disease 1 (PKD1) gene encodes a novel protein with multiple cell recognition domains." Nat Genet **10**(2): 151-160.

Kim, I., Y. Fu, K. Hui, G. Moeckel, W. Mai, C. Li, D. Liang, P. Zhao, J. Ma, X. Z. Chen, A. L. George, Jr., R. J. Coffey, Z. P. Feng and G. Wu (2008). "Fibrocystin/polyductin modulates renal tubular formation by regulating polycystin-2 expression and function." J Am Soc Nephrol **19**(3): 455-468.

Kurbegovic, A., O. Cote, M. Couillard, C. J. Ward, P. C. Harris and M. Trudel (2010). "Pkd1 transgenic mice: adult model of polycystic kidney disease with extrarenal and renal phenotypes." Hum Mol Genet **19**(7): 1174-1189.

Kurbegovic, A. and M. Trudel (2013). "Progressive development of polycystic kidney disease in the mouse model expressing Pkd1 extracellular domain." Hum Mol Genet **22**(12): 2361-2375.

Lanoix, J., V. D'Agati, M. Szabolcs and M. Trudel (1996). "Dysregulation of cellular proliferation and apoptosis mediates human autosomal dominant polycystic kidney disease (ADPKD)." Oncogene **13**(6): 1153-1160.

Lantinga-van Leeuwen, I. S., J. G. Dauwerse, H. J. Baelde, W. N. Leonhard, A. van de Wal, C. J. Ward, S. Verbeek, M. C. Deruiter, M. H. Breuning, E. de Heer and D. J. Peters (2004). "Lowering of Pkd1 expression is sufficient to cause polycystic kidney disease." Hum Mol Genet **13**(24): 3069-3077.

Lu, W., B. Peissel, H. Babakhanlou, A. Pavlova, L. Geng, X. Fan, C. Larson, G. Brent and J. Zhou (1997). "Perinatal lethality with kidney and pancreas defects in mice with a targetted Pkd1 mutation." Nat Genet **17**(2): 179-181.

Masyuk, A. I., B. Q. Huang, C. J. Ward, S. A. Gradilone, J. M. Banales, T. V. Masyuk, B. Radtke, P. L. Splinter and N. F. LaRusso (2010). "Biliary exosomes influence cholangiocyte regulatory mechanisms and proliferation through interaction with primary cilia." Am J Physiol Gastrointest Liver Physiol **299**(4): G990-999.

Mochizuki, T., G. Wu, T. Hayashi, S. L. Xenophontos, B. Veldhuisen, J. J. Saris, D. M. Reynolds, Y. Cai, P. A. Gabow, A. Pierides, W. J. Kimberling, M. H. Breuning, C. C. Deltas, D. J. Peters and S. Somlo (1996). "PKD2, a gene for polycystic kidney disease that encodes an integral membrane protein." Science **272**(5266): 1339-1342.

Natoli, T. A., T. C. Gareski, W. R. Dackowski, L. Smith, N. O. Bukanov, R. J. Russo, H. Husson, D. Matthews, P. Piepenhagen and O. Ibraghimov-Beskrovnaya (2008). "Pkd1 and Nek8 mutations affect cell-cell adhesion and cilia in cysts formed in kidney organ cultures." Am J Physiol Renal Physiol **294**(1): F73-83.

Oppenheimer, E. H. and J. R. Esterly (1975). "Pathology of cystic fibrosis review of the literature and comparison with 146 autopsied cases." Perspect Pediatr Pathol **2**: 241-278.

Pennekamp, P., C. Karcher, A. Fischer, A. Schweickert, B. Skryabin, J. Horst, M. Blum and B. Dworniczak (2002). "The ion channel polycystin-2 is required for left-right axis determination in mice." Curr Biol **12**(11): 938-943.

Pritchard, L., J. A. Sloane-Stanley, J. A. Sharpe, R. Aspinwall, W. Lu, V. Buckle, L. Strmecki, D. Walker, C. J. Ward, C. E. Alpers, J. Zhou, W. G. Wood and P. C. Harris (2000). "A human PKD1 transgene generates functional polycystin-1 in mice and is associated with a cystic phenotype." Hum Mol Genet **9**(18): 2617-2627.

Rossetti, S., S. Burton, L. Strmecki, G. R. Pond, J. L. San Millan, K. Zerres, T. M. Barratt, S. Ozen, V. E. Torres, E. J. Bergstralh, C. G. Winearls and P. C. Harris (2002). "The position of the polycystic kidney disease 1 (PKD1) gene mutation correlates with the severity of renal disease." J Am Soc Nephrol **13**(5): 1230-1237.

Rossetti, S., D. Chauveau, V. Kubly, J. M. Slezak, A. K. Saggar-Malik, Y. Pei, A. C. Ong, F. Stewart, M. L. Watson, E. J. Bergstralh, C. G. Winearls, V. E. Torres and P. C. Harris (2003). "Association of mutation position in polycystic kidney disease 1 (PKD1) gene and development of a vascular phenotype." Lancet **361**(9376): 2196-2201.

Thivierge, C., A. Kurbegovic, M. Couillard, R. Guillaume, O. Cote and M. Trudel (2006). "Overexpression of PKD1 causes polycystic kidney disease." Mol Cell Biol **26**(4): 1538-1548.

Tokhunts, R., S. Singh, T. Chu, G. D'Angelo, V. Baubet, J. A. Goetz, Z. Huang, Z. Yuan, M. Ascano, Y. Zavros, P. P. Therond, S. Kunes, N. Dahmane and D. J. Robbins (2010). "The full-length unprocessed hedgehog protein is an active signaling molecule." J Biol Chem **285**(4): 2562-2568.

Wang, E., H. M. Hsieh-Li, Y. Y. Chiou, Y. L. Chien, H. H. Ho, H. J. Chin, C. K. Wang, S. C. Liang and S. T. Jiang (2010). "Progressive renal distortion by multiple cysts in transgenic mice expressing artificial microRNAs against Pkd1." J Pathol **222**(3): 238-248.

Ward, C. J., H. Turley, A. C. Ong, M. Comley, S. Biddolph, R. Chetty, P. J. Ratcliffe, K. Gattner and P. C. Harris (1996). "Polycystin, the polycystic kidney disease 1 protein, is expressed by epithelial cells in fetal, adult, and polycystic kidney." Proc Natl Acad Sci U S A **93**(4): 1524-1528.

Weston, B. S., S. Jeffery, I. Jeffrey, S. F. Sharaf, N. Carter, A. Saggar-Malik and R. G. Price (1997). "Polycystin expression during embryonic development of human kidney in adult tissues and ADPKD tissue." Histochem J **29**(11-12): 847-856.

Woodward, O. M., Y. Li, S. Yu, P. Greenwell, C. Wodarczyk, A. Boletta, W. B. Guggino and F. Qian (2010). "Identification of a polycystin-1 cleavage product, P100, that regulates store operated Ca entry through interactions with STIM1." PLoS One **5**(8): e12305.

Wu, G., G. S. Markowitz, L. Li, V. D. D'Agati, S. M. Factor, L. Geng, S. Tibara, J. Tuchman, Y. Cai, J. H. Park, J. van Adelsberg, H. Hou, Jr., R. Kucherlapati, W. Edelmann and S. Somlo (2000). "Cardiac defects and renal failure in mice with targeted mutations in Pkd2." Nat Genet **24**(1): 75-78.

Wu, G., X. Tian, S. Nishimura, G. S. Markowitz, V. D'Agati, J. H. Park, L. Yao, L. Li, L. Geng, H. Zhao, W. Edelmann and S. Somlo (2002). "Trans-heterozygous Pkd1 and Pkd2 mutations modify expression of polycystic kidney disease." Hum Mol Genet **11**(16): 1845-1854.

Yang, B., N. D. Sonawane, D. Zhao, S. Somlo and A. S. Verkman (2008). "Small-molecule CFTR inhibitors slow cyst growth in polycystic kidney disease." J Am Soc Nephrol **19**(7): 1300-1310.

Yu, S., K. Hackmann, J. Gao, X. He, K. Piontek, M. A. Garcia-Gonzalez, L. F. Menezes, H. Xu, G. G. Germino, J. Zuo and F. Qian (2007). "Essential role of cleavage of Polycystin-1 at G protein-coupled receptor proteolytic site for kidney tubular structure." Proc Natl Acad Sci U S A **104**(47): 18688-18693.

FIGURE LEGENDS

Figure 1. Expression analysis of Polycystin-1 in *Pkd1* transgenic kidneys at birth.

Western blots of total kidney extract at birth (P0) from *$Pkd1^{Null}$* **(A)**, *$Pkd1_{TAG}$* **(B)** and *$SBPkd1_{TAG}$* **(C)** lines. While the *$Pkd1^{Null}$* kidneys do not show detectable levels of Pc1, at birth all transgenic lines here within express more Pc1 than wild-type kidneys. Gapdh or Tubulin were used as loading controls. Quantification of Pc1 was normalized to the loading wild-type control using Image Quant. Fold: fold induction *vs* control wild-type age-matched kidneys. Tg: transgene. *Pkd1*: endogenous *Pkd1*. ''-'': absent; #18 and 26: *$Pkd1_{TAG}$* transgenic lines; #3 and 41: *$SBPkd1_{TAG}$* transgenic lines.

Figure 2. ***Pkd1* RNA expression in the kidneys of different transgenic compounds at birth.**

Quantitative analysis of Pkd1 expression by Q-PCR **(A)** *$Pkd1_{TAG}$* and **(B)** *$SBPkd1_{TAG}$* lines on *$Pkd1^{-/-}$* genetic background using two sets of primers at each end of *Pkd1* transcript. When compared to the endogenous wild-type *Pkd1*, *$Pkd1^{-/-}$;$Pkd1_{TAG}$* 18 and 26 compounds showed ~8-20-fold and *$Pkd1^{-/-}$;$SBPkd1_{TAG}$* 3 and 41 ~1.5-15fold increase, respectively. For the high copies lines, *$Pkd1^{-/-}$; $Pkd1_{TAG}$ 26* and *$Pkd1^{-/-}$;$SBPkd1_{TAG}$* 41, the 3' end expression was slightly increased when compared to the 5' end which suggest possible presence of additional transcripts at the 3'end of the Pkd1 locus. *Pkd1* expression levels were normalized to endogenous S16 transcript and wild-type was set as calibrator 1. 5: primers in *Pkd1* exons 1 and 2; 3: primers in *Pkd1* exons 39 and 40.

Figure 3. Kidney morphometrics at PO, P5, P10 and P30

(A) KBW of both *$Pkd1^{-/-}$;$Pkd1_{TAG}$* 18 and 26 compounds is significantly different from *$Pkd1^{-/-}$* and analogous to the wild-type kidneys at P0, P10 and P30.
(B) KBW in both *$Pkd1^{-/-}$;$SBPkd1_{TAG}$* 3 and 41 is significantly different from *$Pkd1^{-/-}$* at P0. At P5, the lower transgene copy *$SBPkd1_{TAG}$* 3 line has tendency to have

enlarged kidneys, although it did not reach significance until P10. For the high copy line *SBPkd1$_{TAG}$* 41 KBW is very similar to controls at least until P10. At P30 however, the kidneys are almost double of the normal size and reached statictical significance when compared to the wild-type kidneys of the same age. n: number of mice analyzed; ''#''; when compound significatively different *vs Pkd1$^{-/-}$*; ''&'': when compound significatif different *vs Pkd1$^{+/+}$* at the corresponding age. The data was considered as significatively different when p value <0.05 using Student T test by Excell software (2;3) where 2 genotypes were compared among each other.

Figure 4. Renal and extrarenal manifestations in *Pkd1$^{-/-}$; Pkd1$_{extra}$ 39* compound at birth

(A) Western blots of total kidney extract at birth (P0) from *Pkd1$_{extra}$ 39* 2-copy transgenic line showed stabilized *Pc1$_{extra}$* truncated protein. Gapdh was used as loading control. Tg: transgene. *Pkd1*: endogenous *Pkd1*. ''-'': absent.

(B) Quantitative analysis of Pkd1 expression by Q-PCR on *Pkd1$^{-/-}$* genetic background using two sets of primers at each end of *Pkd1* transcript. Using 5' end primers, *Pkd1$^{-/-}$;Pkd1$_{extra}$39* compound showed ~2fold higher expression when compared to the wild-type *Pkd1$^{+/+}$* kidneys whereas 3' primers showed similar expression to *Pkd1^{Null}* consistent with absence of 3' end in *Pkd1$_{extra}$* transgene.

(C) Ratio of the kidney weight to body weight (KBW) in percentage of *Pkd1$^{-/-}$;Pkd1$_{extra}$ 39* is analogous to the the *Pkd1$^{-/-}$* (*left graph*) correlating with the very similar cyst % coverage at P0 (*righ graph*) for both genotypes.

(D) At P0, the kidneys and pancreas of *Pkd1$^{-/-}$;Pkd1$_{extra}$ 39* are overtly cystic and very similar to the typical phenotype of *Pkd1$^{-/-}$* mice. Images are representative of ''n'', n being the number of mice analyzed. H&E staining. Magnification, 10X. Scale bar, 100μm.

(E) Unlike *Pkd1$^{+/+}$* and *Pkd1$^{-/-}$;Pkd1$_{TAG}$ 26*, the *Pkd1$^{-/-}$;Pkd1$_{extra}$ 39* compound does not show detectable levels of Endo H resistant form of Pc1. N: non-treated; P: PNGase treated; E: EndoH treated. Actin was used as loading control.

Figure 5. Complete rescue of renal and extrarenal histology in *Pkd1$^{-/-}$; Pkd1$_{TAG}$* compound

(A) Similar to previously published observations in *Pkd1$_{TAG}$18* transgenic line, the *Pkd1$^{-/-}$; Pkd1$_{TAG}$18* compound also shows no obvious anomalies until at least 7-8 months, the latest time-point analyzed.
(B) The *Pkd1$^{-/-}$; Pkd1$_{TAG}$26* shows grossly normal renal and extrarenal histology at P0, P10 and P30 and is very similar to *Pkd1$_{TAG}$26* at the coresponding age. Images are representative of ''n'', n being the number of mice analyzed. H&E staining. Magnification, 20X. Scale bar, 100um.

Figure 6. Progression of adult renal and extrarenal phenotype in high copy *Pkd1$^{-/-}$; Pkd1$_{TAG}$26* compound

Analysis of kidney histology at different ages from 2 to 16months showed normal kidneys at early adulthood with kidney cystogenesis occuring adulthood, albeit later than in *Pkd1$_{TAG}$26* transgenic line. Kidney cysts that occured earlier were associated with homozygocity of the *Pkd1$_{TAG}$* transgene in *Pkd1$^{+/-}$;Pkd1$_{TAG}$26* mice and presumably for *Pkd1$^{-/-}$; Pkd1$_{TAG}$26*. Overt liver phenotype notably liver cysts were absent at all points. Occasionaly, pancreas manifested an adipose-like morphology. See text for further details. H&E staining. Magnification, 20X. Scale bar, 100μm.

Figure 7. Incomplete rescue of *Pkd1$^{-/-}$* kidney cystogenesis by *SBPkd1$_{TAG}$* transgenes

***(A)* a)** Already at birth, the low copy renal-specific *Pkd1$^{-/-}$;SBPkd1$_{TAG}$3* compound presents microscopic kidney cysts but no pancreatic cysts or liver anomalies. Pancreatic cysts are visible at P5 where kidney cysts become even macroscopically detectable. At P10 both pancreatic and kidney cysts seem bigger in size with almost no normal surrounding parenchyma that seems replaced by fibrotic/mesenchymal-like tissue. Liver anomalies are never observed until P10, the latest point analyzed. Magnification, 20X. Bar scale: 100μm.

b) At P10, staining with Sirius Red and by immunofluorescence using antibody against smooth muscle actin shows increased signal surrounding the cysts in the pancreas. Multiple nuclei of the cystic epithelia were positive for Ki67, marker for proliferating cells. Representative images for ''n'' number of mice analyzed. H&E staining. Magnification, 20X for all but 2 images at the bottom (Magnification, 40X). Bar scale: 100μm.

(B) From P0 to P10, the high copy renal-specific *Pkd1$^{-/-}$;SBPkd1$_{TAG}$41* compound shows some tubular dilatations and smaller cysts. This tubular phenotype does not seem to progress enormously untill P10. From P10 to P30, kidneys become very cystic and presents also in some cases important hydroneprosis (asterisk). Hepatic or pancreatic cystic phenotypes are not observed. Of note, infiltrations (§), fibrotic (arrows) and adipose-like regions (arrowhead) are observed at some extent in the liver and pancreas, respectively. H&E staining. Magnification, 20X for all images except the hydronephrosis at P30 (5X) and renal and extrarenal histology of 3-4 month-old mice (10X). Bar scale, 100μm.

Figure 8. Fully penetrant hepatic phenotype in the *Pkd1$^{V/V}$;Pkd1* transgenic mice

(A) The GPS cleavage-defective *Pkd1$^{V/V}$* mutant allele leads to dilatations at P10 and evident liver cysts at P30, the endpoint for this mouse model. The *Pkd1$_{extra}$39* transgene that recapitulates Pc1 NTF cleaved product is unable to not rescue the *Pkd1$^{V/V}$* liver phenotype.

(B) At P30, the high copy kidney-specific *Pkd1$^{V/V}$;SBPkd1$_{TAG}$41* compound also presents anomalies *i.e.,* important dilatations spread in a branched-tree pattern which become increased in size, completely invasive at ~3months of age.

(C) The high-copy systemic *Pkd1$^{V/V}$;Pkd1$_{TAG}$26* compound rescues significantly the *Pkd1$^{V/V}$* liver phenotype at P10 and P30. In contrast to the *Pkd1$^{-/-}$; Pkd1$_{TAG}$26* compound (Fig.7), at P30 few small cystic clustered-like structures around biliary ducts can be already observed in *Pkd1$^{V/V}$;Pkd1$_{TAG}$26*, at 4months become obvious and 7 months completely penetrant in females. Cystic clusters seem smaller and less

numerous in *Pkd1$^{V/V}$;Pkd1$_{TAG}$26* males, but at the later point become as invasive as in females. n, number of mice analyzed. F: female; M: male. H&E staining. Magnification, 5X. Scale bar, 100 μm.

Figure 9. Expression analysis of Pc1 in *Pkd1* transgenic compounds on *Pkd1$^{-/-}$* and *Pkd1$^{V/V}$* genetic backgrounds

Western blots using 7e12 highly specific mouse monoclonal against Pc1 on total protein extracts from kidney, liver and pancreas.

(A) In the kidney at P0, expression of Pc1 is either very similar or significantly increased in low- and high-copy *SBPkd1$_{TAG}$* and *Pkd1$_{TAG}$* transgenes on the *Pkd1$^{-/-}$* genetic background.

(B,C) In the pancreas and liver at P0, the low kidney-specific *Pkd1$^{-/-}$; SBPkd1$_{TAG}$3* compound lacks detectable Pc1 expression. Two systemic *Pkd1$_{TAG}$* lines (18 and 26) provide increased Pc1 expression in these two extrarenal tissues of *Pkd1$^{-/-}$* mice. Pc1 expression of similar amplitude to the wild-type tissues was also detected in kidney-specific high copy *Pkd1$^{-/-}$;SBPkd1$_{TAG}$41*.

(D) Comparison of expression pattern of Pc1 in the kidney, liver and pancreas at birth in *Pkd1$^{-/-}$; Pkd1$_{TAG}$18* binary mice to Pc1 in wild-type kidneys. Simialr to Pc1, regulation of β-Tubulin expression also seems to be tissue-dependent at this stage.

(E-F) Expression of Pc1 in the kidney **(E)** and liver **(F)** of high-copy renal overexpressor *Pkd1$^{-/-}$;SBPkd1$_{TAG}$41* compound at P0, P10 and P30. The elevated kidney expression is sustained throughout all ages tested, and this increase seems to follow endogenous Pc1 pattern, with highest levels at birth and lower in adulthood. When compared to the kidneys at any point, the liver shows lower expression levels but similarly to kidneys, these levels decrease also with age. Of note, in the liver *Pkd1$^{-/-}$; SBPkd1$_{TAG}$ 41* express low but somewhat comparable levels to the wild-type liver (n=1).

(G) Similar to the results of Pc1 expression in the liver on *Pkd1$^{-/-}$* background **(F)**, the SBPkd1$_{TAG}$ 41 transgene appears to lead to comparable overall Pc1 levels in the liver on *Pkd1$^{V/V}$* background. The *Pkd1$_{TAG}$26* transgene provides also abundant hepatic

Pc1 expression in *Pkd1*$^{V/V}$ mutant. For all blots, Gapdh, β–Actin or β-Tubulin were used as loading controls. If not directly in the figure, the age and tissue details are specified under the blot. If not stated otherwise, the same quantity of protein extract was loaded on the gel.

Supplementary Figure 1. Schematic representation of previously described mouse models used in this study.

Pkd1$_{TAG}$ and *SBPkd1*$_{TAG}$ are two transgenic systemic or kidney specific expressors respectively of murin full-lenght genomic *Pkd1*. *Pkd1*$_{extra}$ is a transgenic expressor of murine *Pkd1* N-terminal extracelluar domain that mimics a human non-sense mutation (F3043X) in the GPS domain. *Pkd1*$^{V/V}$ is a knock-in allele in the critical residu (HLT3041V) that completely abrogates the Pc1 cleavage in the GPS site. SB: Regulatory elements composed of enhancer SV40 and β-globin promoter.

Fig1.

A.

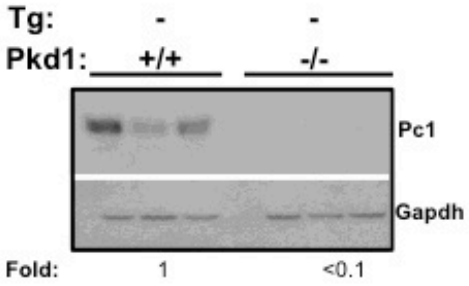
Tg: - -
Pkd1: +/+ -/-
Pc1
Gapdh
Fold: 1 <0.1

B.

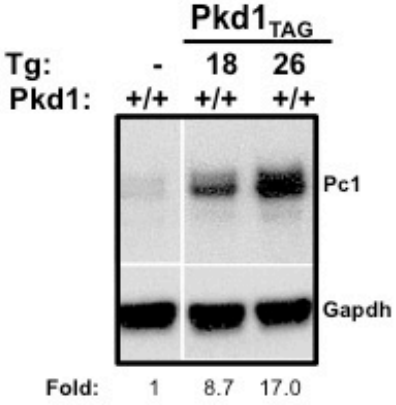
Pkd1TAG
Tg: - 18 26
Pkd1: +/+ +/+ +/+
Pc1
Gapdh
Fold: 1 8.7 17.0

C.

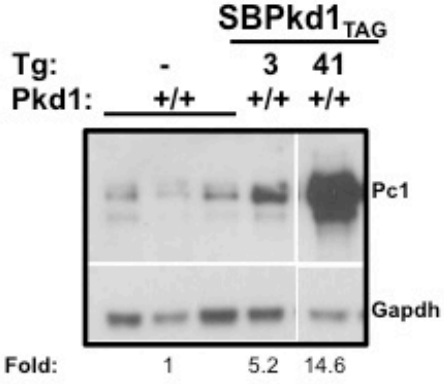
SBPkd1TAG
Tg: - 3 41
Pkd1: +/+ +/+ +/+
Pc1
Gapdh
Fold: 1 5.2 14.6

Fig2.

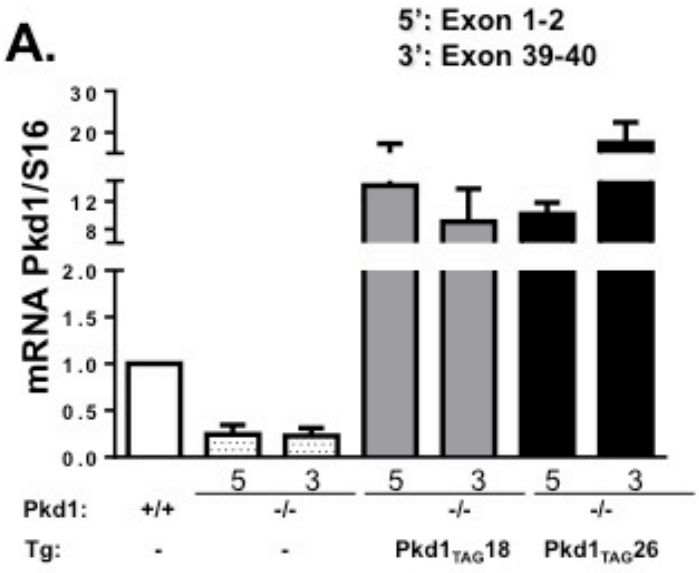
A.
5': Exon 1-2
3': Exon 39-40
mRNA Pkd1/S16
30
20
12
8
2.0
1.5
1.0
0.5
0.0
5
3
5
3
5
3
Pkd1:
+/+
-/-
-/-
-/-
Tg:
-
-
Pkd1TAG18
Pkd1TAG26

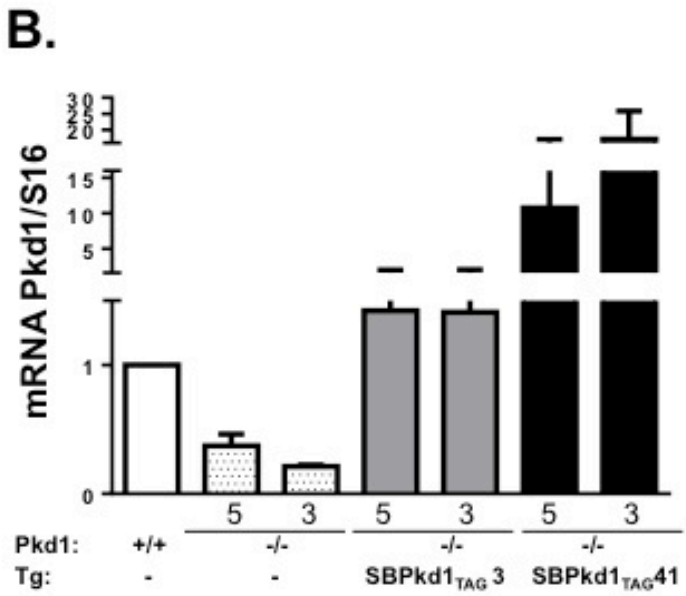
B.
mRNA Pkd1/S16
30
20
15
10
5
1
0
5
3
5
3
5
3
Pkd1:
+/+
-/-
-/-
-/-
Tg:
-
-
SBPkd1TAG3
SBPkd1TAG41

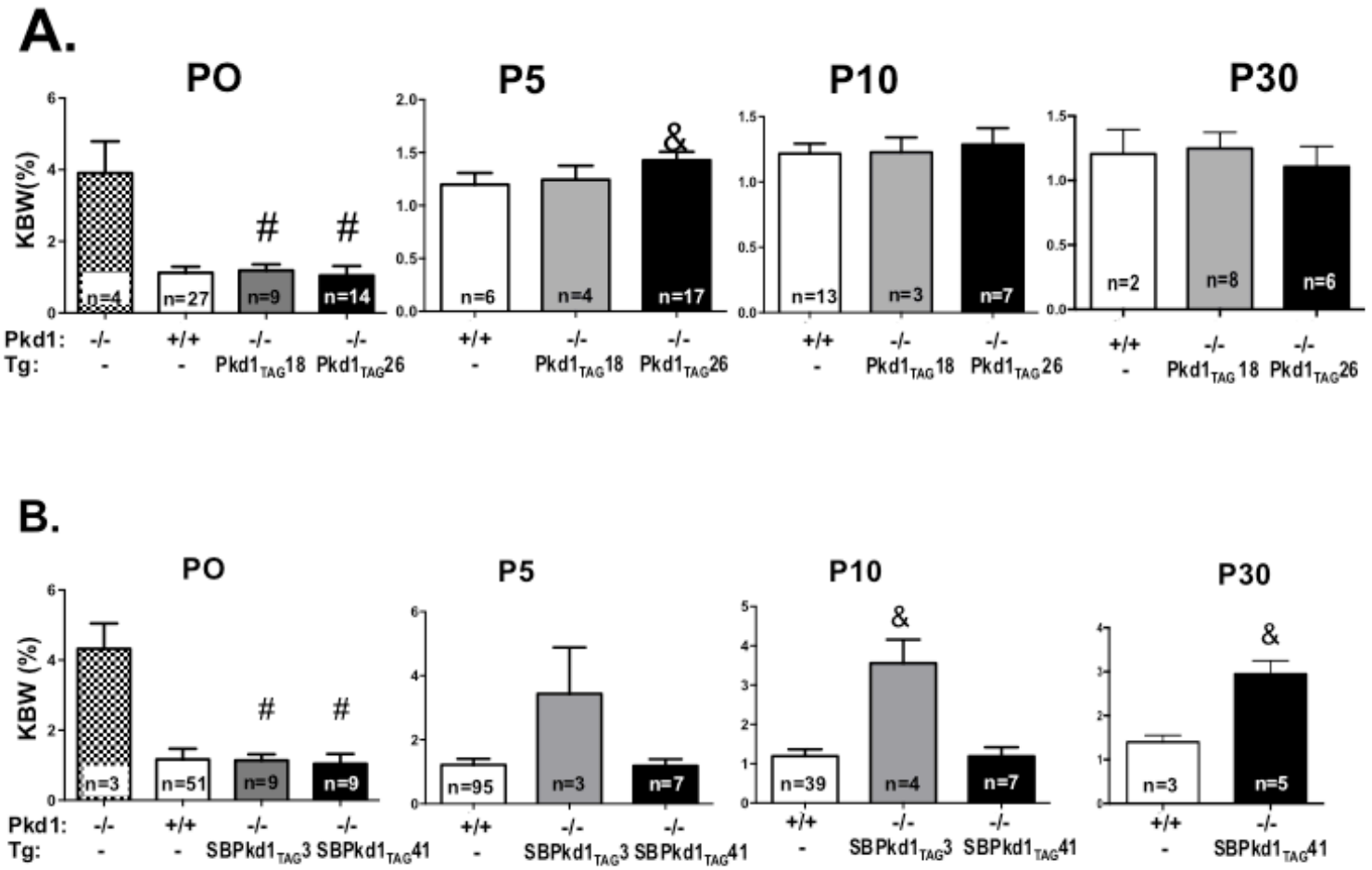
A.
PO
P5
P10
P30
KBW(%)
n=4
n=27
n=9
n=14
n=6
n=4
n=17
n=13
n=3
n=7
n=2
n=8
n=6
#
#
&
Pkd1: -/- +/+ -/- -/- +/+ -/- -/- +/+ -/- -/- +/+ -/- -/-
Tg: - - Pkd1TAG18 Pkd1TAG26 - Pkd1TAG18 Pkd1TAG26 - Pkd1TAG18 Pkd1TAG26 - Pkd1TAG18 Pkd1TAG26
B.
PO
P5
P10
P30
KBW (%)
n=3
n=51
n=9
n=9
n=95
n=3
n=7
n=39
n=4
n=7
n=3
n=5
#
#
&
&
Pkd1: -/- +/+ -/- -/- +/+ -/- -/- +/+ -/- -/- +/+ -/- -/-
Tg: - - SBPkd1TAG3 SBPkd1TAG41 - SBPkd1TAG3 SBPkd1TAG41 - SBPkd1TAG3 SBPkd1TAG41 - SBPkd1TAG41

Fig3.

Fig4.

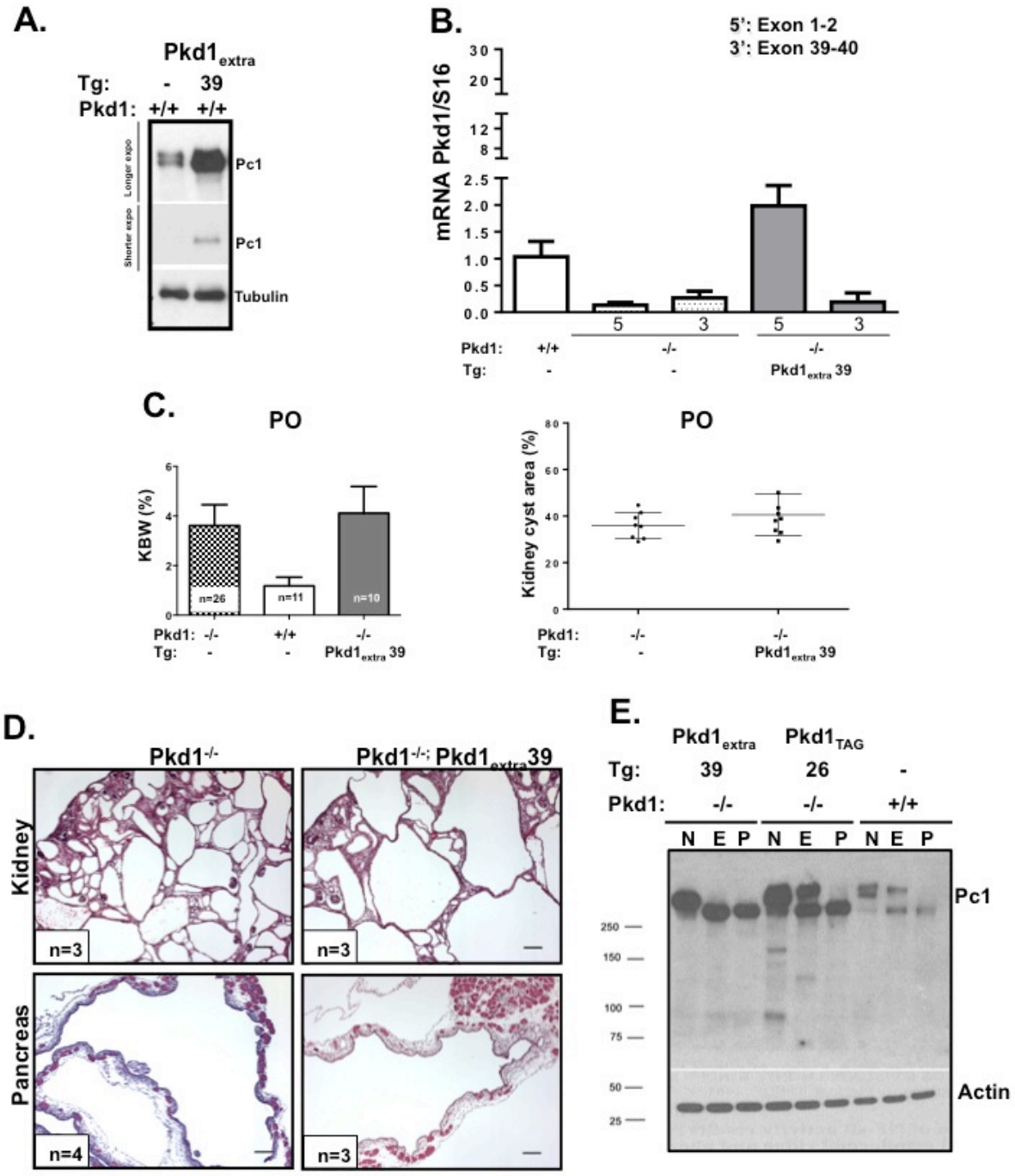
A.
Pkd1extra
Tg: - 39
Pkd1: +/+ +/+
Longer expo
Shorter expo
Pc1
Pc1
Tubulin
B.
5': Exon 1-2
3': Exon 39-40
mRNA Pkd1/S16
30
20
12
8
2.5
2.0
1.5
1.0
0.5
0.0
5
3
5
3
Pkd1: +/+ -/- -/-
Tg: - - Pkd1extra 39
C.
PO
KBW (%)
6
4
2
0
n=26
n=11
n=10
Pkd1: -/- +/+ -/-
Tg: - - Pkd1extra 39
PO
Kidney cyst area (%)
80
60
40
20
0
Pkd1: -/- -/-
Tg: - Pkd1extra 39
D.
Pkd1-/-
Pkd1-/-; Pkd1extra39
Kidney
Pancreas
n=3
n=3
n=4
n=3
E.
Pkd1extra Pkd1TAG
Tg: 39 26 -
Pkd1: -/- -/- +/+
N E P N E P N E P
250
150
100
75
50
25
Pc1
Actin

Fig5A.

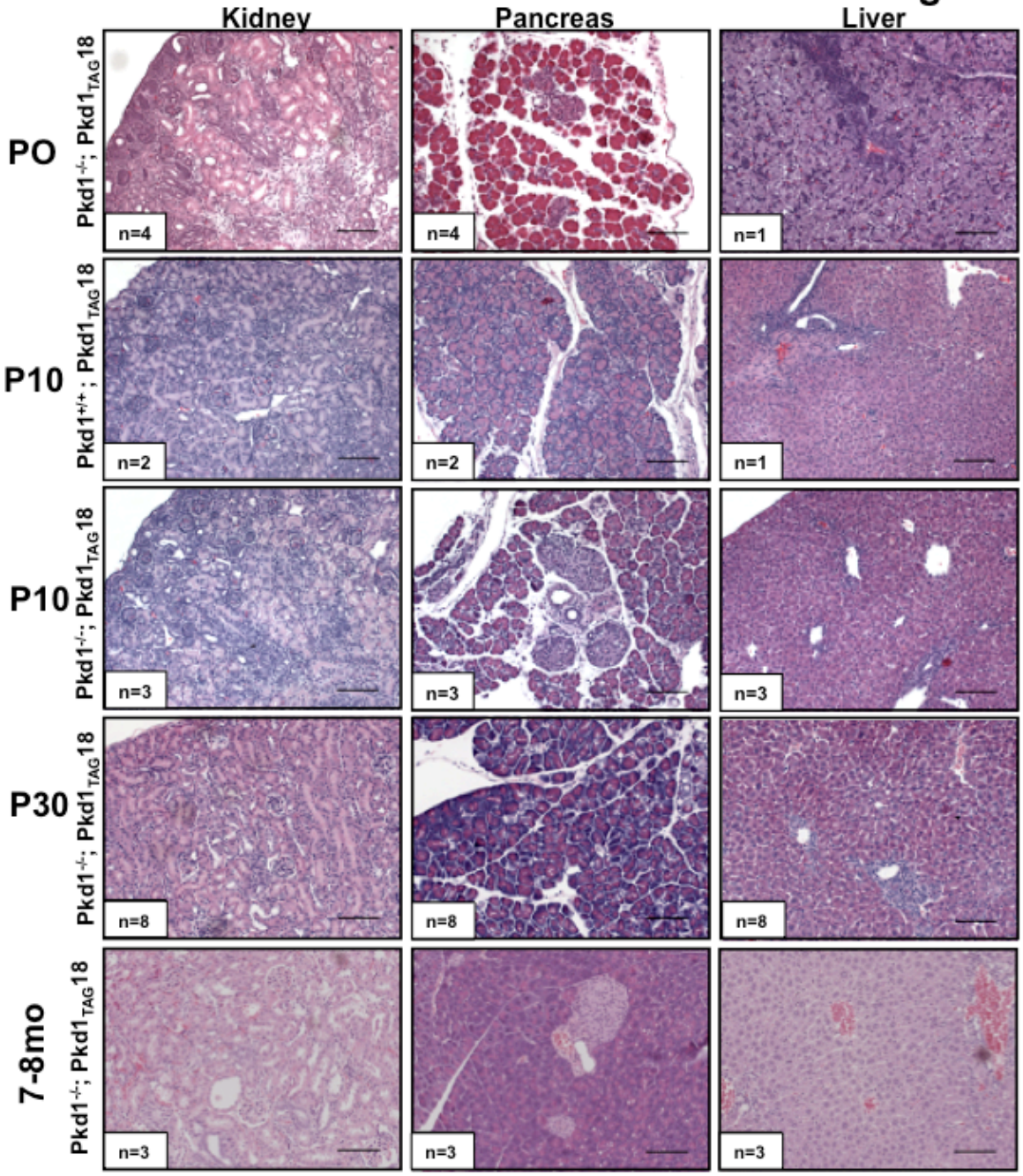
Kidney
Pancreas
Liver
P0
P10
P10
P30
7-8mo
Pkd1-/-; Pkd1TAG18
Pkd1+/+; Pkd1TAG18
Pkd1-/-; Pkd1TAG18
Pkd1-/-; Pkd1TAG18
Pkd1-/-; Pkd1TAG18
n=4
n=4
n=1
n=2
n=2
n=1
n=3
n=3
n=3
n=8
n=8
n=8
n=3
n=3
n=3

Fig5B.

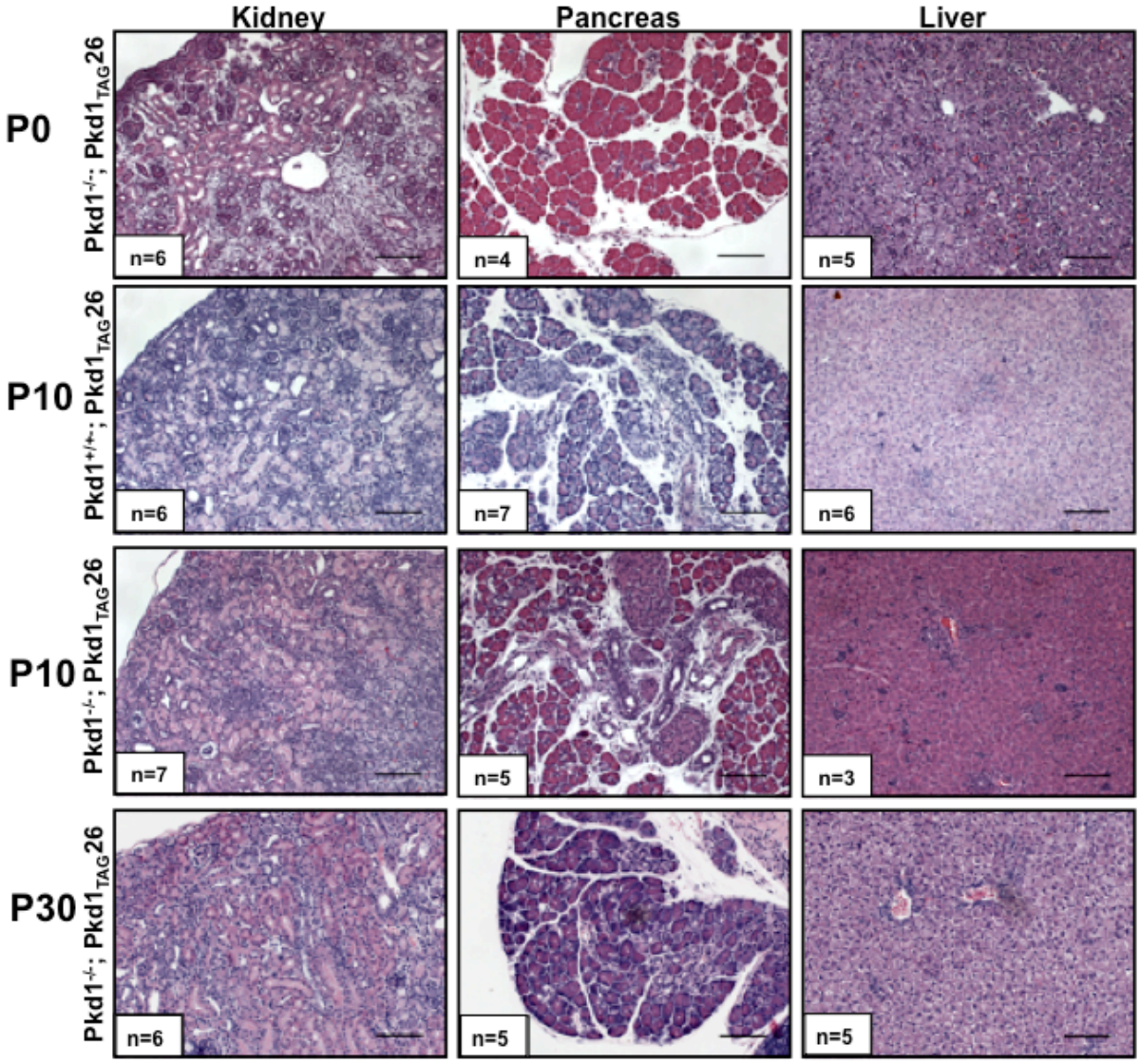
Kidney
Pancreas
Liver
P0
Pkd1-/-; Pkd1TAG26
n=6
n=4
n=5
P10
Pkd1+/+; Pkd1TAG26
n=6
n=7
n=6
P10
Pkd1-/-; Pkd1TAG26
n=7
n=5
n=3
P30
Pkd1-/-; Pkd1TAG26
n=6
n=5
n=5

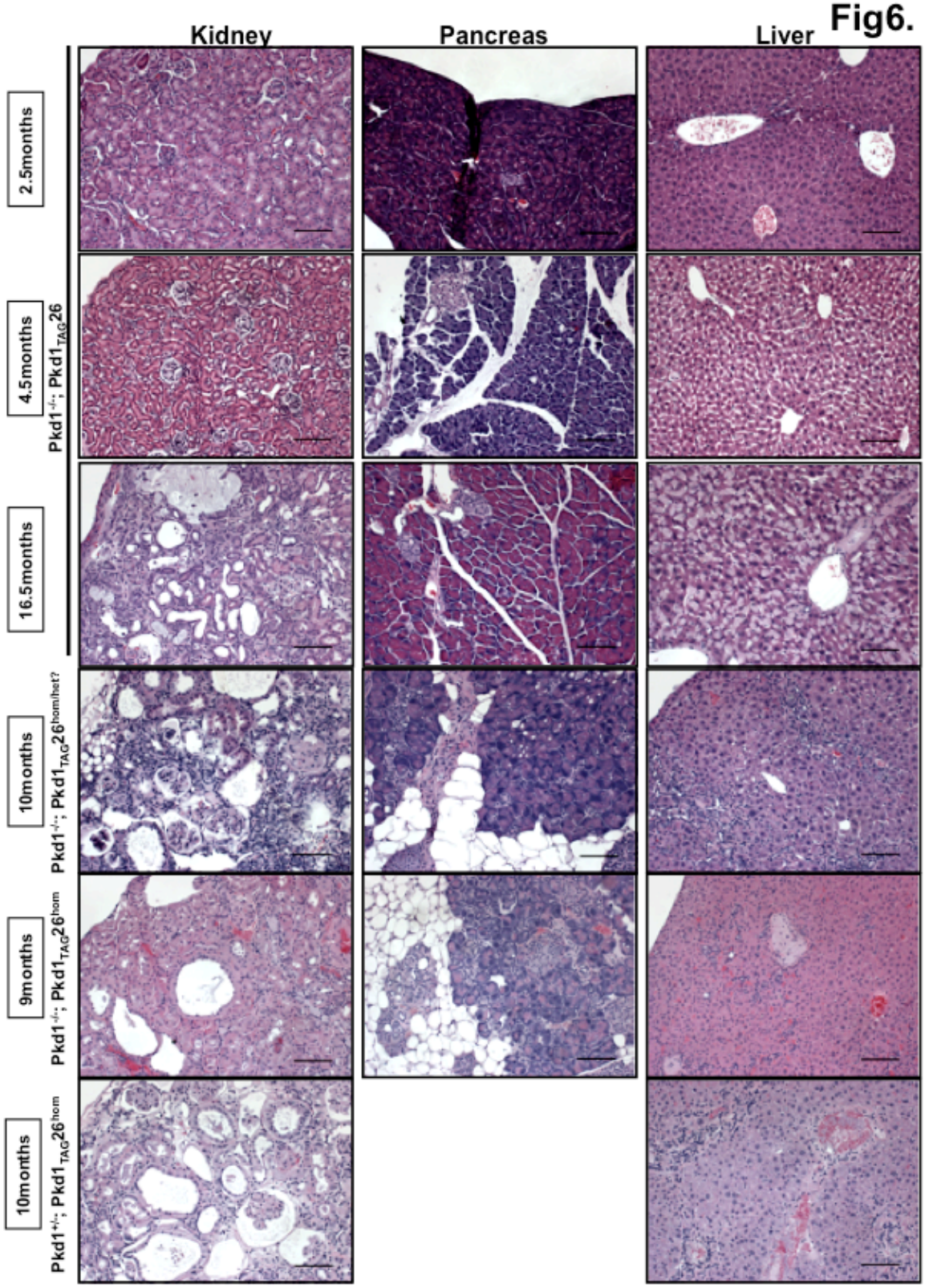
Fig6.
Kidney
Pancreas
Liver
2.5months
4.5months
16.5months
10months
9months
10months
Pkd1+/-; Pkd1TAG26hom
Pkd1-/-; Pkd1TAG26hom
Pkd1-/-; Pkd1TAG26hom/het?
Pkd1-/-; Pkd1TAG26

Fig7A.

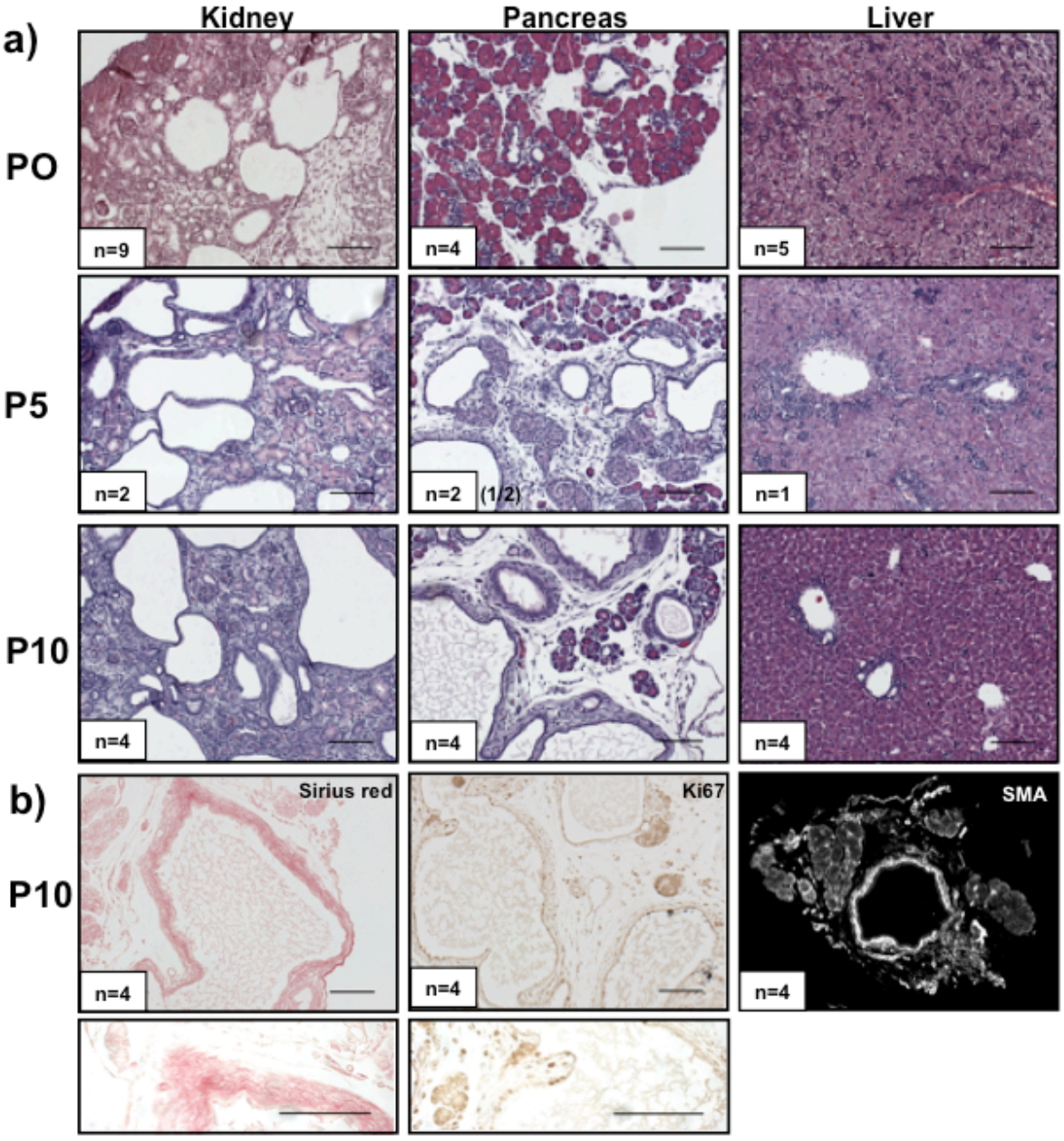
a)
Kidney
Pancreas
Liver
PO
P5
P10
n=9
n=4
n=5
n=2
n=2 (1/2)
n=1
n=4
n=4
n=4
b)
P10
Sirius red
Ki67
SMA
n=4
n=4
n=4

Fig7B.

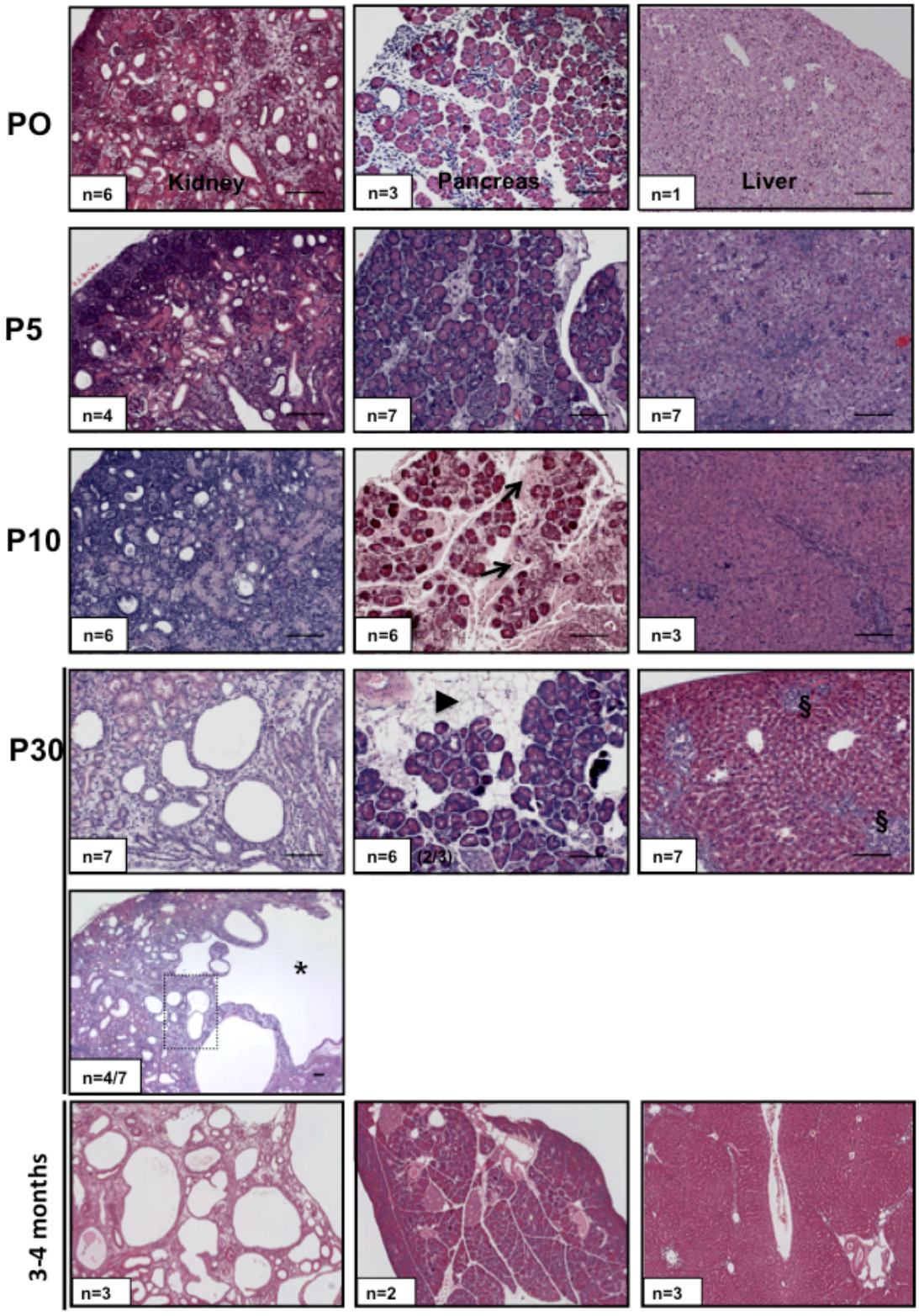
PO
P5
P10
P30
3-4 months
Kidney
Pancreas
Liver
n=6
n=3
n=1
n=4
n=7
n=7
n=6
n=6
n=3
n=7
n=6 (2/3)
n=7
n=4/7
n=3
n=2
n=3
§
§
*

Fig8.

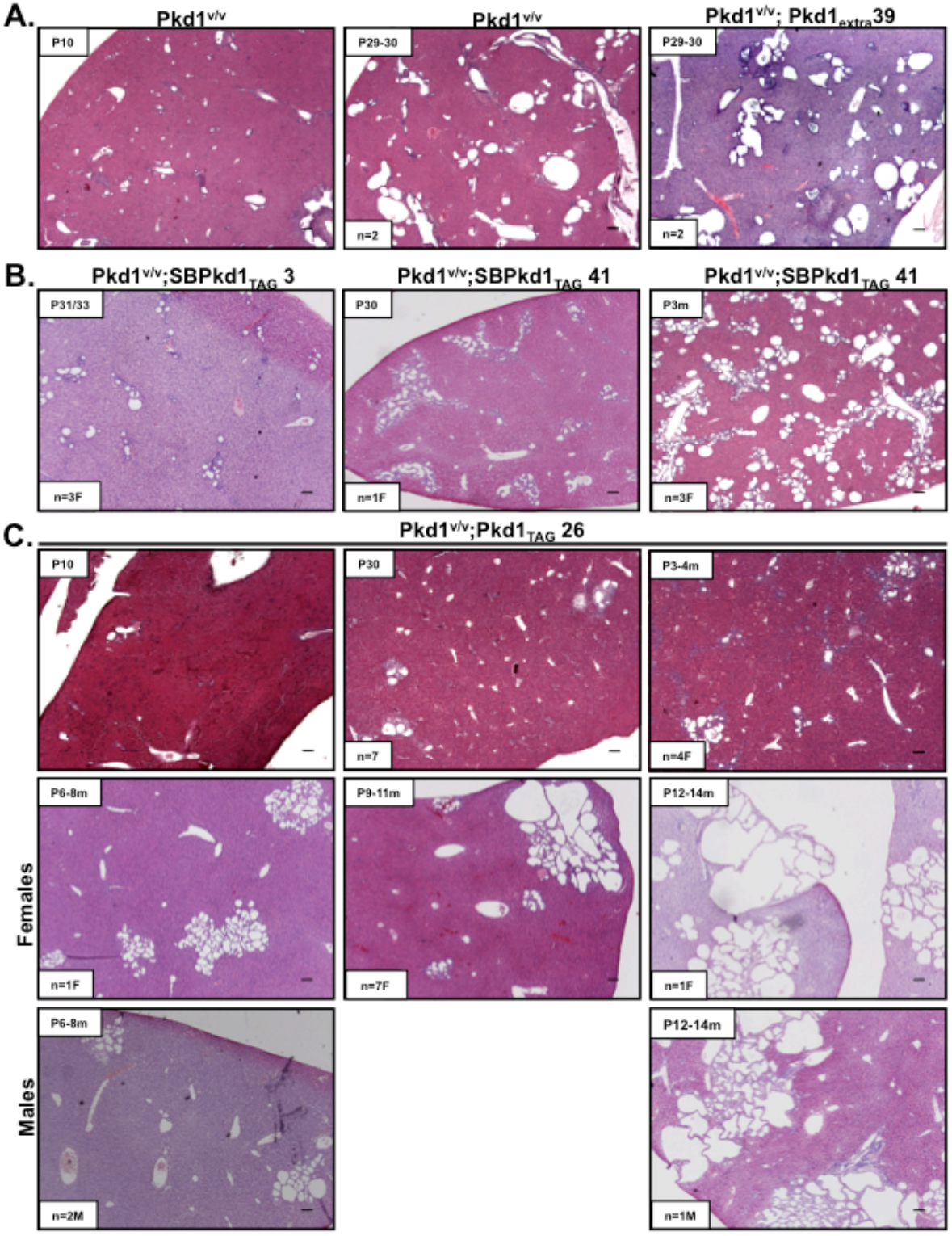
A.
Pkd1v/v
P10
Pkd1v/v
P29-30
n=2
Pkd1v/v; Pkd1extra39
P29-30
n=2
B.
Pkd1v/v;SBPkd1TAG 3
P31/33
n=3F
Pkd1v/v;SBPkd1TAG 41
P30
n=1F
Pkd1v/v;SBPkd1TAG 41
P3m
n=3F
C.
Pkd1v/v;Pkd1TAG 26
P10
P30
n=7
P3-4m
n=4F
Females
P6-8m
n=1F
P9-11m
n=7F
P12-14m
n=1F
Males
P6-8m
n=2M
P12-14m
n=1M

Fig9.

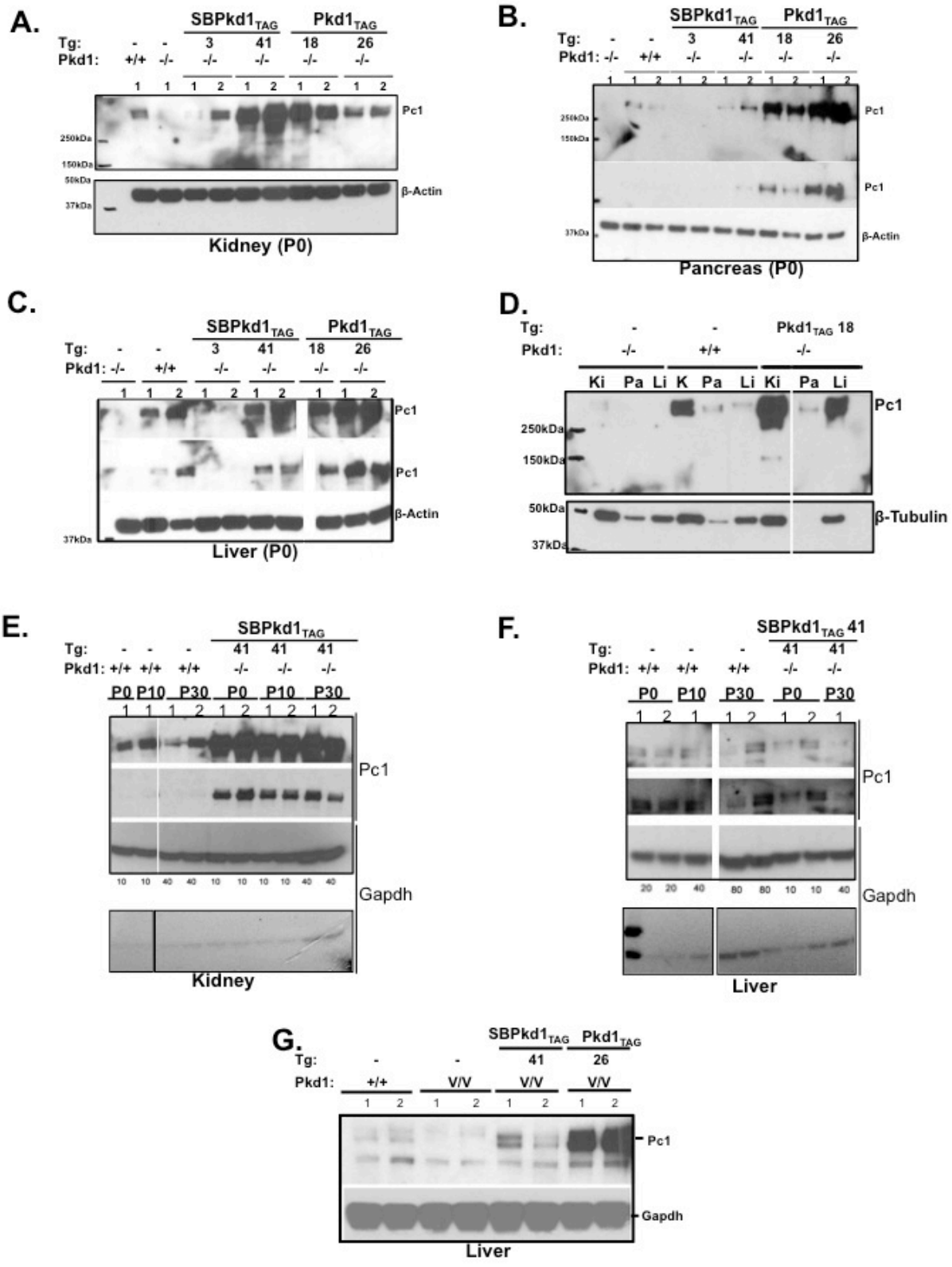
A.
SBPkd1TAG
Pkd1TAG
Tg:
Pkd1:
Pc1
β-Actin
Kidney (P0)
B.
Pancreas (P0)
C.
Liver (P0)
D.
Ki Pa Li K Pa Li Ki Pa Li
β-Tubulin
E.
P0 P10 P30 P0 P10 P30
Gapdh
Kidney
F.
Liver
G.
V/V

Supp Fig1.

Pkd1$_{TAG}$

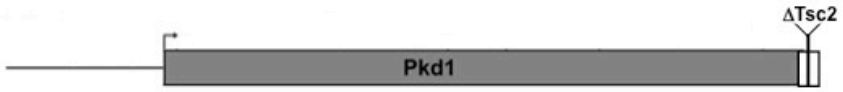

SBPkd1$_{TAG}$

Pkd1$_{extra}$

Pkd1$^{V/V}$

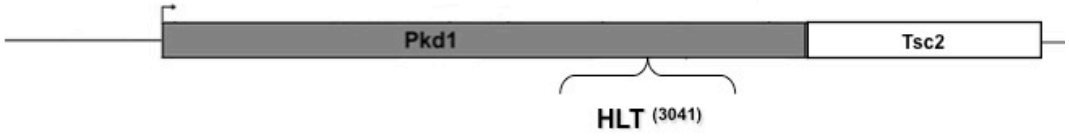

LIST OF ABBREVIATIONS

LOF: Loss of function

ADPKD: autosomal dominant polycystic kidney disease

PKD: polycystic kidney disease

Pc1: murine polycystin-1

GPS: GPCR proteolysis site

NTF: N-terminal fragment

CTF: C-terminal fragment

CHAPTER IX - DISCUSSION AND PERSPECTIVES

Our first article (**Chapter IV**) focused on the discrepancy among proposed ADPKD pathogenetic mechanisms that could have critical implications for the development of safe and efficient therapeutic approaches. We demonstrated that increased expression of *Pkd1*/Pc1 in BAC transgenic $Pkd1_{TAG}$ mice was sufficient to induce kidney cystogenesis *in vivo* but also many other important life-threatening extrarenal anomalies, one of which is liver cysts, the most common human extrarenal manifestation. Importantly, the expression levels of *Pkd1* directly correlated with the severity of kidney disease. The lower *Pkd1* levels lead to later onset while higher levels resulted in more severe adult PKD pathogenesis. Therefore, our data strongly excluded loss-of-function as the sole responsible pathogenetic mechanism for ADPKD. We were also the first group to show that primary cilia structure was altered and longer by increased expression of Pc1. In contrast to the shorter or lack of cilia being associated with cystic kidney disease, we report the elongation of the primary cilium in the kidney in our *Pkd1* gene increase orthologous mouse model. Our characterization of the renal and extrarenal phenotype was associated with increased levels of proliferation, fibrosis and c-myc expression in both kidney and liver. Together, our findings in *Pkd1* gene increase mouse model, which closely parallel those in human ADPKD, strongly suggest the involvement of *Pkd1* gene dosage in ADPKD pathogenesis.

In the second article **(Chapter V)**, our goal was to analyze the human *Pkd1* mutation and gain insight into the function of Pc1 extracellular domain using transgenesis in mice. Our study showed that reproducing the human *Pkd1* truncating mutation which mimics NTF-like GPS cleaved product in mice, termed $Pkd1_{extra}$ for extracellular domain of Pc1, results in late-onset progressive PKD. This model reproduced typical human renal PKD phenotypes starting with cellular anomalies (fibrosis and potential downstream signaling) and moving to the onset and progression of kidney cystogenesis. Similar to $Pkd1_{TAG}$, the kidney phenotype in $Pkd1_{extra}$ was associated with increased levels of c-myc oncogene. Finally, we found that increase in mutated

Pc1 enhanced the stability of the second most important polycystin in ADPKD, Pc2, which supports a possible cross-talk between different members of the polycystin family and PC1/PC2 protein complex. Results from *Pkd1*$_{extra}$ thus suggest that not all truncated human mutations act as loss-of-function variants. Together with *Pkd1*$_{TAG}$ and previously published *SBPkd1*$_{TAG}$, *Pkd1*$_{extra}$ represents an invaluable model to study ADPKD pathogenesis and to assess putative therapies.

In the third article **(Chapter VI)**, by thoroughly characterizing the endogenous murine Pc1, we discovered a new and as of yet unrecognized GPS cleaved Pc1 isoform identified as Pc1^{deN} standing for detached NTF. We found that following GPS cleavage *in vivo,* which seems to occur very early in the ER or cis-Golgi, the Pc1 CTF subunit is critical for further trafficking of the Pc1 NTF. Additionally, the function of CTF in chaperoning the trafficking of NTF was validated by using Pc1 mutants with mutations at either the proximal or the distal end of the CTF Pc1 fragment but unaffected GPS/GAIN domain for proper cleavage at GPS site. On this basis, and with data from genetic complementation studies of uncleavable Pc1 mutant *(Pkd1*$^{V/V}$*)* with transgenic mice mimicking the NTF fragment or the full-length Pc1, we propose a very detailed model of Pc1 biogenesis and trafficking process. Altogether, this work shed light on Pc1 biogenesis *in vivo* and importantly leads to the proposal of a novel therapeutic avenue in ADPKD. In line with what is proposed for rescuing of CFTR folding and maturation by molecular and pharmacological chaperones in CF pathogenesis, direct targeting of Pc1 and GPS cleavage by chaperones represents an alternative and very promising therapeutic approach for ADPKD.

In the fourth article (**Chapter VII**), we assessed the impact of kidney injury in the progression of kidney cellular changes and downstream signaling dynamics by acute kidney ischemia in mice. We found that relatively shortly after IRI (~3wks), the kidneys undergo hypoplasia. Long-term reperfusion leads to increased levels of interstitial fibrosis, infiltrates and kidney cysts with increased expression of Pc1, Pc2, Tuberin, active β-catenin, c-Myc and phospho-Erk. Contrary to the reduced levels of Pc1 and Pc2 being associated with higher susceptibility to kidney injury in several murine

models, increased levels of Pc1 or Pc1 NTF-like protein in two different adult onset *PKD1* gene orthologous models (the $Pkd1_{TAG}$ and $Pkd1_{extra}$) did not result in accentuated cystogenesis. Our findings extend the concept of ADPKD being a ‘’futile kidney repair’’ state. Furthermore, we provide important insight into the chronic consequences of acute kidney injury potentially relevant beyond ADPKD and for the human kidney transplantation field.

In the last article (**Chapter VIII**), our objective was to expand the analysis of the ADPKD pathogenetic mechanism in the liver and pancreas using genetic complementation experiments in mice. We showed that our previously published kidney specific high *Pkd1* expressor ($SBPkd1_{TAG}$ line) was able to completely rescue the kidney cystogenesis in *Pkd1* loss-of-function mice until P10 whereas the lower *Pkd1* expressor reproduced the hypomorphic phenotype with renal cysts. This finding provided additional evidence for dosage of wild-type *Pkd1* gene as the ADPKD pathogenetic mechanism. However, even though the Pc1 extrarenal expression in adult tissues of $Pkd1^{-/-}$; $SBPkd1_{TAG}$ binary compound was very low, our expression analysis of Pc1 at P0, P10 and P30 suggested sufficient amounts in the high kidney expressor that may correct the phenotype in liver and pancreas until P30. The $SBPkd1_{TAG}$ transgene still developed severe kidney cysts and significant hydronephrosis by P30. However, the kidney, liver and pancreatic phenotypes were completely corrected in $Pkd1^{-/-}$ by systemic full-length $Pkd1_{TAG}$ transgene. These comparisons therefore suggested a possible temporal and/or spatial regulation of SB elements that does not completely overlap with the endogenous *Pkd1* promoter. Importantly, crossing of our two *Pkd1* GOF transgenic mice with the uncleaved $Pkd1^{V/V}$ mutant, revealed an important implication of the uncleaved Pc1 form in the liver. In comparison to $Pkd1^{-/-}$;$Pkd1_{TAG}$ compound, the $Pkd1^{V/V}$;$Pkd1_{TAG}$ developed a progressive liver cluster-like cystogenesis, macroscopically visible very early at 3 months and, as observed in human disease, was more severe in females than in males. Altogether, this analysis further supported the gene dosage PKD pathogenetic mechanism. Additionally, our findings point to the importance of a relative abundance

of cleaved and unprocessed full-length Pc1 forms (rate and dynamics of the cleavage) that need to be tightly regulated for proper adult liver homeostasis.

ADPKD pathogenetic mechanism (s)

ADPKD is an autosomal genetic disease that is generally diagnosed in adults and leads to ESRD at ≈ 50 years of age. The major gene responsible is *PKD1* which is highly expressed in embryonic wild-type kidneys and in extrarenal structures such as the liver, with expression drastically decreasing after birth (**Chapter I: S-5.1, 5.2**). The pathogenetic mechanisms underlying human ADPKD cystogenesis remain poorly understood and controversial. Even though all cells in the kidney contain the same germ-line mutation, only a minority of nephrons forms cysts. Observation in human ADPKD showed that *PKD1*/PC1 continues to be heavily expressed at levels comparable to embryonic kidneys, while a significant minority of cysts presents LOH somatic mutations (**Chapter I: S-5.4**). In parallel, observation of kidney cystogenesis in a couple of *Pkd1* inactivation mouse models, detection of somatic mutations and loss-of-heterozygosity, although in only a minority of human cysts, could be indicative of loss-of-function and second-hit theory as the pathogenetic mechanism in ADPKD, in principle similar to the cancerogenesis, and more relevant to the kidney, the Wilms tumor. The two-hit hypothesis implies that ADPKD could behave as a recessive pathology at the cellular level with the requirement of additional homozygous mutations in the *Pkd1* locus, which would result in complete loss of function.

Many examples can be provided that are not explained by LOF theory exclusively. ADPKD mutations may not all be inactivating in nature (loss-of-function). In contrast to late adult onset in human PKD, *Pkd1* LOF mice develop very early *in utero* onset of renal cysts. The extrarenal hepatic phenotype or human disease progression is not reproduced in *Pkd1* LOF models. Rather, $Pkd1^{-/-}$ consistently develop pancreatic cysts, a phenotype rarely reported in human ADPKD. Even though normally more prevalent in the kidneys than in other tissues, the frequency of somatic mutations causing loss-of-function should be very high to account for severe human PKD cystogenesis.

Inactivation of *Pkd1* (LOF) in adult kidneys would be expected to be more severe and consistent.

There is also evidence for LOF and two-hit theory not being directly associated with cystogenesis or an altered cellular phenotype. For instance, generation of chimeric mice with wild-type and *Pkd1*$^{-/-}$ cells showed that, at an early stage of the disease, kidney cysts form from either wild-type or *Pkd1*$^{-/-}$ cells, *i.e.,* not only from the *Pkd1* inactivated cells as would be expected by a LOF model (Nishio, Hatano et al. 2005). In iPS cells isolated from ADPKD patients, the second hit can occur but does not contribute to the observed phenotype of resulting PC2 mislocalization (Freedman, Lam et al. 2013). In human ADPKD tissues and derived immortalized cells, two cysts with the same *PKD1* germline mutation behave in the same way but only one cyst has been shown to encounter an additional somatic hit (Nauli, Rossetti et al. 2006). Because somatic mutations are rather rare, found in only minority of human cysts and not always correlating with altered cellular pathology, additional mechanism(s) other than LOF are probably more prevalent than a sole loss-of-function model.

Herein, we provide direct evidence that *Pkd1* LOF is not the sole mechanism. Our previously published data from *SBPkd1*$_{TAG}$ with overexpression of native murine Pc1 associated with kidney cystogenesis in adult stage and now additional *Pkd1*$_{TAG}$ mice that reproduce human adult kidney and extrarenal progressive disease are both consistent with a gene dosage mechanism and thus provide probably the most authentic orthologous models of human ADPKD (**Chapter IV**) (Thivierge, Kurbegovic et al. 2006) (Kurbegovic, Côté et a. 2010). We showed that increased expression of murine Pc1 (in transgenic mice and on a *Pkd1*$^{-/-}$ genetic background) is able to induce kidney cystogenesis (**Chapter IV, VIII**). This transgenic Pc1 behaves as the wild-type endogenous Pc1 protein: **1)** it has exactly the same aa sequence; **2)** traffics like endogenous Pc1 and is secreted in the urinary exosomes (**Chapter IV, VIII**); **3)** it is cleaved at GPS/GAIN domain with all tethered and detached Pc1 isoforms (**Chapter VI**); **4)** it rescues/complements *Pkd1* loss-of-function (**Chapter VIII**) and finally **5)** is able to interact with Pc2 (**Chapter VI, App.XV**). Therefore, increase in wild-type endogenous-like *Pkd1*/Pc1 in mice is pathogenetic.

One independent group previously attempted a similar overexpression experiment using *PKD1*-PAC that also contained *TSC2* and probably some other neighbor genes (Pritchard, Sloane-Stanley et al. 2000). Given that *TSC2* heterozygous mice show kidney cysts and large deletions of *PKD1* and adjacent *TSC2* gene in human TSC2/PKD1 contiguous syndrome are more severe than PKD1 mutations alone, *TSC2* might have contributed to the phenotype (**Table 7**) (Brook-Carter, Peral et al. 1994, Longa, Scolari et al. 1997, Onda, Lueck et al. 1999). Although inconclusive about whether *PKD1* overexpression alone causes the phenotype since a possible interplay and contribution by the cystogenic *TSC2* gene, this team suggested that overexpression of human *PKD1* gene in mice may lead to kidney cystogenesis. We designed, generated and characterized the phenotype of the transgenic mice with murine *Pkd1* endogenous promoter without interference of *Tsc2* carried in a bacterial artificial chromosome. Furthermore, for the first time, we provided a detailed report on the role of increased *Pkd1*/Pc1 on extrarenal phenotypes with insights into direct downstream cellular alterations (calcium homeostasis, interstitial fibrosis, ciliary structure, proliferation index, c-myc expression). Overall, *Pkd1* GOF is analogous to the human disease. $Pkd1_{TAG}$ does not show obvious kidney development anomalies, and the phenotype is rather manifested by slow progression extended in months and leading to ESRD in late adulthood with the panoply of extrarenal defects.

Our results correlate with *Pkd2*/Pc2 gene decrease and gene increase that are both cystogenic in mice and in fact altogether firmly support the gene dosage mechanism for ADPKD disease (**Chapter I: Table 8A**). From the data obtained by generating the $Pkd1_{extra}$ transgenic mice and recent work from others, we also propose that some *PKD1* human mutations are not inactivating but rather partially functional hypomorphs or potentially acting as dominant negatives previously dismissed (Harris 2010). Finally, *PKD1* gene dosage increase is pathogenic together with complete LOF. Our studies in mice show that Pc1 levels are critical and provide important information and raise concerns about direct targeting of *Pkd1* endogenous levels.

A couple of fundamental questions arise from the gene dosage/gene increase mechanism. First of all, by which mechanism could the wild-type *Pkd1*/Pc1 become

increased and/or stabilized in human ADPKD? And second, what would be the functional mechanistic consequences of higher *Pkd1*/Pc1 abundance?

Hypothetically, endogenous *Pkd1/Pc1* might act as an autosensor and when generally decreased, such as in the heterozygous haploinsufficient state, the cell would try to compensate through an autoregulatory loop via a Pc1 C terminal tail. Consistently, the PC1 CT tail was suggested to undergo cleavage through a RIP process and to translocate into the nucleus for potential regulation of gene transcription (Chauvet, Tian et al. 2004). However, direct transcriptional regulation of *Pkd1* by Pc1 has not yet been shown; this will be possible using methods such as CHIP for direct binding of Pc1 on the *Pkd1* locus when the proper antibodies become available. An alternative explanation would be through downstream modulators. Decreased levels of Pc1 by heterozygous mutation might modulate p53 or β-catenin expression, both shown to directly bind to the *Pkd1* promoter (Rodova, Islam et al. 2002), and consequently stimulate its own transcription. Our data of upregulation of β-catenin and one of its direct downstream targets, the oncogene c-myc, in both *Pkd1* dosage increase and *Pkd1* dosage reduce, support this hypothesis (**App. IIIA**). In addition, overexpression of Pc1 in the SBM c-myc overexpressor, together with c-myc and Pc2 increase in perinatal *Pkd1* gene decrease or adult *Pkd1* gene increase kidneys, implies a possible feed-back regulatory mechanistic loop **(App. IIIB-D, XV, Chapter IV).** Furthermore, some of the early PKD alterations are chromosomal alterations and instability. Pc1 was shown to interact with PC2/ID2 (**Table 3,4**) (Li, Luo et al. 2005) and to regulate cell cycle progression, and is also expressed in the cilia, an organelle whose formation and resorption are directly dictated and dependent on the progression and stage of the cell cycle. Abnormal cell cycle and chromosomal control can lead to chromosomal duplication resulting potentially in overall *Pkd1* increase. This is less probable since *Pkd1* gene duplication is very rare in ADPKD (~1%) (**Chapter I: Table 2**). Finally, as suggested for some new members of the nephrocystins family, PC1 might eventually be involved in the DNA repair process (Chaki, Airik et al. 2012, Zhou, Otto et al. 2012). Since transgenic *Pkd1* completely rescues the $Pkd1^{-/-}$ phenotype and based on direct correlation of *Pkd1* copy number with severity of the cystogenesis in $Pkd1_{TAG}$ kidneys,

the excess of *Pkd1* gene in transgenic mice probably does not lead to increase in frequency of inactivating somatic mutations, although this was not assessed.

To answer the second part questioning the functional relevance of increased *Pkd1*/Pc1, we need to consider the putative functions of PC1.

Calcium homeostasis

Pc1 has been suggested to be involved in a protein complex with the generally accepted Ca (2+)-permeable cation channel, Pc2, at the primary cilia for regulation of calcium influx. Therefore, it is possible that an excess of Pc1/Pc2 complexes in the *Pkd1* transgenic context affect calcium influx, levels and homeostasis. Our unpublished data indeed show increased levels of Pc2 in *Pkd1* gene increase cystic kidneys (**App. XV, unpublished data AS,KS)**, which could lead to increased PC1/PC2 complexes and in parallel, potentially to increased intracellular calcium levels. The excess Pc1 should localize at the primary cilia and cause an increase in Pc2 channel activity at the same localization to form functional calcium channel complexes with the endpoint of more intracellular calcium influx. However, the ciliary transgenic Pc1/endogenous Pc2 co-localization in an *in vivo* overexpression system has not been assessed yet because of a lack of biochemical tools. Ongoing generation of transgenic mice with V5 N-terminal tagged murine Pc1 will facilitate elaboration of this question (**unpublished data, AK,KD**). $Pc1_{TAG}$ and $SBPkd1_{TAG}$ transgenes are expected to localize in the primary cilia given the proposed critical role of Pc1 in the cilia, their ability to fully complement the $Pkd1^{-/-}$ phenotype and also based on recently published immunofluorescence data indicating $Pc1^{H/F}$ transgene ability to localize in the primary cilia by (**Chapter VIII**) (Fedeles, Tian et al. 2011). We would predict an increase of influx of calcium in conditions where PC1 is overexpressed as suggested by *in vitro* studies. Overexpression of C-terminal Pc1 tail in Xenopus oocytes resulted in increased Cl^- and Ca^{2+} permeable calcium channels (Chernova, Vandorpe et al. 2005). If overexpression of Pc1 does not lead necessarily to more functional Pc1/Pc2 complex channels, then Pc1 would need the ability to regulate this process alone. In fact, one group showed that Pc1 can induce calcium levels independently of Pc2 and proposed

that PC1 transduces the intracellular signal via changes in ionic currents (Babich, Zeng et al. 2004), whereas a mutant lacking the extracellular domain (2900aa) or using antibodies against PKD extracellular motifs blocked or reduced the signal. Our data shows that *Pkd1*$_{TAG}$ model develops kidney stones with calcifications and calcium deposits detected microscopically by von Kossa staining and macroscopically in the cardiac intrinsic wall (**Chapter IV**). Although it is not known yet if this happens through a PC1/PC2 complex or PC1 alone, our *in vivo* data correlate with the proposal that PC1 is implicated in calcium homeostasis regulation.

cAMP and ciliogenesis

In ADPKD epithelia, a decrease in intracellular calcium was suggested to correlate with an increase in cAMP levels and subsequent downstream activation of MAPK/ERK signaling (Yamaguchi, Wallace et al. 2004). Interestingly, both decrease in calcium and increase in cAMP levels were shown to cause the elongation of the cilia in cell culture using Gd^{3+} and forskolin respectively (Besschetnova, Kolpakova-Hart et al. 2010). Our findings using two *Pkd1* increase mouse models, under systemic and kidney specific regulatory elements, validate *in vitro* studies. We supply evidence that the ciliary structure and increased cAMP in the transgenic kidneys might be very early events of cystogenesis with potential causative implications based on detection of longer cilia prior to overt cystogenesis (**Chapter IV, unpublished data JC**). Rather than evaluating cilia length as an average where subtle differences would not be appreciated, the length of the primary cilia in kidney epithelial cells of both *Pkd1* GOF models were classified in increments of 1-2μm by two different approaches, immunofluorescence and electron microscopy with the help of Dr. Gattone from Indiana PKD imaging core (**Chapter IV, preliminary data, OC).** Longer cilia in *Pkd1* GOF models appear in contrast to few reports on cilia length of *Pkd1/Pkd2* models described as unchanged or slightly shorter/reduced in human ADPKD or derived immortalized cells (Nauli, Rossetti et al. 2006) (Xu, Rossetti et al. 2007) or completely absent in some ciliopathies (**Chapter I: Table 7**). The most recent reports are confirming our findings of structural ciliary defects in PKD in kidney and liver of the *Pkd1*^{R3277C} hypomorph (Hopp, Ward et al. 2012) and in the kidneys of some other

ciliary cystogenic proteins such as *Nek8*/*Nphp9*, *Bbs4*, *Pkd1 heterozygous* and *Pkd1*/*Tsc1* double heterozygous mice (Mokrzan, Lewis et al. 2007, Sohara, Luo et al. 2008, Bonnet, Aldred et al. 2009). The implication of Pc1 in the elongation of the primary cilia is unknown. Based on our data and previously published reports, we propose a couple of possible explanations: **1)** As mentioned here above, it is highly probable that the role of PC1 directly involves regulation of cAMP and/or calcium levels; **2)** Pc1 was reported or suggested to interact with proteins implicated in ciliogenesis such as Rab8 and Bbs (**Table 3,4**). This is consistent with findings of overexpression of Rab8 that result in longer cilia (Nachury, Loktev et al. 2007). **3)** The kidney repair process was associated with longer cilia (Verghese, Weidenfeld et al. 2008) and PC1 was suggested to act as a sensor for kidney injury and ADPKD as a disease of ''futile renal repair'' (Weimbs 2007).

The reduction in calcium levels and inversely increased cAMP are both associated with ADPKD and longer cilia *in vitro*. The predicted calcium increase in $Pkd1_{TAG}$ and longer cilia in precystic transgenic mice would seem somewhat at odds considering that Pc1 overexpression also leads to increased levels of cAMP at ~1month, age at which almost no cysts can be detected (**Chapter IV, preliminary data, AK, JC**). It remains to be tested if calcium changes, if any, follow the cAMP deregulation. It is possible that Pc1 increases cAMP levels (dependent on or independently of Pc2), and the interaction and localization of Pc1/Pc2/Rab complex to the cilia, with the final outcome of ciliary elongation in kidney epithelial cells. This could be followed by an increase of calcium levels, presumably not in sufficient amounts to have a negative effect on ciliogenesis but rather on other pathways since Pc1 is an enormous protein with most certainly a multitude of cilia-independent functions with functional implications.

A novel concept arose recently from very simple but highly reproducible observations concerning ciliogenesis and could be of great interest for ADPKD. Primary cilia are highly sensitive to changes of the nutrients in the environment. Precisely, the cilia length is induced shortly after serum deprivation in cell culture systems and this is associated with activation of autophagy (Pampliega, Orhon et al. 2013). Since ciliogenesis and autophagy seem to involve common molecular machinery, this would

imply that ciliopathies are unable to activate autophagy. Cilia elongation was proposed to result from blocked autophagy that affects the stability of *Ift20*. Given that autophagy was reported defective in LOF *Pkd1*$^{-/-}$ MEFs (Rowe, Chiaravalli et al. 2013), this would suggest longer cilia and increased *Ift20* levels in this *Pkd1* LOF mouse model, although this was never reported in a quantitative manner. It would be interesting to verify if Ift20 is more stable in *Pkd1* GOF models with elongated primary cilium potentially through direct association with Ift20. Sustained longer cilia from pre-cystic stage in *Pkd1*$_{TAG}$ and *SBPkd1*$_{TAG}$ (**Chapter IV**, **and unpublished data, OC**) could concentrate important signaling pathways directly regulated by the cilia such as Wnts and Hedgehog and allow their abnormal activation. This is supported with the data of targeting the main components of Wnt signalling (β-catenin, c-myc, Wnt9b, APC) and of Shh cascade (Gli3 transcriptional effector) being associated with kidney cystogenesis (**Table 7**). In the lab, we have shown that the canonical Wnt pathway was in fact altered in GOF *Pkd1* model with longer cilia using the TcfLacZ reporter mice and a biochemical approach (**App. III**) (Couillard 2008). One of the future studies will examine Shh pathway activation in longer cilia mouse models (*i.e.,* GOF) using for example a knock-in *Patch1; LacZ* reporter mouse. The findings of Ma *et al*. are consistent with this concept that suggested an existence of a cilia cyst promoting factor and excluded cAMP, mTOR or MAPK/ERK but not Wnt or Shh (Ma, Tian et al. 2013). When cilia formation was abrogated, the authors were able to rescue *Pkd1* and *Pkd2* loss-of-function kidney and liver polycystic disease. Our *Pkd1* GOF that displays longer kidney epithelial cilia may have stimulation of cilia cyst promoting factor; that still remains to be identified, but could be one of the main players responsible for cyst formation. Isolation of the cilia from *Pkd1*$_{TAG}$ kidneys might help identify this possibly enriched ‘’X’’ factor. Since the cilia does not seem to be affected in *Pkd1* LOF models, the cilia dependent stimulating pathway may be still functional but limited in this specific mouse model. This observation reflects some of the limitations of this early onset PKD mimicking the human ADPKD pathogenesis.

PC1 in a multiprotein complex at the membrane

ADPKD is considered to be a ciliopathy since PC1 is expressed in the primary cilia and when mutated leads to polycystic phenotype in the kidneys.

It is generally believed that the flow directs, through primary cilia, the planar cell polarity and proper OCD. Recently shown for IFT88 in zebrafish but also most likely applicable for other ciliary proteins such as PC1/PC2, the PCP and OCD could be regulated in a cilia-independent manner (Borovina and Ciruna 2013). The non-responsiveness following flow/shear stress of epithelia from the *Pkd1*$^{-/-}$ kidneys could also be indirect. Generation and characterization of a PC1 mutant with altered ciliary but otherwise normal intracellular distribution will help assess a direct role of PC1 in the cilia. Nonetheless, many ciliogenic proteins (eg.Ift, Kif) have been suggested to have important if not critical cilia-independent roles (Brown, Maier et al. 2005, Bananis, Nath et al. 2004, Borovina and Ciruna 2013, Robert, Margall-Ducos et al. 2007, Finetti, Paccani et al. 2009, Delaval, Bright et al. 2011). Besides primary cilium, there is also a lot of evidence for PC1 function in a cilia-independent but also developmentally regulated manner. In very early studies, PC1/Pc1 was mainly observed at cell junctions, which correlates with its transmembrane topology. *In vitro* studies suggest Pc1 implication in cell-adhesion mediated via its N-terminal extracellular domain that allows binding to proteins of the adhesion complex or of the extracellular matrix (**Table 3**). Antibodies against PKD domains of Pc1 abrogate cell-cell interaction in MDCK monolayers (Ibraghimov-Beskrovnaya, Bukanov et al. 2000). In addition, the Pc1 cell-adhesion complex is disrupted in human ADPKD primary cells and its main component, the E-cadherin, is deleted from the membrane and replaced by mesenchymal N-cadherin (Roitbak, Ward et al. 2004). Presence of Pc1 EndoH resistant form in *Pkd1*$_{TAG}$ but also partially in adult N-terminal extracellular domain expressor *Pkd1*$_{extra}$ kidneys and exosomal localization support the ability of Pc1/Pc1$_{extra}$ post-ER trafficking and its role in post-ER compartments such as the plasma membrane (**Chapter V**). Absence of ciliary length changes in *Pkd1*$_{extra}$ mice, contrary to the *Pkd1*$_{TAG}$, is explained by a lack of the targeting ciliary sequence in *Pkd1*$_{extra}$

transgene, and may be responsible for the difference in onset and extrarenal manifestations in these two murine models.

Therefore, other than regulating the primary cilia, calcium and cAMP homeostasis, one of the first patho-cellular consequences of mutated PC1 may implicate trafficking defects to the membrane or lack of proper protein complexes formed as proposed for other ‘’gene dosage’’ pathologies. As pointed out by Pritchard *et al*., two other genetic disorders have been described as ‘’gene dosage’’ pathologies where both gene increase and decrease are pathogenic (Pritchard, Sloane-Stanley *et al*. 2000). Pelizaeus-Merzbacher disease (PMD) and Darier’s disease (DD) are clinically heterogeneous diseases with significant variability. These two pathologies are caused by mutations that include genomic duplication, deletions and point mutations in PLP1 and ATP2A2 genes encoding for PLP (an important myelin sheet component) and SERCA2 proteins (calcium pump for influx from cytosol to ER), respectively (Willard and Riordan 1985, Ellis and Malcolm 1994, Thomson, Montague et al. 1997, Sakuntabhai, Ruiz-Perez et al. 1999). Similar to *Pkd1* and *Pkd2*, inactivation or transgenesis of *Plp* in mice both lead to similar phenotypes (neurological in this case), although more severe and more relevant to human disease when overexpressed (Karim, Barrie et al. 2010). Duplication of *PLP* in human, the most common type of human mutation, sometimes even in a far distant region on the same chromosome, was suggested to potentially affect the flanking genes with modifier effect (Sistermans, de Coo et al. 1998). Targeting the *Plp* gene (upregulation and downregulation) leads to altered distribution, localization and protein dynamics of *Plp*, mainly blocked in the ER, endosomes/lysosomes, autophagosomes, that subsequently lowers its interaction with cholesterol and integration to lipid rafts at the membrane of axonomal myelin sheets (Karim, Barrie et al. 2010). A cholesterol-rich diet rescues the PMD phenotype in transgenic mice without decreasing overall levels of *Plp* but rather by helping to distribute it to the myelin membrane (Saher, Rudolphi et al. 2012). It is assumed that inappropriate *Plp* levels affect protein complexes in trafficking to a functional destination such as the plasma membrane. Other similarities between PC1, PLP and SERCA proteins such as a role in calcium homeostasis, cell adhesion and,

interestingly a beneficial outcome of curcumin in both, a mutant PMD but also in *Pkd1* deficient mouse model, point to similar pathogenic mechanisms (Leonhard, van der Wal et al. 2011, Yu, Morimura et al. 2012).

However, unlike PLP, we showed that transgenic $Pc1_{TAG}$ does not accumulate in the ER based on EndoH resistance of GPS cleaved forms and its secretion in the urinary exosomes (**Chapter IV, VI, VIII, App. XV**). Thus, few possibilities could explain this normal trafficking of the transgenic Pc1. First, the trafficking process to the membrane of Pc1 itself is independent of other proteins of the same complex. Second, partners of the Pc1 multiprotein complex may be regulated (at the transcriptional or translational level) by an excess of Pc1/mutant Pc1 for adaptation and formation of appropriate stoichiometry. Third, Pc1 and Pc1 mutants could successfully traffic by ‘’quenching’’ other Pc1 isoforms or non-related proteins (**App. X**). We show that Pc1 affects stability (and possibly distribution) of Pc2. A similar effect on other partners of the multicomplex is possible (eg. Pc2, fibrocystin). Consequently, the activation of developmental pathways such as Shh and Wnt in the adult mouse models would follow with a possible feed-back regulatory mechanism on Pc1 expression. Consistent with this prediction, the *Pkd1* gene dosage decrease would not produce any functional Pc1 containing complex, with detrimental effects on the stability of the above-mentioned candidates. Our results in **Chapter VI** allow us to propose a hypothetical model of PC1 apical/basal *vs* cilia implications at different stages of development and homeostasis, taking into account the GPS cleaved and uncleaved forms of Pc1.

Independence of PC1 multicomplex (PC2) in ADPKD

When considering the relationship between polycystins in particular, one might question if **1)** one polycystin affects another (or other PKD protein) in regards to its stability, abundance, post-translational modification/phosphorylation or function, or, if **2)** only one limiting gene dictates many, if not all, PKD proteins (ADPKD and ARPKD). Our results show that Pc1 can affect Pc2 abundance. This was demonstrated by $Pkd1_{extra}$ mutant and *Pkd1* gene dosage increase, which both result in increased levels of Pc2 in the kidneys (**Chapter V, App. XV, unpublished data, AS**). It is possible that

Pc2 stabilization occurs through direct or indirect interaction between $Pc1_{TAG}$/$Pc1_{extra}$ and Pc2. In fact, by immunoprecipitation we showed that high $Pc1_{TAG}$ directly interacts with endogenous Pc2 at birth, at P10 and in adults (**Chapter V, App. XV**). Excess Pc1 increased interaction with Pc2, although this interaction seemed rapidly saturated (**App. XV**). Paradoxically, the *Pkd1* loss-of-function also seems to lead to increased levels of Pc2. Therefore, stabilization of Pc2 could also be indirect via most likely one of the Pc1 immediate downstream effectors. Given that both *Pkd1* LOF and GOF also increase c-myc expression levels; we therefore favor a Pc1/c-Myc/Pc2/PC1/PC2 complex feedback axis (**App. IIIC, D**). Even though transgenic *Pkd1* was shown to be unable to rescue Pc2 loss-of-function (**Table 8A, 8B**) (Fedeles, Tian et al. 2011) and was suggestive of lack of functional redundancy, Pc1 and Pc2 co-dependence is reported by multiple studies (**Chapter I: S-4.3**). Direct interaction of Pc1 with Pc2 and its role in Pc2 stability and abundance does not completely exclude the possibility that this interaction *per se* is not critical. Overall, our findings together with other groups all suggest interdependence although probably not absolute of polycystins.

Kidney repair, ER stress and ADPKD

In ADPKD, additional stimuli, genetic or non-genetic, were suggested to be required in addition to the inherited heterozygous mutation. ADPKD is a very heterogeneous, completely penetrant but a highly variable and very focal disease with only ~5% of nephrons being affected, that eventually leads to ESRD by destroying the normal parenchyma. Alteration of the renal flow during acute kidney injury caused by toxins, medications, aging-related process and diet (glucose) are some of these stimuli postulated to contribute to the manifestation of the disease.

We showed an impressive overlap between cellular changes implicated in PKD using *Pkd1* gene increase and kidney damage/repair following kidney ischemia. The overlap starts from the presence of elongated cilia to induction of Pc1 and Pc2 expression, and finally, implication of common, mostly developmental, downstream signalling pathways (mTOR/Tsc2-cell size and proliferation, c-myc, ERK, SMA/collagens) (**Chapter VII**). However, since neither model, $Pkd1_{extra}$ nor $Pkd1_{TAG}$, is more cystic when subjected to

kidney injury, our data suggests a presence of necessary common protective elements, which in this case is the amino-terminal extracellular Pc1 ectodomain. Moreover, adult kidney stem cells were shown to contribute to the process of cellular recovery and repair. Pc1 was shown to be expressed in multipotent ES and pluripotent iPS cells and thus could be expressed in adult kidney stem cells for functional involvement during the kidney repair process (Guillaume, D'Agati et al. 1999, Freedman, Lam et al. 2013). Sensing of the damage signal via primary cilia, differentiation of stem cells into epithelial tubular cells, their subsequent migration and integration into the existent damaged tubules could all be affected in *Pkd1* LOF and *Pkd1* GOF conditions allowing a more/less severe defense repair mechanism through cell proliferation, fibrosis and eventually cysts (**Chapter VII**). Our data also clearly provides evidence for implication of gene dosage of Pc1 and Pc2 as a long-term consequence of acute kidney injury. Observations of sustained and elevated expression of polycystins following IRI, associated with long-term fibrosis prior to cystogenesis and eventually formation of kidney cysts is consistent with the role of Pc1 in these processes and noticeably, a *PKD1/PKD2* gene dosage increase mechanism in human polycystic kidney disease. We propose that the $Pkd1_{TAG}$ transgenic mice are recapitulating on their own these cellular conditions that are not synergetic *i.e.,* exacerbated with identical additional stimuli that occurs during kidney repair.

Moreover, the oxidative stress that is normally induced by ischemia is a well-documented inducer and enhancer of ER stress and vice versa (Reviewed in Yoshida 2007). Aged kidneys need supplementary control against ER stress because they are subject to increased ER stress but paradoxically express lower levels of chaperones which eventually leads to accumulation of missfolded proteins and kidney fibrosis in aged models (Takeda, Kume et al. 2013, Tanjore, Lawson et al. 2013, Inagi 2010). Our *Pkd1* mouse models develop later onset of adult ADPKD associated with increased interstitial fibrosis, one of the main characteristics of the human ADPKD disease. Although highly unlikely in $Pkd1_{TAG}$ model, since it completely rescues the *Pkd1* loss-of-function and shows significant EndoH resistant Pc1 form (**Chapter VIII**), the suggested mechanism of ER stress and accumulation of misfolded Pc1 protein could

apply more to the *Pkd1*$_{extra}$ transgenic mutant. In fact, our *Pkd1*$_{extra}$ is highly EndoH sensitive with smaller amounts of PNGase resistance, which indicates higher abundance in the ER or in the cis-Golgi (**Chapter V**). Similar to *Pkd1*$_{extra}$, other human truncating Pc1 mutations could become stabilized and partially accumulate in the ER to activate ER stress response. Additional evidence for ER stress and Pc1 mutants is provided by the recent paper that made an association between ER stress and enhanced Pc2 stability (Yang, Zheng et al. 2013). It is possible that ER stress mechanisms are activated even prior to cystogenesis in PKD. First, Pc2 is also increased during reperfusion not only in late but also in very early stages following kidney ischemia. Second, increase of Pc2 could be detected even in the pre-cystic *Pkd1*$_{extra}$ kidneys (**Chapter V, VII**). It is possible that activation of chaperones or inhibitors of proteasome shown beneficial in *Pkd1* gene decrease mouse models (Fedeles, Tian et al. 2011) would also be successful in our adult ADPKD models. Future studies will assess the implication of the ER stress pathway in pre-cystic and cystic *Pkd1*$_{TAG}$ and *Pkd1*$_{extra}$ models and the effect of modulation of *Pkd2*. During kidney injury, the upper Pc1 corresponding to the PNGase-resistant form seemed more pronounced or the only one present (even in non-IRI at the same age). Thus, it is not necessarily PC1/PC2 accumulation in the ER that follows the ischemia/ER stress. PC1 is shown to localize to the membrane and, as proposed from *in vitro* studies, interact with extracellular proteins to induce anomalies in the extracellular matrix directly or by inducing collagen secretion as proposed in zebrafish (Mangos, Lam et al. 2010).

Finally, ER stress was also shown as a potential activator for RIP cleavage (Zhang, Shen et al. 2006, Ye, Rawson et al. 2000) whereas Pc1 is postulated to undergo RIP and nuclear translocation, although its functional significance is unknown (**Chapter I, S-6.2**) (Chauvet, Tian et al. 2004). Therefore, it is possible that Pc1 gets further activated following ER stress.

PC1 biogenesis, cleavage and PC1 isoforms

The coexistence of the full-length PC1 with the GPS/GAIN cleaved products is complex and likely provides dependent developmental and tissue-specific putative functions. The PC1 cleavage at its GPS/GAIN domain was proposed to occur through an autoproteolytic mechanism *i.e.,* enzyme-independent followed by conformational changes that might be influenced by environments, pH, ligand/protein binding. In the literature, it was shown that the GPS cleavage generates NTF and CTF subunits of Pc1 that tether non-covalently. The functional relevance of the GPS cleavage in PC1 was first tested by generation of *Pkd1*$^{V/V}$ knock-in with a single critical mutation in the cleavage site that prevents the generation of cleaved forms (Yu, Hackmann et al. 2007). The GPS cleavage was previously suggested to be an ubiquitous but developmentally regulated process which may partially explain the lack of cystic phenotype in *Pkd1*$^{V/V}$ before birth. In contrast to the full-length uncleaved PC1 with indispensable functions *in utero* and during kidney development, it is the cleaved form of PC1 that is critical in renal homeostasis and particularly in distal tubular segments since proximal and glomeruli appear unaffected.

Our study (**Chapter VI**) showed that the GPS cleavage leads not only to NTF and CTF tethered forms but also to an independent, detached NTF molecule named Pc1^{deN}. We showed that *in vivo* GPS cleavage occurs very early after synthesis since both NTF and CTF EndoH-sensitive forms are detected, probably in the ER/cis-Golgi. We demonstrate that further trafficking of the NTF cleaved fragment relies on intact Pc1 CTF. This finding was supported by the fact that NTF forms of two PC1 mutants, one in the proximal and the other in distal part of the CTF, are unable to become PNGase resistant. This C-terminal tail contains the ciliary signal sequence and putative PC2 interactive domain and could explain the requirement of intact CTF (**Chapter I:S-4.3 and 5.3.3.2**) (Ward, Brown-Glaberman et al. 2011). Biochemical analysis and genetic complementation of *Pkd1*$^{V/V}$ mice allowed us to conclude that CTF has an indispensable role following GPS cleavage *in vivo.* These results are suggestive of Pc1 requirement to undergo GPS cleavage in order to acquire a novel function but also to down-regulate the full-length Pc1 native levels.

Although the efficiency or dynamics of the cleavage were not quantitatively investigated, our CTF mutants (proximal and distal) are cleaved at the GPS cleavage site, which indicates that these mutations do not affect the folding, at least in the GAIN domain. It is also possible that lower than optimal efficiency of the GPS cleavage correlates with disproportional homeostatic levels of the cleaved and uncleaved products. Given a dynamic nature of the cleavage, complex but flexible structural characteristics of the PC1 extracellular domain and environmental constraints on the PC1 structure, the altered balance and/or relative ratio between PC1 GPS cleaved and PC1 uncleaved full-length in ADPKD kidneys but also liver **(See below)** could be critical and explain the highly variable phenotypes in human.

The data on the NTF-like extracellular fragment (*Pc1*$_{extra}$) with partial PNGase sensitivity may seem contradictory to those on complete absence of the *Pkd1*$_{extra}$ PNGase resistant form on *Pkd1*$^{V/V}$ genetic background (**Chapter V, VI**). This comparison actually revealed an interesting concept about Pc1 biogenesis and commonalities with other aGPCRS. We showed that the transgenic Pc1$_{extra}$ that mimics a human truncating mutation is partially EndoH resistant and therefore able to exit the ER in the *Pkd1*$^{+/+}$ context *i.e.,* with endogenous cleaved products being present. However, *Pkd1*$_{extra}$ was completely EndoH sensitive on cleavage deprived *Pkd1*$^{V/V}$ genetic background. Analogous to *in vitro* ability for tethering of co-transfected soluble NTF-like (E3020X Pc1 mutant) and CTF constructs (Qian, Boletta et al. 2002), the immunoprecipitation of Pc1 CTF revealed increased NTF pull-down when the Pc1$_{extra}$ transgene was present (**App. X**) (Silva, Lelianova et al. 2009). This strongly suggests that some Pc1$_{extra}$ molecules could indeed interact with endogenous Pc1 CTF fragment. It would be very interesting to verify if Pc1 NTF or Pc1$_{extra}$ could cross-associate not only with Pc1 as shown herein but also with some other members of aGPCR as reported for GPR56 and latrophilin, two different families of GPCRs (Silva, Lelianova et al. 2009). In light of Pc1$_{extra}$ partial accumulation in the ER, association of Pc1$_{extra}$ with endogenous CTF and increased Pc2 levels, we can propose at least two different mechanisms by which Pc1$_{extra}$ could lead to cystogenesis: by inducing ER stress and stabilizing Pc2 (or other PKD proteins) and/or by affecting the endogenous

wild-type Pc1/Pc2 stoichiometry by directly binding to the endogenous cleaved fragments of Pc1 (**Chapter V, App. X**).

Finally, based on *in vitro* data and numerous similarities between PC1 and aGPCRs, it is highly probable that Pc1 products have independent activities such as those suggested for latrophilin (Promel, Frickenhaus et al. 2012) and Flamingo (Steimel, Wong et al. 2010), are generating via shedding a potentially functional soluble ectodomain as proposed for BAI1,2,3, latrophilin, CD97, GPR124, GPR116 and GPR126, and contain a GPS independent proteolytic site and/or additional processings at their N-terminal tail (**App. IV**) (Reviewed in Langenhan, Aust et al. 2013, Krasnoperov, Deyev et al. 2009).

Extrarenal homeostasis: Role of PC1 cleavage particularly in the liver

In many aspects, the liver is similar to the kidney in that it relies on fetal developmental processes, both are somewhat branching ductal structures and both at some point require reparative processes. Acute liver injury induces cholangiocytes/hepatoblasts or even trans-differentiation of the hepatocytes for proper regeneration while chronic injury and repair rely on HPC (hepatic progenitor cells). Liver and kidney are the two most exposed organs to toxins, waste, hormones, and medications. They eliminate these endogenous and exogenous toxic molecules through secretion or reabsorption, and their development continues after birth.

Our study (**Chapter VIII**) leads to important insight into the role of GPS cleavage in the liver by mouse genetic complementation of the *Pkd1*$^{V/V}$ GPS uncleaved knock-in mutant. We discovered that, similarly to the kidney, *Pkd1* GPS/GAIN cleavage acts as a limiting factor in PKD liver disease. Our data is in agreement with a recent paper that showed a critical role of *Pkd1* gene in many PKD kidney and liver diseases, although the relevance of the GPS cleavage in this paper was not specifically addressed (**Chapter VIII**) (Fedeles, Tian et al. 2011). Fedeles *et al.* showed that overall total *Pkd1* dosage was critical in polycystic liver disease (PLD) caused by two genes, Sec63 or glucosidase IIβ (Prkcsh), in mice. Both of these proteins are involved in control of protein folding, translocation, export and the quality control pathway from the ER to the

membrane. Inactivation of either gene using pCX-CreER resulted in liver cysts while overexpression of *Pkd1* (and not *Pkd2*) was able to completely rescue the liver phenotype. Importantly, in the kidney cells *in vitro*, Prkcsh inactivation led to decreased Pc1 (~48%) (Fedeles, Tian et al. 2011). Thus, the authors concluded that this *Prkcsh* gene ''*mediates cystic disease by effectively reducing functional PC1 protein dosage*'' dependent on Pc2. Our data on Pc1 regulating the stability of Pc2 in the kidney and studies of others on Pc2 positively regulating the GPS cleavage point to Pc1 cleavage and Pc2 implication in the liver as well (**Chapter V, App. XV, unpublished data AS**) (Chapin, Rajendran et al. 2010). Indeed, Pc2 involvement in the liver is supported by studies with *Pkd2* hypomorph and *Pkd2* unstable (WS) mutants, which were both associated with liver cysts (Kim, Li et al. 2008, Stroope, Radtke et al. 2010). Severe cystogenesis observed in the liver of our binary $Pkd1^{uncleavedV/V}$;$SBPkd1_{TAG}$ mice (but not $Pkd1^{Loss\text{-}of\text{-}function\text{-}/\text{-}}$;$SBPkd1_{TAG}$) is highly suggestive of a role of PC1 GPS cleavage and, more specifically, of uncleaved Pc1 form for liver homeostasis. Importantly, this comparison suggests a potentially critical ratio between Pc1 uncleaved *vs* cleaved forms. $Pkd1^{V/V}$; $SBPkd1_{TAG}$ does not seem to behave as a ''hypomorph'' in the liver since $Pkd1^{-/-}$; $SBPkd1_{TAG}$ at the same age did not develop anomalies. We propose that $Pc1^{V}$ in $Pkd1^{V/V}$; $Pkd1_{TAG}$ compound might also be detrimental for long-term homeostasis, as these mice develop liver cysts obvious from 3 months of age. This would be possible through long-term accumulation of $Pc1^{V}$ or localized suboptimal cleavage that could occur with time. ADPKD being an adult disease, the rate of flow and the components of the flow could influence the stability and cleavage of PC1 in both organs. We hypothesize that the resulting abundance of uncleaved *vs* cleaved products provided by $SBPkd1_{TAG}$ and $Pkd1_{TAG}$ forms dictates the severity and progression of the kidney and liver phenotype.

Our morphological observations of the liver phenotype suggest interrelation between ADPKD (*PKD1*, PC1) and ARPKD (*PKHD1*, FPC) genes in this tissue. ARPKD liver cysts seem continuous/connected with the biliary tree and with an early, rapid onset (Mazyuk, Huang et al. 2004); $Pkd1^{V/V}$; $SBPkd1_{TAG}$ reproduces early onset ARPKD-like liver phenotype while $Pkd1^{V/V}$; $Pkd1_{TAG}$ seems more like the ADPKD liver phenotype

with independent, later onset, big isolated cystic clusters (**Chapter VIII**). Indeed, many commonalities exist between the liver and kidney ADPKD and ARPKD, such as implication of cAMP/ERK/MAPK axes, PC2, primary cilia, exosomes, and modulation of ARPKD phenotype by ADPKD genes in mice and human (Masyuk, Masyuk et al. 2006, Garcia-Gonzalez, Menezes et al. 2007, Kim, Fu et al. 2008, Hogan, Manganelli et al. 2009, Masyuk, Huang et al. 2010). Interestingly, ARPKD *Pkhd1* gene was reported to also regulate Pc2 stability and accordingly, Pc2 is downregulated in *Pkhd1* inactivated mice (Kim, Fu et al. 2008). A decrease in Pc2 is expected to result in inefficient and suboptimal Pc1 GPS cleavage and liver cysts, which is consistent with our data in **Chapter VIII** (Chapin, Rajendran et al. 2010, Fedeles, Tian et al. 2011). Surprisingly, the *Pkd1F/H-BAC* expression was not able to rescue either the liver phenotype in the ARPKD $Pkhd1^{del4}$ mutant nor the kidney phenotype in $Pkd2^{flox/flox}$*;Pkhd1Cre* mice, although the decrease of *Pkd1* worsened the liver ARPKD cysts (Fedeles, Tian et al. 2011). Even though this extensively flagged *Pkd1*-BAC transgene (at both N and C-termini, 3 copies of transgene) was stated to rescue $Pkd1^{-/-}$ kidney until 12 months of age and allowed Pc1 trafficking to the primary cilia, it is unknown if these protein tags alter Pc1 structure or if they allow sufficient expression in the liver for improvement of hepatic cystogenesis, in order to address a possible cross-talk with ADPKD. Nevertheless, our data demonstrate that GPS cleavage of Pc1 is important for liver homeostasis. Whether Pc2 and FPC are directly involved remains to be elucidated.

Additional complexity at the transcriptional level of *Pkd1* and *SBPkd1* gene

Since regulatory elements of any gene can sometimes be found very far or even on another chromosome, it was of critical importance to choose the proper regulatory region to drive the expression of our *Pkd1* transgenes. About 25kb of 5' regulatory region contained in the original BAC and used for generation of transgenic mice was sufficient for proper renal and extrarenal expression (**Chapter IV, VIII**). The pattern of RNA expression by QPCR in $Pkd1_{TAG}$ transgenic mice was analogous to the endogenous *Pkd1* and, importantly, *Pkd1* loss-of-function renal and extrarenal phenotypes were corrected by *Pkd1-BAC* transgene.

Regarding the kidney specific ‘’SB’’ regulatory elements, we showed that this promoter also confers a developmental- and spatial gene expression. The ‘’SB’’ regulatory elements consist of the SV40 enhancer and an adult β-globin promoter. Initially unexpected, this promoter was shown to confer high levels of expression in the kidney and when used upstream of the c-myc coding region, leads to renal cystogenesis in the SBM mouse model without extrarenal anomalies (Trudel, D'Agati et al. 1991). Renal anomalies are reported as early as e16.5 and e17.5 such as glomerular and tubular cysts (Trudel, Barisoni et al. 1998). Cysts in this young SBM mouse model (birth-3wks) originate from collecting (51%), proximal (39%) and distal tubules (7%) and in older mice (1,5-4months) from proximal (50%), collecting (20%) or distal tubules (10%)(D'Agati and Trudel 1992). Together with other studies in our lab, this work provided evidence for tissue specificity of the SB promoter in the kidney. In addition, based on cysts in particular cell types, SBM mice pointed, although indirectly, to the type/origin of tubules expressing the gene under the control of the SB elements.

Here, we provide further evidence and information for the ‘’SB’’ temporal and tissue specific expression when used upstream of the *Pkd1* gene. *SBPkd1*$_{TAG}$ *c*onfers sufficient and appropriate *Pkd1* expression until at least P10 and shows complete kidney rescue in *Pkd1*$^{-/-}$*;SBPkd1*$_{TAG}$*41* compound. Afterwards, renal expression driven by the ‘’SB’’ elements does not follow the *Pkd1* endogenous pattern. *Pkd1*$^{-/-}$*;SBPkd1*$_{TAG}$ develop severe cystogenesis (fast progression from P10-P30) and hydronephrosis by P30 only to die suddenly at ~P33 possibly due to extrarenal defects, while *Pkd1*$^{-/-}$*;Pkd1*$_{TAG}$ mice are normal at this age. While *Pkd1*$^{-/-}$*;SBPkd1*$_{TAG}$ kidneys are cystic, there are no cysts in the pancreatic ducts or hepatic biliary epithelial cell cysts. Conditional *Pkd1* gene decrease using MMTVCre or Mx1Cre leads to occasional cysts at 10wks or very cystic liver at 10 months, respectively (Piontek, Huso et al. 2004, Takakura, Contrino et al. 2008). Therefore, reduced Pc1 expression in *Pkd1*$^{-/-}$*;SBPkd1*$_{TAG}$ livers could be delaying or ‘’rescuing’’ the phenotype. Since immunostaining in mouse tissues using currently available Pc1 antibodies is not conclusive by us and many other groups (**Chapter I**), future studies using cell sorting or laser capture microscopy for isolation of specific structures will definitively help

further characterization of SB elements in *SBPkd1*$_{TAG}$ transgenic and binary renal and extrarenal tissues. A reporter transgenic mice consisting of *LacZ* gene downstream of SB regulatory elements produced in our lab should also contribute in addressing some of the concerns.

In the case of endogenous *Pkd1* transcriptional complexity, our findings lead us to predict alternative transcript(s) in the *Pkd1* gene towards the 3' end in the vicinity of exon39-40 (**App. II**). The low-copy full-length transgenic expressor (*Pkd1*$_{TAG}$ line 6) and both high and low expressors of the extracellular domain (*Pkd1*$_{extra}$ lines) are all unable to rescue the *Pkd1* loss-of-function (**App. II, Chapter VIII**). Interestingly, they all show decreased amounts of the 3' end transcript by QPCR while the full-length *Pkd1*$_{TAG}$ transgene transcript is increased when compared to wild-type non-transgenic kidneys by Northern blot (**App. II, Chapter IV**) (Trudel M 2011). The inverse abundance of the 3' end with full-lengh *Pkd1* transcript was also stated for *Pkd1* gene dosage hypomorph model, although its functional relevance was not directly tested (Lantinga-van Leeuwen, Dauwerse et al. 2004, Happe, van der Wal et al. 2013). Unpublished studies by Bacallao's group are addressing the role of these 3' end transcript(s) in cell systems that seem to be related to the regulation of fibrosis (Kher 2002, Bacallao 2011). Therefore, previously unrecognized *Pkd1* transcripts might be direct modulators of PKD pathogenesis and eventual targets for therapies. This work awaits further investigation.

PC1 functional implications: GPS cleavage and exosomes

Our *in vivo* data on Pc1 endogenous processing and trafficking uncovered novel complexity of this already problematic protein with direct relevance to the human disease.

Relative ratio of PC1 cleaved and uncleaved products. We showed that GPS cleavage and abundance of endogenous cleaved and full-length Pc1 proteins are developmentally regulated. The scenario of GPS uncleaved and cleaved products competing for the same downstream signaling pathways is appealing. The rate and efficiency of the cleavage and relative ratio of cleaved *vs* uncleaved proteins would

then be critical to maintain the proper homeostatic balance of specific signaling pathways. The full-length uncleaved Pc1 was shown to inactivate β-catenin through stabilization of ubiquitin-ligase JADE-1, whereas the cleaved CTF fragment does the opposite (Foy, Chitalia et al. 2012). This is somewhat inconsistent with high levels of β-catenin/Wnt canonical pathway in earlier stages of kidney development or at birth, which become undetectable in adult stage (**App. XI**) and highest expression of uncleaved Pc1 form before birth (Castelli, Boca et al. 2013). In addition, the GPS cleavage was suggested to be a pre-requisite for Pc1 ciliary membrane localization (Chapin, Rajendran et al. 2010) while the primary cilia is implicated in switching from β-catenin dependent/canonical to β-catenin independent/non-canonical Wnt pathway (Simons, Gloy et al. 2005). Therefore, it still remains to be determined whether it is the competitive or independent mechanism that explains the relationship between different Pc1 products.

Role of PC1 and PC2 in the endoplasmic reticulum. Some of the early studies suggested an essential role of the PC1/PC2 complex and of Pc2 in calcium regulation in the ER, but at that time the Pc1 cleavage was unknown. Our studies did not directly address and cannot exclude a role of uncleaved or cleaved forms of Pc1 in the ER. Since GPS uncleaved and cleaved Pc1 forms are present in the ER, although uncleaved is presumed prevalent, both could be involved to some extent in Ca^{2+} regulation. ER stabilization of the human truncating mutations as we showed by $Pc1_{extra}$ could alter this specific ER function, potentially through interaction and interference with some ER resident calcium channels such as polcystin-2 or Pc1 isoforms (**Chapter V, App. X, App. XV**).

Potential exosomal role of polcystin-1 in the kidney and liver. Urinary exosomes from healthy individuals, ARPKD patients and ARPKD mouse model were shown to express ADPKD and ARPKD causative proteins (Pisitkun, Shen et al. 2004, Hogan, Manganelli et al. 2009, Masyuk, Huang et al. 2010). Here, we show here increased Pc1 in mouse urinary exosomes, characterized by a specific exosomal marker Alix, in two ADPKD mouse models, $Pkd1_{TAG}$ 26 and $Pkd1_{extra}$ mice and also

exosomes secreted from MEFs in culture (**Chapter IV, V**). Since urinary exosomes have been shown to interact and bud with the primary cilia for autocrine or paracrine signaling (Hogan, Manganelli et al. 2009), it is possible that cystogenesis observed in both models is in part caused by a yet uncharacterized role of Pc1 in exosomes. In the future, this may be directly addressed by incubation of secreted $Pc1_{TAG}$ or $Pc1_{extra}$ containing exosomes with wild-type cells and analyzing the effect on cell morphology, phenotype and downstream signaling or by inhibiting Pc1 exosomal secretion. Higher abundance of $Pc1_{TAG}$ than $Pc1_{extra}$ in urinary exosomes could correlate with much faster and severe cystogenesis and manifestation of extrarenal anomalies in *Pkd1*$_{TAG}$ when compared to *Pkd1*$_{extra}$ mouse models.

From our data that demonstrates increased Pc1 in exosomes from the *Pkd1/Pkd1*$_{extra}$ transgenic mice, several additional propositions can actually be made. The role in the exosomes was linked to Wnt and ERK/MAP kinase pathways in cancer and tissues other than kidney, which are also important downstream players shown to be active in ADPKD kidney cystogenesis. If β-catenin/Wnt downregulation occurs through an unorthodox manner by exosomal secretion as shown in cancer cells, then one would expect to have less β-catenin/Wnt pathway activity in our PKD mouse models (Chairoungdua, Smith et al. 2010). The evidence of c-myc overexpression, a direct downstream target of β-catenin, in both of these models points to a rather different mechanism in kidney epithelial cells (**Chapter IV, V, App. III**). In addition, our data show that both β-catenin and myc are upregulated in *Pkd1*$^{-/-}$ and *SBPkd1*$_{TAG}$ kidneys and inactivation of c-Myc in the *SBPkd1*$_{TAG}$ overexpressing model partially rescues kidney cystogenesis (**App. III**) (Couillard 2008). It cannot be excluded that Pc1 containing exosomes are a way to regulate basal intracellular Pc1 levels or sequester pathways other than Wnts such as TGFβ for myofibroblast formation, as described in cancer. Additional arguments that support this hypothesis can be retrieved from studies on interactions between biliary exosomes and liver cholangiocytes. Based on pre-cystic elongation of the cilia in *Pkd1*$_{TAG}$ kidney epithelia and exosomal ability to bud with the cilium, we propose further elongation of the cilia by a process of budding of extracellular exosomal vesicles to the cilia, and predict an increased

autocrine/paracrine exosomal budding and ciliary signaling. Our budding-causative cilia elongation would not necessarily require IFTs/BBsome, although their relative abundance would need to be tested. Longer cilia in Nphp3/pcy, Nphp9/Nek8 and R4227X mutants have been recently reported (Bergmann, Fliegauf et al. 2008, Smith, Bukanov et al. 2006, Hopp, Ward et al. 2012) and when assessed not necessarily associated with increased levels of Pc1 or exosomal secretion of Pc1 (Hopp, Ward et al. 2012).

As we proposed for the kidney, exosomal localization of Pc1 could also play a very important role in the liver, which is indeed supported by several findings. First, rat and mouse normal biliary duct cholangiocytes (NBC) express Pc1 (Masyuk, Huang et al. 2010). Second, when biliary exosomes are incubated with isolated NBC, the exosomes attach to the cilia and cause a decrease in phospho-ERK, mir-15A and proliferation levels. Finally, PCK rat (ARPKD) and *Pkhd1*$^{del2/del2}$ mutants both showed increased number of biliary exosomes by EM, but importantly, also accumulation of Pc1 in the second liver disease mouse model (**Chapter I: Table 6, 8C**) (Masyuk, Huang et al. 2010). Furthermore, the number of exosomes per cilia and number of cilia with attached exosomes were both shown to increase in these ARPKD models. Our findings of Pc1 increase in urinary exosomes secreted from the kidney of *Pkd1*$_{TAG}$ mice are somewhat consistent with these reports, although a different mechanism may be functional in the kidney and liver. Since many mutants (*Pkd2*$^{WS25/-}$, *Pkhd1*^{del2}, *Pkd1*$^{V/V}$, *Pkd1*$_{TAG}$, *Pkd1*$^{V/V}$*;Pkd1*$_{TAG}$ and *Pkd1*$^{V/V}$*;SBPkd1*$_{TAG}$) reproduce very similar phenotypes in liver cholangiocytes, PKD pathogenesis could in fact be mediated through exosomes and downstream MAPK signaling. Pc2 has been directly linked with ERK pathway where Pc2 overexpression leads to an increase in phospho-Erk levels (Park, Sung et al. 2009). We show that Pc1 overexpression also leads to increased Pc2 and phospho-Erk levels (**App. XV**). Next, since ADPKD and ARPKD seem to have interrelated pathologies at multiple levels that probably interact in common protein networks, inactivation of one of the members from the complex (eg. *Pkhd1*) could induce abnormal exosomal secretion of others due to altered complex stoichiometry (eg. Pc1 in *Pkhd1*^{del2} mutant), with most likely adverse intracellular and extracellular functions.

Finally, we also showed that *Pkd1*$_{TAG}$ transgenic mice develop liver cysts associated with increased proliferation in late adulthood (**Chapter IV**). Analogous to the human ADPKD, at least in the liver of *Pkd1*$_{TAG}$*26* and *Pkd1*$^{V/V}$*; Pkd1*$_{TAG}$ line, females are more severely affected than males. This penetrance of cystogenesis, which prevails in females, can be explained by the fact that ‘’estrogen-sensitive cells’’/cholangiocytes *i.e.,* epithelial cells of the liver that develop cysts, express high levels of estrogen receptors (ER). Accordingly, the exosomal/ERK pathway in liver cystogenesis with estrogen receptor signaling is shown to have pivotal implications in proliferation of the biliary duct epithelia via ERK/Src signaling axis.

Finally, as suggested for blood cells and *in vitro* epithelial cells, excess of Pc1 could mediate stronger adhesion to the cilia or/and interaction with a specific ligand on exosome-recipient cells. It needs to be determined whether this stronger interaction takes place in Pc1 overexpressing cells and if it is causative of cilia-dependent mechanisms *i.e.,* increasing cAMP-ERK signaling critical for proliferation of the cholangiocytes. The functional significance of Pc1 exosomal secretion remains to be confirmed but is a very compelling concept for a focal cystic disease in tubular ductal structures (kidney and liver) where one type of tubule or duct may secrete diffusible factors that can interact with another type further on. Understanding the role of Pc1 in exosomes could eventually modulate design for an alternative therapeutic approach in ADPKD disease through delivery of specific molecules since exosomes are ‘’*similar to liposomes could be their ability to cross the blood-brain barrier, making them a true systemic signalling carrier* ‘’ (Graner, Alzate et al. 2009).

Insight into ADPKD mutations and therapeutic approaches

In this thesis, we demonstrate that the proper dosage of *Pkd1* levels must be achieved for kidney homeostasis. Human ADPKD expresses sustained and increased *Pkd1*/Pc1 levels in the majority of cysts, while a minority of cysts lack *Pkd1*/Pc1 expression. The overexpression of *Pkd1* is pathogenetic, in addition to complete absence or reduced levels of Pc1 (**Chapter I, IV, Table 8A, B**). Modulation of *Pkd1* levels to a homeostatic threshold is likely to be difficult to impossible as a therapeutic approach. Therefore,

either gene or protein/antibody therapy against ADPKD do not seem to be realistic alternatives for now.

Our study addressing the GPS cleavage and PC1 biogenesis *in vivo* uncovered a new alternative approach for correction of *PKD1* human mutations by rescuing/''chaperoning'' the C-terminal fragment and rescuing the GPS cleavage. Thus, this kind of rescue could potentially become applicable to many other *PKD1* GPS cleavage deficient mutants that act as functional hypomorphs with less Pc1 (cleaved or uncleaved) at proper localizations (membrane, cilia, ER) in both the kidney and liver.

We also provide further evidence for implication of c-myc/β-catenin/Wnt pathway as important target for ADPKD (**Chapter IV, V, App. III.A, B**) (Emami, Nguyen et al. 2004, Lepourcelet, Chen et al. 2004, Huang, Cheng et al. 2006, Handeli and Simon 2008, Delmore, Issa et al. 2011). Inhibitors targeting the BET domain of c-myc or interaction with its partner Max are under intensive investigation *in vitro* and *in vivo* with promising results in the cancer field that could be extrapolated and eventually used for ADPKD (Huang, Cheng et al. 2006, Delmore, Issa et al. 2011). Finally, we offer to the scientific community a few indispensible orthologous PKD models to actually test these therapies for translational studies of the human pathology.

Closure statements with short summary of findings

The key findings of this study encompass multiple levels, starting from the fundamental understanding of the ADPKD pathogenetic mechanism in renal and extrarenal tissues, to the generation of relevant mouse models for the study of human disease by overexpression of the full-length and humanized *Pkd1* mutation, and finally, ending with the characterization of *in vivo* biogenesis of the major ADPKD causative agent, Pc1. Taken together, and summarized in **Fig. 3**, we believe that the findings of this thesis lead to a better understanding of human ADPKD and make a critical contribution by providing novel concepts and tools to study and test ultimate therapeutic therapies for this devastating disease.

Figure 3. Summary of novel findings of this thesis integrated with published data

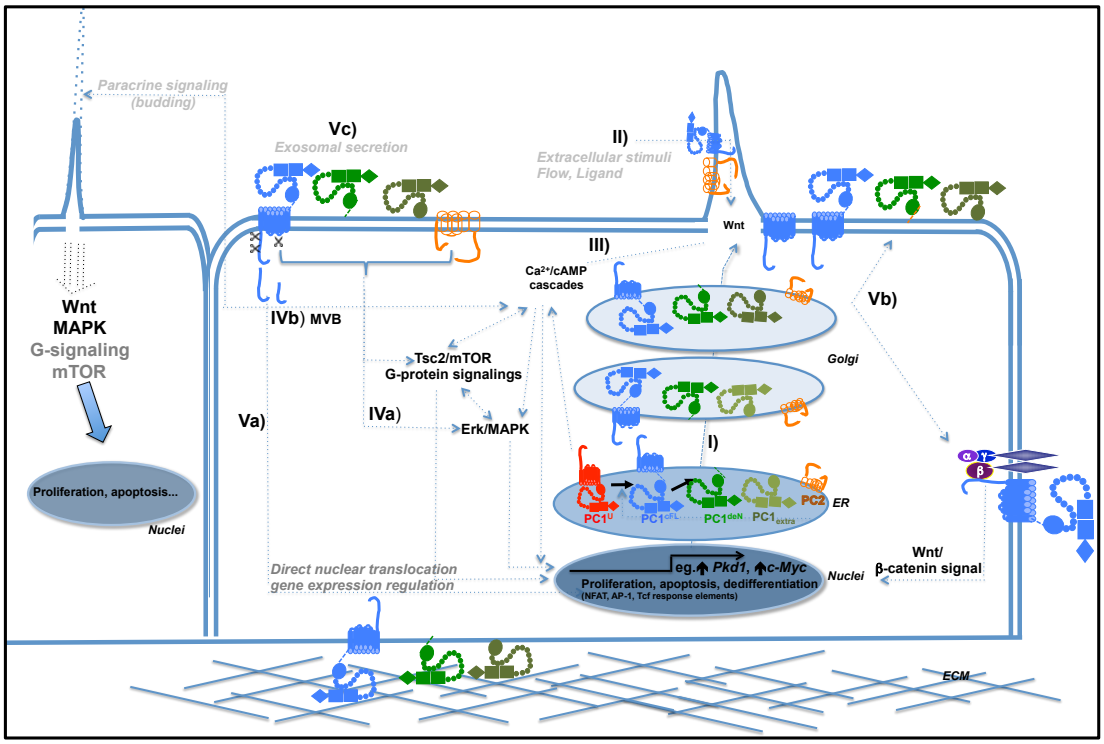

Legend: Schematic representation of PC1 biogenesis, proposed putative roles (wild-type and mutant PC1) and identified downstream factors. (I) Pc1 is cleaved in the ER at the GPS motif. In vivo, this cleavage generates NTF and CTF subunits that are tethered together, and a newly identified detached NTF product, named $Pc1^{deN}$ (**Ch. VI**). The NTF-like $Pc1_{extra}$ mutant accumulates in the ER, but can also partially escape the ER presumably via cross-interaction with an endogenous CTF, Pc2 or other unrelated molecule (**Ch. V, App. X**). Pc2 localizes to the ER but also at the plasma membrane and becomes stabilized following ER stress (Yang, Zheng et al. 2013). **(II)** Pc1 was suggested to act as a sensor in the primary cilia and as a signaling transducer in a calcium dependent or independent fashion (e.g Wnt). Pc1 sensing in the primary cilia or at the non-ciliary membrane may be responsible for **(III)** an increase of cAMP levels in the *Pkd1* GOF mice (our unpublished data). The cAMP increase correlates with stimulation of phospho-ERK levels, higher proliferation and elongation of the cilia in $Pkd1_{TAG}$ kidneys (**Ch. IV, App. XV**). **(IVa)** Both, $Pkd1_{extra}$ and $Pkd1_{TAG}$ mice, show increased Pc2 levels that possibly result in increased Pc1, $Pc1_{extra}$/Pc2 complexes in the cilia or the non-ciliary membrane (**Ch. V, App. XV**). Consistently, Pc2 overexpression was previously associated with activation of Erk and elevated proliferation (Park, Sung et al. 2009). At the membrane, Pc1 and Pc2 may also be endocytosed and fused to MVB for exosomal secretion and eventual intercellular paracrine communication **(IVb) (Ch. IV, V)**. Pc2 was also shown to enhance the GPS Pc1 cleavage **(Va)** (Chapin, Rajendran et al. 2010). Other sequential processing was proposed for Pc1, and some of the resulting shorter CTF products were shown to translocate to the nucleus (**Ch.I: S-6**). Nuclear Pc1 may directly affect several important signaling pathways (NFAT, AP1, Wnt/β-catenin, STAT, etc). The Wnt pathway seems very important in PKD. Pc1 was shown to directly interact with β-catenin, the main component of canonical Wnt signaling and involved in cell proliferation **(Vb) (Table 3).** C-myc, a downstream effector of the β-catenin pathway, is upregulated in $Pkd1_{TAG}$, $Pkd1_{extra}$ and $SBPkd1_{TAG}$ kidneys (**Ch. IV, V, App. III**). Hypothetically, based on overexpression of c-myc being associated with cystogenesis and enhanced *Pkd1*/Pc1 levels, c-Myc could regulate *Pkd1* gene expression to influence the *Pkd1/Pkd2* homeostatic dosage (**App. III**). Paracrine exosomal cellular intercommunication was proposed for both Wnt and MAPK pathways, two pathways associated with ADPKD, and $Pc1_{TAG}$, $Pc1_{extra}$ and Pc2 are detected in the exosomes **(Vc) (Ch. IV, V)**. It is possible that other signals/pathways, known to be modulated by Pc1, are also transmitted/affected in the kidney epithelial cells via exosomes. This scheme reflects regrouped information about the implication of Pc1 in epithelial cells of the kidney and the liver, two organs affected by the cystogenic phenotype of ADPKD, except the report about the exosomal Wnt effect, which was described in cancer cells. ECM: extracellular matrix, Ch: Chapitre, App: appendix.

CHAPTER X – SIGNIFICANCE OF THE WORK

Problematic: Understanding the ADPKD pathogenetic mechanism is of critical importance for developing therapeutic strategies but is still under a lot of investigation. The *Pkd1* gene decrease mouse models are numerous and lead to rapid PKD but diverge in important aspects of the human ADPKD: they do not completely recapitulate the slow progression of the human kidney disease, and they do not manifest some important extrarenal defects or sustained *PKD1*/PC1 expression observed in humans. Therefore, although attractive, the *PKD1* LOF mechanism might not be the sole explanation for ADPKD. Complexity of the polycystin-1 protein (PC1) gene product responsible for this most common human genetic disease is impressive as well: starting from its bilinear structure (N- and C- terminal cleaved fragments, NTF and CTF, in cell adhesion and intracellular signaling, respectively), presence of potential *PKD1*/PC1 isoforms, lack of ligand/orphan, unavailable functional biochemical tools, low abundance of the protein, temporal and spatial regulation of the gene and protein expression pattern to association with numerous very important signaling pathways. All of these characteristics together make it quite challenging to study ADPDK for translational impact and explain to some extent the unsatisfying results from current clinical studies in humans.

Discoveries: In this thesis, we generated an *in vivo* mouse model that reproduces both human renal and extrarenal disease by *Pkd1* transgenesis. Our work not only offers a new, relevant and orthologous working *in vivo* tool but is also informative about human ADPKD pathogenetic mechanism. This work clearly demonstrates that an increase of endogenous wild-type *Pkd1* levels, in addition to *Pkd1* loss-of-function, is sufficient for PKD cystic pathogenesis, and implies a *Pkd1* dosage/balance regulation. Mimicking a human truncating mutation that consisted of Pc1 extracellular domain in mice lead to later onset of ADPKD. Both these PKD models, *Pkd1* gene increase and *Pkd1* truncating mutant, were associated with alterated c-myc and Pc2 expression levels, which supports their role as downstream modulators in ADPKD, Pc1/Pc2 interdependence and suggests their more general implication in polycystic kidney disease. Our work also further provides evidence for

increasing complexity of Pc1 by GPS cleavage with discovery of a novel detached Pc1 isoform. We identified this new endogenous CTF-independent NTF form as a predominant Pc1 molecule on the cell surface *in vivo*. Biochemical analysis led us to uncover interdependence in the trafficking of endogenous Pc1 cleaved and detached forms and their functional importance in the kidney. Furthermore, a crucial role of Pc1 GPS cleavage products and more specifically the Pc1 uncleaved form was also demonstrated for adult liver homeostasis. Finally, we showed the involvement of some common signaling pathways in kidney injury process (early and late stages) and ADPKD using our *Pkd1* transgenic models. Unlike *Pkd1*/*Pkd2* gene decrease, severity of the *Pkd1* increase phenotype was not significantly accentuated following IRI presumably due to the pre-conditioned cellular conditions.

Importance: This thesis covered a couple of facets of the ADPKD problematic by generating *in vivo* genetic tools and applying them to the human pathogenetic mechanism, renal and extrarenal phenotypes, PC1 biogenesis and downstream effectors and signaling. Given that both *Pkd1* gene increase and *Pkd1* truncated human mutation were associated with PKD, gene therapy or modulation of *PKD1* levels might be a very delicate task and ineffective for some ADPKD patients. For prevention of ADPKD, therapies might require adjustments depending on the type and position of the mutation and mutational defect. Since symptoms are most frequently detected at very progressed stages of the disease, targeting the modulators such as c-myc and Pc2, common to all our PKD models and human ADPKD, could improve treatment for ADPKD patients, whose only current choice is dialysis or transplantation. It is also very encouraging that eventual therapeutic approaches might be expanded to an even bigger number of patients based on discovery of parallel pathways in AKI and ADPKD. Finally, this study highlights the importance of studing various mouse models for a broader view (LOF and GOF) of this complex human disease and for assessing novel therapies.

CHAPTER XI - CITATIONS

(1994). "The polycystic kidney disease 1 gene encodes a 14 kb transcript and lies within a duplicated region on chromosome 16. The European Polycystic Kidney Disease Consortium." Cell **77**(6): 881-894.

Abdul-Majeed, S., B. C. Moloney and S. M. Nauli (2012). "Mechanisms regulating cilia growth and cilia function in endothelial cells." Cell Mol Life Sci **69**(1): 165-173.

Abdul-Majeed, S. and S. M. Nauli (2011). "Dopamine receptor type 5 in the primary cilia has dual chemo- and mechano-sensory roles." Hypertension **58**(2): 325-331.

Ahrabi, A. K., F. Jouret, E. Marbaix, C. Delporte, S. Horie, S. Mulroy, C. Boulter, R. Sandford and O. Devuyst (2010). "Glomerular and proximal tubule cysts as early manifestations of Pkd1 deletion." Nephrol Dial Transplant **25**(4): 1067-1078.

Antiga, L., M. Piccinelli, G. Fasolini, B. Ene-Iordache, P. Ondei, S. Bruno, G. Remuzzi and A. Remuzzi (2006). "Computed tomography evaluation of autosomal dominant polycystic kidney disease progression: a progress report." Clin J Am Soc Nephrol **1**(4): 754-760.

Anyatonwu, G. I., M. Estrada, X. Tian, S. Somlo and B. E. Ehrlich (2007). "Regulation of ryanodine receptor-dependent calcium signaling by polycystin-2." Proc Natl Acad Sci U S A **104**(15): 6454-6459.

Arac, D., G. Aust, D. Calebiro, F. B. Engel, C. Formstone, A. Goffinet, J. Hamann, R. J. Kittel, I. Liebscher, H. H. Lin, K. R. Monk, A. Petrenko, X. Piao, S. Promel, H. B. Schioth, T. W. Schwartz, M. Stacey, Y. A. Ushkaryov, M. Wobus, U. Wolfrum, L. Xu and T. Langenhan (2012). "Dissecting signaling and functions of adhesion G protein-coupled receptors." Ann N Y Acad Sci **1276**: 1-25.

Arac, D., A. A. Boucard, M. F. Bolliger, J. Nguyen, S. M. Soltis, T. C. Sudhof and A. T. Brunger (2012). "A novel evolutionarily conserved domain of cell-adhesion GPCRs mediates autoproteolysis." EMBO J **31**(6): 1364-1378.

Arcasoy, M. O. and P. G. Gallagher (1995). "Hematologic disorders and nonimmune hydrops fetalis." Semin Perinatol **19**(6): 502-515.

Arnould, T., E. Kim, L. Tsiokas, F. Jochimsen, W. Gruning, J. D. Chang and G. Walz (1998). "The polycystic kidney disease 1 gene product mediates protein kinase C alpha-dependent and c-Jun N-terminal kinase-dependent activation of the transcription factor AP-1." J Biol Chem **273**(11): 6013-6018.

Atala, A., M. R. Freeman, J. Mandell and D. R. Beier (1993). "Juvenile cystic kidneys (jck): a new mouse mutation which causes polycystic kidneys." Kidney Int **43**(5): 1081-1085.

Attanasio, M., N. H. Uhlenhaut, V. H. Sousa, J. F. O'Toole, E. Otto, K. Anlag, C. Klugmann, A. C. Treier, J. Helou, J. A. Sayer, D. Seelow, G. Nurnberg, C. Becker, A. E. Chudley, P. Nurnberg, F. Hildebrandt and M. Treier (2007). "Loss of GLIS2 causes nephronophthisis in humans and mice by increased apoptosis and fibrosis." Nat Genet **39**(8): 1018-1024.

Audrezet, M. P., E. Cornec-Le Gall, J. M. Chen, S. Redon, I. Quere, J. Creff, C. Benech, S. Maestri, Y. Le Meur and C. Ferec (2012). "Autosomal dominant polycystic kidney disease: comprehensive mutation analysis of PKD1 and PKD2 in 700 unrelated patients." Hum Mutat **33**(8): 1239-1250.

Babich, V., W. Z. Zeng, B. I. Yeh, O. Ibraghimov-Beskrovnaya, Y. Cai, S. Somlo and C. L. Huang (2004). "The N-terminal extracellular domain is required for polycystin-1-dependent channel activity." J Biol Chem **279**(24): 25582-25589.

Bacallao, R., McClintiock, J.N., Kurbegovic, A., Trudel, M. (2011). Transcriptional complexity of the PKD1 gene. Polycystic kidney disease: From bench to bedside, Saxtons River, Vermont, USA.

Bakeberg, J. L., R. Tammachote, J. R. Woollard, M. C. Hogan, H. F. Tuan, M. Li, J. M. van Deursen, Y. Wu, B. Q. Huang, V. E. Torres, P. C. Harris and C. J. Ward (2011). "Epitope-tagged Pkhd1 tracks the processing, secretion, and localization of fibrocystin." J Am Soc Nephrol **22**(12): 2266-2277.

Bananis, E., S. Nath, K. Gordon, P. Satir, R. J. Stockert, J. W. Murray and A. W. Wolkoff (2004). "Microtubule-dependent movement of late endocytic vesicles in vitro: requirements for Dynein and Kinesin." Mol Biol Cell **15**(8): 3688-3697.

Barr, M. M. (2003). "Super models." Physiol Genomics **13**(1): 15-24.

Barr, M. M. and P. W. Sternberg (1999). "A polycystic kidney-disease gene homologue required for male mating behaviour in C. elegans." Nature **401**(6751): 386-389.

Bastos, A. P., K. Piontek, A. M. Silva, D. Martini, L. F. Menezes, J. M. Fonseca, Fonseca, II, G. G. Germino and L. F. Onuchic (2009). "Pkd1 haploinsufficiency increases renal damage and induces microcyst formation following ischemia/reperfusion." J Am Soc Nephrol **20**(11): 2389-2402.

Battini, L., S. Macip, E. Fedorova, S. Dikman, S. Somlo, C. Montagna and G. L. Gusella (2008). "Loss of polycystin-1 causes centrosome amplification and genomic instability." Hum Mol Genet **17**(18): 2819-2833.

Beauchemin, H., M. J. Blouin and M. Trudel (2004). "Differential regulatory and compensatory responses in hematopoiesis/erythropoiesis in alpha- and beta-globin hemizygous mice." J Biol Chem **279**(19): 19471-19480.

Bergmann, C., J. von Bothmer, N. Ortiz Bruchle, A. Venghaus, V. Frank, H. Fehrenbach, T. Hampel, L. Pape, A. Buske, J. Jonsson, N. Sarioglu, A. Santos, J. C. Ferreira, J. U. Becker, R. Cremer, J. Hoefele, M. R. Benz, L. T. Weber, R. Buettner and K. Zerres (2011). "Mutations in multiple PKD genes may explain early and severe polycystic kidney disease." J Am Soc Nephrol **22**(11): 2047-2056.

Bergmann, C., M. Fliegauf, N. O. Bruchle, V. Frank, H. Olbrich, J. Kirschner, B. Schermer, I. Schmedding, A. Kispert, B. Kranzlin, G. Nurnberg, C. Becker, T. Grimm, G. Girschick, S. A. Lynch, P. Kelehan, J. Senderek, T. J. Neuhaus, T. Stallmach, H. Zentgraf, P. Nurnberg, N. Gretz, C. Lo, S. Lienkamp, T. Schafer, G. Walz, T. Benzing, K. Zerres and H. Omran (2008). "Loss of nephrocystin-3 function can cause embryonic lethality, Meckel-Gruber-like syndrome, situs inversus, and renal-hepatic-pancreatic dysplasia." Am J Hum Genet **82**(4): 959-970.

Bertuccio, C. A., H. C. Chapin, Y. Cai, K. Mistry, V. Chauvet, S. Somlo and M. J. Caplan (2009). "Polycystin-1 C-terminal cleavage is modulated by polycystin-2 expression." J Biol Chem **284**(31): 21011-21026.

Besschetnova, T. Y., E. Kolpakova-Hart, Y. Guan, J. Zhou, B. R. Olsen and J. V. Shah (2010). "Identification of signaling pathways regulating primary cilium length and flow-mediated adaptation." Curr Biol **20**(2): 182-187.

Beyenbach, K. W., H. Skaer and J. A. Dow (2010). "The developmental, molecular, and transport biology of Malpighian tubules." Annu Rev Entomol **55**: 351-374.

Bhunia, A. K., K. Piontek, A. Boletta, L. Liu, F. Qian, P. N. Xu, F. J. Germino and G. G. Germino (2002). "PKD1 induces p21(waf1) and regulation of the cell cycle via direct activation of the JAK-STAT signaling pathway in a process requiring PKD2." Cell **109**(2): 157-168.

Bihoreau, M. T., I. Ceccherini, J. Browne, B. Kranzlin, G. Romeo, G. M. Lathrop, M. R. James and N. Gretz (1997). "Location of the first genetic locus, PKDr1, controlling autosomal dominant polycystic kidney disease in Han:SPRD cy/+ rat." Hum Mol Genet **6**(4): 609-613.

Boletta, A., F. Qian, L. F. Onuchic, A. K. Bhunia, B. Phakdeekitcharoen, K. Hanaoka, W. Guggino, L. Monaco and G. G. Germino (2000). "Polycystin-1, the gene product of PKD1, induces resistance to apoptosis and spontaneous tubulogenesis in MDCK cells." Mol Cell **6**(5): 1267-1273.

Bonnet, C. S., M. Aldred, C. von Ruhland, R. Harris, R. Sandford and J. P. Cheadle (2009). "Defects in cell polarity underlie TSC and ADPKD-associated cystogenesis." Hum Mol Genet **18**(12): 2166-2176.

Borovina, A. and B. Ciruna (2013). "IFT88 Plays a Cilia- and PCP-Independent Role in Controlling Oriented Cell Divisions during Vertebrate Embryonic Development." Cell Rep **5**(1): 37-43.

Bouchard, M., A. Souabni, M. Mandler, A. Neubuser and M. Busslinger (2002). "Nephric lineage specification by Pax2 and Pax8." Genes Dev **16**(22): 2958-2970.

Boucher, C. A., H. H. Ward, R. L. Case, K. S. Thurston, X. Li, A. Needham, E. Romero, D. Hyink, S. Qamar, T. Roitbak, S. Powell, C. Ward, P. D. Wilson, A. Wandinger-Ness and R. N. Sandford (2011). "Receptor protein tyrosine phosphatases are novel components of a polycystin complex." Biochim Biophys Acta **1812**(10): 1225-1238.

Boulter, C., S. Mulroy, S. Webb, S. Fleming, K. Brindle and R. Sandford (2001). "Cardiovascular, skeletal, and renal defects in mice with a targeted disruption of the Pkd1 gene." Proc Natl Acad Sci U S A **98**(21): 12174-12179.

Brasier, J. L. and E. P. Henske (1997). "Loss of the polycystic kidney disease (PKD1) region of chromosome 16p13 in renal cyst cells supports a loss-of-function model for cyst pathogenesis." J Clin Invest **99**(2): 194-199.

Brem, G., R. Wanke, E. Wolf, T. Buchmuller, M. Muller, B. Brenig and W. Hermanns (1989). "Multiple consequences of human growth hormone expression in transgenic mice." Mol Biol Med **6**(6): 531-547.

Breuer, W. V., E. Mack and A. Rothstein (1988). "Activation of K+ and Cl- channels by Ca2+ and cyclic AMP in dissociated kidney epithelial (MDCK) cells." Pflugers Arch **411**(4): 450-455.

Brill, S. R., K. E. Ross, C. J. Davidow, M. Ye, J. J. Grantham and M. J. Caplan (1996). "Immunolocalization of ion transport proteins in human autosomal dominant polycystic kidney epithelial cells." Proc Natl Acad Sci U S A **93**(19): 10206-10211.

Brook-Carter, P. T., B. Peral, C. J. Ward, P. Thompson, J. Hughes, M. M. Maheshwar, M. Nellist, V. Gamble, P. C. Harris and J. R. Sampson (1994). "Deletion of the TSC2 and PKD1 genes associated with severe infantile polycystic kidney disease--a contiguous gene syndrome." Nat Genet **8**(4): 328-332.

Brown, C. L., K. C. Maier, T. Stauber, L. M. Ginkel, L. Wordeman, I. Vernos and T. A. Schroer (2005). "Kinesin-2 is a motor for late endosomes and lysosomes." Traffic **6**(12): 1114-1124.

Brown, M. S. and J. L. Goldstein (1997). "The SREBP pathway: regulation of cholesterol metabolism by proteolysis of a membrane-bound transcription factor." Cell **89**(3): 331-340.

Brown, T. (2013). "Tolvaptan Not Recommended for ADPKD." Medscape Medical News.

Bui-Xuan, E. F., Q. Li, X. Z. Chen, C. A. Boucher, R. Sandford, J. Zhou and N. Basora (2006). "More than colocalizing with polycystin-1, polycystin-L is in the centrosome." Am J Physiol Renal Physiol **291**(2): F395-406.

Cadieux, C., R. Harada, M. Paquet, O. Cote, M. Trudel, A. Nepveu and M. Bouchard (2008). "Polycystic kidneys caused by sustained expression of Cux1 isoform p75." J Biol Chem **283**(20): 13817-13824.

Cai, Y., G. Anyatonwu, D. Okuhara, K. B. Lee, Z. Yu, T. Onoe, C. L. Mei, Q. Qian, L. Geng, R. Wiztgall, B. E. Ehrlich and S. Somlo (2004). "Calcium dependence of polycystin-2 channel activity is modulated by phosphorylation at Ser812." J Biol Chem **279**(19): 19987-19995.

Cai, Y., Y. Maeda, A. Cedzich, V. E. Torres, G. Wu, T. Hayashi, T. Mochizuki, J. H. Park, R. Witzgall and S. Somlo (1999). "Identification and characterization of polycystin-2, the PKD2 gene product." J Biol Chem **274**(40): 28557-28565.

Cano-Gauci, D. F., H. H. Song, H. Yang, C. McKerlie, B. Choo, W. Shi, R. Pullano, T. D. Piscione, S. Grisaru, S. Soon, L. Sedlackova, A. K. Tanswell, T. W. Mak, H. Yeger, G. A. Lockwood, N. D. Rosenblum and J. Filmus (1999). "Glypican-3-deficient mice exhibit developmental overgrowth and some of the abnormalities typical of Simpson-Golabi-Behmel syndrome." J Cell Biol **146**(1): 255-264.

Carpenter, C., A. A. Honkanen, H. Mashimo, K. A. Goss, P. Huang, M. C. Fishman, M. Asaad, C. R. Dorso and H. Cheung (1996). "Renal abnormalities in mutant mice." Nature **380**(6572): 292.

Castelli, M., M. Boca, M. Chiaravalli, H. Ramalingam, I. Rowe, G. Distefano, T. Carroll and A. Boletta (2013). "Polycystin-1 binds Par3/aPKC and controls convergent extension during renal tubular morphogenesis." Nat Commun **4**: 2658.

Casuscelli, J., S. Schmidt, B. DeGray, E. T. Petri, A. Celic, E. Folta-Stogniew, B. E. Ehrlich and T. J. Boggon (2009). "Analysis of the cytoplasmic interaction between polycystin-1 and polycystin-2." Am J Physiol Renal Physiol **297**(5): F1310-1315.

Cebotaru, V., L. Cebotaru, H. Kim, M. Chiaravalli, A. Boletta, F. Qian and W. B. Guggino (2014). "Polycystin-1 negatively regulates Polycystin-2 expression via the aggresome/autophagosome pathway." J Biol Chem **289**(10): 6404-6414.

Chacon-Heszele, M. F., D. Ren, A. B. Reynolds, F. Chi and P. Chen (2012). "Regulation of cochlear convergent extension by the vertebrate planar cell polarity pathway is dependent on p120-catenin." Development **139**(5): 968-978.

Chae, S. W., E. Y. Cho, M. S. Park, K. B. Lee, H. Kim and U. Kim (2006). "Polycystin-1 expression in fetal, adult and autosomal dominant polycystic kidney." J Korean Med Sci **21**(3): 425-429.

Chai, O. H., C. H. Song, S. K. Park, W. Kim and E. S. Cho (2013). "Molecular regulation of kidney development." Anat Cell Biol **46**(1): 19-31.

Chairoungdua, A., D. L. Smith, P. Pochard, M. Hull and M. J. Caplan (2010). "Exosome release of beta-catenin: a novel mechanism that antagonizes Wnt signaling." J Cell Biol **190**(6): 1079-1091.

Chaki, M., R. Airik, A. K. Ghosh, R. H. Giles, R. Chen, G. G. Slaats, H. Wang, T. W. Hurd, W. Zhou, A. Cluckey, H. Y. Gee, G. Ramaswami, C. J. Hong, B. A. Hamilton, I. Cervenka, R. S. Ganji, V. Bryja, H. H. Arts, J. van Reeuwijk, M. M. Oud, S. J. Letteboer, R. Roepman, H. Husson, O. Ibraghimov-Beskrovnaya, T. Yasunaga, G.

Walz, L. Eley, J. A. Sayer, B. Schermer, M. C. Liebau, T. Benzing, S. Le Corre, I. Drummond, S. Janssen, S. J. Allen, S. Natarajan, J. F. O'Toole, M. Attanasio, S. Saunier, C. Antignac, R. K. Koenekoop, H. Ren, I. Lopez, A. Nayir, C. Stoetzel, H. Dollfus, R. Massoudi, J. G. Gleeson, S. P. Andreoli, D. G. Doherty, A. Lindstrad, C. Golzio, N. Katsanis, L. Pape, E. B. Abboud, A. A. Al-Rajhi, R. A. Lewis, H. Omran, E. Y. Lee, S. Wang, J. M. Sekiguchi, R. Saunders, C. A. Johnson, E. Garner, K. Vanselow, J. S. Andersen, J. Shlomai, G. Nurnberg, P. Nurnberg, S. Levy, A. Smogorzewska, E. A. Otto and F. Hildebrandt (2012). "Exome capture reveals ZNF423 and CEP164 mutations, linking renal ciliopathies to DNA damage response signaling." Cell **150**(3): 533-548.

Chan, Y. M. and Y. N. Jan (1999). "Presenilins, processing of beta-amyloid precursor protein, and notch signaling." Neuron **23**(2): 201-204.

Chang, C. P., B. W. McDill, J. R. Neilson, H. E. Joist, J. A. Epstein, G. R. Crabtree and F. Chen (2004). "Calcineurin is required in urinary tract mesenchyme for the development of the pyeloureteral peristaltic machinery." J Clin Invest **113**(7): 1051-1058.

Chang, M. Y., C. M. Kuok, Y. C. Chen, S. J. Ryu, Y. C. Tian, Y. H. Wu-Chou, F. J. Tseng and C. W. Yang (2010). "Comparison of intracerebral hemorrhage and subarachnoid hemorrhage in patients with autosomal-dominant polycystic kidney disease." Nephron Clin Pract **114**(2): c158-164.

Chang, M. Y. and A. C. Ong (2012). "Mechanism-based therapeutics for autosomal dominant polycystic kidney disease: recent progress and future prospects." Nephron Clin Pract **120**(1): c25-34; discussion c35.

Chang, M. Y., E. Parker, S. Ibrahim, J. R. Shortland, M. E. Nahas, J. L. Haylor and A. C. Ong (2006). "Haploinsufficiency of Pkd2 is associated with increased tubular cell

proliferation and interstitial fibrosis in two murine Pkd2 models." Nephrol Dial Transplant **21**(8): 2078-2084.

Chapin, H. C., V. Rajendran and M. J. Caplan (2010). "Polycystin-1 surface localization is stimulated by polycystin-2 and cleavage at the G protein-coupled receptor proteolytic site." Mol Biol Cell **21**(24): 4338-4348.

Chapman, A. B., D. Rubinstein, R. Hughes, J. C. Stears, M. P. Earnest, A. M. Johnson, P. A. Gabow and W. D. Kaehny (1992). "Intracranial aneurysms in autosomal dominant polycystic kidney disease." N Engl J Med **327**(13): 916-920.

Chapman, A. B., K. Stepniakowski and F. Rahbari-Oskoui (2010). "Hypertension in autosomal dominant polycystic kidney disease." Adv Chronic Kidney Dis **17**(2): 153-163.

Chapman, A. B., V. E. Torres, R. D. Perrone, T. I. Steinman, K. T. Bae, J. P. Miller, D. C. Miskulin, F. Rahbari Oskoui, A. Masoumi, M. C. Hogan, F. T. Winklhofer, W. Braun, P. A. Thompson, C. M. Meyers, C. Kelleher and R. W. Schrier (2010). "The HALT polycystic kidney disease trials: design and implementation." Clin J Am Soc Nephrol **5**(1): 102-109.

Charron, A. J., R. L. Bacallao and A. Wandinger-Ness (2000). "ADPKD: a human disease altering Golgi function and basolateral exocytosis in renal epithelia." Traffic **1**(8): 675-686.

Charron, A. J., S. Nakamura, R. Bacallao and A. Wandinger-Ness (2000). "Compromised cytoarchitecture and polarized trafficking in autosomal dominant polycystic kidney disease cells." J Cell Biol **149**(1): 111-124.

Chauvet, V., X. Tian, H. Husson, D. H. Grimm, T. Wang, T. Hiesberger, P. Igarashi, A. M. Bennett, O. Ibraghimov-Beskrovnaya, S. Somlo and M. J. Caplan (2004).

"Mechanical stimuli induce cleavage and nuclear translocation of the polycystin-1 C terminus." J Clin Invest **114**(10): 1433-1443.

Chen, J., K. Futami, D. Petillo, J. Peng, P. Wang, J. Knol, Y. Li, S. K. Khoo, D. Huang, C. N. Qian, P. Zhao, K. Dykema, R. Zhang, B. Cao, X. J. Yang, K. Furge, B. O. Williams and B. T. Teh (2008). "Deficiency of FLCN in mouse kidney led to development of polycystic kidneys and renal neoplasia." PLoS One **3**(10): e3581.

Chen, W. C., Y. S. Tzeng and H. Li (2008). "Gene expression in early and progression phases of autosomal dominant polycystic kidney disease." BMC Res Notes **1**: 131.

Chen, X. Z., P. M. Vassilev, N. Basora, J. B. Peng, H. Nomura, Y. Segal, E. M. Brown, S. T. Reeders, M. A. Hediger and J. Zhou (1999). "Polycystin-L is a calcium-regulated cation channel permeable to calcium ions." Nature **401**(6751): 383-386.

Cheng, L. T., S. Nagata, K. Hirano, S. Yamaguchi, S. Horie, J. Ainscough and T. Tada (2012). "Cure of ADPKD by selection for spontaneous genetic repair events in Pkd1-mutated iPS cells." PLoS One **7**(2): e32018.

Chernova, M. N., D. H. Vandorpe, J. S. Clark and S. L. Alper (2005). "Expression of the polycystin-1 C-terminal cytoplasmic tail increases Cl channel activity in Xenopus oocytes." Kidney Int **68**(2): 632-641.

Chi, L., A. Galtseva, L. Chen, R. Mo, C. C. Hui and N. D. Rosenblum (2013). "Kif3a Controls Murine Nephron Number Via GLI3 Repressor, Cell Survival, and Gene Expression in a Lineage-Specific Manner." PLoS One **8**(6): e65448.

Chitalia, V. C., R. L. Foy, M. M. Bachschmid, L. Zeng, M. V. Panchenko, M. I. Zhou, A. Bharti, D. C. Seldin, S. H. Lecker, I. Dominguez and H. T. Cohen (2008). "Jade-1 inhibits Wnt signalling by ubiquitylating beta-catenin and mediates Wnt pathway inhibition by pVHL." Nat Cell Biol **10**(10): 1208-1216.

Choi, S. Y., M. F. Chacon-Heszele, L. Huang, S. McKenna, F. P. Wilson, X. Zuo and J. H. Lipschutz (2013). "Cdc42 Deficiency Causes Ciliary Abnormalities and Cystic Kidneys." J Am Soc Nephrol 24(9):1435-50.

Choi, Y. H., A. Suzuki, S. Hajarnis, Z. Ma, H. C. Chapin, M. J. Caplan, M. Pontoglio, S. Somlo and P. Igarashi (2011). "Polycystin-2 and phosphodiesterase 4C are components of a ciliary A-kinase anchoring protein complex that is disrupted in cystic kidney diseases." Proc Natl Acad Sci U S A **108**(26): 10679-10684.

Cogswell, C., S. J. Price, X. Hou, L. M. Guay-Woodford, L. Flaherty and E. C. Bryda (2003). "Positional cloning of jcpk/bpk locus of the mouse." Mamm Genome **14**(4): 242-249.

Cornec-Le Gall, E., M. P. Audrezet, J. M. Chen, M. Hourmant, M. P. Morin, R. Perrichot, C. Charasse, B. Whebe, E. Renaudineau, P. Jousset, M. P. Guillodo, A. Grall-Jezequel, P. Saliou, C. Ferec and Y. Le Meur (2013). "Type of PKD1 Mutation Influences Renal Outcome in ADPKD." J Am Soc Nephrol **24**(6): 1006-1013.

Côté, O. (2009). Analyse fonctionelle de la polycystine-1 et de son domaine intracellulaire dans le développement de la polykystose rénale autosomique dominante. M.Sc Thesis, Université de Montréal.

Couillard, M. (2008). c-Myc dans le développement rénal et polykystose rénale autosomique dominante. Ph.D. thesis, Université de Montréal.

Cowley, B. D., Jr., S. Gudapaty, A. L. Kraybill, B. D. Barash, M. A. Harding, J. P. Calvet and V. H. Gattone, 2nd (1993). "Autosomal-dominant polycystic kidney disease in the rat." Kidney Int **43**(3): 522-534.

Crocker, J. F., A. G. Stewart, J. M. Sparling and M. E. Bruneau (1976). "Steroid-induced polycystic kidneys in the newborn rat." Am J Pathol **82**(2): 373-380.

D'Agati, V. and M. Trudel (1992). "Lectin characterization of cystogenesis in the SBM transgenic model of polycystic kidney disease." J Am Soc Nephrol **3**(4): 975-983.

Dalagiorgou, G., C. Piperi, U. Georgopoulou, C. Adamopoulos, E. K. Basdra and A. G. Papavassiliou (2013). "Mechanical stimulation of polycystin-1 induces human osteoblastic gene expression via potentiation of the calcineurin/NFAT signaling axis." Cell Mol Life Sci 70(1):167-80.

Dang, Y., B. Liu, P. Xu, P. Zhu, Y. Zhai, M. Liu and X. Ye (2014). "Gpr48 deficiency induces polycystic kidney lesions and renal fibrosis in mice by activating Wnt signal pathway." PLoS One **9**(3): e89835.

Daoust, M. C., D. M. Reynolds, D. G. Bichet and S. Somlo (1995). "Evidence for a third genetic locus for autosomal dominant polycystic kidney disease." Genomics **25**(3): 733-736.

Davidow, C. J., R. L. Maser, L. A. Rome, J. P. Calvet and J. J. Grantham (1996). "The cystic fibrosis transmembrane conductance regulator mediates transepithelial fluid secretion by human autosomal dominant polycystic kidney disease epithelium in vitro." Kidney Int **50**(1): 208-218.

Dedoussis, G. V., Y. Luo, P. Starremans, S. Rossetti, A. J. Ramos, H. F. Cantiello, E. Katsareli, P. Ziroyannis, K. Lamnissou, P. C. Harris and J. Zhou (2008). "Co-inheritance of a PKD1 mutation and homozygous PKD2 variant: a potential modifier in autosomal dominant polycystic kidney disease." Eur J Clin Invest **38**(3): 180-190.

Delaval, B., A. Bright, N. D. Lawson and S. Doxsey (2011). "The cilia protein IFT88 is required for spindle orientation in mitosis." Nat Cell Biol **13**(4): 461-468.

Delmas, P., H. Nomura, X. Li, M. Lakkis, Y. Luo, Y. Segal, J. M. Fernandez-Fernandez, P. Harris, A. M. Frischauf, D. A. Brown and J. Zhou (2002). "Constitutive activation of G-proteins by polycystin-1 is antagonized by polycystin-2." J Biol Chem **277**(13): 11276-11283.

Delmore, J. E., G. C. Issa, M. E. Lemieux, P. B. Rahl, J. Shi, H. M. Jacobs, E. Kastritis, T. Gilpatrick, R. M. Paranal, J. Qi, M. Chesi, A. C. Schinzel, M. R. McKeown, T. P. Heffernan, C. R. Vakoc, P. L. Bergsagel, I. M. Ghobrial, P. G. Richardson, R. A. Young, W. C. Hahn, K. C. Anderson, A. L. Kung, J. E. Bradner and C. S. Mitsiades (2011). "BET bromodomain inhibition as a therapeutic strategy to target c-Myc." Cell **146**(6): 904-917.

Delous, M., L. Baala, R. Salomon, C. Laclef, J. Vierkotten, K. Tory, C. Golzio, T. Lacoste, L. Besse, C. Ozilou, I. Moutkine, N. E. Hellman, I. Anselme, F. Silbermann, C. Vesque, C. Gerhardt, E. Rattenberry, M. T. Wolf, M. C. Gubler, J. Martinovic, F. Encha-Razavi, N. Boddaert, M. Gonzales, M. A. Macher, H. Nivet, G. Champion, J. P. Bertheleme, P. Niaudet, F. McDonald, F. Hildebrandt, C. A. Johnson, M. Vekemans, C. Antignac, U. Ruther, S. Schneider-Maunoury, T. Attie-Bitach and S. Saunier (2007). "The ciliary gene RPGRIP1L is mutated in cerebello-oculo-renal syndrome (Joubert syndrome type B) and Meckel syndrome." Nat Genet **39**(7): 875-881.

Dere, R., P. D. Wilson, R. N. Sandford and C. L. Walker (2010). "Carboxy terminal tail of polycystin-1 regulates localization of TSC2 to repress mTOR." PLoS One **5**(2): e9239.

Dinchuk, J. E., B. D. Car, R. J. Focht, J. J. Johnston, B. D. Jaffee, M. B. Covington, N. R. Contel, V. M. Eng, R. J. Collins, P. M. Czerniak and et al. (1995). "Renal abnormalities and an altered inflammatory response in mice lacking cyclooxygenase II." Nature **378**(6555): 406-409.

Dowdle, W. E., J. F. Robinson, A. Kneist, M. S. Sirerol-Piquer, S. G. Frints, K. C. Corbit, N. A. Zaghloul, G. van Lijnschoten, L. Mulders, D. E. Verver, K. Zerres, R. R. Reed, T. Attie-Bitach, C. A. Johnson, J. M. Garcia-Verdugo, N. Katsanis, C. Bergmann and J. F. Reiter (2011). "Disruption of a ciliary B9 protein complex causes Meckel syndrome." Am J Hum Genet **89**(1): 94-110.

Dressler, G. R. (2009). "Advances in early kidney specification, development and patterning." Development **136**(23): 3863-3874.

Dressler, G. R., J. E. Wilkinson, U. W. Rothenpieler, L. T. Patterson, L. Williams-Simons and H. Westphal (1993). "Deregulation of Pax-2 expression in transgenic mice generates severe kidney abnormalities." Nature **362**(6415): 65-67.

Drummond, I. A. (2005). "Kidney development and disease in the zebrafish." J Am Soc Nephrol **16**(2): 299-304.

Drummond, I. A., A. Majumdar, H. Hentschel, M. Elger, L. Solnica-Krezel, A. F. Schier, S. C. Neuhauss, D. L. Stemple, F. Zwartkruis, Z. Rangini, W. Driever and M. C. Fishman (1998). "Early development of the zebrafish pronephros and analysis of mutations affecting pronephric function." Development **125**(23): 4655-4667.

Du, J., M. Ding, S. Sours-Brothers, S. Graham and R. Ma (2008). "Mediation of angiotensin II-induced Ca2+ signaling by polycystin 2 in glomerular mesangial cells." Am J Physiol Renal Physiol **294**(4): F909-918.

Duning, K., D. Rosenbusch, M. A. Schluter, Y. Tian, K. Kunzelmann, N. Meyer, U. Schulze, A. Markoff, H. Pavenstadt and T. Weide (2010). "Polycystin-2 activity is controlled by transcriptional coactivator with PDZ binding motif and PALS1-associated tight junction protein." J Biol Chem **285**(44): 33584-33588.

Eker, R. (1954). "Familial renal adenomas in Wistar rats; a preliminary report." Acta Pathol Microbiol Scand **34**(6): 554-562.

Ellis, D. and S. Malcolm (1994). "Proteolipid protein gene dosage effect in Pelizaeus-Merzbacher disease." Nat Genet **6**(4): 333-334.

Emami, K. H., C. Nguyen, H. Ma, D. H. Kim, K. W. Jeong, M. Eguchi, R. T. Moon, J. L. Teo, H. Y. Kim, S. H. Moon, J. R. Ha and M. Kahn (2004). "A small molecule inhibitor of beta-catenin/CREB-binding protein transcription [corrected]." Proc Natl Acad Sci U S A **101**(34): 12682-12687.

Elzinga LW, B. W. (1996). Miscellaneous renal and systemic complications of autosomal dominant polycystic kidney disease including infection In: Polycystic Kidney Disease. Oxford, United Kingdom, Oxford University Press.

Engbretson, B. G. and L. C. Stoner (1987). "Flow-dependent potassium secretion by rabbit cortical collecting tubule in vitro." Am J Physiol **253**(5 Pt 2): F896-903.

Evan, A. P. and K. D. Gardner, Jr. (1979). "Nephron obstruction in nordihydroguaiaretic acid-induced renal cystic disease." Kidney Int **15**(1): 7-19.

Everson, G. T. (1993). "Hepatic cysts in autosomal dominant polycystic kidney disease." Am J Kidney Dis **22**(4): 520-525.

Fain, P. R., K. K. McFann, M. R. Taylor, M. Tison, A. M. Johnson, B. Reed and R. W. Schrier (2005). "Modifier genes play a significant role in the phenotypic expression of PKD1." Kidney Int **67**(4): 1256-1267.

Fedeles, S. V., X. Tian, A. R. Gallagher, M. Mitobe, S. Nishio, S. H. Lee, Y. Cai, L. Geng, C. M. Crews and S. Somlo (2011). "A genetic interaction network of five genes for human polycystic kidney and liver diseases defines polycystin-1 as the central determinant of cyst formation." Nat Genet **43**(7): 639-647.

Fick, G. M., A. M. Johnson and P. A. Gabow (1994). "Is there evidence for anticipation in autosomal-dominant polycystic kidney disease?" Kidney Int **45**(4): 1153-1162.

Field, S., K. L. Riley, D. T. Grimes, H. Hilton, M. Simon, N. Powles-Glover, P. Siggers, D. Bogani, A. Greenfield and D. P. Norris (2011). "Pkd1l1 establishes left-right asymmetry and physically interacts with Pkd2." Development **138**(6): 1131-1142.

Filmer, R. B., F. A. Carone, R. G. Rowland and J. R. Babcock (1973). "Adrenal corticosteroid-induced renal cystic disease in the newborn hamster." Am J Pathol **72**(3): 461-472.

Finetti, F., S. R. Paccani, M. G. Riparbelli, E. Giacomello, G. Perinetti, G. J. Pazour, J. L. Rosenbaum and C. T. Baldari (2009). "Intraflagellar transport is required for polarized recycling of the TCR/CD3 complex to the immune synapse." Nat Cell Biol **11**(11): 1332-1339.

Fischer, E., E. Legue, A. Doyen, F. Nato, J. F. Nicolas, V. Torres, M. Yaniv and M. Pontoglio (2006). "Defective planar cell polarity in polycystic kidney disease." Nat Genet **38**(1): 21-23.

Flaherty, L., E. C. Bryda, D. Collins, U. Rudofsky and J. C. Montogomery (1995). "New mouse model for polycystic kidney disease with both recessive and dominant gene effects." Kidney Int **47**(2): 552-558.

Fogelgren, B., S. Y. Lin, X. Zuo, K. M. Jaffe, K. M. Park, R. J. Reichert, P. D. Bell, R. D. Burdine and J. H. Lipschutz (2011). "The exocyst protein Sec10 interacts with Polycystin-2 and knockdown causes PKD-phenotypes." PLoS Genet **7**(4): e1001361.

Foggensteiner, L., A. P. Bevan, R. Thomas, N. Coleman, C. Boulter, J. Bradley, O. Ibraghimov-Beskrovnaya, K. Klinger and R. Sandford (2000). "Cellular and subcellular

distribution of polycystin-2, the protein product of the PKD2 gene." J Am Soc Nephrol **11**(5): 814-827.

Follit, J. A., L. Li, Y. Vucica and G. J. Pazour (2010). "The cytoplasmic tail of fibrocystin contains a ciliary targeting sequence." J Cell Biol **188**(1): 21-28.

Foy, R. L., V. C. Chitalia, M. V. Panchenko, L. Zeng, D. Lopez, J. W. Lee, S. V. Rana, A. Boletta, F. Qian, L. Tsiokas, K. B. Piontek, G. G. Germino, M. I. Zhou and H. T. Cohen (2012). "Polycystin-1 regulates the stability and ubiquitination of transcription factor Jade-1." Hum Mol Genet. 15;21(26):5456-71.

Freedman, B. S., A. Q. Lam, J. L. Sundsbak, R. Iatrino, X. Su, S. J. Koon, M. Wu, L. Daheron, P. C. Harris, J. Zhou and J. V. Bonventre (2013). "Reduced Ciliary Polycystin-2 in Induced Pluripotent Stem Cells from Polycystic Kidney Disease Patients with PKD1 Mutations." J Am Soc Nephrol 24(10);1571-86.

Friedberg, V. (1955). "[Studies on fetal urine secretion]." Gynaecologia **140**(1): 34-45.

Fry, J. L., Jr., W. E. Koch, J. C. Jennette, E. McFarland, F. A. Fried and J. Mandell (1985). "A genetically determined murine model of infantile polycystic kidney disease." J Urol **134**(4): 828-833.

Fu, L., G. Wang, M. M. Shevchuk, D. M. Nanus and L. J. Gudas (2011). "Generation of a mouse model of Von Hippel-Lindau kidney disease leading to renal cancers by expression of a constitutively active mutant of Hif1αlpha." Cancer Res **71**(21): 6848-6856.

Gabow, P. A. (1993). "Autosomal dominant polycystic kidney disease." Am J Kidney Dis **22**(4): 511-512.

Gallagher, A. R., A. Cedzich, N. Gretz, S. Somlo and R. Witzgall (2000). "The polycystic kidney disease protein PKD2 interacts with Hax-1, a protein associated with the actin cytoskeleton." Proc Natl Acad Sci U S A **97**(8): 4017-4022.

Gallagher, A. R., S. Hoffmann, N. Brown, A. Cedzich, S. Meruvu, D. Podlich, Y. Feng, V. Konecke, U. de Vries, H. P. Hammes, N. Gretz and R. Witzgall (2006). "A truncated polycystin-2 protein causes polycystic kidney disease and retinal degeneration in transgenic rats." J Am Soc Nephrol **17**(10): 2719-2730.

Garcia-Gonzalez, M. A., L. F. Menezes, K. B. Piontek, J. Kaimori, D. L. Huso, T. Watnick, L. F. Onuchic, L. M. Guay-Woodford and G. G. Germino (2007). "Genetic interaction studies link autosomal dominant and recessive polycystic kidney disease in a common pathway." Hum Mol Genet **16**(16): 1940-1950.

Garcia-Gonzalez, M. A., P. Outeda, Q. Zhou, F. Zhou, L. F. Menezes, F. Qian, D. L. Huso, G. G. Germino, K. B. Piontek and T. Watnick (2010). "Pkd1 and Pkd2 are required for normal placental development." PLoS One **5**(9).

Gattone, V. H., 2nd, X. Wang, P. C. Harris and V. E. Torres (2003). "Inhibition of renal cystic disease development and progression by a vasopressin V2 receptor antagonist." Nat Med **9**(10): 1323-1326.

Geng, L., W. Boehmerle, Y. Maeda, D. Y. Okuhara, X. Tian, Z. Yu, C. U. Choe, G. I. Anyatonwu, B. E. Ehrlich and S. Somlo (2008). "Syntaxin 5 regulates the endoplasmic reticulum channel-release properties of polycystin-2." Proc Natl Acad Sci U S A **105**(41): 15920-15925.

Geng, L., C. R. Burrow, H. P. Li and P. D. Wilson (2000). "Modification of the composition of polycystin-1 multiprotein complexes by calcium and tyrosine phosphorylation." Biochim Biophys Acta **1535**(1): 21-35.

Geng, L., D. Okuhara, Z. Yu, X. Tian, Y. Cai, S. Shibazaki and S. Somlo (2006). "Polycystin-2 traffics to cilia independently of polycystin-1 by using an N-terminal RVxP motif." J Cell Sci **119**(Pt 7): 1383-1395.

Geng, L., Y. Segal, A. Pavlova, E. J. Barros, C. Lohning, W. Lu, S. K. Nigam, A. M. Frischauf, S. T. Reeders and J. Zhou (1997). "Distribution and developmentally regulated expression of murine polycystin." Am J Physiol **272**(4 Pt 2): F451-459.

Geng, L., Y. Segal, B. Peissel, N. Deng, Y. Pei, F. Carone, H. G. Rennke, A. M. Glucksmann-Kuis, M. C. Schneider, M. Ericsson, S. T. Reeders and J. Zhou (1996). "Identification and localization of polycystin, the PKD1 gene product." J Clin Invest **98**(12): 2674-2682.

Giamarchi, A., S. Feng, L. Rodat-Despoix, Y. Xu, E. Bubenshchikova, L. J. Newby, J. Hao, C. Gaudioso, M. Crest, A. N. Lupas, E. Honore, M. P. Williamson, T. Obara, A. C. Ong and P. Delmas (2010). "A polycystin-2 (TRPP2) dimerization domain essential for the function of heteromeric polycystin complexes." EMBO J **29**(7): 1176-1191.

Gogusev, J., I. Murakami, M. Doussau, L. Telvi, A. Stojkoski, P. Lesavre and D. Droz (2003). "Molecular cytogenetic aberrations in autosomal dominant polycystic kidney disease tissue." J Am Soc Nephrol **14**(2): 359-366.

Gonzalez-Perrett, S., K. Kim, C. Ibarra, A. E. Damiano, E. Zotta, M. Batelli, P. C. Harris, I. L. Reisin, M. A. Arnaout and H. F. Cantiello (2001). "Polycystin-2, the protein mutated in autosomal dominant polycystic kidney disease (ADPKD), is a Ca2+-permeable nonselective cation channel." Proc Natl Acad Sci U S A **98**(3): 1182-1187.

Goodman, T., H. C. Grice, G. C. Becking and F. A. Salem (1970). "A cystic nephropathy induced by nordihydroguaiaretic acid in the rat. Light and electron microscopic investigations." Lab Invest **23**(1): 93-107.

Grantham, J. J. (1990). "Polycystic kidney disease: neoplasia in disguise." Am J Kidney Dis **15**(2): 110-116.

Grantham, J. J., A. B. Chapman and V. E. Torres (2006). "Volume progression in autosomal dominant polycystic kidney disease: the major factor determining clinical outcomes." Clin J Am Soc Nephrol **1**(1): 148-157.

Grantham, J. J., J. L. Geiser and A. P. Evan (1987). "Cyst formation and growth in autosomal dominant polycystic kidney disease." Kidney Int **31**(5): 1145-1152.

Grantham, J. J., R. Mangoo-Karim, M. E. Uchic, M. Grant, W. A. Shumate, C. H. Park and J. P. Calvet (1989). "Net fluid secretion by mammalian renal epithelial cells: stimulation by cAMP in polarized cultures derived from established renal cells and from normal and polycystic kidneys." Trans Assoc Am Physicians **102**: 158-162.

Gresh, L., E. Fischer, A. Reimann, M. Tanguy, S. Garbay, X. Shao, T. Hiesberger, L. Fiette, P. Igarashi, M. Yaniv and M. Pontoglio (2004). "A transcriptional network in polycystic kidney disease." EMBO J **23**(7): 1657-1668.

Griffin, M. D., V. E. Torres, J. P. Grande and R. Kumar (1996). "Immunolocalization of polycystin in human tissues and cultured cells." Proc Assoc Am Physicians **108**(3): 185-197.

Griffin, M. D., D. A. O'Sullivan, V. E. Torres, J. P. Grande, Y. S. Kanwar and R. Kumar (1997). "Expression of polycystin in mouse metanephros and extra-metanephric tissues." Kidney Int **52**(5): 1196-1205.

Grimm, D. H., Y. Cai, V. Chauvet, V. Rajendran, R. Zeltner, L. Geng, E. D. Avner, W. Sweeney, S. Somlo and M. J. Caplan (2003). "Polycystin-1 distribution is modulated by polycystin-2 expression in mammalian cells." J Biol Chem **278**(38): 36786-36793.

Grimm, D. H., A. Karihaloo, Y. Cai, S. Somlo, L. G. Cantley and M. J. Caplan (2006). "Polycystin-2 regulates proliferation and branching morphogenesis in kidney epithelial cells." J Biol Chem **281**(1): 137-144.

Guay-Woodford, L. M. (2003). "Murine models of polycystic kidney disease: molecular and therapeutic insights." Am J Physiol Renal Physiol **285**(6): F1034-1049.

Guay-Woodford, L. M., E. C. Bryda, B. Christine, J. R. Lindsey, W. R. Collier, E. D. Avner, P. D'Eustachio and L. Flaherty (1996). "Evidence that two phenotypically distinct mouse PKD mutations, bpk and jcpk, are allelic." Kidney Int **50**(4): 1158-1165.

Guay-Woodford, L. M. and R. A. Desmond (2003). "Autosomal recessive polycystic kidney disease: the clinical experience in North America." Pediatrics **111**(5 Pt 1): 1072-1080.

Guillaume, R., V. D'Agati, M. Daoust and M. Trudel (1999). "Murine Pkd1 is a developmentally regulated gene from morula to adulthood: role in tissue condensation and patterning." Dev Dyn **214**(4): 337-348.

Guillaume, R. and M. Trudel (2000). "Distinct and common developmental expression patterns of the murine Pkd2 and Pkd1 genes." Mech Dev **93**(1-2): 179-183.

Guillaume, R. (2000). Caractérisation de l'expression des gènes Pkd1 et Pkd2. Ph.D., Université de Montréal.

Guo, D. F., A. M. Beyer, B. Yang, D. Y. Nishimura, V. C. Sheffield and K. Rahmouni (2011). "Inactivation of Bardet-Biedl syndrome genes causes kidney defects." Am J Physiol Renal Physiol **300**(2): F574-580.

Guo, L., M. Chen, N. Basora and J. Zhou (2000). "The human polycystic kidney disease 2-like (PKDL) gene: exon/intron structure and evidence for a novel splicing mechanism." Mamm Genome **11**(1): 46-50.

Hakroush, S., M. J. Moeller, F. Theilig, B. Kaissling, T. P. Sijmonsma, M. Jugold, A. L. Akeson, M. Traykova-Brauch, H. Hosser, B. Hahnel, H. J. Grone, R. Koesters and W. Kriz (2009). "Effects of increased renal tubular vascular endothelial growth factor (VEGF) on fibrosis, cyst formation, and glomerular disease." Am J Pathol **175**(5): 1883-1895.

Hanaoka, K., O. Devuyst, E. M. Schwiebert, P. D. Wilson and W. B. Guggino (1996). "A role for CFTR in human autosomal dominant polycystic kidney disease." Am J Physiol **270**(1 Pt 1): C389-399.

Hanaoka, K., F. Qian, A. Boletta, A. K. Bhunia, K. Piontek, L. Tsiokas, V. P. Sukhatme, W. B. Guggino and G. G. Germino (2000). "Co-assembly of polycystin-1 and -2 produces unique cation-permeable currents." Nature **408**(6815): 990-994.

Handeli, S. and J. A. Simon (2008). "A small-molecule inhibitor of Tcf/beta-catenin signaling down-regulates PPARgamma and PPARdelta activities." Mol Cancer Ther **7**(3): 521-529.

Happe, H., W. N. Leonhard, A. van der Wal, B. van de Water, I. S. Lantinga-van Leeuwen, M. H. Breuning, E. de Heer and D. J. Peters (2009). "Toxic tubular injury in kidneys from Pkd1-deletion mice accelerates cystogenesis accompanied by dysregulated planar cell polarity and canonical Wnt signaling pathways." Hum Mol Genet **18**(14): 2532-2542.

Happe, H., A. M. van der Wal, D. C. Salvatori, W. N. Leonhard, M. H. Breuning, E. de Heer and D. J. Peters (2013). "Cyst expansion and regression in a mouse model of polycystic kidney disease." Kidney Int **83**(6): 1099-1108.

Harris, P. C. (2010). "What is the role of somatic mutation in autosomal dominant polycystic kidney disease?" J Am Soc Nephrol **21**(7): 1073-1076.

Harris, P. C., K. T. Bae, S. Rossetti, V. E. Torres, J. J. Grantham, A. B. Chapman, L. M. Guay-Woodford, B. F. King, L. H. Wetzel, D. A. Baumgarten, P. J. Kenney, M. Consugar, S. Klahr, W. M. Bennett, C. M. Meyers, Q. J. Zhang, P. A. Thompson, F. Zhu and J. P. Miller (2006). "Cyst number but not the rate of cystic growth is associated with the mutated gene in autosomal dominant polycystic kidney disease." J Am Soc Nephrol **17**(11): 3013-3019.

Hartman, T. R., D. Liu, J. T. Zilfou, V. Robb, T. Morrison, T. Watnick and E. P. Henske (2009). "The tuberous sclerosis proteins regulate formation of the primary cilium via a rapamycin-insensitive and polycystin 1-independent pathway." Hum Mol Genet **18**(1): 151-163.

Hassane, S., W. N. Leonhard, A. van der Wal, L. J. Hawinkels, I. S. Lantinga-van Leeuwen, P. ten Dijke, M. H. Breuning, E. de Heer and D. J. Peters (2010). "Elevated TGFbeta-Smad signalling in experimental Pkd1 models and human patients with polycystic kidney disease." J Pathol **222**(1): 21-31.

Hateboer, N., M. A. v Dijk, N. Bogdanova, E. Coto, A. K. Saggar-Malik, J. L. San Millan, R. Torra, M. Breuning and D. Ravine (1999). "Comparison of phenotypes of polycystic kidney disease types 1 and 2. European PKD1-PKD2 Study Group." Lancet **353**(9147): 103-107.

Hateboer, N., B. Veldhuisen, D. Peters, M. H. Breuning, J. L. San-Millan, N. Bogdanova, E. Coto, M. A. van Dijk, A. R. Afzal, S. Jeffery, A. K. Saggar-Malik, R. Torra, D. Dimitrakov, I. Martinez, S. S. de Castro, M. Krawczak and D. Ravine (2000). "Location of mutations within the PKD2 gene influences clinical outcome." Kidney Int **57**(4): 1444-1451.

Haycraft, C. J., P. Swoboda, P. D. Taulman, J. H. Thomas and B. K. Yoder (2001). "The C. elegans homolog of the murine cystic kidney disease gene Tg737 functions in a ciliogenic pathway and is disrupted in osm-5 mutant worms." Development **128**(9): 1493-1505.

Haze, K., H. Yoshida, H. Yanagi, T. Yura and K. Mori (1999). "Mammalian transcription factor ATF6 is synthesized as a transmembrane protein and activated by proteolysis in response to endoplasmic reticulum stress." Mol Biol Cell **10**(11): 3787-3799.

Heinrich, A. C., R. Pelanda and U. Klingmuller (2004). "A mouse model for visualization and conditional mutations in the erythroid lineage." Blood **104**(3): 659-666.

Herron, B. J., W. Lu, C. Rao, S. Liu, H. Peters, R. T. Bronson, M. J. Justice, J. D. McDonald and D. R. Beier (2002). "Efficient generation and mapping of recessive developmental mutations using ENU mutagenesis." Nat Genet **30**(2): 185-189.

Hidaka, S., V. Konecke, L. Osten and R. Witzgall (2004). "PIGEA-14, a novel coiled-coil protein affecting the intracellular distribution of polycystin-2." J Biol Chem **279**(33): 35009-35016.

Hiesberger, T., Y. Bai, X. Shao, B. T. McNally, A. M. Sinclair, X. Tian, S. Somlo and P. Igarashi (2004). "Mutation of hepatocyte nuclear factor-1beta inhibits Pkhd1 gene expression and produces renal cysts in mice." J Clin Invest **113**(6): 814-825.

Hiesberger, T., E. Gourley, A. Erickson, P. Koulen, C. J. Ward, T. V. Masyuk, N. F. Larusso, P. C. Harris and P. Igarashi (2006). "Proteolytic cleavage and nuclear translocation of fibrocystin is regulated by intracellular Ca2+ and activation of protein kinase C." J Biol Chem **281**(45): 34357-34364.

Hiesberger, T., X. Shao, E. Gourley, A. Reimann, M. Pontoglio and P. Igarashi (2005). "Role of the hepatocyte nuclear factor-1beta (HNF-1beta) C-terminal domain in Pkhd1 (ARPKD) gene transcription and renal cystogenesis." J Biol Chem **280**(11): 10578-10586.

Hocher, B., C. Thone-Reineke, P. Rohmeiss, F. Schmager, T. Slowinski, V. Burst, F. Siegmund, T. Quertermous, C. Bauer, H. H. Neumayer, W. D. Schleuning and F. Theuring (1997). "Endothelin-1 transgenic mice develop glomerulosclerosis, interstitial fibrosis, and renal cysts but not hypertension." J Clin Invest **99**(6): 1380-1389.

Hoffmeister, H., K. Babinger, S. Gurster, A. Cedzich, C. Meese, K. Schadendorf, L. Osten, U. de Vries, A. Rascle and R. Witzgall (2011). "Polycystin-2 takes different routes to the somatic and ciliary plasma membrane." J Cell Biol **192**(4): 631-645.

Hogan, M. C., L. Manganelli, J. R. Woollard, A. I. Masyuk, T. V. Masyuk, R. Tammachote, B. Q. Huang, A. A. Leontovich, T. G. Beito, B. J. Madden, M. C. Charlesworth, V. E. Torres, N. F. LaRusso, P. C. Harris and C. J. Ward (2009). "Characterization of PKD protein-positive exosome-like vesicles." J Am Soc Nephrol **20**(2): 278-288.

Hogan, M. C., T. V. Masyuk, L. J. Page, V. J. Kubly, E. J. Bergstralh, X. Li, B. Kim, B. F. King, J. Glockner, D. R. Holmes, 3rd, S. Rossetti, P. C. Harris, N. F. LaRusso and V. E. Torres (2010). "Randomized clinical trial of long-acting somatostatin for autosomal dominant polycystic kidney and liver disease." J Am Soc Nephrol **21**(6): 1052-1061.

Holland, P. M., A. Milne, K. Garka, R. S. Johnson, C. Willis, J. E. Sims, C. T. Rauch, T. A. Bird and G. D. Virca (2002). "Purification, cloning, and characterization of Nek8, a novel NIMA-related kinase, and its candidate substrate Bicd2." J Biol Chem **277**(18): 16229-16240.

Hopp, K., C. J. Ward, C. J. Hommerding, S. H. Nasr, H. F. Tuan, V. G. Gainullin, S. Rossetti, V. E. Torres and P. C. Harris (2012). "Functional polycystin-1 dosage governs autosomal dominant polycystic kidney disease severity." J Clin Invest **122**(11): 4257-4273.

Hossain, Z., S. M. Ali, H. L. Ko, J. Xu, C. P. Ng, K. Guo, Z. Qi, S. Ponniah, W. Hong and W. Hunziker (2007). "Glomerulocystic kidney disease in mice with a targeted inactivation of Wwtr1." Proc Natl Acad Sci U S A **104**(5): 1631-1636.

Hou, X., M. Mrug, B. K. Yoder, E. J. Lefkowitz, G. Kremmidiotis, P. D'Eustachio, D. R. Beier and L. M. Guay-Woodford (2002). "Cystin, a novel cilia-associated protein, is disrupted in the cpk mouse model of polycystic kidney disease." J Clin Invest **109**(4): 533-540.

Hu, J., Y. K. Bae, K. M. Knobel and M. M. Barr (2006). "Casein kinase II and calcineurin modulate TRPP function and ciliary localization." Mol Biol Cell **17**(5): 2200-2211.

Hu, J. and M. M. Barr (2005). "ATP-2 interacts with the PLAT domain of LOV-1 and is involved in Caenorhabditis elegans polycystin signaling." Mol Biol Cell **16**(2): 458-469.

Hu, M. C., T. D. Piscione and N. D. Rosenblum (2003). "Elevated SMAD1/beta-catenin molecular complexes and renal medullary cystic dysplasia in ALK3 transgenic mice." Development **130**(12): 2753-2766.

Huan, Y. and J. van Adelsberg (1999). "Polycystin-1, the PKD1 gene product, is in a complex containing E-cadherin and the catenins." J Clin Invest **104**(10): 1459-1468.

Huang, M. J., Y. C. Cheng, C. R. Liu, S. Lin and H. E. Liu (2006). "A small-molecule c-Myc inhibitor, 10058-F4, induces cell-cycle arrest, apoptosis, and myeloid differentiation of human acute myeloid leukemia." Exp Hematol **34**(11): 1480-1489.

Hughes, J., C. J. Ward, R. Aspinwall, R. Butler and P. C. Harris (1999). "Identification of a human homologue of the sea urchin receptor for egg jelly: a polycystic kidney disease-like protein." Hum Mol Genet **8**(3): 543-549.

Hughes, J., C. J. Ward, B. Peral, R. Aspinwall, K. Clark, J. L. San Millan, V. Gamble and P. C. Harris (1995). "The polycystic kidney disease 1 (PKD1) gene encodes a novel protein with multiple cell recognition domains." Nat Genet **10**(2): 151-160.

Hurd, T., W. Zhou, P. Jenkins, C. J. Liu, A. Swaroop, H. Khanna, J. Martens, F. Hildebrandt and B. Margolis (2010). "The retinitis pigmentosa protein RP2 interacts with polycystin 2 and regulates cilia-mediated vertebrate development." Hum Mol Genet **19**(22): 4330-4344.

Husson, H., P. Manavalan, V. R. Akmaev, R. J. Russo, B. Cook, B. Richards, D. Barberio, D. Liu, X. Cao, G. M. Landes, C. J. Wang, B. L. Roberts, K. W. Klinger, S. A. Grubman, D. M. Jefferson and O. Ibraghimov-Beskrovnaya (2004). "New insights into ADPKD molecular pathways using combination of SAGE and microarray technologies." Genomics **84**(3): 497-510.

Huston, J., 3rd, V. E. Torres, P. P. Sulivan, K. P. Offord and D. O. Wiebers (1993). "Value of magnetic resonance angiography for the detection of intracranial aneurysms in autosomal dominant polycystic kidney disease." J Am Soc Nephrol **3**(12): 1871-1877.

Ibraghimov-Beskrovnaya, O., N. O. Bukanov, L. C. Donohue, W. R. Dackowski, K. W. Klinger and G. M. Landes (2000). "Strong homophilic interactions of the Ig-like domains of polycystin-1, the protein product of an autosomal dominant polycystic kidney disease gene, PKD1." Hum Mol Genet **9**(11): 1641-1649.

Ibraghimov-Beskrovnaya, O., W. R. Dackowski, L. Foggensteiner, N. Coleman, S. Thiru, L. R. Petry, T. C. Burn, T. D. Connors, T. Van Raay, J. Bradley, F. Qian, L. F.

Onuchic, T. J. Watnick, K. Piontek, R. M. Hakim, G. M. Landes, G. G. Germino, R. Sandford and K. W. Klinger (1997). "Polycystin: in vitro synthesis, in vivo tissue expression, and subcellular localization identifies a large membrane-associated protein." Proc Natl Acad Sci U S A **94**(12): 6397-6402.

Ikeda, M., P. Fong, J. Cheng, A. Boletta, F. Qian, X. M. Zhang, H. Cai, G. G. Germino and W. B. Guggino (2006). "A regulatory role of polycystin-1 on cystic fibrosis transmembrane conductance regulator plasma membrane expression." Cell Physiol Biochem **18**(1-3): 9-20.

Inagi, R. (2010). "Endoplasmic reticulum stress as a progression factor for kidney injury." Curr Opin Pharmacol **10**(2): 156-165.

Islam, M. R., T. Jimenez, C. Pelham, M. Rodova, S. Puri, B. S. Magenheimer, R. L. Maser, C. Widmann and J. P. Calvet (2010). "MAP/ERK kinase kinase 1 (MEKK1) mediates transcriptional repression by interacting with polycystic kidney disease-1 (PKD1) promoter-bound p53 tumor suppressor protein." J Biol Chem **285**(50): 38818-38831.

Islam, M. R., S. Puri, M. Rodova, B. S. Magenheimer, R. L. Maser and J. P. Calvet (2008). "Retinoic acid-dependent activation of the polycystic kidney disease-1 (PKD1) promoter." Am J Physiol Renal Physiol **295**(6): F1845-1854.

Janaswami, P. M., E. H. Birkenmeier, S. A. Cook, L. B. Rowe, R. T. Bronson and M. T. Davisson (1997). "Identification and genetic mapping of a new polycystic kidney disease on mouse chromosome 8." Genomics **40**(1): 101-107.

Jena, N., C. Martin-Seisdedos, P. McCue and C. M. Croce (1997). "BMP7 null mutation in mice: developmental defects in skeleton, kidney, and eye." Exp Cell Res **230**(1): 28-37.

Jeon, J. O., K. H. Yoo and J. H. Park (2007). "Expression of the Pkd1 gene is momentously regulated by Sp1." Nephron Exp Nephrol **107**(2): e57-64.

Jiang, S. T., Y. Y. Chiou, E. Wang, H. K. Lin, Y. T. Lin, Y. C. Chi, C. K. Wang, M. J. Tang and H. Li (2006). "Defining a link with autosomal-dominant polycystic kidney disease in mice with congenitally low expression of Pkd1." Am J Pathol **168**(1): 205-220.

Jonassen, J. A., J. San Agustin, J. A. Follit and G. J. Pazour (2008). "Deletion of IFT20 in the mouse kidney causes misorientation of the mitotic spindle and cystic kidney disease." J Cell Biol **183**(3): 377-384.

Jonassen, J. A., J. SanAgustin, S. P. Baker and G. J. Pazour (2012). "Disruption of IFT complex A causes cystic kidneys without mitotic spindle misorientation." J Am Soc Nephrol **23**(4): 641-651.

Jou, T. S. and W. J. Nelson (1998). "Effects of regulated expression of mutant RhoA and Rac1 small GTPases on the development of epithelial (MDCK) cell polarity." J Cell Biol **142**(1): 85-100.

Jou, T. S., E. E. Schneeberger and W. J. Nelson (1998). "Structural and functional regulation of tight junctions by RhoA and Rac1 small GTPases." J Cell Biol **142**(1): 101-115.

Jurczyk, A., A. Gromley, S. Redick, J. San Agustin, G. Witman, G. J. Pazour, D. J. Peters and S. Doxsey (2004). "Pericentrin forms a complex with intraflagellar transport proteins and polycystin-2 and is required for primary cilia assembly." J Cell Biol **166**(5): 637-643.

Kaimori, J. Y., Y. Nagasawa, L. F. Menezes, M. A. Garcia-Gonzalez, J. Deng, E. Imai, L. F. Onuchic, L. M. Guay-Woodford and G. G. Germino (2007). "Polyductin undergoes

notch-like processing and regulated release from primary cilia." Hum Mol Genet **16**(8): 942-956.

Kamura, K., D. Kobayashi, Y. Uehara, S. Koshida, N. Iijima, A. Kudo, T. Yokoyama and H. Takeda (2011). "Pkd1l1 complexes with Pkd2 on motile cilia and functions to establish the left-right axis." Development **138**(6): 1121-1129.

Kang, H. S., J. Y. Beak, Y. S. Kim, R. Herbert and A. M. Jetten (2009). "Glis3 is associated with primary cilia and Wwtr1/TAZ and implicated in polycystic kidney disease." Mol Cell Biol **29**(10): 2556-2569.

Kanwar, Y. S. and F. A. Carone (1984). "Reversible changes of tubular cell and basement membrane in drug-induced renal cystic disease." Kidney Int **26**(1): 35-43.

Karihaloo, A., F. Koraishy, S. C. Huen, Y. Lee, D. Merrick, M. J. Caplan, S. Somlo and L. G. Cantley (2011). "Macrophages promote cyst growth in polycystic kidney disease." J Am Soc Nephrol **22**(10): 1809-1814.

Karim, S. A., J. A. Barrie, M. C. McCulloch, P. Montague, J. M. Edgar, D. L. Iden, T. J. Anderson, K. A. Nave, I. R. Griffiths and M. McLaughlin (2010). "PLP/DM20 expression and turnover in a transgenic mouse model of Pelizaeus-Merzbacher disease." Glia **58**(14): 1727-1738.

Karner, C., K. A. Wharton, Jr. and T. J. Carroll (2006). "Planar cell polarity and vertebrate organogenesis." Semin Cell Dev Biol **17**(2): 194-203.

Karner, C. M., R. Chirumamilla, S. Aoki, P. Igarashi, J. B. Wallingford and T. J. Carroll (2009). "Wnt9b signaling regulates planar cell polarity and kidney tubule morphogenesis." Nat Genet **41**(7): 793-799.

Katsuyama, M., T. Masuyama, I. Komura, T. Hibino and H. Takahashi (2000). "Characterization of a novel polycystic kidney rat model with accompanying polycystic liver." Exp Anim **49**(1): 51-55.

Keith, D. S., V. E. Torres, B. F. King, H. Zincki and G. M. Farrow (1994). "Renal cell carcinoma in autosomal dominant polycystic kidney disease." J Am Soc Nephrol **4**(9): 1661-1669.

Kelley, K. A., N. Agarwal, S. Reeders and K. Herrup (1991). "Renal cyst formation and multifocal neoplasia in transgenic mice carrying the simian virus 40 early region." J Am Soc Nephrol **2**(1): 84-97.

Kher, R. V. A., Janet; Wandinger Ness, Angela; Charron, Audra J.; Bacallao, Robert (2002). A second transcript encoded by the PKD1 gene locus codes for vascular matrix protein. J Am Soc Nephrol. **13:** 110a.

Kim, E., T. Arnould, L. Sellin, T. Benzing, N. Comella, O. Kocher, L. Tsiokas, V. P. Sukhatme and G. Walz (1999). "Interaction between RGS7 and polycystin." Proc Natl Acad Sci U S A **96**(11): 6371-6376.

Kim, E., T. Arnould, L. K. Sellin, T. Benzing, M. J. Fan, W. Gruning, S. Y. Sokol, I. Drummond and G. Walz (1999). "The polycystic kidney disease 1 gene product modulates Wnt signaling." J Biol Chem **274**(8): 4947-4953.

Kim, H., W. Jeong, K. Ahn, C. Ahn and S. Kang (2004). "Siah-1 interacts with the intracellular region of polycystin-1 and affects its stability via the ubiquitin-proteasome pathway." J Am Soc Nephrol **15**(8): 2042-2049.

Kim, I., T. Ding, Y. Fu, C. Li, L. Cui, A. Li, P. Lian, D. Liang, D. W. Wang, C. Guo, J. Ma, P. Zhao, R. J. Coffey, Q. Zhan and G. Wu (2009). "Conditional mutation of Pkd2

causes cystogenesis and upregulates beta-catenin." J Am Soc Nephrol **20**(12): 2556-2569.

Kim, I., Y. Fu, K. Hui, G. Moeckel, W. Mai, C. Li, D. Liang, P. Zhao, J. Ma, X. Z. Chen, A. L. George, Jr., R. J. Coffey, Z. P. Feng and G. Wu (2008). "Fibrocystin/polyductin modulates renal tubular formation by regulating polycystin-2 expression and function." J Am Soc Nephrol **19**(3): 455-468.

Kim, I., C. Li, D. Liang, X. Z. Chen, R. J. Coffy, J. Ma, P. Zhao and G. Wu (2008). "Polycystin-2 expression is regulated by a PC2-binding domain in the intracellular portion of fibrocystin." J Biol Chem **283**(46): 31559-31566.

Kim, J., J. E. Lee, S. Heynen-Genel, E. Suyama, K. Ono, K. Lee, T. Ideker, P. Aza-Blanc and J. G. Gleeson (2010). "Functional genomic screen for modulators of ciliogenesis and cilium length." Nature **464**(7291): 1048-1051.

Kim, K., I. Drummond, O. Ibraghimov-Beskrovnaya, K. Klinger and M. A. Arnaout (2000). "Polycystin 1 is required for the structural integrity of blood vessels." Proc Natl Acad Sci U S A **97**(4): 1731-1736.

Kimura, K., A. Wakamatsu, Y. Suzuki, T. Ota, T. Nishikawa, R. Yamashita, J. Yamamoto, M. Sekine, K. Tsuritani, H. Wakaguri, S. Ishii, T. Sugiyama, K. Saito, Y. Isono, R. Irie, N. Kushida, T. Yoneyama, R. Otsuka, K. Kanda, T. Yokoi, H. Kondo, M. Wagatsuma, K. Murakawa, S. Ishida, T. Ishibashi, A. Takahashi-Fujii, T. Tanase, K. Nagai, H. Kikuchi, K. Nakai, T. Isogai and S. Sugano (2006). "Diversification of transcriptional modulation: large-scale identification and characterization of putative alternative promoters of human genes." Genome Res **16**(1): 55-65.

Kleymenova, E., O. Ibraghimov-Beskrovnaya, H. Kugoh, J. Everitt, H. Xu, K. Kiguchi, G. Landes, P. Harris and C. Walker (2001). "Tuberin-dependent membrane localization

of polycystin-1: a functional link between polycystic kidney disease and the TSC2 tumor suppressor gene." Mol Cell **7**(4): 823-832.

Kobayashi, A., K. M. Kwan, T. J. Carroll, A. P. McMahon, C. L. Mendelsohn and R. R. Behringer (2005). "Distinct and sequential tissue-specific activities of the LIM-class homeobox gene Lim1 for tubular morphogenesis during kidney development." Development **132**(12): 2809-2823.

Kobayashi, T., Y. Hirayama, E. Kobayashi, Y. Kubo and O. Hino (1995). "A germline insertion in the tuberous sclerosis (Tsc2) gene gives rise to the Eker rat model of dominantly inherited cancer." Nat Genet **9**(1): 70-74.

Kobayashi, T., M. Nishizawa, Y. Hirayama, E. Kobayashi and O. Hino (1995). "cDNA structure, alternative splicing and exon-intron organization of the predisposing tuberous sclerosis (Tsc2) gene of the Eker rat model." Nucleic Acids Res **23**(14): 2608-2613.

Kolpakova-Hart, E., B. McBratney-Owen, B. Hou, N. Fukai, C. Nicolae, J. Zhou and B. R. Olsen (2008). "Growth of cranial synchondroses and sutures requires polycystin-1." Dev Biol **321**(2): 407-419.

Kolpakova-Hart, E., C. Nicolae, J. Zhou and B. R. Olsen (2008). "Col2-Cre recombinase is co-expressed with endogenous type II collagen in embryonic renal epithelium and drives development of polycystic kidney disease following inactivation of ciliary genes." Matrix Biol **27**(6): 505-512.

Kottgen, M., T. Benzing, T. Simmen, R. Tauber, B. Buchholz, S. Feliciangeli, T. B. Huber, B. Schermer, A. Kramer-Zucker, K. Hopker, K. C. Simmen, C. C. Tschucke, R. Sandford, E. Kim, G. Thomas and G. Walz (2005). "Trafficking of TRPP2 by PACS proteins represents a novel mechanism of ion channel regulation." EMBO J **24**(4): 705-716.

Kottgen, M., B. Buchholz, M. A. Garcia-Gonzalez, F. Kotsis, X. Fu, M. Doerken, C. Boehlke, D. Steffl, R. Tauber, T. Wegierski, R. Nitschke, M. Suzuki, A. Kramer-Zucker, G. G. Germino, T. Watnick, J. Prenen, B. Nilius, E. W. Kuehn and G. Walz (2008). "TRPP2 and TRPV4 form a polymodal sensory channel complex." J Cell Biol **182**(3): 437-447.

Kottgen, M., A. Hofherr, W. Li, K. Chu, S. Cook, C. Montell and T. Watnick (2011). "Drosophila sperm swim backwards in the female reproductive tract and are activated via TRPP2 ion channels." PLoS One **6**(5): e20031.

Koulen, P., Y. Cai, L. Geng, Y. Maeda, S. Nishimura, R. Witzgall, B. E. Ehrlich and S. Somlo (2002). "Polycystin-2 is an intracellular calcium release channel." Nat Cell Biol **4**(3): 191-197.

Krasnoperov, V., I. E. Deyev, O. V. Serova, C. Xu, Y. Lu, L. Buryanovsky, A. G. Gabibov, T. A. Neubert and A. G. Petrenko (2009). "Dissociation of the subunits of the calcium-independent receptor of alpha-latrotoxin as a result of two-step proteolysis." Biochemistry **48**(14): 3230-3238.

Kreidberg, J. A., M. J. Donovan, S. L. Goldstein, H. Rennke, K. Shepherd, R. C. Jones and R. Jaenisch (1996). "Alpha 3 beta 1 integrin has a crucial role in kidney and lung organogenesis." Development **122**(11): 3537-3547.

Kuehn, E. W., M. N. Hirt, A. K. John, P. Muehlenhardt, C. Boehlke, M. Putz, A. G. Kramer-Zucker, M. Bashkurov, P. S. van de Weyer, F. Kotsis and G. Walz (2007). "Kidney injury molecule 1 (Kim1) is a novel ciliary molecule and interactor of polycystin 2." Biochem Biophys Res Commun **364**(4): 861-866.

Kurbegovic, A. (2006). Étude in vivo du rôle du domaine extracellulaire de la polycystine-1. M. Sc. thesis, Université de Montréal.

Kurbegovic, A., O. Cote, M. Couillard, C. J. Ward, P. C. Harris and M. Trudel (2010). "Pkd1 transgenic mice: adult model of polycystic kidney disease with extrarenal and renal phenotypes." Hum Mol Genet **19**(7): 1174-1189.

Kurbegovic, A. and M. Trudel (2013). "Progressive development of polycystic kidney disease in the mouse model expressing Pkd1 extracellular domain." Hum Mol Genet **22**(12): 2361-2375.

Kurbegovic, A., H. Kim, H. Xu, S. Yu, J. Cruanes, R. L. Maser, A. Boletta, M. Trudel and F. Qian (2014). "Novel Functional Complexity of Polycystin-1 by GPS Cleavage In Vivo: Role in Polycystic Kidney Disease." Mol Cell Biol **34**(17): 3341-3353.

Kwon, M., T. S. Pavlov, K. Nozu, S. A. Rasmussen, D. V. Ilatovskaya, A. Lerch-Gaggl, L. M. North, H. Kim, F. Qian, W. E. Sweeney, Jr., E. D. Avner, J. B. Blumer, A. Staruschenko and F. Park (2012). "G-protein signaling modulator 1 deficiency accelerates cystic disease in an orthologous mouse model of autosomal dominant polycystic kidney disease." Proc Natl Acad Sci U S A **109**(52): 21462-21467.

Lager, D. J., Q. Qian, R. J. Bengal, M. Ishibashi and V. E. Torres (2001). "The pck rat: a new model that resembles human autosomal dominant polycystic kidney and liver disease." Kidney Int **59**(1): 126-136.

Lal, M., X. Song, J. L. Pluznick, V. Di Giovanni, D. M. Merrick, N. D. Rosenblum, V. Chauvet, C. J. Gottardi, Y. Pei and M. J. Caplan (2008). "Polycystin-1 C-terminal tail associates with beta-catenin and inhibits canonical Wnt signaling." Hum Mol Genet **17**(20): 3105-3117.

Langenhan, T., G. Aust and J. Hamann (2013). "Sticky signaling--adhesion class G protein-coupled receptors take the stage." Sci Signal **6**(276): re3.

Lanoix, J., V. D'Agati, M. Szabolcs and M. Trudel (1996). "Dysregulation of cellular proliferation and apoptosis mediates human autosomal dominant polycystic kidney disease (ADPKD)." Oncogene **13**(6): 1153-1160.

Lantinga-van Leeuwen, I. S., J. G. Dauwerse, H. J. Baelde, W. N. Leonhard, A. van de Wal, C. J. Ward, S. Verbeek, M. C. Deruiter, M. H. Breuning, E. de Heer and D. J. Peters (2004). "Lowering of Pkd1 expression is sufficient to cause polycystic kidney disease." Hum Mol Genet **13**(24): 3069-3077.

Lantinga-van Leeuwen, I. S., W. N. Leonhard, A. van der Wal, M. H. Breuning, E. de Heer and D. J. Peters (2007). "Kidney-specific inactivation of the Pkd1 gene induces rapid cyst formation in developing kidneys and a slow onset of disease in adult mice." Hum Mol Genet **16**(24): 3188-3196.

Lebeau, C., K. Hanaoka, M. L. Moore-Hoon, W. B. Guggino, R. Beauwens and O. Devuyst (2002). "Basolateral chloride transporters in autosomal dominant polycystic kidney disease." Pflugers Arch **444**(6): 722-731.

Lee, J. E., M. H. Park and J. H. Park (2004). "The gene expression profile of cyst epithelial cells in autosomal dominant polycystic kidney disease patients." J Biochem Mol Biol **37**(5): 612-617.

Lee, S. O., T. Masyuk, P. Splinter, J. M. Banales, A. Masyuk, A. Stroope and N. Larusso (2008). "MicroRNA15a modulates expression of the cell-cycle regulator Cdc25A and affects hepatic cystogenesis in a rat model of polycystic kidney disease." J Clin Invest **118**(11): 3714-3724.

Lehtonen, S., A. Ora, V. M. Olkkonen, L. Geng, M. Zerial, S. Somlo and E. Lehtonen (2000). "In vivo interaction of the adapter protein CD2-associated protein with the type 2 polycystic kidney disease protein, polycystin-2." J Biol Chem **275**(42): 32888-32893.

Leonhard, W. N., A. van der Wal, Z. Novalic, S. J. Kunnen, R. T. Gansevoort, M. H. Breuning, E. de Heer and D. J. Peters (2011). "Curcumin inhibits cystogenesis by simultaneous interference of multiple signaling pathways: in vivo evidence from a Pkd1-deletion model." Am J Physiol Renal Physiol **300**(5): F1193-1202.

Lepourcelet, M., Y. N. Chen, D. S. France, H. Wang, P. Crews, F. Petersen, C. Bruseo, A. W. Wood and R. A. Shivdasani (2004). "Small-molecule antagonists of the oncogenic Tcf/beta-catenin protein complex." Cancer Cell **5**(1): 91-102.

Li, A., X. Tian, S. W. Sung and S. Somlo (2003). "Identification of two novel polycystic kidney disease-1-like genes in human and mouse genomes." Genomics **81**(6): 596-608.

Li, H., I. A. Findlay and D. N. Sheppard (2004). "The relationship between cell proliferation, Cl- secretion, and renal cyst growth: a study using CFTR inhibitors." Kidney Int **66**(5): 1926-1938.

Li, H. P., L. Geng, C. R. Burrow and P. D. Wilson (1999). "Identification of phosphorylation sites in the PKD1-encoded protein C-terminal domain." Biochem Biophys Res Commun **259**(2): 356-363.

Li, K. J., A. L. Shiau, Y. Y. Chiou, Y. T. Yo and C. L. Wu (2005). "Transgenic overexpression of prothymosin alpha induces development of polycystic kidney disease." Kidney Int **67**(5): 1710-1722.

Li, Q., Y. Dai, L. Guo, Y. Liu, C. Hao, G. Wu, N. Basora, M. Michalak and X. Z. Chen (2003). "Polycystin-2 associates with tropomyosin-1, an actin microfilament component." J Mol Biol **325**(5): 949-962.

Li, Q., N. Montalbetti, P. Y. Shen, X. Q. Dai, C. I. Cheeseman, E. Karpinski, G. Wu, H. F. Cantiello and X. Z. Chen (2005). "Alpha-actinin associates with polycystin-2 and regulates its channel activity." Hum Mol Genet **14**(12): 1587-1603.

Li, Q., N. Montalbetti, Y. Wu, A. Ramos, M. K. Raychowdhury, X. Z. Chen and H. F. Cantiello (2006). "Polycystin-2 cation channel function is under the control of microtubular structures in primary cilia of renal epithelial cells." J Biol Chem **281**(49): 37566-37575.

Li, X., C. R. Burrow, K. Polgar, D. P. Hyink, G. L. Gusella and P. D. Wilson (2008). "Protein kinase X (PRKX) can rescue the effects of polycystic kidney disease-1 gene (PKD1) deficiency." Biochim Biophys Acta **1782**(1): 1-9.

Li, X., Y. Luo, P. G. Starremans, C. A. McNamara, Y. Pei and J. Zhou (2005). "Polycystin-1 and polycystin-2 regulate the cell cycle through the helix-loop-helix inhibitor Id2." Nat Cell Biol **7**(12): 1202-1212.

Li, X., B. S. Magenheimer, S. Xia, T. Johnson, D. P. Wallace, J. P. Calvet and R. Li (2008). "A tumor necrosis factor-alpha-mediated pathway promoting autosomal dominant polycystic kidney disease." Nat Med **14**(8): 863-868.

Li, Y., J. M. Wright, F. Qian, G. G. Germino and W. B. Guggino (2005). "Polycystin 2 interacts with type I inositol 1,4,5-trisphosphate receptor to modulate intracellular Ca2+ signaling." J Biol Chem **280**(50): 41298-41306.

Liang, G., Q. Li, Y. Tang, K. Kokame, T. Kikuchi, G. Wu and X. Z. Chen (2008). "Polycystin-2 is regulated by endoplasmic reticulum-associated degradation." Hum Mol Genet **17**(8): 1109-1119.

Liang, G., J. Yang, Z. Wang, Q. Li, Y. Tang and X. Z. Chen (2008). "Polycystin-2 down-regulates cell proliferation via promoting PERK-dependent phosphorylation of eIF2alpha." Hum Mol Genet **17**(20): 3254-3262.

Lienkamp, S. S., K. Liu, C. M. Karner, T. J. Carroll, O. Ronneberger, J. B. Wallingford and G. Walz (2012). "Vertebrate kidney tubules elongate using a planar cell polarity-dependent, rosette-based mechanism of convergent extension." Nat Genet **44**(12): 1382-1387.

Lin, F., T. Hiesberger, K. Cordes, A. M. Sinclair, L. S. Goldstein, S. Somlo and P. Igarashi (2003). "Kidney-specific inactivation of the KIF3A subunit of kinesin-II inhibits renal ciliogenesis and produces polycystic kidney disease." Proc Natl Acad Sci U S A **100**(9): 5286-5291.

Little, M. H. and A. P. McMahon (2012). "Mammalian kidney development: principles, progress, and projections." Cold Spring Harb Perspect Biol **4**(5).

Liu, G., S. Myers, X. Chen, J. J. Bissler, R. R. Sinden and M. Leffak (2012). "Replication fork stalling and checkpoint activation by a PKD1 locus mirror repeat polypurine-polypyrimidine (Pu-Py) tract." J Biol Chem **287**(40): 33412-33423.

Liu, S., W. Lu, T. Obara, S. Kuida, J. Lehoczky, K. Dewar, I. A. Drummond and D. R. Beier (2002). "A defect in a novel Nek-family kinase causes cystic kidney disease in the mouse and in zebrafish." Development **129**(24): 5839-5846.

Lo, S. H., Q. C. Yu, L. Degenstein, L. B. Chen and E. Fuchs (1997). "Progressive kidney degeneration in mice lacking tensin." J Cell Biol **136**(6): 1349-1361.

Lohning, C., U. Nowicka and A. M. Frischauf (1997). "The mouse homolog of PKD1: sequence analysis and alternative splicing." Mamm Genome **8**(5): 307-311.

Longa, L., F. Scolari, A. Brusco, C. Carbonara, S. Polidoro, B. Valzorio, P. Riegler, N. Migone and R. Maiorca (1997). "A large TSC2 and PKD1 gene deletion is associated with renal and extrarenal signs of autosomal dominant polycystic kidney disease." Nephrol Dial Transplant **12**(9): 1900-1907.

Losekoot, M., C. A. Ruivenkamp, A. P. Tholens, J. E. Grimbergen, L. Vijfhuizen, S. Vermeer, H. B. Dijkman, E. A. Cornelissen, E. M. Bongers and D. J. Peters (2012). "Neonatal onset autosomal dominant polycystic kidney disease (ADPKD) in a patient homozygous for a PKD2 missense mutation due to uniparental disomy." J Med Genet **49**(1): 37-40.

Low, S. H., S. Vasanth, C. H. Larson, S. Mukherjee, N. Sharma, M. T. Kinter, M. E. Kane, T. Obara and T. Weimbs (2006). "Polycystin-1, STAT6, and P100 function in a pathway that transduces ciliary mechanosensation and is activated in polycystic kidney disease." Dev Cell **10**(1): 57-69.

Lowden, D. A., G. W. Lindemann, G. Merlino, B. D. Barash, J. P. Calvet and V. H. Gattone, 2nd (1994). "Renal cysts in transgenic mice expressing transforming growth factor-alpha." J Lab Clin Med **124**(3): 386-394.

Lu, W., X. Fan, N. Basora, H. Babakhanlou, T. Law, N. Rifai, P. C. Harris, A. R. Perez-Atayde, H. G. Rennke and J. Zhou (1999). "Late onset of renal and hepatic cysts in Pkd1-targeted heterozygotes." Nat Genet **21**(2): 160-161.

Lu, W., B. Peissel, H. Babakhanlou, A. Pavlova, L. Geng, X. Fan, C. Larson, G. Brent and J. Zhou (1997). "Perinatal lethality with kidney and pancreas defects in mice with a targetted Pkd1 mutation." Nat Genet **17**(2): 179-181.

Lu, W., X. Shen, A. Pavlova, M. Lakkis, C. J. Ward, L. Pritchard, P. C. Harris, D. R. Genest, A. R. Perez-Atayde and J. Zhou (2001). "Comparison of Pkd1-targeted

mutants reveals that loss of polycystin-1 causes cystogenesis and bone defects." Hum Mol Genet **10**(21): 2385-2396.

Luyten, A., X. Su, S. Gondela, Y. Chen, S. Rompani, A. Takakura and J. Zhou (2010). "Aberrant regulation of planar cell polarity in polycystic kidney disease." J Am Soc Nephrol **21**(9): 1521-1532.

Ma, M., X. Tian, P. Igarashi, G. J. Pazour and S. Somlo (2013). "Loss of cilia suppresses cyst growth in genetic models of autosomal dominant polycystic kidney disease." Nat Genet **45**(9): 1004-1012.

Ma, R., W. P. Li, D. Rundle, J. Kong, H. I. Akbarali and L. Tsiokas (2005). "PKD2 functions as an epidermal growth factor-activated plasma membrane channel." Mol Cell Biol **25**(18): 8285-8298.

MacKay, K., L. J. Striker, C. A. Pinkert, R. L. Brinster and G. E. Striker (1987). "Glomerulosclerosis and renal cysts in mice transgenic for the early region of SV40." Kidney Int **32**(6): 827-837.

Madsen, O. D., J. Jensen, N. Blume, H. V. Petersen, K. Lund, C. Karlsen, F. G. Andersen, P. B. Jensen, L. I. Larsson and P. Serup (1996). "Pancreatic development and maturation of the islet B cell. Studies of pluripotent islet cultures." Eur J Biochem **242**(3): 435-445.

Magenheimer, B. S., P. L. St John, K. S. Isom, D. R. Abrahamson, R. C. De Lisle, D. P. Wallace, R. L. Maser, J. J. Grantham and J. P. Calvet (2006). "Early embryonic renal tubules of wild-type and polycystic kidney disease kidneys respond to cAMP stimulation with cystic fibrosis transmembrane conductance regulator/Na(+),K(+),2Cl(-) Co-transporter-dependent cystic dilation." J Am Soc Nephrol **17**(12): 3424-3437.

Magistroni, R., N. He, K. Wang, R. Andrew, A. Johnson, P. Gabow, E. Dicks, P. Parfrey, R. Torra, J. L. San-Millan, E. Coto, M. Van Dijk, M. Breuning, D. Peters, N. Bogdanova, G. Ligabue, A. Albertazzi, N. Hateboer, K. Demetriou, A. Pierides, C. Deltas, P. St George-Hyslop, D. Ravine and Y. Pei (2003). "Genotype-renal function correlation in type 2 autosomal dominant polycystic kidney disease." J Am Soc Nephrol **14**(5): 1164-1174.

Makita, R., Y. Uchijima, K. Nishiyama, T. Amano, Q. Chen, T. Takeuchi, A. Mitani, T. Nagase, Y. Yatomi, H. Aburatani, O. Nakagawa, E. V. Small, P. Cobo-Stark, P. Igarashi, M. Murakami, J. Tominaga, T. Sato, T. Asano, Y. Kurihara and H. Kurihara (2008). "Multiple renal cysts, urinary concentration defects, and pulmonary emphysematous changes in mice lacking TAZ." Am J Physiol Renal Physiol **294**(3): F542-553.

Malhas, A. N., R. A. Abuknesha and R. G. Price (2002). "Interaction of the leucine-rich repeats of polycystin-1 with extracellular matrix proteins: possible role in cell proliferation." J Am Soc Nephrol **13**(1): 19-26.

Mangoo-Karim, R., M. Uchic, C. Lechene and J. J. Grantham (1989). "Renal epithelial cyst formation and enlargement in vitro: dependence on cAMP." Proc Natl Acad Sci U S A **86**(15): 6007-6011.

Mangoo-Karim, R., M. E. Uchic, M. Grant, W. A. Shumate, J. P. Calvet, C. H. Park and J. J. Grantham (1989). "Renal epithelial fluid secretion and cyst growth: the role of cyclic AMP." FASEB J **3**(14): 2629-2632.

Mangos, S., P. Y. Lam, A. Zhao, Y. Liu, S. Mudumana, A. Vasilyev, A. Liu and I. A. Drummond (2010). "The ADPKD genes pkd1a/b and pkd2 regulate extracellular matrix formation." Dis Model Mech **3**(5-6): 354-365.

Manning, D. K., M. Sergeev, R. G. van Heesbeen, M. D. Wong, J. H. Oh, Y. Liu, R. M. Henkelman, I. Drummond, J. V. Shah and D. R. Beier (2013). "Loss of the ciliary kinase Nek8 causes left-right asymmetry defects." J Am Soc Nephrol **24**(1): 100-112.

Mao, Y., J. Mulvaney, S. Zakaria, T. Yu, K. M. Morgan, S. Allen, M. A. Basson, P. Francis-West and K. D. Irvine (2011). "Characterization of a Dchs1 mutant mouse reveals requirements for Dchs1-Fat4 signaling during mammalian development." Development **138**(5): 947-957.

Marciano, D. K., P. R. Brakeman, C. Z. Lee, N. Spivak, D. J. Eastburn, D. M. Bryant, G. M. Beaudoin, 3rd, I. Hofmann, K. E. Mostov and L. F. Reichardt (2011). "p120 catenin is required for normal renal tubulogenesis and glomerulogenesis." Development **138**(10): 2099-2109.

Markoff, A., N. Bogdanova, M. Knop, C. Ruffer, H. Kenis, P. Lux, C. Reutelingsperger, V. Todorov, B. Dworniczak, J. Horst and V. Gerke (2007). "Annexin A5 interacts with polycystin-1 and interferes with the polycystin-1 stimulated recruitment of E-cadherin into adherens junctions." J Mol Biol **369**(4): 954-966.

Markowitz, G. S., Y. Cai, L. Li, G. Wu, L. C. Ward, S. Somlo and V. D. D'Agati (1999). "Polycystin-2 expression is developmentally regulated." Am J Physiol **277**(1 Pt 2): F17-25.

Masyuk, A. I., B. Q. Huang, C. J. Ward, S. A. Gradilone, J. M. Banales, T. V. Masyuk, B. Radtke, P. L. Splinter and N. F. LaRusso (2010). "Biliary exosomes influence cholangiocyte regulatory mechanisms and proliferation through interaction with primary cilia." Am J Physiol Gastrointest Liver Physiol **299**(4): G990-999.

Masyuk, A. I., T. V. Masyuk, P. L. Splinter, B. Q. Huang, A. J. Stroope and N. F. LaRusso (2006). "Cholangiocyte cilia detect changes in luminal fluid flow and transmit them into intracellular Ca2+ and cAMP signaling." Gastroenterology **131**(3): 911-920.

McDonald, A. T., J. F. Crocker, S. C. Digout, S. C. McCarthy, S. R. Blecher and D. E. Cole (1990). "Glucocorticoid-induced polycystic kidney disease--a threshold trait." Kidney Int **37**(3): 901-908.

Menezes, L. F., Y. Cai, Y. Nagasawa, A. M. Silva, M. L. Watkins, A. M. Da Silva, S. Somlo, L. M. Guay-Woodford, G. G. Germino and L. F. Onuchic (2004). "Polyductin, the PKHD1 gene product, comprises isoforms expressed in plasma membrane, primary cilium, and cytoplasm." Kidney Int **66**(4): 1345-1355.

Menezes, L. F., F. Zhou, A. D. Patterson, K. B. Piontek, K. W. Krausz, F. J. Gonzalez and G. G. Germino (2012). "Network analysis of a Pkd1-mouse model of autosomal dominant polycystic kidney disease identifies HNF4alpha as a disease modifier." PLoS Genet **8**(11): e1003053.

Merrick, D., H. Chapin, J. E. Baggs, Z. Yu, S. Somlo, Z. Sun, J. B. Hogenesch and M. J. Caplan (2012). "The gamma-secretase cleavage product of polycystin-1 regulates TCF and CHOP-mediated transcriptional activation through a p300-dependent mechanism." Dev Cell **22**(1): 197-210.

Metcalf, D., S. Mifsud, L. Di Rago, N. A. Nicola, D. J. Hilton and W. S. Alexander (2002). "Polycystic kidneys and chronic inflammatory lesions are the delayed consequences of loss of the suppressor of cytokine signaling-1 (SOCS-1)." Proc Natl Acad Sci U S A **99**(2): 943-948.

Michaud, J., P. Russo, A. Grignon, L. Dallaire, D. Bichet, D. Rosenblatt, E. Lamothe and M. Lambert (1994). "Autosomal dominant polycystic kidney disease in the fetus." Am J Med Genet **51**(3): 240-246.

Miller, M. M., D. M. Iglesias, Z. Zhang, R. Corsini, L. Chu, I. Murawski, I. Gupta, S. Somlo, G. G. Germino and P. R. Goodyer (2011). "T-cell factor/beta-catenin activity is

suppressed in two different models of autosomal dominant polycystic kidney disease." Kidney Int **80**(2): 146-153.

Milutinovic, J., P. F. Rust, P. J. Fialkow, L. Y. Agodoa, L. A. Phillips, T. G. Rudd and S. Sutherland (1992). "Intrafamilial phenotypic expression of autosomal dominant polycystic kidney disease." Am J Kidney Dis **19**(5): 465-472.

Mochizuki, T., Y. Saijoh, K. Tsuchiya, Y. Shirayoshi, S. Takai, C. Taya, H. Yonekawa, K. Yamada, H. Nihei, N. Nakatsuji, P. A. Overbeek, H. Hamada and T. Yokoyama (1998). "Cloning of inv, a gene that controls left/right asymmetry and kidney development." Nature **395**(6698): 177-181.

Mokrzan, E. M., J. S. Lewis and K. Mykytyn (2007). "Differences in renal tubule primary cilia length in a mouse model of Bardet-Biedl syndrome." Nephron Exp Nephrol **106**(3): e88-96.

Moller, S., M. D. Croning and R. Apweiler (2001). "Evaluation of methods for the prediction of membrane spanning regions." Bioinformatics **17**(7): 646-653.

Montell, C., L. Birnbaumer and V. Flockerzi (2002). "The TRP channels, a remarkably functional family." Cell **108**(5): 595-598.

Morgan, D., L. Turnpenny, J. Goodship, W. Dai, K. Majumder, L. Matthews, A. Gardner, G. Schuster, L. Vien, W. Harrison, F. F. Elder, M. Penman-Splitt, P. Overbeek and T. Strachan (1998). "Inversin, a novel gene in the vertebrate left-right axis pathway, is partially deleted in the inv mouse." Nat Genet **20**(2): 149-156.

Morham, S. G., R. Langenbach, C. D. Loftin, H. F. Tiano, N. Vouloumanos, J. C. Jennette, J. F. Mahler, K. D. Kluckman, A. Ledford, C. A. Lee and O. Smithies (1995). "Prostaglandin synthase 2 gene disruption causes severe renal pathology in the mouse." Cell **83**(3): 473-482.

Morishita, Y., T. Matsuzaki, M. Hara-chikuma, A. Andoo, M. Shimono, A. Matsuki, K. Kobayashi, M. Ikeda, T. Yamamoto, A. Verkman, E. Kusano, S. Ookawara, K. Takata, S. Sasaki and K. Ishibashi (2005). "Disruption of aquaporin-11 produces polycystic kidneys following vacuolization of the proximal tubule." Mol Cell Biol **25**(17): 7770-7779.

Moser, M., S. Dahmen, R. Kluge, H. Grone, J. Dahmen, D. Kunz, H. Schorle and R. Buettner (2003). "Terminal renal failure in mice lacking transcription factor AP-2 beta." Lab Invest **83**(4): 571-578.

Moser, M., S. Matthiesen, J. Kirfel, H. Schorle, C. Bergmann, J. Senderek, S. Rudnik-Schoneborn, K. Zerres and R. Buettner (2005). "A mouse model for cystic biliary dysgenesis in autosomal recessive polycystic kidney disease (ARPKD)." Hepatology **41**(5): 1113-1121.

Moy, G. W., L. M. Mendoza, J. R. Schulz, W. J. Swanson, C. G. Glabe and V. D. Vacquier (1996). "The sea urchin sperm receptor for egg jelly is a modular protein with extensive homology to the human polycystic kidney disease protein, PKD1." J Cell Biol **133**(4): 809-817.

Moyer, J. H., M. J. Lee-Tischler, H. Y. Kwon, J. J. Schrick, E. D. Avner, W. E. Sweeney, V. L. Godfrey, N. L. Cacheiro, J. E. Wilkinson and R. P. Woychik (1994). "Candidate gene associated with a mutation causing recessive polycystic kidney disease in mice." Science **264**(5163): 1329-1333.

Munn, C. A. (1886). "Note on a Method of obtaining Uric Acid Crystals from the Malpighian Tubes of Insects and from the Nephridium of Pulmonate Mollusca." J Physiol **7**(2): 128-129.

Murcia, N. S., W. G. Richards, B. K. Yoder, M. L. Mucenski, J. R. Dunlap and R. P. Woychik (2000). "The Oak Ridge Polycystic Kidney (orpk) disease gene is required for left-right axis determination." Development **127**(11): 2347-2355.

Muto, S., A. Aiba, Y. Saito, K. Nakao, K. Nakamura, K. Tomita, T. Kitamura, M. Kurabayashi, R. Nagai, E. Higashihara, P. C. Harris, M. Katsuki and S. Horie (2002). "Pioglitazone improves the phenotype and molecular defects of a targeted Pkd1 mutant." Hum Mol Genet **11**(15): 1731-1742.

Nachury, M. V., A. V. Loktev, Q. Zhang, C. J. Westlake, J. Peranen, A. Merdes, D. C. Slusarski, R. H. Scheller, J. F. Bazan, V. C. Sheffield and P. K. Jackson (2007). "A core complex of BBS proteins cooperates with the GTPase Rab8 to promote ciliary membrane biogenesis." Cell **129**(6): 1201-1213.

Nagao, S., T. Ushijima, M. Kasahara, T. Yamaguchi, M. Kusaka, J. Matsuda, M. Nagao and H. Takahashi (1999). "Closely linked polymorphic markers for determining the autosomal dominant allele (Cy) in rat polycystic kidney disease." Biochem Genet **37**(7-8): 227-235.

Nagao, S., T. Watanabe, N. Ogiso, T. Marunouchi and H. Takahashi (1995). "Genetic mapping of the polycystic kidney gene, pcy, on mouse chromosome 9." Biochem Genet **33**(11-12): 401-412.

Nakayama, K., K. Nakayama, I. Negishi, K. Kuida, H. Sawa and D. Y. Loh (1994). "Targeted disruption of Bcl-2 alpha beta in mice: occurrence of gray hair, polycystic kidney disease, and lymphocytopenia." Proc Natl Acad Sci U S A **91**(9): 3700-3704.

Natoli, T. A., T. C. Gareski, W. R. Dackowski, L. Smith, N. O. Bukanov, R. J. Russo, H. Husson, D. Matthews, P. Piepenhagen and O. Ibraghimov-Beskrovnaya (2008). "Pkd1 and Nek8 mutations affect cell-cell adhesion and cilia in cysts formed in kidney organ cultures." Am J Physiol Renal Physiol **294**(1): F73-83.

Natoli, T. A., L. A. Smith, K. A. Rogers, B. Wang, S. Komarnitsky, Y. Budman, A. Belenky, N. O. Bukanov, W. R. Dackowski, H. Husson, R. J. Russo, J. A. Shayman, S. R. Ledbetter, J. P. Leonard and O. Ibraghimov-Beskrovnaya (2010). "Inhibition of glucosylceramide accumulation results in effective blockade of polycystic kidney disease in mouse models." Nat Med **16**(7): 788-792.

Nauli, S. M., F. J. Alenghat, Y. Luo, E. Williams, P. Vassilev, X. Li, A. E. Elia, W. Lu, E. M. Brown, S. J. Quinn, D. E. Ingber and J. Zhou (2003). "Polycystins 1 and 2 mediate mechanosensation in the primary cilium of kidney cells." Nat Genet **33**(2): 129-137.

Nauli, S. M., X. Jin, W. A. AbouAlaiwi, W. El-Jouni, X. Su and J. Zhou (2013). "Non-motile primary cilia as fluid shear stress mechanosensors." Methods Enzymol **525**: 1-20.

Nauli, S. M., S. Rossetti, R. J. Kolb, F. J. Alenghat, M. B. Consugar, P. C. Harris, D. E. Ingber, M. Loghman-Adham and J. Zhou (2006). "Loss of polycystin-1 in human cyst-lining epithelia leads to ciliary dysfunction." J Am Soc Nephrol **17**(4): 1015-1025.

Nauta, J., M. A. Goedbloed, H. V. Herck, D. A. Hesselink, P. Visser, R. Willemsen, R. P. Dokkum, C. J. Wright and L. M. Guay-Woodford (2000). "New rat model that phenotypically resembles autosomal recessive polycystic kidney disease." J Am Soc Nephrol **11**(12): 2272-2284.

Nechiporuk, T., T. E. Fernandez and V. Vasioukhin (2007). "Failure of epithelial tube maintenance causes hydrocephalus and renal cysts in Dlg5-/- mice." Dev Cell **13**(3): 338-350.

Newby, L. J., A. J. Streets, Y. Zhao, P. C. Harris, C. J. Ward and A. C. Ong (2002). "Identification, characterization, and localization of a novel kidney polycystin-1-polycystin-2 complex." J Biol Chem **277**(23): 20763-20773.

Nguyen, H. Q., D. M. Danilenko, N. Bucay, M. L. DeRose, G. Y. Van, A. Thomason and W. S. Simonet (1996). "Expression of keratinocyte growth factor in embryonic liver of transgenic mice causes changes in epithelial growth and differentiation resulting in polycystic kidneys and other organ malformations." Oncogene **12**(10): 2109-2119.

Nickel, C., T. Benzing, L. Sellin, P. Gerke, A. Karihaloo, Z. X. Liu, L. G. Cantley and G. Walz (2002). "The polycystin-1 C-terminal fragment triggers branching morphogenesis and migration of tubular kidney epithelial cells." J Clin Invest **109**(4): 481-489.

Nie, X. and L. J. Arend (2013). "Pkd1 is required for male reproductive tract development." Mech Dev 130(11-12):567-76.

Nishimoto, I., T. Okamoto, Y. Matsuura, S. Takahashi, T. Okamoto, Y. Murayama and E. Ogata (1993). "Alzheimer amyloid protein precursor complexes with brain GTP-binding protein G(o)." Nature **362**(6415): 75-79.

Nishimura, D. Y., M. Fath, R. F. Mullins, C. Searby, M. Andrews, R. Davis, J. L. Andorf, K. Mykytyn, R. E. Swiderski, B. Yang, R. Carmi, E. M. Stone and V. C. Sheffield (2004). "Bbs2-null mice have neurosensory deficits, a defect in social dominance, and retinopathy associated with mislocalization of rhodopsin." Proc Natl Acad Sci U S A **101**(47): 16588-16593.

Nishio, S., M. Hatano, M. Nagata, S. Horie, T. Koike, T. Tokuhisa and T. Mochizuki (2005). "Pkd1 regulates immortalized proliferation of renal tubular epithelial cells through p53 induction and JNK activation." J Clin Invest **115**(4): 910-918.

Noguchi, C. T., M. Gladwin, B. Diwan, P. Merciris, R. Smith, X. Yu, G. Buzard, A. Fitzhugh, L. K. Keefer, A. N. Schechter and N. Mohandas (2001). "Pathophysiology of a sickle cell trait mouse model: human alpha(beta)(S) transgenes with one mouse beta-globin allele." Blood Cells Mol Dis **27**(6): 971-977.

Nomura, H., A. E. Turco, Y. Pei, L. Kalaydjieva, T. Schiavello, S. Weremowicz, W. Ji, C. C. Morton, M. Meisler, S. T. Reeders and J. Zhou (1998). "Identification of PKDL, a novel polycystic kidney disease 2-like gene whose murine homologue is deleted in mice with kidney and retinal defects." J Biol Chem **273**(40): 25967-25973.

O'Sullivan, D. A., V. E. Torres, P. A. Gabow, S. N. Thibodeau, B. F. King and E. J. Bergstralh (1998). "Cystic fibrosis and the phenotypic expression of autosomal dominant polycystic kidney disease." Am J Kidney Dis **32**(6): 976-983.

Oatley, P., A. P. Stewart, R. Sandford and J. M. Edwardson (2012). "Atomic force microscopy imaging reveals the domain structure of polycystin-1." Biochemistry **51**(13): 2879-2888.

Oatley, P., M. M. Talukder, A. P. Stewart, R. Sandford and J. M. Edwardson (2013). "Polycystin-2 Induces a Conformational Change in Polycystin-1." Biochemistry 6;52(31):5280-7.

Obara, T., S. Mangos, Y. Liu, J. Zhao, S. Wiessner, A. G. Kramer-Zucker, F. Olale, A. F. Schier and I. A. Drummond (2006). "Polycystin-2 immunolocalization and function in zebrafish." J Am Soc Nephrol **17**(10): 2706-2718.

Obermuller, N., Y. Cai, B. Kranzlin, R. B. Thomson, N. Gretz, W. Kriz, S. Somlo and R. Witzgall (2002). "Altered expression pattern of polycystin-2 in acute and chronic renal tubular diseases." J Am Soc Nephrol **13**(7): 1855-1864.

Ohno, K. and K. Kondo (1989). "A mutant rat with congenital skeletal abnormalities and polycystic kidneys." Jikken Dobutsu **38**(2): 139-146.

Ojeda, J. L., M. A. Ros and J. A. Garcia-Porrero (1986). "Polycystic kidney disease induced by corticoids. A quantitative and qualitative analysis of cell populations in the tubular cysts." Nephron **42**(3): 240-248.

Okajima, D., G. Kudo and H. Yokota (2010). "Brain-specific angiogenesis inhibitor 2 (BAI2) may be activated by proteolytic processing." J Recept Signal Transduct Res **30**(3): 143-153.

Olbrich, H., M. Fliegauf, J. Hoefele, A. Kispert, E. Otto, A. Volz, M. T. Wolf, G. Sasmaz, U. Trauer, R. Reinhardt, R. Sudbrak, C. Antignac, N. Gretz, G. Walz, B. Schermer, T. Benzing, F. Hildebrandt and H. Omran (2003). "Mutations in a novel gene, NPHP3, cause adolescent nephronophthisis, tapeto-retinal degeneration and hepatic fibrosis." Nat Genet **34**(4): 455-459.

Onda, H., A. Lueck, P. W. Marks, H. B. Warren and D. J. Kwiatkowski (1999). "Tsc2(+/-) mice develop tumors in multiple sites that express gelsolin and are influenced by genetic background." J Clin Invest **104**(6): 687-695.

Ong, A. C., P. C. Harris, D. R. Davies, L. Pritchard, S. Rossetti, S. Biddolph, D. J. Vaux, N. Migone and C. J. Ward (1999). "Polycystin-1 expression in PKD1, early-onset PKD1, and TSC2/PKD1 cystic tissue." Kidney Int **56**(4): 1324-1333.

Ong, A. C., C. J. Ward, R. J. Butler, S. Biddolph, C. Bowker, R. Torra, Y. Pei and P. C. Harris (1999). "Coordinate expression of the autosomal dominant polycystic kidney disease proteins, polycystin-2 and polycystin-1, in normal and cystic tissue." Am J Pathol **154**(6): 1721-1729.

Onuchic, L. F., L. Furu, Y. Nagasawa, X. Hou, T. Eggermann, Z. Ren, C. Bergmann, J. Senderek, E. Esquivel, R. Zeltner, S. Rudnik-Schoneborn, M. Mrug, W. Sweeney, E. D. Avner, K. Zerres, L. M. Guay-Woodford, S. Somlo and G. G. Germino (2002). "PKHD1, the polycystic kidney and hepatic disease 1 gene, encodes a novel large protein

containing multiple immunoglobulin-like plexin-transcription-factor domains and parallel beta-helix 1 repeats." Am J Hum Genet **70**(5): 1305-1317.

Oppenheimer, E. H. and J. R. Esterly (1975). "Pathology of cystic fibrosis review of the literature and comparison with 146 autopsied cases." Perspect Pediatr Pathol **2**: 241-278.

Otto, E. A., B. Schermer, T. Obara, J. F. O'Toole, K. S. Hiller, A. M. Mueller, R. G. Ruf, J. Hoefele, F. Beekmann, D. Landau, J. W. Foreman, J. A. Goodship, T. Strachan, A. Kispert, M. T. Wolf, M. F. Gagnadoux, H. Nivet, C. Antignac, G. Walz, I. A. Drummond, T. Benzing and F. Hildebrandt (2003). "Mutations in INVS encoding inversin cause nephronophthisis type 2, linking renal cystic disease to the function of primary cilia and left-right axis determination." Nat Genet **34**(4): 413-420.

Palsson, R., C. P. Sharma, K. Kim, M. McLaughlin, D. Brown and M. A. Arnaout (1996). "Characterization and cell distribution of polycystin, the product of autosomal dominant polycystic kidney disease gene 1." Mol Med **2**(6): 702-711.

Pampliega, O., I. Orhon, B. Patel, S. Sridhar, A. Diaz-Carretero, I. Beau, P. Codogno, B. H. Satir, P. Satir and A. M. Cuervo (2013). "Functional interaction between autophagy and ciliogenesis." Nature **502**(7470): 194-200.

Pandey, P., S. Qin, J. Ho, J. Zhou and J. A. Kreidberg (2011). "Systems biology approach to identify transcriptome reprogramming and candidate microRNA targets during the progression of polycystic kidney disease." BMC Syst Biol **5**: 56.

Pang, C. J., W. Lemsaddek, Y. N. Alhashem, C. Bondzi, L. C. Redmond, N. Ah-Son, C. I. Dumur, K. J. Archer, J. L. Haar, J. A. Lloyd and M. Trudel (2012). "Kruppel-like factor 1 (KLF1), KLF2, and Myc control a regulatory network essential for embryonic erythropoiesis." Mol Cell Biol **32**(13): 2628-2644.

Park, E. Y., Y. H. Sung, M. H. Yang, J. Y. Noh, S. Y. Park, T. Y. Lee, Y. J. Yook, K. H. Yoo, K. J. Roh, I. Kim, Y. H. Hwang, G. T. Oh, J. K. Seong, C. Ahn, H. W. Lee and J. H. Park (2009). "Cyst formation in kidney via B-Raf signaling in the PKD2 transgenic mice." J Biol Chem **284**(11): 7214-7222.

Parnell, S. C., B. S. Magenheimer, R. L. Maser and J. P. Calvet (1999). "Identification of the major site of in vitro PKA phosphorylation in the polycystin-1 C-terminal cytosolic domain." Biochem Biophys Res Commun **259**(3): 539-543.

Parnell, S. C., B. S. Magenheimer, R. L. Maser, C. A. Rankin, A. Smine, T. Okamoto and J. P. Calvet (1998). "The polycystic kidney disease-1 protein, polycystin-1, binds and activates heterotrimeric G-proteins in vitro." Biochem Biophys Res Commun **251**(2): 625-631.

Parnell, S. C., B. S. Magenheimer, R. L. Maser, C. A. Zien, A. M. Frischauf and J. P. Calvet (2002). "Polycystin-1 activation of c-Jun N-terminal kinase and AP-1 is mediated by heterotrimeric G proteins." J Biol Chem **277**(22): 19566-19572.

Parnell, S. C., S. Puri, D. P. Wallace and J. P. Calvet (2012). "Protein phosphatase-1alpha interacts with and dephosphorylates polycystin-1." PLoS One **7**(6): e36798.

Parnell, S. C. M., B.S; Maser, R.L.; Havens, M.A.; Magenheimer, L.; Hastings, M.; Calvet J.P (2012). A Single Amino Acid Deletion in the Polycystin-1 (PC1) C-Tail Affects G-Protein Signaling and Causes PKD in Mice. J Am Soc Nephrol. **23:** 48A (FR-OR084).

Patel, H. P., L. Lu, R. T. Blaszak and J. J. Bissler (2004). "PKD1 intron 21: triplex DNA formation and effect on replication." Nucleic Acids Res **32**(4): 1460-1468.

Patel, V., S. Hajarnis, D. Williams, R. Hunter, D. Huynh and P. Igarashi (2012). "MicroRNAs regulate renal tubule maturation through modulation of Pkd1." J Am Soc Nephrol **23**(12): 1941-1948.

Patel, V., L. Li, P. Cobo-Stark, X. Shao, S. Somlo, F. Lin and P. Igarashi (2008). "Acute kidney injury and aberrant planar cell polarity induce cyst formation in mice lacking renal cilia." Hum Mol Genet **17**(11): 1578-1590.

Patel, V., D. Williams, S. Hajarnis, R. Hunter, M. Pontoglio, S. Somlo and P. Igarashi (2013). "miR-17~92 miRNA cluster promotes kidney cyst growth in polycystic kidney disease." Proc Natl Acad Sci U S A **110**(26): 10765-10770.

Paul, B. M., M. B. Consugar, M. Ryan Lee, J. L. Sundsbak, C. M. Heyer, S. Rossetti, V. J. Kubly, K. Hopp, V. E. Torres, E. Coto, M. Clementi, N. Bogdanova, E. de Almeida, D. G. Bichet and P. C. Harris (2014). "Evidence of a third ADPKD locus is not supported by re-analysis of designated PKD3 families." Kidney Int **85**(2): 383-392.

Pazour, G. J., B. L. Dickert, Y. Vucica, E. S. Seeley, J. L. Rosenbaum, G. B. Witman and D. G. Cole (2000). "Chlamydomonas IFT88 and its mouse homologue, polycystic kidney disease gene tg737, are required for assembly of cilia and flagella." J Cell Biol **151**(3): 709-718.

Pazour, G. J., J. T. San Agustin, J. A. Follit, J. L. Rosenbaum and G. B. Witman (2002). "Polycystin-2 localizes to kidney cilia and the ciliary level is elevated in orpk mice with polycystic kidney disease." Curr Biol **12**(11): R378-380.

Pedersen, A., C. Skjong and W. Shawlot (2005). "Lim 1 is required for nephric duct extension and ureteric bud morphogenesis." Dev Biol **288**(2): 571-581.

Pei, Y., Z. Lan, K. Wang, M. Garcia-Gonzalez, N. He, E. Dicks, P. Parfrey, G. Germino and T. Watnick (2012). "A missense mutation in PKD1 attenuates the severity of renal disease." Kidney Int **81**(4): 412-417.

Pei, Y., A. D. Paterson, K. R. Wang, N. He, D. Hefferton, T. Watnick, G. G. Germino, P. Parfrey, S. Somlo and P. St George-Hyslop (2001). "Bilineal disease and trans-heterozygotes in autosomal dominant polycystic kidney disease." Am J Hum Genet **68**(2): 355-363.

Pei, Y., T. Watnick, N. He, K. Wang, Y. Liang, P. Parfrey, G. Germino and P. St George-Hyslop (1999). "Somatic PKD2 mutations in individual kidney and liver cysts support a "two-hit" model of cystogenesis in type 2 autosomal dominant polycystic kidney disease." J Am Soc Nephrol **10**(7): 1524-1529.

Pennekamp, P., C. Karcher, A. Fischer, A. Schweickert, B. Skryabin, J. Horst, M. Blum and B. Dworniczak (2002). "The ion channel polycystin-2 is required for left-right axis determination in mice." Curr Biol **12**(11): 938-943.

Peral, B., A. C. Ong, J. L. San Millan, V. Gamble, L. Rees and P. C. Harris (1996). "A stable, nonsense mutation associated with a case of infantile onset polycystic kidney disease 1 (PKD1)." Hum Mol Genet **5**(4): 539-542.

Perico, N., L. Antiga, A. Caroli, P. Ruggenenti, G. Fasolini, M. Cafaro, P. Ondei, N. Rubis, O. Diadei, G. Gherardi, S. Prandini, A. Panozo, R. F. Bravo, S. Carminati, F. R. De Leon, F. Gaspari, M. Cortinovis, N. Motterlini, B. Ene-Iordache, A. Remuzzi and G. Remuzzi (2010). "Sirolimus therapy to halt the progression of ADPKD." J Am Soc Nephrol **21**(6): 1031-1040.

Perrone, R. D. (1997). "Extrarenal manifestations of ADPKD." Kidney Int **51**(6): 2022-2036.

Persu, A., O. Devuyst, N. Lannoy, R. Materne, G. Brosnahan, P. A. Gabow, Y. Pirson and C. Verellen-Dumoulin (2000). "CF gene and cystic fibrosis transmembrane conductance regulator expression in autosomal dominant polycystic kidney disease." J Am Soc Nephrol **11**(12): 2285-2296.

Persu, A., M. Duyme, Y. Pirson, X. M. Lens, T. Messiaen, M. H. Breuning, D. Chauveau, M. Levy, J. P. Grunfeld and O. Devuyst (2004). "Comparison between siblings and twins supports a role for modifier genes in ADPKD." Kidney Int **66**(6): 2132-2136.

Peters, D. J., L. Spruit, R. Klingel, F. Prins, H. J. Baelde, P. C. Giordano, L. F. Bernini, E. de Heer, M. H. Breuning and J. A. Bruijn (1996). "Adult, fetal, and polycystic kidney expression of polycystin, the polycystic kidney disease-1 gene product." Lab Invest **75**(2): 221-230.

Peters, D. J., A. van de Wal, L. Spruit, J. J. Saris, M. H. Breuning, J. A. Bruijn and E. de Heer (1999). "Cellular localization and tissue distribution of polycystin-1." J Pathol **188**(4): 439-446.

Peters, D. J. and M. H. Breuning (2001). "Autosomal dominant polycystic kidney disease: modification of disease progression." Lancet **358**(9291): 1439-1444.

Phillips, C. L., K. J. Miller, A. J. Filson, J. Nurnberger, J. L. Clendenon, G. W. Cook, K. W. Dunn, P. A. Overbeek, V. H. Gattone, 2nd and R. L. Bacallao (2004). "Renal cysts of inv/inv mice resemble early infantile nephronophthisis." J Am Soc Nephrol **15**(7): 1744-1755.

Piontek, K., L. F. Menezes, M. A. Garcia-Gonzalez, D. L. Huso and G. G. Germino (2007). "A critical developmental switch defines the kinetics of kidney cyst formation after loss of Pkd1." Nat Med **13**(12): 1490-1495.

Piontek, K. B. and G. G. Germino (1999). "Murine Pkd1 introns 21 and 22 lack the extreme polypyrimidine bias present in human PKD1." Mamm Genome **10**(2): 194-196.

Piontek, K. B., D. L. Huso, A. Grinberg, L. Liu, D. Bedja, H. Zhao, K. Gabrielson, F. Qian, C. Mei, H. Westphal and G. G. Germino (2004). "A functional floxed allele of Pkd1 that can be conditionally inactivated in vivo." J Am Soc Nephrol **15**(12): 3035-3043.

Pisitkun, T., R. F. Shen and M. A. Knepper (2004). "Identification and proteomic profiling of exosomes in human urine." Proc Natl Acad Sci U S A **101**(36): 13368-13373.

Polgar, K., C. R. Burrow, D. P. Hyink, H. Fernandez, K. Thornton, X. Li, G. L. Gusella and P. D. Wilson (2005). "Disruption of polycystin-1 function interferes with branching morphogenesis of the ureteric bud in developing mouse kidneys." Dev Biol **286**(1): 16-30.

Pollard, P. J., B. Spencer-Dene, D. Shukla, K. Howarth, E. Nye, M. El-Bahrawy, M. Deheragoda, M. Joannou, S. McDonald, A. Martin, P. Igarashi, S. Varsani-Brown, I. Rosewell, R. Poulsom, P. Maxwell, G. W. Stamp and I. P. Tomlinson (2007). "Targeted inactivation of fh1 causes proliferative renal cyst development and activation of the hypoxia pathway." Cancer Cell **11**(4): 311-319.

Ponting, C. P., K. Hofmann and P. Bork (1999). "A latrophilin/CL-1-like GPS domain in polycystin-1." Curr Biol **9**(16): R585-588.

Praetorius, H. A. and K. R. Spring (2001). "Bending the MDCK cell primary cilium increases intracellular calcium." J Membr Biol **184**(1): 71-79.

Prasad, S., J. P. McDaid, F. W. Tam, J. L. Haylor and A. C. Ong (2009). "Pkd2 dosage influences cellular repair responses following ischemia-reperfusion injury." Am J Pathol **175**(4): 1493-1503.

Preminger, G. M., W. E. Koch, F. A. Fried, E. McFarland, E. D. Murphy and J. Mandell (1982). "Murine congenital polycystic kidney disease: a model for studying development of cystic disease." J Urol **127**(3): 556-560.

Pritchard, L., J. A. Sloane-Stanley, J. A. Sharpe, R. Aspinwall, W. Lu, V. Buckle, L. Strmecki, D. Walker, C. J. Ward, C. E. Alpers, J. Zhou, W. G. Wood and P. C. Harris (2000). "A human PKD1 transgene generates functional polycystin-1 in mice and is associated with a cystic phenotype." Hum Mol Genet **9**(18): 2617-2627.

Promel, S., M. Frickenhaus, S. Hughes, L. Mestek, D. Staunton, A. Woollard, I. Vakonakis, T. Schoneberg, R. Schnabel, A. P. Russ and T. Langenhan (2012). "The GPS motif is a molecular switch for bimodal activities of adhesion class G protein-coupled receptors." Cell Rep **2**(2): 321-331.

Promel, S., T. Langenhan and D. Arac (2013). "Matching structure with function: the GAIN domain of Adhesion-GPCR and PKD1-like proteins." Trends Pharmacol Sci 34(8):470-8.

Puri, S., B. S. Magenheimer, R. L. Maser, E. M. Ryan, C. A. Zien, D. D. Walker, D. P. Wallace, S. J. Hempson and J. P. Calvet (2004). "Polycystin-1 activates the calcineurin/NFAT (nuclear factor of activated T-cells) signaling pathway." J Biol Chem **279**(53): 55455-55464.

Puri, S., M. Rodova, M. R. Islam, B. S. Magenheimer, R. L. Maser and J. P. Calvet (2006). "Ets factors regulate the polycystic kidney disease-1 promoter." Biochem Biophys Res Commun **342**(4): 1005-1013.

Qamar, S., M. Vadivelu and R. Sandford (2007). "TRP channels and kidney disease: lessons from polycystic kidney disease." Biochem Soc Trans **35**(Pt 1): 124-128.

Qian, C. N., J. Knol, P. Igarashi, F. Lin, U. Zylstra, B. T. Teh and B. O. Williams (2005). "Cystic renal neoplasia following conditional inactivation of apc in mouse renal tubular epithelium." J Biol Chem **280**(5): 3938-3945.

Qian, F., A. Boletta, A. K. Bhunia, H. Xu, L. Liu, A. K. Ahrabi, T. J. Watnick, F. Zhou and G. G. Germino (2002). "Cleavage of polycystin-1 requires the receptor for egg jelly domain and is disrupted by human autosomal-dominant polycystic kidney disease 1-associated mutations." Proc Natl Acad Sci U S A **99**(26): 16981-16986.

Qian, F., F. J. Germino, Y. Cai, X. Zhang, S. Somlo and G. G. Germino (1997). "PKD1 interacts with PKD2 through a probable coiled-coil domain." Nat Genet **16**(2): 179-183.

Qian, F., T. J. Watnick, L. F. Onuchic and G. G. Germino (1996). "The molecular basis of focal cyst formation in human autosomal dominant polycystic kidney disease type I." Cell **87**(6): 979-987.

Qian, F., W. Wei, G. Germino and A. Oberhauser (2005). "The nanomechanics of polycystin-1 extracellular region." J Biol Chem **280**(49): 40723-40730.

Qin, S., M. Taglienti, L. Cai, J. Zhou and J. A. Kreidberg (2012). "c-Met and NF-kappaB-dependent overexpression of Wnt7a and -7b and Pax2 promotes cystogenesis in polycystic kidney disease." J Am Soc Nephrol 23(8): 1309-1318.

Qiu, N., Z. Xiao, L. Cao, V. David and L. D. Quarles (2012). "Conditional mesenchymal disruption of pkd1 results in osteopenia and polycystic kidney disease." PLoS One **7**(9): e46038.

Rankin, E. B., J. E. Tomaszewski and V. H. Haase (2006). "Renal cyst development in mice with conditional inactivation of the von Hippel-Lindau tumor suppressor." Cancer Res **66**(5): 2576-2583.

Raphael, K. L., K. A. Strait, P. K. Stricklett, R. L. Miller, R. D. Nelson, K. B. Piontek, G. G. Germino and D. E. Kohan (2009). "Inactivation of Pkd1 in principal cells causes a more severe cystic kidney disease than in intercalated cells." Kidney Int **75**(6): 626-633.

Rawson, R. B., N. G. Zelenski, D. Nijhawan, J. Ye, J. Sakai, M. T. Hasan, T. Y. Chang, M. S. Brown and J. L. Goldstein (1997). "Complementation cloning of S2P, a gene encoding a putative metalloprotease required for intramembrane cleavage of SREBPs." Mol Cell **1**(1): 47-57.

Reed, B., I. Helal, K. McFann, W. Wang, X. D. Yan and R. W. Schrier (2012). "The impact of type II diabetes mellitus in patients with autosomal dominant polycystic kidney disease." Nephrol Dial Transplant **27**(7): 2862-2865.

Ricker, J. L., V. H. Gattone, 2nd, J. P. Calvet and C. A. Rankin (2000). "Development of autosomal recessive polycystic kidney disease in BALB/c-cpk/cpk mice." J Am Soc Nephrol **11**(10): 1837-1847.

Robert, A., G. Margall-Ducos, J. E. Guidotti, O. Bregerie, C. Celati, C. Brechot and C. Desdouets (2007). "The intraflagellar transport component IFT88/polaris is a centrosomal protein regulating G1-S transition in non-ciliated cells." J Cell Sci **120**(Pt 4): 628-637.

Rodova, M., M. R. Islam, R. L. Maser and J. P. Calvet (2002). "The polycystic kidney disease-1 promoter is a target of the beta-catenin/T-cell factor pathway." J Biol Chem **277**(33): 29577-29583.

Rodova, M., M. R. Islam, K. R. Peterson and J. P. Calvet (2003). "Remarkable sequence conservation of the last intron in the PKD1 gene." Mol Biol Evol **20**(10): 1669-1674.

Roitbak, T., Z. Surviladze, R. Tikkanen and A. Wandinger-Ness (2005). "A polycystin multiprotein complex constitutes a cholesterol-containing signalling microdomain in human kidney epithelia." Biochem J **392**(Pt 1): 29-38.

Roitbak, T., C. J. Ward, P. C. Harris, R. Bacallao, S. A. Ness and A. Wandinger-Ness (2004). "A polycystin-1 multiprotein complex is disrupted in polycystic kidney disease cells." Mol Biol Cell **15**(3): 1334-1346.

Romagnolo, B., D. Berrebi, S. Saadi-Keddoucci, A. Porteu, A. L. Pichard, M. Peuchmaur, A. Vandewalle, A. Kahn and C. Perret (1999). "Intestinal dysplasia and adenoma in transgenic mice after overexpression of an activated beta-catenin." Cancer Res **59**(16): 3875-3879.

Rosselot, C., L. Spraggon, I. Chia, E. Batourina, P. Riccio, B. Lu, K. Niederreither, P. Dolle, G. Duester, P. Chambon, F. Costantini, T. Gilbert, A. Molotkov and C. Mendelsohn (2010). "Non-cell-autonomous retinoid signaling is crucial for renal development." Development **137**(2): 283-292.

Rossetti, S., S. Burton, L. Strmecki, G. R. Pond, J. L. San Millan, K. Zerres, T. M. Barratt, S. Ozen, V. E. Torres, E. J. Bergstralh, C. G. Winearls and P. C. Harris (2002). "The position of the polycystic kidney disease 1 (PKD1) gene mutation correlates with the severity of renal disease." J Am Soc Nephrol **13**(5): 1230-1237.

Rossetti, S., D. Chauveau, V. Kubly, J. M. Slezak, A. K. Saggar-Malik, Y. Pei, A. C. Ong, F. Stewart, M. L. Watson, E. J. Bergstralh, C. G. Winearls, V. E. Torres and P. C. Harris (2003). "Association of mutation position in polycystic kidney disease 1 (PKD1) gene and development of a vascular phenotype." Lancet **361**(9376): 2196-2201.

Rossetti, S., D. Chauveau, D. Walker, A. Saggar-Malik, C. G. Winearls, V. E. Torres and P. C. Harris (2002). "A complete mutation screen of the ADPKD genes by DHPLC." Kidney Int **61**(5): 1588-1599.

Rossetti, S., M. B. Consugar, A. B. Chapman, V. E. Torres, L. M. Guay-Woodford, J. J. Grantham, W. M. Bennett, C. M. Meyers, D. L. Walker, K. Bae, Q. J. Zhang, P. A. Thompson, J. P. Miller, P. C. Harris and C. Consortium (2007). "Comprehensive molecular diagnostics in autosomal dominant polycystic kidney disease." J Am Soc Nephrol **18**(7): 2143-2160.

Rossetti, S., V. J. Kubly, M. B. Consugar, K. Hopp, S. Roy, S. W. Horsley, D. Chauveau, L. Rees, T. M. Barratt, W. G. van't Hoff, P. Niaudet, V. E. Torres and P. C. Harris (2009). "Incompletely penetrant PKD1 alleles suggest a role for gene dosage in cyst initiation in polycystic kidney disease." Kidney Int **75**(8): 848-855.

Roth, M. G. (1999). "Snapshots of ARF1: implications for mechanisms of activation and inactivation." Cell **97**(2): 149-152.

Rowe, I., M. Chiaravalli, V. Mannella, V. Ulisse, G. Quilici, M. Pema, X. W. Song, H. Xu, S. Mari, F. Qian, Y. Pei, G. Musco and A. Boletta (2013). "Defective glucose metabolism in polycystic kidney disease identifies a new therapeutic strategy." Nat Med **19**(4): 488-493.

Roy, A., A. Kucukural and Y. Zhang (2010). "I-TASSER: a unified platform for automated protein structure and function prediction." Nature Protocols **5**: 725-738.

Rundle, D. R., G. Gorbsky and L. Tsiokas (2004). "PKD2 interacts and co-localizes with mDia1 to mitotic spindles of dividing cells: role of mDia1 IN PKD2 localization to mitotic spindles." J Biol Chem **279**(28): 29728-29739.

Russo, R. J., H. Husson, D. Joly, N. O. Bukanov, N. Patey, B. Knebelmann and O. Ibraghimov-Beskrovnaya (2005). "Impaired formation of desmosomal junctions in ADPKD epithelia." Histochem Cell Biol **124**(6): 487-497.

Saadi-Kheddouci, S., D. Berrebi, B. Romagnolo, F. Cluzeaud, M. Peuchmaur, A. Kahn, A. Vandewalle and C. Perret (2001). "Early development of polycystic kidney disease in transgenic mice expressing an activated mutant of the beta-catenin gene." Oncogene **20**(42): 5972-5981.

Saburi, S., I. Hester, E. Fischer, M. Pontoglio, V. Eremina, M. Gessler, S. E. Quaggin, R. Harrison, R. Mount and H. McNeill (2008). "Loss of Fat4 disrupts PCP signaling and oriented cell division and leads to cystic kidney disease." Nat Genet **40**(8): 1010-1015.

Saher, G., F. Rudolphi, K. Corthals, T. Ruhwedel, K. F. Schmidt, S. Lowel, P. Dibaj, B. Barrette, W. Mobius and K. A. Nave (2012). "Therapy of Pelizaeus-Merzbacher disease in mice by feeding a cholesterol-enriched diet." Nat Med **18**(7): 1130-1135.

Sakuntabhai, A., V. Ruiz-Perez, S. Carter, N. Jacobsen, S. Burge, S. Monk, M. Smith, C. S. Munro, M. O'Donovan, N. Craddock, R. Kucherlapati, J. L. Rees, M. Owen, G. M. Lathrop, A. P. Monaco, T. Strachan and A. Hovnanian (1999). "Mutations in ATP2A2, encoding a Ca2+ pump, cause Darier disease." Nat Genet **21**(3): 271-277.

Salaun, C., G. W. Gould and L. H. Chamberlain (2005). "The SNARE proteins SNAP-25 and SNAP-23 display different affinities for lipid rafts in PC12 cells. Regulation by distinct cysteine-rich domains." J Biol Chem **280**(2): 1236-1240.

Sandford, R., B. Sgotto, S. Aparicio, S. Brenner, M. Vaudin, R. K. Wilson, S. Chissoe, K. Pepin, A. Bateman, C. Chothia, J. Hughes and P. Harris (1997). "Comparative analysis of the polycystic kidney disease 1 (PKD1) gene reveals an integral membrane glycoprotein with multiple evolutionary conserved domains." Hum Mol Genet **6**(9): 1483-1489.

Schaffner, D. L., R. Barrios, C. Massey, E. I. Banez, C. N. Ou, S. Rajagopalan, E. Aguilar-Cordova, R. M. Lebovitz, P. A. Overbeek and M. W. Lieberman (1993). "Targeting of the rasT24 oncogene to the proximal convoluted tubules in transgenic mice results in hyperplasia and polycystic kidneys." Am J Pathol **142**(4): 1051-1060.

Schieren, G., B. Rumberger, M. Klein, C. Kreutz, J. Wilpert, M. Geyer, D. Faller, J. Timmer, I. Quack, L. C. Rump, G. Walz and J. Donauer (2006). "Gene profiling of polycystic kidneys." Nephrol Dial Transplant **21**(7): 1816-1824.

Schietke, R. E., T. Hackenbeck, M. Tran, R. Gunther, B. Klanke, C. L. Warnecke, K. X. Knaup, D. Shukla, C. Rosenberger, R. Koesters, S. Bachmann, P. Betz, G. Schley, J. Schodel, C. Willam, T. Winkler, K. Amann, K. U. Eckardt, P. Maxwell and M. S. Wiesener (2012). "Renal tubular HIF-2alpha expression requires VHL inactivation and causes fibrosis and cysts." PLoS One **7**(1): e31034.

Seeger-Nukpezah, T., D. A. Proia, B. L. Egleston, A. S. Nikonova, T. Kent, K. Q. Cai, H. H. Hensley, W. Ying, D. Chimmanamada, I. G. Serebriiskii and E. A. Golemis (2013). "Inhibiting the HSP90 chaperone slows cyst growth in a mouse model of autosomal dominant polycystic kidney disease." Proc Natl Acad Sci U S A **110**(31): 12786-12791.

Serra, A. L., D. Poster, A. D. Kistler, F. Krauer, S. Raina, J. Young, K. M. Rentsch, K. S. Spanaus, O. Senn, P. Kristanto, H. Scheffel, D. Weishaupt and R. P. Wuthrich (2010). "Sirolimus and kidney growth in autosomal dominant polycystic kidney disease." N Engl J Med **363**(9): 820-829.

Shannon, M. B., B. L. Patton, S. J. Harvey and J. H. Miner (2006). "A hypomorphic mutation in the mouse laminin alpha5 gene causes polycystic kidney disease." J Am Soc Nephrol **17**(7): 1913-1922.

Sharif-Naeini, R., J. H. Folgering, D. Bichet, F. Duprat, I. Lauritzen, M. Arhatte, M. Jodar, A. Dedman, F. C. Chatelain, U. Schulte, K. Retailleau, L. Loufrani, A. Patel, F. Sachs, P. Delmas, D. J. Peters and E. Honore (2009). "Polycystin-1 and -2 dosage regulates pressure sensing." Cell **139**(3): 587-596.

Sharma, N., Z. A. Kosan, J. E. Stallworth, N. F. Berbari and B. K. Yoder (2011). "Soluble levels of cytosolic tubulin regulate ciliary length control." Mol Biol Cell **22**(6): 806-816.

Sherstha, R., C. McKinley, P. Russ, A. Scherzinger, T. Bronner, R. Showalter and G. T. Everson (1997). "Postmenopausal estrogen therapy selectively stimulates hepatic enlargement in women with autosomal dominant polycystic kidney disease." Hepatology **26**(5): 1282-1286.

Shibazaki, S., Z. Yu, S. Nishio, X. Tian, R. B. Thomson, M. Mitobe, A. Louvi, H. Velazquez, S. Ishibe, L. G. Cantley, P. Igarashi and S. Somlo (2008). "Cyst formation and activation of the extracellular regulated kinase pathway after kidney specific inactivation of Pkd1." Hum Mol Genet **17**(11): 1505-1516.

Shillingford, J. M., N. S. Murcia, C. H. Larson, S. H. Low, R. Hedgepeth, N. Brown, C. A. Flask, A. C. Novick, D. A. Goldfarb, A. Kramer-Zucker, G. Walz, K. B. Piontek, G. G. Germino and T. Weimbs (2006). "The mTOR pathway is regulated by polycystin-1, and its inhibition reverses renal cystogenesis in polycystic kidney disease." Proc Natl Acad Sci U S A **103**(14): 5466-5471.

Shillingford, J. M., K. B. Piontek, G. G. Germino and T. Weimbs (2010). "Rapamycin ameliorates PKD resulting from conditional inactivation of Pkd1." J Am Soc Nephrol **21**(3): 489-497.

Silva, J. P., V. Lelianova, C. Hopkins, K. E. Volynski and Y. Ushkaryov (2009). "Functional cross-interaction of the fragments produced by the cleavage of distinct adhesion G-protein-coupled receptors." J Biol Chem **284**(10): 6495-6506.

Simon, E. A., S. Cook, M. T. Davisson, P. D'Eustachio and L. M. Guay-Woodford (1994). "The mouse congenital polycystic kidney (cpk) locus maps within 1.3 cM of the chromosome 12 marker D12Nyu2." Genomics **21**(2): 415-418.

Simons, K. and M. Zerial (1993). "Rab proteins and the road maps for intracellular transport." Neuron **11**(5): 789-799.

Simons, M., J. Gloy, A. Ganner, A. Bullerkotte, M. Bashkurov, C. Kronig, B. Schermer, T. Benzing, O. A. Cabello, A. Jenny, M. Mlodzik, B. Polok, W. Driever, T. Obara and G. Walz (2005). "Inversin, the gene product mutated in nephronophthisis type II, functions as a molecular switch between Wnt signaling pathways." Nat Genet **37**(5): 537-543.

Singla, V. and J. F. Reiter (2006). "The primary cilium as the cell's antenna: signaling at a sensory organelle." Science **313**(5787): 629-633.

Sistermans, E. A., R. F. de Coo, I. J. De Wijs and B. A. Van Oost (1998). "Duplication of the proteolipid protein gene is the major cause of Pelizaeus-Merzbacher disease." Neurology **50**(6): 1749-1754.

Smith, L. A., N. O. Bukanov, H. Husson, R. J. Russo, T. C. Barry, A. L. Taylor, D. R. Beier and O. Ibraghimov-Beskrovnaya (2006). "Development of polycystic kidney disease in juvenile cystic kidney mice: insights into pathogenesis, ciliary abnormalities, and common features with human disease." J Am Soc Nephrol **17**(10): 2821-2831.

Smith, U. M., M. Consugar, L. J. Tee, B. M. McKee, E. N. Maina, S. Whelan, N. V. Morgan, E. Goranson, P. Gissen, S. Lilliquist, I. A. Aligianis, C. J. Ward, S. Pasha, R. Punyashthiti, S. Malik Sharif, P. A. Batman, C. P. Bennett, C. G. Woods, C. McKeown,

M. Bucourt, C. A. Miller, P. Cox, L. Algazali, R. C. Trembath, V. E. Torres, T. Attie-Bitach, D. A. Kelly, E. R. Maher, V. H. Gattone, 2nd, P. C. Harris and C. A. Johnson (2006). "The transmembrane protein meckelin (MKS3) is mutated in Meckel-Gruber syndrome and the wpk rat." Nat Genet **38**(2): 191-196.

Soderdahl, D. W., J. B. Thrasher and K. L. Hansberry (1997). "Bilateral renal cell carcinoma in autosomal dominant polycystic kidney disease. A case report and literature review." Am J Nephrol **17**(1): 96-99.

Sohara, E., Y. Luo, J. Zhang, D. K. Manning, D. R. Beier and J. Zhou (2008). "Nek8 regulates the expression and localization of polycystin-1 and polycystin-2." J Am Soc Nephrol **19**(3): 469-476.

Song, X., V. Di Giovanni, N. He, K. Wang, A. Ingram, N. D. Rosenblum and Y. Pei (2009). "Systems biology of autosomal dominant polycystic kidney disease (ADPKD): computational identification of gene expression pathways and integrated regulatory networks." Hum Mol Genet **18**(13): 2328-2343.

Sorenson, C. M. and N. Sheibani (1999). "Focal adhesion kinase, paxillin, and bcl-2: analysis of expression, phosphorylation, and association during morphogenesis." Dev Dyn **215**(4): 371-382.

Stambolic, V., L. Ruel and J. R. Woodgett (1996). "Lithium inhibits glycogen synthase kinase-3 activity and mimics wingless signalling in intact cells." Curr Biol **6**(12): 1664-1668.

Starremans, P. G., X. Li, P. E. Finnerty, L. Guo, A. Takakura, E. G. Neilson and J. Zhou (2008). "A mouse model for polycystic kidney disease through a somatic in-frame deletion in the 5' end of Pkd1." Kidney Int **73**(12): 1394-1405.

Stayner, C., J. Shields, L. Slobbe, J. M. Shillingford, T. Weimbs and M. R. Eccles (2012). "Rapamycin-mediated suppression of renal cyst expansion in del34 Pkd1-/- mutant mouse embryos: an investigation of the feasibility of renal cyst prevention in the foetus." Nephrology (Carlton) **17**(8): 739-747.

Steimel, A., L. Wong, E. H. Najarro, B. D. Ackley, G. Garriga and H. Hutter (2010). "The Flamingo ortholog FMI-1 controls pioneer-dependent navigation of follower axons in C. elegans." Development **137**(21): 3663-3673.

Stocklin, E., F. Botteri and B. Groner (1993). "An activated allele of the c-erbB-2 oncogene impairs kidney and lung function and causes early death of transgenic mice." J Cell Biol **122**(1): 199-208.

Stokely, M. E., S. Y. Hwang, J. Y. Hwang, B. Fan, M. A. King, K. Inokuchi and P. Koulen (2006). "Polycystin-1 can interact with homer 1/Vesl-1 in postnatal hippocampal neurons." J Neurosci Res **84**(8): 1727-1737.

Streets, A. J., D. J. Moon, M. E. Kane, T. Obara and A. C. Ong (2006). "Identification of an N-terminal glycogen synthase kinase 3 phosphorylation site which regulates the functional localization of polycystin-2 in vivo and in vitro." Hum Mol Genet **15**(9): 1465-1473.

Streets, A. J., B. E. Wagner, P. C. Harris, C. J. Ward and A. C. Ong (2009). "Homophilic and heterophilic polycystin 1 interactions regulate E-cadherin recruitment and junction assembly in MDCK cells." J Cell Sci **122**(Pt 9): 1410-1417.

Streets, A. J., O. Wessely, D. J. Peters and A. C. Ong (2013). "Hyperphosphorylation of polycystin-2 at a critical residue in disease reveals an essential role for polycystin-1-regulated dephosphorylation." Hum Mol Genet **22**(10): 1924-1939.

Stroope, A., B. Radtke, B. Huang, T. Masyuk, V. Torres, E. Ritman and N. LaRusso (2010). "Hepato-renal pathology in pkd2ws25/- mice, an animal model of autosomal dominant polycystic kidney disease." Am J Pathol **176**(3): 1282-1291.

Su, X., K. Driscoll, G. Yao, A. Raed, M. Wu, P. L. Beales and J. Zhou (2014). "Bardet-Biedl syndrome proteins 1 and 3 regulate the ciliary trafficking of polycystic kidney disease 1 protein." Hum Mol Genet **23**(20): 5441-51.

Takahashi, H., J. P. Calvet, D. Dittemore-Hoover, K. Yoshida, J. J. Grantham and V. H. Gattone, 2nd (1991). "A hereditary model of slowly progressive polycystic kidney disease in the mouse." J Am Soc Nephrol **1**(7): 980-989.

Takahashi, H., Y. Ueyama, T. Hibino, Y. Kuwahara, S. Suzuki, K. Hioki and N. Tamaoki (1986). "A new mouse model of genetically transmitted polycystic kidney disease." J Urol **135**(6): 1280-1283.

Takakura, A., L. Contrino, A. W. Beck and J. Zhou (2008). "Pkd1 inactivation induced in adulthood produces focal cystic disease." J Am Soc Nephrol **19**(12): 2351-2363.

Takakura, A., L. Contrino, X. Zhou, J. V. Bonventre, Y. Sun, B. D. Humphreys and J. Zhou (2009). "Renal injury is a third hit promoting rapid development of adult polycystic kidney disease." Hum Mol Genet **18**(14): 2523-2531.

Takakura, A., E. A. Nelson, N. Haque, B. D. Humphreys, K. Zandi-Nejad, D. A. Frank and J. Zhou (2011). "Pyrimethamine inhibits adult polycystic kidney disease by modulating STAT signaling pathways." Hum Mol Genet **20**(21): 4143-4154.

Takayama, H., W. J. LaRochelle, S. G. Sabnis, T. Otsuka and G. Merlino (1997). "Renal tubular hyperplasia, polycystic disease, and glomerulosclerosis in transgenic mice overexpressing hepatocyte growth factor/scatter factor." Lab Invest **77**(2): 131-138.

Takeda, N., S. Kume, Y. Tanaka, Y. Morita, M. Chin-Kanasaki, H. Araki, K. Isshiki, S. Araki, M. Haneda, D. Koya, A. Kashiwagi, H. Maegawa and T. Uzu (2013). "Altered unfolded protein response is implicated in the age-related exacerbation of proteinuria-induced proximal tubular cell damage." Am J Pathol **183**(3): 774-785.

Takiar, V., S. Nishio, P. Seo-Mayer, J. D. King, Jr., H. Li, L. Zhang, A. Karihaloo, K. R. Hallows, S. Somlo and M. J. Caplan (2011). "Activating AMP-activated protein kinase (AMPK) slows renal cystogenesis." Proc Natl Acad Sci U S A **108**(6): 2462-2467.

Talbot, J. J., J. M. Shillingford, S. Vasanth, N. Doerr, S. Mukherjee, M. T. Kinter, T. Watnick and T. Weimbs (2011). "Polycystin-1 regulates STAT activity by a dual mechanism." Proc Natl Acad Sci U S A **108**(19): 7985-7990.

Tanjore, H., W. E. Lawson and T. S. Blackwell (2013). "Endoplasmic reticulum stress as a pro-fibrotic stimulus." Biochim Biophys Acta **1832**(7): 940-947.

Thatava, T., A. S. Armstrong, J. G. De Lamo, R. Edukulla, Y. K. Khan, T. Sakuma, S. Ohmine, J. L. Sundsbak, P. C. Harris, Y. C. Kudva and Y. Ikeda (2011). "Successful disease-specific induced pluripotent stem cell generation from patients with kidney transplantation." Stem Cell Res Ther **2**(6): 48.

Thivierge, C., A. Kurbegovic, M. Couillard, R. Guillaume, O. Cote and M. Trudel (2006). "Overexpression of PKD1 causes polycystic kidney disease." Mol Cell Biol **26**(4): 1538-1548.

Thomson, C. E., P. Montague, M. Jung, K. A. Nave and I. R. Griffiths (1997). "Phenotypic severity of murine Plp mutants reflects in vivo and in vitro variations in transport of PLP isoproteins." Glia **20**(4): 322-332.

Tian, Y., R. Kolb, J. H. Hong, J. Carroll, D. Li, J. You, R. Bronson, M. B. Yaffe, J. Zhou and T. Benjamin (2007). "TAZ promotes PC2 degradation through a SCFbeta-Trcp E3 ligase complex." Mol Cell Biol **27**(18): 6383-6395.

Tiner, W. J., Sr., V. N. Potaman, R. R. Sinden and Y. L. Lyubchenko (2001). "The structure of intramolecular triplex DNA: atomic force microscopy study." J Mol Biol **314**(3): 353-357.

Togawa, A., J. Miyoshi, H. Ishizaki, M. Tanaka, A. Takakura, H. Nishioka, H. Yoshida, T. Doi, A. Mizoguchi, N. Matsuura, Y. Niho, Y. Nishimune, S. Nishikawa and Y. Takai (1999). "Progressive impairment of kidneys and reproductive organs in mice lacking Rho GDIalpha." Oncogene **18**(39): 5373-5380.

Torra, R., C. Badenas, A. Darnell, C. Nicolau, V. Volpini, L. Revert and X. Estivill (1996). "Linkage, clinical features, and prognosis of autosomal dominant polycystic kidney disease types 1 and 2." J Am Soc Nephrol **7**(10): 2142-2151.

Torra, R., C. Nicolau, C. Badenas, S. Navarro, L. Perez, X. Estivill and A. Darnell (1997). "Ultrasonographic study of pancreatic cysts in autosomal dominant polycystic kidney disease." Clin Nephrol **47**(1): 19-22.

Torres, V. E., B. F. King, M. A. McKusick, J. Bjornsson and H. Zincke (2001). "Update on tuberous sclerosis complex." Contrib Nephrol(136): 33-49.

Torres, V. E., X. Wang, Q. Qian, S. Somlo, P. C. Harris and V. H. Gattone, 2nd (2004). "Effective treatment of an orthologous model of autosomal dominant polycystic kidney disease." Nat Med **10**(4): 363-364.

Torres, V. E., P. C. Harris and Y. Pirson (2007). "Autosomal dominant polycystic kidney disease." Lancet **369**(9569): 1287-1301.

Torres, V. E. (2008). "Role of vasopressin antagonists." Clin J Am Soc Nephrol **3**(4): 1212-1218.

Torres, V. E. and P. C. Harris (2009). "Autosomal dominant polycystic kidney disease: the last 3 years." Kidney Int **76**(2): 149-168.

Town, T., J. J. Breunig, M. R. Sarkisian, C. Spilianakis, A. E. Ayoub, X. Liu, A. F. Ferrandino, A. R. Gallagher, M. O. Li, P. Rakic and R. A. Flavell (2008). "The stumpy gene is required for mammalian ciliogenesis." Proc Natl Acad Sci U S A **105**(8): 2853-2858.

Traykova-Brauch, M., K. Schonig, O. Greiner, T. Miloud, A. Jauch, M. Bode, D. W. Felsher, A. B. Glick, D. J. Kwiatkowski, H. Bujard, J. Horst, M. von Knebel Doeberitz, F. K. Niggli, W. Kriz, H. J. Grone and R. Koesters (2008). "An efficient and versatile system for acute and chronic modulation of renal tubular function in transgenic mice." Nat Med **14**(9): 979-984.

Trudel, M., V. D'Agati and F. Costantini (1991). "C-myc as an inducer of polycystic kidney disease in transgenic mice." Kidney Int **39**(4): 665-671.

Trudel, M. and V. D'Agati (1992). "A model of polycystic kidney disease in SBM transgenic mice." Contrib Nephrol **97**: 47-59.

Trudel, M., L. Barisoni, J. Lanoix and V. D'Agati (1998). "Polycystic kidney disease in SBM transgenic mice: role of c-myc in disease induction and progression." Am J Pathol **152**(1): 219-229.

Trudel M, K. A. (2011). Toward understanding Pkd1 cystogenetic mechanism. J Am Soc Nephrol **22:** 59A.

Tsang, T. E., W. Shawlot, S. J. Kinder, A. Kobayashi, K. M. Kwan, K. Schughart, A. Kania, T. M. Jessell, R. R. Behringer and P. P. Tam (2000). "Lim1 activity is required for intermediate mesoderm differentiation in the mouse embryo." Dev Biol **223**(1): 77-90.

Tsiokas, L., T. Arnould, C. Zhu, E. Kim, G. Walz and V. P. Sukhatme (1999). "Specific association of the gene product of PKD2 with the TRPC1 channel." Proc Natl Acad Sci U S A **96**(7): 3934-3939.

Tsiokas, L., E. Kim, T. Arnould, V. P. Sukhatme and G. Walz (1997). "Homo- and heterodimeric interactions between the gene products of PKD1 and PKD2." Proc Natl Acad Sci U S A **94**(13): 6965-6970.

Upadhya, P., E. H. Birkenmeier, C. S. Birkenmeier and J. E. Barker (2000). "Mutations in a NIMA-related kinase gene, Nek1, cause pleiotropic effects including a progressive polycystic kidney disease in mice." Proc Natl Acad Sci U S A **97**(1): 217-221.

Van Adelsberg, J., S. Chamberlain and V. D'Agati (1997). "Polycystin expression is temporally and spatially regulated during renal development." Am J Physiol **272**(5 Pt 2): F602-609.

Van Bodegom, D., Z. Saifudeen, S. Dipp, S. Puri, B. S. Magenheimer, J. P. Calvet and S. S. El-Dahr (2006). "The polycystic kidney disease-1 gene is a target for p53-mediated transcriptional repression." J Biol Chem **281**(42): 31234-31244.

van Keimpema, L., F. Nevens, R. Vanslembrouck, M. G. van Oijen, A. L. Hoffmann, H. M. Dekker, R. A. de Man and J. P. Drenth (2009). "Lanreotide reduces the volume of polycystic liver: a randomized, double-blind, placebo-controlled trial." Gastroenterology **137**(5): 1661-1668 e1661-1662.

Van Maldergem, L., E. Jauniaux, C. Fourneau and Y. Gillerot (1992). "Genetic causes of hydrops fetalis." Pediatrics **89**(1): 81-86.

Van Raay, T. J., T. C. Burn, T. D. Connors, L. R. Petry, G. G. Germino, K. W. Klinger and G. M. Landes (1996). "A 2.5 kb polypyrimidine tract in the PKD1 gene contains at least 23 H-DNA-forming sequences." Microb Comp Genomics **1**(4): 317-327.

Vassilev, P. M., L. Guo, X. Z. Chen, Y. Segal, J. B. Peng, N. Basora, H. Babakhanlou, G. Cruger, M. Kanazirska, C. Ye, E. M. Brown, M. A. Hediger and J. Zhou (2001). "Polycystin-2 is a novel cation channel implicated in defective intracellular Ca(2+) homeostasis in polycystic kidney disease." Biochem Biophys Res Commun **282**(1): 341-350.

Veikkolainen, V., F. Naillat, A. Railo, L. Chi, A. Manninen, P. Hohenstein, N. Hastie, S. Vainio and K. Elenius (2012). "ErbB4 modulates tubular cell polarity and lumen diameter during kidney development." J Am Soc Nephrol **23**(1): 112-122.

Veis, D. J., C. M. Sorenson, J. R. Shutter and S. J. Korsmeyer (1993). "Bcl-2-deficient mice demonstrate fulminant lymphoid apoptosis, polycystic kidneys, and hypopigmented hair." Cell **75**(2): 229-240.

Veldhuisen, B., L. Spruit, H. G. Dauwerse, M. H. Breuning and D. J. Peters (1999). "Genes homologous to the autosomal dominant polycystic kidney disease genes (PKD1 and PKD2)." Eur J Hum Genet **7**(8): 860-872.

Verghese, E., R. Weidenfeld, J. F. Bertram, S. D. Ricardo and J. A. Deane (2008). "Renal cilia display length alterations following tubular injury and are present early in epithelial repair." Nephrol Dial Transplant **23**(3): 834-841.

Vujic, M., C. M. Heyer, E. Ars, K. Hopp, A. Markoff, C. Orndal, B. Rudenhed, S. H. Nasr, V. E. Torres, R. Torra, N. Bogdanova and P. C. Harris (2010). "Incompletely penetrant PKD1 alleles mimic the renal manifestations of ARPKD." J Am Soc Nephrol **21**(7): 1097-1102.

Wahl, P. R., A. L. Serra, M. Le Hir, K. D. Molle, M. N. Hall and R. P. Wuthrich (2006). "Inhibition of mTOR with sirolimus slows disease progression in Han:SPRD rats with autosomal dominant polycystic kidney disease (ADPKD)." Nephrol Dial Transplant **21**(3): 598-604.

Wakabayashi, T., S. Fujita, Y. Ohbora, T. Suyama, N. Tamaki and S. Matsumoto (1983). "Polycystic kidney disease and intracranial aneurysms. Early angiographic diagnosis and early operation for the unruptured aneurysm." J Neurosurg **58**(4): 488-491.

Waldherr, R., K. Zerres, A. Gall and H. Enders (1989). "Polycystic kidney disease in the fetus." Lancet **2**(8657): 274-275.

Walz, G., K. Budde, M. Mannaa, J. Nurnberger, C. Wanner, C. Sommerer, U. Kunzendorf, B. Banas, W. H. Horl, N. Obermuller, W. Arns, H. Pavenstadt, J. Gaedeke, M. Buchert, C. May, H. Gschaidmeier, S. Kramer and K. U. Eckardt (2010). "Everolimus in patients with autosomal dominant polycystic kidney disease." N Engl J Med **363**(9): 830-840.

Wang, X., A. V. Koulov, W. A. Kellner, J. R. Riordan and W. E. Balch (2008). "Chemical and biological folding contribute to temperature-sensitive DeltaF508 CFTR trafficking." Traffic **9**(11): 1878-1893.

Wang, E., H. M. Hsieh-Li, Y. Y. Chiou, Y. L. Chien, H. H. Ho, H. J. Chin, C. K. Wang, S. C. Liang and S. T. Jiang (2010). "Progressive renal distortion by multiple cysts in transgenic mice expressing artificial microRNAs against Pkd1." J Pathol **222**(3): 238-248.

Wang, W. J., H. G. Tay, R. Soni, G. S. Perumal, M. G. Goll, F. P. Macaluso, J. M. Asara, J. D. Amack and M. F. Tsou (2013). "CEP162 is an axoneme-recognition

protein promoting ciliary transition zone assembly at the cilia base." Nat Cell Biol **15**(6): 591-601.

Wang, Q., X. Q. Dai, Q. Li, Z. Wang, R. Cantero Mdel, S. Li, J. Shen, J. C. Tu, H. Cantiello and X. Z. Chen (2012). "Structural interaction and functional regulation of polycystin-2 by filamin." PLoS One **7**(7): e40448.

Wang, S., Y. Luo, P. D. Wilson, G. B. Witman and J. Zhou (2004). "The autosomal recessive polycystic kidney disease protein is localized to primary cilia, with concentration in the basal body area." J Am Soc Nephrol **15**(3): 592-602.

Wang, S., J. Zhang, S. M. Nauli, X. Li, P. G. Starremans, Y. Luo, K. A. Roberts and J. Zhou (2007). "Fibrocystin/polyductin, found in the same protein complex with polycystin-2, regulates calcium responses in kidney epithelia." Mol Cell Biol **27**(8): 3241-3252.

Wang, X., V. Gattone, 2nd, P. C. Harris and V. E. Torres (2005). "Effectiveness of vasopressin V2 receptor antagonists OPC-31260 and OPC-41061 on polycystic kidney disease development in the PCK rat." J Am Soc Nephrol **16**(4): 846-851.

Wang, X., Y. Wu, C. J. Ward, P. C. Harris and V. E. Torres (2008). "Vasopressin directly regulates cyst growth in polycystic kidney disease." J Am Soc Nephrol **19**(1): 102-108.

Wanke, R., E. Wolf, G. Brem and W. Hermanns (2001). "[Role of podocyte damage in the pathogenesis of glomerulosclerosis and tubulointerstitial lesions: findings in the growth hormone transgenic mouse model of progressive nephropathy]." Verh Dtsch Ges Pathol **85**: 250-256.

Wann, A. K. and M. M. Knight (2012). "Primary cilia elongation in response to interleukin-1 mediates the inflammatory response." Cell Mol Life Sci **69**(17): 2967-2977.

Ward, C. J., M. C. Hogan, S. Rossetti, D. Walker, T. Sneddon, X. Wang, V. Kubly, J. M. Cunningham, R. Bacallao, M. Ishibashi, D. S. Milliner, V. E. Torres and P. C. Harris (2002). "The gene mutated in autosomal recessive polycystic kidney disease encodes a large, receptor-like protein." Nat Genet **30**(3): 259-269.

Ward, C. J., H. Turley, A. C. Ong, M. Comley, S. Biddolph, R. Chetty, P. J. Ratcliffe, K. Gattner and P. C. Harris (1996). "Polycystin, the polycystic kidney disease 1 protein, is expressed by epithelial cells in fetal, adult, and polycystic kidney." Proc Natl Acad Sci U S A **93**(4): 1524-1528.

Ward, C. J., D. Yuan, T. V. Masyuk, X. Wang, R. Punyashthiti, S. Whelan, R. Bacallao, R. Torra, N. F. LaRusso, V. E. Torres and P. C. Harris (2003). "Cellular and subcellular localization of the ARPKD protein; fibrocystin is expressed on primary cilia." Hum Mol Genet **12**(20): 2703-2710.

Ward, H. H., U. Brown-Glaberman, J. Wang, Y. Morita, S. L. Alper, E. J. Bedrick, V. H. Gattone, 2nd, D. Deretic and A. Wandinger-Ness (2011). "A conserved signal and GTPase complex are required for the ciliary transport of polycystin-1." Mol Biol Cell **22**(18): 3289-3305.

Watnick, T. J., Y. Jin, E. Matunis, M. J. Kernan and C. Montell (2003). "A flagellar polycystin-2 homolog required for male fertility in Drosophila." Curr Biol **13**(24): 2179-2184.

Watnick, T. J., K. B. Piontek, T. M. Cordal, H. Weber, M. A. Gandolph, F. Qian, X. M. Lens, H. P. Neumann and G. G. Germino (1997). "An unusual pattern of mutation in

the duplicated portion of PKD1 is revealed by use of a novel strategy for mutation detection." Hum Mol Genet **6**(9): 1473-1481.

Watnick, T. J., V. E. Torres, M. A. Gandolph, F. Qian, L. F. Onuchic, K. W. Klinger, G. Landes and G. G. Germino (1998). "Somatic mutation in individual liver cysts supports a two-hit model of cystogenesis in autosomal dominant polycystic kidney disease." Mol Cell **2**(2): 247-251.

Weatherbee, S. D., L. A. Niswander and K. V. Anderson (2009). "A mouse model for Meckel syndrome reveals Mks1 is required for ciliogenesis and Hedgehog signaling." Hum Mol Genet **18**(23): 4565-4575.

Weavers, H., S. Prieto-Sanchez, F. Grawe, A. Garcia-Lopez, R. Artero, M. Wilsch-Brauninger, M. Ruiz-Gomez, H. Skaer and B. Denholm (2009). "The insect nephrocyte is a podocyte-like cell with a filtration slit diaphragm." Nature **457**(7227): 322-326.

Wei, Q., K. Bhatt, H. Z. He, Q. S. Mi, V. H. Haase and Z. Dong (2010). "Targeted deletion of Dicer from proximal tubules protects against renal ischemia-reperfusion injury." J Am Soc Nephrol **21**(5): 756-761.

Wei, W., K. Hackmann, H. Xu, G. Germino and F. Qian (2007). "Characterization of cis-autoproteolysis of polycystin-1, the product of human polycystic kidney disease 1 gene." J Biol Chem **282**(30): 21729-21737.

Weimbs, T. (2007). "Polycystic kidney disease and renal injury repair: common pathways, fluid flow, and the function of polycystin-1." Am J Physiol Renal Physiol **293**(5): F1423-1432.

Weston, B. S., C. Bagneris, R. G. Price and J. L. Stirling (2001). "The polycystin-1 C-type lectin domain binds carbohydrate in a calcium-dependent manner, and interacts with extracellular matrix proteins in vitro." Biochim Biophys Acta **1536**(2-3): 161-176.

Weston, B. S., S. Jeffery, I. Jeffrey, S. F. Sharaf, N. Carter, A. Saggar-Malik and R. G. Price (1997). "Polycystin expression during embryonic development of human kidney in adult tissues and ADPKD tissue." Histochem J **29**(11-12): 847-856.

White, J. G., Southgate, E., Thomson, J.N., and Brenner, S. (1986). The structure of the nervous system of the nematode Caenorhabditis elegans: the mind of a worm, Phil. Trans. R. Soc. Lond. **:** 1–340.

Williams, S. S., P. Cobo-Stark, L. R. James, S. Somlo and P. Igarashi (2008). "Kidney cysts, pancreatic cysts, and biliary disease in a mouse model of autosomal recessive polycystic kidney disease." Pediatr Nephrol **23**(5): 733-741.

Willard, H. F. and J. R. Riordan (1985). "Assignment of the gene for myelin proteolipid protein to the X chromosome: implications for X-linked myelin disorders." Science **230**(4728): 940-942.

Wilson, P. D. (1997). "Epithelial cell polarity and disease." Am J Physiol **272**(4 Pt 2): F434-442.

Wilson, P. D. (2004). "Polycystic kidney disease." N Engl J Med **350**(2): 151-164.

Wilson, P. D., L. Geng, X. Li and C. R. Burrow (1999). "The PKD1 gene product, "polycystin-1," is a tyrosine-phosphorylated protein that colocalizes with alpha2beta1-integrin in focal clusters in adherent renal epithelia." Lab Invest **79**(10): 1311-1323.

Wilson, P. D., J. T. Norman, N. T. Kuo and C. R. Burrow (1996). "Abnormalities in extracellular matrix regulation in autosomal dominant polycystic kidney disease." Contrib Nephrol **118**: 126-134.

Wilson, C., S. Idziaszczyk, J. Colley, V. Humphreys, C. Guy, J. Maynard, J. R. Sampson and J. P. Cheadle (2005). "Induction of renal tumorigenesis with elevated levels of somatic loss of heterozygosity in Tsc1+/- mice on a Blm-deficient background." Cancer Res **65**(22): 10179-10182.

Wilson, C., S. Idziaszczyk, L. Parry, C. Guy, D. F. Griffiths, E. Lazda, R. A. Bayne, A. J. Smith, J. R. Sampson and J. P. Cheadle (2005). "A mouse model of tuberous sclerosis 1 showing background specific early post-natal mortality and metastatic renal cell carcinoma." Hum Mol Genet **14**(13): 1839-1850.

Wodarczyk, C., G. Distefano, I. Rowe, M. Gaetani, B. Bricoli, M. Muorah, A. Spitaleri, V. Mannella, P. Ricchiuto, M. Pema, M. Castelli, A. E. Casanova, L. Mollica, M. Banzi, M. Boca, C. Antignac, S. Saunier, G. Musco and A. Boletta (2010). "Nephrocystin-1 forms a complex with polycystin-1 via a polyproline motif/SH3 domain interaction and regulates the apoptotic response in mammals." PLoS One **5**(9): e12719.

Wodarczyk, C., I. Rowe, M. Chiaravalli, M. Pema, F. Qian and A. Boletta (2009). "A novel mouse model reveals that polycystin-1 deficiency in ependyma and choroid plexus results in dysfunctional cilia and hydrocephalus." PLoS One **4**(9): e7137.

Woodward, O. M., Y. Li, S. Yu, P. Greenwell, C. Wodarczyk, A. Boletta, W. B. Guggino and F. Qian (2010). "Identification of a polycystin-1 cleavage product, P100, that regulates store operated Ca entry through interactions with STIM1." PLoS One **5**(8): e12305.

Woollard, J. R., R. Punyashtiti, S. Richardson, T. V. Masyuk, S. Whelan, B. Q. Huang, D. J. Lager, J. vanDeursen, V. E. Torres, V. H. Gattone, N. F. LaRusso, P. C. Harris and C. J. Ward (2007). "A mouse model of autosomal recessive polycystic kidney disease with biliary duct and proximal tubule dilatation." Kidney Int **72**(3): 328-336.

Wu, G., V. D'Agati, Y. Cai, G. Markowitz, J. H. Park, D. M. Reynolds, Y. Maeda, T. C. Le, H. Hou, Jr., R. Kucherlapati, W. Edelmann and S. Somlo (1998). "Somatic inactivation of Pkd2 results in polycystic kidney disease." Cell **93**(2): 177-188.

Wu, G., G. S. Markowitz, L. Li, V. D. D'Agati, S. M. Factor, L. Geng, S. Tibara, J. Tuchman, Y. Cai, J. H. Park, J. van Adelsberg, H. Hou, Jr., R. Kucherlapati, W. Edelmann and S. Somlo (2000). "Cardiac defects and renal failure in mice with targeted mutations in Pkd2." Nat Genet **24**(1): 75-78.

Wu, G., X. Tian, S. Nishimura, G. S. Markowitz, V. D'Agati, J. H. Park, L. Yao, L. Li, L. Geng, H. Zhao, W. Edelmann and S. Somlo (2002). "Trans-heterozygous Pkd1 and Pkd2 mutations modify expression of polycystic kidney disease." Hum Mol Genet **11**(16): 1845-1854.

Wu, M., C. Yang, B. Tao, S. Bu and L. M. Guay-Woodford (2013). "The Ciliary Protein Cystin Forms a Regulatory Complex with Necdin to ModulateMyc Expression." PLoS One **8**(12): e83062.

Wu, W., S. Kitamura, D. M. Truong, T. Rieg, V. Vallon, H. Sakurai, K. T. Bush, D. R. Vera, R. S. Ross and S. K. Nigam (2009). "Beta1-integrin is required for kidney collecting duct morphogenesis and maintenance of renal function." Am J Physiol Renal Physiol **297**(1): F210-217.

Wu, Y., X. Q. Dai, Q. Li, C. X. Chen, W. Mai, Z. Hussain, W. Long, N. Montalbetti, G. Li, R. Glynne, S. Wang, H. F. Cantiello, G. Wu and X. Z. Chen (2006). "Kinesin-2 mediates physical and functional interactions between polycystin-2 and fibrocystin." Hum Mol Genet **15**(22): 3280-3292.

Xiao, Z., M. Dallas, N. Qiu, D. Nicolella, L. Cao, M. Johnson, L. Bonewald and L. D. Quarles (2011). "Conditional deletion of Pkd1 in osteocytes disrupts skeletal mechanosensing in mice." FASEB J **25**(7): 2418-2432.

Xiao, Z., S. Zhang, L. Cao, N. Qiu, V. David and L. D. Quarles (2010). "Conditional disruption of Pkd1 in osteoblasts results in osteopenia due to direct impairment of bone formation." J Biol Chem **285**(2): 1177-1187.

Xiao, Z., S. Zhang, B. S. Magenheimer, J. Luo and L. D. Quarles (2008). "Polycystin-1 regulates skeletogenesis through stimulation of the osteoblast-specific transcription factor RUNX2-II." J Biol Chem **283**(18): 12624-12634.

Xu, C., S. Rossetti, L. Jiang, P. C. Harris, U. Brown-Glaberman, A. Wandinger-Ness, R. Bacallao and S. L. Alper (2007). "Human ADPKD primary cyst epithelial cells with a novel, single codon deletion in the PKD1 gene exhibit defective ciliary polycystin localization and loss of flow-induced Ca2+ signaling." Am J Physiol Renal Physiol **292**(3): F930-945.

Xu, G. M., S. Gonzalez-Perrett, M. Essafi, G. A. Timpanaro, N. Montalbetti, M. A. Arnaout and H. F. Cantiello (2003). "Polycystin-1 activates and stabilizes the polycystin-2 channel." J Biol Chem **278**(3): 1457-1462.

Xu, G. M., T. Sikaneta, B. M. Sullivan, Q. Zhang, M. Andreucci, T. Stehle, I. Drummond and M. A. Arnaout (2001). "Polycystin-1 interacts with intermediate filaments." J Biol Chem **276**(49): 46544-46552.

Xu, H., J. Shen, C. L. Walker and E. Kleymenova (2001). "Tissue-specific expression and splicing of the rat polycystic kidney disease 1 gene." DNA Seq **12**(5-6): 361-366.

Xu, M., L. Ma, P. J. Bujalowski, F. Qian, R. B. Sutton and A. F. Oberhauser (2013). "Analysis of the REJ Module of Polycystin-1 Using Molecular Modeling and Force-Spectroscopy Techniques." J Biophys **2013**: 525231.

Xu, N., J. F. Glockner, S. Rossetti, D. Babovich-Vuksanovic, P. C. Harris and V. E. Torres (2006). "Autosomal dominant polycystic kidney disease coexisting with cystic fibrosis." J Nephrol **19**(4): 529-534.

Yamaguchi, T., S. J. Hempson, G. A. Reif, A. M. Hedge and D. P. Wallace (2006). "Calcium restores a normal proliferation phenotype in human polycystic kidney disease epithelial cells." J Am Soc Nephrol **17**(1): 178-187.

Yamaguchi, T., D. P. Wallace, B. S. Magenheimer, S. J. Hempson, J. J. Grantham and J. P. Calvet (2004). "Calcium restriction allows cAMP activation of the B-Raf/ERK pathway, switching cells to a cAMP-dependent growth-stimulated phenotype." J Biol Chem **279**(39): 40419-40430.

Yang, B., N. D. Sonawane, D. Zhao, S. Somlo and A. S. Verkman (2008). "Small-molecule CFTR inhibitors slow cyst growth in polycystic kidney disease." J Am Soc Nephrol **19**(7): 1300-1310.

Yang, J., W. Zheng, Q. Wang, C. Lara, S. Hussein and X. Z. Chen (2013). "Translational up-regulation of polycystic kidney disease protein PKD2 by endoplasmic reticulum stress." FASEB J **27**(12);4998-5009.

Yates, L. L., J. Papakrivopoulou, D. A. Long, P. Goggolidou, J. O. Connolly, A. S. Woolf and C. H. Dean (2010). "The planar cell polarity gene Vangl2 is required for mammalian kidney-branching morphogenesis and glomerular maturation." Hum Mol Genet **19**(23): 4663-4676.

Ye, J., R. B. Rawson, R. Komuro, X. Chen, U. P. Dave, R. Prywes, M. S. Brown and J. L. Goldstein (2000). "ER stress induces cleavage of membrane-bound ATF6 by the same proteases that process SREBPs." Mol Cell **6**(6): 1355-1364.

Yoder, B. K., X. Hou and L. M. Guay-Woodford (2002). "The polycystic kidney disease proteins, polycystin-1, polycystin-2, polaris, and cystin, are co-localized in renal cilia." J Am Soc Nephrol **13**(10): 2508-2516.

Yoder, B. K., A. Tousson, L. Millican, J. H. Wu, C. E. Bugg, Jr., J. A. Schafer and D. F. Balkovetz (2002). "Polaris, a protein disrupted in orpk mutant mice, is required for assembly of renal cilium." Am J Physiol Renal Physiol **282**(3): F541-552.

Yoo, K. H., T. Y. Lee, M. H. Yang, E. Y. Park, Y. J. Yook, H. S. Lee and J. H. Park (2008). "NCAM as a cystogenesis marker gene of PKD2 overexpression." BMB Rep **41**(8): 593-596.

Yoo, K. H., Y. H. Sung, M. H. Yang, J. O. Jeon, Y. J. Yook, Y. M. Woo, H. W. Lee and J. H. Park (2007). "Inactivation of Mxi1 induces Il-8 secretion activation in polycystic kidney." Biochem Biophys Res Commun **356**(1): 85-90.

Yook, Y. J., Y. M. Woo, M. H. Yang, J. Y. Ko, B. H. Kim, E. J. Lee, E. S. Chang, M. J. Lee, S. Lee and J. H. Park (2012). "Differential Expression of PKD2-Associated Genes in Autosomal Dominant Polycystic Kidney Disease." Genomics Inform **10**(1): 16-22.

Yoshida, H. (2007). "ER stress and diseases." FEBS J **274**(3): 630-658.

Yu, L. H., T. Morimura, Y. Numata, R. Yamamoto, N. Inoue, B. Antalfy, Y. Goto, K. Deguchi, H. Osaka and K. Inoue (2012). "Effect of curcumin in a mouse model of Pelizaeus-Merzbacher disease." Mol Genet Metab **106**(1): 108-114.

Yu, J., T. J. Carroll and A. P. McMahon (2002). "Sonic hedgehog regulates proliferation and differentiation of mesenchymal cells in the mouse metanephric kidney." Development **129**(22): 5301-5312.

Yu, Q. H. and Q. Yang (2009). "Diversity of tight junctions (TJs) between gastrointestinal epithelial cells and their function in maintaining the mucosal barrier." Cell Biol Int **33**(1): 78-82.

Yu, S., K. Hackmann, J. Gao, X. He, K. Piontek, M. A. Garcia-Gonzalez, L. F. Menezes, H. Xu, G. G. Germino, J. Zuo and F. Qian (2007). "Essential role of cleavage of Polycystin-1 at G protein-coupled receptor proteolytic site for kidney tubular structure." Proc Natl Acad Sci U S A **104**(47): 18688-18693.

Yuajit, C., S. Homvisasevongsa, L. Chatsudthipong, S. Soodvilai, C. Muanprasat and V. Chatsudthipong (2013). "Steviol reduces MDCK Cyst formation and growth by inhibiting CFTR channel activity and promoting proteasome-mediated CFTR degradation." PLoS One **8**(3): e58871.

Yuajit, C., C. Muanprasat, A. R. Gallagher, S. V. Fedeles, S. Kittayaruksakul, S. Homvisasevongsa, S. Somlo and V. Chatsudthipong (2014). "Steviol retards renal cyst growth through reduction of CFTR expression and inhibition of epithelial cell proliferation in a mouse model of polycystic kidney disease." Biochem Pharmacol **88**(3): 412-421.

Yuasa, T., A. Takakura, B. M. Denker, B. Venugopal and J. Zhou (2004). "Polycystin-1L2 is a novel G-protein-binding protein." Genomics **84**(1): 126-138.

Yuasa, T., B. Venugopal, S. Weremowicz, C. C. Morton, L. Guo and J. Zhou (2002). "The sequence, expression, and chromosomal localization of a novel polycystic kidney disease 1-like gene, PKD1L1, in human." Genomics **79**(3): 376-386.

Zatti, A., V. Chauvet, V. Rajendran, T. Kimura, P. Pagel and M. J. Caplan (2005). "The C-terminal tail of the polycystin-1 protein interacts with the Na,K-ATPase alpha-subunit." Mol Biol Cell **16**(11): 5087-5093.

Zeier, M., P. Fehrenbach, S. Geberth, K. Mohring, R. Waldherr and E. Ritz (1992). "Renal histology in polycystic kidney disease with incipient and advanced renal failure." Kidney Int **42**(5): 1259-1265.

Zhang, M. Z., W. Mai, C. Li, S. Y. Cho, C. Hao, G. Moeckel, R. Zhao, I. Kim, J. Wang, H. Xiong, H. Wang, Y. Sato, Y. Wu, Y. Nakanuma, M. Lilova, Y. Pei, R. C. Harris, S. Li, R. J. Coffey, L. Sun, D. Wu, X. Z. Chen, M. D. Breyer, Z. J. Zhao, J. A. McKanna and G. Wu (2004). "PKHD1 protein encoded by the gene for autosomal recessive polycystic kidney disease associates with basal bodies and primary cilia in renal epithelial cells." Proc Natl Acad Sci U S A **101**(8): 2311-2316.

Zhang, K., X. Shen, J. Wu, K. Sakaki, T. Saunders, D. T. Rutkowski, S. H. Back and R. J. Kaufman (2006). "Endoplasmic reticulum stress activates cleavage of CREBH to induce a systemic inflammatory response." Cell **124**(3): 587-599.

Zhang, Y., J. Wada, A. Yasuhara, I. Iseda, J. Eguchi, K. Fukui, Q. Yang, K. Yamagata, T. Hiesberger, P. Igarashi, H. Zhang, H. Wang, S. Akagi, Y. S. Kanwar and H. Makino (2007). "The role for HNF-1beta-targeted collectrin in maintenance of primary cilia and cell polarity in collecting duct cells." PLoS One **2**(5): e414.

Zhang, Y. (2008). "I-TASSER server for protein 3D structure prediction." BMC Bioinformatics **9**: 40.

Zhao, H., H. Kegg, S. Grady, H. T. Truong, M. L. Robinson, M. Baum and C. M. Bates (2004). "Role of fibroblast growth factor receptors 1 and 2 in the ureteric bud." Dev Biol **276**(2): 403-415.

Zhao, Y., J. L. Haylor and A. C. Ong (2002). "Polycystin-2 expression is increased following experimental ischaemic renal injury." Nephrol Dial Transplant **17**(12): 2138-2144.

Zhou, W., E. A. Otto, A. Cluckey, R. Airik, T. W. Hurd, M. Chaki, K. Diaz, F. P. Lach, G. R. Bennett, H. Y. Gee, A. K. Ghosh, S. Natarajan, S. Thongthip, U. Veturi, S. J. Allen, S. Janssen, G. Ramaswami, J. Dixon, F. Burkhalter, M. Spoendlin, H. Moch, M. J. Mihatsch, J. Verine, R. Reade, H. Soliman, M. Godin, D. Kiss, G. Monga, G. Mazzucco, K. Amann, F. Artunc, R. C. Newland, T. Wiech, S. Zschiedrich, T. B. Huber, A. Friedl, G. G. Slaats, J. A. Joles, R. Goldschmeding, J. Washburn, R. H. Giles, S. Levy, A. Smogorzewska and F. Hildebrandt (2012). "FAN1 mutations cause karyomegalic interstitial nephritis, linking chronic kidney failure to defective DNA damage repair." Nat Genet **44**(8): 910-915.

Zhou, X., L. X. Fan, W. E. Sweeney, Jr., J. M. Denu, E. D. Avner and X. Li (2013). "Sirtuin 1 inhibition delays cyst formation in autosomal-dominant polycystic kidney disease." J Clin Invest **123**(7): 3084-3098.

Zullo, A., D. Iaconis, A. Barra, A. Cantone, N. Messaddeq, G. Capasso, P. Dolle, P. Igarashi and B. Franco (2010). "Kidney-specific inactivation of Ofd1 leads to renal cystic disease associated with upregulation of the mTOR pathway." Hum Mol Genet **19**(14): 2792-2803.

CHAPTER XII - APPENDIX

I) *Pkd1*$_{extra}$ transgene on *Pkd1*$^{-/-}$ genetic background (recapitulating *Pkd1*$_{extra}$ knock-in)

Mouse Genotype	Pkd1 expression n	*5′*	n	*3′*
Pkd1$_{EXTRA39}$; Pkd1$^{+/+}$	**6**	2.21 ± 0.67[a]	**7**	0.90 ± 0.43
Pkd1$_{EXTRA39}$; Pkd1$^{+/-}$	**6**	1.64 ± 0.29[b]	**3**	0.37 ± 0.17[d]
Pkd1$_{EXTRA39}$; Pkd1$^{-/-}$	**5**	1.99 ± 0.38[c]	**4**	0.19 ± 0.17
Pkd1$^{+/+}$	**6**	1.03 ± 0.29	**6**	1.03 ± 0.24
Pkd1$^{+/-}$	**7**	0.65 ± 0.15*	**6**	0.84 ± 0.26
Pkd1$^{-/-}$	**4**	0.13 ± 0.05***	**4**	0.27 ± 0.12**
TG vs nonTG:	a p < 0.01; b p < 0.0002; c p < 0.0005; d p < 0.02			
Pkd1$^{+/+}$ vs Pkd1$^{+/-}$ or Pkd1$^{-/-}$:	* p < 0.02; **p ≤ 0.0002, *** p <0.0005			

Legend: *Pkd1* RNA expression analysis and characterization of the phenotype in *Pkd1*$^{-/-}$*; Pkd1*$_{extra}$ mice (line 39) at birth. A. Quantitative renal expression of *Pkd1* gene at birth using primers at 5' (exon1/2) and 3' (exon39/40) end (**See also Chapter VIII**). Analysis at the 5' end showed significantly enhanced *Pkd1* expression in *Pkd1*$^{+/+}$*; Pkd1*$_{extra}$, *Pkd1*$^{+/-}$*; Pkd1*$_{extra}$ and *Pkd1*$^{-/-}$*; Pkd1*$_{extra}$ relative to their non-transgenic controls. Within the *Pkd1*$_{extra}$ on any *Pkd1* endogenous background there is no significant difference. In the non-transgenic control group, expression of *Pkd1*$^{+/-}$ and *Pkd1*$^{-/-}$ relative to *Pkd1*$^{+/+}$ was significantly decreased. Analysis at 3' showed that only *Pkd1*$^{+/-}$*; Pkd1*$_{extra}$ was statistically different from their non-transgenic controls. Data are presented as average of $\Delta\Delta$Ct ± standard deviation when compared to *Pkd1*$^{+/+}$ wild-type group (set as 1). n: number of mice analyzed. p values when transgenic compared with non-transgenic: a, p < 0.01; b, p < 0.0002; c, p < 0.0005; d, p < 0.02. p values when *Pkd1*$^{+/+}$ compared with *Pkd1*$^{+/-}$ or *Pkd1*$^{-/-}$: * p < 0.02; **p ≤ 0.0002, *** p < 0.0005. See also **Chapter VIII** for further phenotypical characterization and comparison of expression with other *Pkd1* transgenic lines.

II) *Pkd1$_{TAG}$* transgene on *Pkd1$^{-/-}$* genetic background

A.

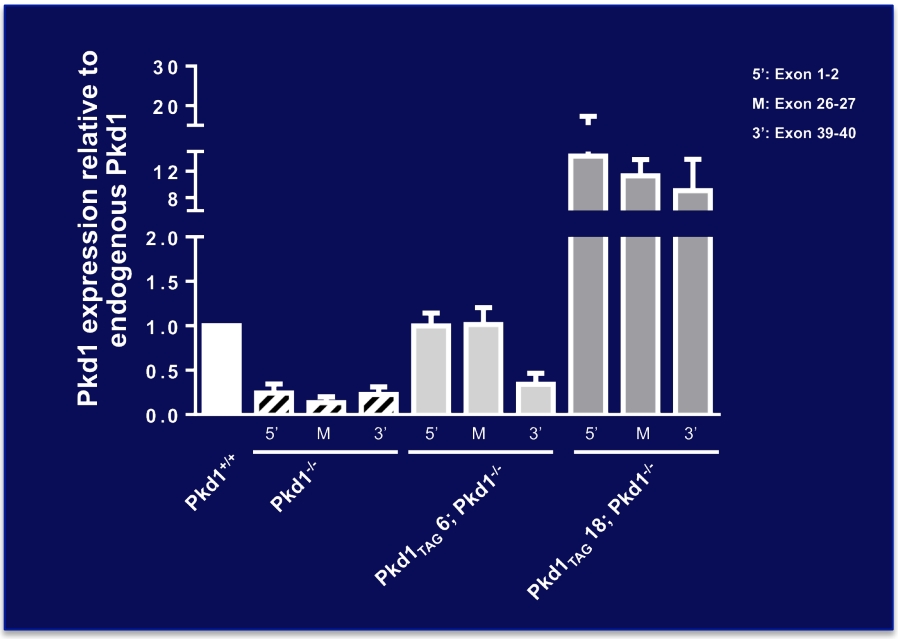

B.

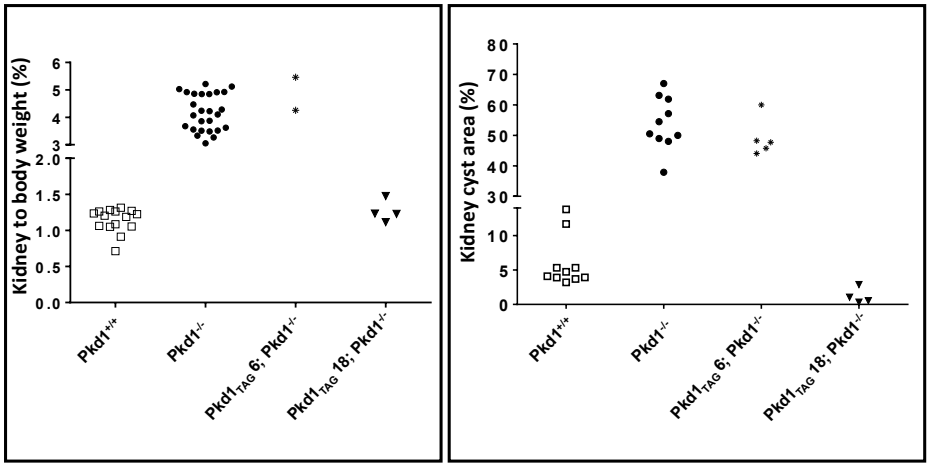

C.

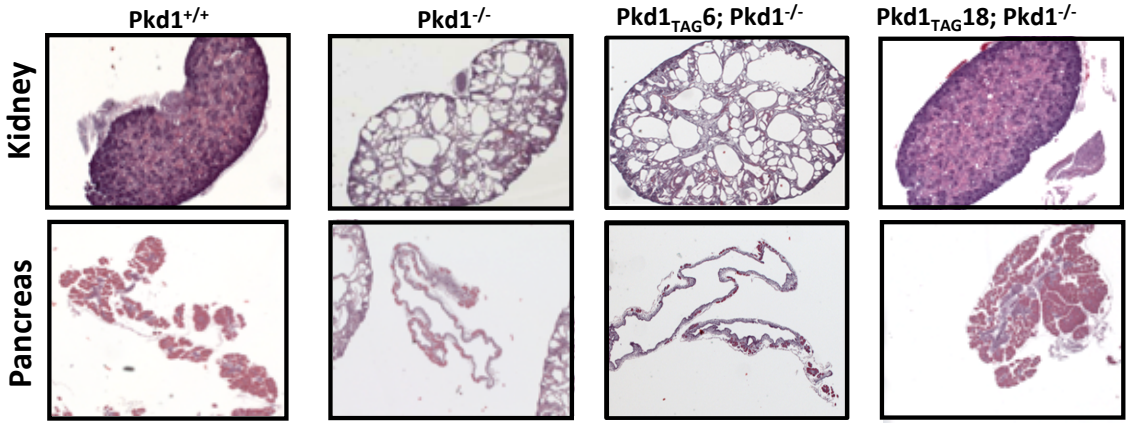

Legend: *Pkd1* RNA expression analysis and characterization of the phenotype in *Pkd1*$^{-/-}$; *Pkd1*$_{TAG}$ mice at birth, including the low copy expressor, the *Pkd1*$_{TAG}$*6* transgenic line. A. Comparison of *Pkd1* expression of high (*Pkd1*$_{TAG}$*18*) and low (*Pkd1*$_{TAG}$*6*) systemic *Pkd1* expressors on *Pkd1*$^{-/-}$ background at birth by Q-PCR**. B.** Kidney to body ratio (KBW) and cyst index area of *Pkd1*$_{TAG}$*6; Pkd1*$^{-/-}$ are analogous to the *Pkd1*$^{-/-}$ mice, while those of high expressor are significantly different and similar to wild-type control. **C.** In comparison to the high transgene expressor (*Pkd1*$_{TAG}$*18; Pkd1*$^{-/-}$) that showed no evidence of renal or pancreatic cystogenesis (**Chapter VIII**), the low expressor (*Pkd1*$_{TAG}$*6; Pkd1*$^{-/-}$) mice developed renal and pancreatic cystic phenotype. Of note, there is an absence of liver phenotype in all mice. The lack of ability of *Pkd1*$_{TAG}$*6* the transgene to rescue *Pkd1*$^{-/-}$ cystogenesis could be explained by a decrease in 3' *Pkd1* transcript shown in A. The complexity and potentially multiple transcripts and alternative splicing at the 3' end of *Pkd1* gene have been previously evoked, and abnormal relative expression of any of these 3' transcripts could be responsible for some of the observed phenotypes (**Also App. VIII, Chapter I-Section 3.1.1&7.1.2.1**).

III) Wnt pathway in PKD

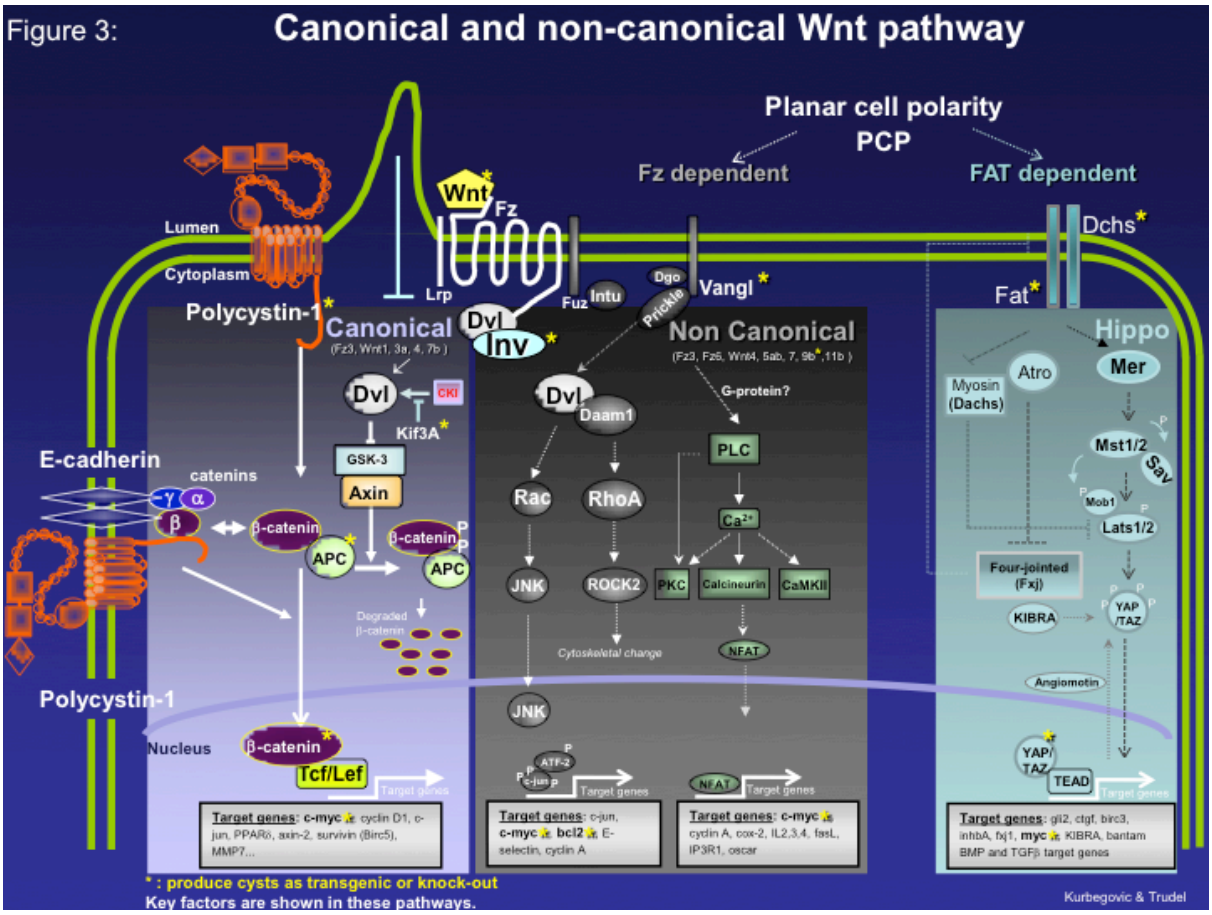

Legend: Schematic illustration of canonical/β-catenin and non-canonical/PCP Wnt pathway and the downstream effectors. Yellow star: Inactivation of these genes or their overexpression was associated in the literature with kidney cysts. PCP: planar cell polarity. Template adapted and modified from Martin Couillard.

III.A) Active β-catenin protein expression in *Pkd1 dosage increase or decrease* kidneys

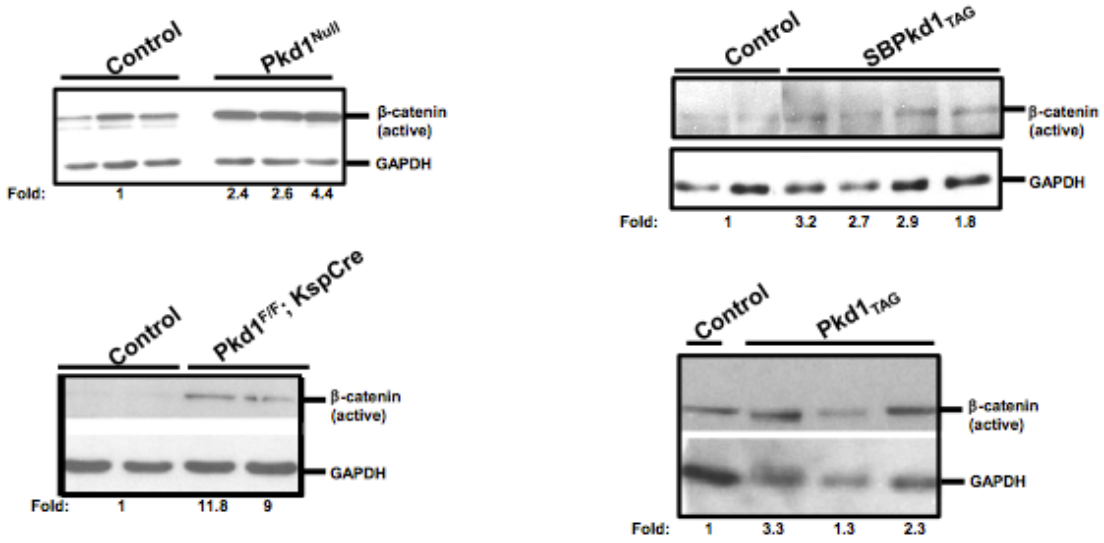

Legend: Expression analysis of the active form of β-catenin protein in the kidneys of *Pkd1* dosage increase or dosage decrease. Western blots on total kidney extracts in *Pkd1* dosage decrease (two left panels) and dosage increase mouse models (two right panels) using ABC antibody that recognizes a non-phospho 92kDa active form of β-catenin (residus Ser37 or Thr41), normally phosphorylated by GSK-3β and targeted for degradation. ***Active β-catenin levels were increased in the kidneys of all four mice models. These results, together with the data from Couillard et al. strongly support an involvement of canonical Wnt pathway in PKD.*** Gapdh served as a loading control. Active β-catenin levels were normalized to Gapdh and the average obtained for control mice was set as 1. ImageQuant software was used for quantification.

III.B) c-Myc expression analysis in *Pkd1* dosage increase or decrease kidneys

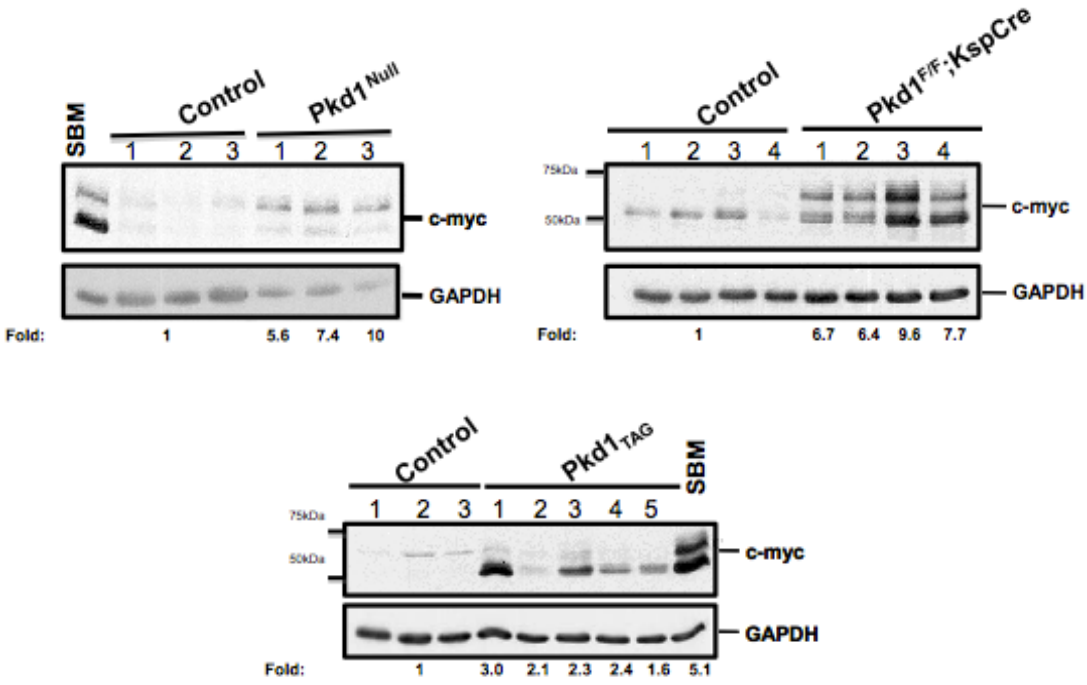

Legend: Protein expression analysis of a direct downstream target of canonical Wnt pathway, the c-myc oncogene, in *Pkd1* dosage decrease and *Pkd1* dosage increase. *Upper, left.* Immunoblot of c-myc on newborn renal tissues from *Pkd1*$^{-/-}$ mice (n=3) in comparison to negative wild-type controls and to one SBM transgenic kidney as positive control. Expression of c-myc was increased in all three *Pkd1*$^{-/-}$ samples analysed and ranged from ~5- to ~10-fold relative to endogenous levels. ***Upper, right***. Immunoblot of c-myc on kidneys from mice with kidney conditionally-ablated *Pkd1* (n=4) in comparison to negative wild-type age-matched controls at P10. Expression of c-myc was induced from 6.7- to 9.6-fold in *Pkd1*$^{F/F}$*; KspCre* mice relative to controls. ***Lower panel.*** Adult kidneys from the *Pkd1*$_{TAG}$ *26* mouse line (n=5) were monitored for c-myc protein expression by immunoblot in comparison to age-matched controls (n=3) and to one SBM transgenic c-myc mouse line that develops PKD. Renal expression of c-myc was increased from 1.6- to 3.0-fold above negative controls and slightly lower than in SBM mice. ***These findings demonstrate consistently increased c-myc expression in all Pkd1 mouse models tested and, together with the data from Couillard et al. strongly support c-myc as a downstream, direct or indirect, modulator of polycystic kidney disease.*** Rabbit monoclonal antibody against c-myc was used in this study and recognizes a c-myc product band of ~60kDa.

III.C) Possible C-myc / PC1 feedback loop

A. **B.**

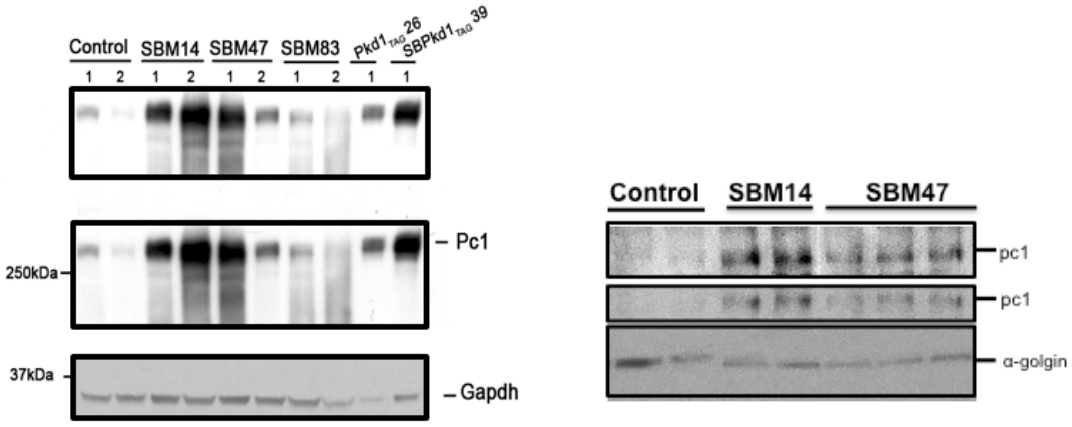

Legend: Expression of polycystin-1 in kidney-specific overexpressor of c-myc, the SBM mouse model by Western blot. A. Expression of Pc1 in adult kidneys of three different SBM transgenic lines was compared to levels of Pc1 in normal non-transgenic (control) and *Pkd1*/Pc1 overexpressing murine kidneys (*Pkd1*$_{TAG}$ and *SBPkd1*$_{TAG}$ transgenic lines). Gapdh served as a loading control to confirm the equal loading on a gradient 4-12% Bis-Tris Invitrogen gel. **B.** Additional adult kidneys samples were analysed for Pc1 expression on 5% Tris-Glycine gels. Control, n=2; SBM 14, n=2; SBM47, n=3. α–Golgin served as a loading control. Two blots of Pc1 represent two different expositions. ***This analysis shows that c-myc overexpression can trigger, directly or indirectly, upregulation of Pc1.*** Control: non-transgenic kidneys of the same genetic background. SBM14, 47 and 81: PKD mouse model, three transgenic lines overexpressing c-myc in the kidneys. *Pkd1*$_{TAG}$ and *SBPkd1*$_{TAG}$: PKD1 mouse models with systemic and kidney-specific Pc1 overexpression, respectively.

III.D) C-myc / Pc2 axes

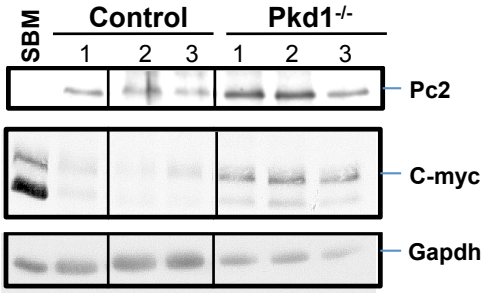

Legend: Protein expression analysis of c-myc and polycystin-2 in *Pkd1*^{Null} (*Pkd1*$^{-/-}$) kidneys at birth by Western blot. The *Pkd1*$^{-/-}$ loss-of-function mouse model, which has increased c-myc expression, also shows upregulation of Pc2 in comparison to the wild-type controls. ***Thus, together with App. III.C, this data suggest a probable Pc1-c-myc-Pc2 axis or Pc1/Pc2 calcium complex-cmyc signaling and/or feedback regulation (See App. XV).*** Gapdh was used as a control for equal loading.

1-4: 4 different mice of indicated genotype. SBM: PKD adult mouse model by kidney specific overexpression of c-myc.

III.E) Wnt non-canonical pathway - Inactivation of *Rac1* in the kidneys

A.

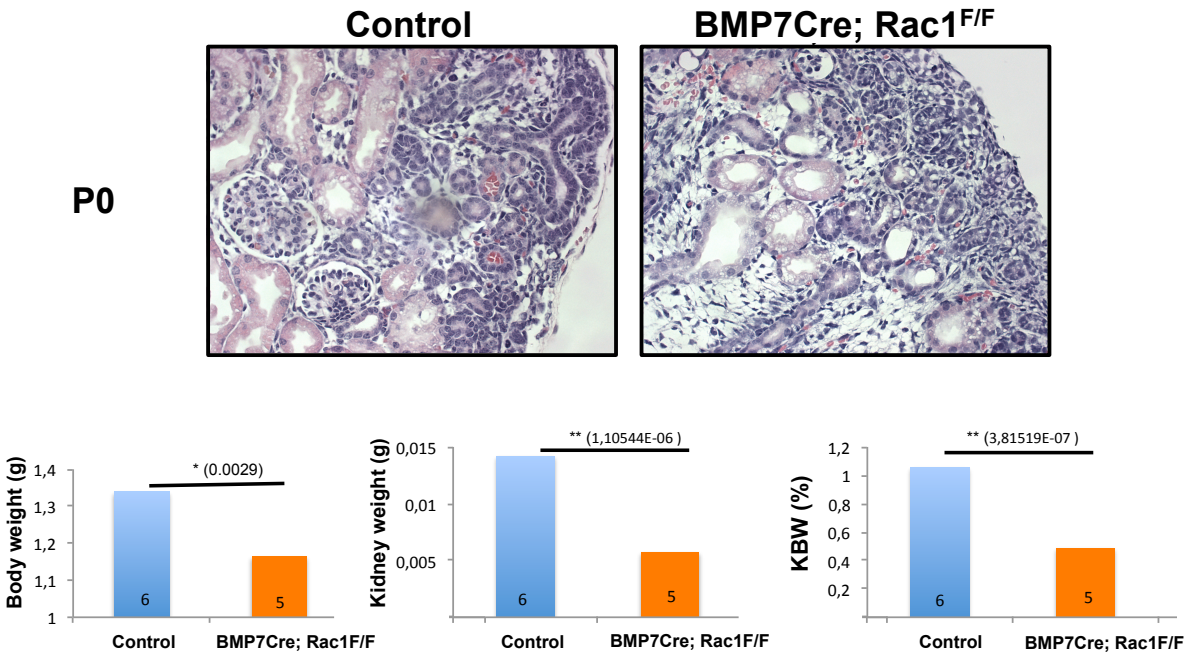

B.

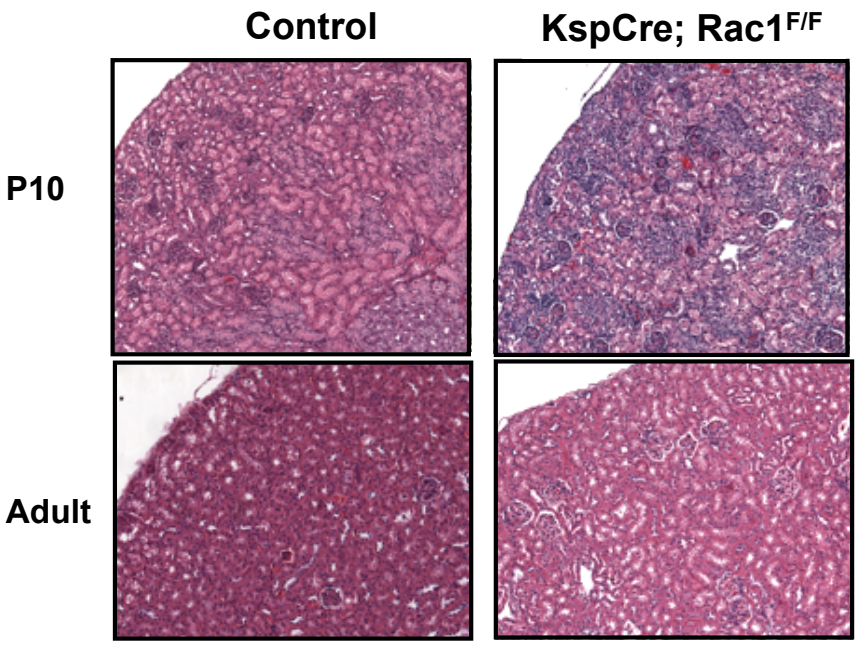

Legend: Early and late inactivation of *Rac1* gene specifically in the kidneys. *A. Inactivation of Rac1 by BMP7Cre leads to hypoplasic kidneys.* Mating between *BMP7Cre; Rac1$^{fl/+}$* and *Rac1$^{fl/+}$* mice

were accomplished specifically to avoid any risk of obtaining homozygous knock-in BMP7Cre pups that on their own were shown to develop hypoplasic pups. At birth, all pups (in grams), kidneys (grams) and kidney to body ratio (%) were significantly smaller in *Rac1* conditionally inactivated mice than in controls. In the mutant kidneys at birth, we could observe lesser number of matured tubules, no S shaped bodies, a lot of non-induced metanephric mesenchyme and some, but much smaller number of glomeruli, indicating that the nephrogenesis has stopped. Therefore, the nephron seem to be formed but kidneys contain much fewer nephrons. In the control wild-type kidneys, the nephrogenesis is still continuing after birth as observed by UB branching and presence in the ''T'' shapped structure. Of note, the significant reduction in the total body weight of *BMP7Cre; Rac1*$^{F/F}$ mice is most probably caused by the extrarenal expression of BPM7Cre construct. ***Convergent extension (a branch of non-canonical Wnt pathway) and altered kidney branching could be responsible for renal hypoplasia in this mouse model (App. III). B. Inactivation of Rac1 by KspCre does not lead to any obvious alterations in post-natal renal histology.*** Renal sections from *Rac1* ablated mice using KspCre (*KspCre; Rac1*$^{F/F}$) at post-natal day (P10) and adult stage do not exhibit morphologic alterations in comparison to the wild-type control kidneys. Of note, *BMP7Cre* is expressed very early in epithelial cells of the UB, while KspCre is expressed later in collecting/distal structures. To determine its relevance in PKD, *Rac1* can be now inactivated in PKD LOF and GOF mouse models using for example *KspCre*. *In collaboration with Dr. Jean-François Côté, IRCM*.

IV) Position of the centrosome in *Pkd1$_{TAG}$* dosage increase kidney epithelial cells

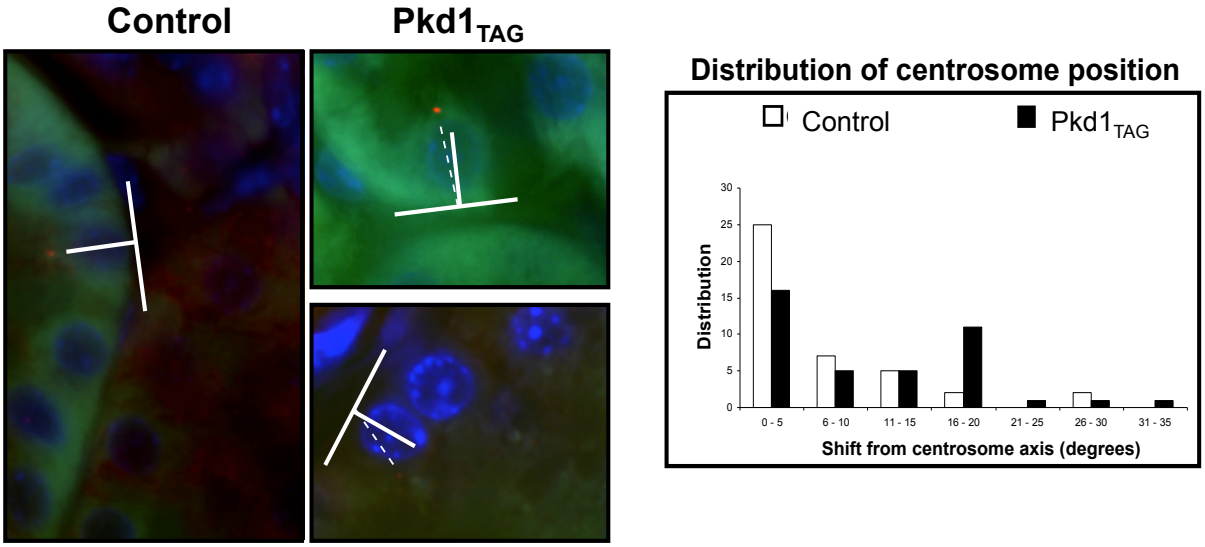

Legend: Centrosome position defect in *Pkd1* dosage increase kidneys by stereoimaging. Centrosome should be typically located at the center of the apical end of each renal epithelial cell. The majority of control wild-type cells have their centrosome at the tip of a line drawn through the nucleus and perpendicular to the basal membrane (white T indicated). In *Pkd1* dosage increase (*Pkd1$_{TAG}$26*), several epithelial cells were significantly shifted from the perpendicular angle. Centrosomes of *Pkd1$_{TAG}$26* epithelial cells are often displaced from the center to the lateral junction of the cells (indicated by the dashed line). This finding suggests misorientation of mitotic spindle and PCP defects. At least 10 non-overlapping regions (100X magnification) and 0.4 μm Z-stacks were deconvoluted. Centrosome position and angles of deviation were measured using Imaris software. Immunofluorescence staining was with 30μm renal sections using anti-γ-tubulin (red color: centrosome, generous gift of Dr. William Zhang, IRCM) and DAPI (blue color: nuclei) and a DM6000 microscope. Prepared by Anthonio Scalia and Almira Kurbegovic.

V) Assessing the functional role of PC1 GPS cleavage in the kidney using *SBPkd1$_{TAG}$* mice (*Pkd1$^{V/V}$* background) *Collaboration with Dr. Feng, University of Maryland School of Medicine*

V.A) Expression and characterization of the kidney phenotype at P10

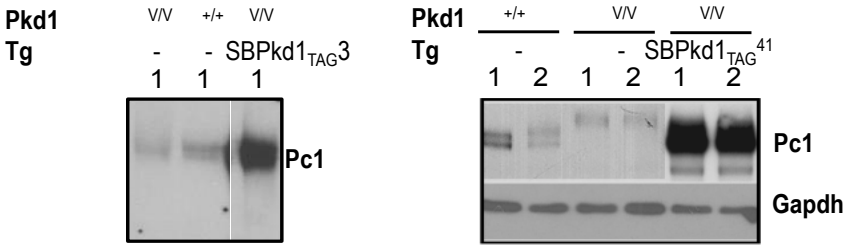

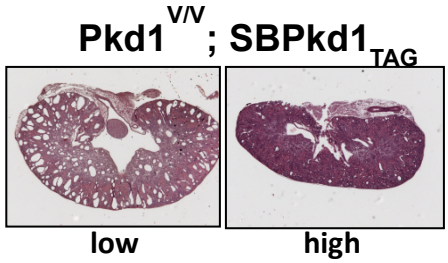

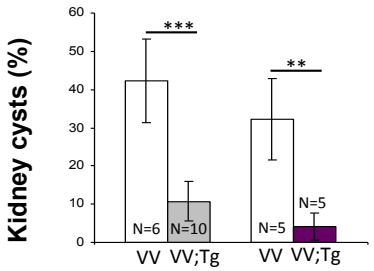

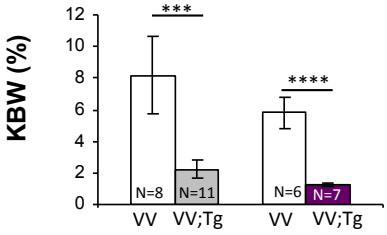

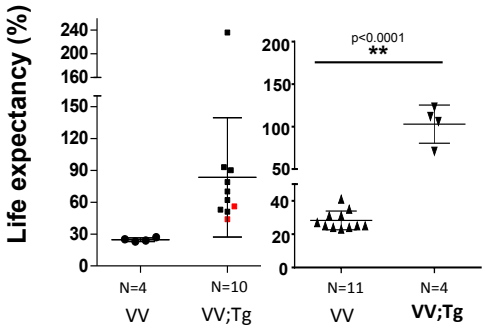

Legend: Pc1 expression analysis, kidney morphometric at P10 and life expectancy in kidney specific *Pkd1* transgenes on *Pkd1*$^{V/V}$ genetic background. Pc1 expression in the binary kidneys, (the low-copy (line *SBPkd1*$_{TAG}$*3*) and high-copy (line *SBPkd1*$_{TAG}$*41*), and their controls (most upper pannel) at P10. Both lines express increased Pc1 levels in comparison to the *Pkd1*$^{+/+}$ and *Pkd1*$^{V/V}$ control kidneys. KBW (kidney to body weight ratio), cyst area percentage (%) and life expectancy (in days) were significantly changed in the kidneys of *Pkd1*$^{V/V}$ by the low-copy and high-copy kidney specific *Pkd1* expressors. Line *SBPkd1*$_{TAG}$*3* had significantly important effect on *Pkd1*$^{V/V}$ cystogenesis while the high *SBPkd1*$_{TAG}$*41* expressor rescued almost completely. *Pkd1*$^{V/V}$ life expectancy was extended from ~1 month to 3-4 months by these kidney specific *Pkd1* transgenes. ***Pkd1 kidney specific or systemic transgenic expressors behave similarily on Pkd1*$^{V/V}$ *and Pkd1*$^{-/-}$ *genetic backgrounds, however with some significant differences regarding the extrarenal phenotype and life expectancy (Chapter VI, VIII, App.VB).*** ''N'' indicates number of mice analyzed. VV: *Pkd1*$^{V/V}$; VV; Tg: *Pkd1*$^{V/V}$*; SBPkd1*$_{TAG}$*3* (left group, low copy) and *SBPkd1*$_{TAG}$*41* (right group, high copy). *SBPkd1*$_{TAG}$: kidney specific *Pkd1* transgenic mouse. Gapdh was used as a loading control. 1,2: number of mice analyzed.

V.B) Progression of the PKD in kidney specific *Pkd1* expressor (*SBPkd1$_{TAG}$*) on *Pkd1$^{V/V}$* background

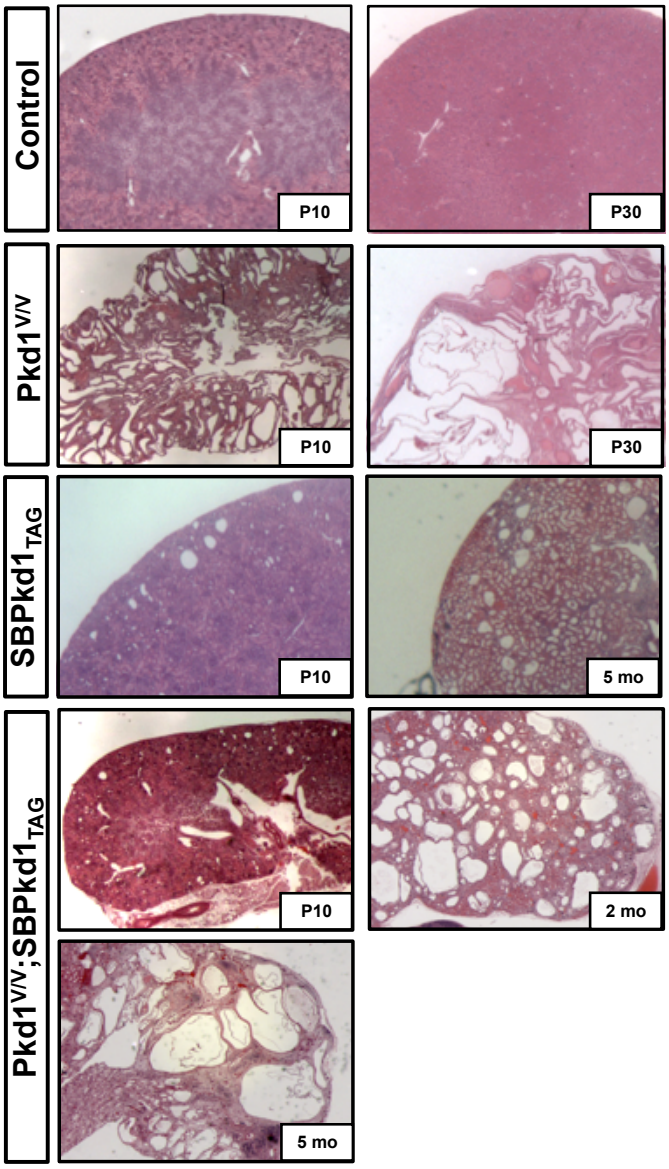

Legend: Histologic analysis of *Pkd1$^{v/v}$* kidneys in comparison to wild-type control at P10 and P30. At P10, *Pkd1$^{v/v}$* show multiple cysts that increase in size and number with age (life expectancy ~P25-30). Similarly to high-copy kidney specific *SBPkd1$_{TAG}$41* expressor, the *Pkd1$^{v/v}$; SBPkd1$_{TAG}$41* compound showed very few anomalies at P10 and display a significant rescue of the *Pkd1$^{V/V}$* kidney phenotype and extended lifespan. At ~2 months of age, the kidneys of *Pkd1$^{v/v}$; SBPkd1$_{TAG}$41* compound were however very cystic and later at 5 months (the oldest mice obtained) overtly cystic. Thus, together kidney and liver phenotype in these binary mice (progression of liver phenotype is described in **Chapter VIII**) were probably the cause of early death.

V.C) Cyst origin in kidney specific *Pkd1* expressor (*SBPkd1$_{TAG}$*) on *Pkd1$^{V/V}$* background

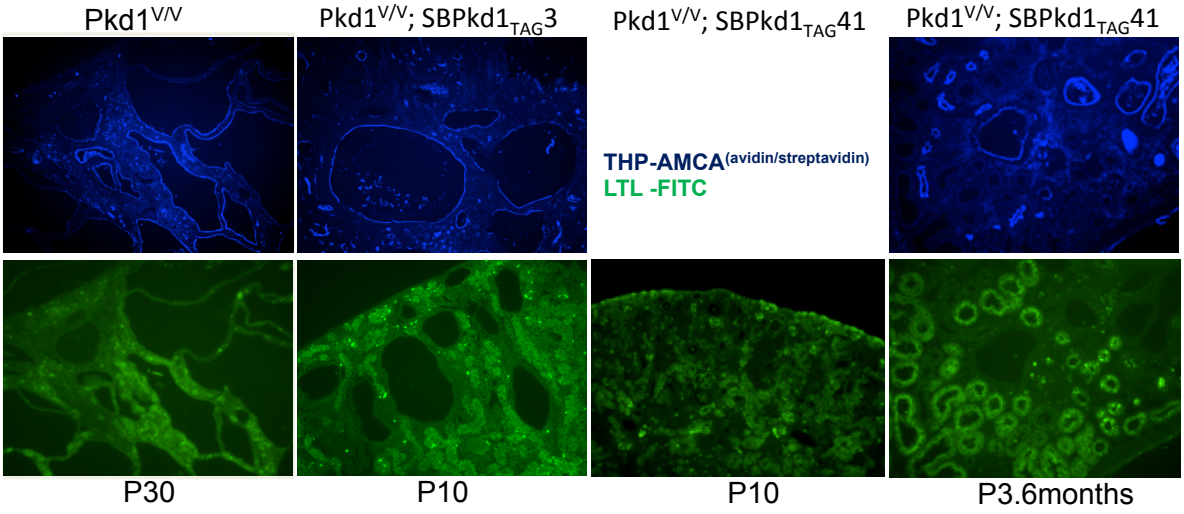

Legend: Origin of kidney cysts in *Pkd1$^{V/V}$; SBPkd1$_{TAG}$3* or *Pkd1$^{V/V}$; SBPkd1$_{TAG}$41* binary mice by immunofluorescence. LTL coupled to FITC was used for identification of proximal tubules and THP/AMCA for detection of both thick ascending limb (TAL) and distal convoluted tubule (DCT). At P30, the end point for *Pkd1$^{V/V}$* mouse model, that probably succomb due to the kidney failure, the *Pkd1$^{V/V}$* kidney cysts are mainly of the distal segment origin, as previously described (Yu, Hackmann et al. 2007). The lack of total rescue of the *Pkd1$^{V/V}$* kidney phenotype by low kidney specific *SBPkd1$_{TAG}$3* transgene at P10 does not seem to be due to the cysts in the proximal tubules by the transgene. The cysts that occur at P10 in *Pkd1$^{V/V}$; SBPkd1$_{TAG}$ 3* are still mainly THP^{+} and LTL^{-}. Hence, the *SBPkd1$_{TAG}$3* mouse line probably does not provide a sufficient expression of the transgene in THP positive segments. As for the *SBPkd1$_{TAG}$41* line, that significantly rescues *Pkd1$^{V/V}$* kidney cystogenesis at P10, the LTL positive dilatations/cysts are obvious much later, at P3.6months. Together, this data suggest that ***for the higher kidney specific expressor, at P10, the transgene is expressed enough in almost all kidney segments required, and in the later stage, some expression of the transgene in the proximal tubules may contribute slightly to the Pkd1$^{V/V}$ kidney cystogenesis. Since invasive cysts still occur in the Pkd1$^{V/V}$; SBPkd1$_{TAG}$ 41, either the transgene is not expressed in specific type of tubular segments, or not enough in adult stage, or it is the transgene overexpression that contributes significantly to cystogenesis at this later point.*** Those hypotheses are tested by genetic complementation studies of *Pkd1$^{-/-}$* by *SBPkd1$_{TAG}$* and *Pkd1$_{TAG}$* transgenes (**Chapter VIII**). The age of mice are indicated below the panels. LTL*: Lectin Lotus tetragonolobus*; THP: Tamm-Horsfall protein; AMCA: aminomethyl coumarin acetate (AMCA) blue fluorescent dye; FITC: Fluorescein isothiocyanate.

V.D) Effect of gene dosage by the *Pkd1* transgene on *Pkd1*$^{V/V}$ background

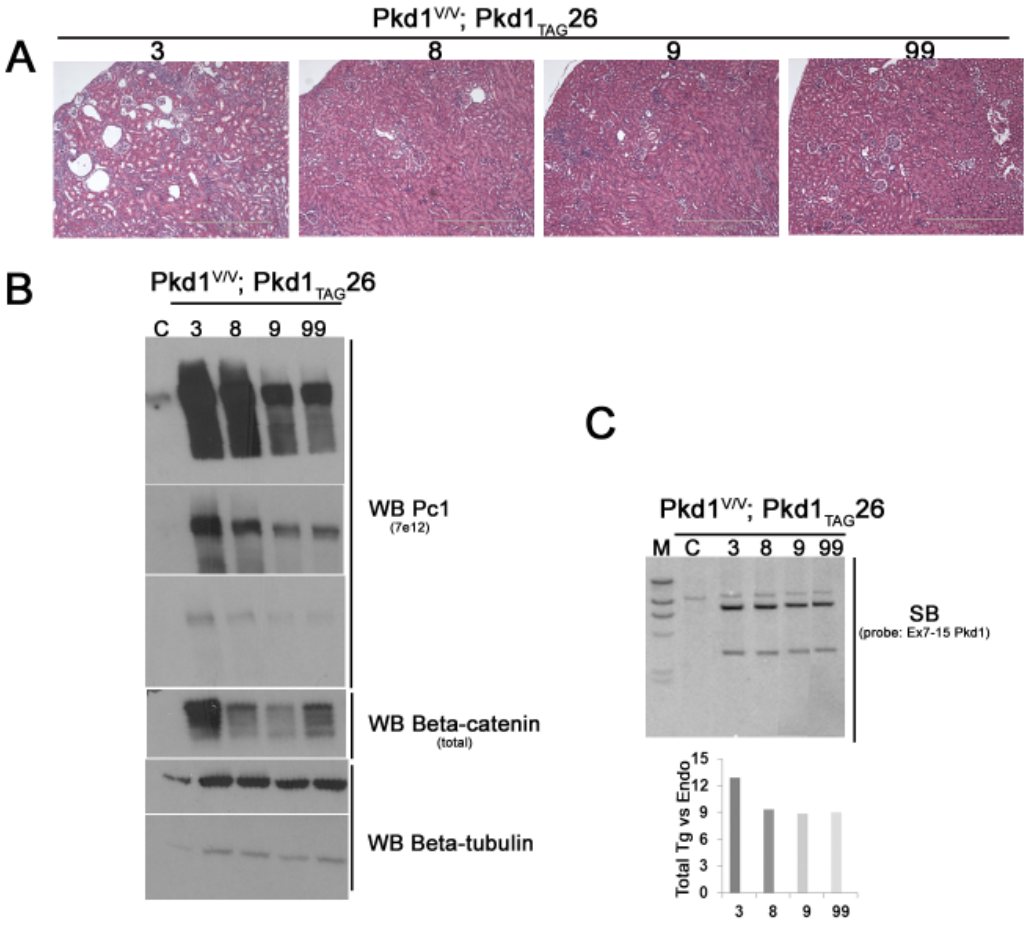

Legend: Kidney histology of *Pkd1*$^{V/V}$*; Pkd1*$_{TAG}$*26* mice (n=3: #3, 8, 9) and one littermate *Pkd1*$^{V/+}$*; Pkd1*$_{TAG}$*26* control (n=1, #99) at ~3months of age. While two *Pkd1*$^{V/V}$*; Pkd1*$_{TAG}$*26* mice did not show any discernable kidney anomalies, one mouse showed mild cystic phenotype (**A**, #3). These mice were regenotyped using frozen kidneys by a Southern blot (SB), using EcoRI digest and ex7-15 *Pkd1* probe. The transgene copy number was quantifed by PhosphoImager as a total transgene versus endogenous *Pkd1* **(C)**. The cystic mice corresponded to the higher copy number (almost 2-fold increase in comparison to other mice), and is hence, most likely homozygous for the *Pkd1*$_{TAG}$ transgene. The Western blot was carried out on these same mice to verify if increased number of copies correlated with increased *Pkd1* expression **(B)**. ***Indeed, the cystic mice showed highest Pc1 expression, consistent with gene dosage of Pkd1 in ADPKD cystogenesis.*** Of note, hybridation of the lower part of the WB membrane with β-catenin (total) antibody revealed increased levels, consistent with implication of Wnt-canonical pathway in ADPKD (**App. III**). β-Tubulin was used as loading control. H&E staining. Bar 500 μm.

V.E) Liver fibrosis in *Pkd1* renal and systemic high transgenic expressors on *Pkd1*$^{V/V}$ background

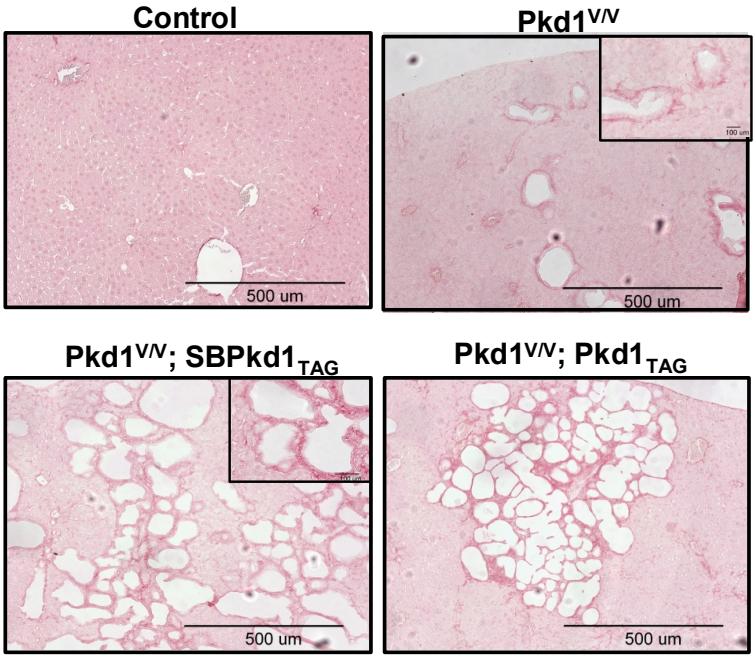

Legend: Evaluation of collagen levels and localization by Sirius Red staining on liver sections from adult wild-type control *Pkd1*$^{+/+}$, *Pkd1*$^{V/V}$ and *Pkd1* kidney-specific *SBPkd1*$_{TAG}$ *41* or systemic *Pkd1*$_{TAG}$ *26* on *Pkd1*$^{V/V}$ genetic background. Both *Pkd1*$^{V/V}$*; SBPkd1*$_{TAG}$*41* and *Pkd1*$^{V/V}$*; Pkd1*$_{TAG}$*26* lines showed significant increase of collagen deposition in the cystic regions of the liver. The pre-cystic biliary duct networks also appear surrounded with a more intense fibrotic/collagen enriched signal.

Overall conclusions about the section App. V and Chapters VI&VIII: *SBPkd1*$_{TAG}$ and *Pkd1*$_{TAG}$ transgenes can substantially rescue the *Pkd1*$^{V/V}$ renal phenotype extending their lifespan to ~3months and > 1 year respectively. For the kidney specific transgene, this lifespan extension for *Pkd1*$^{V/V}$ seems longer than for *Pkd1*$^{-/-}$ background, hence the uncleaved Pc1 form could be functional not only in embryonic but also in later adult stage as well. Expression of Pc1 in *Pkd1*$_{TAG}$ liver abrogated significantly the biliary cysts normally detected in *Pkd1*$^{V/V}$ liver. Significant rescue of renal phenotype in *Pkd1*$^{V/V}$ mice by *SBPkd1*$_{TAG}$ transgene uncovered a major role of Pc1 cleavage in liver biliary system. Importantly, together the absence of liver phenotype in *Pkd1*$^{-/-}$ mice combined with the markedly invasive biliary cysts in *Pkd1*$^{V/V}$ and the mildly but consistently affected *Pkd1*$^{V/V}$*; Pkd1*$_{TAG}$ suggest that presence of uncleavable Pc1 is responsible for the liver phenotype.

VI) Inactivation of *Pkd1* in red blood cells

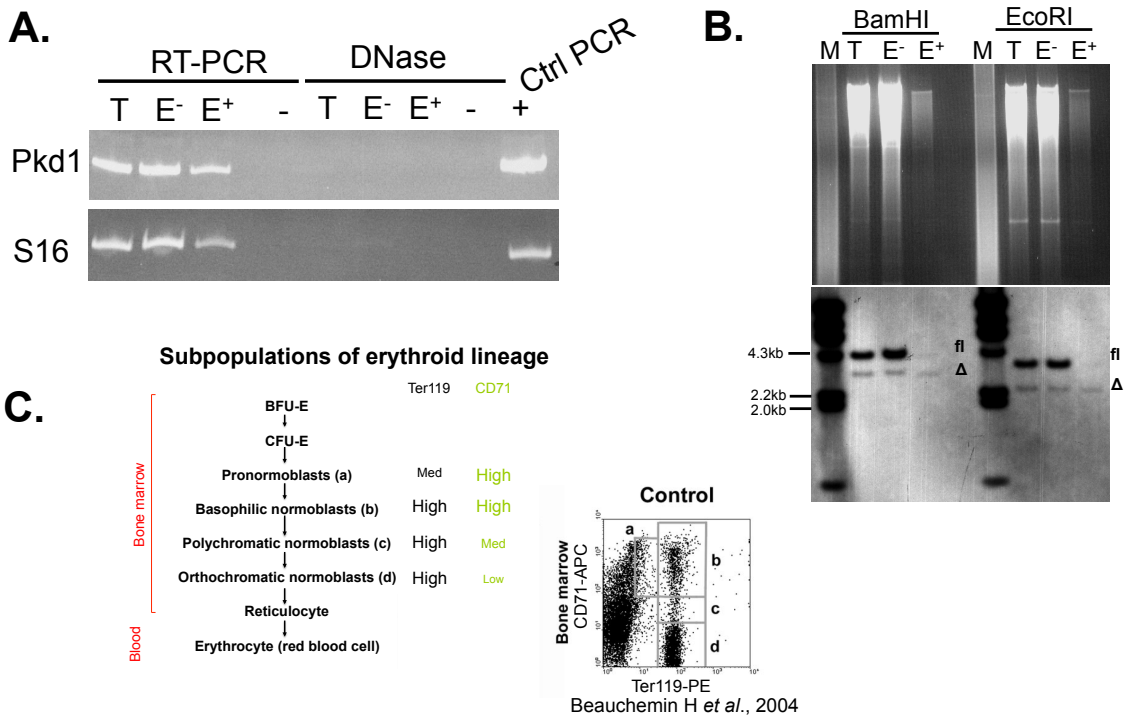

Mice	n	Proerythroblasts (region a) (%)	Basophilic erythroblast (region b) (%)	Polychromatophilic erythroblasts (region c) (%)	Orthochromatophilic erythroblasts (region d) (%)
Pkd1fl/fl	3	3.8 ± 0.4	23.3 ± 4.2	4.9 ± 3.0	10.3 ± 1.1
Pkd1fl/fl; EpoRCre+/in	3	4.6 ± 0.8	18.1 ± 0.6	7.2 ± 2.7	10.4 ± 2.0

Legend: PC1 expression was previously reported in red blood cells. To gain insight into the role of PC1 specifically in red blood cells, independently of any potential input of polycystic kidney disease, the *Pkd1* was conditionally inactivated in red blood cells using highly efficient and erythroid-specific *EpoRCre* knock-in mice and $Pkd1^{flox}$ allele (Heinrich, Pelanda et al. 2004, Piontek, Huso et al. 2004, Pang, Lemsaddek et al. 2012).

(A) We first confirmed that *Pkd1* is indeed expressed in erythroid cells by RT-PCR using 5' end *Pkd1* primers (ex1/ex2). Erythroid-specific Ter119+ (E+) cells were obtained from bone marrow by FACS using Ter119-PE antibody and magnetic anti-PE microbeads following MACS or Easysep capture. T: total cells from bone marrow; E^-: Ter119 negative population; E^+: Ter119 positive cell population. -: H20 negative PCR control; Ctrl PCR: positive control for *Pkd1* expression, $Pkd1_{TAG}$ transgenic brain tissue.

(B) We then analyzed the recombination efficiency by Southern blot on DNA from bone marrow of *Pkd1*$^{fl/fl}$*; EpoRCre* mice (total or sorted by MACS). The recombination was very high, almost total, as only the deleted (Δ) band was observed in Ter119+ population shown by two different restriction enzymes and *Pkd1* ex4-6 probe, and consistent with previous studies (Heinrich, Pelanda et al. 2004). Expected bands for BamHI (flox: ~3.3kb; Δ: ~2.3kb) and EcoRI (flox: ~3.6kb; Δ: ~2,7kb). M: Lambda HindIII DNA ladder.

(C) Co-staining with CD71 and Ter119 markers is a tool to identify different cell types during erythroid differentiation, from BFU, CFU, PE, EB, EP, EA to mature red blood cells, *i.e.,* the erythrocytes (Beauchemin, Blouin et al. 2004). EpoR is expressed in CFU, BFU and PE; Tert119 is expressed from PE to mature red blod cells and CD71 expression is increasing from CE to EA. Consistent with an absence of erythroid anomalies, such as haemoglobin levels and erythrocyte morphology, in *Pkd1*^{de34} loss-of-function mouse mutant (Lu, Shen et al. 2001), our preliminary data suggest that *Pkd1*$^{fl/fl}$*; EpoRCre* adult mice do not have a significant defect in erythroid differentiation in the bone marrow by FACS analysis, albeit a non significant tendency towards a decrease in basophilic and increased polychromatophilic erythroblasts. ***This observation suggests that Pkd1 does not have a significant role in adult medullary erythropoiesis.*** In addition, RBC (red blood cell count) and retics (%) in *EpoRCre; Pkd1*$^{fl/fl}$ (n=4) were similar to control mice (n=2) (unpublished data HF, MMS). This may not be the case for *Pkd2* gene that was reported to be highly expressed, even more than Pc1, in red blood cells (Markowitz, Cai et al. 1999). BFU: burst-forming unit; CFU: colony-forming unit, PE: proerythroblast; EB: erythroblast basophile; EP: erythroblast polychromatophile; EA: erythroblast acidophile.

VII) Impact of exogenous cAMP in *Pkd1* dosage reduce and increase *ex vivo*

A.

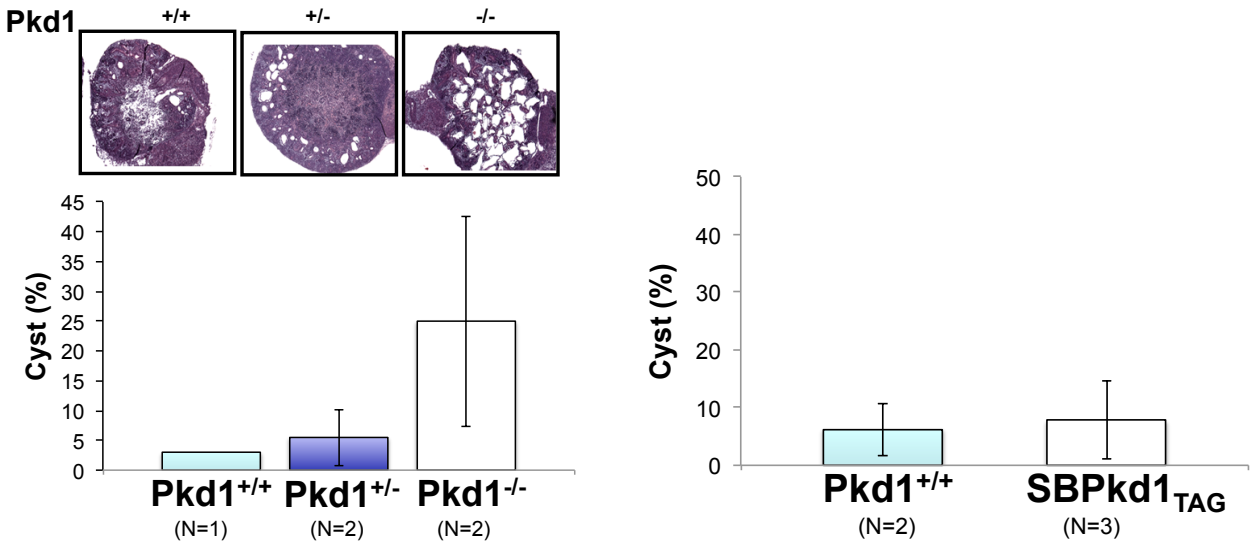

B.

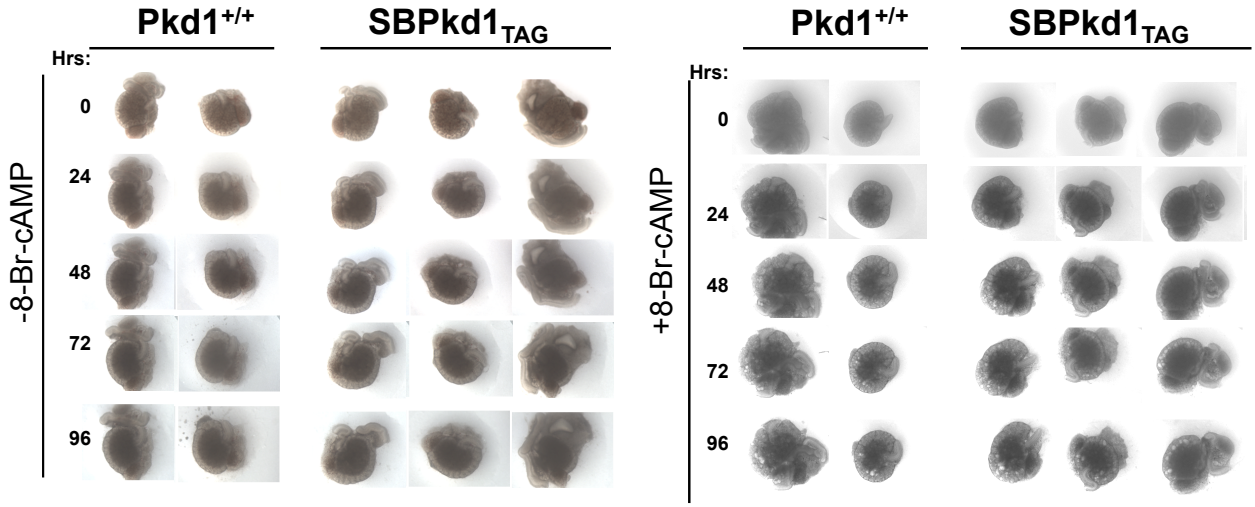

Legend: cAMP impact on kidney explants from *Pkd1* dosage reduce (A, left) and *Pkd1* gene increase *Pkd1* mouse models (A right, B). Kidney explants *ex vivo* were removed at E14.5, incubated 24 hours on filters and then treated with cAMP (+8-Br-cAMP) for 96 hours or left untreated (-8-Br-cAMP). Pictures were taken in the beginning of the treatment and every 24 hours for a period of 4 days, last day corresponding to E19.5, fixed in formalin and stained with H&E. Incubation with cAMP for 96 hours resulted in few cysts in the kidneys from the wild-type mice, while the treatment of *Pkd1*$^{-/-}$ kidneys caused consistently severe cystogenesis showed by an increased cystic index and kidney histology analysis (H&E) (**A**). The haploinsufficient *Pkd1*$^{+/-}$ kidneys also showed kidney cysts but much less than *Pkd1*$^{-/-}$. **The**

***Pkd1* LOF (*Pkd1*$^{-/-}$) kidneys are thus hyper-responsive to cAMP levels consistent with the previous studies** (Magenheimer, St John et al. 2006). In contrast to inactivation of *Pkd1*, our preliminary study suggests that overexpression of *Pkd1* (*SBPkd1*$_{TAG}$, line 39) does not result in the same cellular response nor magnitude to alteration of cAMP levels in embryonic kidney culture (**A, right panel and B**), although more mice will be required to confirm this observation unequivocally. The images were taken using Axiophot microscope. *SBPkd1*$_{TAG}$: kidney specific overexpressor, line 39. N=number of mice of particular genotype.

VIII) Expected Pc1 product(s) in *Pkd1* dosage reduce mouse models

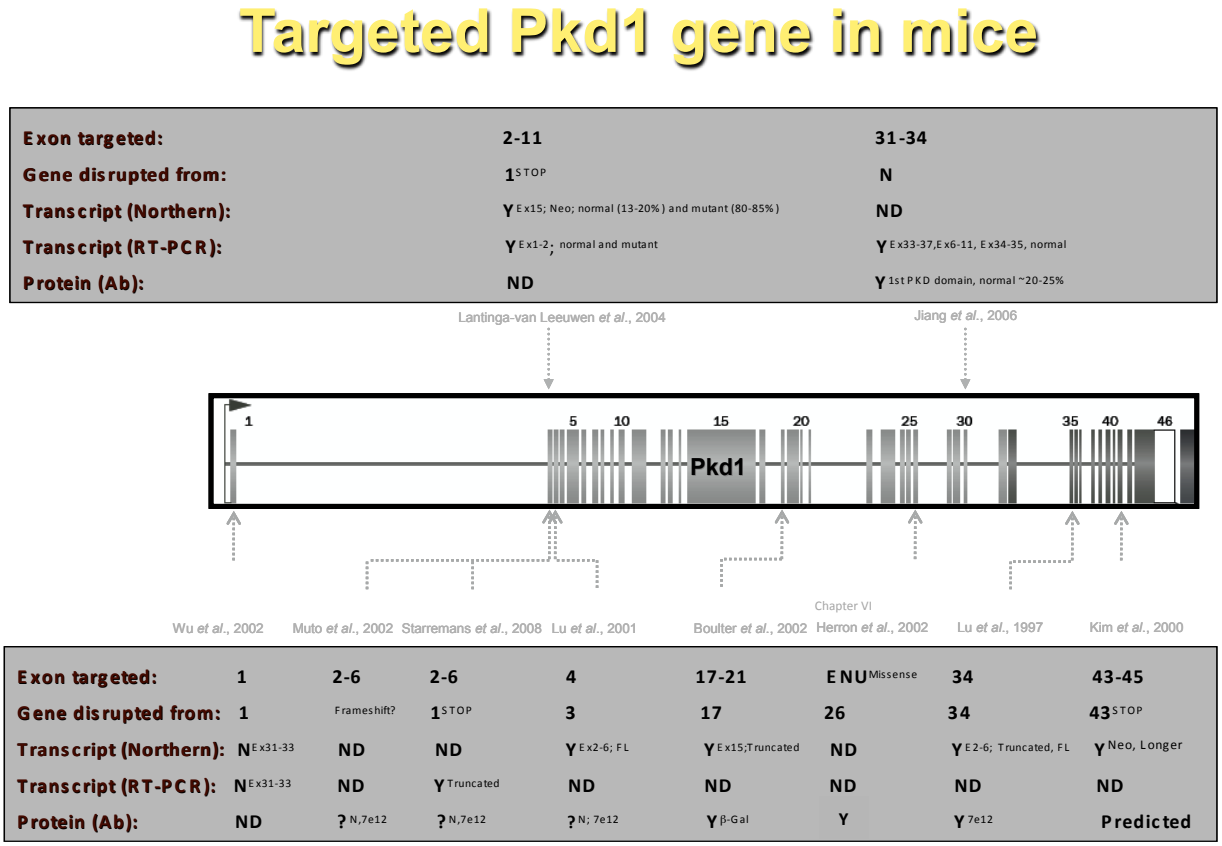

Legend: Schematic summary of different *Pkd1* ''loss-of-function'' (Lower gray panel) and two hypomorph *Pkd1* mouse models (Upper gray panel) with expression of putative residual Pc1 proteins (**Also See Table 8A**). Although these mouse models are often refered to as ''null'', implying complete absence of any form of a targeted gene, in many cases a truncated Pc1 protein, or even a protein of similar size to the full-length endogenous Pc1 is reported, predicted or might have been produced, but was undetected due to the choice of antibody that targets the deleted region. This observation could explain why these *Pkd1* ''null'' mice differ in many aspects: onset, progression of kidney disesase and divergence in extrarenal manifestations. It is thus possible that generated truncated Pc1 products are partially functional in mice, but also in human ADPKD. ND: not determined. ?: Not sure since antibody could not detect possible residual protein. N: no. Y: yes. $7^{e}12$: mouse monoclonal Pc1 antibody against N-terminal LRR domain of Pc1 (ex2-4).

References: (Wu, Tian et al. 2002) (Muto, Aiba et al. 2002) (Starremans, Li et al. 2008) (Lu, Shen et al. 2001) (Boulter, Mulroy et al. 2001) (Herron, Lu et al. 2002) (Lu, Peissel et al. 1997) (Kim, Drummond et al. 2000) (Jiang, Chiou et al. 2006) (Lantinga-van Leeuwen, Dauwerse et al. 2004).

IX) Temperature-sensitivity assay for *Pkd1*$_{extra}$ protein trafficking in MEFs

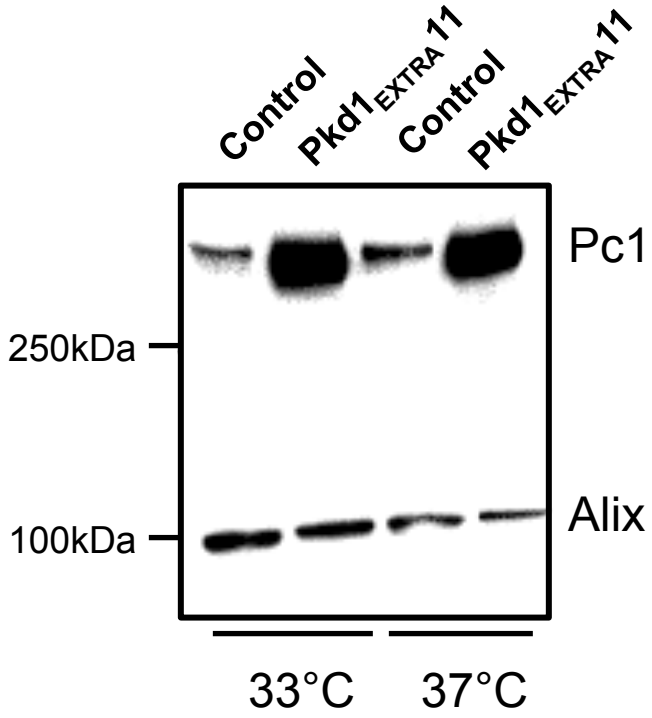

Legend: Effect of low temperature on Pc1 and Pc1$_{extra}$ intracellular trafficking. The CFTR ΔF508 mutants with folding defects have been shown in some reports to traffic properly from the ER (but not in others) when submitted to lower temperature. The mechanism for this is unknown, but it was proposed to occur through kinetic thermodynamic stability or specific biological components that vary between cell types and different temperatures, 2nd being more accepted by (Wang, Koulov et al. 2008), which might also explain the discrepancy in different reports. Hopp *et al.* have recently showed that this could be the case for some of the *Pkd1* human mutants. A *Pkd1* hypomorph R3277 mutant was found to traffic more efficiently out of the ER into the exosomes of primary CD cells when cells were incubated at lower temperature, at 33°C (Hopp, Ward et al. 2012). Reproducing the experiment using MEFs derived from *Pkd1*$_{extra}$11 or wild-type embryos, that already localize in the exosomes even at the high 37°C, we observed that both *Pkd1*$_{extra}$ 11, but also the wild-type Pc1 exosomal levels, if anything were upregulated at non-permissive 37°C, when normalized to Alix, the exosomal resident protein. ***It is noteworthy that this potentially inverse effect of temperature on Pc1 trafficking could be specific to MEF cells.*** CD: collecting ducts; MEFs: mouse embryonic fibroblasts; ER: endoplasmic reticulum.

X) Possible cross-interaction between transgenic polycystin1$_{extra}$ NTF-like protein and endogenous polycystin-1 CTF fragment

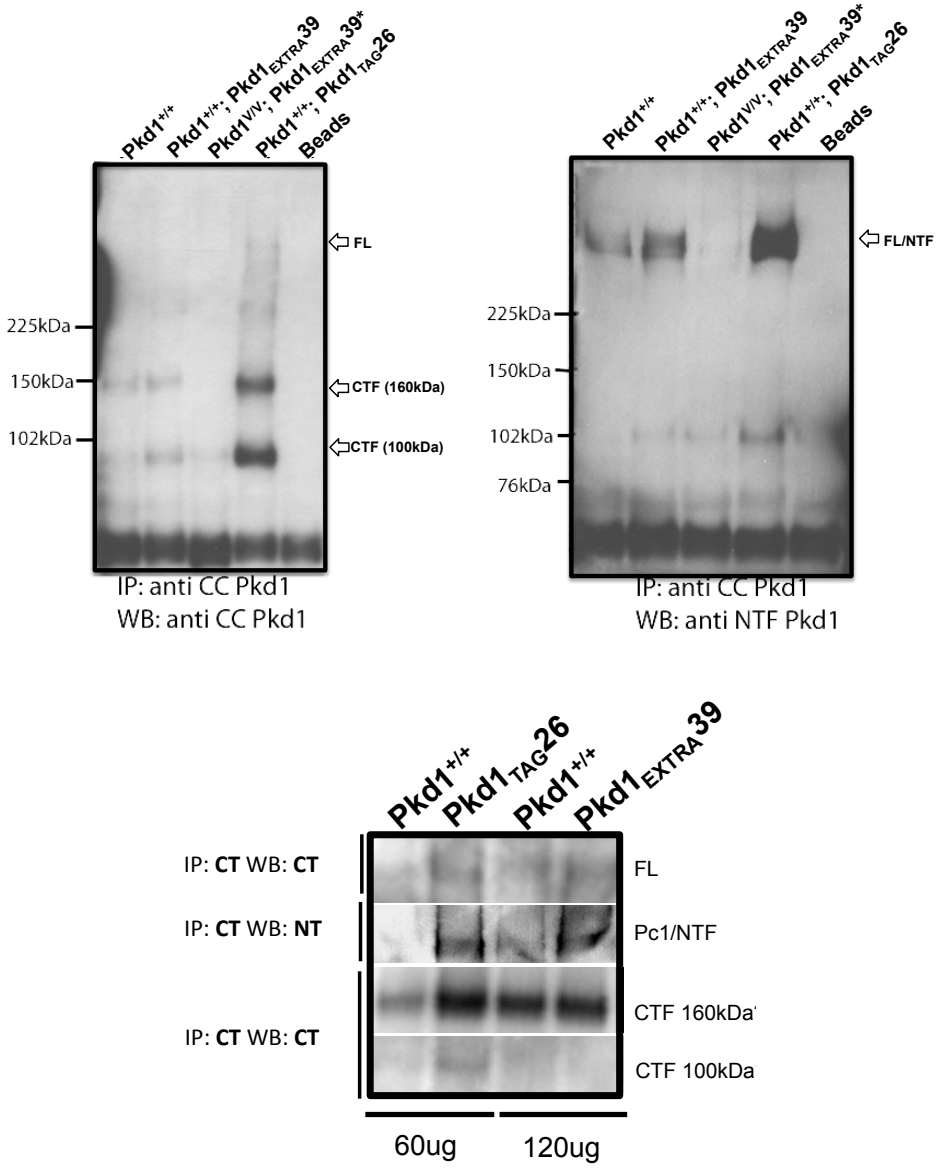

Legend: **Immunoprecipitation (IP) using C-terminal Pc1 chicken antibody and immunoblot detection (WB) with C-terminal Pc1 rabbit polyclonal antibody (left upper panel) or N-terminal Pc1 mouse monoclonal antibody (right upper panel) using P10 total kidney extract or MEFs (lower panel).**

(Upper panels) After immunoprecipitation and hybridization using C-terminal Pc1 antibody, the *Pkd1*$^{+/+}$ wild-type kidneys show at least two CTF fragments: GPS-cleaved ~160 kDa and GPS independent ~100kDa forms (**Chapter I, Section 4.1**). The full-length (FL) Pc1 is very low to undetectable. *Pkd1*

overexpressor (*Pkd1*$_{TAG}$ transgenic) show an increase of both CTF forms but very little full-length protein, which suggests that the Pc1 GPS-cleavage is very efficient and a constitutive process. As expected, *Pkd1*$^{V/V}$*; Pkd1*$_{EXTRA}$*39* compound (*Pkd1* NTF-like fragment on *Pkd1*$^{V/V}$ endogenous background) does not show a 160kDa CTF due to the absence of cleavage by ''V'' mutation, but does contain a 100kDa CTF cleaved product, provided by the ''V'' allele (**Chapter I, Section 4.1.1.2.3**).

When immunoprecipitated and hybridized with N-terminal Pc1 antibody, that recognizes the NTF GPS-cleaved form as well as the uncleaved full-length Pc1, protein extracts from the *Pkd1*$^{+/+}$*; Pkd1*$_{EXTRA}$*39* kidneys **(*upper right)*** and MEFs ***(lower panel)*** showed more interaction than *Pkd1*$^{+/+}$ suggestive of an ***in vivo interaction between Pc1$_{extra}$ and endogenous Pc1 CTF fragment.*** This ''cross-interaction'' appears partial in the kidneys since Pc1$_{EXTRA}$ is expressed to almost similar levels to Pc1$_{TAG}$ while this latest IP-ed much more than Pc1$_{EXTRA}$. An interaction between CTF and NTF subunits among unrelated aGPCRs, latrophilin and GPR, was reported by (Silva, Lelianova et al. 2009). In collaboration with Dr. Qian Feng, University of Maryland, School of Medicine.

On the left side of each panel are indicated molecular weights of the protein marker (BIORAD Kaleidoscope). Of note, for kidney extracts 700 μg of protein was used except for *Pkd1*$^{V/V}$*; Pkd1*$_{EXTRA}$*39* (420μg). Beads served as negative control. Similar results were obtained from 2 independent experiments for the total kidney extracts.

XI) Analysis of temporal regulation of renal *Pkd1* expression in wild-type and two *Pkd1* transgenic mice

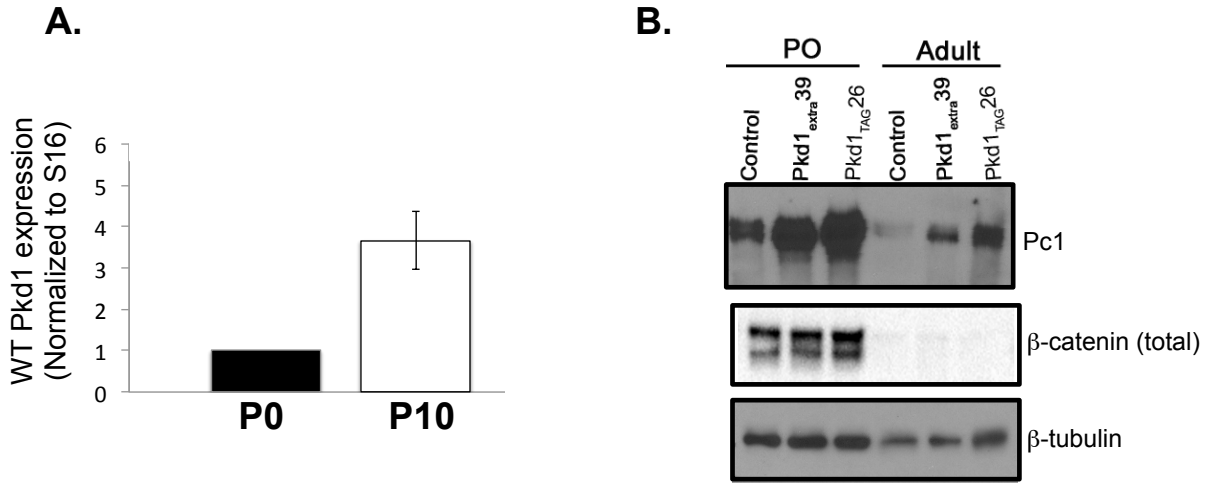

Legend: *Pkd1*/Pc1 kidney expression in wild-type (QPCR, A) and two transgenic *Pkd1*$_{extra}$ and *Pkd1*$_{TAG}$ mice at different ages (Western blot, B).

(A) Although the full-length 14kb *Pkd1* transcript was reported to peak at around E17 and to decrease to almost undetectable levels at birth, our Q-PCR analysis showed that 3' *Pkd1* murine transcript is still increasing few days after birth. Hence, potentially 3' *Pkd1* alternative transcript may have an independent role in kidney homeostasis (**Also see App.II**).

(B) Expression of both, Pc1 and β-catenin, decreases after birth and drops to very low levels in adulthood. This pattern of expression is consistent with Pc1 and β-catenin being two developmentally regulated genes whose expression needs to be switched off after developmental and highly proliferative periods (Geng, Segal et al. 1997). Furthermore, Pc1 expression is time-dependent in both wild-type and *Pkd1* transgenic mice which is supportive of presence of all regulatory elements required for appropriate temporal regulation of expression of *Pkd1* in our BAC-transgenes. Levels of Pc1 expression in adult *Pkd1*$_{TAG}$ PKD mice seem similar to those in wild-type mouse kidneys at birth. This is consistent with comparable PC1 levels in human adult ADPKD and human fetal normal kidney. Q-PCR analysis (MxPro3005P) was performed using 3' *Pkd1* primers in exon 39 and 40. For Western blot, we used 7^{e}12 mouse monoclonal Pc1 antibody against N-terminal LRR domain of Pc1. Equal loading of protein in P0 and adult protein extracts (9μg) was ensured by Bradford assay.

XII) Comparative analysis of specific PC1 and Pc1 motifs from GAIN domain to C terminus end

A .

	www.ensembl.org		Predicted by previous studies			
	Human (PC1)	**Mouse (Pc1)**	**Human (PC1)**	**Human (PC1)**	**Human (PC1)**	**Mouse (Pc1)**
GAIN domain (≈REJ+GPS) ≈320aa						
GPS domain	3011-3060	3003-3052				
Cleavage site H↓LT	3048↓3049	3040↓3041				
			Sandford *et al.*,1997 (1)	Hughes *et al.*, 1995 (2)	Chauvet *et al.*, 2004 (3)	Ward *et al.*, 2011 (4)
TM domain I	3073-3095	3065-3087	3075-3095	2580-2600		
TM domain II	3283-3302	3275-3294	3281-3301	2691-2713		
TM domain III	3322-3344	3314-3336	3323-3343	3075-3095		
TM domain IV	3556-3578	3547-3569	3559-3579	3323-3343		
TM domain V	3588-3610	3883-3905	3582-3602	3281-3301		
TM domain VI	3671-3690	3926-3948	3669-3689	3559-3579		
TM domain VII	3895-3917	3968-3990	3895-3915	3582-3602		
TM domain VIII	3937-3959	4016-4038	3934-3953	3669-3689		
TM domain IX	3979-4000	NI	3994-4014	3895-3911		
TM domain X	4026-4048	NI	4027-4045	4028-4048		
TM domain XI	NI	NI	4084-4104	4056-4076		
Cytosolic C-terminus	4048-4302/3	4038-4293	4105-4302 (deduction)	4077-4302 (deduction)		
NLS	—	—	—	—	4134-4154 (3) **LRRLRL….KVR**	4124-4144
Coiled-coil domain	4229-4249 (20aa)	4219-4239 (20aa)	4193-4248 (3)		Chapter I, Table 8	Chapter I, Table 8
Ciliary targeting signal	—	—	—	—	4296-4302	4287-4293 (4) **KVHPSST** Last 7aa

B.

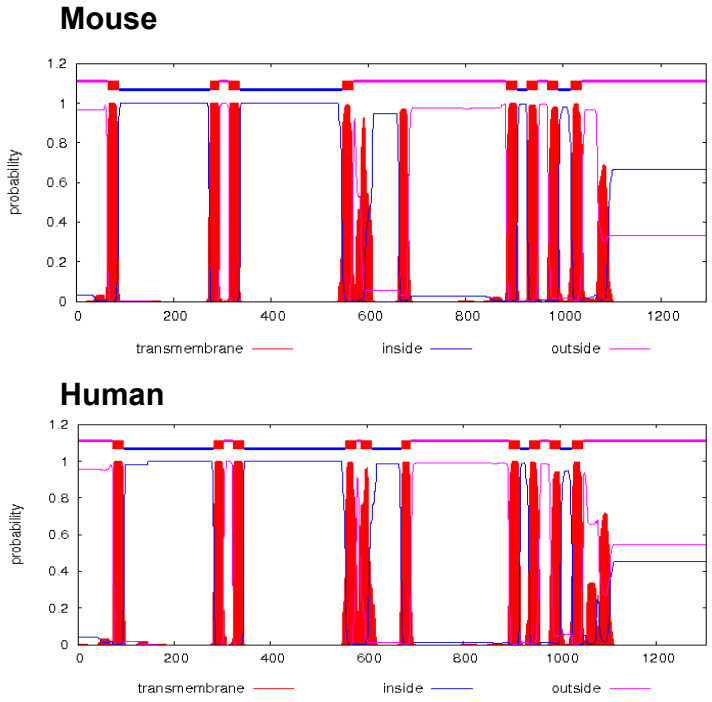

Legend: Comparison of amino acid position and localization for different Pc1 domains focusing specifically on TM, GPS, coiled-coil, NLS and ciliary targeting signal.

(A) Sequence compilation from the public database (www.ensembl.org) and comparison with the published predictions using different softwares. (1) In this study, Coils version 2.2 (ISREC Bioinformatic group, http://ulrec3.unil.ch/software/COILS-form.html) served for the coiled coil prediction. **(2)** TopPred II program was used in this case for the transmembrane topology. Hydrophobicity higher then 1.4 identified 10TM domains. One domain (TMII) was considered as a possible TM domain. **(3-4)** Localization of the NLS and ciliary targeting signal was identified by biochemical, mutagenic and functional assays. Published structures were considered "provisional" and the proposed topology needed further studied with antibodies and cristallography for confirmation. **References:** (Sandford, Sgotto et al. 1997) (Hughes, Ward et al. 1995) (Chauvet, Tian et al. 2004) (Ward, Brown-Glaberman et al. 2011).

(B) TMHMM software prediction of putative transmembrane domains in murine and human sequence of polycystin-1 protein. This server was chosen because it was rated as ‘*’best in an independent comparison of programs for prediction of TM helices’’* (Moller, Croning et al. 2001) (http://www.cbs.dtu.dk/services/TMHMM/). Of note, position ‘’0’’ was set as amino acid 3000 of Pc1. Instead of submitting the entire PC1 sequence of 4302aa, only aa3000 and onward were analyzed since the input for this software could not be longer than 2500aa. NLS: nuclear localisation sequence; TM: transmembrane domain; GAIN: G-protein-coupled receptor (GPCR) autoproteolysis-inducing domain; REJ: receptor for egg jelly domain; GPS: GPCR proteolysis site; aa: amino acid. NI: not identified by the software chosen in a particular study.

XIII) Prediction of GAIN domain in polycystin-1

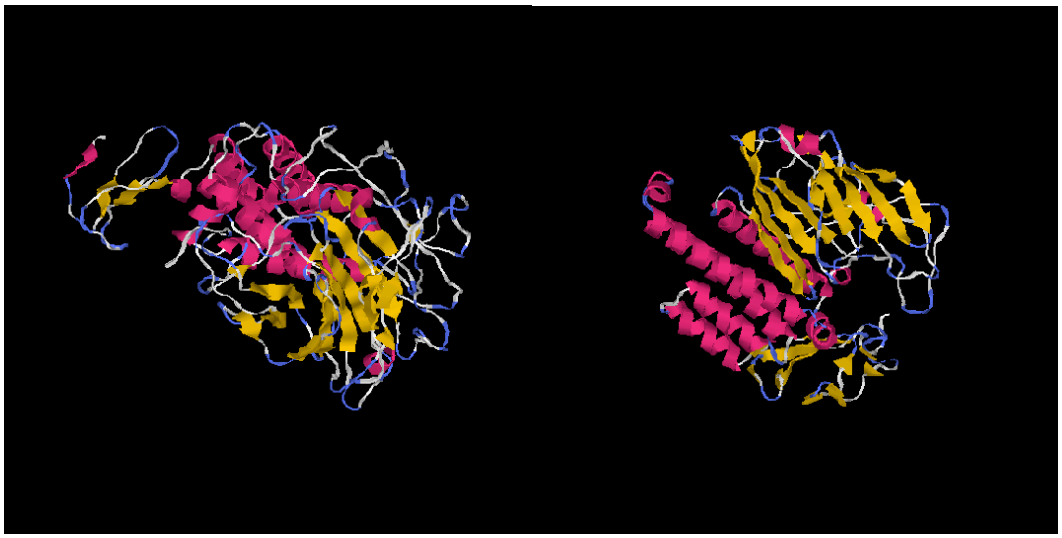

Left: 3D structure of Pc-1 predicted by TASSER software. Selected model 1, C-score=-2.48.

Sequence query (**GAIN domain of mouse PC1**):

VPWLHSLTASVLPGLLKQADPQHVIEYSLALITVLNEYEQAPDVSEPNVEQQLRAQMRKNITETLISLRVN
TVDDIQQITAALAQCMVSSRELMCRSCLKKMLQKLEGMMRILQAETTEGTLTPTTIADSILNITGDLIHLAS
LDMQGPQPLELGVEPPSLMVASKAYNLSSALMRILMRSRVLNEEPLTLAGEEIVALGKRSDPLSLLCYGK
ALGPSCHFSIPEAFSGALSNLSDVVQLIFLVDSNPFPFGYISNYTVSTKVASMAFQTQTGTQIPIEQLAAE
RAITVKVPNNSDQAAQSSHNPVGSTIVQPQTSVSAVVTADNSNPQAGLHLRITYTVLNERYLSAEPEPYL
AVYLHSVSQPNEYNCSASRRISLEVLEGADHRLYTFFIAPGTGTLDRSYYLNLTSHFHWSALEVSVGLYT
SLCQYFSEEMMMWRTEGIVPLEETSPSQAVCLTRHLTAFGASLFVPPSHVQFIFPE

Right: 3D structure of CL1 predicted by TASSER software. Selected model 1, C-score=0.37.

Sequence query (**GAIN domain of Cl1 mouse aa460-489**):

RPPAPNLHVSPELFCEPREVRRVQWPATQQGMLVERPCPKGTRGIASFQCLPALGLWNPRGPDLSNC
TSPWVNQVAQKIKSGENAANIASELARHTRGSIYAGDVSSSVKLMEQLLDILDAQLQALRPIERESAGKN
YNKMHKRERTCKDYIKAVVETVDNLLRPEALESWKDMNATEQVHTATMLLDVLEEGAFLLADNVREPA
RFLAAKQNVVLEVTVLNTEGQVQELVFPQEYPSENSIQLSANTIKQNSRNGVVKVVFILYNNLGLFLSTE
NATVKLAGEAGTGGPGGASLVVNSQVIAASINKESSRVFLMDPVIFTVAHLEAKNHFNANCSFWNYSER
SMLGYWSTQGCRLVESNKTHTTCACSHLTNFAVLMAHREIYQGRI

Legend: 3D structure prediction of murine polycystin-1 and CL1 GAIN domain by I-TASSER server. As shown for CL1 and BAI by crystallography, a similar structural conformation and β–sheets/αhelix compositions was also predicted by TASEER online protein structure and function prediction software for murine Cl1 (**right**) and Pc1 (**left**) (**Chapter I, Section 4.1.1.1**) (Arac, Boucard et al. 2012). BMC Bioinformatics, vol 9, 40 (2008). A Roy, A Kucukural, Y Zhang. I-TASSER: a unified platform for automated protein structure and function prediction. Nature Protocols, 5: 725-738 (2010) (Zhang 2008, Roy, Kucukural et al. 2010).

XIV) Potential additional cleavage site at N-terminus of polycystin-1

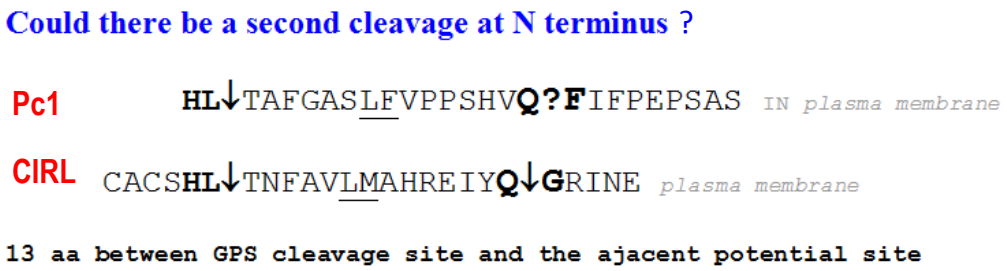

Legend: Protein sequence alignment of the murine Pc1 and CI-1 (CIRL) in search for a potential additional cleavage site. In addition to the GPS cleavage site, latrophilin/CIRL (arrow on the left) was suggested to undergo an additional cleavage between the GPS motif and first TM domain thus generating a soluble CIRL NTF fragment (arrow on the right). The uncleaved latrophilin can traffic to the membrane and can be processed at this second site *in vitro* and *in vivo*. Given some similarity between Pc1 and CIRL sequence, it is possible that Pc1 also contains a GPS independent cleavage site(s) at its N-terminus that could result in soluble PC1 NTF with functional significance. HLT: GPS cleavage site; ?: putative GPS independent additional N-terminal cleavage site in PC1. Q↓G identified as CLTR cleavage site by mass spectrometry (Krasnoperov, Deyev et al. 2009).

XV) Relative abundance and interaction between polycystins in *Pkd1$_{TAG}$* mice

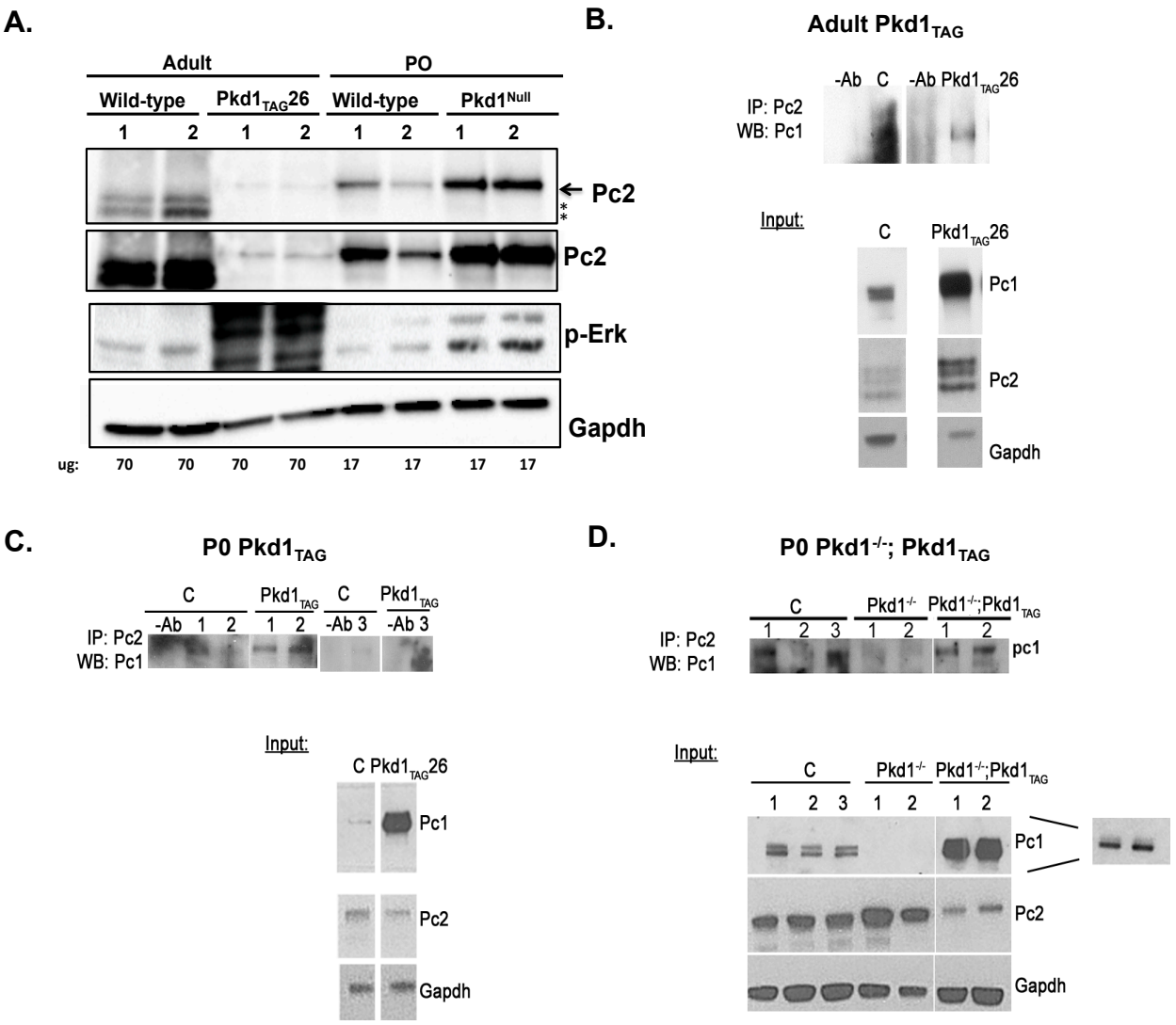

Legend: A) Increased phospho-Erk and Pc2 levels in the cystic kidneys of *Pkd1$_{TAG}$* gene increase and *Pkd1$^{-/-}$* gene decrease mouse models. *Additional bands of unknown origin (lower than 130kDa expected for Pc2) which appear when we use an anti-rat Pc2 monoclonal antibody and when Pc2 levels are very low *i.e.,* adult stage. Gapdh was used as loading control. Because of developmentally regulated decreasing expression of Pc2, more protein extract was used for the adult stage (70μg) than for the post-natal kidneys (17μg). **B-D)** Interaction of Pc2 and endogenous Pc1 and/or Pc1$_{TAG}$ in the kidneys at P0 (**C,D**), P10 (**Chapter V, Suppl. Fig.3**) and in adult stage by immunoprecipitation (**B**). Pc1/Pc2 interaction was detected in the wild-type control kidneys at all ages analyzed, which supports the presence of endogenous Pc1/Pc2 protein complex. Importantly, similarly to the control kidneys, at P0 we also detected an interaction between transgenic Pc1$_{TAG}$ and endogenous Pc2 on *Pkd1$^{-/-}$* genetic background (*Pkd1$^{-/-}$; Pkd1$_{TAG}$*) (**D**). However, even though Pc1/Pc2 interaction was higher in *Pkd1$_{TAG}$* transgenic kidneys at P0, P10 and adult stage, Pc2/Pc1$_{TAG}$ interaction did not seem extensively higher

than normal endogenous Pc1/Pc2 interaction suggesting a possible saturation of Pc2 by Pc1. Correlating with the preliminary data from (Côté 2009), Pc2 levels seem slightly decreased by *Pkd1*$_{TAG}$ transgene at early non-cystic stage (P0 and P10), which become increased in the cystic adult stage (**A**). Specific conditions for these experiments were: **IP starting material**- 200-300μg for P0 and 600μg for adult; **Input material**- 3.5% for P0 and 8% for adult kidneys.

C: Control wild-type age-matched kidneys; *Pkd1*$^{-/-}$ kidneys were used as negative control for Pc1/Pc2 interaction given undetectable Pc1 levels; *Pkd1*$_{TAG}$: *Pkd1*$_{TAG}$ transgenic line #26 that expresses high levels of *Pkd1*/Pc1; ''- Ab'': Control conditions where Pc2 antibody step was omitted during IP procedure for assessing potential non-specific binding to the beads.

XVI) Laparotomy of *Pkd1*$_{TAG}$ at ESRD

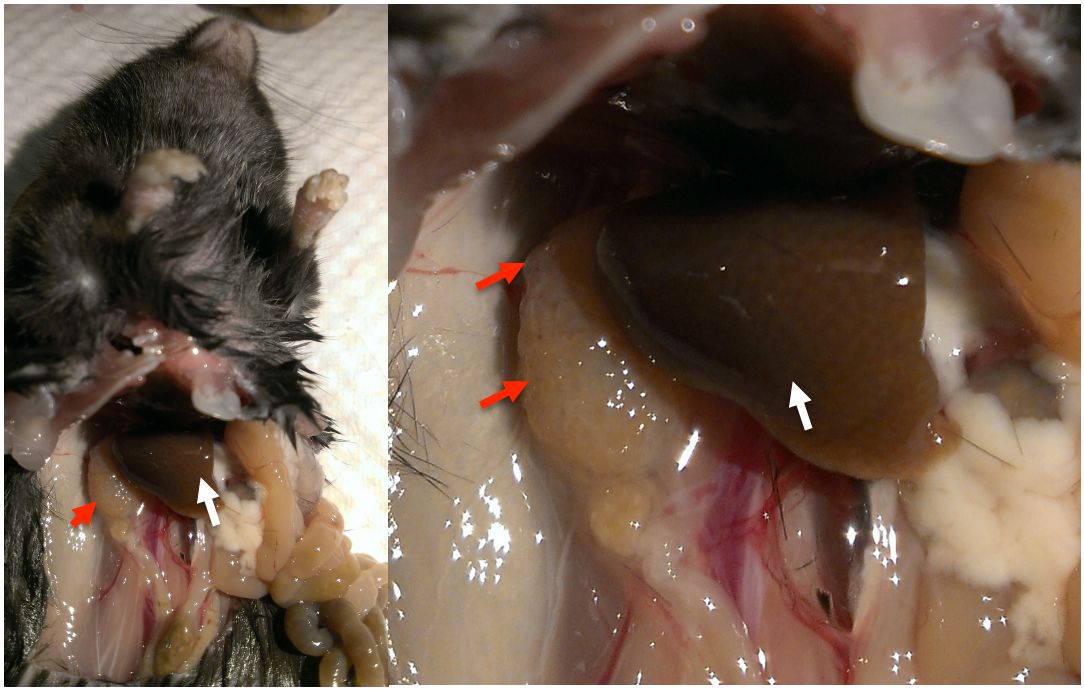

Legend: Pkd1$_{TAG}$ mice laparotomy. Note the presence of bosselated pale cystic kidneys (red arrows) and absence of liver anomalies (white arrows) in 6 months-old female from transgenic line#26 at ESRD (12^{e}generation C57Bl6/J genetic background). The mouse was sacrificed because it was showing signs of distress *i.e.,* curved body and limited movements. Photo taken by digital camera HTC.